UNIVERSITY OF KWAZULU-NATAL

DEVELOPMENT OF A NOVEL APPARATUS FOR VAPOUR-LIQUID EQUILIBRIUM MEASUREMENTS AT MODERATE PRESSURES

2006

PRASHANT REDDY

DEVELOPMENT OF A NOVEL APPARATUS FOR VAPOUR-LIQUID EQUILIBRIUM MEASUREMENTS AT MODERATE PRESSURES

by

PRASHANT REDDY

A thesis submitted in fulfillment of the academic requirements for the degree of Doctor of Philosophy in the School of Chemical Engineering at the University of KwaZulu-Natal, Durban.

DECEMBER 2006

ABSTRACT

In this work, a novel experimental apparatus has been designed, constructed and commissioned for the measurement of VLE at pressures up to 750 kPa and temperatures up to 600 K. The project undertaken represents a complete re-working of the design of Harris (2004), which was plagued by irregularities in the equipment operation and in the acquisition of experimental data. As in the work of Harris (2004), the design of the apparatus presented here is based upon the highly successful glass VLE still design of Raal (Raal and Muhlbauer, 1998). The novel apparatus is principally constructed from machined 316 stainless steel and features sight glasses in strategic positions to allow for an observation of the fluid flow characteristics in specific sections of the apparatus. The key criteria that encompassed the design of the equipment were expediency, operational efficiency and versatility in the acquisition of reliable VLE data.

An initial test of the performance of the equipment was achieved through the measurement of pure-component vapour pressures of selected hydrocarbons (n-alkanes and a cycloalkane) and alkanols. The test system for vapour-liquid equilibrium (P-T-x-y) measurements with the novel apparatus was that of cyclohexane + ethanol at a pressure of 40 kPa. Good agreement between the literature and the experimental data was observed. Isobars for the cyclohexane + ethanol system at 69.8 kPa, 97.7 kPa and 150 kPa were also measured. The latter constitutes new data that have been measured for this system. Novel vapour-liquid equilibrium data were also obtained for the systems of 1-propanol + 2-butanol, 1-propanol + n-dodecane and 2-butanol + n-dodecane at temperatures of 373.15 K, 393.15 K and 423.15 K. For the very high relative volatility alkanol + n-dodecane systems, uncertainties in the measurement of the vapour phase (y) resulted in only P-T-x experimental data being presented here, where the vapour phase composition was computed with the Wilson equation.

The theoretical treatment of the experimental VLE data was achieved through a combination of the gamma-phi and the phi-phi approaches in the fitting of the VLE data to various thermodynamic models. In the gamma-phi method, a variety of activity coefficient models (Wilson, T-K Wilson, NRTL, UNIQUAC and modified UNIQUAC) together with the truncated virial equation of state were employed to find the best fit for the data. In the phi-phi method, the isothermal data sets were treated with the Peng-Robinson-Stryjek-Vera equation of state with the original Huron-Vidal (HV) and the modified Huron-Vidal mixing rules (MHV1 and MHV2) in the correlative procedure. Thermodynamic consistency testing was also performed with the Direct Test of Van Ness (1995) to assess the quality of the experimental P-T-x-y VLE data sets measured in this study.

PREFACE

The work described in this thesis was performed in the School of Chemical Engineering at the University of KwaZulu-Natal, Durban, from January, 2004 to December, 2006, under the supervision of Prof. D. Ramjugernath and Prof. J.D. Raal.

I, Prashant Reddy, declare that to the best of my knowledge, the work contained in this thesis is indeed my own work, unless stated otherwise in the text. This thesis has not been submitted for degree purposes, in part or whole, to any other tertiary institution.

Prashant Reddy

As the candidate's supervisor, I, Prof. D. Ramjugernath, have approved this thesis for submission.

Prof D. Ramjugernath

As the candidate's co-supervisor, I, Prof. J.D Raal, have approved this thesis for submission.

Prof J.D. Raal

ACKNOWLEDGEMENTS

The success of this project can be attributed to the combined efforts of many individuals in their demonstrated willingness to render invaluable advice and assistance for the successful completion of many of the challenging tasks that were an inherent feature of this work. In particular, I would like to unequivocally extend my sincerest gratitude to the individuals mentioned below and would like to apologize in advance for any inadvertent omissions.

- My supervisors, Prof. D. Ramjugernath and Prof. J.D. Raal, for affording me the opportunity to undertake this project under their expert tutelage.

- My parents and family, for their unwavering support and indispensable role in my personal and professional life.

- The mechanical workshop staff in the School of Chemical Engineering. In particular, Mr Ken Jack and Mr Les Henwood for sharing their expertise on many occasions for the design and the fabrication of the apparatus and for exploring the limits between "theory and practice".

- The computer and electronics workshop staff in the School of Chemical Engineering. In particular, Mr Dhavaraj Naidoo, Mr Preyothen Nayager and Mr Colin Mandri.

- My friends and colleagues: Etienne Wilson, Jason Knock, Anne Megne Motchelaho, Prebantha Moodley, Rinay Bhownath, Minal Soni, Sudhir Pillay, Shameer Hareepersad, Scott Clifford, Tyrone McKnight, Yash Nannoolal, Mkokheli Ndlovu, Niri Naidu and Ayanda Khanyile for their friendship and support during both joyful and tumultuous times.

- The technical and sales staff of Wika Instruments, Kaytherm, Labworld, Temperature Controls, Johannesburg Valve and Fitting Co. and Separations. In particular, Desi Naidoo, Kevin Wickee, Serina Thamanna, Elias Thomas and Vivian Naidoo for their advice.

- Themesha Khan, Iordan Ignatov and Jeremy Thurgood from the School of Electronic Engineering at UKZN for their assistance in modifying the VALVECON program.

- The National Research Foundation (NRF) of South Africa and the University of KwaZulu-Natal Scholarships Office for financial support.

CONTENTS

FIGURES

CHAPTER 2:

CHAPTER 3:

CHAPTER 4:

CHAPTER 6:

CHAPTER 7:

CHAPTER 8:

APPENDIX A:

APPENDIX C:

TABLES

CHAPTER 3:

CHAPTER 5:

CHAPTER 6:

CHAPTER 7:

CHAPTER 8:

APPENDIX A:

APPENDIX B:

APPENDIX C:

PHOTOGRAPHS

CHAPTER 4:

NOTATION

SYMBOLS

a	Cubic EOS pure component energy parameter, adjustable parameter in correlating equations, number of points in a data set
a_{mn}	UNIFAC interaction parameter between groups m and n
A	Molar Helmholtz free energy, adjustable parameter in correlating equations, GC chromatogram peak area, cubic EOS constant
A_{ij}	Adjustable interaction parameter in G^E correlating equations
b	Cubic EOS covolume parameter, adjustable parameter in correlating equations, number of points in a data set
B	Virial EOS second virial coefficient, adjustable parameter in correlating equations, cubic EOS constant
B_{ij}	Virial EOS cross second virial coefficient
c	Cubic EOS Volume translation parameter
C	Virial EOS third virial coefficient, adjustable parameter in correlating equations
d_{ij}	EOS mixing rule binary interaction parameter
D	Adjustable parameter in correlating equations, WSMR simplifying term
E_0	Adjustable parameter in correlating equations
f	Fugacity
g_{ij}	Adjustable interaction parameter in the NRTL equation, two-fluid theory Gibbs free energy
G	Molar Gibbs free energy
G_{ij}	Constant or function in the Wilson and NRTL equations.
H	Molar enthalpy
k_{ij}	EOS mixing rule binary interaction parameter
K	Phase equilibrium constant
l_i	Simplifying term in the UNIQUAC equation

m	Number of points in a data set
M	General mixture property
M_W	Molar mass
n	Number of points in a data set, total number of moles in the system
p	Number of points in a data set
P	Pressure
P_D	Deviation pressure in the method of Maher and Smith (1979)
P_{vap}	Pure component vapour pressure
q	Molecular surface area parameter for the UNIQUAC and UNIFAC equations, feed composition in flash calculations, MHV1 and MHV2 constants
q′	Molecular surface area parameter for the modified UNIQUAC equation
Q	WSMR simplifying term
Q_k	UNIFAC group area parameter
r	Molecular size parameter for the UNIQUAC and UNIFAC equations, number of points in a data set
R	Universal gas constant
R_k	UNIFAC group size parameter
s	Adjustable parameter in correlating equations
S	Molar entropy, summation for the vapour phase composition
t	Number of points in a data set
T	Temperature
T_b	Normal boiling point temperature
R	Universal gas constant
R_D	Radius of gyration
u_{ij}	Adjustable interaction parameter in the UNIQUAC equation
V	Molar volume

V_W	Hard-core van der Waals volume
x	Liquid phase mole fraction, Wagner equation independent variable
X_m	UNIFAC group mole fraction
y	Vapour phase mole fraction
z	Lattice coordination number, liquid or vapour mole fraction, effective volume fraction in the Wohl expansion, overall composition
Z	Molar compressibility correction factor
Z_{RA}	Modified Rackett equation parameter

GREEK SYMBOLS

α	Vapour pressure correlation for cubic EOS, parameter in the MHV1 and MHV2 mixing rules, adjustable parameter in correlating equations
α_{ij}	Non-randomness parameter for the NRTL equation, relative volatility
β	Constant or function in the T-K Wilson equation, simplifying term in the WSMR and TCMR models
β_v	Constant or function in the T-K Wilson equation
χ	Simplifying term for the WSMR and TCMR models
δ_{ij}	Simplifying term for the second virial coefficients, composition-dependent term in the CDMR model
ε	Predefined tolerance for the convergence of the residual quantities in the minimization routines
ε_p	Pressure-dependent term in the Gibbs-Duhem equation
ε_T	Temperature-dependent term in the Gibbs-Duhem equation
Φ_i	Nonideality term in the LPVLE gamma-phi method, constant or function in the UNIQUAC equation, polarity factor in the Tarakad-Danner method
ϕ	Fugacity coefficient
γ	Activity coefficient

η_{ij}	Association or solvation factor for the Hayden and O'Connell method
λ_{ij}	Adjustable interaction parameter in the Wilson and T-K Wilson equations
κ	Parameter in the cubic EOS $\alpha(T_R, \omega)$ correlation
Λ_{ij}	Constant or function in the Wilson and the T-K Wilson equations
μ	Chemical potential, dipole moment
θ_i	Constant or function in the UNIQUAC and UNIFAC equations
ρ	Density
σ	Cubic EOS numerical constant, molecular size parameter for the Hayden and O'Connell method
τ_{ij}	Constant or function in the NRTL and UNIQUAC equations.
ω	Acentric factor
ξ	Local volume fraction in the Wilson equation
ψ	Function for the enthalpy of vapourization from vapour pressure correlations
ψ_{mn}	UNIFAC group interaction parameter

SUPERSCRIPTS

calc	Calculated quantity
C	Combinatorial contribution in the UNIQUAC and UNIFAC equations
exp	Experimental quantity
E	Excess quantity
D	Dimerized molecular contribution in the Hayden and O'Connell method
F	Free molecular contribution in the Hayden and O'Connell method
nr	Non-random portion of the Helmholtz free energ
o	Standard state
r	Reference state value
R	Residual contribution in the UNIQUAC and UNIFAC equations, residual

sat	Saturation state pure component quantity
L	Liquid phase
V	Vapour phase
∞	Infinite dilution

SUBSCRIPTS

c	Critical state property
cij	Pseudo-critical property
i	Component identity
j	Component identity
k	Component identity
m	Mixture
old	Old value for a variable in an iteration sequence
new	New or current value for a variable in an iteration sequence
r	Reduced variable
ref	Reference state value
o	Zero pressure state
vdW	van der Waals
∞	Infinite pressure state

OVERBARS

-	Partial molar property

ABBREVIATIONS

AADP	Absolute average deviation
ASOG	Analytical solution of groups
BWR	Benedict-Webb-Rubin EOS
BWRS	Benedict-Webb-Rubin-Starling EOS
CDDMR	Composition-dependent and density-dependent MR
CDLCMR	Composition-dependent local composition MR
CDMR	Composition-dependent MR
CMR	Classical MR
DDLCMR	Density-dependent local composition MR
DIMR	Density-independent MR
DIPPR	Design Institute for Physical Property Data
DDB	Dortmund Data Bank
EOS	Equation/s of state
FID	Flame ionization detector
G^E	Excess molar Gibbs free energy
GC	Gas chromatography/gas chromatograph
GC EOS	Group contribution EOS
GLE	Gas-liquid equilibria
HPVLE	High-pressure vapour-liquid equilibria
HV	Huron-Vidal MR
HVID	Huron-Vidal infinite dilution activity coefficient MR
HVOS	Huron-Vidal-Orbey-Sandler MR
ID	Inner diameter
IRP	Infinite-reference pressure
LCMR	Local composition mixing rule

LCVM	Linear combination of the HV and MHV1 models
LEMF	Local effective mole fraction activity coefficient model
LLE	Liquid-liquid equilibria
LPVLE	Low-pressure vapour-liquid equilibria
MHV1	Modified Huron-Vidal first-order MR
MHV2	Modified Huron-Vidal second-order MR
MR	Mixing rule/s
OD	Outer diameter
OF	Objective function
NRP	No-reference pressure
NRTL	Non-random two-liquid activity coefficient model
PC	Personal computer
PR	Peng-Robinson EOS
PRSV	Peng-Robinson-Stryjek-Vera EOS
PVT	Pressure-Volume-Temperature
PRSK	Predictive-Soave-Redlich-Kwong model
QSVC	Quadratic second virial coefficient condition
RK	Redlich-Kwong EOS
RMSD	Root mean square deviation
SLE	Solid-liquid equilibria
SRK	Soave-Redlich-Kwong EOS
SS	Stainless steel
t-mPr EOS	Translated and modified PR EOS
TC test	Thermodynamic Consistency test
TCB	Twu-Coon and Bluck MR
TCD	Thermal conductivity detector
T-K Wilson	Tsuboka-Katayama Wilson activity coefficient model

UNIFAC	UNIQUAC functional group activity coefficient model
UNIQUAC	Universal quasi-chemical activity coefficient model
UNIWAALS	UNIFAC G^E model and van der Waals EOS combined approach
vdW	van der Waals MR
VLE	Vapour-liquid equilibria
VLLE	Vapour-liquid-liquid equilibria
VT-SRK	Volume-translated SRK EOS
VT-PR	Volume-translated PR EOS
WSMR1	Wong-Sandler MR
WSMR2	Reformulated Wong-Sandler MR
ZRP	Zero-reference pressure

"Classical thermodynamics made a deep impression upon me. It is the only physical theory of universal content concerning which I am convinced that, within the framework of the applicability of its basic concepts, it will never be overthrown" , Albert Einstein, physicist and theoretical scientist (1879 - 1955).

CHAPTER ONE

INTRODUCTION

Contemporary trends in the field of phase equilibrium thermodynamics indicate a burgeoning interest or concentration of efforts in the development of predictive thermodynamic models (Gmehling, 2003; Jaubert *et al.*, 2004; Vetere, 2004) and molecular simulation (Deiters *et al.*, 1999; Sandler, 2003) to enable the acquisition of quantitative estimates of the phase equilibrium properties of a system; most notably vapour-liquid equilibria. This aversion to experimental measurements can be attributed to high costs, long time periods, undesirable phenomena and numerous experimental difficulties (Van't Hoff *et al.*, 2004) which have plagued researchers over the course of the last century; coupled with advances in computational efficiency and the sheer magnitude of chemical compounds and combinations thereof requiring thermodynamic characterization. However, not only does the measurement of vapour-liquid equilibria serve as the framework for the development, validation and continual modification of predictive or computational thermodynamics, it remains an integral part of the successful design of a large number of industrial thermal separation processes (distillation, extractive distillation, azeotropic distillation and flash operations).

It is widely acknowledged that the greatest capital investment and operating costs in the oil refining, petrochemical, chemical and related industries (gas processing, pharmaceutical, *etc.*) are frequently incurred in the design of the separation step. Despite the high-energy consumption of distillation, the latter accounts for 90% of all thermal separation processes in the chemical industry due to the numerous advantages of distillation over other methods (Gmehling *et al.*, 1999). Consequently, the optimal design of separation sequences, control strategies and more significantly the separation equipment itself (as in the sizing of distillation columns) for an industrial separation process is a task of tremendous importance for the process engineer as its successful completion weighs heavily upon the economics of the entire chemical plant. In addition to transport, physical and thermo-chemical data of the components in the mixture to be separated, a vital ingredient for the proper realization of the separation step is a reliable knowledge of the phase equilibrium properties (vapour-liquid equilibrium) of the system. The ideal scenario is the availability of a thermodynamically consistent set of vapour-liquid equilibrium data at the pressure, temperature and composition range for the operating or working conditions of the process. Since this is infrequently the case, an alternative approach has been the use of the correlative approach (if a minimal amount of experimental data is

available) or predictive thermodynamic models (in the complete absence of any experimental data) in process simulators.

Critical evaluations and commentary on the use of predictive thermodynamic models in process simulators for the design of industrial separation processes (Wakeham *et al.*, 2000; Barnicki, 2002; Chen *et al.*, 2004) has yielded that a "blindfolded approach" to the use of the above *i.e.* neglecting small errors between predicted and experimental values can translate into significant errors in distillation column design, which can severely compromise the economy and the efficiency of the separation process. It is therefore of the utmost importance to ensure the availability of a sufficiently large database of reliable experimental data, not only as a direct means for the design of separation equipment, but to improve the predicted results and confidence in the predictive capability (Chen *et al.*, 2004) of underlying models of process simulators, such as the UNIFAC (Dortmund) approach (Kato and Gmehling, 2005), to allow for the accurate design of separation processes.

Traditional low-pressure dynamic recirculating stills possess considerable advantages over other vapour-liquid equilibrium measurement techniques (*e.g.* static methods), in their respective pressure ranges, such as low investment costs, simple operation and expediency in furnishing a full VLE data set of P-T-x-y measurements; an example of which is the highly successful contemporary low-pressure VLE glass still design of Raal (Raal and Muhlbauer, 1998). A survey of vapour-liquid equilibrium that has been published in open literature and data from a variety of reliable literature sources (Dortmund Data Bank, 1999; Hirata *et al.*, 1975) yields a relative void in the availability of published vapour-liquid equilibrium data in the moderate-pressure range (0.1 MPa < P $\leq$ 1 MPa) for industrially relevant systems. The above pressure range is particularly applicable to the design of separation equipment as there are a number of distillation sequences whose operating conditions fall within this range.

There have been very few effective designs based on traditional low-pressure VLE stills that have been developed to address the above deficiency in the current phase equilibrium data pool. The work of Harris (2004) represented an initial attempt at such a design in our laboratories at the Thermodynamics Research Unit at the University of KwaZulu-Natal, where the equipment was to measure VLE data at pressures up to 30 MPa and temperatures up to 700 K. However, as a result of an overambitious pressure range and an oversight of key design and operational considerations, there were serious concerns over the operational efficiency and quality of data produced. Consequently using the design and associated flaws of the equipment of Harris (2004) as a benchmark for the necessary modifications, a novel apparatus has been developed in our laboratories to allow for the measurement of vapour pressures and vapour-liquid

equilibrium data for pressures up to 750 kPa and temperatures up to 600 K. Despite an unavoidable diminution of the operating pressure range (as a result of thinner stainless steel vessel walls and the inclusion of glass inserts), this design represents a significant improvement to that of its predecessor. As with the design of Harris, the design of the novel equipment has been based on the successful design of the low-pressure liquid and vapour condensate recirculating still of Raal (Raal and Muhlbauer, 1998). An initial test of the performance of the equipment was conducted through the measurement of the pure component vapour pressures of cyclohexane, n-heptane, n-octane, ethanol and 1-propanol.

The investigation of the vapour-liquid equilibria of mixtures containing hydrocarbons and alkanols is of considerable importance as such systems are industrially relevant for the design of separation processes and from a theoretical point of view, for the development and validation of liquid phase thermodynamic models (Peleteiro *et al.*, 2001; Darwish and Al-Anber, 1997). In this work, the types of binary mixtures investigated were of the following combinations: cycloalkane + alkanol, alkanol + n-alkane and alkanol + alkanol systems. The chemical components corresponding to the above that were studied are the systems of cyclohexane + ethanol, 1-propanol + 2-butanol, 1-propanol + n-dodecane and 2-butanol + n-dodecane. Both isobaric and isothermal measurements were obtained for the relevant systems in the low and moderate-pressure regions to demonstrate the versatility of the apparatus. The alkanol + n-dodecane systems studied, for which no VLE data is currently available in open literature, proved particularly challenging to measure (especially for the vapour phase composition) due to the very high relative volatility of the system. Consequently, only experimental P-T-x data were reliably obtained and the vapour phase composition (y) was computed in a BUBL P calculation with the Wilson equation. The latter served to highlight that the traditional difficulties experienced in the measurement of these types of systems with conventional dynamic recirculating VLE stills are indeed quite challenging to address, as these could not be circumvented despite the innovative novel features that were incorporated in the VLE apparatus presented in this study.

The raw experimental vapour pressure and vapour-liquid equilibrium data were subjected to theoretical treatment in the form of data correlation and thermodynamic consistency testing. The data reduction for the vapour-liquid equilibrium data was achieved through both the indirect (gamma-phi) and direct (phi-phi) approaches where a variety of activity coefficient models, equations of state and mixing rules were employed to correlate the data. Thermodynamic consistency testing was performed on the P-T-x-y experimental data with the Direct Test of Van Ness (1995) to allow for a rigourous assessment of the quality of the data measured.

The content of the research presented in this work allows for invaluable insight into the design principles and considerations inherent in the quite challenging task of designing phase equilibrium measurement equipment (assisted by providing critical commentary in tracing the origins of the early VLE still designs) and provides an extensive coverage of the theoretical aspects of VLE treatment to provide a holistic view on the contemporary state of vapour-liquid equilibrium measurements in the low and moderate-pressure regimes.

CHAPTER TWO

A REVIEW OF THE CLASSIFICATION AND DEVELOPMENT OF VAPOUR-LIQUID EQUILIBRIUM EQUIPMENT

2.1 Introduction

The task of designing VLE measurement equipment is quite arduous and requires great insight due to the complex nature of the phase equilibrium behaviour of real systems, some of which exhibit complex phenomena (azeotropes, retrograde behaviour, *etc.*). This coupled with the wide ranges of pressures (less than 1 kPa to over 100 MPa) and temperatures (200 - 700 K) over which VLE data has to be measured, further complicates the design criteria. Additionally, the nature of the system to be investigated (in terms of surface tension, latent heat, relative volatility, viscosity, thermal stability, *etc.*) plays a major role in determining the final design of the VLE equipment by imposing restrictions upon its range of applicability.

Scientific forays into the optimal design of equipment for the accurate measurement of VLE of various systems has been a gradual, steady progression of extending existing ideas and inventing new ones for new purposes over the course of the last 100 years. The impossible task of designing a "universal" VLE still, suitable for all temperature and pressure ranges (Rogalski and Malanowski, 1980), as well as chemical systems and type of data required, has resulted in the development and classification of distinct types of VLE stills and many variations thereof.

A contemporary classification of VLE equipment can be based on the type of operation (static or dynamic), mode of operation (isobaric or isothermal or isopleth), operating conditions (high, moderate or low-pressure), variable measurement (P-T-x-y) and method of phase determination (analytical or synthetic). The distinction amongst high, medium and low-pressure VLE is of course appropriate in a relative sense (Dohrn and Brunner, 1995) as it depends on an arbitrary assignment of the lower limit.

There are many comprehensive reviews of experimental methods and equipment for low-pressure VLE and to a lesser extent, except in recent reviews, high-pressure VLE measurement

in various literature sources as in the monographs by Hala *et al.* (1967), Malanowski (1982a, 1982b), Deiters and Schneider (1986), Abbott (1986) and Raal and Muhlbauer (1994, 1998).
In this review chapter, a brief treatment of HPVLE methods will be presented with the objective of establishing theoretical and experimental considerations that are common to HPVLE and LPVLE methods. Greater emphasis will be placed upon the development of dynamic recirculating type VLE stills for low and moderate pressures, which comprises the field of interest to the author. For an in-depth review of the classification and development of the different types of HPVLE measurement methods, Appendix A can be consulted.

2.2 Classification of HPVLE equipment

A basic classification scheme for high-pressure VLE equipment, adapted from that of Raal and Muhlbauer (1998), is shown in Figure 2.1. The basis of the broad classification scheme is the means by which an equilibrium condition is established *i.e.* whether the equilibrium phases *i.e.* vapour or liquid or both are circulated through the equilibrium still (dynamic) or simply coexist in the environment of a closed, agitated equilibrium cell (static). Special methods in the form of dynamic recirculating VLE stills are also included in this classification.

Sub-division of the static method for VLE determination is based on whether the equilibrium phase/s (usually vapour phase) is/are sampled (analytical) or not (synthetic). Static equipment can also be constant-volume cells or variable-volume cells, where for the latter; the pressure of the system can be varied due to the movement of a piston present in the cell. Synthetic static equipment can be further classified as being a visual synthetic method, non-visual method or the synthetic method using material balances. Static equipment that combines features from both the analytical and the synthetic types are classified as "combined static methods".
Dynamic methods involve the sampling of the equilibrium phases and are consequently classified as being analytical, with no subdivisions in this regard. Dynamic methods can, however, be sub-divided based on which of the equilibrium phases is circulated (vapour, liquid or both) through the equilibrium cell and the rate of circulation. The two principle sub-divisions, based on the above criteria for dynamic method classification, as shown in Figure 2.1 are single pass or flow methods and phase recirculation methods. Flow methods are traditionally either single vapour pass (semi-flow), also known as pure gas circulation (Fornari *et al.* 1990), or single vapour and liquid pass (continuous flow) methods and involve the steady metered flow of vapour (at a regulated pressure) or vapour and liquid (at a regulated temperature), respectively, in a single pass through the equilibrium cell. This method apparently allows for a rapid equilibration time when compared with other methods.

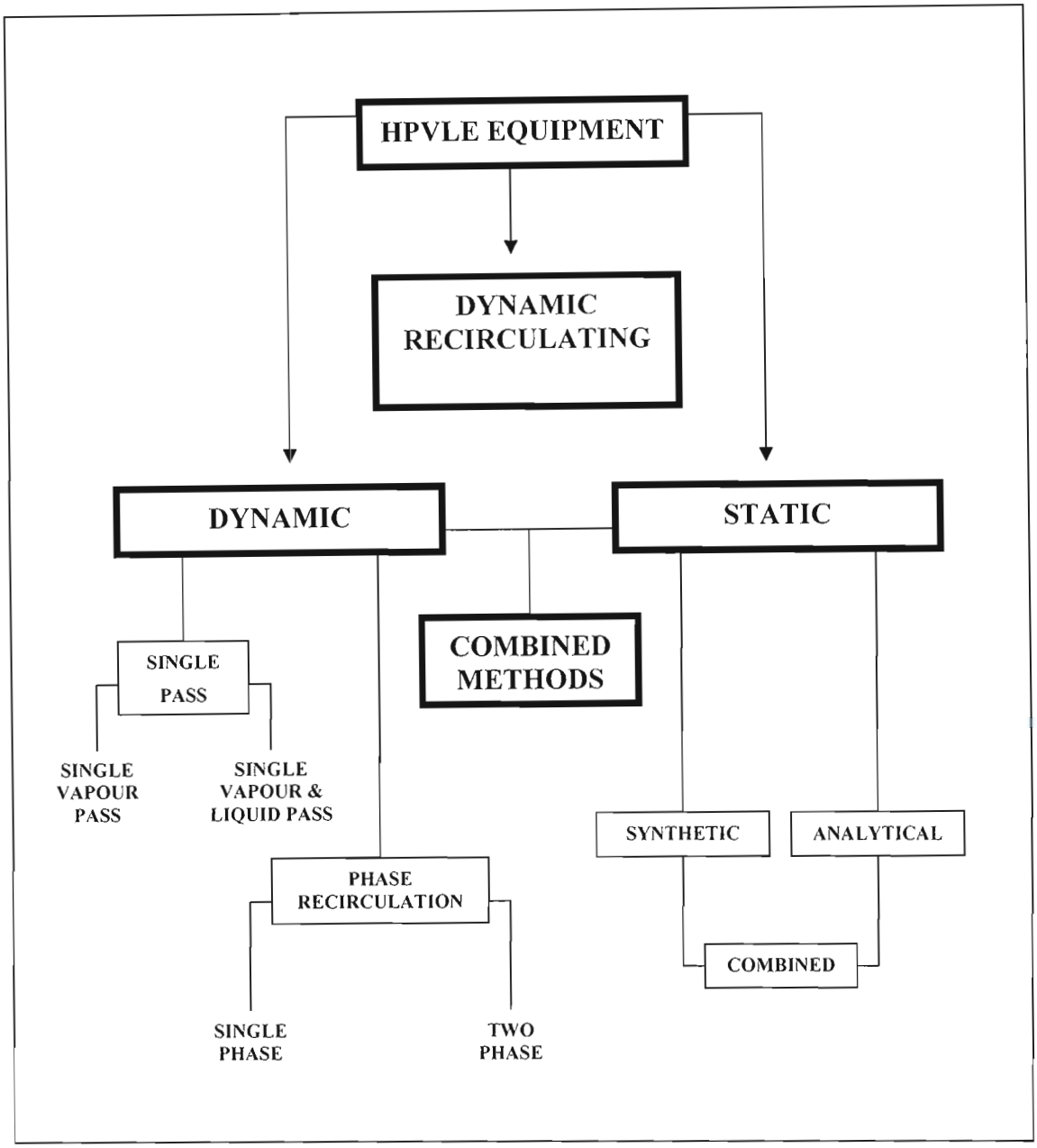

Figure 2.1. Classification scheme for HPVLE equipment.

As opposed to the flow methods, in recirculation methods, as its name applies, a single phase or both phases is/are continuously withdrawn from the equilibrium cell and recirculated until equilibrium has been established. Dynamic methods can be used to obtain isothermal or isobaric data and static methods can be used to obtain isobars and more commonly, isotherms as well as isopleths, for the synthetic static type, since the method inherently involves a closed system that contains accurately known amounts of system components.

Contemporary dynamic recirculating VLE stills are usually based upon liquid and vapour condensate recirculation and to a lesser extent, the condensate recirculation LPVLE method, where the latter are classified as traditionally low-pressure (subatmospheric) VLE measurement methods. Consequently, the separate classification of this method stems from the fact that it is usually excluded from a traditional HPVLE classification scheme for dynamic methods due to its different operational principles and a limited pressure range. These methods are different from conventional HPVLE phase recirculation methods, as the equilibrium still is equipped with an electrically heated reboiler, which generates a vapour-liquid mixture which is transported via the "vapour-lift" or "thermal-lift" principle through a Cottrell pump to the equilibrium chamber, where equilibration and phase disengagement occur.

The phases are "recirculated" in a different manner, without pneumatic or magnetic pumps (dynamic HPVLE phase recirculation methods), as the vertical positioning of the exiting streams of the disengaged phases above the reboiler *i.e.* the hydrostatic head, is used for the necessary pressure differential for the return of the phases to the reboiler, where the phases are mixed and brought to a boil once more. In this fashion, the liquid and vapour condensate phases are continuously transported or recirculated from the equilibrium chamber in external recirculation loops, with appropriate static sampling points, and then once again boiled in the reboiler, until a steady state has been reached.

These types of VLE equipment can be used for the acquisition of both isothermal and isobaric data; however, in its normal mode of operation, isobaric data is usually obtained. In dynamic HPVLE methods, the equilibrium chamber and associated equipment represents a temperature-controlled zone, consequently in the normal mode of operation for the latter, the acquisition of isothermal data is favoured. It is imperative that a clear distinction is made between traditional HPVLE dynamic methods and dynamic recirculating VLE stills (previously restricted to subatmospheric conditions), due to the latter method, through ingenious and innovative designs having found limited applicability in superatmospheric determinations.

There have been a few designs of these types of stills with suitable materials of construction to allow for efficient operation at elevated pressures, such as that of Wiesniewska *et al.* (1993). This technique, coupled with the latter possibility (of higher pressures) serves as the basis of the experimental work of the author, which will be elaborated on later in this chapter and in the text.

There are many variations of the classification scheme for VLE equipment as evident in the review papers of other authors such as Fornari *et al.* (1990) and Dohrn and Brunner (1995), whose criterion for the broad classification of VLE equipment is the means of phase determination *i.e.* direct sampling methods (DSM) or indirect sampling methods (ISM).

Consequently, the classification scheme for HPVLE equipment can take different forms, depending on what the author considers to be the most distinctive aspects of VLE design.

There can also be many variations in the design of a VLE measurement apparatus by combining the operational principles of the different types of equipment (static and dynamic), shown in the separate categories in Figure 2.1, into a single hybrid VLE measurement apparatus. An example of such a deviation from conventional classification is the development of a static equilibrium cell in the Thermodynamic Research Unit at the University of KwaZulu-Natal, which features internal circulation through the sampling valves as described in detail by Raal and Muhlbauer (1998). This novel feature allows for the equal ease in the acquisition of isobaric, isothermal and isoplethic phase equilibrium data since its design is a hybrid of the dynamic and static methods, combining the advantages of both methods.

2.3 Common features of Analytical HPVLE equipment

Analytical HPVLE equipment (shown schematically in Figure 2.2) incorporate the use of direct sampling techniques for phase composition determination. As such, there are some fundamental similarities between static and dynamic analytical VLE equipment. The features of dynamic recirculating VLE stills are not represented in this diagram and will be dealt with separately in a later section. The diagram in Figure 2.2 excludes the auxiliary equipment and other ancillary aspects of the design of dynamic and static equipment. The latter are considered as unnecessary in representing general analytical VLE equipment, which consists of the following features (Raal and Muhlbauer, 1998), listed below:

(a) An *equilibrium cell* or chamber, which is the heart of the apparatus, within which the equilibrium condition between the phases is established.

(b) A suitable *environment* that ensures that isothermal or adiabatic conditions are maintained within the equilibrium cell, for isothermal determinations. This controlled environment can take the form of a thermal regulating fluid in the form of air (Legret *et al.*, 1981), inert gases (Rogers and Prausnitz, 1970), water (Katayama, 1975), oil (Schotte, 1980) or a metal jacket (Ng and Robinson, 1978).

(c) A means for effective *agitation* of the contents of the equilibrium cell to facilitate the attainment of equilibrium.

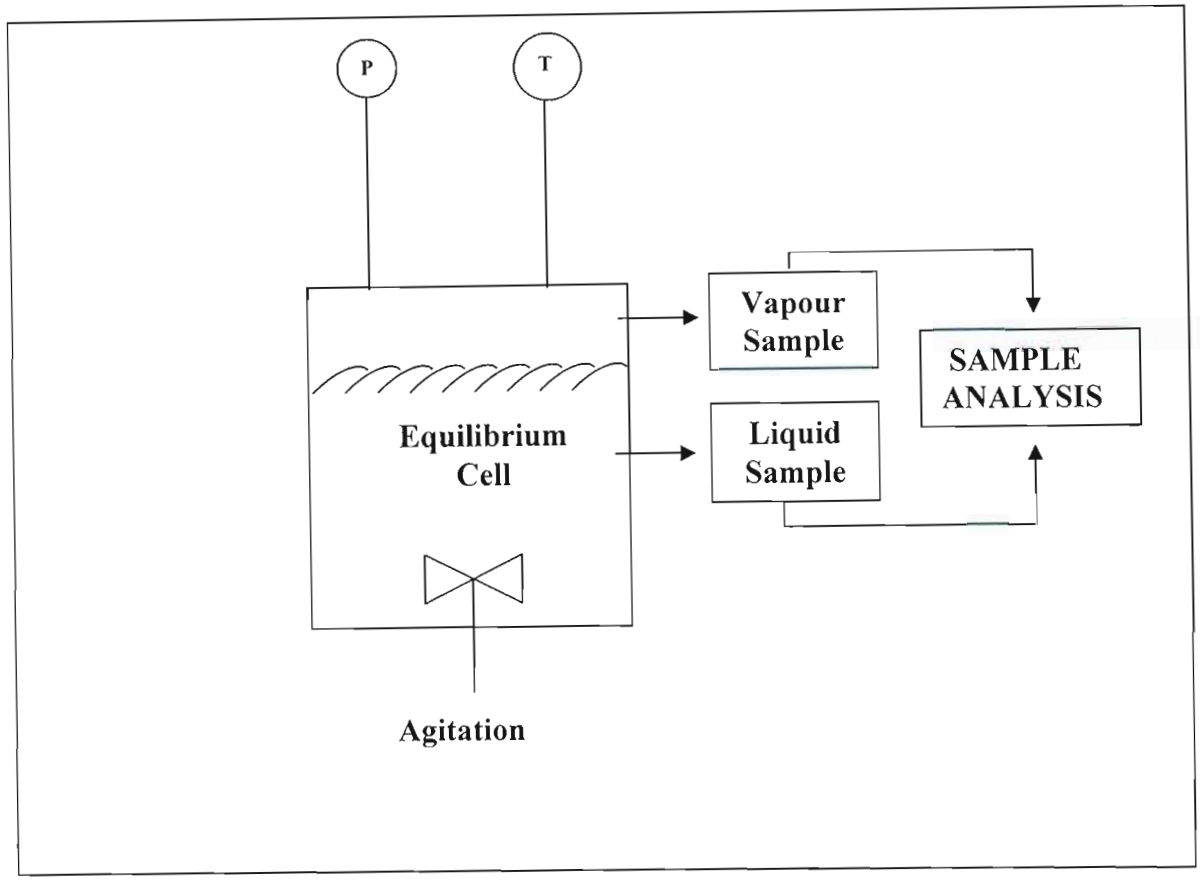

Figure 2.2. Features of typical Analytical HPVLE equipment.

Static and dynamic methods employ different mechanisms to fulfil this important requirement for VLE determinations, which of course forms the basis of their fundamental difference as VLE measurement methods. Typically, in static methods, agitation devices such as an internal magnetic stirrer (Kolbe and Gmehling, 1985) or mechanical rocking of the equilibrium cell (Huang *et al.*, 1985) are techniques that are used to assist in equilibrium attainment.
Dynamic methods use phase circulation methods (pumps to serve for agitation and mixing of the cell contents). However, there is some overlap as a few vapour circulation methods also incorporate the use of an internal magnetic stirrer in the equilibrium cell (Freitag and Robinson, 1986).

(d) Methods for the *accurate analysis* of the liquid and/or vapour samples. This can be achieved principally by two means *i.e.* "external" and *in situ* analysis. Equipment based on external analyses have provisions for sampling facilities at appropriate sample points; withdrawal from which allows for subsequent external analysis of the phase equilibrium compositions through the use of quantitative techniques such as gas chromatography. Dynamic methods (except the single vapour pass) are particularly amenable to the above, due to their circulating operation

facilitating sample withdrawal (recirculation sampling loops), whilst static methods require special sampling interventions in the apparatus for withdrawing liquid and/or vapour samples. An important consideration in sample withdrawal is that the equilibrium not be disturbed during the sample withdrawal, which is more serious for static methods, where volume changes are quite undesirable. Sample withdrawal and analysis can be eliminated with *in situ* analysis under pressure, where optical means such as spectroscopic methods (Kaiser *et al.*, 1992) are employed. However, the use of these techniques is often complicated by the need for time-consuming high-pressure calibrations *e.g.* for infrared analysis. The incorporation of vibrating tube densitometers in the recirculation loop of dynamic HPVLE methods allows for the density of the circulated equilibrium phase to be determined accurately. The only consideration is that of the pulsation of the pump affecting the reading (Wendland *et al.*, 1993), which can be eliminated by turning the pump off.

(e) *Thermal and pressure sensors*, which have been properly calibrated, are required for the accurate measurement of the cell temperature and pressure. Measurement of temperature is often achieved through the use of platinum resistance thermometers, thermocouples and too a lesser extent thermistors and quartz thermometers (frequently used for calibration purposes). For the measurement of system pressure, mechanical pressure gauges and electronic pressure sensors (transducers, transmitters) are the most commonly used. Dead weight piston gauges have been more commonly used as standards against which the primary sensing devices are calibrated. Monitoring of the pressure and temperature throughout the run is important for establishing when the "plateau region" *i.e.* equilibrium has been reached.

(f) The incorporation of an effective means to visually or optically observe the phase behaviour in the equilibrium chamber (sight glasses, cameras, *etc.*) are a novel feature for the direct observation of phase separation and multiple phase formation. This feature is an integral part of visual static synthetic methods.

2.4 Classification of experimental HPVLE variables

A useful classification of experimental variables was made by Deiters and Schneider (1986), who distinguished between "density" and "field" variables in their review of high-pressure VLE methods. "Densities" are extensive variables whose property values (mole fraction, density, *etc.*) are not the same in the co-existing equilibrium phases. "Fields" are intensive variables whose values (temperature, pressure, *etc.*) are the same throughout entire system in the equilibrium phases. In HPVLE, measurement of fields or intensive variables poses much less

problems for accurate measurement than densities, especially in the determination of accurate values for the vapour phase compositions. Of course, in the synthetic or indirect method, this problem of uncertainty in the measurement of fields is completely eliminated.

2.5 Experimental challenges in the determination of HPVLE

The challenges encountered by experimenters in the field of VLE have been reviewed by Raal and Muhlbauer (1994, 1998) and can be summarised below as the following:

(a) Criteria for the establishment of equilibrium

The establishment of a true equilibrium condition for a non-reacting system necessitates that there are no thermal or material exchanges with the environment and that there be no internal macroscopic changes due to any gradients (pressure, temperature, compositions and densities) within the system, with respect to time. In other words, a steady state condition with $\frac{dx}{dt} = 0$, where x is a measurable system variable, is required.

The attainment of the equilibrium condition is indeed adversely affected by the cumulative effect of the minor fluctuations of experimental parameters (pressure, temperature, volume, *etc.*), which with even attempts at strict control, often cannot be perfectly maintained at constant values (within the detectable limits of the system), coupled with the limitations of the experimenter and the methods employed. An example of an experimental limitation for ensuring an equilibrium condition is the effect of the incorporation of stirring or agitation in the equilibrium vessel. Although, stirring or agitation improves contact between the phases to speed up the attainment of equilibrium, the effects of "fluid friction" and the subsequent thermal gradients generated in the liquid phase are not negligible. Consequently, a true equilibrium is probably never reached or maintained (Raal and Muhlbauer, 1998) due to the unceasing small changes in the surroundings, difficulties in experimental control and "retarding resistances" in fluid flow and interfacial contact.

The steady state condition is "judged" to have been attained by the experimenter when the system temperature, pressure and phase compositions (densities, refractive index, infrared spectra, *etc.*) remain stable *i.e.* there is no detected change in these system properties for an appreciable time interval.

Experimenters such as Rigas *et al.* (1958) and Fredenslund *et al.* (1973) based their criterion for the establishment of a state of equilibrium as being a constant system pressure. Fredenslund

et al. (1973) in this regard, considered a change in pressure of less than 0.05% in 30 minutes as being sufficient to serve as an indication of equilibrium.

The experimental "assumption" of an attainment of equilibrium is therefore dependent upon the measurement accuracies and capabilities of the thermal and pressure sensors together with the analytical measuring devices (densitometers, gas chromatographs) for phase compositions.

(b) Control of experimental variables

As mentioned in the previous paragraph, in practice it is almost impossible to maintain system variables of pressure, temperature and volume at constant values throughout the course of the experiment. Usually, a "setpoint" or predetermined value for a system variable, with as low a tolerance (dead-band) as possible is the common control strategy. The greater the deviations of the system pressure or temperature from the control value, the greater the difficulty in obtaining reliable phase equilibrium data, due to the intimate relationship between system variables such as temperature and pressure.

Pressure control can be achieved through the use of electronic shut-off valves (on-off) or control valves (regulating). Electromagnetic valves such as solenoid valves have found widespread use in pressure control systems and with the advent of proportional solenoid valves, economically constructed pressure controllers are now possible. Shut-off valves are able to control the system pressure *i.e.* maintain a "setpoint" by opening to a lower or higher pressure source to stabilise the system pressure, which is between these two limits. The opening of the valves can be fine-tuned by pulse-width modulation and the use of manual control valves in conjunction with the solenoid valves. Proportional valves are able to regulate the system pressure through the control of the flow rate of an inert gas into the system, where the flow characteristics of the valve are proportional to the current delivered to the valve. The control of pressure is thus dependent upon the limitations of the response time of the pressure feedback and control unit and the pulsation of the valve. Leaks in the equipment would be detrimental to pressure control and welds, fittings and junctions in the equipment are the major sources of leaks in this regard.

Temperature control is commonly achieved through the use of a thermostat in the form of an isothermal fluid bath, where the temperature of the fluid is regulated through the use of a feedback system; the temperature of the system is monitored by a thermal sensor and then relayed to a control unit, which then adjusts the heating element current. Internal and external vacuum jacketing of the equilibrium cell (Rogalski *et al.*, 1980) is another effective means for minimisation of heat losses.

The use of external insulation material (Fibrefax®, polyurethane foam, *etc.*) is also employed to insulate the equilibrium cell from thermal contact with its environment. The loss or gain of heat from the surroundings is a major impediment in obtaining isothermal conditions for the equilibrium cell. There should therefore be no gradients or paths for any conductive or radiative heat transfer (AC heaters) to or from the equilibrium cell. Strategies for accurate temperature monitoring (such as multiple temperature sensors) and control in the equilibrium cell have traditionally been the preserve of those experimenters employing static methods.

(c) Accurate measurement of temperature and pressure

With the availability of highly accurate, linear and robust pressure and temperature sensors, the accuracy of the variable readings are often limited by the resolution (number of decimal places) of the respective instrument display units or multimeter readings. Consequently, display units, the proper mounting of the sensor, good signal conditioning and noise interferences, *etc.* and not the sensor itself, often limit the accuracy of pressure and temperature readings. Additionally, the calibration of the thermal and pressure sensors are also quite often a limiting factor for the accuracy of the respective measurements.

(d) Withdrawal and handling of samples prior to analysis

Difficulty is experienced for the withdrawal of samples from a system, which is either at a very high pressure or low pressure. For the analysis of samples in an HPVLE determination, the equilibrium state attained for the sample in the cell (pressure, temperature, compositions) differs from its initial state in its entry to an analytical measuring device *e.g.* gas chromatograph. Care must be taken to preserve the integrity of the withdrawn sample. This is to ensure that it remains representative of the equilibrium condition throughout the analytical procedure.

To minimize the effects of a large pressure drop and change in the interior volume of the cell during sampling, different strategies were employed. Some experimenters (Aroyan and Katz, 1951) employed controlled injections of compressed mercury into a pressure control cylinder or buffer tank coupled to the equilibrium cell during sampling. Sampling through capillaries (Heintz and Streett, 1983) and specialized valves (Lauret *et al.*, 1994) to ensure minimization of sample sizes and hence changes in cell volume were also employed.

The problem of ensuring representative samples is also exacerbated for mixtures of components with widely varying volatilities or volatile/non-volatile mixtures, as there is preferential flashing of the more volatile components during sampling and also partial condensation of the heavier components in the sample lines. To this end, complex homogenisation techniques employed by

Rogers and Prausnitz (1970), Ng and Robinson (1978) and Wagner and Wichterle (1987) have been reported in the literature.

(d) Analysis of withdrawn phases

A wide variety of analytical techniques are available for the quantification of the equilibrium phases. These techniques include refractometry, densitometry, spectroscopy, mass spectrometry and chromatographic methods. The latter of these methods, gas chromatography, is the most popular. It is however, characterised by the need to calibrate the detector (thermal conductivity or flame ionisation detectors) as the detector response varies with column effluent composition, and the nature of substance. In particular, the proper analysis of high-pressure gas or gas-liquid mixtures presents a great problem for researchers, as the detector response factor varies greatly across the mole fraction range for the gas. To this end, a precision volumetric calibration device has been developed in our research group (Raal and Muhlbauer, 1998) for the preparation of highly-accurate standard gas or gas-liquid mixtures.

2.6 Classification and development of LPVLE Recirculation Methods

The popularity of dynamic recirculating VLE stills is clearly evident in the observation that data measured with these stills accounts for a significant fraction of the pool of published low-pressure VLE data (Raal and Muhlbauer, 1998). This can be attributed to the method providing a fairly rapid, inexpensive and reliable means for measuring VLE data.
However, despite the above, the method and its continual developments has been a source of severe criticism from many researchers advocating the use of other methods such as the static method (Abbott, 1978). Marsh (1989) commented that despite the many modifications to the basic design, the quality of the data obtained has not been significantly improved. The traditional and even contemporary areas of concern about this method are essentially the attainment of an equilibrium state which "differs infinitesimally from the true equilibrium state", pressure and temperature control difficulties, superheating of the equilibrium phases and phase sampling uncertainties.

The results of comparative studies (Malanowski, 1975) on the quality of VLE data obtained from different types of LPVLE methods has quite clearly affirmed the ability of the dynamic recirculating method to produce reliable data.

There have been many extensive reviews of the development of experimental methods for the measurement of low-pressure vapour-liquid equilibria and these can be found in the works of Hala *et al.* (1967), Malanowski (1982a), Abbott (1986) and that of Raal and Muhlbauer (1998). However, the author considers it a necessary exercise to profoundly trace the significant developments of low-pressure dynamic VLE methods from the beginning of the 20th century till present to illustrate the founding principles of these methods and the contemporary state of the field of LPVLE measurements. The important aspects of the design of the various types of equipment provided in the monographs above coupled with direct references to the original journal publications will be presented in detail to allow for greater insight into the novel designs, modifications and theoretical considerations inherent in the design of low-pressure dynamic recirculating VLE measurement equipment so as to facilitate an understanding of how these ideas have contributed to the design of the equipment presented in this study.

2.6.1 Classification of LPVLE Recirculating equipment

A contemporary classification of low-pressure VLE equipment (Malanowski, 1982a) is based upon the number of phases to be recirculated and the phase condition (condensed or vapourized) of the recirculated stream, as shown diagrammatically in Figure. 2.3.

The fundamental operational principle of the many recirculation methods is the continuous phase disengagement of the equilibrium vapour and liquid phases under isothermal or more commonly, isobaric conditions and the recirculation of either or both the vapour and the liquid phases in various ways (condensed or vapourized) back to the reboiler, where the mixture is boiled again.

The circulated phases eventually reach a steady material state *i.e.* constant composition, which should correspond with a constant temperature and pressure state as indicated by the respective sensors. It is usual practice for provisions for sampling both phases to be incorporated into the still design so that a full data set *i.e.* P-T-x-y can be furnished. The vapour phase recirculation method, especially, differs from other low-pressure recirculation methods as it involves the use of a pump and in its normal mode of operation it is used to measure isothermal data.

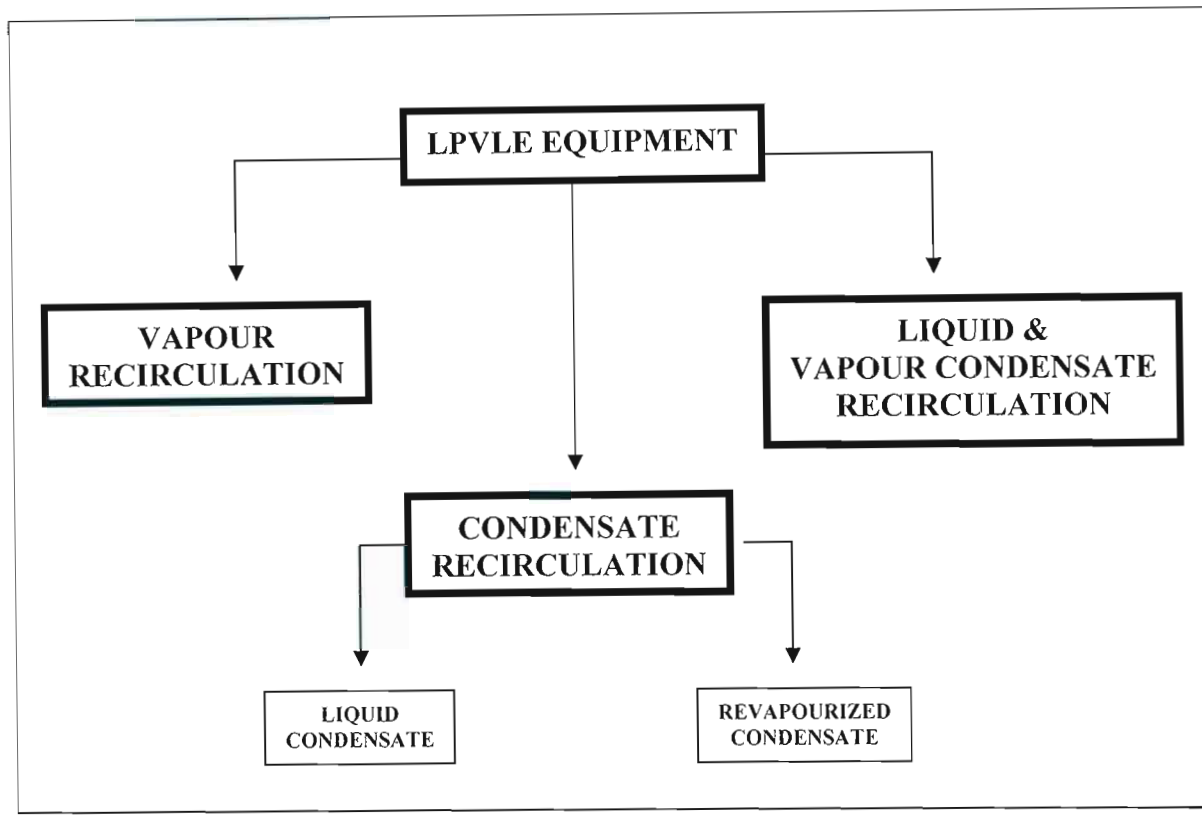

Figure 2.3. Classification scheme for LPVLE Recirculating equipment.

2.6.2 Features of typical LPVLE Recirculating equipment.

A diagrammatic representation of the key features of LPVLE recirculating equipment of the liquid phase and vapour condensate type is shown in Figure 2.4.

The liquid phase and vapour condensate recirculation method is indeed the most common and most successful LPVLE recirculating still design. The latter was consequently chosen as the most appropriate model for low-pressure recirculating equipment. With regards to the other types of methods, which are antiquated and no longer in use, further elaboration will be provided in the respective sections highlighting their development.

Due to some similarities between high-pressure and low-pressure VLE measurement methods, most of the considerations mentioned in Section 2.3 are also applicable here, however, the operational and functional design principles of LPVLE stills are fundamentally different to that of HPVLE methods and can be summarized as follows:

(a) A *reboiler or boiling section* is required to provide sufficient heat input to initiate and also perpetuate boiling of the mixture; usually under constant-pressure conditions.

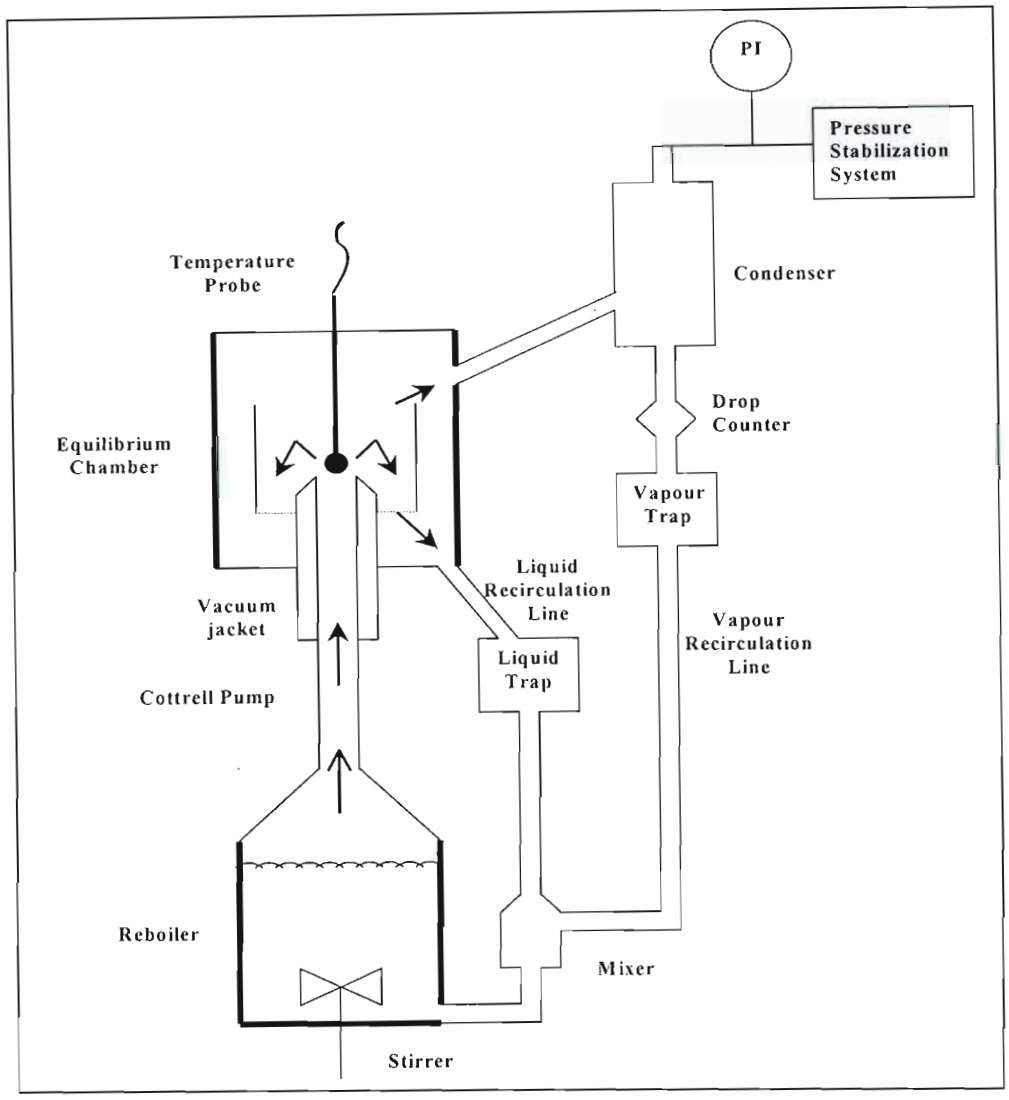

Figure 2.4. Schematic of a LPVLE Recirculating apparatus.

Two types of heating duties can normally be distinguished *i.e.* internal and external heating. External heating (shown as darkened regions around the reboiler) ensures that the influence of the external environment in the form of temperature gradients is negated together with maximizing energy efficiency.

The internal heating provides the bulk of the heating duty as it is positioned so as to be in intimate contact with the fluid (not shown in the diagram) and allows for the rapid, smooth and controlled boiling of the mixture. The appropriate use of nichrome wire windings, heating tapes, cartridge heaters and various other types of heating elements (with provision for variable energy input) are employed to achieve the steady state boiling of the recirculated mixture.

(b) A means of *agitation* of the returning vapour condensate and liquid phase mixture serves to allow for intimate phase contacting to prevent concentration gradients and hence flashing of the lighter components upon re-entry into the reboiler. This is usually achieved with magnetically coupled internal stirrers and/or specially designed mixing sections in the return line, as shown in Figure 2.10. This is especially important for systems that exhibit a high relative volatility.

(c) The intermediate section between the reboiler and equilibrium chamber in the form of the *Cottrell tube or pump* (Cottrell, 1919), to allow for the transport of the superheated mixture via the "thermal-lift principle" to temperature probe well in the equilibrium chamber. The Cottrell tube has in the past been designed such that it enters at the side of the equilibrium chamber (as will be shown later in the many illustrations of the early designs). This design illustrated in the diagram shows the vacuum jacketed Cottrell tube entering through centre of the base of the equilibrium chamber, a design that has been favoured in recent designs (Raal and Muhlbauer, 1998). The Cottrell tube is a feature that is traditionally unique to ebulliometric (Swietolawski, 1945) and liquid phase and vapour condensate recirculation methods; however, modifications to the Othmer-type stills have featured this (Zudkevitch, 1992). Consequently, vapour recirculation and condensate recirculation equipment consist of a single chamber (as there is no Cottrell tube or separate chamber for equilibration to occur in), which is partitioned into the "liquid phase container" and the equilibrium chamber directly above it (Malanowski, 1982a).

(d) The design of the *equilibrium chamber* is crucial as proper phase contacting and subsequent disengagement occurs here and it has been subject to many modifications over the years. The equilibrium chamber can be packed or unpacked, where in the latter design, the Cottrell tube is considered as being sufficient to achieve phase equilibrium. It is imperative that the equilibrium chamber is maintained in a proper adiabatic state to ensure that erroneous phase compositions and temperature readings are not obtained.
Various strategies such as "vacuum jacketing", simple "draft boxes" or covering the chamber with insulating materials (shown as darkened regions in the diagram) are employed in this regard. The temperature probe is mounted in an appropriate position at the vapour-liquid disengagement interface in the equilibrium chamber to allow for the equilibrium temperature to be determined.

(e) *Heat exchangers* are very important auxiliary features in the equipment. For vapour phase recirculation method, no condensation of the vapour phase occurs; consequently no condensing facilities are required as the vapour phase is maintained (in a separate bath) at a temperature higher than that of the equilibrium cell.

For condensate recirculation stills, both phases enter the still as liquid phases. In revapourized condensate recirculation, the vapour phase condensate is revapourized prior to re-entry into the equilibrium chamber, whereas in the liquid condensate recirculation, the vapour phase condensate re-enters the equilibrium chamber in a liquid state. In some early designs, the use of liquid phase coolers (Brown, 1952) and sampling receiver coolers (Heertjies, 1960) has also been employed. The top of the condenser has been favoured in the majority of still designs for pressure connections *i.e.* to the atmosphere or to a suitable pressure regulating system.

(f) *Sampling ports or traps* serve to provide minimal holdup of the condensed phases to allow for sampling through static ports via septa or other appropriate sampling techniques (sampling valves, sample loops, *etc.*) where there is minimal disturbance of the still operation due to sampling. A drop counter, which leads into the vapour condensate trap, was a popular feature incorporated into the designs of early LPVLE stills, and still in use today, for providing an indication of the rate of condensation or flow of the vapour condensate and approach to the equilibrium condition.

2.6.3 Criteria for the proper design of LPVLE Recirculating equipment

The principles, upon which a properly designed recirculating still should be based, adapted from Malanowski (1982a), can be listed as follows below:

(a) The final design and form of the VLE still should be *as simple as possible*, eliminating many unnecessary design complications, especially with regards to the sampling of the vapour and liquid phases. Associated with design complications are additional costs; consequently a simple yet effective design is optimal.

(b) The requirement for the filling or charging of the still with the chemical components, for a single run, should be fulfilled by fairly *small sample volumes*. This is especially important for expensive or rare chemicals.

(c) Provisions for *the monitoring of experimental variables* (pressure and temperature) should allow for high accuracy. This has been discussed above in Section 2.3 (e).

(d) The *time required for the attainment of a steady state* should be short for the determination of single point. However, this factor, although related to the design of the equipment, is also highly dependent upon the nature of the system under study with regards to heat capacities, latent heat, relative volatilities, *etc.*

(e) There should ideally be no *partial condensation of the vapour stream* on the walls of the temperature sensor or in the equilibrium chamber prior to phase disengagement and sampling. Any attempts to prevent the partial condensation of the vapour phase should also not result in overheating of the temperature sensor.

(f) *Entrainment of liquid droplets in the exiting vapour streams* must be prevented through proper design. This serious problem is also shared by single pass HPVLE dynamic methods (discussed in Appendix A).

(g) The recirculated streams of vapour (or its condensate) and liquid (at different temperatures and compositions) should be *mixed thoroughly* to ensure that flashing or differential vapourization of the more volatile components (secondary evaporation) does not occur when the mixture is boiled again. If this condition is not properly prevented, the phases will never reach a true steady state and this is consequently a very important consideration in the design of any recirculating method.
This point proved to be a major undoing in the design of the equipment of Harris (2004). Consequently, internal stirring or mixing sections must be incorporated into the equipment design for reliable phase equilibrium determinations.

(h) The *flow and compositions of the recirculated phases* should remain constant once steady-state boiling has been achieved, to ensure that a steady state condition can be reached.

(i) There should be no *pockets or voids* in the equipment design, which would allow for dead volumes or the accumulation of material, out of the recirculation pathway.

(j) The provision for the *withdrawal of samples* without the disturbance of the equilibrium condition is also an important consideration for the design of the equipment to obtain representative samples. There should also be minimal holdup of the recirculating streams in the sample traps together with stirring to ensure homogeneity of the extracted samples.

2.6.4 Development of LPVLE Recirculation Methods

2.6.4.1 Vapour Recirculation Methods

The first experimenter to employ the use of this method was Inglis (1906) due to the apparent uncertainties in obtaining a steady-state with flow-type or single pass methods. Inglis (1906) investigated isothermal distillation of mixtures of nitrogen and oxygen and argon and oxygen.

The general principles of this method are shown in Figure 2.5. Although it was originally a low-pressure method, it was the basis for the HPVLE dynamic vapour recirculation method (see Appendix A), where the use of vapour recirculation pump is also employed, as in the original method where a vapour pump is used to recirculate the vapour phase through the sedentary liquid phase in the equilibrium chamber.

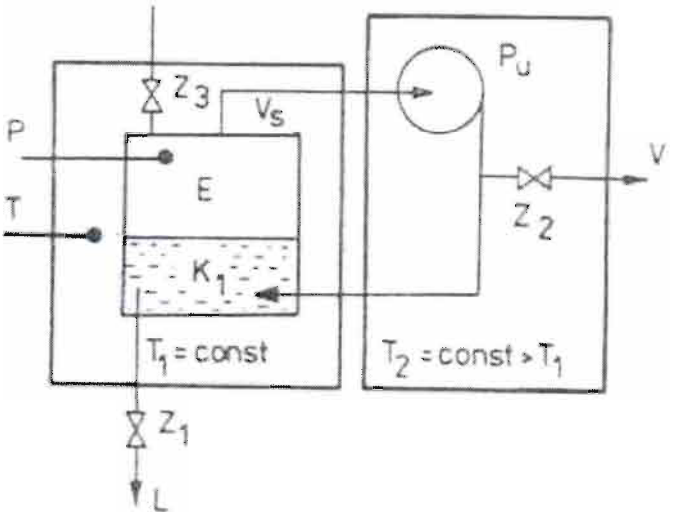

Figure 2.5. Schematic of a Vapour Recirculation apparatus: **E**, equilibrium chamber; $\mathbf{K_1}$, liquid phase container; **P**, pressure sensor; **T**, temperature sensor; $\mathbf{T_1}$,$\mathbf{T_2}$, constant-temperature baths; $\mathbf{V_s}$, vapour path; $\mathbf{Z_1}$, liquid phase(**L**) sampling valve; $\mathbf{Z_2}$, vapour phase sampling valve, $\mathbf{Z_3}$, valve for degassing.

The vapour recirculation method was the only low-pressure recirculating method that employed the use of a vapour pump to create the pressure differential required for the recirculation of the phase and is thus the only method affected by pressure drop, pump limitations, *etc.*, as was summarized previously for HPVLE phase recirculation methods. It has largely been replaced by other low-pressure recirculating methods for LPVLE determinations and on the other hand, it has been modified extensively for HPVLE determinations, as mentioned above.

2.6.4.2 Condensate Recirculation Methods

Vapour Condensate Recirculation

The first stills with vapour condensate recirculation were those of Yamaguchi (1913) and that of Sameshima (1918), which were modifications of the still of Carveth (1899). The most important modification implemented in the equipment of Sameshima (1918) was the condensate trap, with a 10 cm^3 capacity that allowed for continuous circulation of the small quantity of the condensed vapour phase. This was an improvement on earlier methods, which required rather large liquid volumes. Included in this category is perhaps the most famous of all VLE stills (Malanowski, 1982a), although burdened with major shortcomings, in the form of the Othmer Still.

Equipment of Othmer (1928)

Othmer attempted in 1928 to remedy the errors considered to be responsible for the principal inaccuracies of the vapour condensate recirculation method at that time. These were identified as partial fractionation of the evolving vapours on the cooler parts of the apparatus and errors resulting from a changing composition of the liquid phase in the boiler.

In his glass still design (shown in Figure 2.6), Othmer had intended to develop an apparatus which would be simple, compact, require small liquid volumes and provide accurate results given a short equilibration time. At the base of the still was a sample cock, for the drainage of samples of boiling liquid. At the top of the still, a thistle tube with a stop cock was blown to allow for the charging of the still. Above the liquid in the still, was a vapour tube that featured an elliptical hole near its base to allow for the passage of the generated vapour upwards, which was then "jacketed" with the vapours to allow for thermal equilibrium between the vapour and the inner walls of the vapour tube to be established; to prevent the partial condensation of the vapours inside the tube.

A thermometer, suitably supported (rubber, cork or Pyrex® stopper) was inserted into the vapour tube via the top. The vapours then moved up **B**, where the condensate and remaining vapour were passed through a condenser and a drop counter; the condensate then collected in a sample reservoir, from where the condensate overflow was recirculated through the overflow tube.

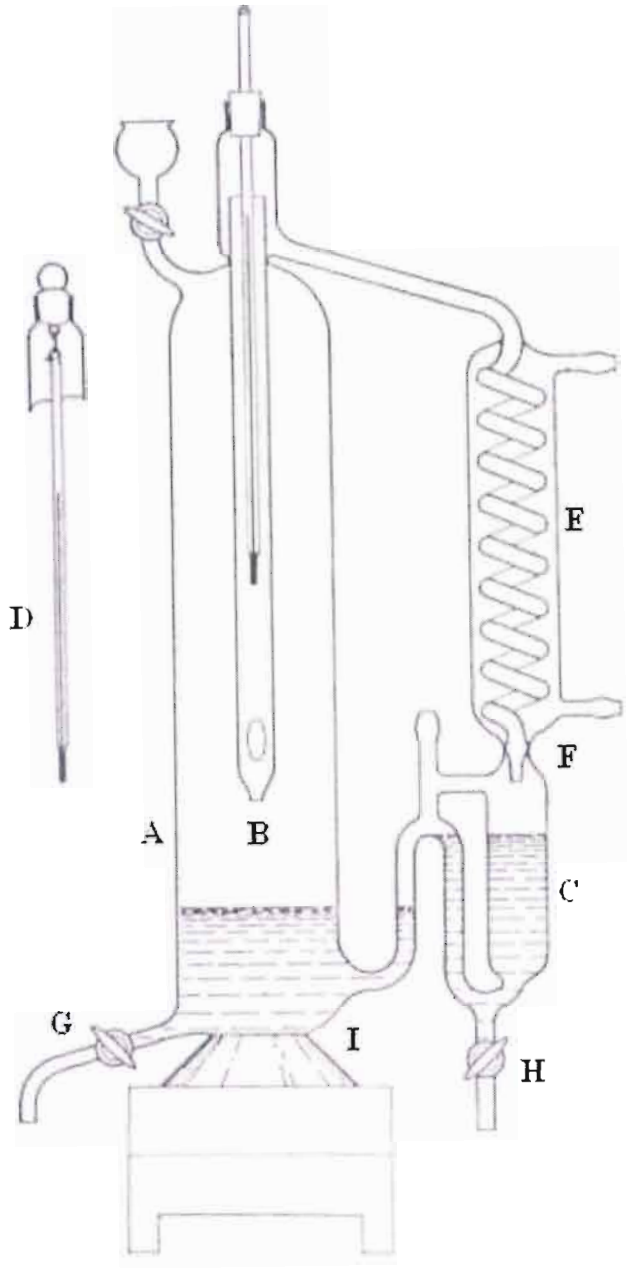

Figure 2.6. Apparatus of Othmer (1928): **A**, boiling chamber; **B**, vapour tube; **C**, vapour condensate receiver; **D**, thermometer; **E**, condenser; **F**, drop counter; **G**, liquid sampling valve; **H**, vapour condensate sample cock; **I**, heater.

The base of the condensate trap had a stopcock for withdrawal of vapour condensate samples. The first amount of condensate was discarded due to uncertainty. A constant temperature reading, as detectable by the thermometer, was taken to be an indication of a steady state; however, a further precaution taken by Othmer was to allow several circulations of the vapour condensate through the condensate the trap prior to any sampling. Equilibrium times were roughly 30 to 60 minutes.

The many potential sources of errors in the design of the Othmer VLE apparatus and these can be summarised below as follows:

(a) The determination of the *equilibrium temperature was inaccurate* as the temperature of a phase transition is most accurately obtained at the interface of equilibrium mixture *i.e.* vapour-liquid interface of the phases and not in just one of either of the two phases (binary). If it were to be immersed in the boiling liquid phase, the effects of superheating the liquid phase would result in erroneous measurements and conversely, immersion in the vapour phase, which is subject to many heat losses in its path, would also result in incorrect measurements.
There were also uncertainties as to whether the vapour above the boiling liquid was truly in a state of equilibrium due to effects such as superheating the vapour phase, splash evaporation on the sides of a heated vessel, *etc.*

(b) The *absence of any stirring mechanism in the boiling chamber* resulted in the creation of concentration gradients when the relatively cold vapour condensate stream (richer in the more volatile stream) returned to the boiling vessel, where it was insufficiently mixed with the boiling liquid. This resulted in the flashing of the lower boiling cooler condensate stream, producing a vapour that differed from its true equilibrium composition as it contained an excess of the more volatile component.
The assumption that boiling itself (especially in the absence of an internal heater) was sufficient for the mixing of inhomogeneous streams is invalid, especially when the temperature difference of the two streams was large, as is always the case for a boiling liquid and its condensed vapour. Consequently, in light of the above, the goal of Othmer to design an apparatus where the composition of the liquid in the boiling chamber would remain constant "by returning to the boiling liquid the same amount of each constituent as is being evolved in the vapour by means of the overflow", equilibrium had not been achieved. Othmer (1928), himself had stated in the journal article, that it was observed that the temperature had "decreased slightly" when the vapour condensate stream returned to the still.

(c) The problem of *partial condensation of the vapour phase* had not been avoided in the design of the apparatus as the possibility of partial condensation on the walls of the boiling vessel (with which the vapour was not in thermal equilibrium) still existed, together with the fact that the vapour jacket that these vapours formed around the vapour tube could not completely prevent the partial condensation of vapour phase in the vapour tube moving upwards towards the condenser.

This situation is indeed made quite worse for high-boiling systems (Hala, 1967) as heat loss and partial condensation becomes more significant as the temperature difference between the vapour and the wall temperature increases. The problem of partial condensation is extremely difficult to eliminate. If the upper part of the still were to be insulated or heated with nichrome wire to prevent partial condensation of the vapour, this would result in superheating the walls of the still and the possibility of producing non-equilibrium vapour due to the "splash evaporation" of the boiling liquid droplets thrown onto the superheated walls and this non-equilibrium total evaporation of liquid droplets (richer in the heavier component) on the vessel walls must be avoided.

(d) The *size of the condensate trap was too large* to allow for rapid circulation of the vapour condensate, which is crucial to prevent any unnecessary holdup of the recirculated phase. This ensures that a rapid approach to equilibrium is obtained where there is steady-state boiling of a constant-composition mixture, with minimal holdup in the recirculation lines and in the boiling chamber. In this regard, the principle of the design of the condensate trap of Sameshima (1918) with an 8 cm^3 capacity should have been employed into the design of Othmer's apparatus. An additional comment here is that the vapour condensate trap should also incorporate stirring of the condensed phase to ensure that there are no concentration gradients.

(e) There should *ideally be internal and external heating* of the boiler vessel to ensure that smooth steady boiling of the mixture occurs. In the design of Othmer, there was only external heating of the base of the still; which is very inefficient heat transfer to the still contents. Internal heating (cartridge heaters, platinum wires, *etc.*) allows for more rapid heating and also provides nucleation sites.

(f) The last and possibly most blatant flaw in this design was that the *sampling of the liquid phase from the boiling vessel* did not allow for true determination of the equilibrium liquid composition. The liquid mixed with the some of the returning vapour condensate during the withdrawal of the liquid sample and as soon as boiling is terminated at the end of the run.
There was also partial condensation of any vapour present, further contributing to erroneous composition values for the liquid phase. Consequently, it was noted by researchers such as Ellis (1952) that the Othmer still boiling point curve lies inside those curves, where the VLE data sets have been acquired by stills where the liquid phase is sampled prior to mixing with the condensate.

In light of the above, there have been more than a hundred different kinds of modifications to this original flawed design of Othmer (1928) to address the many drawbacks listed above.

In one type of modification of the Othmer still that has incorporated the option of a Cottrell tube, this has allowed for the acquisition of data of better quality. It should be noted, however, that despite the hundreds of modifications to the original design, thermodynamic consistency tests indicate that the data obtained by these methods are indeed of poor quality (Malanowski, 1982a) and some authors (Raal and Muhlbauer, 1998) strongly advise against the use of this method for accurate determinations. The work of Zudkevitch (1992) can be referred to for a more current review of the flaws and modifications of Othmer stills.

Revapourized Condensate recirculation

In revapourized condensate recirculation, the vapour phase is initially condensed in a cooler and then transferred to a receiver or container, from where it is transferred to a heated section, where flash vapourization of the condensate is effected. The flashed condensate is then returned to the equilibrium chamber in the form of a vapour. The original idea for this type of circulation was conceived by Chilton (1935) and the first successful design of a still of this type was developed by Jones *et al.* (1943).

With the development of the Othmer still (1928) and its many subsequent modifications, came a plethora of published data of poor quality. The statistical error analysis of the data indicated that the flashing of the improperly mixed and the cooler returning vapour condensate stream in the boiler was the principal flaw (Hala, 1967). Consequently, it was apparent that the mixing of the circulating vapour stream and the boiling liquid had to be improved upon to improve both the operation of the still and the quality of the data. Various strategies were employed to achieve this in the form of internal stirrers and heaters to eliminate concentration gradients and non-equilibrium vapourization of the condensate stream. The design of Jones *et al.* (1943) served to incorporate a mixing principle where the revapourized vapour condensate would be made to bubble through the boiling liquid phase until equilibrium was achieved.

Equipment of Jones et al. (1943)

The design of the apparatus of Jones *et al.* (1943) was motivated, in an analogous fashion to that of Othmer (1928), by the need to eliminate the inherent sources of error in preceding equipment designs. The two principle sources of error were identified in the study as being the production of a non-equilibrium vapour from the boiling liquid surface due to concentration gradients and the improper mixing of the returning vapour recirculation stream and the liquid in the still, resulting in flashing.

The still of Jones *et al.* (1943), known as the Jones-Colburn still, is shown in Figure 2.7. It was constructed entirely out of Pyrex® to allow for observation of the liquid levels in the apparatus. An important design consideration by Jones *et al* was the use of a "flash boiler" or vapourizer to rapidly flash the recirculating vapour condensate into vapour. This flash boiler was in the form of an electrically heated tube, the operation of which served to ensure that a constant steady liquid level would be maintained in the residue chamber, in accordance with the condensate chamber, where the fixed overflow level ensured constant liquid levels. There were three separate temperature-controlled zones in the apparatus in the form of the residue chamber (**A**), vapour line(**C**) and the flash boiler (**G**).

The vapour line connecting the residue chamber to the overhead condenser was heated to a higher temperature than that of the vapour exiting the residue chamber to prevent any partial condensation or refluxing. The superheated vapour could then be transported to the overhead condenser and entered the U-tube condensate receiver, from where the flow of the condensate, under its own hydrostatic head, passed through the three-way stopcock and the capillary tube.

The function of the capillary tube was to allow for a smooth, controlled flow of the vapour condensate into the flash boiler to ensure a constant vapourization rate (proportional to flow of liquid).

When a steady-state had been attained (15 to 40 minutes), the pressure was equalized and the samples of the liquid and the condensate were extracted from the two-way stopcocks at the base of the residue chamber and the condensate receiver, respectively.

Unfortunately, as with the design of Othmer (1928), the design of Jones *et al.*, which did allow for the acquisition of much more accurate results, was also plagued with significant flaws that were not taken into consideration by the researchers. Some of these flaws can be summarised below:

(a) The most significant shortcoming of this apparatus was the apparent difficulty in achieving the optimal operation of the still by *balancing the heating losses in the various sections*, which is quite crucial in maintaining adiabatic conditions in the still. The correct heat input into the residue chamber resistance coil was crucial to the correct operation of the still to compensate for the heat losses that occur.

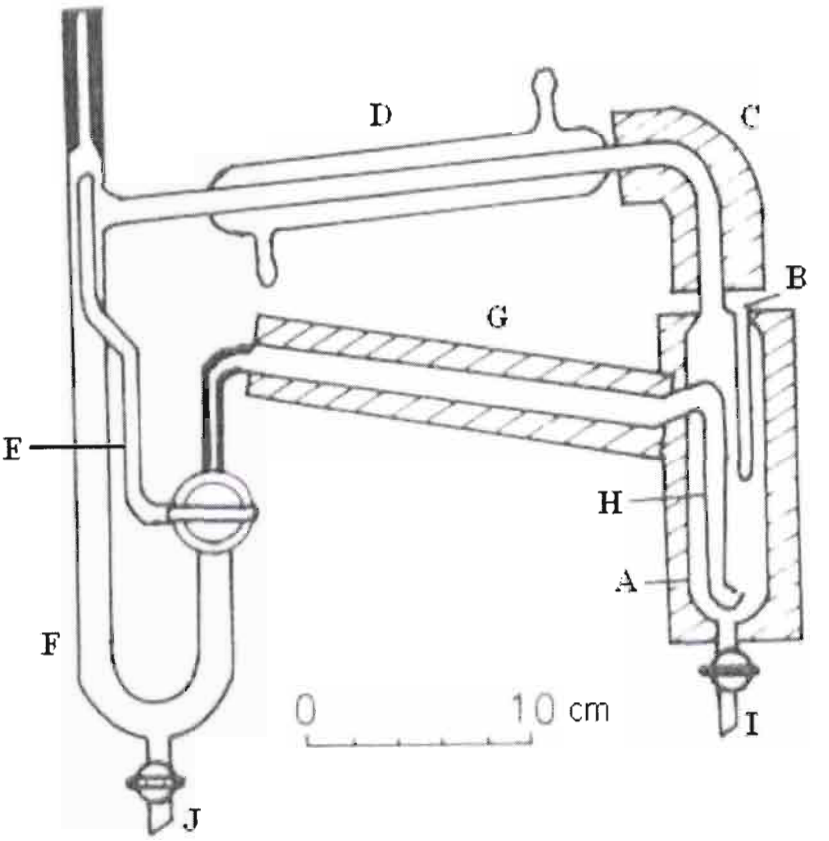

Figure 2.7. Apparatus of Jones *et al.* (1943): **A**, residue chamber; **B**, thermowell; **C**, superheated vapour take-off tube; **D**, vapour condenser; **E**, pressure equalizing tube; **F**, vapour condensate chamber; **G**, vapour condensate flash boiler; **H**, vapour bubbler; **I**, **J**, sampling cocks.

Insufficient heating (due to low heat input) of the residue chamber meant that the rate of vapour generation from the residue chamber would indeed be too slow to perpetuate the circulation of the vapour phase, since the vapour the returning vapour phase would gradually start condensing to a point where circulation would stop. If the heat input to the still is too high, then the rate of circulation of the vapour phase would be too high and there would be an overload of the liquid condensate in the flash boiler resulting in improper flashing of the condensate *en route* to the residue chamber.

(b) If the spiral was wound incorrectly, this created *vertical temperature gradients* (Raal and Muhlbauer, 1998) that resulted in incorrect vapour phase compositions, especially in the residue chamber, where heat losses along the thermowell or sample line must be compensated for by the heating spiral.

The installation of the external windings was difficult over the ends and irregular projections of glass vessels. The windings created hotspots, favouring thermal decomposition or partial

evaporation, and Hipkin *et al.* (1954) claimed that "precise control" of the heat input to the windings was extremely difficult.

(c) The bubbling of the vapour phase upwards through the liquid *created pressure gradients* due to the pressure drops in the apparatus. This pressure drop, which was a result of the holdup in the residue chamber, compromised the accuracy of the equilibrium pressure and temperature measurements.

(d) The *measurement of the equilibrium temperature* was imprecise as a result of the thermal sensor not being isolated from the bulk heating of the residue chamber by the heating spiral. Consequently, the equilibrium temperature obtained is influenced by the amount of heat input into the heating spiral.

The original design of Jones *et al.* resulted in more than 60 modifications in the 1940's and 1950's. However, as a result of the difficulties associated with the operation of these types of VLE stills, this type of method steadily declined in popularity, despite the claims of the early researchers that the sound theoretical principles of revapourized condensate recirculation outweighed the operational disadvantages (Hipkin and Myers, 1954). These sound theoretical principles were based on the excellent contacting and mixing between the vapour and liquid phases.

Notable modifications of the VLE still were those that were made independently by Hipkin and Meyers (1954) and Raal *et al.* (1972); discussion of the latter will be deferred to a later section since it is considered as a "hybrid method".

Equipment of Hipkin and Meyers (1954)

The equipment of Hipkin and Meyers (1954) is shown in Figure 2.8. A comparison of the latter equipment with that of Jones *et al.* (1943) yields fundamental differences in the design and the operation of the still. In the latter design, an external vapour jacket is used, in place of heating wire spirals, to maintain adiabatic conditions in the contactor, which has been one of the most controversial aspects of this type of still design. The use of an external vapour or liquid jacket around the equilibrium section of the apparatus inspired the later designs of the "self-lagging" still of Rose and Williams (1955) and the apparatus of Yerazunis *et al.* (1964).

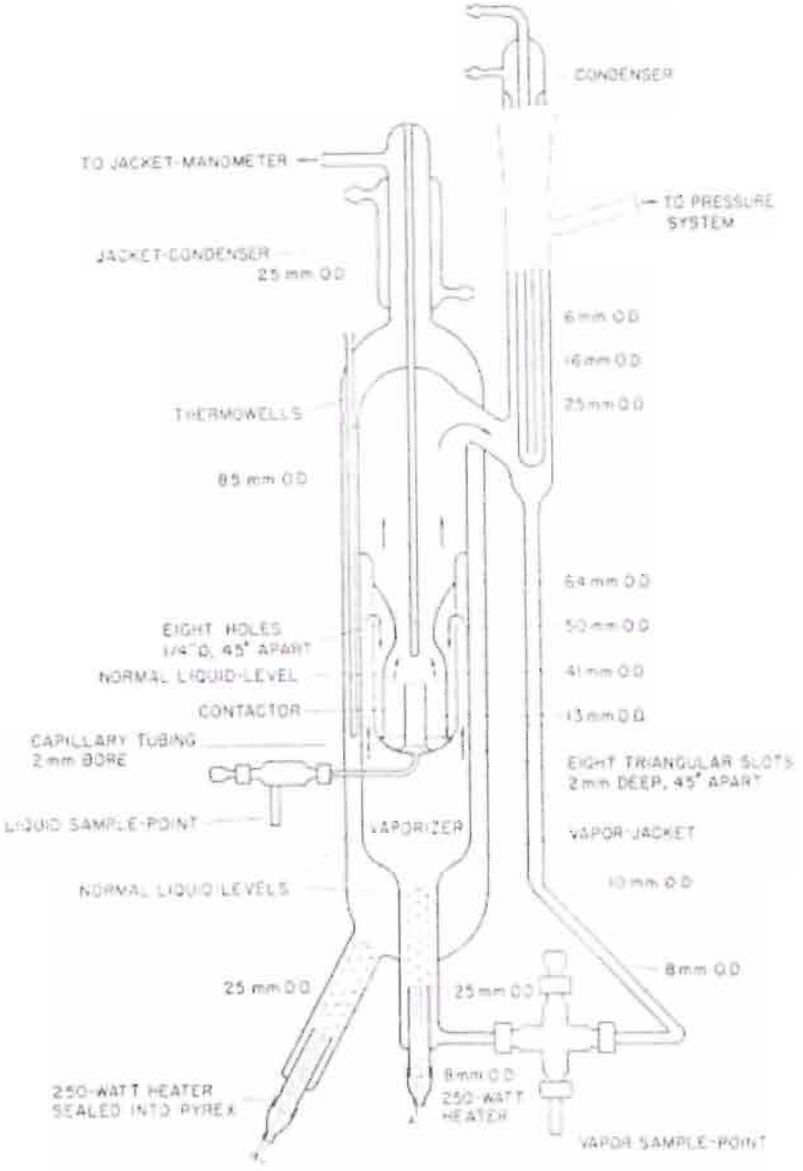

Figure 2.8. Apparatus of Hipkin and Meyers (1954).

Three bayonet-type heaters were used in the apparatus, where the heating elements were fused into a borosilicate glass tube. The heaters were ring-sealed directly into the body of the still. Two of the heaters were sealed into the vapour jacket and the third in the vapourizer. The vapour jacket enclosed all the parts of the still, except the condenser and the condensate return line.

In the operation of the still, the mixture was charged to the contactor and vapourizer of the still. In the operation of the vapour jacket at the start of each run proceeded with the evacuation of the jacket, boiling of the liquid and regulation of the jacket temperature during the run with a temperature controller. Heat input was then provided to the vapourizer to initiate boiling and the

vapours that were passed through annular spaces, bubbled through eight small holes and mixed with the liquid in the contactor. The contactor featured a centre tube, which was open at both ends. It allowed for a rather diminished application of Cottrell's principle of thermal lift for circulation and also allowed for liquid sampling, as it lead to a liquid sample valve. The top of the contactor was shaped into a Venturi to allow boiling liquid and vapour to impinge upon the copper-constantan thermocouple in the thermowell for measurement of the equilibrium temperature. The vapour was then totally condensed in the condenser, which was at the top of the condensate recirculation line, and then returned to the condenser, where it was vapourized again to ensure recirculation

2.6.4.3 Liquid and Vapour Condensate Recirculation Methods

The genesis of liquid phase and vapour recirculation methods can be attributed to the early ideas and designs of two researchers in the form of Cottrell (1919) and Swietolawski (1924). Due to the quite considerable improvement in the quality of the results obtained by this method over the others and the simplicity of the still design and operation, liquid and vapour condensate recirculation fast became the method of choice for many researchers and many subsequent modifications were made.

It is not the purpose or within the scope of this review to cover a large majority of the modifications but to focus on the important ones which have over the years served as important contributions to the field and as an inspiration to the designs of other researchers in their quest for a perfectly operating still. Although the ebulliometric method has been traditionally used for the measurement of boiling points or for total pressure measurements only, it is included in this classification due to the intimate relationship and common founding principles of the two methods. Where the discrepancies between the methods are necessary, this will be clearly stressed in the text.

Equipment of Cottrell (1919)

As mentioned above, the fundamental contribution of Cottrell to the field has been an integral part of the successful development of this method for LPVLE measurements. The original idea of Cottrell for the development of an apparatus for the accurate measurement of the boiling point temperature of solutions was devised by Cottrell in 1910. It was only in 1919 that Cottrell published the details of the apparatus, as persuaded by Washburn (1919), who further modified the apparatus. The design of the apparatus of Cottrell is shown in Figure 2.9.

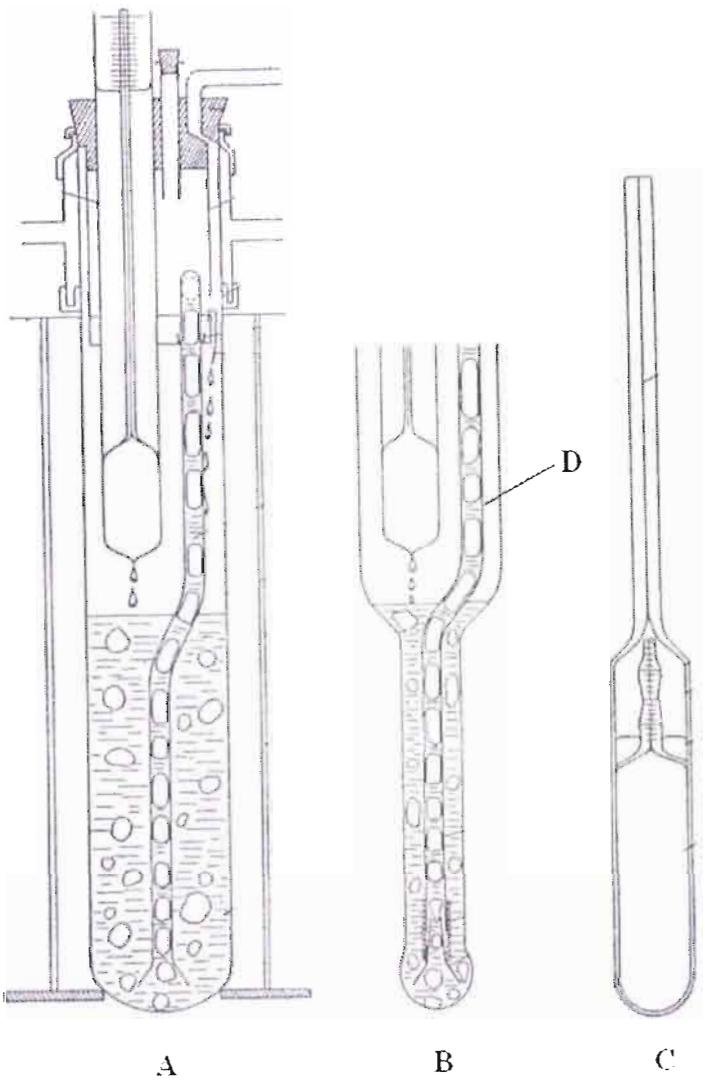

Figure 2.9. Apparatus of Cottrell (1919).

Cottrell identified the errors associated with the immersion of the thermometer in the body of the boiling liquid to determine the boiling point of solutions due to effects such as superheating, the pressure differential, *etc.* It was proposed by Cottrell instead that the thermometer be placed in the vapour phase, where the boiling action of the liquid phase be used to propel the liquid, which would deposit as a thin film over the thermometer. In the apparatus of Cottrell, the large test tube **A** served as the body of the still, in which the liquid was resident and brought to a boil in. The flat-bottomed test tube **B** was designed with two holes in its base, through which the Beckmann thermometer **C** and the pump tube **D** were "loosely" inserted, and is supported in **A** by means of a stopper in the neck of **A**.

The operation of the still commenced with the boiling of the liquid in A and in an analogous fashion to air-lift pumps, the bubbles of the vapour phase propelled a "broken stream" of

superheated liquid up the pump tube and into **B** *i.e.* a thermal-lift pump (the Cottrell pump). The amount of liquid in **A** must be considerably larger than that in **D** to ensure that there is a smooth, uninterrupted operation and the heat input (though the flame) must be adjusted to ensure enough of the vapour bubbles pass up **D**. The liquid in **B** then passed down the thermometer stem and was returned to the boiling mixture.

Cottrell himself identified the inherent flaws of his equipment in the form of superheating of the phases, pressure fluctuations, and uncertainties in temperature measurement with the Beckmann thermometer. However, the most important part of the work of Cottrell was in the application of the thermal-lift principle with the "Cottrell pump", which was incorporated into the designs of many researchers.

Equipment of Swietolawski and Romer (1924)

Swietolawski and Romer (1924) quite significantly further elaborated upon the novel ideas and developments for the accurate measurement of the boiling points of pure liquids and solutions put forward by Cottrell (1919) and Washburn (1919). This culminated in the design of a still, whose original design is shown in Figure 2.10, which was claimed by a few researchers (Leslie *et al.*, 1968) to be the most accurate for the determination of boiling points in the pressure range of 5 - 200 kPa.

The application of heat to the bulb in the form of **A** brings the solution to boil and the principle of the "thermal lift" of the vapour bubbles and liquid mixture up the Cottrell tube (**B**) was then applied. The superheated mixture was then discharged sideways into the equilibrium chamber, represented by (**B**), as shown in the diagram. The liquid then equilibrated with the vapour phase present to generate an equilibrium temperature, which was then measured with the externally insulated temperature probe which is surrounded by a tube (**C**) to prevent any heat losses. A condenser (**D**) is strategically located at the base, to ensure that the vapour condenses at this point and is returned, together with the liquid stream to the boiler.

There were quite a few fundamental flaws and limitations which were inherent in the pioneering design of Swietolawski, however, it was used only for the measurement of boiling points, as in the case of Cottrell's (1919) apparatus. Only later on did Swietolawski (1929) formally present the idea of separating the streams of vapour condensate and liquid to allow for the collections of samples of the phases. However, the latter design principle was for a different type of apparatus in the form of the flow-type (Malanowski, 1982a).

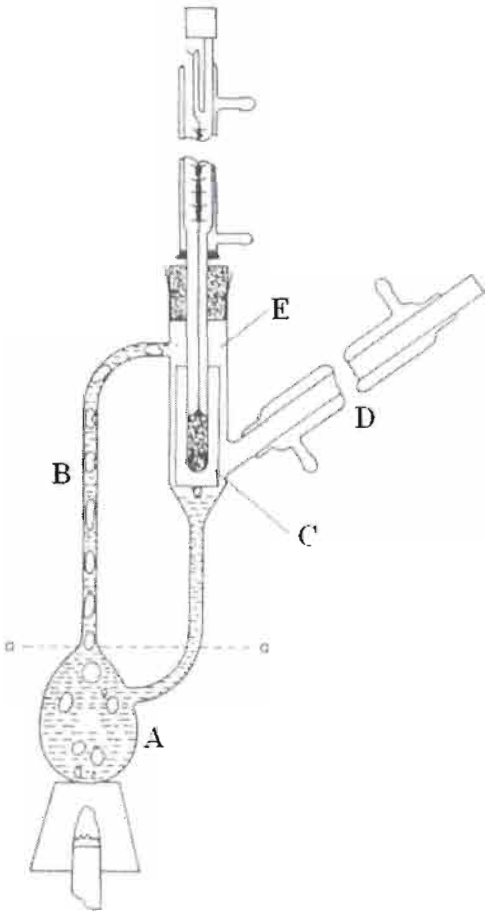

Figure 2.10. Apparatus of Swietolawski and Romer (1924): **A**, boiling chamber; **B**, Cottrell tube; **C**, insulating tube; **D**, condenser; **E**, equilibrium chamber.

Equipment of Lee (1931)

The design of Lee was the first circulating still with a Cottrell pump to feature provisions for the withdrawal of samples of liquid and vapour condensate. However, the phase sampling could not be achieved without disturbance of the operating conditions, as a temporary increase in pressure was necessary to stop circulation during sampling.

The equipment of Lee is shown in Figure 2.11. As is apparent from the diagram, the equipment had the feature of the provision of a suitable interface for the separation of the superheated mixture thermally-lifted through the Cottrell tube (**B**) through the action of a heater at the base of the liquid phase container (**A**). In the equilibrium chamber, the liquid separated from the vapour (but not concurrently) through the perforations in the tube.

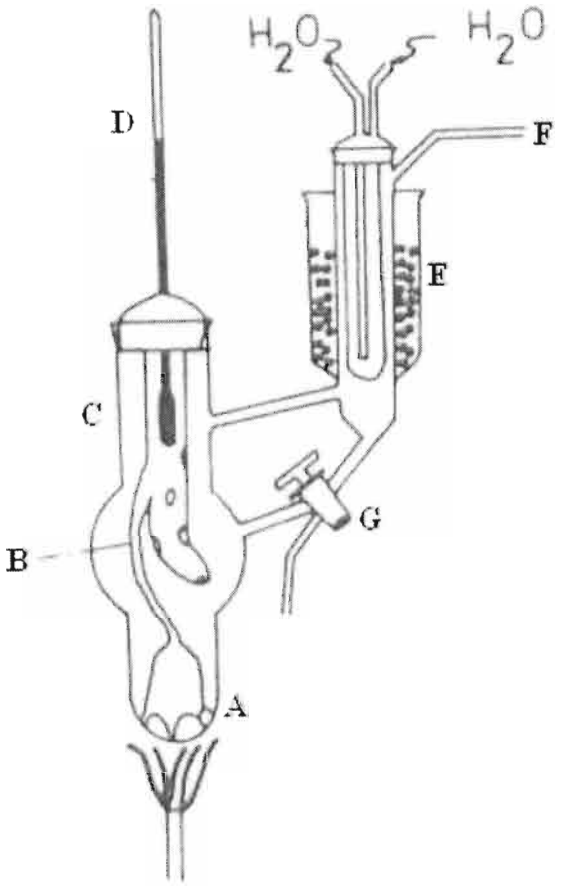

Figure 2.11. Apparatus of Lee (1931): **A**, liquid phase container; **B**, Cottrell tube; **C**, equilibrium chamber; **D**, temperature sensor; **E**, condenser; **F**, pressure connection; **G**, vapour condensate sample cock.

The less dense vapour phase then disengaged from the liquid phase and was then condensed in **E**, which featured an internally-cooled water jacket and connections to the pressure stabilization system. The condensed phase was then sampled from the sampling point represented in the diagram by **G**.

The design of Lee featured the novelty of disengaging and sampling the phases, however, without the interruption of the operation of the still, which was a crucial hindrance in its design. This is quite important as the interruption of the operation of the apparatus to withdraw samples of the phases will in most cases adversely affect the determination of the true equilibrium compositions. Other flaws of the design included a poor interface for the equilibration of the vapour-liquid mixture, incorrect liquid sampling from the boiling chamber, as in the design of Othmer (1928), and incorrect temperature measurement.

Equipment of Gillespie (1946)

In accordance with the objective of improving the design and operation of Lee (1931), Gillespie made two very important modifications to design of the recirculating still. The first of these modifications related to an improved interface (to be separate from the boiling chamber) for the disengagement of the two equilibrium phases *i.e.* a vapour-liquid separating chamber and also the simplification of allowing for sampling without disturbing the continuous operation of the still.

The Gillespie still is widely acknowledged by many researchers as being the first still of the liquid and vapour recirculation type as providing acceptable results (Hala *et al.*, 1967). The original design of the still is shown in Figure 2.12, was constructed entirely of glass. As a form of external heating, a heating spiral (resistance wire) was wound around the 100 cm^3 capacity boiling vessel (**A**) and the internal heater was made from thin platinum wire. The internal heater assembly consisted of the platinum spiral, immersed in the solution, and the lead wires, which were fused through a ground glass stopper, to heavier platinum wires.

The purpose of the internal heater was to promote the nucleation of vapour bubbles for smooth and steady boiling, which was considered as being sufficient for the agitation of the contents of the boiling chamber *i.e.* the mixing of the streams. The vapour bubbles from the boiling mixture then carried a broken stream of liquid up the Cottrell tube (**B**), which was then squirted against the thermowell (**C**) from the side, and the vapour-liquid mixture passed into the disengagement chamber, where separation of the phases was achieved.

The equilibrium liquid was returned to the boiling chamber and the equilibrium vapour was then totally condensed along a downward passage by the two condensers (**F**), and then collected in the receiver (**G**), from where the overflow passed into the condensate return line, and mixed, through the drop counter (**E**), with the returning liquid stream in the liquid return line *en route* to the boiling chamber.

The return stream (liquid and vapour condensate) entered the boiling chamber via a capillary, to allow for a smooth constant flow of the return stream and constant liquid levels during boiling. With the attainment of equilibrium, samples of liquid and vapour condensate were then obtained from the sample cocks (**K**) and (**H**), respectively, without the interruption of the operation of the still.

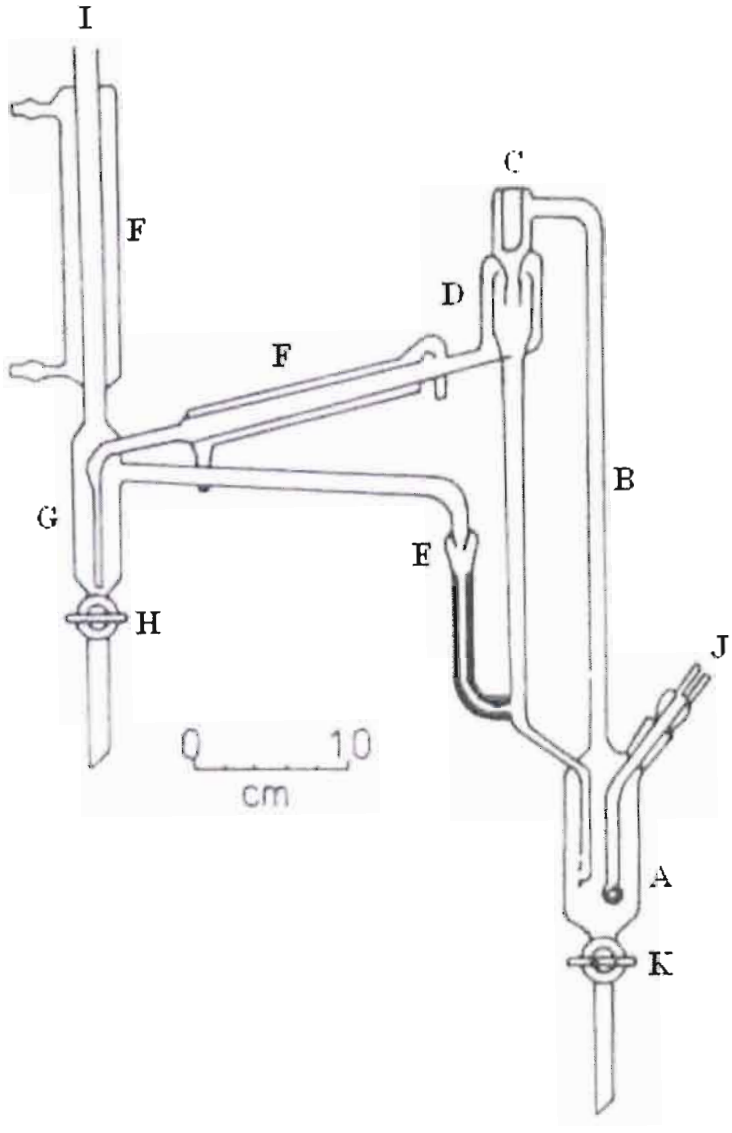

Figure 2.12. Apparatus of Gillespie (1946): **A**, boiling chamber; **B**, Cottrell tube; **C**, thermowell; **D**, vapour-liquid separator section; **E**, drop counter; **F**, condensers; **G**, vapour condensate trap; **H**, vapour condensate sampling cock; **I**, pressure connection; **J**, internal heater; **K**, liquid sample cock.

The limitations or flaws of the Gillespie still can be listed below as follows:

(a) The most blatant flaw was indeed the *incorrect sampling of the liquid phase* from the boiling chamber, which resulted in erroneous liquid phase composition determinations. The liquid that resided in the boiling chamber was not representative of the liquid that achieved equilibrium with the vapour phase in the disengagement chamber, as it had contained some of the vapour condensate, which had been recirculated back into the chamber through the condensate line.

For accurate liquid phase compositions, provision has to made for the collection and sampling of the liquid phase exiting the equilibrium chamber for true liquid phase composition measurements.

(b) The sampling of the phases during a run *affected the operation of the still* by interrupting the circulation. Consequently, even though a sample could be withdrawn from the still during its continuous operation, this did indeed affect the proper operation of the still. This was due to the use of stopcocks, which altered liquid levels, causing pressure fluctuations (if connected to a manostat) and compromising the equilibrium phase composition measurements.

(c) The assumptions which were made by many early researchers (Hala *et al.*, 1967), which can be mentioned at this juncture, was that the *Cottrell tube was a sufficient mechanism for the attainment of equilibrium* between the vapour and liquid phases. This is not justified, as the maximum concurrent contacting of the phases is required for sufficient interphase mass transfer between the respective phases, which must also be in thermal (temperature) and mechanical (pressure) equilibrium.
The Cottrell tube provides short contact times and a limited contacting interface for the phases and is consequently primarily only for the transport of the superheated mixture to a disengagement interface (appreciable contact time and interfacial area), where proper equilibrium can be achieved.

(d) The *equilibrium chamber should ideally be insulated* or surrounded by a vacuum jacket, especially for high-boiling systems, to ensure adiabatic conditions in the equilibrium chamber. This is due to the occurrence of heat losses, which leads to partial condensation, before the vapour exits the disengagement chamber. In the later designs of VLE stills by Altsheler (1951) and Scatchard *et al.* (1952), the silvered evacuated jacket was employed to prevent heat losses from the equilibrium chamber (Hala *et al.*, 1967).

(e) The *vapour bubbles generated by the internal heater* cannot be considered as sufficient for the perfect mixing of the hot liquid and cold return stream in the boiling chamber. Some form of mechanical agitation, is much more desirable to eliminate thermal and concentration gradients.

(f) The relatively *long equilibrium time for this apparatus* has been quoted by researchers. Othmer (1948) claimed that it exceeded 40 hours. Decreasing the size of the vapour receiver will assist in this respect, by decreasing the holdup.

Gillespie tested the apparatus for the possible entrainment of liquid droplets in the exiting vapour phase (Hala *et al.*, 1967) as a function of heat input (circulation rate) and the results proved that entrainment was negligible, even at high circulation rates. There were quite a few subsequent modifications made to the original design of Gillespie by researchers attempting to overcome its inherent limitations outlined above (Hala *et al.*, 1967).

Equipment of Brown (1952)

In accordance with the personal recommendations of Gillespie, the work of Brown and Ewald featured the development of a still with quite notable and important modifications to the design of Gillespie (1946). The initial modifications (Brown and Ewald, 1950) served to address the errors in the liquid phase sampling from the boiler and the necessity for the addition of collector or liquid trap below the disengagement chamber. In later work due to operating difficulties with the initial still, Brown realized that further modifications were necessary and redesigned the still.

The design of the Brown still, shown in Figure 2.13, as modified from an earlier still, in addition to the features of the Gillespie still had electromagnetic valves (**E, L**) , vapour (**M**) and liquid sample collectors (**M**) and a liquid cooler (**I**). In this design, the internal heater was located in a central position, within the body of liquid in the boiler, as opposed to other designs where the heater was mounted in a sideways fashion. The latter alteration to the design of the boiler was to ensure continuous nucleation, smooth boiling and proper operation of the Cottrell pump down to pressures as low as 7 kPa (Malanowski, 1982a).

It was also necessary for the researchers to re-design the sample collecting system *i.e.* eliminate the use of stop cocks, which might cause sample contamination due to the stop cock grease. In this design, the liquid sample collector, in the form of a detachable vial, was placed directly below the disengagement chamber, and the filling of the vial was actuated electrically with electromagnetic valves.

The same arrangement on the vapour condensate side was retained for sample collection. These electromagnetic valves served to allow for the proper withdrawal of liquid and vapour condensate samples without the interruption of the continuous circulation of the still.

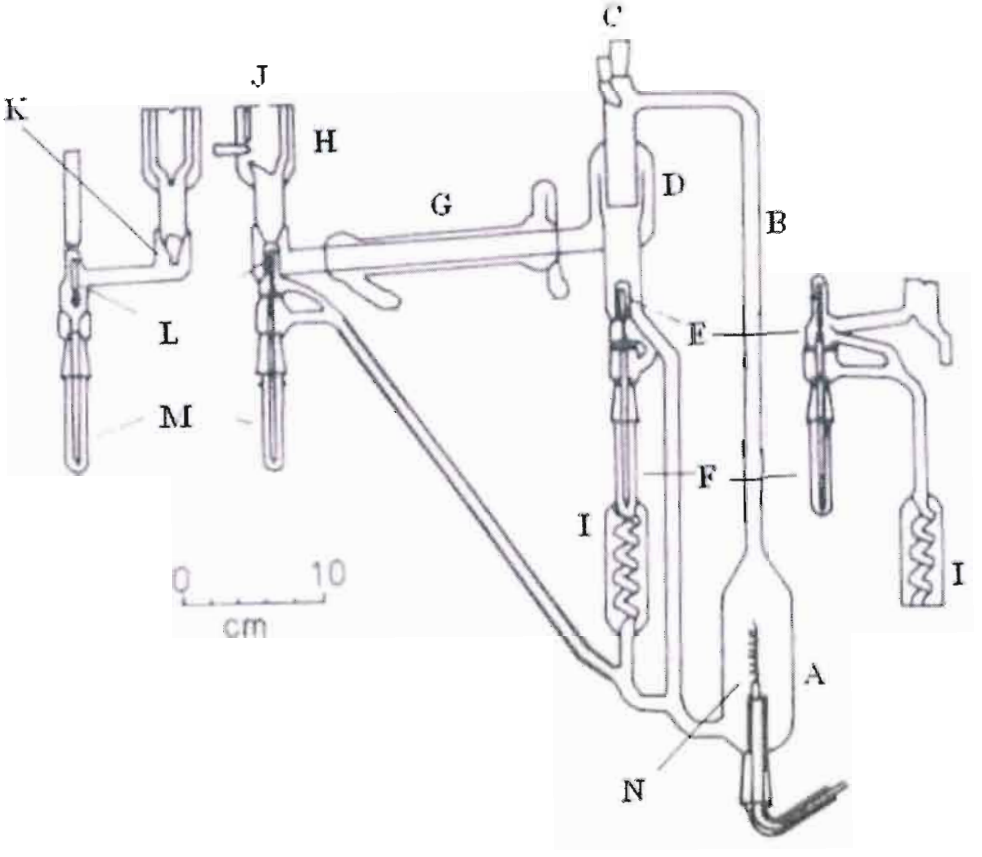

Figure 2.13. Apparatus of Brown (1952): **A**, boiling chamber; **B**, Cottrell tube; **C**, thermowell; **D**, vapour-liquid separator; **E**, liquid sampling valve; **F**, liquid sample traps; **G**,**H**, condenser; **I**, liquid phase cooler; **J**, pressure connection; **K**, drop counter; **L**, vapour condensate sampling valve; **M**, vapour condensate sample trap; **N**, internal heater.

In response to an observation in the earlier design where flashing occurred when the condensate is mixed with the liquid stream, especially for systems with high relative volatilities, a liquid cooling section was added, to cool the liquid stream before it mixed with the returning condensate stream. Due to holdup in the liquid cooler, only a portion of the liquid stream was cooled through one leg and the other return leg led directly back into the boiler.

The Brown still (1952) provided very precise results, even for systems with high relative volatilies (Hala *et al.*, 1967). Two significant drawbacks of the still were the long equilibrium times (as long as four hours) and the large initial charge required (200 cm^3 of liquid sample). As with the Gillespie still, the equilibrium chamber was not protected against heat losses.

Equipment of Ellis (1952)

A very insightful paper was published by Ellis, who identified the shortcomings of other VLE stills such as those of Othmer (1928) and Gillespie (1946) on the basis of theoretical and practical principles. Ellis identified some key considerations with regards to design of an optimal still. The most significant of these was the "adiabatic equilibrium coil" to ensure optimal contacting of the vapour-liquid mixture, which Ellis had incorporated into the design.
It must be noted that the notion of an "equilibrium coil" in this design was a feature that would formally serve to perform the function of both the Cottrell pump and the vapour-liquid contacting and disengagement interface. The design of the Ellis still is shown in Figure 2.14.

In the boiling chamber, on the surface of the glass wall surrounding the heater unit in **A**, vapour bubbles were generated on the heated surface and the boiled mixture then passed upwards into the equilibrium coil **(B)**. The equilibrium coil was made up of three spiral turns of 8 mm glass tubing and was in an arrangement that ensured that most of the coil was immersed in the liquid in the still body.
The vapour-liquid mixture travelling upwards in the coil eventually impinges upon the thermometer well **(E)**, the base of which has a hole, to allow for the disengagement of the liquid phase from the vapour phase. The separated liquid then drained into the still body, from where it re-entered the boiling chamber, where it mixed with returning condensate and was boiled again.

The disengaged vapours travel upwards along the inner tube, in which a thermometer in **(F)** measured the vapour temperature. To prevent partial condensation of the vapours in this section, the outer part of the still **(D)** around the vapours (including around the equilibrium coil) was heated with resistance wire to ensure that the temperature at junction **(F)** was higher than that at junction **(E)** *i.e.* superheating the vapour prevented partial condensation. The superheated vapour was then condensed due to the cold finger **(H),** collected in the condensate receiver **(K)**, from where it was sampled, and the overflow returned to the boiling chamber through the capillary inlet (shown as a darkened and narrow section in Figure 2.14), which ensured that backflow was minimal and the smooth flow of the returning condensate.

Equilibrium was judged to have been attained when the boiling stabilized to within 0.1 K for an hour and the condensate drop rate (taken from the condenser tip) was approximately 40 - 70 drops per minute.

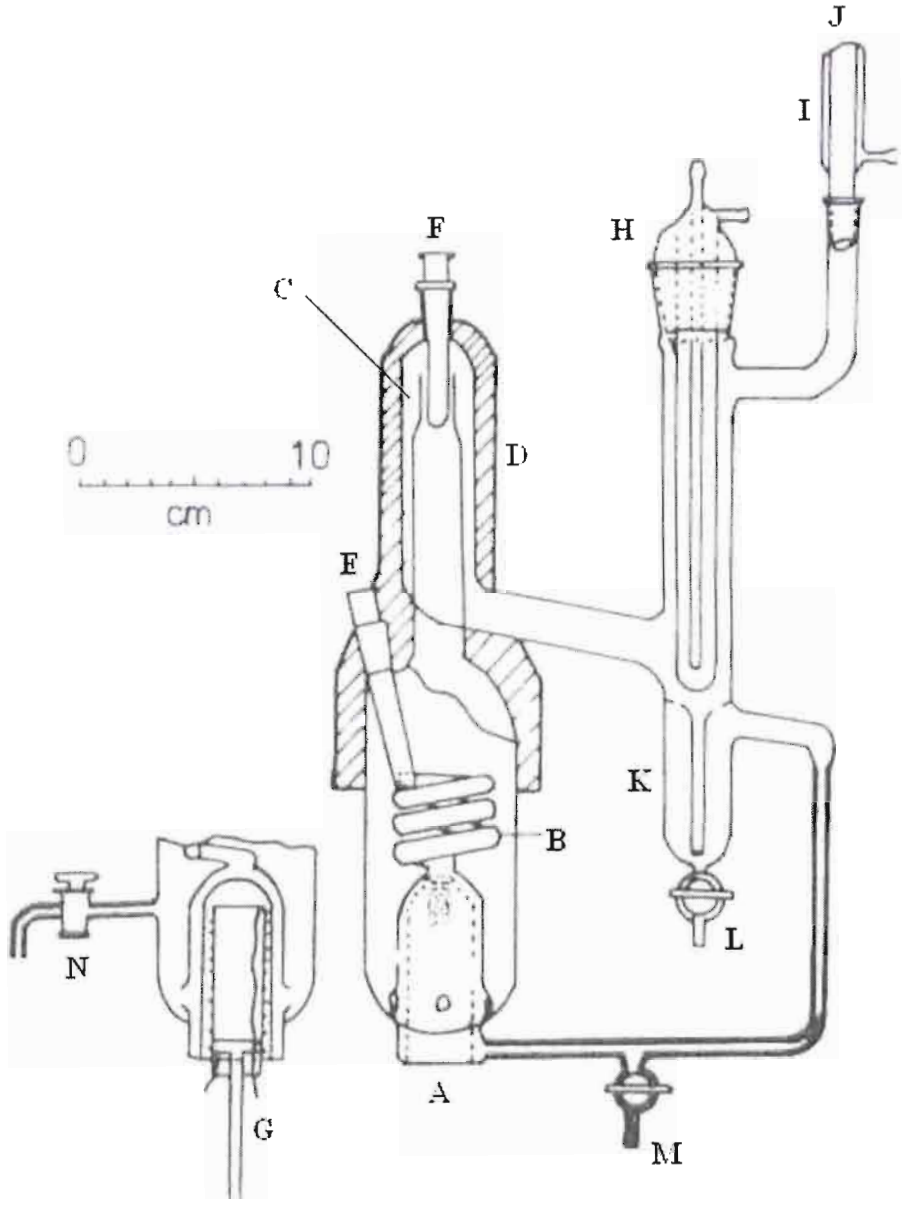

Figure 2.14. Apparatus of Ellis (1952): **A**, boiling chamber; **B**, Cottrell Tube; **C**, vapour-liquid separator; **D**, heating section; **E,F**, thermowell; **G**, internal heater; **H,I**, condenser; **J**, pressure stabilizing connection; **K**, vapour condensate sample trap; **L**, vapour condensate sample cock; **M**, still drain valve; **N**, liquid sample cock.

During the operation of the still, samples were continuously withdrawn. Although the Ellis still was found to provide results that were in close agreement with the various model correlations, there were still flaws in the design of the equipment. Most notable are the following:

(a) The *liquid sampling point was improperly devised* as the assumption that the contents of the still body was entirely that of the disengaged liquid phase returning from the equilibrium coil is

invalid. The outwardly expanded holes in the base of the boiling tube cannot completely prevent the mixing of the returning condensate, at any time, with contents of the still body.
Also, the partial condensation of any vapours on the wall, below the heated section, would return to the liquid in the still. Coupled with the above, there was no agitation in the still body, and the existence of concentration gradients was definite.

(b) The vapour bubbles that were generated by the heater surface in the boiling chamber were *not sufficient for the mixing* of a cooler returning condensate stream and the hot boiling liquid; hence the possibility of flashing existed. Mechanical stirring and even heating of the returning condensate stream should have been employed.

(c) The three spiral turns of glass *tubing as the equilibrium coil* were not sufficient to guarantee equilibrium for the vapour-liquid mixture, as even with the increased holdup in the spirals, the area for interfacial contact of the phases would still not be sufficient.

(d) The *temperature measurement was incorrect,* as the mounting of the thermometer well in the heated section of the apparatus would give erroneous measurements.

(e) The *holdup of the vapour phase was quite large*, with regards to the transport of the phase through the equilibrium coil, up the heated section, through a nearly horizontal intermediate section, collecting as condensate in a considerably over-sized receiver and returning through a capillary line.

Equipment of Scatchard and Ticknor (1952)

The still of Scatchard and Ticknor shown in Figure 2.15, had a rather unusual design and consisted of a boiling chamber (**A**) with a suitable internal heater, a curved Cottrell pump (**B**), an equilibrium chamber (**C**), thermowell (**D**), condenser (**E**), liquid cooler (**H**), liquid take-off tube (**K**), condensate take-off tube (**J**), common return line (**I**) and appropriate sample points for the vapour condensate (**F**) and liquid samples (**G**).

There were three important features of this still. The first related to an idea borrowed from the design of Altsheler *et al.* (1951) where it was recognized that some sort of lagging or insulation was required to ensure that adiabatic conditions were maintained in the equilibrium chamber (as in the form of a silvered evacuated jacket). The second related to the dire need to increase the interfacial area and holdup time for the proper contacting of the phases and the recognition that the Cottrell pump was not a sufficient mechanism to ensure equilibrium.

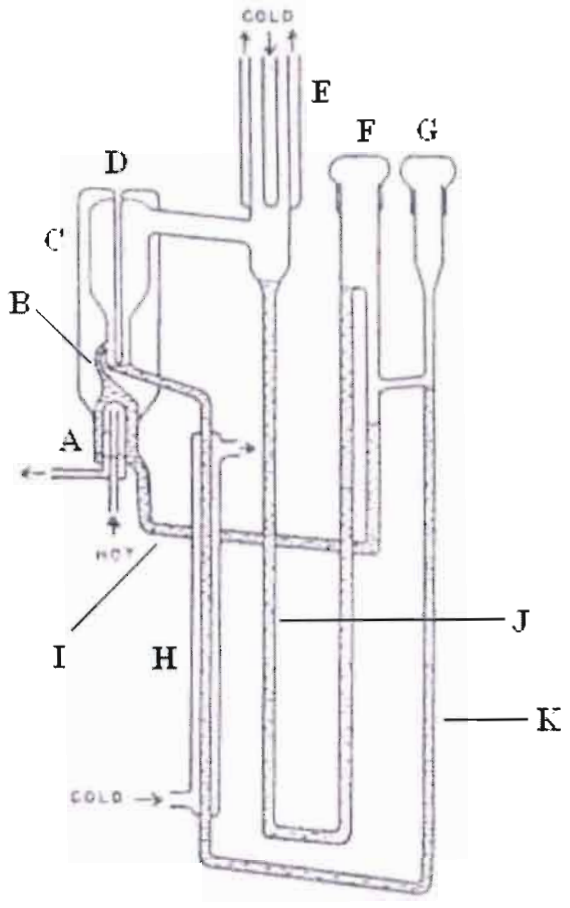

Figure 2.15. Apparatus of Scatchard and Ticknor (1952): **A**, boiling chamber; **B**, Cottrell pump; **C**, equilibrium chamber; **D**, thermowell; **E**, condenser; **F**, liquid sample point; **G**, vapour condensate sample point; **H**, liquid cooler; **I**, common return line; **J**, condensate take-off tube; **K**, liquid take-off tube.

This was implemented by the authors in their design in the form of a wound glass spiral mounted around the base of the thermowell. The third feature was the union of the two streams of liquid and vapour condensate along an appreciable length and the pre-heating of this stream prior to re-entry into the boiler to slightly below the mixture boiling point. The latter served to help to negate the effect of any concentration gradients and flashing of the more volatile components.

The simplicity of the design of the equipment, the precise results obtained with it and the small sample volumes required (about 45 cm^3) were attributes of this still design.

Equipment of Rose and Williams (1955)

Rose and Williams developed a modified Gillespie still, in which the sampling of liquid phase was from a receiver, placed below the equilibrium chamber, and not from the contents of the

boiler liquid, as in original design of the Gillespie still (Gillespie *et al.*, 1946). Rose and Williams recognized the importance of maintaining an adiabatic environment for the Cottrell tube, equilibrium chamber and the liquid trap. It was decided that instead of controlled heating, the upper sections of the equipment should be "automatically self-lagging" *i.e.* it should be a "self-lagging still". In this still, the equilibrium liquid stream would be used to jacket or lag the Cottrell tube. The final design of the self-lagging equilibrium still is shown in Figure 2.16.

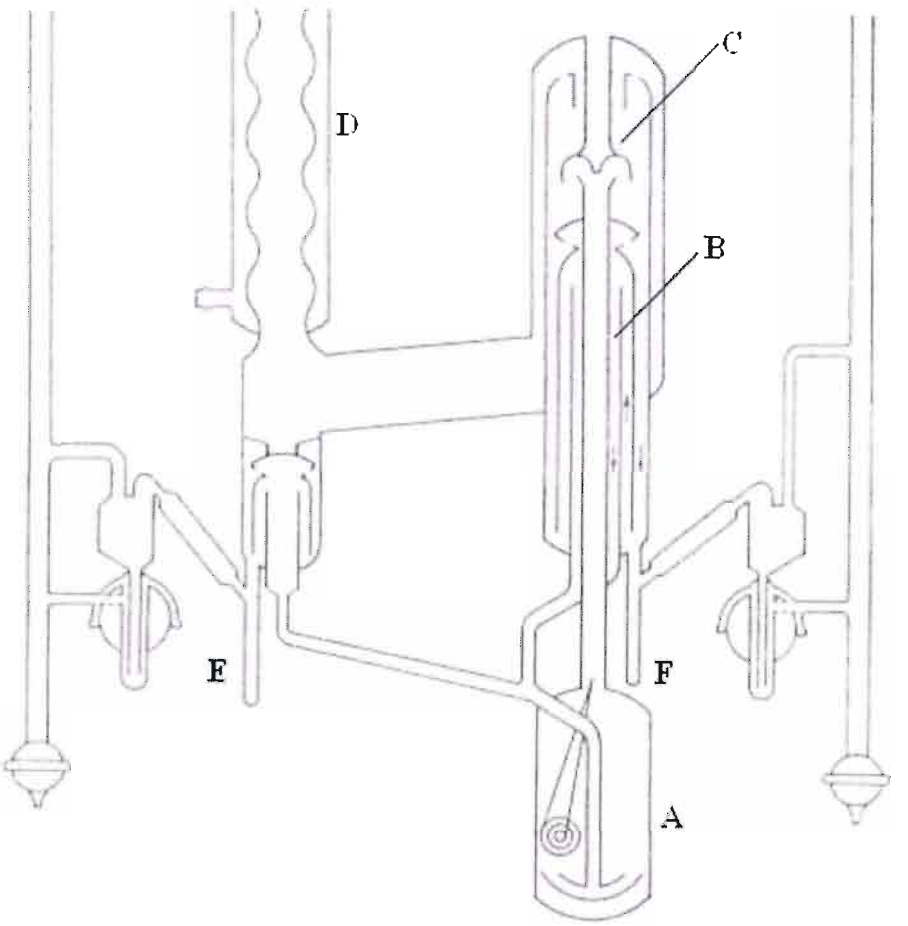

Figure 2.16. Apparatus of Rose and Williams (1955): **A**, boiling chamber; **B**, Cottrell tube; **C**, vapour-liquid separator; **D**, condenser; **E**, vapour condensate trap; **F**, liquid sample trap.

The most important parts of the apparatus are the boiling chamber (**A**) with an external and internal heater, the Cottrell tube (**B**), liquid trap (**F**), condensate trap (**E**) and the condenser (**D**). The external heater consisted of Nichrome wire wound around asbestos tape on the boiler wall; which was then covered with more asbestos tape. The internal heater was the same as in the design of Gillespie. As opposed to other designs, the Cottrell tube was centrally located about the equilibrium chamber, termed the entrainment separator, emphasizing the fact that early researchers did not feel that anything in addition to the Cottrell tube should be required for the

equilibration of the mixture. The purpose of this section was to merely prevent entrainment of liquid droplets in the vapour phase. This central positioning of the Cottrell tube was important in that the squirted mixture would be angularly symmetrically distributed in the equilibrium chamber, preventing any preferred radial direction for creating concentration gradients (Joseph *et al.*, 2002).

There was a baffle located at the top of the Cottrell tube, which effected the disengagement of the phases, which impinged upon the thermometer well at the base of the baffle. The liquid then flowed through a series of annular spaces of three concentric tubes around the central Cottrell tube. The passage of the liquid through the outermost concentric tube filled the liquid trap, the overflow of which passed up the middle concentric tube. This passage of liquid through the innermost concentric tube *i.e.* in contact with the Cottrell served the purpose of "self-lagging" as a result of its thermal contact with the contents of the Cottrell tube, allowing minimal heat losses, except if a large temperature gradient had existed between the liquid phase and the superheated mixture in the Cottrell tube (which increased with the mixture boiling point). The still was run for a few minutes before the sampling valves were activated, as explained above, and the sample bottles flushed. When equilibrium was attained, the sample bottles were then removed and the samples were analyzed by refractometry. Equilibrium times of approximately 30 minutes were reported.

Rose and Williams also decided to investigate two other sources of error in VLE measurement, that of non-dissipation of superheat along the Cottrell tube and the pressure drop for forcing the vapour up the condenser. It is imperative that the superheated vapour-liquid mixture dissipates its superheat prior to impingement on the thermowell otherwise erroneous measurements are obtained. Erroneous readings may also be obtained since the pressure is measured at the top of the condenser and the temperature is measured in the equilibrium chamber. A large pressure drop in the condenser, due to the condensing of the vapour, results in the boiling point measured in the equilibrium chamber not being the boiling point that corresponds to the pressure that is measured. The investigations of the above two factors by Rose and Williams showed them to be quite small.

The concept of a self-lagging still is a novel idea; however, the design was not exempt from some fundamental flaws. Firstly, the contacting of the phases for equilibration was restricted to the interior area of the Cottrell tube, and the disengagement of the phases by striking a baffle was not very effective, as partial condensation of the exiting vapour occurred on the inner part of the arches of the baffle (see Figure 2.16). For higher temperatures *i.e.* above 423 K, the self-lagging principle was not sufficient to ensure correct still operation; consequently, insulation or

electrical heating is required. However, there were many important considerations mentioned and investigated by the researchers in this work.

Equipment of Heertjes (1960)

The importance of the work of Heertjes was in the borrowing from the principles of fractional distillation in the design of VLE equipment *i.e.* increasing the holdup time for phase contacting and the interfacial area for efficient mass transfer between the contacting phases. Heertjes realized that maintaining isobaric and adiabatic conditions whilst the liquid and vapour are kept in contact long enough to establish equilibrium was extremely important; hence the use of glass Raschig rings in his equipment. The equipment operated on the principle that a saturated vapour would be firstly generated from a liquid mixture; this vapour would then be cooled to yield a vapour and liquid mixture, which was then contacted in an equilibrium section, as described above. The equilibrium temperature could then be measured at the disengagement interface of the equilibrium vapour and liquid phases, which could then be sampled and analysed, when equilibrium was attained.

The apparatus of Heertjes is shown in Figure 2.17. In the beginning of a run, the receivers and the boiling flask were charged with the liquid mixture. The heating of the mixture resulted in the generation of a saturated vapour, which then passed up the vapour transport tube (insulated with asbestos cord to negate partial condensation effects). The vapour phase then discharged into the equilibrium tube, the upper portion of which was not insulated to allow for partial condensation of the vapour. This mixture then flowed concurrently through the equilibrium section, which was packed with glass Raschig rings, to promote the attainment of an equilibrium condition. To ensure adiabatic conditions, this portion of the equilibrium tube was vacuum-jacketed with an inner silver lining. The disengaged vapour travelled through the exit tube to the condenser, where it was cooled and collected in the sample receiver, from where it returned to the boiler. The liquid phase was also collected in a cooled sample trap *en route* back to the boiler. All connections to the atmosphere were via desiccant-filled tubes to prevent the ingress of moisture. Equilibrium times were around 30 minutes as judged by a constant temperature reading.

There were many fundamental flaws inherent in the design of Heertjes equipment and some of these can be summarised as follows:

(a) A concern in the design of a packed section in an equilibrium chamber is the *pressure drop* along the packing, especially if the section is too long and the packing is too compacted.

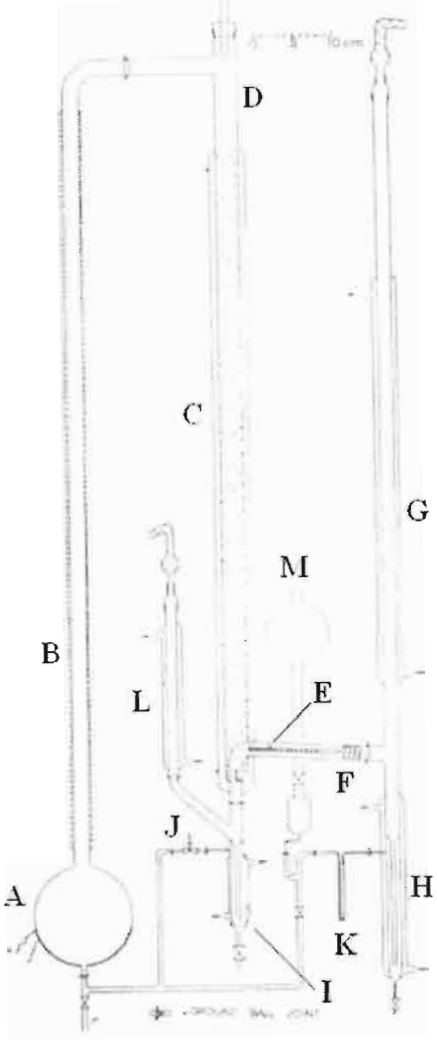

Figure 2.17. Apparatus of Heertjes (1960): **A**, boiling chamber; **B**, vapour take-off tube; **C**, insulated portion of equilibrium tube; **D**, uninsulated portion of equilibrium chamber; **E**, thermometer; **F**, vapour transport tube; **G**, **L**, condenser; **H**, cooled vapour condensate sample trap; **I**, cooled liquid sample trap; **J**, liquid return line; **K**, liquid seal, **M**, sample filling point.

Although details of the length of the packed section are not provided, visual inspection of the diagram (drawn to scale) reveals that the packed section was quite long in relation to the rest of the equipment.

(b) The vapour transport tube should *not be too long* relative to the size of the boiling chamber and in the equipment of Heertjes, the length of the tube was unjustified. The latter would result in excessive holdup coupled with the large size and holdup in the equilibrium section.

(c) The idea of cooling the sample receivers was an excellent one; but the *use of magnetic stirring* in the coolers (to dissipate any concentration gradients in the trap) should have been employed to allow for representative sampling. Also the cooling of these streams necessitates the pre-heating of the return streams (Scatchard, 1952) to allow for thermal and concentration

gradients between the returning streams and the hot boiler liquid to be minimized to prevent flashing and to reduce the heating duties of the reboiler.

(d) The entire equilibrium tube should have been maintained in an adiabatic state, and not have an un-insulated portion, which allowed for the creation of vertical temperature gradients, even though there was a vacuum-insulated section lower down. The formation of the vapour-liquid mixture by heat loss to a thermally-uncontrolled external environment was unacceptable for the generation of an equilibrium mixture.

Equipment of Dvorak and Boublik (1963)

Obtaining accurate VLE data for systems exhibiting high relative volatilities is a challenging task for most researchers. In this regard, Dvorak *et al.* attempted to design a still, which would be particularly suitable for the study of such systems. This design is shown in Figure 2.18.

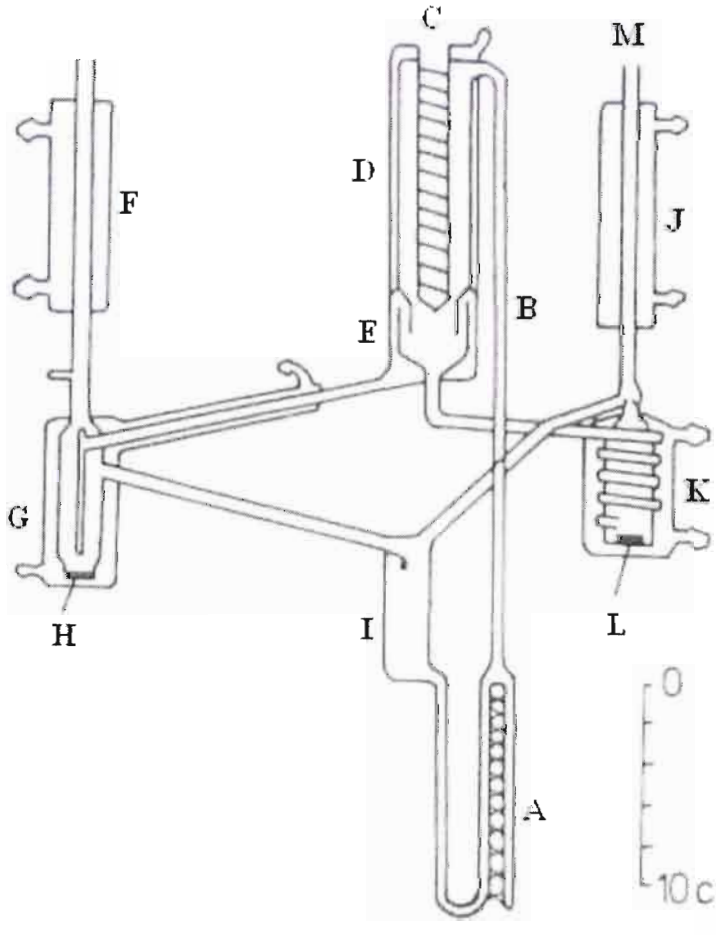

Figure 2.18. Apparatus of Dvorak and Boublik (1963): **A**, boiling chamber; **B**, Cottrell tube; **C**, thermowell; **D**, equilibrium chamber; **E**, vapour-liquid separator; **F**, **J**, condenser; **G**, vapour condensate sample trap; **H**, **L**, magnetic stirrers; **I**, mixing section; **K**, liquid sample trap; **M**, pressure connection.

The design featured mechanically-stirred and cooled sampling traps to ensure the dissipation of concentration gradients, which was an important consideration to obtain representative samples. The design also featured a large static mixing section formed from a union of the returning vapour condensate and liquid streams to allow for premixing of the streams to negate the occurrence of flashing upon the return of the streams to the reboiler. A few flaws of the design related to the reliance on the Cottrell tube for equilibrium to be attained, incorrect temperature measurement and the absence of mechanical stirring in the reboiler. Consequently, due to the above coupled with the inherent limitations of the LPVLE dynamic recirculation method, measurements for high relative volatility systems cannot be advocated with the above design.

Equipment of Yerazunis et al. (1964)

The development of the equipment of Yerazunis *et al.* was influenced by the need to correct the "undesirable features" of an earlier attempt by researchers in the same laboratory to construct a modified Gillespie still (Landwehr *et al.*, 1958) where unsatisfactory sample trap design and the uncertainties in the vapour-liquid disengagement interface resulted in apparent erroneous phase compositions. The layout of the apparatus of Yerazunis *et al.* is shown in Figure 2.19. The equilibrium chamber is magnified in Figure 2.20 to show the details of the most significant features of the design of the equipment.

In this design, the lower part of the Cottrell pump that lead up to the equilibrium chamber was left un-lagged to assist in the dissipation of the superheat from the superheated liquid-vapour mixture travelling up to through the Cottrell pump. The vapour-liquid mixture was then forced concurrently through a short column, which was packed with 1/8 inch Fenske helices. Prior to their work, researchers considered the Cottrell tube as being sufficient for the attainment of the equilibrium condition and the equilibrium chamber (termed the disengagement chamber by many researchers) as serving the purpose for phase disengagement only. The use of the packed section was inspired from the work of Heertjes (1960) and the use of the latter serves to allow for increased contacting of the phases to allow for interfacial mass transfer to occur.

Yerazunis *et al.* distinguished between a local equilibrium and a global equilibrium. In a local equilibrium, the elements of a fluid mixture will establish equilibrium with one another in an improperly designed apparatus, which may not in most instances be representative of the true or global equilibrium. Hence the contributions to the establishment of erroneous local equilibria in various parts of the apparatus due to undesirable effects such as partial condensation, improper mixing *etc.*, must be eliminated or smoothed out.

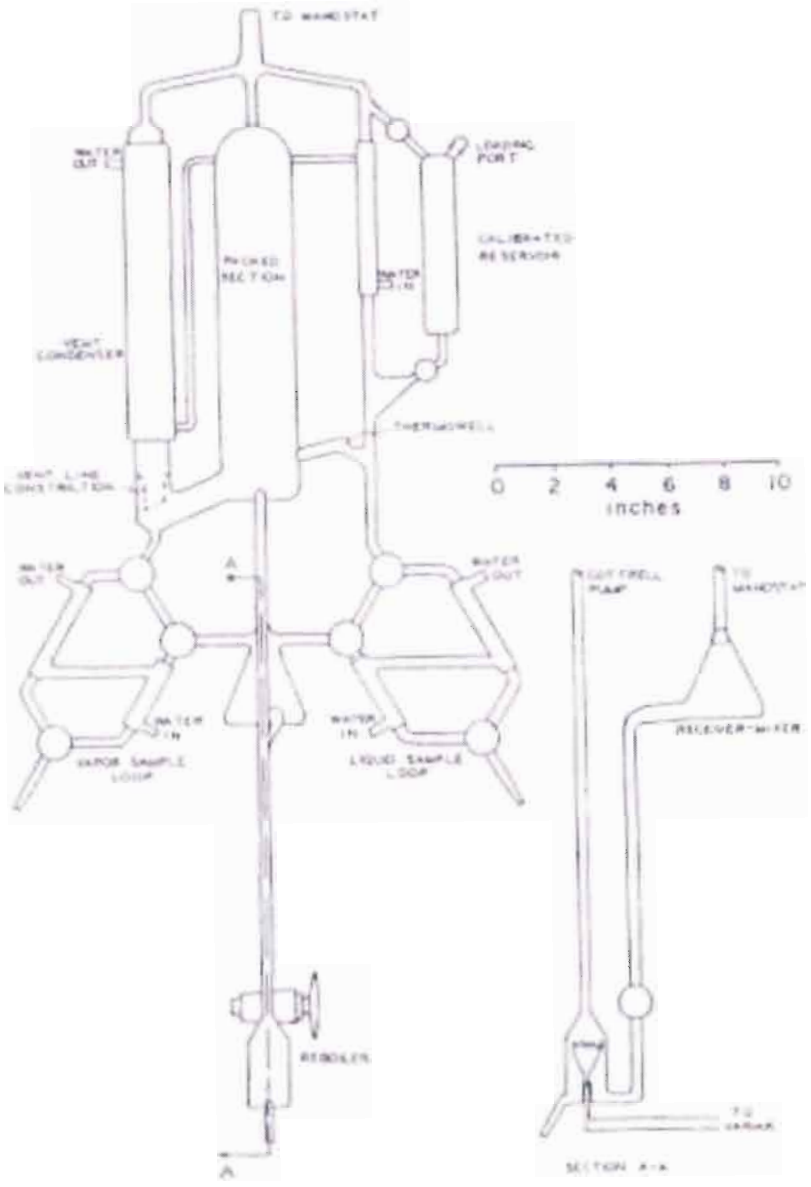

Figure 2.19. Apparatus of Yerazunis *et al.* (1964).

With liquid phase and vapour condensate recirculation, global or gross equilibrium must be achieved in a single pass as the mixture passes through the Cottrell tube from the reboiler through to the equilibrium chamber and then disengages. If global equilibrium cannot be attained in any of the passes (if the vapour-liquid contacting and equilibration interface is inefficient), then continued circulation will not improve the approach to equilibrium (by smoothing out any erroneous local equilibria).

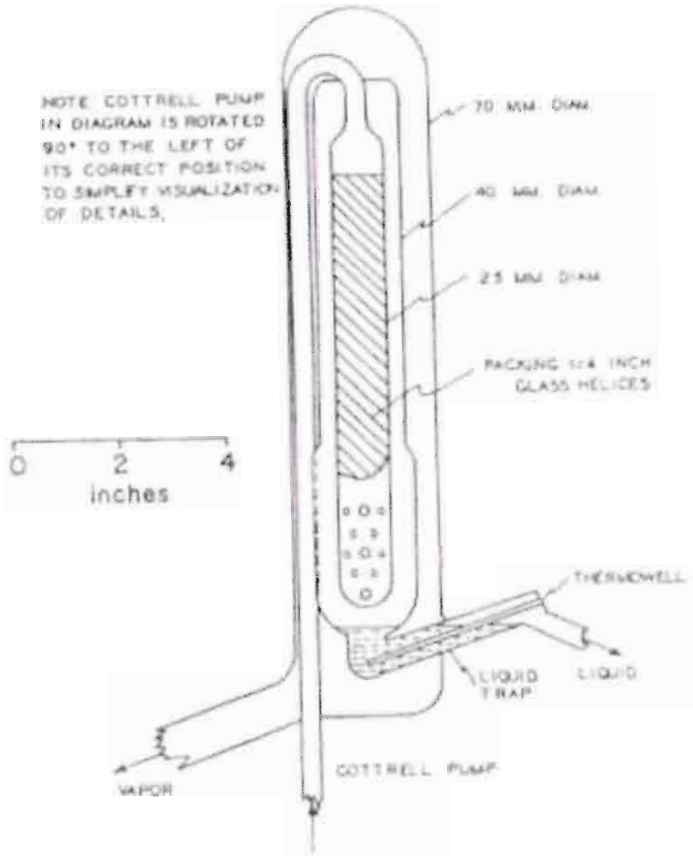

Figure 2.20. Equilibrium chamber of the apparatus of Yerazunis *et al.* (1964).

Yerazunis *et al.* also realized that the use of a Cottrell tube as the principal contacting section for the phases was subject to many uncertainties as the boiling of the mixture in the reboiler results in "chaotic" vapourization and superheating of the liquid phase. The latter would result in the superheated mixture of vapour and liquid travelling up the Cottrell tube at any instant being unrepresentative of the actual equilibrium composition. The packing in the equilibrium chamber allowed for proper mixing of the phases in an adiabatic environment, away from the superheat of the Cottrell tube.

The vapour-liquid mixture then disengaged after its concurrent passage through the concentric holes at the base of the equilibrium chamber. The liquid drained through the holes and collected in a short liquid trap beneath the equilibrium chamber, where the equilibrium temperature was measured, and the overflowed into the liquid sampling loop. The vapour phase flowed upwards around the packed column section inside the equilibrium chamber and then entered the annular space between the outer body of the chamber and the inner glass housing of the equilibrium chamber. In this way the vapour formed a jacket around the entire equilibrium chamber, hence negating heat losses.

This idea of the use of vapour or liquid to form a jacket around the equilibrium chamber was borrowed from the designs of Hipkin and Meyers (1954) and Rose and Williams (1955), respectively. The choice of the vapour phase for the self-lagging of the equilibrium chamber was motivated by the ease of vapour flow manipulation and the energy requirements for the latent heat of condensation of the vapour stream. The vapour stream then passed into a condenser, from where the condensate entered the condensate sampling loop.

The researchers felt that a reworking of the sampling loop design was desirable to maintain a continuous steady flow of the disengaged phase through the sampling loop. To this end, the overflow-type sample receiver had to be eliminated from the design. The use of a three-way by-pass valve allowed for the isolation of samples whilst the still operates continuously. In this way, there is minimal holdup of the phases in their return to the reboiler and also minimal perturbation of the circulating operation of the still.
The use of external water jackets allowed for the cooling of the samples *in situ* prior to sampling, facilitating the handling and negating errors associated with sampling.

Another important feature in the design of Yerazunis *et al.* was the union of the condensate and liquid streams from the sample loops in a receiver (shown from the side in the lower right hand corner of Figure 2.19), which had mechanical agitation, to allow for good mixing prior to re-entry into the reboiler.

Although the work of Yerazunis *et al.* had ushered in a significant era of the advancement of VLE design and data acquisition, a few concerns over the design were inevitable.
The use of the stopcocks in the apparatus had introduced difficulties related to possible contamination due to stopcock grease *i.e.* incompatible materials. Although the sample loop streams were well mixed prior to re-entry into the reboiler, mechanical agitation in the reboiler was necessary to ensure that the returning stream was well mixed with the hot reboiler liquid to prevent any flashing. Consideration should also be accorded to the use of pressure equalizing tubes across the sample loops so as to minimize any pressure drop (due to accumulating liquid) and the internal pressure gradients in the equipment.

Equipment of Raal et al. (1972)

The flaws identified in the Jones-Colburn design (1943) could be overcome through the use of the liquid and vapour phase condensate recirculation method. In the latter method, the transport of the slightly superheated slugs of the vapour-liquid mixture along the Cottrell pump to an adiabatic disengagement interface, allowed for accurate measurement of the equilibrium

temperature. However, Raal *et al* (1972) later postulated that the contacting of the phases in the Jones-Colburn still allowed for a closer approach to equilibrium than those obtainable in liquid and vapour phase recirculation methods, which actually relied only on the Cottrell tube for the attainment of equilibrium. Consequently a novel approach to determining VLE was adopted by Raal *et al.* (1972), who combined the advantageous features of the revapourized condensate recirculation method and the liquid and vapour phase recirculation method in the development of a new apparatus. Although the apparatus of Raal is a hybrid of two different methods; since the design principle of liquid phase and vapour condensate recirculating stills is retained in the design, it has been included in this classification scheme.

The design of the apparatus of Raal *et al.* is shown in Figure 2.21. In this design, the contacting principle of the Jones-Colburn still (Jones *et al.*, 1943) *i.e.* the bubbling of the vapour phase through the liquid phase in the form of a bubbling chamber was coupled with the use of the Cottrell pump, in a design which allowed for adiabatic conditions in the equilibrium chamber and accurate temperature measurement. The inner equilibrium chamber fitted loosely inside the outer chamber such that their alignment produced a uniform annular space of approximately 2 mm. The liquid that was heated in the boiler section *i.e.* the base of the outer chamber by the resistance spiral formed vapour bubbles, which propelled a vapour-liquid mixture upwards through the annular Cottrell pump.

This mixture impinged onto a thermowell, which housed a thermocouple, for the temperature measurement. The "thermally-lifted" mixture also served to maintain the inner chamber at the temperature of the boiling liquid *i.e.* a "self-lagging" effect. At the top of the inner down-comer tube, a simple disengagement interface allowed for phase disengagement.
The liquid passed downwards through the down-comer tube, whilst the vapour phase travelled upwards and then was forced through the annular space between the down-comer and the inner wall of the inner chamber. The vapour then passed through the concentric holes at the base of this annular space and then bubbled through the liquid resident in the inner equilibrium chamber to allow for equilibrium to be attained between the phases. When equilibrium was attained, the vapour phase bubbled through the liquid phase without a change in composition.

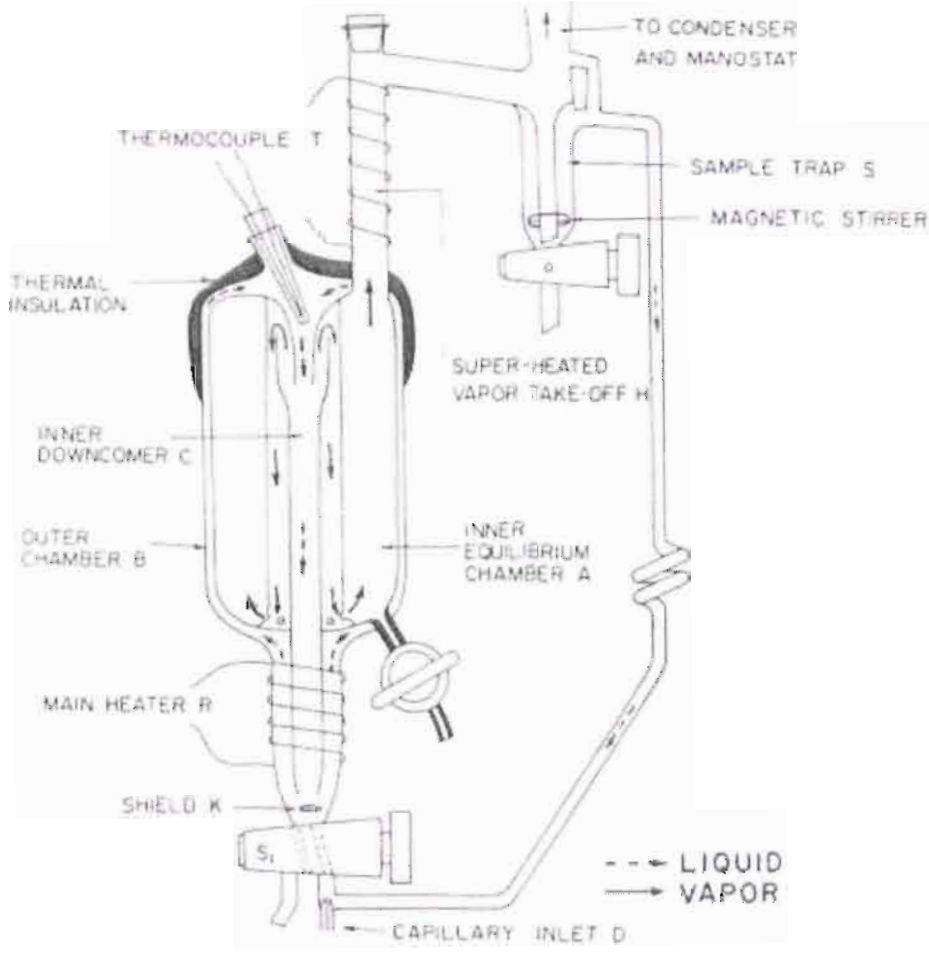

Figure 2.21. Apparatus of Raal *et al.* (1972).

The partial condensation of the vapour stream was in turn prevented by thermal contacting with the equilibrium liquid in the innermost liquid down-comer. This vapour was then superheated in this section to prevent partial condensation. This upper section of the equilibrium chamber was also insulated with a suitable material. The superheated vapour was then condensed and then collected in a magnetically stirred sample trap, which had a pressure equalizer tube. Overflow from the trap returned to the heated section via a return tube, with a short spiral section of two turns, probably to negate back flow and marginally increase holdup.

To eliminate the effects of superheating and bumping in the heated section of the apparatus, which would result in splash vapourization, a stream of fine dry air or nitrogen bubbles was introduced through the capillary inlet projecting into the entry point of the condensate return line. To ensure that the bubbles were directed outwards around and not into the down-comer tube, a shield was placed at the exit point of the down-comer tube. The bubbles also serve to assist in the mixing of the returning condensate with the liquid resident in the heated section.

The typical equilibrium times that were observed for this apparatus were 1.5 to 2.5 hours, depending on the system studied. The condensate sample was obtained from the stirred sample trap.

The theoretical treatment of the data showed that for the highly nonideal systems studied, the data were thermodynamically-consistent. However, there were a few concerns about the VLE apparatus, as summarised below:

(a) There was indeed a *pressure difference between the inner an outer chambers* as a result of the pressure drop in inner chamber as a result of the hydrostatic head of the liquid resident in this chamber. This pressure difference affects the accuracy of the temperature measurement in the outer chamber.

(b) The *backflow of liquid up the down-comer* occurred due to the accumulation of the returning condensate in the heated section. The effectiveness of the shield in preventing the bubbles from travelling up the down-comer is also an important consideration, as this would contribute to the problem of the pressure difference between the inner and outer chambers.

(c) Equilibrium *times were too long*.

(d) The *use of stopcocks* was not the most ideal sampling mechanism, as many researchers had eliminated the use of stopcocks from their design (Brown, 1952).

Equipment of Rogalski and Malanowski (1980)

Ebulliometry was traditionally used for measuring the boiling points of pure substances as in the design of Swietolawski and Romer (1924). The design of liquid phase and vapour condensate recirculation although based on the design of the Swietolawski ebulliometer, developed along different operational principles than the design of ebulliometers, which as mentioned above were principally used for boiling point determinations.

Equilibrium stills for VLE determination required a greater attention to detail with regards to sampling points, equilibrium chambers, disengagement interfaces, *etc.* The above point is stressed at this juncture to illustrate that a few authors have a tendency to use the concepts of the traditional ebulliometric methods and low-pressure VLE methods based on equilibrium stills, interchangeably. The work of Rogalski and Malanowski (1980) clearly highlights the

differences between the two original contexts of the development of ebulliometry and equilibrium stills.

Rogalski and Malanowski decided to modify the original ebulliometer design to allow for the rapid and accurate determination of VLE data in the low-pressure region of a wide range of temperatures. The authors developed two types of stills, one of which is shown in Figure 2.22. The apparatus in Figure 2.22 was employed for the determination of a complete VLE data set in the form of pressure, temperature and both phase compositions *i.e.* (P-T-x-y), as is determined for an equilibrium still. Consequently it is of the analytical type and featured sampling facilities for the quantitative determination of the equilibrium phases.
The other type of apparatus (which is not shown here) was employed for total pressure or boiling point determinations, as for an ebulliometer, where the pressure and temperature of liquid samples of known total composition is determined and the composition of the liquid phase (x) is calculated, yielding an incomplete (P-T-x) data set.

In traditional ebulliometry, there is no actual designation of a reboiler, as instead the boiling section is considered as an extension of the Cottrell tube *i.e.* a single entity (Kneisl *et al.*, 1989). The still in Figure 2.22 featured sampling ports for the vapour condensate (**K**) and liquid (**L**) phases and a heated section (**G**) to prevent the partial condensation of the exiting vapour. In the operation of the still, the initial charge was heated in the boiling chamber or reboiler (**A**) by the electrical heater. The inner walls of the reboiler were sintered with powdered glass, to facilitate boiling through the creation of nucleation sites and minimizing superheating of the liquid by providing an activated, non-uniform surface (Malanowski, 1982a).

To minimise heat losses from the equilibrium chamber *i.e.* maintain adiabatic conditions, the equilibrium chamber (**D**) was housed in a vacuum jacket (**E**). In this design, the authors claim that the steady state was established in the equilibrium chamber, however, on the outside wall of the thermowell.

The determination of an optimal heat input into the reboiler for the transport of the slightly superheated mixture up the Cottrell pump has been a controversial one. Malanowski (1982a) showed that the flow of the condensate through the drop counter can be used a qualitative indicator that the apparatus is functioning optimally.

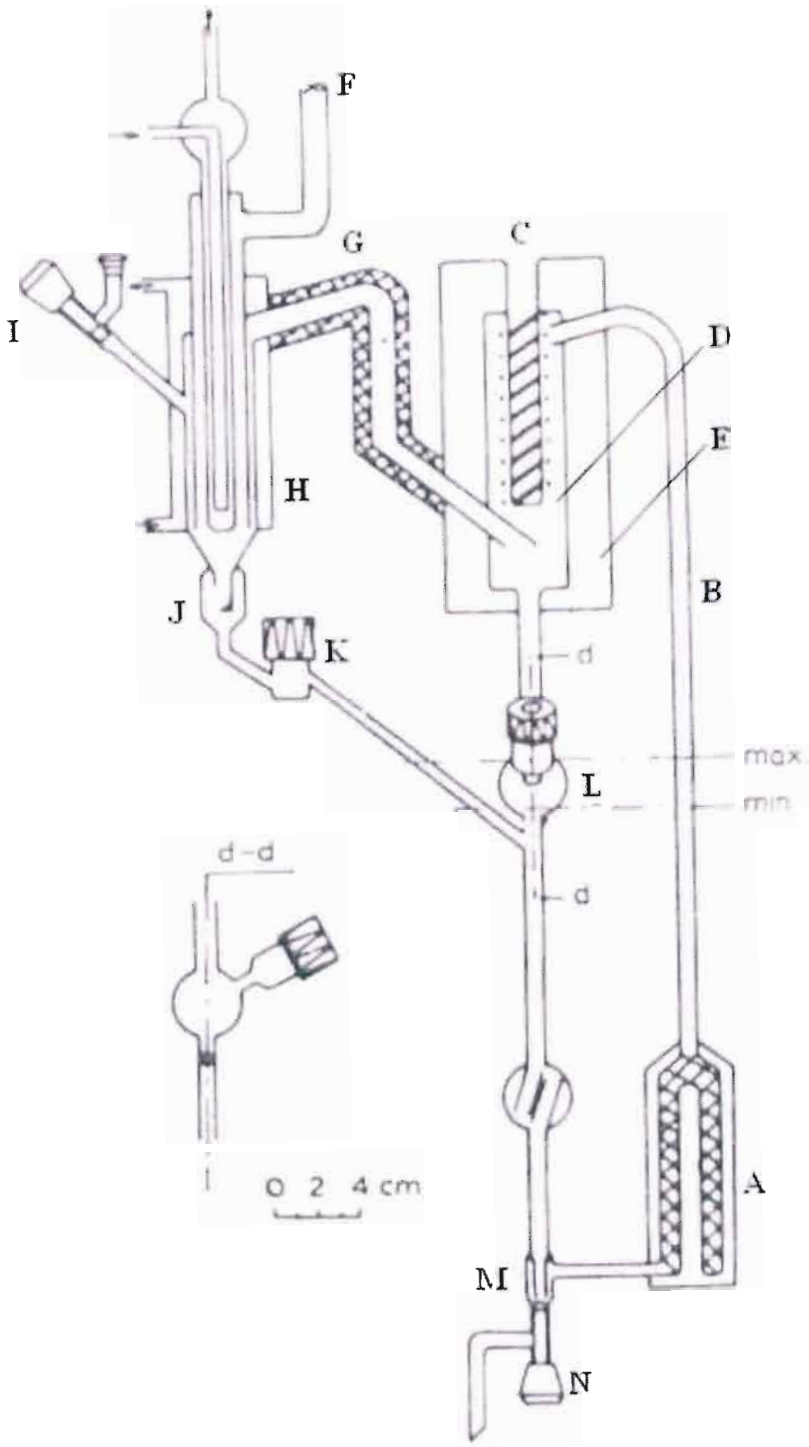

Figure 2.22. Apparatus of Rogalski and Malanowski (1980) for P-T-x-y measurements: **A**, boiling chamber; **B**, Cottrell tube; **C**; thermowell; **D**, equilibrium chamber; **E**, vacuum jacket; **F**, pressure connection; **G**, heated vapour take-off tube; **H**, condenser; **I**, sample filling point; **J**, drop counter; **K**, vapour condensate sample trap; **L**, liquid sample trap; **M**, mixing section; **N**, drain valve.

If a curve of the boiling point versus drops per unit time is examined (Figure 2.23), a "plateau region" is observed for a pure substance (curve 1) and a mixture (curve 2), which is a roughly a horizontal section in the curve and represents the equilibrium or steady state region. The latter is shown as the region between the vertical lines **A** and **B** in Figure 2.23. As can be observed, the plateau region for a pure substance is in most instances slightly flatter (and easier to determine experimentally) than that for the substance in a mixture. Consequently, it is recommended that the plateau region for the pure substances in terms of an optimal drop count (corresponding to line **C**) be determined first, and the drop count lying in the common plateau of the substances can then be used as the constant drop count for the mixture with the component. This method is indeed not applicable where there is a large difference in volatility between the two substances (no common plateau) and where the system is strongly nonideal.

To credit of the efforts of the authors, accurate VLE measurements were obtained by the researchers for the nonideal systems that were investigated and the data also was also shown to compare well to that obtained by the static method.

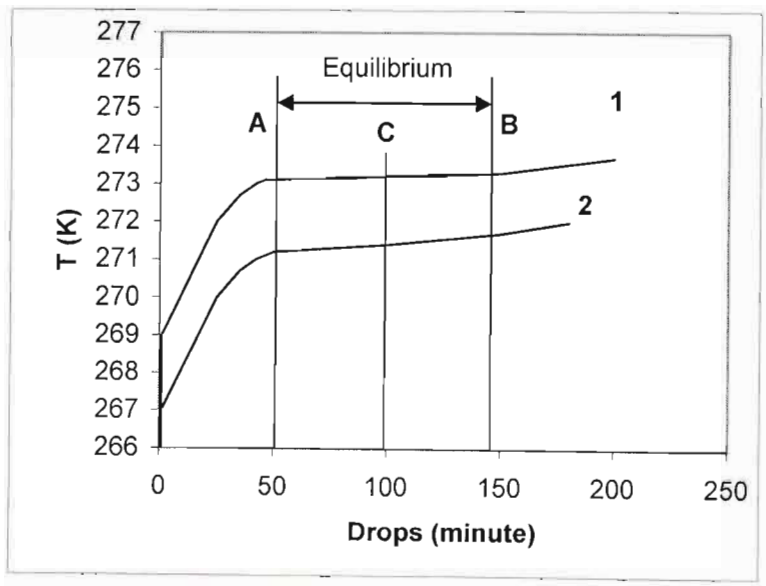

Figure 2.23. Curve of the equilibrium temperature as a function of drop count.

A few criticisms of the method are the following:

(a) In the determination of the equilibrium condition, the authors stated that the latter *was limited to* "determined narrow ranges of the flow of fluid phases" where the heat input to the Cottrell pump is constant for a particular system.

This alludes to internal inconsistency where the equilibrium temperature for isobaric conditions is dependent upon the heat input to the Cottrell pump *i.e.* the circulation rate. It has even been acknowledged (Malanowski, 1982a) that the boiling temperature is a function of the amount of heat input to the Cottrell pump (reboiler) for the Swietolawski ebulliometer. Consequently, stable hydrodynamic conditions have to be maintained in the apparatus for each run with regards to the circulation rate, as indicated by the drop counter, to ensure that reliable or reproducible results are obtained. This translates into the number of drops per minute being kept constant during all the runs. The operation of the ebulliometers therefore requires a great deal of operator skill and experience for reliable VLE results.

(b) The *assumptions in ebulliometry*, as with most of the early researchers in liquid and vapour condensate recirculation, was that the Cottrell tube itself was sufficient for the attainment of the equilibrium condition between the vapour and liquid phases (Olson, 1989). The contacting and disengagement section for the phases in the equilibrium chamber in these types of equipment was poorly designed. Consequently, any attempt to modify ebulliometers for the measurement of VLE must borrow heavily from the design of liquid phase and vapour condensate recirculation stills, which then renders the design an equilibrium still anyway, since equilibrium compositions and not only boiling points (as in the case of ebulliometry) are determined.
Thus the distinction between pure ebulliometry and conventional liquid phase and vapour condensate recirculation is a very fine one, since both are based the same operational principles (Cottrell pump), but are designed for different purposes. However, the terms ebulliometers and VLE equilibrium stills cannot be used interchangeably as was the case for some researchers (Berro *et al.*, 1982).

(d) There was *no stirring in the sample traps* to prevent the creation of concentration gradients, which compromised attempts for representative sampling.

(e) The *design of the vapour take-off tube* from the equilibrium chamber to the condenser was an inefficient one as it results in unnecessary holdup of the vapour phase and in the possible entrainment of the liquid phase in the vapour.

Any attempts to use ebulliometry for the measurement of VLE must incorporate the features of a VLE equilibrium still and most notably, the proper design of a contacting and disengagement section and stirring in the respective parts of the apparatus.

Later modifications of the Rogalski and Malanowksi still included a collaboration of Rogalski with Berro and Peneloux in 1982 in an attempt to address the limitations of the dynamic method or ebulliometry for the measurement of VLE due to the uncertainties in the determination of the phase compositions. A solution was proposed where an *in situ* analysis of the samples, would be performed, hence eliminating sample withdrawal and external analysis.

The coupling of an Anton Paar densimeter to the ebulliometer would allow for online or flow sampling, without disturbing the circulation operation or the equilibrium state established. The design of Berro *et al.* suffered from the same limitations as the original design of Rogalski and Malanowski (1980) and due to the modification, a further limitation *i.e.* the densimeter being *limited to operating temperatures* for the vapour condensate and liquid streams that are higher than 298.15 K was incurred.

Another modification of note but with regards more to the automation of the technique and the auxiliary equipment than the actual still itself was observed in the work of Hiaki *et al.* (1994). In the work of Hiaki *et al.*(1994), a VLE still based on the Rogalski-Malanowski design (1980), with a computer-controlled actuation of two solenoid valves (in conjunction with three surge tanks) for isobaric or isothermal determinations was developed. The equipment modification related to the liquid sampling and return line. The authors had felt that in the original design, the possibility of the backflow of the mixed vapour condensate and liquid stream back into the liquid sampling trap was not compensated for. The principal modification was in the form of an intervention between the return line and sample trap, which would serve as a buffer for fluctuations in the liquid levels.

Raal and Brouckaert (1992)

Twenty years later Raal and Brouckaert revisited the original still design of Raal *et al.* (1972) to determine, in particular, VLE data for systems that exhibited limited miscibility. In this study, Raal and Brouckaert asserted that conventional recirculating stills were inappropriate for such studies as a true equilibrium was difficult to attain and the vapour phase would condense out into a two-phase mixture, when the miscibility limits of the system were exceeded.

The proposed apparatus is shown in Figure 2.24. In a comparison of the still with the previous version (Raal *et al.*, 1972), relatively few but important modifications were made to improve upon the original design.

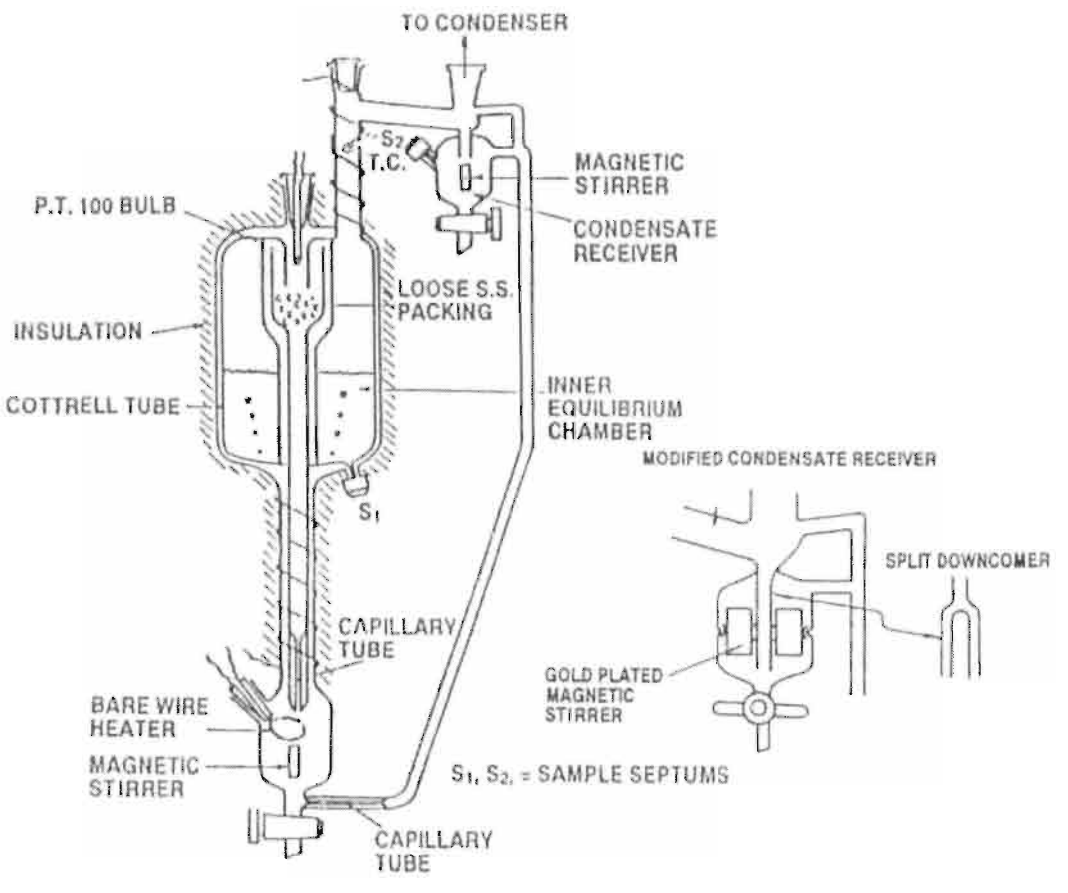

Figure 2.24. Apparatus of Raal and Brouckaert (1992).

The modifications included the use of capillaries in the entry points of the return lines, opposed to fine inert gas bubbles, to smooth the continuous flow of the returning condensate and the liquid stream into the heated section. For the dissipation of any concentration gradients in the boiling chamber or the condensate sample trap, magnetic stirrers were used to provide the necessary agitation. Where partially miscible systems are investigated, a "split down-comer" was used in the condensate trap to facilitate the separation of the phases. An internal heater in the form of a bare wire heater was employed for the rapid and smooth heating of the charged mixture. The annular space available for the transport of the vapour-liquid mixture from the boiler *i.e.* the annular Cottrell tube was decreased from approximately 2 mm in the previous design to 1 mm in the current design. The mixture then enters a separation chamber, which is packed with loose stainless steel packing to assist in the equilibration and the disengagement of the phases.

As mentioned for the earlier apparatus of Raal *et al.* (1972), the fluid flowed adjacent to the outside (Cottrell pump mixture) and the inside (inner vapour down comer) of the inner

equilibrium chamber to allow for adiabatic conditions. Raal *et al.*(1972) decided to also use insulation around the Cottrell tube to minimize any heat losses to the environment.
The above modifications helped to optimize the design for the study of highly nonideal and for partially miscible systems; however, the problem of the pressure drop between the down comer and the inner equilibrium chamber due to the hydrostatic head of the liquid in the latter was not addressed. This can have a deleterious effect on the equilibrium temperature measurements, as the pressure of the equilibrium mixture, measured in the inner equilibrium chamber, will not always necessarily be thermodynamically consistent with the measured temperature at the disengagement section. There should be a pressure equalization mechanism incorporated into the design of the apparatus to ensure that there are no internal pressure gradients that result in thermodynamically inconsistent pressure and temperature measurements.

Raal (1998)

One of the most recent successful developments in the field of LPVLE measurement has been achieved by the Thermodynamics Research Unit at the University of KwaZulu-Natal in the form of a highly refined computer-controlled dynamic VLE still. The VLE still is capable of acquiring both isobaric and isothermal and has been designed in the same mould as that of Hiaki *et al.* (1994) in terms of the design and in the efficient operation of the pressure and temperature feedback/control system. The design of the glass still, however, features many additional novel modifications to enable the acquisition of reliable thermodynamically consistent data based on sound operating principles.

The design of the still of Raal, as described in the text of Raal and Muhlbauer (1998), is shown in Figure 2.25. The reboiler (**A**) features both internal and external heaters. The external heater serves to mainly compensate for any heat losses to the external environment in maintaining the boiling temperature, whilst the internal heater has the more important role of ensuring precise control over the circulation rate and for the creation of nucleation sites for smooth, rapid and continuous boiling.
The contents of the reboiler are also mechanically agitated to ensure that the dissipation of any concentration gradients occurs and the possibility of the flashing of the volatile components in the return stream is negated. The Cottrell tube (**E**) is vacuum jacketed (**D**) to minimize any heat loss by the vapour-liquid mixture transported by the vapour-lift principle.

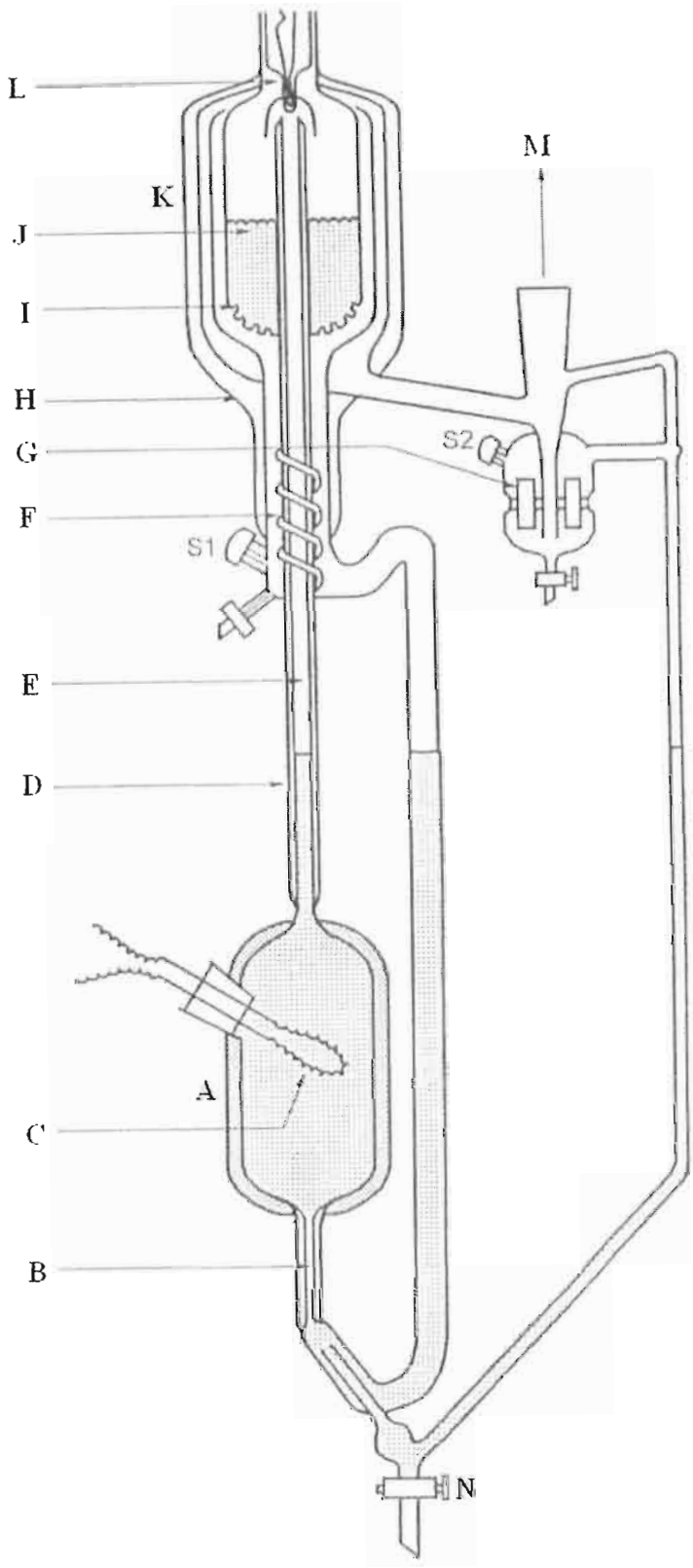

Figure 2.25. Apparatus of Raal (1998): **A**, reboiler; **B**, capillary; **C**, internal heater; **D**, **H**, vacuum jacket; **E**, Cottrell tube; **F**, s/s mixing spiral (liquid phase); **G**, magnetic stirrer (vapour condensate); **I**, drain holes; **J**, s/s wire mesh packing; **K**, equilibrium chamber; **L**, temperature sensor; **M**, inlet for the condenser and the pressure regulating system; **N**, drain valve, S_1, liquid sampling point; S_2, vapour condensate sample point.

The vacuum jacket also serves to ensure that any superheat from the vapour-liquid mixture in the Cottrell tube is not transferred to the equilibrium mixture. The equilibrium chamber (**K**) is angularly symmetric about the Cottrell tube, as in the design of Rose and Williams (1955). This ensures that there is no preferential radial direction for the equilibrating mixture of vapour and liquid to pass through in the packed section in **J** (to prevent any concentration or temperature gradients).

This design is also more efficient than the sideways entry of the Cottrell tube as in the apparatus of Rogalski and Malanowski (1980) as it makes the equipment more compact in design and operation. The mixture then discharges into a packed equilibrium chamber in which the vapour and liquid phases are forced concurrently downwards. The packing material used is rolled 3 mm stainless steel wire mesh cylinders.

As discussed previously (Yerazunis *et al.*, 1964), the packing material serves to improve the approach of the phases to a true equilibrium by allowing for an increased interfacial contacting of the phases for mass transfer and increased contact time for the phases on freshly created surfaces as the mixture flows concurrently towards the base of the packed section. Pressure drop along the packing of the equilibrium chamber is an important consideration and with the open structure of the mesh cylinders, a very low pressure drop is experienced.

The Pt-100 temperature sensor (**L**) is inserted via a glass stopper in a tapered opening at the top of the equilibrium chamber, into the base of the packed section of the equilibrium chamber, where the phases disengage. This is the most appropriate point as it is the termination point for the contacting of the phases and the commencement of phase disengagement. This ensures that maximum contacting of the phases has occurred for equilibrium to be attained between the phases before the equilibrium temperature is measured.

The equilibrium mixture then disengages as it passes through small holes at the base of the equilibrium chamber. The liquid mixture then flows in a downward path and is mixed as it passes along a stainless steel winding or mixing spiral and accumulates, with a short residence time, in a liquid trap ($\mathbf{S_1}$). The disengaged equilibrium vapour then flows upwards around the equilibrium chamber. In this fashion, the equilibrium vapour insulates or serves as lagging to ensure that adiabatic conditions are maintained in the equilibrium chamber as in the design of Yerazunis *et al.* (1964). The vacuum jacket (**H**) formed in the annular space between the outermost and the middle concentric tube provides additional insulation of the equilibrium chamber.

The equilibrium vapour is condensed in the condenser attached at point (**M**) in the apparatus, from the condensate collects in magnetically stirred condensate trap ($\mathbf{S_2}$). Liquid and condensate samples are extracted from the sample traps through suitable septa with a gas-tight syringe, without disturbing the established equilibrium.

The liquid and vapour condensate streams are then returned separately in their respective return lines. Any backflow into the sample traps were compensated for, in the later modified design of Joseph (2001), which features a "siphon break" tube to prevent the above. However, there is a capillary section (**B**) at the base of the reboiler, which serves to negate backflow and allow for the smooth flow of the returning stream into the reboiler.

The systems measured with this apparatus include that of cyclohexane + ethanol (Joseph *et al.*, 2002) and diacetyl with toluene and cyclohexane (Joseph *et al.*, 2001). The data obtained was shown to compare favourably with that obtainable in the literature and was also shown to be thermodynamically consistent.

A comprehensive review has been provided for both high and low-pressure VLE measurement equipment. The design and operation of traditional high-pressure VLE equipment has shown to necessitate high capital costs for equipment development, require the use of expensive auxiliary equipment (metering pumps, valves, sensors, thermostats, *etc.*), require complicated sampling systems (capillaries, multi-port gas chromatographic valves), incur time-consuming operating procedures (degassing, evacuation, *etc.*) and also require long equilibration times.

In contrast to HPVLE measurement methods, LPVLE methods usually involve the construction of equipment which is relatively of a simple, compact design (with glass being the most obvious choice for subatmospheric measurements), simple operating procedures, small sample sizes and shorter equilibrium times. However, the pressure and temperature ranges of such equipment are severely restricted to moderate conditions (subatmospheric and less than 473.15 K) therefore the range for VLE data acquisition by such methods has been quite limited. Consequently, it has been desirable to develop methods that are based on the operational principles and associated design of LPVLE methods for use at higher pressures and /or temperatures to obtain VLE data in fairly cost-effective, rapid and simple way.

2.7 Development of LPVLE methods for higher pressures and temperatures

In the comprehensive reviews by Fornari *et al.* (1990), Dohrn and Brunner (1995) and Christov and Dohrn (2002) of high-pressure VLE equipment (with 1 MPa as the lower limit), less than 5 pieces of equipment amongst the hundreds listed, for the time period of 1978 to 1999, are based on the design of traditional LPVLE methods. This attests to the difficulty experienced by many researchers in attempting to extrapolate traditional low-pressure still designs to cope with the rigours of elevated pressures and temperatures.

In Section 2.5 the development of low-pressure methods was reviewed and in this section, the modification of similar types equipment for studies at higher pressures and temperatures will be dealt with. The two types of traditionally low-pressure designs that have been most popular as the templates for superatmospheric studies are the vapour condensate recirculating stills (Othmer-type), especially predominant in the early designs, and the liquid and vapour condensate recirculating stills. The inherent flaws of the designs presented below will not be elaborated upon due to the extensive coverage of the subject matter in the previous section and will be left to the intuition of the reader to ascertain. The design criteria and considerations for the use of LPVLE methods at higher pressures and temperatures will be dealt separately below.

2.7.1 Designs for elevated pressures

The first type of recirculating equilibrium still used for high-pressure determinations was based on the vapour condensate recirculation method and a detailed discussion of the apparatus will be presented below, together with the later designs.

Equipment of Scheeline and Gilliland (1939)

Scheeline and Gilliland considered the two most common HPVLE methods in that time in the form of the static method and the "dew and bubble-point" method to be undoubtedly associated with a superfluous amount of experimental difficulties. The success of the use of equilibrium VLE stills at atmospheric pressure it was believed would allow it to be also applicable to high-pressure measurements up to the critical region.

Initial considerations that arose for the design of the equipment related to the viewing of the cell contents and the accurate control of the system pressure. The former design consideration was

necessitated by the need to ensure that the complete flashing of the liquid phase or the partial condensation of the vapour phase did not occur, together with the need to observe the critical region behaviour of the system studied. With regards to pressure control, the use of an inert gas to pressurize the system contents was not favoured due to concerns over the solubility of the gas in the mixture (creating a ternary mixture) and consequently pressure control was achieved with controlled heat input into the still with the aid of a mercury switch.

The equipment is shown in Figure 2.26. The equilibrium VLE still was constructed from gauge-glass tubing which was closed at one end. A bottom heater was coiled around the base of the equilibrium still to bring the mixture to a boil. The top or open end of the tubing was sealed with a packing gland with a rubber and Neoprene® composite gasket. The Neoprene® portion of the gasket was in contact with the hydrocarbon vapours; a necessary consideration for chemical compatibility.

The opposite closed end of the glass tubing was slotted into a steel base, where lead wool and rubber sheet was used to prevent glass-steel contact. To secure the glass in the packing gland, three tie rods were used. A steel ruler was placed adjacent to the still to measure the liquid level.

The packing gland, which was machined from a steel hexagon, featured four silver-soldered tubes that entered the equilibrium still through the steel top. These were the still sampling line (steel hypodermic tubing), a suitable thermowell (copper tube sealed at one end), vapour exit line (copper tube) and the liquid return line from the trap (seamless steel tubing), which only extended only halfway into the steel top.
To prevent any partial condensation of the vapour on the inner walls of the still, a stream of electrically heated air was blown into the annular space between a loosely fitted Pyrex® jacket, used to surround the still, and the outer wall of the still.

The condenser was constructed from copper tubing and did not contain any internal cooling jackets or tubing and was instead cooled by "natural air convection". The vapour condensate trap was also constructed from glass tubing, sealed at one end, and the packing gland, steel base and the tie rods were arranged in a similar fashion to that of the equilibrium still, except for the inverted positioning.

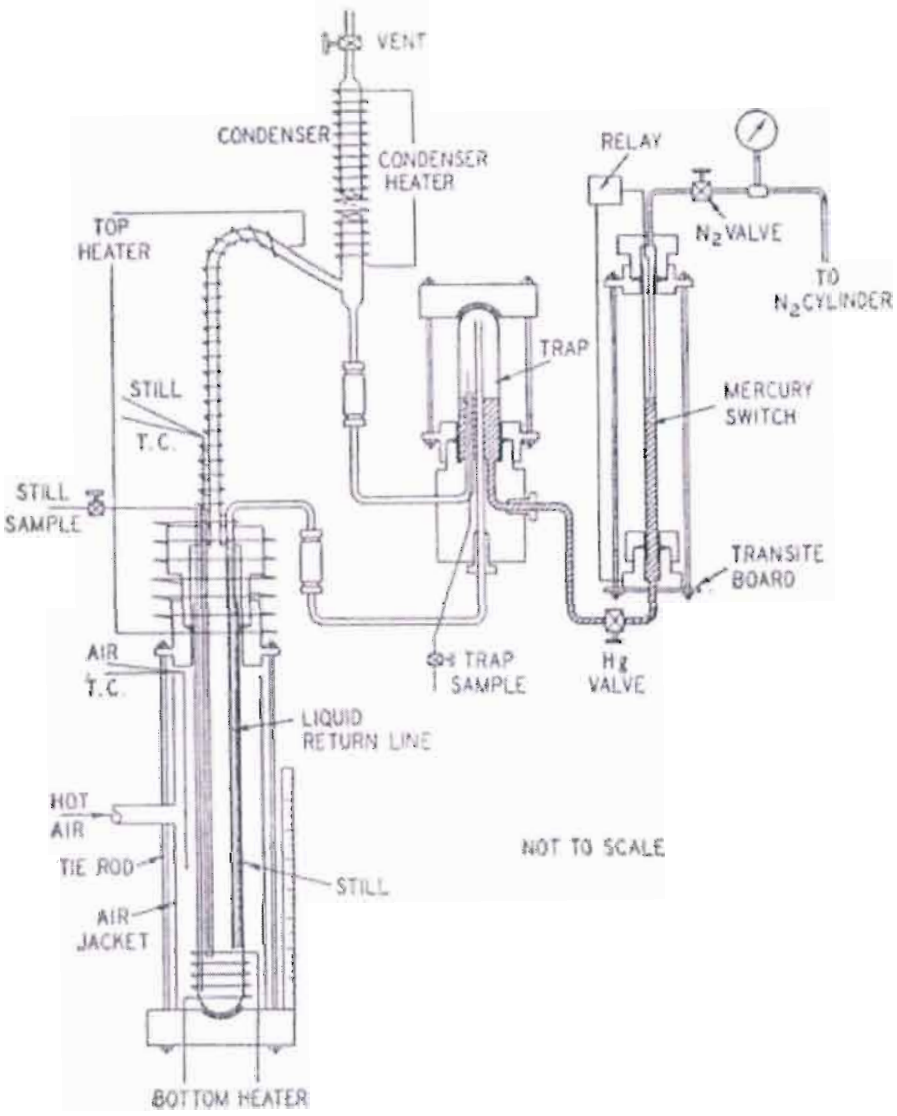

Figure 2.26. Apparatus of Scheeline and Gilliland (1939).

The system investigated by the researchers was that of isobutylene and propane. The authors reported equilibrium times of 15 minutes. The equilibrium still (liquid) and the trap (vapour condensate) samples were withdrawn into glass sampling bulbs. The pressure capacity of the entire apparatus was 10.3 MPa with the failure of the glass body described as being "infrequent" and being attributed to the over-tightening of the packing gland. Tests for possible entrainment of liquid droplets in the vapour phase were performed and no entrainment was observed even for conditions of vigorous boiling.

Equipment of Griswold et al. (1943)

The modified high-pressure VLE apparatus of Griswold *et al.* was based on the operational principles of the low pressure Othmer vapour condensate recirculating still, as in the earlier work of Scheeline and Gilliland (1939), whose equipment was principally constructed from glass, for which sealing was achieved through the use of gaskets and packing glands. Griswold *et al.* considered the above two design criteria as undesirable, who opted for an all-metal construction to ensure that there would be no concerns about the structural integrity of the material of construction and the chemical compatibility of the gasket material with the systems studied.

The final design of the still was the culmination of three prior attempts and is shown in Figure 2.27. The entire apparatus was constructed from metal in the form of extra-heavy and double-extra-heavy pipe, machined steel monoblocs, sheet iron and steel tubing. The entire apparatus was insulated with 85% magnesia lagging. The reboiler consists of a circulation pipe and a collar on one end, which was essentially a welded sheet iron ring. The purpose of the circulation pipe and the collar was to ensure that there was sufficient mixing of the vapour condensate return stream and the boiler liquid contents.

The main body, or what can be described as the equilibrium chamber, had the largest volume of the sections in the apparatus. This design criterion was in accordance with the objectives of obtaining sufficient vapour space above the liquid contents to minimize any entrainment of liquid droplets in the exiting vapour stream. To compensate for any heat losses that might occur on the walls of the equilibrium chamber *i.e.* to prevent refluxing, a winding of Nichrome wire around a layer of asbestos, was used to heat the equilibrium chamber. The equilibrium chamber was heated at a temperature that was 3 - 4 K higher than the equilibrium temperature.

The vapour take-off tube had a vent valve for the evacuation of the apparatus and directed the vapour into the condenser. The variable lengths of the condenser sections allowed for a variable surface area available for the total condensation of the sample. The design allowed for both the condensing surface and the coolant fluid to be varied to suit the system and the operating temperature to ensure that excellent control over the system temperature could be achieved. Since the use of an inert gas to pressurize the system was not favoured, isothermal conditions were maintained in the apparatus by balancing heat input and heat removal from the system by adjusting the reboiler heating voltage (from the variable-voltage transformers) and the flow rate of the coolant fluid, respectively.

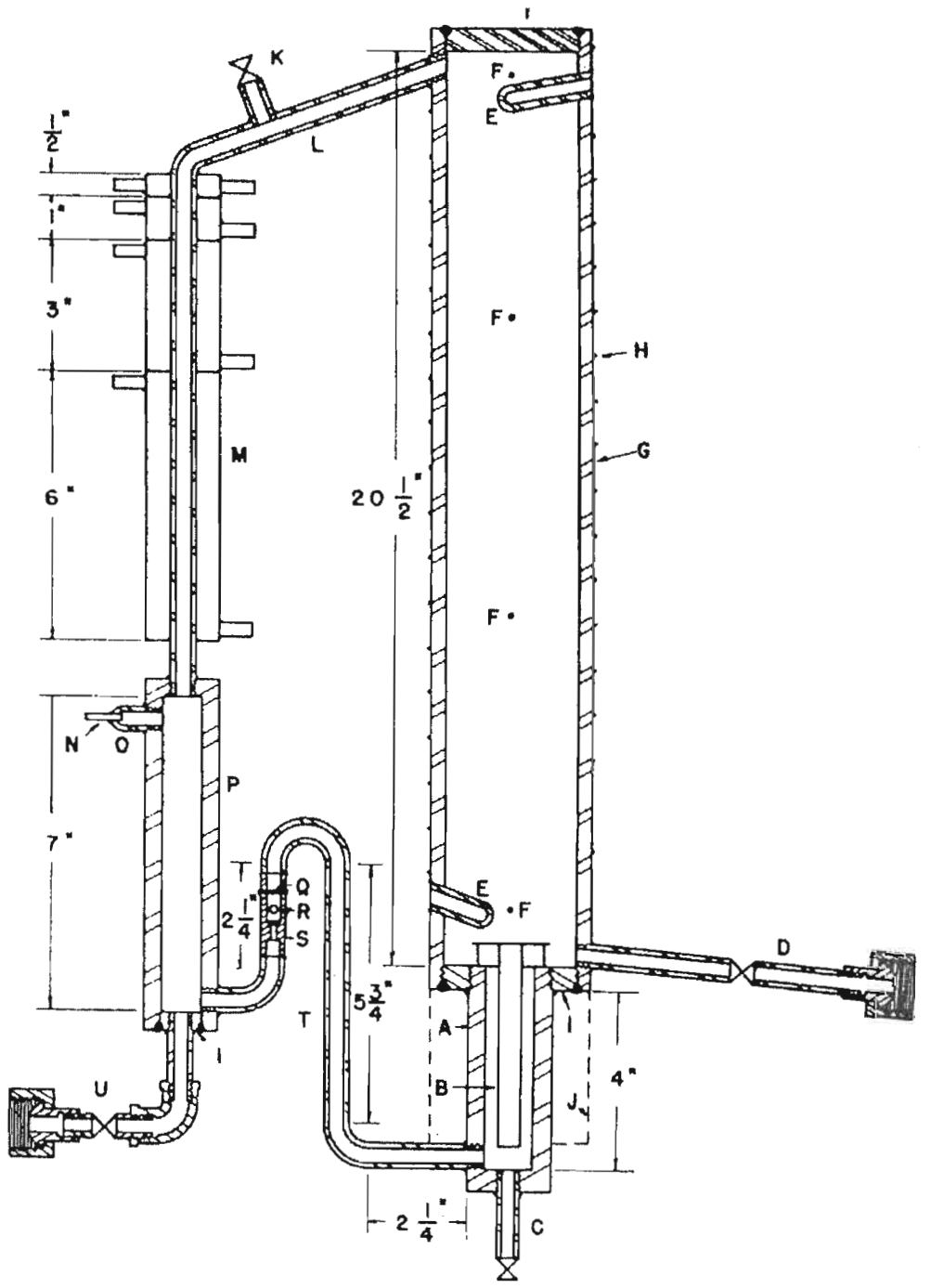

FIGURE 1

A—Heater leg of still.
B—Circulation pipe.
C—Drain.
D—Liquid sample outlet.
E—Thermowells.
F—Wall thermocouples.
G—Main body.
H—Compensating heater winding.
I—End plugs of still and vapor condensate chamber.
J—Position of alundum heater winding holder. (Norton No. MD28278, Alundum RA 98.)
K—Evacuation vent.
L—Vapor line.
M—Condenser shell.
N—Capillary steel pressure gauge tubing.
O—¼" extra heavy pipe nipple.
P—Vapor condensate chamber.
Q—Ball check valve stop.
R—3/16" steel ball check valve.
S—Body and seat of check valve.
T—Vapor condensate return line.
U—Vapor sample outlet.
All valves are ¼" size drop-forged steel, 3000 p.s.i max. working pressure. (Henry Vogt Machine Co., Louisville Ky.)

Figure 2.27. Apparatus of Griswold *et al.* (1943).

The vapour condensate sample was withdrawn at the base of the condensate chamber through a sampling line passing through the threaded and welded end-cap. The condensate return line contained a vertically mounted ball check valve, to prevent the backflow of the boiler contents into the condensate chamber.

The vapour condensate and liquid sampling lines terminated in female connections to allow for the attachment of sampling bombs, which have a capacity of 30 cm^3 and 60 cm^3, respectively. Equilibrium times of around five hours were reported by the researchers, who showed that the rate of circulation had a minimal effect on the equilibrium phase compositions.

Equipment of Othmer and Morely (1946)

A high-pressure version of the original design of the condensate recirculating Othmer apparatus (1928) was developed by Othmer, together with Morely in 1946, for operation at pressures up to 3.5 MPa. The means of pressurizing the system was in the form of an inert gas (nitrogen), since the pressure range of the experiments (below 1.4 MPa) would not introduce any significant errors (estimated below 0.7 %) into the measurements.

The apparatus of Othmer and Morely essentially consisted of a reboiler, condenser, condensate reservoir, trap and surge. The equipment, shown in Figure 2.28 was constructed from stainless steel and the individual parts were welded together.

When the mixture in the reboiler was brought to a boil, the generated vapours jacketted the walls of the vapour tube after the trapped air had been removed through the vent valve. Liquid samples, in the usual fashion for Othmer-type equipment, were withdrawn at the base of the reboiler through a liquid sample valve. The equipment was insulated through the use of a one-inch layer of 85% magnesia insulation. The vapours that passed up through the vapour tube and the top of the boiler entered a condenser consisting of several turns of stainless steel pipe housed in an iron pipe condenser box. The vapours were totally condensed and collected in the condensate receiver after passing through a drip indicator. The reservoir was constructed from cast stainless steel and had two sight glasses (front and back) to allow for visual observation and control of the circulation rate. A pressure equalizer tube was used to ensure that there were no pressure gradients between the condensate reservoir and the trap due to the hydrostatic head of the accumulating liquid.

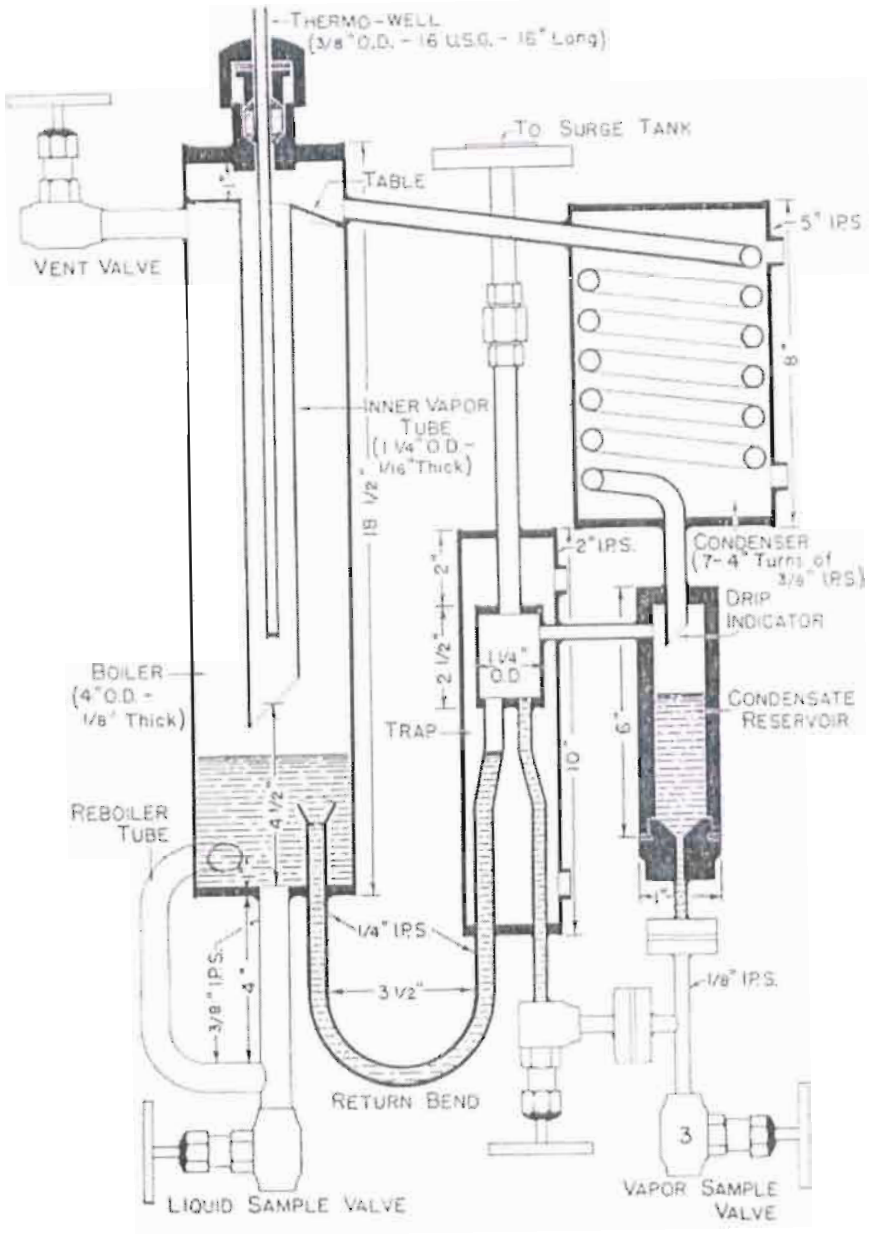

Figure 2.28. Apparatus of Othmer and Morely (1946).

There was a union tee at the base of the condensate reservoir, where one leg allowed for the withdrawal of a sample through the vapour sample valve and the other leg (at an angle of 90 °) allowed for the recirculation of the condensate into the trap. The trap was water-jacketed to cool the condensate. The purpose of the trap was to maintain a constant liquid level in the reservoir and as an overflow vessel to smooth out any fluctuations in the boiling action or liquid flow. The trap was connected to a surge tank via a valve located in the vent line of the trap. The surge tank was constructed from stainless steel and was slightly inclined to allow any condensate to drip back into the trap.

The authors reported equilibrium times of around 2 - 3 hours. A double valve metal bomb was attached to the sample valve and was used for the rapid and simultaneous liquid and condensate sample withdrawals so as to minimize the effect of flashing as a result of the pressure reduction.

Equipment of Gelus et al. (1949)

Gelus *et al.* (1949) followed on from the work of Scheeline and Gilliland (1939) in attempting to negate the apparent uncertainties associated with the vapour condensate recirculation method in its applicability to higher pressures.

The equipment was principally constructed from steel due to concerns over the high-temperature strength of glass and problems due to sealing difficulties (packing glands, gaskets, *etc.*). The maximum operating pressure was 3.5 MPa. The recirculation apparatus is shown in Figure 2.29. Steel pipe was used throughout for the body, stainless steel valves being used. All parts of the equipment were heavily insulated except for the ballast vessel and the vacuum system. The boiler was constructed from a standard steel pipe section with the ends being plugged, welded and fitted with pipe connections. The lower end was covered with baked ceramic cement, around which two heating elements were mounted. The upper section of the boiler was insulated with asbestos cloth around which a heating element is wound. A baffle system was used in the boiler to promote good mixing of the liquid contents.

A magnified internal section of the boiler is shown in Figure 2.30 to provide details of the baffle system. The annular space served as the "vapour-lift pump", as being analogous to the low-pressure design of Raal *et al.* (1972), which propelled a vapour-liquid mixture upwards and the mixture then hit against the upper baffles. The upper baffles (annular and conical), in addition to preventing liquid droplet entrainment, also served to allow for contacting between the hot rising vapours and the liquid, which returned to the base of the boiler by dropping through the centre of the baffles. The baffle at the base of the boiler at the condensate return line inlet served to prevent the returning stream from interfering with the circulation rate of the boiler contents and to some extent promote good mixing with the boiler contents. The vapour take-off line from the boiler and the condenser are heated, which can be used to reduce the circulation or boil-up rate if desired.

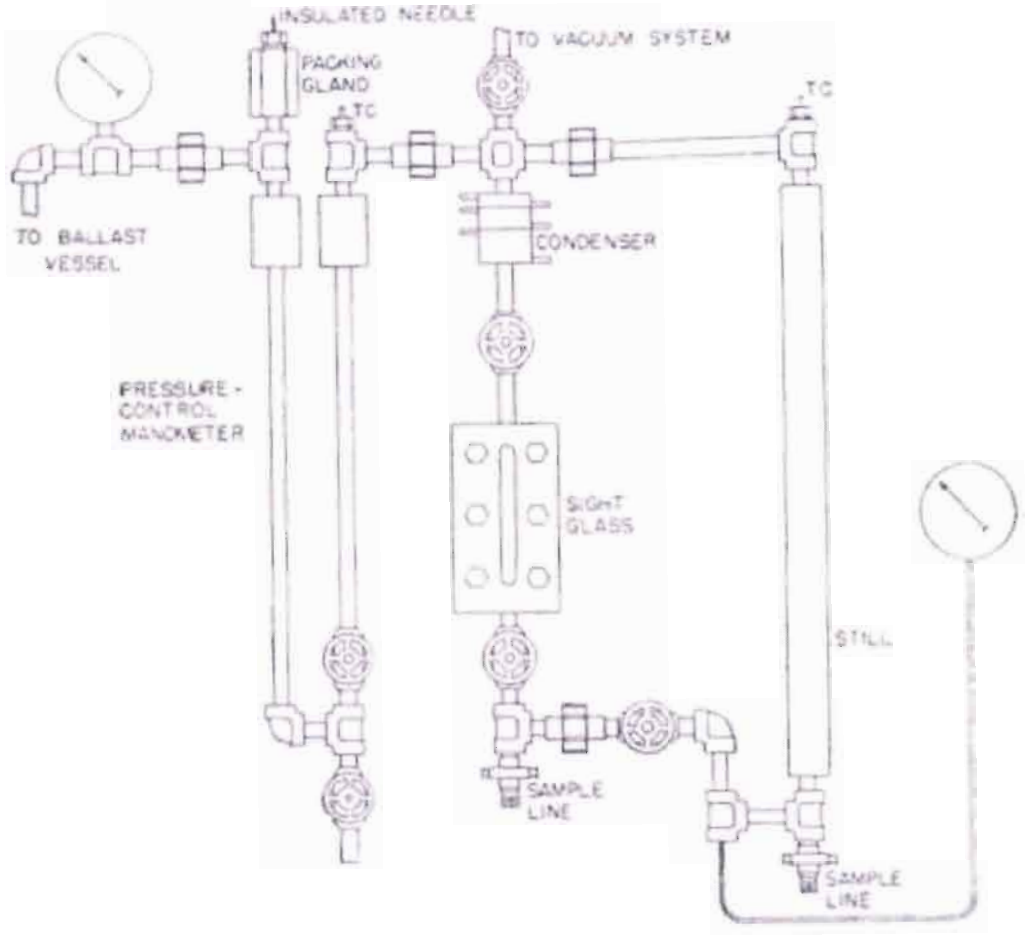

Figure 2.29. Apparatus of Gelus *et al.* (1949).

The condenser was principally divided into three sections in accordance with the heating and cooling requirements of systems of varying volatilities and for control over the boiling rates. The pipe union cross and the still side of the control U-tube were heated to prevent any partial condensation of the vapour in the vacuum line or mercury lines.

The condensate sample was collected in a trap with 20 cm^3 capacity with a sight glass. In the normal operation of the still, the boiler was charged with sufficient material (at least 150 cm^3) such that the still contained sufficient charge corresponding to the centre of the sight glass. A sample was taken from the trap through the use of an isolating valve between the condensate return line and the boiler.

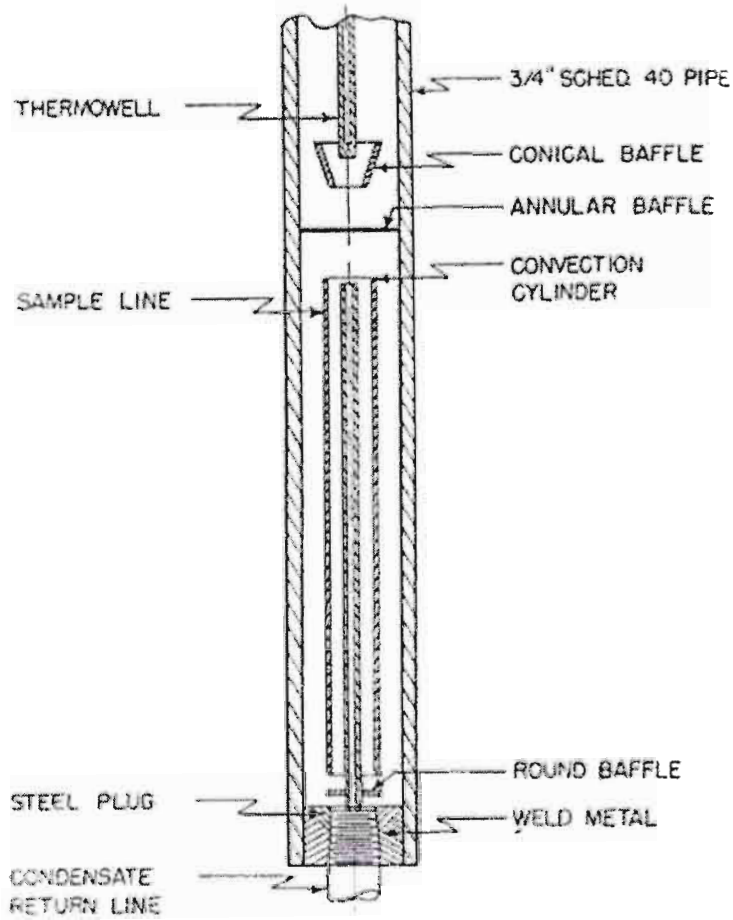

Figure 2.30. Magnified section of the boiler of the apparatus of Gelus *et al.* (1949).

Equipment of Zieborak (1964)

The equipment of Zieborak represented the first attempt at the design of an ebulliometer based on the original design of Swietolawski (1924), to withstand conditions of elevated temperatures and pressures. Although, as mentioned previously that there is undoubtedly a clear distinction between ebulliometry and VLE recirculation methods, the analogous operating principles of the two warrants the inclusion of this equipment design in this review. The temperature range of the apparatus was 347 - 495 K and the equipment could withstand pressures up to 2.5 MPa.

The metal ebulliometer design of Zieborak is shown in Figure 2.31. Since the latter is a traditional ebulliometric-type design, there are no provisions for sampling since the measurement of boiling points is the desired outcome.

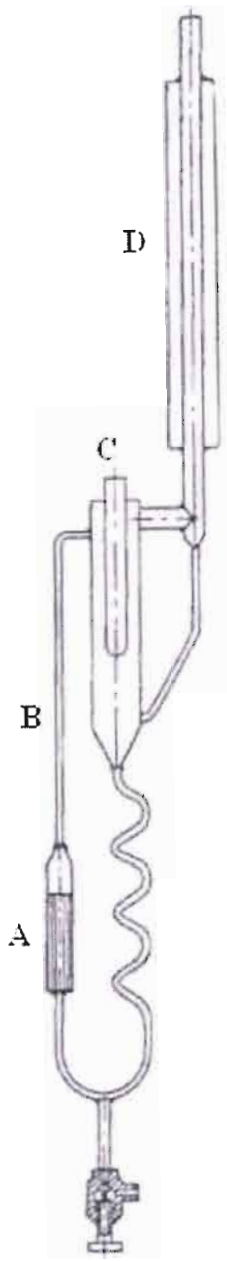

Figure 2.31. Ebulliometric apparatus of Zieborak (1964): **A**, boiling chamber; **B**, Cottrell tube; **C**, thermowell; **D**, condenser.

The design and principle of operation is analogous to that of the Swietolawski ebulliometer (1924) design, however, with a few modifications. One of these modifications was the use of steel capillaries (0.5mm diameter) in the boiling chamber (**A**) to smooth the flow of the return liquid and to limit backflow of the boiler contents. The contents of the boiling chamber were heated with a heating mantle mounted onto outside of the boiling chamber. The equilibrium temperature was measured with a platinum resistance thermometer housed in the thermowell (**C**) in the equilibrium chamber.

Equipment of Nagahama and Hirata (1976)

The equipment of Nagahama and Hirata had combined features of both the Othmer-type and the liquid and vapour recirculating-type equilibrium stills. There were two types of pressure control strategies that were used, in the form of compressed nitrogen and a heat input control, which of course depended on the pressure range that was studied. The equipment design is shown in Figure 2.32.

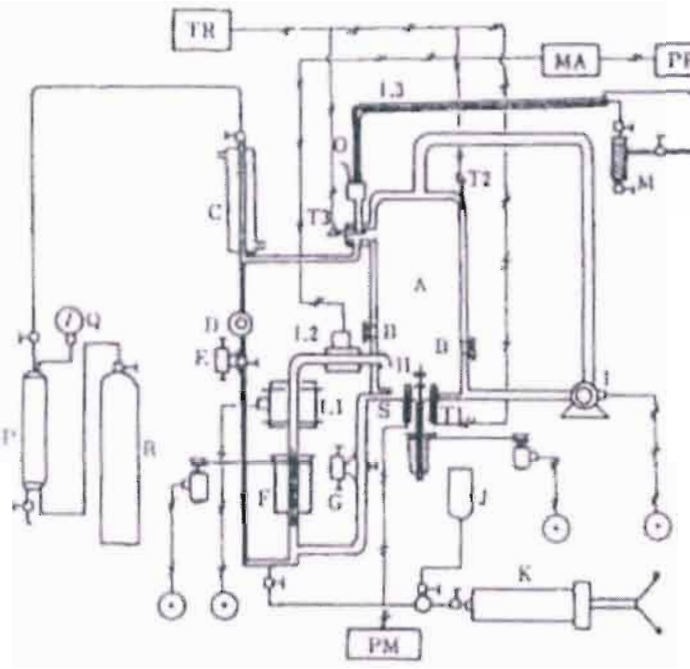

A	:	Vapor–liquid contacting cell	N	:	Pressure transducer
B	:	Sight glass	O	:	Rupture disk for safety
C	:	Condenser	P	:	N_2 gas surge tank
D	:	Drop counter	Q	:	Bourdon tube
E	:	Vapor sampling cell	R	:	Compressed N_2 gas reservoir
G	:	Liquid sampling cell	S	:	Copper–constantan thermocouple
H	:	Agitaitor	T1–T3	:	P_T resistance thermometer
I	:	Blower & heater		:	valve
J	:	Sample reservoir		:	Variable resistor
K	:	Charge pump		:	Electric wire
L1	:	Main heater	TR	:	Temperature recorder
L2	:	Control heater	PRC	:	Pressure recorder & controller
L3	:	Heater	MA	:	Magnetic amplifier
M	:	Vapor/mercury separator	PM	:	Potentiometer

Figure 2.32. Apparatus of Nagahama and Hirata (1976).

As for a typical Othmer-type apparatus, the boiler and the equilibrium chamber were combined into a single vapour-liquid contacting cell with appropriately positioned sight-glasses and the liquid phase samples would be withdrawn from the cell. However, unlike typical Othmer-type apparatus, both phases were recirculated in separate lines and then combined in their re-entry into the cell. The cell also featured an internal stirrer to assist in ensuring the generation of equilibrium vapours.

Equipment of Olson (1989)

Later developments in the use of ebulliometers for the determination of boiling points and as well as modified ebulliometers for VLE determinations included the efforts of researchers such as Olson (1989) to demonstrate the industrial applicability of the ebulliometric VLE method. Olson demonstrated the use of the technique for pressures up to 2 MPa with the design of a metal apparatus which had appropriately positioned sight glasses. The design of the apparatus is shown in Figure 2.33.

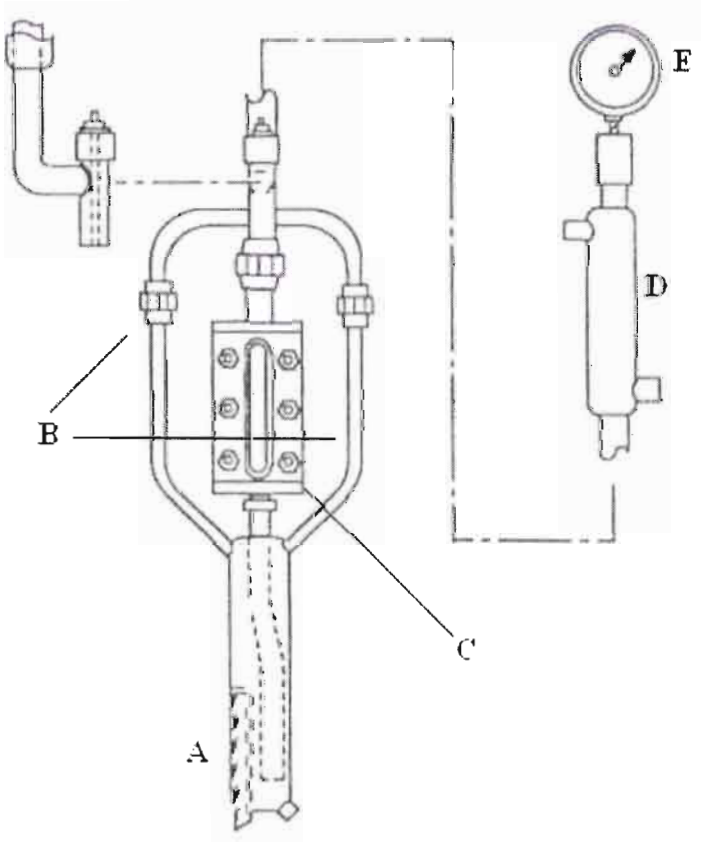

Figure 2.33. Apparatus of Olson (1989): **A**, boiling chamber; **B**, twin-arm Cottrell tube; **C**, the sight glass section; **D**, condenser; **E**, pressure gauge.

As can be observed from the design, the vapour lift pump or Cottrell pump consisted of two arms *i.e.* a "twin-arm design". The boiled mixture first passed up through the two arms of the ebulliometer and impinged upon the thermal sensor in the thermowell. The vapour is condensed and mixed with the liquid as it returns to the reboiler through the section fitted with the sight glass, which allows for visual observation of the circulation rate. The pressure connections were made through the top of the condenser and pressure control in the system was achieved through the use of compressed nitrogen and a backpressure regulator.

Data was obtained for the dichlorosilane + trichlorosilane binary system for the pressure range of 0.7 - 2 MPa. This pressure range comes into question as the concerns over the solubility of the nitrogen in the binary system, forming a ternary system, were expressed by early researchers such as Scheeline and Gilliland (1936) and Othmer (1946), who opted for alternative pressure control strategies or diminished pressure ranges, respectively.

Equipment of Wisniewska et al. (1993)

The equipment of Wisniewska *et al.* was based on the design of the Rogalski-Malanowski glass ebulliometers (Rogalski and Malanowski, 1980) that were modified for VLE measurement. The equipment was developed to withstand pressures up to 3 MPa but was checked up to a pressure of 5 MPa. Its development, as was the case for Olson (1989) was also inspired by a dire need for VLE data in the range of 0.1 - 3 MPa by a fast and reliable VLE measurement method.

The entire medium pressure ebulliometer apparatus, shown in Figure 2.34, was constructed from stainless steel, with the exception of the drop counter, which was constructed of thick-walled glass tubing to allow for visual observation of the circulation. As for the design upon which it was based *i.e.* the Rogalski-Malanowski still (1980), the boiler and the Cottrell tube were considered as a single entity (**A**). Special attention had to be paid to the design of the drop counter, the sampling valves and the feed valve in superatmospheric determinations.

The needle valves were constructed to minimize dead volumes where the body of the valve was filled with the condensate or liquid mixture at all times during the operation. As in the design of Rogalski and Malanowski (1980), a suitable mixing section in the return line to the reboiler was incorporated; however, there was still no mechanical agitation in the reboiler or the sample traps. Also, the sideways entry of the Cottrell tube in the equilibrium chamber, the design of the equilibrium chamber itself and the transport of the vapour to the condenser at the disengagement interface were unchanged.

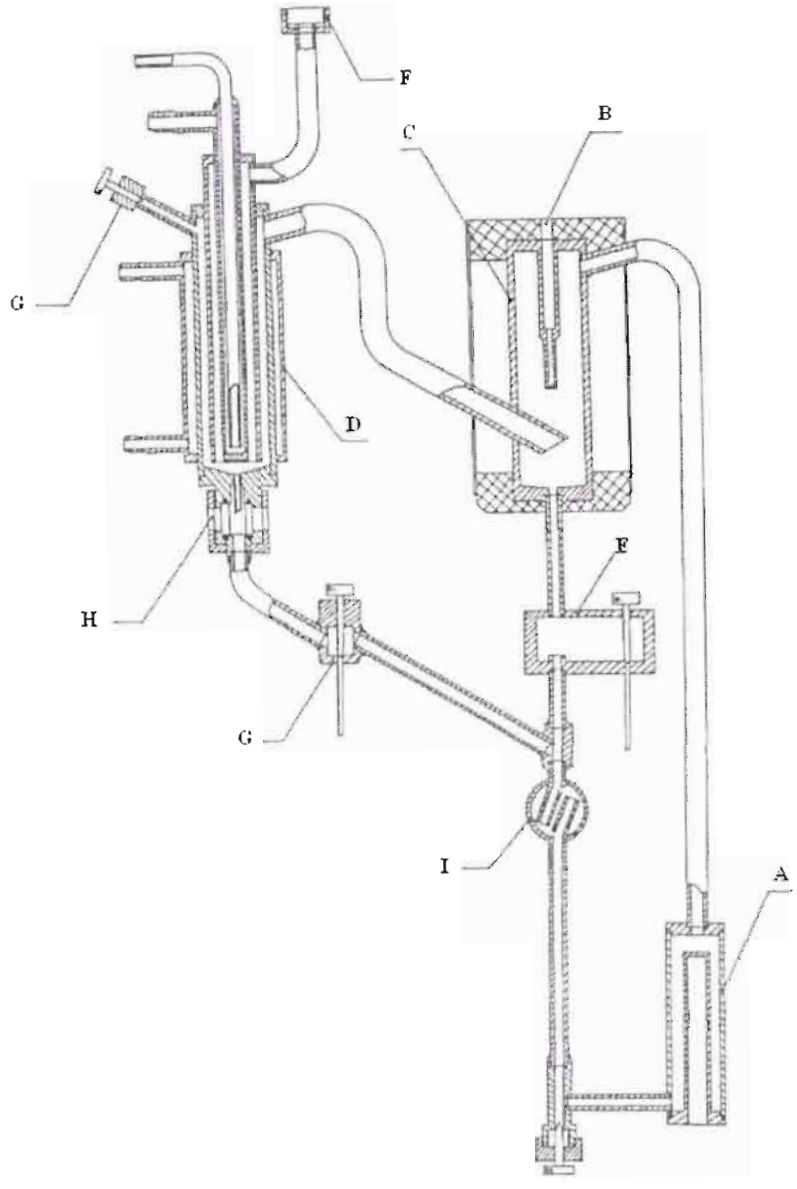

Figure 2.34. Apparatus of Wisniewska *et al.* (1993): **A**, boiling chamber; **B**, thermowell; **C**, equilibrium chamber; **D**, condenser; **E**, liquid sample trap; **F**, pressure connection; **G**, sample filling point; **H**, drop counter; **I**, mixing section.

The pressure stabilization system (shown in Figure 2.35) consisted of a nitrogen cylinder (**A**), a buffer tank (**J**) and regulating valves (**B**). The use of nitrogen as the pressurizing gas placed a restriction upon the operating range of the equipment to those pressures where the solubility of nitrogen in the system was negligible. The design of the pressure stabilization system was also not optimal as the nitrogen cylinder should be directly linked to the buffer tank and the pressure distributor (**C**) be taken off the buffer tank.

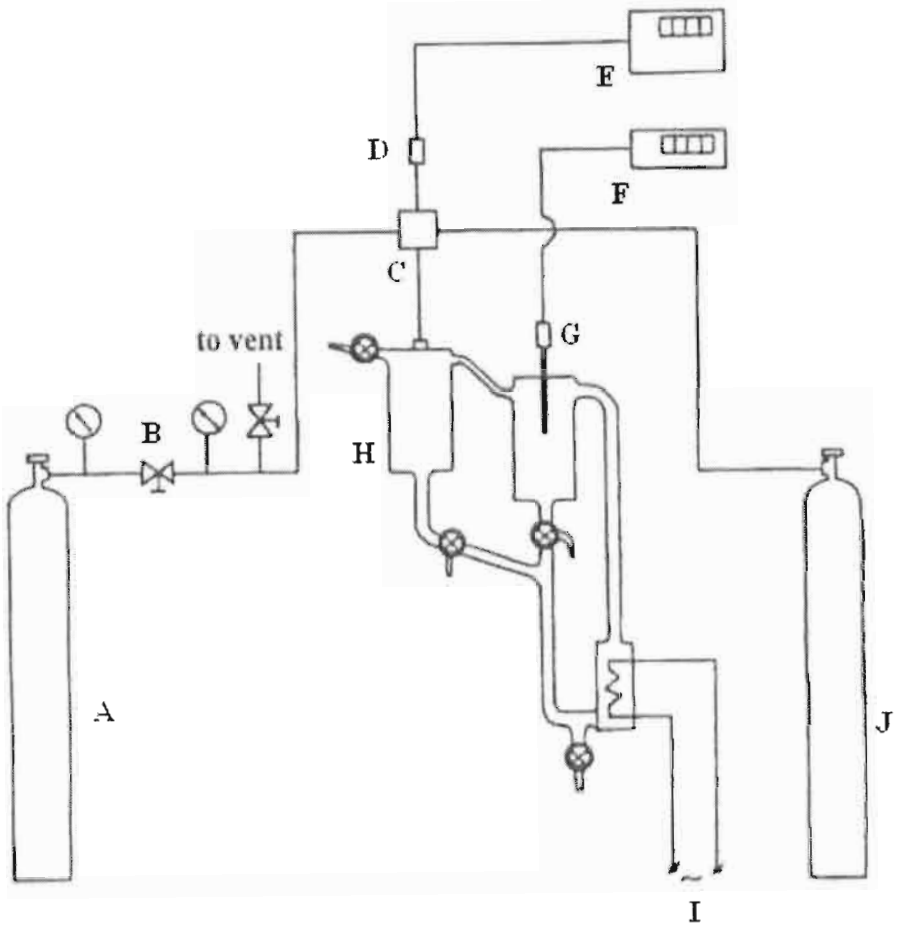

Figure 2.35. Pressure stabilization system of the equipment of Wisniewska *et al.* (1993): A, compressed nitrogen; **B**, pressure reduction valves; **C**, pressure distributor; **D**, pressure transducer; **E,F**, digital display; **G**, temperature sensor; **H**, ebulliometer; **I**, stabilizing power system; **J**, pressure buffer tank.

The authors reported equilibrium times of around 1 hour for the benzene + heptane and the benzene + cycloheptane binary systems studied. Samples of the liquid and vapour condensate were withdrawn using glass-sampling vessels, connected to the valve via a septum.
The sampling vessels and the external part of the valve were evacuated first and cooled with liquid nitrogen.

Equipment of Harris (2004)

The development of the VLE measurement equipment of Harris (2004) in the laboratories of the Thermodynamic Research Unit at the University of KwaZulu-Natal, was motivated by the need for the measurement of high-temperature VLE in the low to moderate-pressure regions chiefly for industrial applications. It was based on the operational principles of the design of Raal (Raal and Muhlbauer, 1998).

The still was constructed from machined 316 stainless steel and was designed to operate between the temperatures of 300 - 700 K and pressures between 0.1kPa - 30 MPa. The details of this equipment and its design flaws will be discussed in greater detail in Chapter 4, as it serves as the basis for the construction of a new moderate-pressure VLE apparatus by the author.

The trends that have been observed with regards to the extrapolation of LPVLE methods to elevated pressure ranges quite clearly indicate the difficulties that arise when such a task is propositioned. The need for transparency in high-pressure stills necessitates the incorporation of sight glasses or windows that not only diminish the structural integrity but introduce sealing problems (Griswold *et al.*, 1943). Also the requirement of a pressurizing medium such as fixed gas results in concerns over the solubility of the gas at higher pressures due to concerns over the solubility of the gas in the system. This necessitates often complicated and expensive alternative control strategies. It is indeed quite interesting to note that the use of the vapour condensate recirculation method has proven to be the most popular for extrapolation to higher pressures; probably due to only one phase *i.e.* the less dense vapour phase, being circulated.

2.7.2 Designs for elevated temperatures

Experimental measurement of accurate pure component vapour pressures and binary VLE data at high temperatures has typically been the domain of high molecular weight hydrocarbons, most notably, n-alkanes (Chirico *et al.* 1989) and polycyclic aromatic hydrocarbons (Gupta *et al.*, 1991) Due to the inherent propensity of these compounds to undergo thermally-induced oligomerization or polymerization and decomposition reactions, the above task has often been met with failure. The high-pressure continuous flow dynamic (Joyce *et al.*, 1999) and static methods (Morgan and Kobayashi, 1994) featured quite prominently amongst researchers investigating systems at high temperatures. There have been very few designs based on LPVLE methods that have been employed in high-temperature studies.

Equipment of Haynes and Van Winkle (1954)

One of the early forays into the study of vapour-liquid equilibria of higher molecular weight aromatic + alkane mixtures was that of Haynes and Van Winkle, who employed the use of a Jones-Colburn-type still. Of particular interest to the research group was the overall study of VLE behaviour of systems containing high-boiling hydrocarbons at subatmospheric pressures.

As discussed in the previous chapter, this type of apparatus is quite challenging to effectively control to allow for the acquisition of reliable VLE results. The authors designed the still with distinct thermally-controlled zones to ensure that in the operation of the still, the revapourized vapour condensate circulation was optimal. The research output from the group with regards to the vapour liquid equilibria of high-boiling hydrocarbons (alkanes, alkenes and polynuclear aromatics) was quite significant (Hirata *et al.*, 1975) and contributed greatly to the body of knowledge of the VLE characteristics of these types of systems.

Equipment of Myers and Fenske (1955)

Myers and Fenske (1955) identified the importance of addressing the issue of the lack of vapour pressure data for high-boiling hydrocarbons to allow for optimal processing of the high-boiling distillation column bottoms. To this end, an apparatus based on the Othmer-type still was then constructed to allow for the acquisition of vapour pressures and vapour-liquid equilibrium data in the range of 0.1 mmHg to atmospheric pressure.

The apparatus of Myers and Fenske and its important features are shown in Figure 2.36. The principal construction material for the apparatus was chosen to be stainless steel (even though operation would be in the low-pressure region) to ease concerns over safe operation since high temperatures would be attained in the studies. A few considerations that influenced the design of the equipment related to the design of the reboiler and also ensuring even heating and proper mixing of the boiling liquid. With regards to the former, a reboiler with a large cross-sectional area was favoured to minimize the effect of the hydrostatic head of liquid in the reboiler in terms of its contribution to any superheating and "bumping" of the liquid mixture at low pressures. For the latter, a novel "combination heater and stirrer "was employed to allow for immersion heating and mechanical agitation in a single unit. Another consideration was that of the ease of disassembling of the apparatus with regards to cleaning (residues) and maintenance (change of gaskets). Consequently, the top of the reboiler was flanged, with a Teflon® gasket and brass compression fitting being used to provide the seal. A tempered glass window, shown in the upper half of Figure 2.36, allowed for visual observation of the contents of the interior of the still.

A variable-volume condensate cup was another notable feature of the equipment. The volume of the cup was varied through the use of an aluminium plug in the cup, with a Teflon® spring-loaded valve (manually operated with a rod) that can me raised or lowered to control the return flow rate of the condensate.

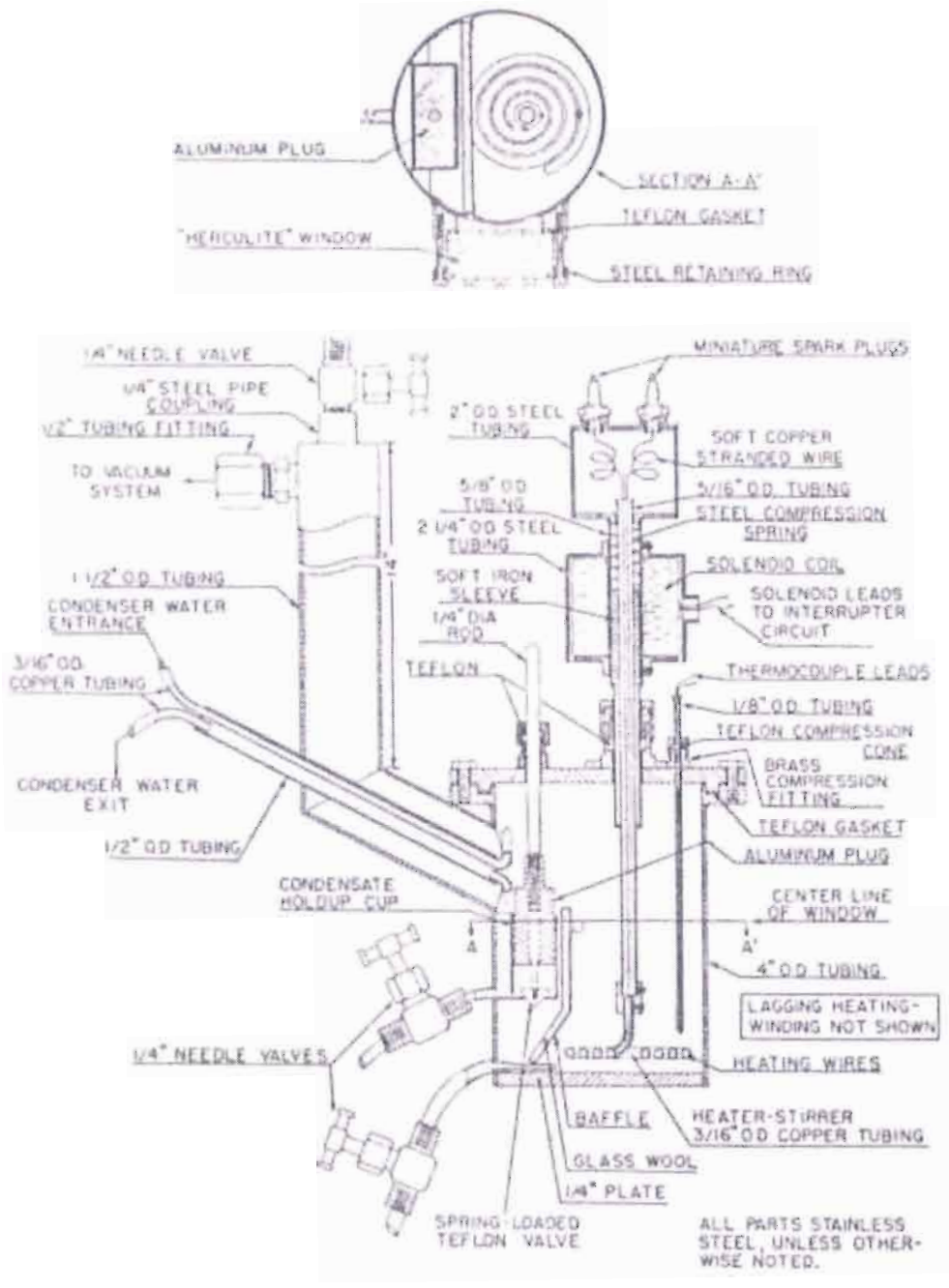

Figure 2.36. Apparatus of Myers and Fenske (1955).

The equipment essentially shares the same flaws as in the original design of Othmer (1928), however, the incorporation of a combination heater-stirrer unit and the variable-volume distillate cup were novel features. If the apparatus were to be used for measuring binary or multicomponent VLE, and not just pure component vapour pressures, it would be shown to be seriously flawed. Equilibrium times of 4 to 5 minutes were reported by the authors, who used the experimental data obtained to construct vapour pressure charts for 26 different hydrocarbons including hexadecane, octadecane and eicosane.

Equipment of Coon et al. (1989)

A comparative study was undertaken by Coon *et al.* with regards to activity coefficients obtained from solid-liquid equilibrium (SLE) and vapour-liquid equilibrium experiments. The compounds investigated were polynuclear aromatic hydrocarbons, which were combined with tetralin and decalin (solvents), to form combinations of binary mixtures. Isothermal results had also been obtained at temperatures of 160 °C and 180 °C for polynuclear aromatic hydrocarbon systems that included biphenyl, naphthalene, anthracene, carbazole and dibenzofuran.

The experimental apparatus for the determination of VLE was a commercially developed Stage-Mueller VLE still, constructed by Fischer Labor-und-verfahrenstechnik. The still featured a silvered vacuum jacket to prevent heat losses. The cooling system of the VLE still was that of a "closed" one where excellent control over the temperature of the cooling fluid in the still was made possible so as to prevent any loss of volatile material through the condenser to the vacuum system and also any solidification of the high-boiling component in the condenser. An analysis of the results and the conclusions reached by the authors interestingly enough revealed that the vapour liquid equilibrium studies are "not the best method for obtaining activity coefficient data" for systems containing polynuclear aromatic compounds and related structures.

The experimental difficulties that were experienced by the researchers were cited as follows:

(a) The *solidification of the less volatile* component in the condensers if the temperature was too low.

(b) The *loss of the more volatile* component to the vacuum system if the condenser temperature was too high.

(c) Due to *the considerable relative volatility* of the systems studied, "temperature swings" in the equilibrium cell were experienced as a result of changes in the charge mixture composition returning to the heater.

(d) The *dilution of the samples* was deemed as necessary to prevent solidification during the gas chromatographic analysis. This compromised the accuracy of the quantitative analysis of the liquid and vapour mole fractions as the detection limits of the detector are approached in the above.

In terms of the difficulties experienced , points **(a)** and **(b)** are valid in that when a system which exhibits high relative volatility *i.e.* when the boiling points of the two substances differ substantially or when one component is in great excess (for studies at or near the infinitely dilute region), control of the condenser fluid temperature is extremely difficult to satisfy both requirements in **(a)** and **(b)**. The temperature swings experienced by the authors probably relate to flaws in the equipment design *i.e.* absence of stirring in the boiler chamber and an absence of heating in the return line. The results obtained by the authors with the VLE method was quite scattered and statistical treatment of the data revealed that the predictions of VLE using SLE derived parameters from UNIQUAC with the SLE experimental data was more useful than the reverse procedure.

The brief description of equipment designs and considerations in the measurement of high-temperature VLE dealt with above provides sufficient indication of the great challenges that researchers are faced in such a task. Since the high molecular weight hydrocarbons studied were frequently solids at room temperature, this necessitated special procedures for the initial charging of the mixtures and preventing any solidification in any part of the apparatus during a run. Of course with the greatest concern/s in the study being thermally-induced polymerizations and/or decompositions, an unenviable burden of monitoring the integrity of the components as a function of time (Joyce *et al.*, 1999) is necessitated for high-temperature investigations.

2.8 Conclusion

In this review chapter, a fairly comprehensive review of the various types of VLE measurement equipment has been presented to illustrate the complex nature of this field. The early designs of the VLE measurement equipment have been elaborated upon so as to provide meaningful insight into the ingenuity of researchers who have either borrowed existing ideas or employed the use of sheer innovation to improve upon designs of that era, which assisted in ushering the current designs used in laboratories worldwide. A clear distinction between high-pressure and low-pressure VLE equipment was initially emphasized to later facilitate an understanding of the extrapolation of the use of the latter for application in moderate to high-pressure studies, as this is especially pertinent to the work of the author. The systematic accumulation of the theoretical considerations and practical design criteria from this review, especially in the design of LPVLE equipment, has inherently contributed to the success of the design of the equipment presented in this work.

CHAPTER 3

THEORETICAL TREATMENT OF VAPOUR PRESSURE AND VAPOUR-LIQUID EQUILIBRIUM DATA

3.1 Introduction

The practical aspects involved in the measurement of the vapour pressures and vapour-liquid equilibrium data *i.e.* the multitude of equipment designs and experimental considerations, have been dealt with extensively in Chapter 2. It is the purpose of this chapter then to illustrate the step that follows the acquisition of the raw experimental data in the form of the application of theoretical methods (thermodynamic or mathematical models) for the treatment of the data. Traditionally, this has taken the form of model parameter fitting or correlation, thermodynamic consistency testing and development of predictive methods. The first of these two approaches will be treated in great detail in this review chapter as a comprehensive study of predictive methods is not relevant to the objectives of this study.

As mentioned earlier, the sheer magnitude of novel chemical systems requiring thermophysical property characterization for process development is a daunting task for any self-respecting experimental thermodynamicist. In accordance with the above, there have been two approaches to facilitate the task of the process engineer requiring accurate knowledge of the thermodynamic behaviour of the system in the form of correlation (based on a limited data set) and prediction (no experimental phase equilibrium data).
Correlation operates on the basis that some experimental data is required; however, it eases the burden of requiring experimental data at the actual operating conditions of the system. The latter involves the construction of a thermodynamic model with a flexible framework (empirical or semi-theoretical) which incorporates adjustable parameters that are to be determined from the experimental data set by suitable regression techniques. Once these models have been properly parameterised, interpolation and extrapolation can be performed.

The development of predictive methods based on classical thermodynamic models is along the lines of the fulfilment of an ideal scenario; the representation of the thermodynamic behaviour of a system with a suitable model requiring no experimental data. Without any recourse to experimentation, the VLE data for the system can be obtained from the pure component properties of the mixture components. Models that have been based on the group contribution

concept such as ASOG (Wilson and Deal, 1962) and especially, UNIFAC (Fredenslund *et al.*, 1977) and modified UNIFAC (Weidlich and Gmehling, 1987; Larsen *et al.*, 1987) have demonstrated excellent reliability and a wide range of applicability (Gmehling, 1999) in recent times. These methods are of great applicability when the component molecules can be readily fragmented into constitutional functional groups for which parameter values are available. Such methods are subject to continual revision and extension and constitute an active and important area of research in contemporary phase equilibrium thermodynamics.

Accurate phase equilibrium data are of unparalleled importance for the design of the separation step in industrial processes; the use of inaccurate data can severely compromise the operational efficiency and economic feasibility of the entire process. In the event of the availability of a full P-T-x-y data set, an effective and rigourous assessment of the accuracy of the experimental VLE data in the form of thermodynamic consistency testing is a worthwhile exercise. Several methods have been proposed for the verification of the consistency of VLE data sets in addition to the satisfaction of the basic thermodynamic constraints of the Gibbs-Duhem equation as a fundamental criterion for ensuring the thermodynamic consistency of a data set. An effective approach in the application of thermodynamic consistency testing has often been achieved through the systematic combination of different and complementary consistency tests in the overall evaluation of a data set (Moon *et al.*, 1991).

The content of this chapter is heavily biased towards the theoretical treatment of VLE data as opposed to pure component vapour pressures as the former is inherently theoretically more complex than the latter. Greater emphasis will also be placed upon the use of correlative as opposed to predictive methods in VLE data treatment as this approach is of greater relevance to the author's field of study. For a review of the fundamental thermodynamic relations presented in this review, the texts of Sandler (1999), Smith *et al.* (2001) or Elliot and Lira (1999) can be consulted.

3.2 Correlation of Vapour Pressure data

3.2.1 Overview

The accurate representation of the pure component properties (vapour pressures, phase molar volumes) is an integral part of the process of modelling the phase equilibria of binary and multi-component mixtures. Consequently, it is imperative that equations relating the thermophysical properties of pure components as a function of temperatures be accurate over the region of

interest. There are two popular methods for the correlation of vapour pressure as a function of temperature. The first of these, discussed below, consists of methods that are either purely empirical or based on the integration of the Clausius-Clapeyron equation and the second is based on the equation of state method, which will be dealt with at a later stage for the treatment of vapour-liquid equilibria. The latter can be employed to correlate the saturation pressure of pure compounds over a wide temperature range (from the triple point to the critical point). A third, but largely overlooked approach for the correlation of vapour pressures, is based on the derivation of equations through the use of statistical mechanics; an example of which is the Abrams-Massaldi-Prausnitz equation (1974).

3.2.2 Vapour Pressure correlations

The first family of equations for the correlation of vapour pressures, apart from the empirical relations, is based on an expression relating the equilibrium condition between the vapour and liquid phases of a pure component, known as the Clausius-Clapeyron equation:

$$\frac{d \ln P_{vap}}{d(1/T)} = -\frac{\Delta H_v}{R\Delta Z_v} \tag{3.1}$$

where P_{vap} is the compound saturated vapour pressure, T is the temperature, R is the universal gas constant and ΔH_v and ΔZ_v are the differences in the enthalpies and compressibility factors of the saturated vapour and liquid phases, respectively. A large number of vapour pressure correlation equations are based on an integration of Equation (3.1). The simplest exact solution to Equation (3.1) requires the assumption that the $\frac{\Delta H_v}{R\Delta Z_v}$ term is a constant and not dependent on temperature. Both ΔH_v and ΔZ_v decrease with increasing temperature and have weak temperature dependencies except near the critical point.

With a constant of integration *i.e.* A , Equation (3.1) becomes the following:

$$\ln P_{vap} = A - \frac{B}{T} \tag{3.2}$$

where $B = \frac{\Delta H_v}{R\Delta Z_v}$. This form of the equation is sometimes known as the Clapeyron equation and is suitable for the representation of saturation pressures over small temperature intervals not exceeding 20 K (Malanowski and Anderko, 1992), even when ΔH_v is temperature-dependent.

Over large temperature ranges, the equation represents vapour pressures quite poorly (Reid *et al.*, 1987).

Antoine (1888a, 1888b) proposed a simple empirical modification of the Clapeyron equation in the form of a three-parameter equation, shown below in Equation (3.3).

$$\ln P_{vap} = A - \frac{B}{T+C} \tag{3.3}$$

where A, B and C are constants and for $C = 0$, Equation (3.3) reverts to the Clapeyron equation. The Antoine equation is perhaps the most popular vapour pressure correlating equation for low-pressure VLE studies and Antoine constants have been tabulated for more than 8000 organic compounds (Malanowski and Anderko, 1992). The Antoine equation can be used to accurately correlate vapour pressures for non-associating organic compounds over the pressure range of 1-200 kPa. When used for the representation of associating compound vapour pressures, the range of applicability *i.e.* pressure is reduced (for alkanols it is limited to 5 - 80 kPa).

The adjustable parameters or constants of the Antoine equation are empirical and the only reliable means of determining them is through the regression of experimental data (Reid *et al.*, 1987) as advocated by Malanowski and Anderko (1992), who are guarded against the use of Antoine constants that are obtained by mathematical treatments. Each set of parameter values should be associated with temperature or pressure limits and the constants should ideally never be used outside these limits. Extrapolation outside the stated limits can sometimes produce erroneous results as a result of the Antoine equation often being incapable of reproducing the correct shape of the vapour pressure curve over the entire temperature range.

Other popular three-parameter empirical equations include those of Miller (4.4) and Cox (4.5). The modified Miller equation was found by some researchers to provide a more accurate fit to experimental data than the Antoine equation (Reid *et al.*, 1987).

$$\ln P_{vapr} = -\frac{A}{T_r}\left[1 - T_r^2 + B\left(3 + T_r\right)\left(1 - T_r\right)^3\right] \tag{3.4}$$

where $T_r = \frac{T}{T_c}$ and $P_{vapr} = \frac{P_{vap}}{P_c}$ and P_c and T_c are the critical pressures and temperatures, respectively. The adjustable parameters in the Miller equation, shown above, are A, B and P_c.

The parameter P_c is an empirical parameter that exhibits large deviations from the real critical pressure and hence cannot be used for its prediction.

The Cox equation was found by Osborn and Scott (1978, 1979) to be capable of "adequately" representing vapour pressures from the triple point pressure to 0.3 MPa and for extrapolations with "reasonable precision" over a 50 K range. This was in comparison with the Antoine equation that could not successfully be used by the authors for extrapolation outside the experimental range. The Cox equation was used in the following form by Chirico *et al.* (1989):

$$\ln\left[\frac{P_{vap}}{P_{ref}}\right] = \left[1 - \left(\frac{T_{ref}}{T}\right)\right] \exp\left(A + BT + CT^2\right) \tag{3.5}$$

where P_{ref} and T_{ref} refer to a reference pressure and a reference temperature, respectively. For a reference substance, P_{ref} and T_{ref} represent an accurately known point on the vapour pressure curve of the substance *e.g.* the normal boiling point of the substance. The adjustable parameters, as for the Antoine equation, are A, B and C .

The three-parameter equations, discussed above, are generally not suitable for the representation of vapour pressures over a wide range of temperatures from the triple point to the critical point. In an attempt to improve upon the use of empirical equations to represent vapour pressures, the number of adjustable parameters or constants in the equations was increased.

One of the most popular of these equations was the Frost-Kalkwarf equation (Malanowski and Anderko, 1992) or the Harlecher-Braun equation (Sandler, 1999). This relation, shown as Equation (3.6), has 4 adjustable parameters in the form of A, B, C and D.

$$\ln P_{vap} = A + \frac{B}{T} + C \ln T + D \frac{P_{vap}}{T^2} \tag{3.6}$$

The Frost-Kalkwarf equation was derived on the basis that the enthalpy of vapourization, ΔH_v, is a linear function of temperature and that the change in volume term between the vapour and liquid phases, ΔV_v, can be estimated from the van der Waals equation of state. Due to the form of the equation, the vapour pressure must be solved for iteratively.

A modification of the Frost-Kalkwarf correlation was the form used by the DIPPR Compilation Project (Daubert and Jones, 1990) as follows:

$$\ln P_{vap} = A + \frac{B}{T} + C \ln T + DT^{E} \tag{3.7}$$

where A, B, C and D. are adjustable parameters and E is assigned a value of either 2 or 6, depending on which value gives a better fit of the experimental data. Equation (3.7) with $E = 6$ is also known as the Riedel equation (Sandler, 1999). The fitting procedure for the equation involves either a constrained (at the critical point) or unconstrained (with a fit only over the experimental data range) fit. The constrained fit is necessitated due to requirement that the thermodynamically correct "slight S-shape" should be obtained for the vapour pressure curve between the critical and normal boiling points. This is achieved with positive values for A and D together with negative values for B and C. In an unconstrained fit, there is no assurance that the sign rule will hold, even with accurate experimental data. The above equation was used extensively by the DIPPR Compilation Project for the correlation of the vapour pressures of many industrially relevant chemical substances (Daubert and Jones, 1990).

It has also been found to be advantageous to generalize the vapour pressure relations through the law of corresponding states *i.e.* through the use of reduced variables. An excellent example of this is one of the most highly recommended vapour pressure correlation equations in the form of the Wagner equation shown below:

$$\ln P_{vapr} = \frac{Ax + Bx^{1.5} + Cx^{3} + Dx^{6}}{T_r} \tag{3.8}$$

From Equation (3.8), A, B, C and D are the adjustable parameters and the independent variable *i.e.* $x = (1 - T_r)$ is a measure of the distance from the critical point. The above form is known as the "3 - 6" form of the Wagner equation since the base x associated with the coefficients C and D, is raised to the exponential powers of 3 and 6, respectively. An alternative form *i.e.* the "2.5 - 5" Wagner equation was employed by researchers such as Morgan and Kobayashi (1994) in fitting vapour pressure data. The Wagner equation is considered as being highly efficient (Malanowski and Anderko, 1992) and as being the only empirical equation capable of accurately representing experimental data with a few constants from $T_r = 0$ to the critical point. However, one should be guarded against possible inconsistent thermodynamic behaviour with

regards to the shape of the vapour pressure curve, whilst giving an accurate fit to the experimental data.

Unlike the Antoine equation, the Wagner equation may be used to safely extrapolate outside the experimental data range due to the manner in which the constants have been determined. However, the Wagner equation may not extrapolate well below reduced temperatures of 0.5.

Some researchers (Vetere, 1991) noted that the D parameter is important for obtaining excellent correlations with highly accurate experimental data. However, for data that is not reliable, the D - term can in most cases be ignored, without greatly affecting the fitting of the data.

The equations presented above *i.e.* Equations (3.2) - (3.8) have in common that their adjustable parameters are all purely empirical, as the latter have no theoretical significance in terms of molecular parameters or interactions. One attempt to address this lack of physical significance of the parameters was by Abrams *et al.* (1974). They employed the use of the kinetic theory of polyatomic fluids developed by Moelwyn-Hughes (1961) to formulate a vapour pressure equation (AMP) with the same algebraic form as the empirical equation suggested by Miller (1964). The derivation of the AMP equation will not be presented here as it is beyond the scope of the author's work and the pertinent equations will merely be presented below as follows:

$$\ln P = A + \frac{B}{T} + C \ln T + DT + ET^2 \tag{3.9}$$

where

$$A = \ln\left[\frac{R}{V_W}\right] + \left[s - \frac{1}{2}\right] \ln\left[\frac{E_0}{R}\right] - \ln[(s-1)!] + \ln\alpha \tag{3.10}$$

$$B = -\frac{E_0}{R} \tag{3.11}$$

$$C = \frac{3}{2} - s \tag{3.12}$$

$$D = \frac{s-1}{\left[\frac{E_0}{R}\right]} \tag{3.13}$$

$$E = \frac{(s-3)(s-1)}{2\left(\frac{E_0}{R}\right)^2} \tag{3.14}$$

The two adjustable parameters of the AMP equation as shown in Equations (3.10) - (3.14) are s and E_0. The hard-core van der Waals volume (V_W) is obtained from the group-contribution correlation of Bondi (1968) and α is a proportionality constant (independent of the nature of the liquid), and determined empirically to be equal to 0.0966. R is the universal gas constant (82.06 $cm^3.atm.mol^{-1}.K^{-1}$) such that $\left(\frac{E_0}{R}\right)$ is given in K, P is in atm and T in K. Therefore, as opposed to the original form of the Miller equation (1964) with five adjustable parameters in the form of A, B, C, D and E, the AMP equation has only two adjustable parameters *i.e.* s and E_0. The parameter s is a function of the size, shape and flexibility of the molecule and was shown to increase with chain length and to decrease as the shape of the molecule became more globular or branched. The parameter E_0 is an indication of the strength of the intermolecular forces; hence it was observed that E_0 for a normal alcohol was larger than that for a normal alkane of the same chain length. When the E_0 parameter was differentiated with respect to temperature, it was shown that the parameter corresponded with the enthalpy of vapourization of the hypothetical or model fluid at T = 0.

A comparative study conducted by the authors with experimental values and those obtained from the Antoine correlation showed that excellent representation of the vapour pressures of pure liquids from 10 - 1500 mmHg could be achieved with the AMP equation. The authors also concluded that since molecular size and flexibility are taken into consideration in the kinetic theory, the equation should perform well for liquids with large molecules.

3.2.3 Modelling experimental Vapour Pressure data

There are essentially two correlation strategies for the fitting of the experimental vapour pressure data to vapour pressure equations *i.e.* a constrained and an unconstrained fitting approach. Malanowski and Anderko (1992) advocate that the constrained correlation approach should in theory produce results that are more accurate than those obtained by an unconstrained approach, since for the former relation the known or reliably predictable physical behaviour of the system is incorporated into the fitting procedure as a constraint. This would be particularly effective where the experimental data set is characterised by a great deal of uncertainty *e.g.* when the investigated compound is prone to undergoing degradation at higher temperatures. It

is imperative that the correlations obtained are both accurate (small residuals) and thermodynamically consistent in terms of the observed behaviour of the saturation curve *i.e.* the slight S- shape of the curve between the triple and critical points. As mentioned above, the "constrained fit" approach was utilized by the DIPPR Compilation Project (Daubert and Jones, 1990) to ensure that the slight S-shape of the saturation was obtained for the DIPPR modified Frost- Kalkwarf correlating equation shown in Equation (3.7). The use of an unconstrained fit by the author was justified in this work as the conditions for the compounds investigated were always far from the critical point; hence no consideration of the proper shape of the saturation curve near critical conditions was necessitated.

With regards to the use of the correlating equations, the comparative studies illustrated in the works of Malanowski and Anderko (1992) and Reid *et al.* (1987) have shown that the Antoine equation is suitable for pressure measurements in the 5 - 200 kPa range for non-associating or weakly associating chemicals (for strongly polar compounds this range is reduced). The Wagner equation was considered as much more suitable for higher and wider pressure ranges *i.e.* for conditions nearing the critical (as $T_r \rightarrow 1$).

The Antoine, Cox, Wagner, Frost-Kalkwarf and modified Frost-Kalkwarf vapour pressure correlations were chosen for the modelling of the experimental vapour pressures obtained in this work. Since the vapour pressures in this study were measured at low pressures, far away from the critical region, the use of the equation of state method for vapour pressure correlation was not justified. Also the use of the equation of state method, as discussed in Section (3.5.3.2), does not allow for an explicit solution of pressure *i.e.* it involves iterative calculations. The mathematical computational software, MATLAB® (version 7.0.1), was used to perform the fitting of the experimental data to a variety of correlation equations using the Nelder-Mead Simplex algorithm. A discussion of the functions and the features of the Optimization Toolbox are available from the online Mathworks® resources.

The objective function used was simply the difference between the experimentally measured vapour pressure $\left(P^{exp}\right)$ and that predicted $\left(P^{calc}\right)$ from the various vapour correlations presented above, as shown below:

$$OF = \sum_{i=1}^{n} \left(P^{exp} - P^{calc}\right)_i^2 \qquad (3.15)$$

Since it was a direct fit, no iterational loops were involved.

3.3 Thermodynamic Consistency Testing of Vapour Pressure data

(a) The *computation of the enthalpy of vapourization* (ΔH_v) from the fit of the vapour pressure data using the gradient of $\left[\frac{d \ln P_{vap}}{d(1/T)}\right]$ allows for the thermodynamic consistency of the vapour pressure data to be assessed. Malanowski and Anderko (1992) suggested that the difference between the computed and measured values (by calorimetry) should be within 0.1 - 0.4 % of the measured value.

The following simple treatment (Reid *et al.*, 1987) allows for the estimation of ΔH_v from the vapour pressure correlations dealt with in Section (3.2.2), where a dimensionless constant ψ is defined (using reduced variables) and derived as follows:

$$\psi \equiv \frac{\Delta H_v}{RT_c \Delta Z_v} = \frac{-d \ln P_{vapr}}{d(1/T_r)} \tag{3.16}$$

Consequently by differentiating the various vapour pressure equations, expressions for ψ can be obtained. For the Antoine and the Wagner equations, respectively, the following two forms are obtained:

$$\psi = \frac{B}{T_c}\left[\frac{T_r}{T_r + C/T_c}\right] \tag{3.17}$$

$$\psi = -a + bx^{0.5}(0.5x - 1.5) + cx^2(2x - 3) + dx^5(5x - 6) \tag{3.18}$$

To use the above two relations, the relevant constants must first be obtained (from data fitting or literature values) from the vapour pressure equations *i.e.* Equations (3.2) and (3.8) to evaluate the term on the right-hand side of Equation (3.16). The ΔH_v is then obtained from the term on the left-hand side of Equation (3.8) through the use of values for ΔZ_v. This thermodynamic consistency testing *i.e.*comparison of computed and experimental ΔH_v values, was employed in the vapour pressure measurement work of Chirico *et al.* (1989).

(b) In the study of *compounds that are thermally sensitive*, the data has to be rigorously tested to ensure that the effects of thermal decomposition or polymerization do not adversely affect the quality of the data set. The DIPPR Compilation Project (Daubert and Jones, 1990) performed

the qualitative testing of the data set for such effects with a plot of $\ln P$ versus $(1/T)$ for the data set with Equation (3.7). The graphical analysis of such a plot shows whether the chemical substance is decomposing or polymerizing at elevated temperatures. If the slope of the graphical plot increases in an exponential fashion with increasing temperature, thermal decomposition is indicated (see Figure 3.1). Conversely, if the slope decreases in an exponential fashion, then polymerization is indicated.

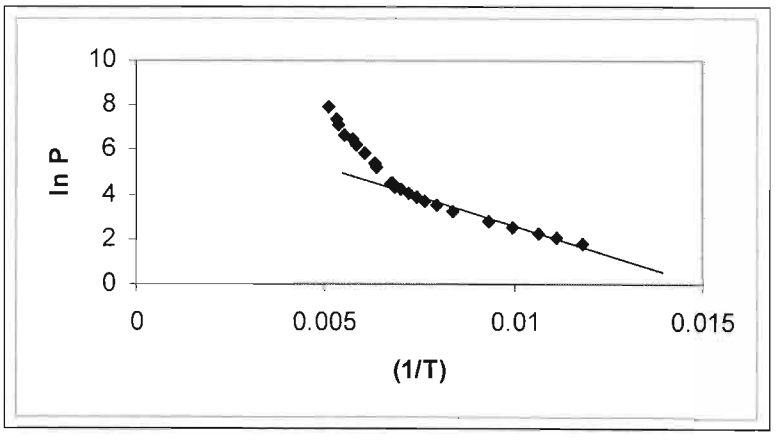

Figure 3.1. Plot of ln P versus (1/T) displaying the onset of thermal decomposition at elevated temperatures.

(c) With regards to *constrained data fitting* (Malanowski and Anderko, 1992), the constrained fit is assessed through the observation that an appropriate plot of versus $\frac{\Delta H_v}{\Delta Z_v}$ versus T_r, or via differentiation, a minimum must be observed in the 0.8 - 0.9 reduced temperature range.

An additional test (Daubert and Jones, 1990) is that for a line drawn on a $\ln P$ versus $(1/T)$ plot between the melting point and the critical point, a positive deviation for all the data points from the line should be observed. This test is known as the "line rule" plot. In this study, the graphical test in **(b)** was employed to test the vapour pressure data.

3.4 Prediction of Pure Component Vapour Pressures

3.4.1 Overview

The vapour pressure correlations presented above serve to allow for the estimation of vapour pressures through the application of the experimentally-derived correlation parameters in an

appropriate pressure and temperature range or by generalizing the constants through the use of suitable reference points on the vapour pressure curve (normal boiling point and critical point). However, the true essence or value of a predictive method lies in the fact that ideally only pure component properties of the chemicals of interest are required to predict physico-chemical properties. These types of methods, which includes group-contribution methods, are of great applicability when experimental difficulties or uncertainties supersede the acquisition of reliable experimental data, which subsequently also excludes the possibility of the use of correlating equations for interpolation or extrapolation purposes. Although equation of state methods are also used for predictive purposes, discussion of this approach will be deferred to a later more generalized discussion of the equation of state method.

3.4.2 Vapour Pressure predictive models

Two notable and popular truly predictive vapour pressure expressions are those of Riedel and Gomez-Thodos (Reid *et al.*, 1987). The latter can be represented as follows:

$$\ln P_r = \beta\left[\frac{1}{T_r^m} - 1\right] + \gamma\left[T_r^7 - 1\right] \tag{3.19}$$

where the constants in Equation (3.19) *i.e.* β, γ and m are related to one another through an expression for the normal boiling point (T_b) as follows:

$$\gamma = ah + b\beta \tag{3.20}$$

where

$$a = \frac{1 - T_{br}^{-1}}{T_{br}^7 - 1} \tag{3.21}$$

$$b = \frac{1 - T_{br}^m}{T_{br}^7 - 1} \tag{3.22}$$

$$h = T_{br}\left[\frac{\ln\left(\frac{P_c}{1.01325}\right)}{1 - T_{br}}\right] \tag{3.23}$$

The use of the Gomez-Thodos method involves division of compounds into the following classes: non-polar, polar non-associating, polar associating or hydrogen-bonded compounds.

For non-polar compounds:

$$\beta = -4.26700 - \frac{221.79}{h^{2.5}\exp\left(0.0384h^{2.5}\right)} + \frac{3.8126}{\exp\left(\frac{2272.44}{h^3}\right)} + \Delta^* \tag{3.24}$$

$$m = 0.78425\exp(0.089315h) - \frac{8.5217}{\exp(0.74826h)} \tag{3.25}$$

where $\Delta^* = 0$, except for He($\Delta^* = 0.41815$), H_2 ($\Delta^* = 0.19904$) and Ne ($\Delta^* = 0$) and γ is obtained from Equation (3.20).

For polar non-associating compounds:

$$m = 0.466\,T_c^{0.166} \tag{3.26}$$

$$\gamma = 0.08594\exp\left(7.462 \times 10^{-4} T_c\right) \tag{3.27}$$

For polar hydrogen-bonded compounds:

$$m = 0.0052\,M_w^{0.29} T_c^{0.72} \tag{3.28}$$

$$\gamma = \frac{2.464}{M_w}\exp\left(9.8 \times 10^{-6} M_w T_c\right) \tag{3.29}$$

where M_w is the molar mass and β is obtained from Equation (4.18) for polar non-associating and polar associating compounds.

As mentioned previously, the constants of vapour pressure correlations can be generalized to allow for predictive capability to be imparted to the original form of the correlation. Vetere (1991) attempted such a treatment for the "3 - 6" form of the Wagner equation, as shown in Equation (3.8), after drawing on the work of McGarry (1983). It was shown that by subjecting the Wagner equation to thermodynamic constraints when correlating a narrow data set, the accuracy of the correlation can significantly be improved. The constraints and the assumptions

that Vetere adopted in formulating a predictive expression for the Wagner equation involved setting $D = 0$, as in Equation (3.30), and employing the use of just two sets of experimental data in the form of the normal boiling point and the critical constants (T_c and P_c).

$$\ln P_{vapr} = \frac{A(1 - T_r) + B(1 - T_r)^{1.5} + C(1 - T_r)^3}{T_r} \tag{3.30}$$

Vetere employed the use of the Riedel factor (Equation (3.31)) at T_c to show that α_c was related to the A term in the Wagner equation as shown in Equation (3.32).

$$\alpha(T_r) = \frac{d\log(P_r)}{d\log(T_r)} \tag{3.31}$$

$$A = -\alpha_c \tag{3.32}$$

Equation (3.30) was then applied at the normal boiling point and Equation (3.32) was substituted to give the following:

$$C = \frac{\alpha_c - H - B(1 - T_{br})^{0.5}}{(1 - T_{br})^2} \tag{3.33}$$

where the H - term was introduced by Miller (1963) and defined as:

$$H = \frac{T_{br} \ln P_c}{1 - T_{br}} \tag{3.34}$$

where P_c is in atm.

By applying equations (3.30) and (3.31) at the normal boiling point, α_b can be obtained:

$$\alpha_b = \ln P_c + \alpha_c - 1.5B(1 - T_{br})^{0.5} - 3C(1 - T_{br})^2 \tag{3.35}$$

By inserting Equation (3.33) into Equation (3.35), an expression for B can be obtained:

$$B = \frac{\alpha_b + 2\alpha_c - 3H - \ln P_c}{1.5\left(1 - T_{br}\right)^{0.5}} \tag{3.36}$$

An examination of Equations (3.32) and (3.36) reveals that evaluation of the constants B and C is achievable through knowledge of only two values of the Riedel parameter *i.e.* at the normal boiling point (α_b) and at the critical point (α_c). In this way, the entire vapour pressure curve can be predicted through the use of these two parameters. These can be obtained through the use of the following generalized relations based on normal boiling point and critical conditions.

The following is proposed for α_c:

$$\alpha_c = -0.294 + 1.1708\left(\frac{T_{br} \ln P_c}{1 - T_{br}}\right) \tag{3.37}$$

A generalized correlation for α_b is much more difficult to obtain and instead a ratio of α_b / α_c is presented for each family of compounds in terms of the reduced boiling point as follows:

For hydrocarbons:

$$\left[\frac{\alpha_b}{\alpha_c}\right] = 2.7305 - 2.0325T_{br} \tag{3.38}$$

For alkanols:

$$\left[\frac{\alpha_b}{\alpha_c}\right] = 3.6775 - 3.2500T_{br} \tag{3.39}$$

For organic acids:

$$\left[\frac{\alpha_b}{\alpha_c}\right] = 2.0575 - 1.0500T_{br} \tag{3.40}$$

For glycols:

$$\left[\frac{\alpha_b}{\alpha_c}\right] = 1.8850 - 1.3333T_{br} \tag{3.41}$$

For all other polar substances:

$$\left[\frac{\alpha_b}{\alpha_c}\right] = 3.0042 - 2.4211T_{br} \tag{3.42}$$

Vetere then proceeded to test the novel predictive method for nearly 50 compounds of different chemical identities against a few other predictive methods to allow for an effective evaluation of the performance of the equation. Vetere concluded that the overall performance of the equation was superior to that of the other literature methods; however, Vetere also acknowledged that the Wagner equation's strong sensitivity with regards to the α_b parameter was indeed a flaw in the predictive approach with the Wagner equation.

Another predictive method that has been developed from a correlative one is based on the AMP equation, which has been discussed above in Equations (3.9) - (3.14). Macknick and Prausnitz (1979) developed a group contribution scheme for the evaluation of the s and the E_0 parameters, which in the predictive method, represent the number of equivalent oscillators per molecule and the enthalpy of vaporization of the hypothetical liquid, respectively. The three molecular parameters *i.e.* s, E_0 and V_W are determined as follows:

$$s = \sum_{i=1}^{n} n_i s_i \tag{3.43}$$

$$\frac{E_o}{R} = \sum_{i=1}^{n} n_i \left[\frac{\varepsilon_{oi}}{R}\right] \tag{3.44}$$

$$V_w = \sum_{i=1}^{n} n_i V_{wi} \tag{3.45}$$

where s_i, ε_{oi} and V_{wi} are the contributions from the group of type i and n_i is the number of groups of that type in the molecule. It should also be mentioned that a significant breakthrough

in the prediction of vapour pressures of nonelectrolyte organic compounds via the group contribution method has been achieved within our research group in the form of the work of Nannoolal *et al.* (2006).

3.5 Correlation of Vapour-Liquid Equilibria

3.5.1 Overview

The correlation or reduction of binary or multicomponent VLE data allows for the development of an effective empirical or semi-theroretical thermodynamic framework for the interpretation and quantification of observed phase equilibrium behaviour, which is an invaluable exercise for process engineers and thermodynamicists alike. The development of a mathematical model for the thermodynamic behaviour of the system greatly facilitates the task of the design or process engineer involved in the development of large-scale fluid separation operations that are based on the classical phase contacting processes of distillation (fractional and solvent-enhanced), adsorption, stripping and solvent extraction (Prausnitz *et al.*, 1980). The acquisition of binary interaction parameters from VLE data for a binary system can be used for the calculation of industrially-relevant multicomponent phase equilibria.

For thermodynamicists, the development of a theoretical framework for interpreting the phase equilibrium of the system allows for a means of developing predictive methods, where the use of fundamental component or mixture properties can be used to calculate or predict the phase equilibrium characteristics of the system.The use of predictive methods is especially favoured for studying the VLE behaviour of chemical systems under severe operating conditions (extremely high temperatures and/or pressures), where the data that is acquired will be subject to great uncertainty (Raal and Muhlbauer, 1998).

The equilibrium condition is expressed directly through the equality of the chemical potentials, which for a binary system consisting of a vapour and liquid phase at the same temperature and pressure, is the relation shown in Equation (3.46) for each component (i) in the mixture.

$$\mu_i^L = \mu_i^V \tag{3.46}$$

However, the use of the relation shown in Equation (3.46) for the direct computation of the equilibrium relation is impractical and it is through the isofugacity criterion, shown in Equation (3.47), that the equilibrium condition can be expressed in terms of the experimentally accessible

variables of pressure, temperature, volume and phase composition and the nonideal behaviour of the phases can be expressed through auxiliary functions.

$$f_i^V = f_i^L \tag{3.47}$$

Consequently, the modelling of the experimental VLE data is based on the use of suitable mathematical relations that incorporate adjustable or empirical parameters to best satisfy the isofugacity criterion. In addition to the use of efficient algorithms and statistical techniques for the actual data reduction procedure, there are two other factors that are crucial for the accurate modelling of the data. The first relates to the accuracy of the data, which can be assessed through the use of thermodynamic consistency testing (only for P-T-x-y), to be dealt with later on, and the second concerns the selection of a suitable thermodynamic model or method for satisfying the isofugacity criterion to represent the thermodynamic behaviour of the system.

There have traditionally been two approaches or methods for the correlation of VLE data in the form of the direct or phi-phi (ϕ_i - ϕ_i) method and the indirect or gamma-phi (γ_i - ϕ_i) method. The methods differ in terms of the auxiliary functions *i.e.* the activity coefficient (γ_i) and the fugacity coefficient (ϕ_i) used to represent the nonideal behaviour of the vapour and liquid phases. The ϕ_i - ϕ_i method employs the use of an equation of state with reliable mixing rules to represent the vapour (ϕ_i) and liquid phases (ϕ_i) and the γ_i - ϕ_i method treats both phases separately *i.e.* an activity coefficient or G^E model for the liquid phase (γ_i) and an equation of state for the vapour phase (ϕ_i). For the treatment of a binary mixture, the binary interaction parameters are incorporated into the mixing rules for the equation of state and into the G^E model to characterize the specific interactions between pairs of components.

Raal and Muhlbauer (1998) describe the emergence of an additional approach to those above in the form of the modern direct method to address the limitations of the ϕ_i - ϕ_i approach in dealing with the higher density of the liquid phase and with complex polar systems. These incorporate the activity coefficient approach into the treatment of the component fugacities via the EOS mixing rules and will be discussed at a later stage.

In terms of the γ_i - ϕ_i model, there is a further distinction in the type of equation of state employed in the treatment of the vapour phase with regards to the pressure range. The n-parameter virial equation of state usually suffices as an adequate treatment for the vapour phase up to pressures of 1.5 and 5 MPa with the two and three-parameter truncated forms, respectively

(Smith and Van Ness, 1975). However, for higher pressures, the vapour phase nonideality is treated with more accurate cubic or complex equations of state. In the discussion of the γ_i - ϕ_i method, preference is given to the low to moderate-pressure approach as this is relevant to the operating range of the author.

The use of the ϕ_i - ϕ_i and γ_i - ϕ_i approaches, each with its own advantages and disadvantages, has been dealt with extensively by many researchers (Raal and Muhlbauer, 1998) and comprises the bulk of this chapter.

3.5.2 The Gamma-Phi (γ_i - ϕ_i) Method

3.5.2.1 Overview

The γ_i - ϕ_i method, also known as the activity coefficient approach involves the use of two distinct auxiliary functions to separately represent nonideal behaviour of the liquid and vapour phases in the isofugacity expression.

With regards to the vapour phase, nonideal behaviour for a component i in the mixture is expressed through the use the fugacity coefficient, which is defined below:

$$\phi_i^V = \frac{f_i^V}{f_i^o} = \frac{f_i^V}{Py_i} \tag{3.48}$$

where ϕ_i^V is the fugacity coefficient of component i in the vapour phase , f_i^V is the fugacity of component i in the vapour phase, f_i^o is the standard-state fugacity of the vapour phase, P is the total system pressure and y_i is the vapour phase composition. The fugacity coefficient depends on pressure, temperature and in a multicomponent mixture on the mole fractions of all the other components in the vapour phase (y_j).

For the liquid phase treatment in the in the γ_i - ϕ_i approach, the nonideal behaviour is lumped into the activity coefficient term and defined in an analogous fashion to the fugacity coefficient, below as follows:

$$\gamma_i = \frac{f_i^L}{f_i^o x_i} \tag{3.49}$$

In Equation (3.49), γ_i is the activity coefficient of component i, f_i^L is the fugacity of component i in the liquid phase, f_i^o is the standard-state fugacity of the liquid phase and x_i is the liquid phase composition. The activity coefficient depends on temperature, pressure (to a lesser extent) and the component mole fraction in the liquid phase.

The pressure dependence of the activity coefficient at low to moderate pressures is very weak and is usually ignored, however, for higher pressures this dependence has to be accounted for (in the HPVLE γ_i - ϕ_i approach).Prausnitz *et al.* (1980) described the use of an adjusted activity coefficient, $\gamma_i^{(P^r)}$, shown in Equation (3.50), as a correction for the pressure dependency of the activity coefficient γ_i, defined in Equation (3.49), for correlating VLE data with the isothermal form of the Gibbs-Duhem equation (where dP and dT are set equal to zero). The γ_i value at the system pressure (P) can be related to the γ_i value at an arbitary reference pressure *i.e.* (P^r). In this way, the adjusted activity coefficient is independent of the experimental pressure and can be used in both the isobaric and isothermal Gibbs-Duhem equation.

$$\gamma_i^{(P^r)} = \gamma_i \exp\left[\int_P^{P^r} \frac{\overline{V}_i^L}{RT} dP\right] \tag{3.50}$$

where $\overline{V}_i^L$ is the partial liquid molar volume of component i.

An examination of Equations (3.48) and (3.49) reveals that the only difference between the two equations is indeed the manner in which the reference state is defined *i.e.* the choice of reference fugacities. For the vapour phase, the reference fugacity (f_i^o) is that of the partial pressure of an ideal gas in a mixture (Py_i) and the fugacity coefficient evaluates to a value of unity for ideal gas conditions.

The normalization of the activity coefficient (specification of a state in which the γ_i value is unity) can either follow the symmetric or unsymmetric convention with regards to the state of the components presents. If both components are condensable (for LPVLE measurements), the symmetric convention can be used, as shown below:

$$\gamma_i \to 1 \text{ as } x_i \to 1 \tag{3.51}$$

However, the presence of a supercritical or noncondensable component in the liquid solution necessitates an unsymmetric normalization convention with regards to the two components, where for the noncondensable component the following applies:

$$\gamma_i^* \rightarrow 1 \text{ as } x_i \rightarrow 0 \tag{3.52}$$

where γ_i^* denotes that the definition is applicable to supercritical components. The presence of a supercritical component and the resulting normalization represented by Equation (3.52) in fact violates the theoretical framework of the γ_i - ϕ_i approach with regards to the treatment of the liquid phase.

In the event that the liquid phase contains only condensable components, a suitable standard state for the components is obtained through an integration of the expression in Equation (3.53).

$$RT \ln \frac{f_i^o}{P} = \int_0^P \left[\overline{V}_i^L - \frac{RT}{P} \right] dP \tag{3.53}$$

where R is the universal gas constant, T is the system temperature, P is the system pressure, f_i^o is the standard-state fugacity for the liquid phase and $\overline{V}_i^L$ is the partial molar volume for the component i. The above integral is then split into two parts *i.e.* from a pressure of zero to the saturation pressure and from the saturation pressure to the system pressure (the effect of compressing the liquid) in the form of Equation (3.54) and (3.55).

$$RT \ln \frac{f_i^{sat}}{P_i^{sat}} = \int_0^{P_i^{sat}} \left[\overline{V}_i - \frac{RT}{P} \right] dP \tag{3.54}$$

$$RT \ln \frac{f_i^o}{P} = \int_{P_i^{sat}}^P \left[\overline{V}_i^L - \frac{RT}{P} \right] dP \tag{3.55}$$

After rearrangement and simplification, the above two expressions evaluate to Equation (3.56).

$$f_i^o = \phi_i^{sat} P_i^{sat} \exp\left[\int_{P_i^{sat}}^P \frac{V_i^L}{RT} dP \right] \tag{3.56}$$

where P_i^{sat} is the saturated vapour pressure of the pure liquid i at the temperature T of the

system, ϕ_i^{sat} is the fugacity coefficient of the pure saturated vapour i at P_i^{sat} and temperature T and V_i^L is the liquid molar volume of pure liquid i at T (for a condensable component at the system temperature $V_i^L = \overline{V}_i^L$).

The difficulty of the γ_i - ϕ_i approach in the treatment of a supercritical component is clearly evident in the expression for the standard-state liquid fugacity, which is valid only for the symmetric normalization in Equation (3.51), as the existence of a pure supercritical liquid is a physical impossibility (Prausnitz *et al.*, 1980). Even with the introduction of a hypothetical or imaginary standard state for a pure supercritical liquid, determination of liquid phase fugacities through extrapolation from imaginary vapour pressures is an unattractive solution. A further discussion of the treatment of supercritical components in phase equilibrium computations is available in works of Raal and Muhlbauer (1998) and Prausnitz *et al.* (1980).

The exponential of the bracketed term in Equation (3.56) is known as the Poynting correction and is generally insignificant at low to moderate pressures, but increases significantly with an increase in pressure or at lower temperatures (as the pressure dependency of the liquid molar volume increases). Generally, V_i^L is assumed to be independent of pressure so as to simplify calculations, as in Equation (3.57).

$$f_i^o = \phi_i^{sat} P_i^{sat} \exp\left[\frac{V_i^L}{RT}\left(P - P_i^{sat}\right)\right] \tag{3.57}$$

The above is only justified when liquids are incompressible for small, isothermal changes in pressure. When the difference between the system pressure and saturation pressure of the liquid is not considerable, the Poynting correction is close to unity and is omitted and since the gas is essentially an ideal gas at saturation pressure (not applicable to carboxylic acids and strongly associating compounds), $\phi_i^{sat} = 1$. With these two assumptions, $f_i^o = P_i^{sat}$.

Substituting Equation (3.57) into Equation (3.49), applying the isofugacity criterion in Equation (3.46) and simplifying, yields the following working equation for the γ_i - ϕ_i computation of vapour-liquid equilibria:

$$y_i P \Phi_i = x_i \gamma_i P_i^{sat} \tag{3.58}$$

From Equation (3.58), a new simplifying term *i.e.* Φ_i, has been introduced.

The Φ_i term can be quantified as follows:

$$\Phi_i = \left(\frac{\phi_i^V}{\phi_i^{sat}}\right) \exp\left[\frac{V_i^L}{RT}\left(P_i^{sat} - P\right)\right] \tag{3.59}$$

An examination of Equations (3.58) and (3.59) for the computation of the equilibrium condition yields an interrelation between the experimentally accessible variables and the auxiliary functions that are used to quantify the vapour phase and liquid phase nonidealities in the form of the fugacity coefficient and the activity coefficient, respectively. The term Φ_i contains, in addition to the Poynting correction, the ϕ_i^{sat} and ϕ_i^V terms. For the evaluation of the Poynting correction factor, a suitable equation for the volume of the saturated liquid phase as a function of temperature is required. The Rackett correlation, as modified by Spencer and Danner (1972) is recommended in various literature sources (Reid *et al.*, 1987) for the estimation of liquid molar volumes.

3.5.2.2 Calculation of the vapour phase nonideality

As mentioned above, in the γ_i - ϕ_i approach it is the liquid phase nonideal behaviour that is correlated through the activity coefficient with the various models of the excess Gibbs energy as a function of composition. Consequently, all vapour phase nonideal behaviour *i.e.* the fugacity coefficients, have to be determined indirectly or in an independent way. To this end, an equation of state relating the PVT properties of the fluid is required to enable the suitable calculation of the vapour phase fugacities. Equations of state are often most conveniently written in terms of the compressibility factor (Z), which for an ideal gas, is defined as:

$$Z = Z_o = \frac{PV_m}{RT} = 1 \tag{3.60}$$

The above defines the limiting value of Z as zero density is approached. The theoretically-based truncated virial equation of state is the preferred choice for the representation of the vapour phase nonideality in the γ_i - ϕ_i approach for pressures below 0.5 MPa (Abbott, 1986). The virial equation of state was derived from a statistical mechanical framework and consequently has a sound theoretical basis for the representation of properties of pure gases and mixtures. The equation, as its name implies, is actually an expression for the compressibility correction factor as a McLaurin power series as function of density (reciprocal molar volume) in the form of the

volume explicit Leiden version or in the pressure-explicit form, known as the Berlin form. These two forms are shown below as Equations (3.61) and (3.62), respectively.

$$Z = 1 + \frac{B}{\overline{V}} + \frac{C}{\overline{V}^2} + \ldots\ldots \tag{3.61}$$

where $\overline{V}$ is the molar volume, B is the second virial coefficient and C is the third virial coefficient.

$$Z = 1 + B'P + C'P^2 + \ldots\ldots \tag{3.62}$$

The second (B') and third (C') virial coefficients in the above pressure-explicit expansion are related to those in the volume-explicit expansion in Equation (3.61) through Equations (3.63) and (3.64), shown below:

$$B' = \frac{B}{RT} \tag{3.63}$$

$$C' = \frac{C - B^2}{(RT)^2} \tag{3.64}$$

It must be remembered that for the expressions in (3.63) and (3.62) to be exact, the two power series shown above in Equations (3.61) and (3.62) have to retain the form of mathematically infinite Taylor series. However, to simplify the calculations and due to the lack of reliable experimental or predicted higher virial coefficients, the virial equation of state is for the most part usually truncated at the second virial coefficient. This results in a discrepancy (Malanowski and Anderko, 1992) between the values obtained through the use of Equations (3.61) and (3.62), which is typically 5 %. More importantly, this truncation strictly renders the virial equation of state applicable at low to moderate pressures. The virial equation can in principle be used at higher pressures; however, a larger number of virial coefficients (knowledge of which is highly limited) are required to correctly represent the PVT properties of fluids.

The virial equation is also limited to the treatment of only a single phase as the compressibility correction factor is not differentiable at the phase boundary between the one-phase and the two-phase regions. This is clearly visualized in the isotherms of the virial equation (Walas, 1985), which do not possess the S-shape (a characteristic for a proper equation of state for both

phases). Consequently, even with a large number of terms, it cannot represent liquid phase behaviour or the coexistence of the liquid and vapour phase. The apparent lack of applicability of the virial equation of state to higher pressure ranges necessitates the use of more accurate equations of state such as the cubic-type in HPVLE computations with the γ_i - ϕ_i approach.

As a rough approximation of the pressure range of applicability of the virial equation of state, Prausnitz *et al.* (1980) recommend the following relation as an indication of the latter:

$$P \leq \frac{T}{2} \frac{\sum_{i=1}^{n} y_i P_{c,i}}{\sum_{i=1}^{n} y_i T_{c,i}} \tag{3.65}$$

Despite the limitations of the truncated-virial equation of state, its justification for suitable use in the γ_i - ϕ_i approach stems from its demonstrated superiority over other traditional equations of state (*e.g.* cubic) in the treatment of the vapour phase in the low-pressure region (Sandler *et al.*, 1994). A significant attribute of the virial expansion for gases is the relationship between the virial coefficients and the intermolecular forces *i.e.* for an ideal gas, the intermolecular forces are zero and the compressibility correction factor is unity. For real gases, statistical mechanics can be employed to relate expressions for the virial coefficients to intermolecular forces.
The virial coefficients obtained from Equations (3.61) and (3.62) for pure substances are temperature-dependent only.

For the treatment of mixtures, the mixture second virial coefficient *i.e.* B_{mix} is a function of both the temperature and the concentration of all the mixture components and can be obtained from a statistical-mechanical rigourous concentration dependent mixing rule shown in Equation (3.66).

$$B_{mix} = \sum_{i}^{n} \sum_{j}^{n} y_i y_j B_{ij} \tag{3.66}$$

for the m vapour phase compositions of components i and j and where B_{ij} is the interaction virial coefficient or the cross coefficient that represents the bimolecular interaction between the molecules i and j.

For a binary mixture, this reduces to:

$$B_{mix} = y_1^2 B_{11} + y_1 y_2 B_{12} + y_2^2 B_{22} \tag{3.67}$$

where the B_{11} and B_{22} terms represent the pure component virial coefficients and the B_{12} term is the mixture cross coefficient; all of which are functions of temperature only.

To evaluate the fugacity coefficient terms *i.e.* ϕ_i^{sat} and ϕ_i^V in the Φ_i term in Equation (3.59), the virial equation of state truncated after the second virial coefficient is substituted as shown below into the following:

$$\ln \phi_i = \int_0^P \left[\frac{\overline{V}_i}{RT} - \frac{1}{P} \right] dP \tag{3.68}$$

From equation (3.60),

$$Z - 1 = \frac{BP}{RT} \tag{3.69}$$

Rearrangement and substitution of Equation (3.69) into Equation (3.68) yields the following:

$$\ln \phi_i = \int_0^P \left[\frac{Z-1}{P} \right] dP \tag{3.70}$$

An evaluation of the above for the pure saturated vapour and for the mixture components in the vapour phase, allows for the working equations for ϕ_i^{sat} and ϕ_i^V to be obtained:

$$\ln \phi_i^{sat} = \frac{BP_i^{sat}}{RT} \tag{3.71}$$

$$\ln \phi_i^V = \frac{P}{RT} \left(B_{ii} + y_j^2 \delta_{ij} \right) \tag{3.72}$$

where

$$\delta_{ij} = \left(2B_{ij} - B_{ii} - B_{jj} \right) \tag{3.73}$$

The values of the virial coefficients can be determined from experimental measurements in the form of PVT data, from statistical mechanics where the pair intermolecular energy is quantified through the use of potential functions or empirical or semi-theoretical correlations. There are very few literature sources for experimental virial coefficients, which also display considerable scatter due to the different experimental methods used to obtain them. It has also indeed been acknowledged by many researchers (Meng *et al.*, 2004) that in the older PVT data no attempt to compensate for the effects of physical adsorption was made, producing values that were far too negative for subcritical conditions. The most popular compilations of virial coefficients (Walas, 1985) are those of Dymond and Smith (1980) and Kogan (1968).

Analytical expressions for the prediction or correlation of virial coefficients can essentially be divided into two approaches *i.e.* those that are based purely on the corresponding states or on the extended corresponding states method and those that incorporate statistical mechanical considerations in the calculation of the second virial coefficient. With regards to chemically reacting systems (beyond the scope of this study), a chemical theory of vapour imperfections (Marek, 1955; Prausnitz, 1969; Nothnagel *et al.*, 1973; Prausnitz *et al.*, 1980) is required to calculate fugacity coefficients based on the true equilibrium concentrations *i.e.* equilibrium constants.

The corresponding states principle in its original form was essentially a two-parameter relation with reduced temperature, T_r, and reduced pressure, P_r, as the independent variables and was consequently only applicable to the simple, monoatomic molecules, where the latter did not exhibit size-shape, polarity or association effects.
The work of Pitzer and Curl (1957) was to extend the corresponding states principle to include a third parameter, known as the acentric factor (ω) to account for size-shape effects or the non-spherical nature of nonpolar molecules:

$$\omega = -1.0 - \log\left(P_r^{sat}\right)_{T_r = 0.7} \tag{3.74}$$

where P_r^{sat} is the reduced vapour pressure at a $T_r = 0.7$, since for simple monatomic gases $P_r^{sat} = 1$ at $T_r = 0.7$.

There have been other "third parameters" that have also been proposed by a variety of researchers (Tarakad and Danner, 1977) to characterize the non-sphericity of molecules.

The correlation for the second virial coefficient proposed by Pitzer *et al.* (1957) was the following:

$$\frac{BP_c}{RT_c} = B^{(0)} + \omega B^{(1)} \tag{3.75}$$

where the $B^{(0)}$ and $B^{(1)}$ terms are expressions that are functions of T_r since B is a function of temperature only. The correlation above served as the inspiration for later, more successful correlations (Walas, 1985) such as that of Abbott (Smith and Van Ness, 1975) and Tsonopoulos (1974). The $B^{(0)}$ and $B^{(1)}$ terms for the correlations of Pitzer and Curl, Abbott and Tsonopoulos are presented in Appendix B. The correlations based on the original Pitzer-Curl correlation suffer from the limitations of being applicable only to nonpolar, non-associating gases and more elaborate treatments are required *i.e.* consideration of a fourth parameter or additional terms to extend the corresponding states principle to polar fluids.

Tsonopoulos (1974) correlated second virial coefficients for polar non-associating (ketones, acetaldehyde, acetonitrile, ethers) and polar associating compounds (alkanols, water) through the use of additional terms with empirical parameters in conjunction with the same terms for nonpolar gases (see Appendix B) to obtain the Pitzer-Tsonopoulos correlation:

$$\frac{BP_c}{RT_c} = B^{(0)} + \omega B^{(1)} + B^{(2)} \tag{3.76}$$

The Tsonopoulos correlation provides a very simple, purely empirical approach for correlating complex polar non-associating and associating compounds and has limitations at high values of reduced temperatures, where erroneous results are obtained.

Another corresponding states correlation for polar fluids of note is that of Tarakad and Danner (1977), which is a four-parameter corresponding states method. The four parameters used, apart from the reduced temperature and pressure are the radius of gyration and an empirical polarity factor. The radius of gyration, $\overline{R}$, was used as the third parameter to effectively represent the non-spherical nature of molecules *i.e.* size-shape effects, since the use of the acentric factor as the third parameter does not strictly preclude the effects of polarity on the virial coefficient *i.e.* the acentric factor is influenced by the polar nature of the molecule. A correlation with distinct terms for the size-shape and polarity contributions allows for a true measure of the size-shape effects of polar compounds as a contribution to the second virial coefficient terms. The fourth parameter (Φ_i) was obtained in an empirical fashion by correlating the difference between

polar fluids and also nonpolar fluids of similar size and shape at $T_r = 0.6$. The correlation of Tarakad and Danner was of the following form:

$$\frac{BP_c}{RT_c} = B^{(0)}_{\text{simple fluid}} + B^{(0)}_{\text{size-shape}} + B^{(0)}_{\text{polar correction}} \tag{3.77}$$

The terms for the above correlation are presented in Appendix B. Tarakad and Danner provided values of Φ_i for various classes of compounds in the original journal article. The mixing rule for Φ_{cij} is applicable for polar-polar interactions only and for all other interactions $\Phi_{cij} = 0$. In a comparison of various correlation methods for the second virial coefficient by the authors for 291 binary systems of different compounds, the Tarakad-Danner and Hayden and O'Connell (1975) correlations performed the best. However, the limitations of the purely empirical polarity factor in the Tarakad and Danner approach were evident for systems with strong association effects.

As mentioned above, most of the older PVT data suffered from errors due to adsorption effects, consequently, the older correlations that are based on this data will also be unreliable. Also the corresponding states method only accounts for size-shape effects and dipole moment effects and does not characterize the more complex chemical associations and quantum effects (Meng *et. al.*, 2004). Consequently, data that is obtained from purely empirical approaches with generalized correlations should be used with some degree of apprehension and caution. This certainly advocates the use of predictive methods for second virial coefficients that incorporate elements of statistical mechanical theory together with the extended corresponding states method.

One of the most popular and highly recommended second virial coefficient correlations is that of Hayden and Connell (1975). This approach employs the use of the bound-pair formalism of Stogryn and Hirschfelder (1959) in characterising interactions between molecules as being due to the interactions between like and unlike pairs in molecular configurations that are bound, metastably bound and free pairs.

The pure component and cross virial coefficients are provided as being the sum of two principal contributions:

$$B_{ij} = B^F_{ij} + B^D_{ij} \tag{3.78}$$

The terms in Equation (3.78) are equivalent to the following:

$$B_{ij}^{F} = \left(B_{non-polar}^{F}\right)_{ij} + \left(B_{polar}^{F}\right)_{ij} \tag{3.79}$$

$$B_{ij}^{D} = \left(B_{bound}^{D}\right)_{ij} + \left(B_{metastable}^{D}\right)_{ij} + \left(B_{chemical}^{D}\right)_{ij} \tag{3.80}$$

The superscript "F" refers to those molecular interactions resulting from weak physical forces *i.e.* between relatively "free" molecules and the superscript "D" refers to interactions as a result of strong chemical forces between molecules *i.e.* "bound" or "dimerized" molecules.
The Hayden and O'Connell approach is indeed a complex one, when compared to those that are based purely on the corresponding states method and has found widespread use for a variety of chemical systems (except carboxylic acids) in the calculation of vapour phase nonidealities. This method has been employed for the calculation of both pure component and cross virial coefficients for the measurements in this work and the method in its entirety is presented in Appendix B.

3.5.2.3 Correlation of the liquid phase behaviour with G^E models

In the above paragraphs, the treatment of the experimental thermodynamic variables and vapour phase nonideal behaviour has been dealt with. However, at the heart of the correlation of VLE data with the gamma-phi approach is the use of equations for the correlation of the liquid phase behaviour with composition and to a lesser extent, with temperature (Walas, 1985). Van Ness and Abbott (1982) described the "primary thermodynamic value" of low to moderate-pressure VLE data as being a route to the calculation of the excess Gibbs energy, G^E, *i.e.* data reduction in its pure sense for the development of an expression for the composition dependence of the G^E of a mixture.

The pressure, temperature and composition dependence of the excess Gibbs energy is expressed through the fundamental excess property relation, the original derivation of which can be found in the work of Van Ness (1958), and can be shown as:

$$d\left[\frac{G^E}{RT}\right] = -\left[\frac{H^E}{RT^2}\right]dT + \left[\frac{V^E}{RT}\right]dP + \sum_{i=1}^{n} \ln\gamma_i dx_i \tag{3.81}$$

where G^E, H^E and V^E are the excess molar Gibbs energy, enthalpy and volume, respectively.

Through suitable manipulation of Equation (3.81), as shown by Van Ness (1995), the following form of the Gibbs-Duhem equation in terms of activity coefficients can be obtained:

$$\sum_{i=1}^{n} d \ln \gamma_i x_i = -\left[\frac{H^E}{RT^2}\right] dT + \left[\frac{V^E}{RT}\right] dP \qquad (3.82)$$

An examination of Equation (3.82) allows for the relationship between the activity coefficients and the excess thermodynamic functions to be seen more clearly, where the latter is important for thermodynamic consistency testing.

As can be seen from Equation (3.82), the determination of γ_i values allow for the calculation of excess thermodynamic quantities such as H^E and S^E (since $G^E = H^E - TS^E$). The calculation of the latter two excess thermodynamic quantities from a VLE data set is discussed in Appendix B.

Consequently, using a canonical equation that relates G^E to experimental variables of pressure, temperature and composition allows for a suitable route to the activity coefficient. However, as opposed to canonical equations of state (to be discussed later), which upon differentiation serve to provide the required thermodynamic properties such as fugacity as a function of pressure, temperature and composition, there is no liquid phase model (Smith and Abbott, 1982) that is able to provide a complete thermodynamic description of the system for the liquid phase.

For the treatment of isobaric data, the temperature dependence of the H^E term in equation (4.82) needs to be incorporated into thermodynamic expressions for the activity coefficients (except for athermal solutions). Many authors describe this as a task that is quite inconvenient (Raal and Muhlbauer, 1998), consequently the term is ignored. The treatment of isothermal data is a much easier task as both the H^E and V^E terms can be ignored, where the latter term is considerably smaller than the former. Also, the use of the adjusted activity coefficient in Equation (3.50) is a compensatory effect in this regard.

A common approach for low-pressure VLE data based on the above considerations is to devise suitable expressions based on the relations for the composition dependence of the excess Gibbs energy at constant temperature and pressure *i.e.* Equation (3.83).

$$\left[\frac{\partial\left(\frac{nG^E}{RT}\right)}{\partial n_i}\right]_{T,P,n_j} = \ln\gamma_i \tag{3.83}$$

where $\overline{G}_i^E$ is the partial molar excess Gibbs energy for component i.

Since $\overline{G}_i^E$ is a partial molar property, the use of the summability relation (Smith *et al.*, 2001), for the intensive mixture or solution property of G^E yields the following important expression:

$$\frac{G^E}{RT} = \sum_i^n \ln\gamma_i x_i \tag{3.84}$$

Although it may be implied from the above that activity coefficients derive from excess Gibbs energies, the procedure is actually reversed, as with all other quantities known, Equation (3.58) can be solved for experimental γ_i values, which are then used to compute the $\overline{G}^E$ values.

Although the data reduction procedure can be accomplished by either G^E model-dependent or G^E model-independent methods, a discussion of the latter will be excluded (as it has not been used in this work) and interested readers are referred to the text of Raal and Muhlbauer (1998).

In the G^E model-dependent approach, a suitable analytical relation, is employed to represent G^E primarily as a function of composition and in some models, temperature, to allow for the data reduction of the experimental VLE data set to a set of model parameters. The choice of the analytical equation is of course an integral part of the success of the data reduction procedure and since considerable choice of available models exists in this regard, a judicious approach is often required.

The correlating equations, as with many of the mathematical models of systems in science and engineering are either purely empirical or semi-theoretical. In the empirical approach, the objective is maximum flexibility in terms of fitting a wide variety of systems through the use of mathematical relations such as series expansions of various polynomials, with no consideration of the molecular structure or chemical nature of the components. In stark contrast, the semi-

theoretical approach attempts to provide a simple molecular thermodynamic description of the system behaviour to ensure that the fitted parameters have significance beyond the data set from which they are *i.e.* incorporated into a theoretical framework for the interpretation of liquid phase nonideal behaviour. Many different functional forms for the G^E function have been developed and to date none of these forms have been able to enjoy the status of "universal applicability" *i.e.* capable of representing all types of systems under different conditions.

As mentioned above in the empirical approach is one that is purely mathematical in terms of the use of correlating equations that are typically polynomial expressions, with no consideration of a molecular structure or interaction. These types of equations are generally applicable to binary systems only, however, the Wohl relation (Wohl, 1946), may be an exception in this regard.

The fundamental basis for fitting empirical relations to the mixture property of $\frac{G^E}{RT}$ is that the pure component limits must be obeyed *i.e.* as x_1 and $x_2 \to 0$, G^E must also approach zero.

For a binary mixture, this can be shown as follows:

$$\lim_{\substack{x_1 \to 0 \\ x_2 \to 1}} \left[\frac{G^E}{RT}\right] = \lim_{\substack{x_1 \to 1 \\ x_2 \to 0}} \left[\frac{G^E}{RT}\right] \tag{3.85}$$

Intuitively, from (3.85), the empirical fitting is done to the following:

$$\left[\frac{G^E}{RTx_1x_2}\right] = g(x_1) \tag{3.86}$$

Rearranging Equation (3.86) produces the expression in shown below:

$$\left(\frac{G^E}{RT}\right) = x_1x_2g(x_1) \tag{3.87}$$

where $g(x_1)$ is a relation expressing the composition dependence of the excess Gibbs energy.

The composition dependence of G^E can also be expressed in terms of volume fractions or molecular surface fractions, especially when molecules differ in size or chemical nature, however, this is more pertinent to semi-theoretical methods.

The Margules and Related Equations

This family of equations, proposed by Margules in 1895, are the oldest empirical equations for the compositional dependence of G^E that still have contemporary significance. The simplest empirical approach in the correlation of VLE data using Equation (3.87) is to take the function $g(x_1)$ as being constant, which results in the two-suffix (one-parameter) Margules equation which is shown in Equation (3.88).

$$\left(\frac{G^E}{RT}\right) = Ax_1x_2 \tag{3.88}$$

where A is an empirical constant.

The above relation is also known as the symmetrical or Porter equation (Raal and Muhlbauer, 1998). Mathematically, the above relation predicts that the composition dependence of G^E is a symmetrical function. This is the case for systems that do not deviate greatly from ideality *i.e.* for mixtures of molecules that are chemically and structurally similar. However, for complex systems, a great variety of forms for the composition dependence function of G^E is observed *i.e.* straight horizontal lines, straight non-horizontal lines and various asymmetric curvilinear shapes (Walas, 1985). Consequently, the applicability of Equation (3.88) extends only to its use as a qualitative criterion for the extent of nonideal behaviour of a mixture (Gess *et al.*, 1991) or for obtaining quick estimates of the trends of nonideal behaviour (Raal and Muhlbauer, 1998). Expressions for the activity coefficients for the system components can be obtained through the substitution of an expression for the excess molar Gibbs energy or G^E in Equation (3.88) in the partial differential expression of Equation (3.83), shown below:

$$\ln\gamma_1 = Ax_2^2 \tag{3.89}$$

$$\ln\gamma_2 = Ax_1^2 \tag{3.90}$$

The expressions for the activity coefficients of the other G^E models presented in this review are derived in the same manner. The generalized form of the Margules equations as a power series expansion and its representation with empirical parameters is shown in Appendix B. The most commonly used forms of the Margules equations are the three-suffix (2-parameter) and the four-suffix (3-parameter) equations.

The three-suffix form can be represented as follows:

$$\left(\frac{G^E}{RTx_1x_2}\right) = A_{21}x_1 + A_{12}x_2 \tag{3.91}$$

where

$$\ln\gamma_1 = x_2^2\left[A_{12} + 2x_1(A_{21} - A_{12})\right] \tag{3.92}$$

$$\ln\gamma_2 = x_1^2\left[A_{21} + 2x_2(A_{12} - A_{21})\right] \tag{3.93}$$

The form of the four-suffix Margules equation as used by Van Ness *et al.* (1973) is as follows:

$$\left(\frac{G^E}{RTx_1x_2}\right) = Ax_2 + Bx_1 - Dx_1x_2 \tag{3.94}$$

where

$$\ln\gamma_1 = x_2^2\left[A + 2x_1(B - A - D) + 3Dx_1^2\right] \tag{3.95}$$

$$\ln\gamma_2 = x_1^2\left[B + 2x_2(A - B - D) + 3Dx_2^2\right] \tag{3.96}$$

The four-suffix form was tested extensively with experimental data by Van Ness *et al.* (1973) and was shown to be capable of representing the observed G^E behaviour of real systems. The four-suffix Margules equation generally finds applicability in the thermodynamic consistency testing of VLE data (Gess *et al.*, 1991) and is not usually employed for the actual parameter estimation procedure.

When the lower order equations have been insufficient for the representation of highly nonideal behaviour, series expansions with higher-order terms are used. Higher-order Margules equations in the form of the modified and extended modified Margules equations are well known but have been rarely applied (Abbott and Van Ness, 1975). These have the following respective forms:

$$\left(\frac{G^E}{RTx_1x_2}\right) = A_{21}x_1 + A_{12}x_2 - \frac{\alpha_{12}\alpha_{21}x_1x_2}{\alpha_{12}x_1 + \alpha_{21}x_2} \tag{3.97}$$

$$\left(\frac{G^E}{RTx_1x_2}\right) = A_{21}x_1 + A_{12}x_2 - \frac{\alpha_{12}\alpha_{21}x_1x_2}{\alpha_{12}x_1 + \alpha_{21}x_2 + \eta x_1x_2} \tag{3.98}$$

where α_{12}, α_{21} and η are additional empirical parameters.

The Redlich-Kister expansion (1948b) is roughly similar to that of Margules equations and for the same number of parameters; the Margules and Redlich-Kister expansions are completely equivalent.

The Redlich-Kister expansion can be generalized to the following form:

$$\left(\frac{G^E}{RTx_1x_2}\right) = A_o + \sum_{n=1}^{a} A^n z^n \tag{3.99}$$

where $z = (x_1 - x_2)$ and the value of a (the order of the equation) varies from zero to five (1-6 parameters).

The Redlich-Kister expansion is often used in the following working form:

$$\left(\frac{G^E}{RTx_1x_2}\right) = B + C(x_1 - x_2) + D(x_1 - x_2)^2 + E(x_1 - x_2)^3 + \ldots \tag{3.100}$$

The activity coefficients for the above (with $E = 0$) are the following:

$$\ln\gamma_1 = x_2^2\left[B + C(3x_1 - x_2) + D(x_1 - x_2)(5x_1 - x_2)\right] \tag{3.101}$$

$$\ln\gamma_2 = x_1^2\left[B + C(x_1 - 3x_2) + D(x_1 - x_2)(x_1 - 5x_2)\right] \tag{3.102}$$

An interesting point to note about the Redlich-Kister expansion (Raal and Muhlbauer, 1998) is that the odd-powered expansion terms in Equation (3.100) *i.e.* with the coefficients C and E, when non-zero, produce an asymmetric skewing of an otherwise parabolic shape produced by the B and D terms.

It is important to employ a cautious approach in the correlation of VLE data with higher-order equations as it is imperative that the number of parameters used, unless the polynomials are orthogonal (to be dealt with below), are representative of the completeness, extent and accuracy

of the data set. The use of higher-order equations for the Margules-type expansions can result in an incorrect representation of the experimental data *i.e.* "unjustified oscillations" (Malanowski and Anderko, 1992) such as artificial curvature or inflection points (Raal and Muhlbauer, 1998) as the equation attempts to incorporate random experimental errors into the fitting procedure. Also, with an increase in the number of parameters comes an increase in the inter-correlation or interdependence of the parameters (Gess *et al.*, 1991). This can largely be avoided through the use of the flexible cubic spline functions and orthogonal polynomials, an example of which is the Legendre polynomial expansion:

$$\left(\frac{G^E}{RTx_1x_2}\right) = \left[p_0 + p_1(2x_1 - 1) + p_2(6x_1^2 - 6x_1 + 1) + \ldots\right] \qquad (3.103)$$

where p_k is the coefficient of the Legendre polynomial (in parenthesis) of order k and is the empirical parameter to be determined.

A comparison of the Redlich-Kister and Legendre polynomial expansions reveals that in these expressions, $p_0 = B$ and $p_1 = C$, hence, the Redlich-Kister expansion is considered to be very similar to an orthogonal polynomial. In a Legendre expansion, the regressed coefficients are orthogonal if the data set is large enough to approximate a continuum. Orthogonal coefficients allow for flexibility in the data fitting procedure, as the regressed coefficients are independent of one another *i.e.* the respective parameter values for the Legendre polynomials are the same whether a higher or lower order series is used. The Legendre polynomials as with the other polynomial series mentioned above are used extensively in testing a data set for thermodynamic consistency. The advantages of polynomial expansions over other equations (Walas, 1985) are the flexibility in the values of the model parameters (can be negative or positive) and in the representation of extrema *i.e.* minima and maxima, in the activity coefficient data across the composition range.

The van Laar Equation

The van Laar equation (1910, 1913) was historically the first attempt by a researcher at formally proposing a theory for the liquid phase behaviour. Although it is today regarded as being purely empirical, the original formulation of the theory was based on the van der Waals equation of state. The form of the equation (Abbott and Van Ness, 1975) is based on the linear relationship

between the reciprocal of $\left(\frac{G^E}{RTx_1x_2}\right)$ and the liquid phase composition as shown below in Equation (3.104).

$$\left(\frac{G^E}{RTx_1x_2}\right)^{-1} = \frac{x_1}{A'_{21}} + \frac{x_2}{A'_{12}} \tag{3.104}$$

The expression in Equation (3.104) is equivalent to:

$$\left(\frac{G^E}{RTx_1x_2}\right) = \frac{A'_{12}A'_{21}}{A'_{12}x_1 + A'_{21}x_2} \tag{3.105}$$

where

$$\ln\gamma_1 = A'_{12}\left(\frac{A'_{21}x_2}{A'_{12}x_1 + A'_{21}x_2}\right)^2 \tag{3.106}$$

$$\ln\gamma_2 = A'_{21}\left(\frac{A'_{12}x_1}{A'_{12}x_1 + A'_{21}x_2}\right)^2 \tag{3.107}$$

A discussion of the original formulation of the van Laar equation within the framework of the van der Waals equation of state is deferred to Appendix B.

The three-term van Laar equation can be obtained through the addition of another parameter (η) in the denominator *i.e.*

$$\left(\frac{G^E}{RTx_1x_2}\right) = \frac{A'_{12}A'_{21}}{A'_{12}x_1 + A'_{21}x_2 + \eta x_1x_2A'_{12}A'_{21}} \tag{3.108}$$

The corresponding activity coefficients are as follows:

$$\ln\gamma_1 = A'_{12}\left[\frac{1+\eta A'_{12}x_1^2}{\left(1+\frac{A'_{12}x_1}{A'_{21}x_2}+\eta A'_{12}x_1\right)^2}\right] \tag{3.109}$$

$$\ln\gamma_2 = A'_{21}\left[\frac{1+\eta A'_{21}x_2^2}{\left(1+\frac{A'_{21}x_2}{A'_{11}x_1}+\eta A'_{21}x_2\right)^2}\right] \tag{3.110}$$

Traditional limitations of the Van Laar equation as an empirical equation include an inability to represent systems which have an extrema in the activity coefficient behaviour and the necessity that both the fitted parameters have to be of the same sign to represent the data over the entire composition range (Walas, 1985). To address the former, Null (1980) proposed a modification which involved the use of absolute value functions in the activity coefficient expressions. Raal and Muhlbauer (1998) also report that in some rare instances, parameters of opposite sign can be tolerated, and the denominator can become zero. Another point of note is that systems that correlate well with the Van Laar equation give poor correlations with the Margules relations and *vice versa* (Malanowski and Anderko, 1992).

Generalized Empirical Expressions

A generalized empirical expression can be obtained (Van Ness and Abbott, 1982) to represent the empirical approaches discussed above. This can be expressed as follows:

$$\left(\frac{G^E}{RTx_1x_2}\right) = \frac{A_0+\sum_{n=1}^{a}A_n z^n}{1+\sum_{m=1}^{b}B_m z^m} \tag{3.111}$$

where $z=(x_1 - x_2)$ and A_0, A_n and B_m are empirical constants.

For the various cases *i.e.* combinations of values of a and b in the summations of the polynomial terms in Equation (3.111), the different forms of the Margules empirical equations, the Redlich-Kister expansion, van Laar equation, *etc.*, can be recovered, as dealt with extensively by Van Ness and Abbott (1982).

Wohl Expansion

The last of the empirical approaches to be discussed and one that stands out from the rest, was proposed by Wohl in 1946. Although it is purely an empirical expression, it does deviate from the norm of such expressions as it can be used for multicomponent systems and it attempts to assign some physical significance to the parameters albeit through the use of some primitive assumptions about interactions between molecules. It is actually a series expansion in effective volume fractions (z_i) and it incorporates the parameters q_i and a_{ijk}, where the former is seen as being analogous to the effective size of the molecule and the latter to the interaction energies between the molecules in different combinations.

The general form of the Wohl expansion is the following:

$$\frac{G^E}{RT} = \left(\sum_{i=1}^{n} x_i q_i\right)\left[\sum_{i=1}^{n}\sum_{j=1}^{n} f_{ij} z_i z_j a_{ij} + \sum_{i=1}^{n}\sum_{j=1}^{n}\sum_{k=1}^{n} f_{ijk} z_i z_j z_k a_{ijk} + \ldots.\right] \tag{3.112}$$

where

$$z_i = \frac{x_i q_i}{\sum_{j=1}^{n} x_j q_j} \tag{3.113}$$

$$f_{ijk} = \left[\frac{(m_i + m_j + m_k + \ldots)!}{m_i! m_j! m_k! \ldots}\right] \tag{3.114}$$

where $f_{ijk} = 0$ if all the subscripts are equal and f_{ij} is obtained by removing k.

In particular for a binary system, we have:

$$\frac{G^E}{RT(x_1 q_1 + x_2 q_2)} = 2a_{12} z_1 z_2 + 3a_{112} z_1^2 z_2 + 3a_{122} z_1 z_1^2 + \ldots \tag{3.115}$$

Through the use of the above (truncated at the tertiary interactions), it can be shown how the different empirical functional forms can be obtained from the Wohl expansion with different

assumptions (Gess *et al.*, 1991).This serves to allow an insight into the limitations of the other empirical equations.

Assuming that secondary interactions *i.e.* $(a_{12} = a_{21})$ are dominant over tertiary interactions *i.e.* (a_{112} and a_{122}), Equation (3.115) becomes:

$$\frac{G^E}{RT(x_1q_1 + x_2q_2)} = 2a_{12}z_1z_2 \tag{3.116}$$

Now assuming that the molecules have equal sizes *i.e.* $q_1 = q_2 = q$,

$$\frac{G^E}{RT} = 2a_{12}qx_1x_2 \tag{3.117}$$

The expression in (3.117) can be recognized as the two-suffix Margules equation, shown as Equation (3.88), where $A = 2a_{12}q$ and it can now be clearly seen that the assumption of equal-sized molecules in the two-suffix Margules equation does indeed contribute to its inadequacies in representing nonideal systems. The higher-order Margules equations and other empirical relations can be derived in an analogous fashion, allowing for an insight into the deficiencies of the various empirical approaches on the basis of the assumptions inherent in their derivation.

In the above paragraphs, various empirical correlations have been presented and discussed. However, the empirical approach is inadequate for the treatment of highly nonideal systems and where an insight into molecular thermodynamic phenomena is desired. This is due to following:

(a) The parameters that are obtained *have no actual significance* beyond the data set from which they are obtained. This is as a result of the equation being purely empirical as the model has no theoretical basis, where the equation is not based on molecular thermodynamic model which actually characterizes the interactions between the molecules on the basis of size, shape, interaction energies, *etc.* Also, the use of volume or surface area fractions instead of composition is important when the molecules differ in size or shape. Consequently, the data from empirical correlations are generally not insightful in the validation and development of theories of liquid phase behaviour.

(b) There is *no temperature dependency of the parameters* in the empirical activity coefficient relations *i.e.* the activity coefficient terms do not incorporate the system temperature. With regards to the treatment of isobaric systems, this is a major shortcoming as the polynomial

expansions are incapable of representing polythermal data (Malanowski and Anderko, 1992). This also severely compromises interpolation and extrapolation, together with the development of predictive methods with empirical equation parameters.

(c) Due to the above, empirical models (except for the Wohl expansion) *cannot be used for the treatment of multicomponent systems*, since for these types of mixtures, the binary interaction terms characterising specific interactions between molecular pairs, obtained through statistical mechanical considerations, are required.

As a result of the above, those equations which have a semi-theoretical basis are more widely favoured amongst contemporary researchers and will be dealt with in great detail below. It must be remembered that although these types of equations inherently have a limited theoretical basis at the molecular level, the numerical values of the parameters, as with the empirical approach, can only be obtained through the reduction of experimental data, as the theoretical framework (often plagued by many assumptions) is just too weak for most of the models to allow for the quantification of the parameters from molecular theory, a task which is to be accomplished by predictive methods.

Wilson and Modified Wilson Equations

In 1964, a new expression for the composition dependence of the excess Gibbs energy based on the work of Flory and Huggins (Flory, 1953) was proposed by Wilson. A central concept used in the approach for the description of mixtures was that of "local compositions". Wilson realized that molecules do have a preferential tendency to arrange themselves based on the nature of the energies of interactions between the molecules and it is this "local concentration" of the mixture components that must be considered to describe the interactions between molecules. This was in stark contrast to earlier solution theories, such as the regular solution theory (Scatchard, 1931; Hildebrand and Wood, 1962), where one of the major assumptions was that the arrangement of the molecules was completely random and more importantly that the energies of interaction between any two molecules was independent of any molecules in the vicinity of the interaction, where both of the above were independent of temperature.

In the work of Wilson, an expression was developed for the local compositions through the use of local mole fractions, which were defined through the use of statistical mechanics with the Boltzmann distribution of energies amongst different states.

For a binary mixture of i and j molecules, the local mole fractions are used to describe the probability of the distribution of molecules of j around a central i molecule relative to the probability of the distribution of i molecules around the central i molecule as follows:

$$\frac{x_{ji}}{x_{ii}} = \frac{x_j \exp\left(-\frac{\lambda_{ji}}{RT}\right)}{x_i \exp\left(-\frac{\lambda_{ii}}{RT}\right)} \tag{3.118}$$

In Equation (3.118), x_{ji} is the local mole fraction or probability of finding molecules of type j in the vicinity or around the central i molecule and λ_{ji} is proportional to the potential energies of the interactions between the i and j molecules. Both x_{ij} and λ_{ij} are defined in an analogous manner.

The final form of Wilson's equation as applied to a binary mixture is as follows:

$$\frac{G^E}{RT} = -x_1 \ln(x_1 + \Lambda_{12} x_2) - x_2 \ln(x_2 + \Lambda_{21} x_1) \tag{3.119}$$

where

$$\Lambda_{12} = \frac{V_2}{V_1} \exp\left(-\frac{\lambda_{12} - \lambda_{11}}{RT}\right) \tag{3.120}$$

$$\Lambda_{21} = \frac{V_1}{V_2} \exp\left(-\frac{\lambda_{21} - \lambda_{22}}{RT}\right) \tag{3.121}$$

and $\lambda_{ji} = \lambda_{ii}$.

Consequently, the adjustable parameters are $(\lambda_{12} - \lambda_{11})$ and $(\lambda_{21} - \lambda_{22})$ for a binary mixture. Applying the partial molar property operator allows for the activity coefficients to be obtained:

$$\ln\gamma_1 = -\ln(x_1 + \Lambda_{12} x_2) + x_2\left(\frac{\Lambda_{12}}{x_1 + \Lambda_{12} x_2} - \frac{\Lambda_{21}}{x_2 + \Lambda_{21} x_1}\right) \tag{3.122}$$

$$\ln\gamma_2 = -\ln(x_2 + \Lambda_{21}x_1) - x_1\left(\frac{\Lambda_{12}}{x_1 + \Lambda_{12}x_2} - \frac{\Lambda_{21}}{x_2 + \Lambda_{21}x_1}\right) \qquad (3.123)$$

For a greater insight into the derivation of the Wilson equation, Appendix B can be consulted. As with the other semi-theoretical approaches, the Wilson model is readily extended to include treatment of multicomponent systems, due to these models containing binary interaction terms, which for the Wilson equation is Λ_{ij}. The activity coefficient expressions for multicomponent mixtures are presented in Table 3.1. In addition to being applicable to treating multicomponent mixtures, the parameters of the Wilson equation have limited inbuilt temperature dependence, as in Equations (3.120) and (3.121).

However, the parameter $\left(\frac{\lambda_{ij} - \lambda_{ii}}{RT}\right)$ can be treated as temperature-independent over small temperature intervals facilitating the computation of γ_i from isothermal and isobaric data.

The Wilson equation is also able to represent systems that exhibit positive deviations ($G^E > 0$) and negative deviations ($G^E < 0$) from ideality. Generally, the parameters are negative for negative deviations and positive for positive deviations.

The Wilson equation is generally superior to the empirical equations and other semi-theoretical models for the representation of the liquid phase behaviour of polar non-associating, polar associating and nonpolar molecules. Its flexibility is demonstrated in its ability to treat highly nonideal systems and those with asymmetrical G^E curves. However, there are some significant shortcomings of the Wilson equation, which relate both to the computation of numerical values of the parameters and limitations of the model. Walas (1985) reports that for ($\gamma_i < 1$), there are difficulties that are encountered with regards to the presence of multiple roots and that negative values of the parameters are not allowed for representation of the activity coefficients across the whole composition range. The Wilson equation also cannot represent any extrema in the curves of activity coefficient versus composition. The most significant downfall is the inability of the equation to treat systems that exhibit limited miscibility *i.e.* liquid-liquid equilibria, across the concentration range. There are no values of the adjustable parameters within the mathematical framework of the original Wilson equation that are able to satisfy the conditions for phase splitting, which requires that roots for the mathematical condition of $\left(\frac{\partial^2(\Delta G_{mixing})}{\partial x^2} = 0\right)$ be found, where ΔG_{mixing} is the Gibbs energy of mixing.

Table 3.1. Activity coefficients from G^E models for multicomponent mixtures.

Model	Activity coefficient expression
Wilson	$\ln\gamma_i = -\ln\left(\sum_{j=1}^{m}\Lambda_{ij}x_j\right) + 1 - \sum_{k=1}^{m}\frac{x_k\Lambda_{ki}}{\sum_{j=1}^{m}\Lambda_{kj}x_j}$
T- K Wilson	$\ln\gamma_i = -\ln\left(\sum_{j=1}^{m}\Lambda_{ij}x_j\right) - \sum_{k=1}^{m}\frac{x_k\Lambda_{ki}}{\sum_{j=1}^{m}\Lambda_{kj}x_j} + \ln\left(\sum_{j=1}^{m}\frac{x_jV_j}{V_j}\right) + \sum_{k=1}^{m}x_k\left(\frac{\frac{V_i}{V_k}}{\sum_{j=1}^{m}\frac{V_jx_j}{V_k}}\right)$
NRTL	$\ln\gamma_i = \frac{\sum_{j=1}^{m}\tau_{ji}G_{ji}x_j}{\sum_{k=1}^{m}G_{ki}x_k} + \sum_{j=1}^{m}\frac{x_jG_{ij}}{\sum_{k=1}^{m}G_{kj}x_k}\left(\tau_{ij} - \frac{\sum_{r=1}^{m}x_r\tau_{rj}G_{rj}}{\sum_{k=1}^{m}x_kG_{kj}}\right)$
UNIQUAC	$\ln\gamma_i = \ln\frac{\Phi_i}{x_i} + \frac{z}{2}q_i\ln\frac{\theta_i}{\Phi_i} + l_i - \frac{\Phi_i}{x_i}\sum_{j=1}^{m}x_jlj - q_i\ln\left(\sum_{j=1}^{m}\theta_j\tau_{ji}\right) + q_i - q_i\sum_{j=1}^{m}\frac{\theta_j\tau_{ij}}{\sum_{k=1}^{m}\theta_k\tau_{kj}}$

Wilson attempted to remedy the above flaw inherent in the algebraic form of the equation through the addition of a third empirical constant, C, to account or predict limited miscibility.

$$\frac{G^E}{RT} = C\left[x_1\ln(x_1 + \Lambda_{12}x_2) + x_2\ln(x_2 + \Lambda_{21}x_1)\right] \qquad (3.124)$$

However, the addition of the third parameter, which has no physical significance to molecular properties, only serves to introduce further complexities. For the general multicomponent model, which is based on molecular pairs and binary interaction terms, the model becomes much more complex as C is not readily incorporated into a model with the binary interaction terms, as the former is not related in any specific way to the interactions between the mixture components. Also, the addition of another term increases the parameter interdependence, which is undesirable as it results inevitably in an increase in the number of different parameter value

combinations or sets and makes the regression procedure much more difficult *i.e.* longer computation times.

Probably most successful modification of the Wilson equation to handle partially miscible systems was that of Tsuboka and Katayama (1975), known as the T-K Wilson equation, where for a binary mixture, the excess Gibbs energy is represented as:

$$\frac{G^E}{RT} = x_1 \ln \frac{(x_1 + V_{12}x_2)}{(x_1 + \Lambda_{12}x_2)} + x_2 \ln \frac{(x_2 + V_{21}x_1)}{(x_2 + \Lambda_{21}x_1)} \qquad (3.125)$$

where

$$V_{ij} = \frac{V_j}{V_i} \qquad (3.126)$$

The corresponding activity coefficients are the following:

$$\ln \gamma_1 = \ln \frac{(x_1 + V_{12}x_2)}{(x_1 + \Lambda_{12}x_2)} + (\beta - \beta_v)x_2 \qquad (3.127)$$

$$\ln \gamma_2 = \ln \frac{(x_2 + V_{21}x_1)}{(x_2 + \Lambda_{21}x_1)} - (\beta - \beta_v)x_1 \qquad (3.128)$$

where

$$\beta_v = \frac{V_{12}}{(x_1 + V_{12}x_2)} - \frac{V_{21}}{(x_2 + V_{21}x_1)} \qquad (3.129)$$

$$\beta = \frac{(\Lambda_{12})}{(x_1 + \Lambda_{12}x_2)} - \frac{(\Lambda_{21})}{(x_2 + \Lambda_{21}x_1)} \qquad (3.130)$$

In using the T-K Wilson equation, caution must be exercised when using activity coefficients from vapour-liquid equilibrium data for the prediction of liquid-liquid equilibria, as the latter are very sensitive to the parameter values (Walas, 1985). There is generally good agreement between the Wilson and T-K Wilson equations when the volume ratios (V_{ij}) are close to unity. Another significant modification of the original Wilson equation to handle ternary liquid-liquid

equilibria was that of Huang and Lee (1994), a model which was later shown to be capable of simultaneously representing G^E, H^E and VLE (Huang and Lee, 1996).

The Non-Random Two-Liquid (NRTL) Equation

The NRTL equation was proposed in 1968 by Renon and Prausnitz as an improvement to that of the Wilson equation. The model was based on the "local composition" concept of Wilson (1964) and the two-liquid theory of Scott (Hildebrand and Scott, 1964). The local composition was defined, in an analogous fashion to that of Wilson, as:

$$\frac{x_{ij}}{x_{jj}} = \frac{x_i \exp\left(-\alpha_{ij}\frac{g_{ij}}{RT}\right)}{x_j \exp\left(-\alpha_{ij}\frac{g_{jj}}{RT}\right)} \qquad (3.131)$$

where the g_{ij} term is analogous to the λ_{ij} term used by Wilson to characterize the interaction energies between the binary pairs of component molecules and α_{ij} is the third parameter, which accounts for the non-randomness of the mixture.

For non-random mixtures, α_{ij} was related to the reciprocal of the coordination number (z), which was obtained from the lattice theory of Guggenheim (1952). The lattice theory essentially served to describe the nonidealities (due to size and shape effects) of athermal mixtures where molecules occupy fixed lattice sites. In the lattice theory, each molecule has z neighbours, hence z is actually the number of molecules surrounding or just touching the reference molecule in a lattice structure. Regression of experimental data has produced a wide variety of values for α_{ij} and it is acknowledged that α_{ij} can only be considered strictly as an empirical parameter and not related to molecular interactions; since lattice theory is not used in the development of the NRTL equation. There is much controversy over the optimum values of the non-randomness parameter. With regards to completely random mixtures *i.e.* no "ordering effects", local compositions are equal to overall compositions, giving $\alpha_{ij} = 0$ and for completely non-random mixtures, $\alpha_{ij} = 1$. However, in many experimental regressions, the best values for α_{ij} are often not between 0 and 1. In the original paper, Renon and Prausnitz recommended a range of 0.2 - 0.47, which was dependent upon the chemical nature of the constituents. Malanowski and Anderko (1992) consider typical values as being in the range of -1 to 0.5. For partially miscible and miscible binary mixtures, Marina and Tassios (1973) proposed that a value of -1 produces excellent representation of the data. Walas (1985) conducted an in-depth study of the optimal

values of α_{ij} for a variety of systems and although rather inconclusive, values of 0.3 were recommended for non-aqueous mixtures and 0.4 for aqueous organic mixtures.

The final form of the NRTL equation is as follows:

$$\frac{G^E}{RT} = x_1 x_2 \left[\frac{\tau_{21} G_{21}}{x_1 + G_{21} x_2} + \frac{\tau_{12} G_{12}}{x_2 + G_{12} x_1} \right] \tag{3.132}$$

where

$$\tau_{12} = \frac{(g_{21} - g_{11})}{RT} \tag{3.133}$$

$$\tau_{21} = \frac{(g_{12} - g_{22})}{RT} \tag{3.134}$$

$$G_{21} = \exp(-\alpha_{12} \tau_{21}) \tag{3.135}$$

$$G_{12} = \exp(-\alpha_{12} \tau_{12}) \tag{3.136}$$

The activity coefficient expressions for the NRTL equation can be represented as follows:

$$\ln \gamma_1 = x_2^2 \left[\tau_{21} \left(\frac{G_{21}}{x_1 + G_{21} x_2} \right)^2 + \left(\frac{\tau_{12} G_{12}}{(x_2 + G_{12} x_1)^2} \right) \right] \tag{3.137}$$

$$\ln \gamma_2 = x_1^2 \left[\tau_{12} \left(\frac{G_{12}}{x_2 + G_{12} x_1} \right)^2 + \left(\frac{\tau_{21} G_{21}}{(x_1 + G_{21} x_2)^2} \right) \right] \tag{3.138}$$

When $\alpha_{ij} = 0$, the NRTL equation reduces to one term polynomial equation, obtainable from the generalized empirical equation in (3.111). The Local Effective Mole Fraction equation (LEMF) is the NRTL equation with $\alpha_{ij} = -1$. For more details on the theoretical aspects of the derivation of the NRTL equation, Appendix B can be consulted. As with the Wilson equation, the NRTL equation can be extended to the treatment of multicomponent systems with only the use of binary interaction terms for the molecular pairs. This is shown in Table 3.1. However,

unlike the Wilson equation, the NRTL equation is able to represent liquid-liquid equilibria, together with providing excellent representation of highly nonideal systems.

The interaction energy parameters in the form of $(g_{21} - g_{11})$ and $(g_{12} - g_{22})$ have a limited explicit temperature dependence, as for the Wilson equation. However, the parameters can be regarded as independent of temperature for small temperature intervals. For larger temperature intervals, Renon (1971) suggested that a linear temperature dependence for the parameters be used as follows:

$$\tau_{j,i} = \tau_{j,i}^{(0)} + \tau_{j,i}^{(T)}(T - 273.15) \tag{3.139}$$

$$\alpha_{j,i} = \alpha_{j,i}^{(0)} + \alpha_{j,i}^{(T)}(T - 273.15) \tag{3.140}$$

The correlations in Equations (3.139) and (3.140) serve to only further increase the number of parameters in the correlation *i.e.* from 3 to 6 for each binary mixture. Malanowski and Anderko (1992) express the opinion that despite the above two relations not being theoretically justified, the relations cannot be disproved without sufficient experimental data *i.e.* multiple sets of isothermal data over a large temperature range.

The use of three parameters in the NRTL approach is seen as a downfall of this equation when compared to other semi-theoretical approaches. As discussed before, an increase in the number of parameters only serves to further complicate the model by increasing the interdependence of the parameters and increasing computation time for the correlation.

The Universal Quasi-Chemical (UNIQUAC) Equation

Following on from the work that had preceded them, Abrams and Prausnitz (1975) attempted to combine the attributes of the Wilson and the NRTL equations *i.e.* the local composition concept and the two-fluid theory to produce a two-parameter expression in what could be viewed as an extension of the quasi-chemical lattice theory of Guggenheim (1952), known as the UNIQUAC equation. The equation is actually an approximation of the excess molar Helmholtz energy with that of the excess molar Gibbs energy *i.e.* $A^E \approx G^E$, and is valid as long as the molar volumes of mixing are small, which is satisfied for subcritical conditions.

The proposal of the UNIQUAC model was of great significance as it attempted to distinctly represent the effect of the size and shape of the molecule (entropic or athermal contribution) and

the differing intermolecular interaction energies (energetic or thermal contribution) in a single equation. The former was known as the configurational or combinatorial contribution, which attempted to describe the interactions between molecules of the same type but of different sizes and shapes and the latter was known as the residual contribution, which described interactions between molecules of different chemical natures (Malanowski and Anderko, 1992). Hence the UNIQUAC equation for the excess Gibbs energy of liquid mixtures is the following:

$$G^E = G^E_{combinatorial} + G^E_{residual} \tag{3.141}$$

With regards to the combinatorial contribution for size and shape effects, the three-dimensional lattice representation of the liquid phase, as presented by Guggenheim (1952), was adopted. For a polysegmented molecule, each segment of the molecule occupies a single lattice site to give a total of r_i segments for each molecule of type i. As in the two-fluid theory devised by Scott, an approximation of the interaction energy between a segment in a central lattice site and that of the segments surrounding the central cell is required. Although the coordination number (z) *i.e.* the number of nearest neighbours, is the same for all the segments, consideration has to be given to the different sizes and shapes of molecules. The latter inherently affects the ability of segments of different molecules to interact with each other. Consequently, the exposed surface area available for interaction is important in characterizing athermal interactions. As opposed to the Wilson and NRTL equations, which use local volume fractions in the equation expression, Abrams and Prausnitz used local surface area fractions to more accurately characterize surface interactions between molecules. Consequently, in the athermal case, the contribution to the excess Gibbs energy is governed entirely by considerations of the structure of the molecule only *i.e.* size and shape. There are no chemical interactions to influence the ordering of the molecules in molecular clusters and hence the average local surface area fractions are equal to the total or bulk surface area fractions of the molecules. This is in stark contrast to the Wilson and NRTL derivations, where the energetic interactions and the size/shape effects are lumped into a single term through the local composition concept, where use is made of the Boltzmann constant in the local mole fraction. The average bulk surface area fractions (θ_i) can be represented as:

$$\theta_i = \frac{x_i q_i}{\sum_j^n x_j q_j} = \theta_{ij} \tag{3.142}$$

where θ_i is the bulk surface area fraction of molecule i, θ_{ij} is the surface area fraction of the molecules of i in a region immediately surrounding a central j molecule and q is the surface area

parameter. The term "immediately surrounding" is an arbitrary description defined by the coordination number.

For the residual case, where the chemical identities of the molecules differ vastly, the chemical interactions between the molecules have to be considered and the average local surface area fraction will indeed be influenced by the energies of the interactions between the molecules. By modifying the Wilson expression for the local volume fractions, Abrams and Prausnitz then approximated the average surface area fraction for the athermal case as follows:

$$\frac{\theta_{ji}}{\theta_{ii}} = \frac{\theta_j \exp\left(-\frac{u_{ji}}{RT}\right)}{\theta_i \exp\left(-\frac{u_{ii}}{RT}\right)} \tag{3.143}$$

where u_{ji} is the term which serves to approximates the interaction energy between molecules i and j. From the above, it can be seen that the final form of the UNIQUAC equation can actually be expressed as a combination of two parts, a combinatorial and a residual part. The former *i.e.* the combinatorial part, as mentioned above arises solely from structural considerations and consequently a function of concentration and pure component molecular structural parameters *i.e.* a molecular size parameter (r) and an external surface area parameter (q). The residual part takes into account the interaction energies between the segments of molecules and it is therefore a function of temperature and the interaction energies (u_{ji} - u_{ii}) and is hence dependent upon the properties of the mixture.

For a binary system, these two terms are represented as:

$$\frac{G^E_{combinatorial}}{RT} = x_1 \ln\frac{\Phi_1}{x_1} + x_2 \ln\frac{\Phi_2}{x_2} + \frac{z}{2}\left(q_1 x_1 \ln\frac{\theta_1}{\phi_1} + q_2 x_2 \ln\frac{\theta_2}{\phi_2}\right) \tag{3.144}$$

$$\frac{G^E_{residual}}{RT} = -q_1 x_1 \ln(\theta_1 + \theta_2 \tau_{21}) - q_2 x_2 \ln(\theta_2 + \theta_1 \tau_{12}) \tag{3.145}$$

where the Φ_i term is the average segment fraction of component i, θ_i is the average surface area fraction of molecule i and the τ_{ji} term is an adjustable parameter, containing the energetic interaction terms (u_{ji} and u_{ii}). These are shown in Equations (3.146) and (3.147).

$$\Phi_i = \frac{x_i r_i}{x_1 r_1 + x_2 r_2} \tag{3.146}$$

$$\theta_i = \frac{x_i q_i}{x_1 q_1 + x_2 q_2} \tag{3.147}$$

$$\tau_{ji} = \left[- \frac{\left(u_{ji} - u_{ii}\right)}{RT} \right] \tag{3.148}$$

The activity coefficient expressions, as for the excess Gibbs energy, consist of the combinatorial (γ_i^C) and residual contributions (γ_i^R) in two separate parts as shown below:

$$\ln \gamma_i = \ln \gamma_i^C + \ln \gamma_i^R \tag{3.149}$$

$$\ln \gamma_1^C = \ln \frac{\Phi_1}{x_1} + \frac{z}{2} q_1 \ln \frac{\theta_1}{\Phi_1} + \Phi_2 \left(l_1 - \frac{r_1}{r_2} l_2 \right) \tag{3.150}$$

$$\ln \gamma_1^R = - q_1 \ln\left(\theta_1 + \theta_2 \tau_{21}\right) + \theta_2 q_1 \left(\frac{\tau_{21}}{\theta_1 + \theta_2 \tau_{21}} - \frac{\tau_{12}}{\theta_2 + \theta_1 \tau_{12}} \right) \tag{3.151}$$

and

$$\ln \gamma_2^C = \ln \frac{\Phi_2}{x_2} + \frac{z}{2} q_2 \ln \frac{\theta_2}{\Phi_2} + \Phi_1 \left(l_2 - \frac{r_2}{r_1} l_1 \right) \tag{3.152}$$

$$\ln \gamma_2^R = - q_2 \ln\left(\theta_2 + \theta_1 \tau_{12}\right) + \theta_1 q_2 \left(\frac{\tau_{12}}{\theta_2 + \theta_1 \tau_{12}} - \frac{\tau_{21}}{\theta_1 + \theta_2 \tau_{21}} \right) \tag{3.153}$$

where z is the coordination number (set equal to 10) and l_i is a simplifying term:

$$l_i = \frac{z}{2}\left(r_i - q_i\right) - \left(r_i - 1\right) \tag{3.154}$$

Abrams and Prausnitz defined the size and area parameters as the following:

$$r_i = \frac{V_{wi}}{0.01517} \tag{3.155}$$

$$q_i = \frac{A_{wi}}{2.5 \times 10^8} \tag{3.156}$$

where V_{wi} (m^3/kmol) and A_{wi} (m^3/kmol) are the van der Waals volumes and areas, respectively, that obtained from the method of Bondi (1968).

A much simpler approach for the evaluation of the size (r_i) and the surface (q_i) parameters is achieved by obtaining the parameters as the sum of the molecular structure contributions (R and Q, respectively) of the various functional groups that are present in the molecule *i.e.* the group contribution method (Sandler, 1999). In this method, the R and Q values of a relatively small number of functional groups or sub-groups can be used to obtain the molecular structural parameters of a huge collection of different molecular structures involved in phase equilibrium studies.

In terms of modifications of the equation, Anderson and Prausnitz (1978) proposed later that empirically adjusted values of the surface area parameter q_i be used *i.e.* q_i' in the calculation of $G^E_{residual}$ for mixtures containing water or alkanols to give a better agreement for any mixtures containing these components, especially alkanol + hydrocarbon systems (Prausnitz *et al.*, 1980) For components containing a hydroxyl group, the surface area available for interaction is smaller that the geometric external surface area, which is given by q_i. Consequently, in the modified UNIQUAC equation, the average surface area fraction terms for a binary mixture as follows:

$$\theta_i' = \frac{x_i q_i'}{x_1 q_1' + x_2 q_2'} \tag{3.157}$$

For an in-depth look at other significant modifications of the UNIQUAC equation, the text of Walas (1985) can be consulted, together with the work of Maurer and Prausnitz (1978) and more recently, the work of Wiesniewska-Goclowska and Malanowski (2001).

As was the case with the preceding models based on the "local composition concept", the UNIQUAC equation is readily extendable to the treatment of multicomponent mixtures (shown

in Table 3.1). Although all the factors in the UNIQUAC equation were originally assumed to be temperature-independent, it can be seen from Equation (3.148) that this model has an inbuilt limited explicit temperature dependence. Prausnitz *et al.* (1980) claimed that the interaction energies were "often only weakly dependent on temperature" and it is also mentioned by Reid *et al.* (1987) that the UNIQUAC's parameters quite frequently have indeed a smaller temperature dependence when compared to the other multicomponent models. The accuracy of the model can be further improved by expressing the coordination number (z) in a temperature-dependent form. Skjold-Jorgensen *et al.* (1980) proposed the following quadratic form for a temperature-dependent coordination number:

$$z = 35.2 - 0.1272T - 0.00014T^2 \qquad (3.158)$$

The nominal value of 10 for the coordination number is justified for many liquids under normal conditions (Walas, 1985), however, certain researchers such as Krumins *et al.* (1980) described certain instances where a value of 6 provided more accurate correlations.

The many advantages of the UNIQUAC equation include the treatment of multicomponent mixtures, the inbuilt temperature dependence, applicability to liquid-liquid equilibria and possible superior representation of highly nonideal or complex mixtures consisting of widely differing components. However, even with its greater algebraic complexity and more sound theoretical basis, it is often inferior in the representation of vapour-liquid equilibrium data of moderately nonideal systems to simpler models (Walas, 1985).

Simplifications of G^E Models for binary mixtures

It is often the case that the use of more than one adjustable parameter in a correlating equation for a binary mixture is not justified due to the data set being quite scattered or the size of the data set being quite limited (Malanowski and Anderko, 1992). Although there are correlating equations such as the one-parameter Margules equation, shown in Equation (3.88), which meet the above requirement, it has been shown that the real binary systems do not exhibit a symmetric behaviour with regards to the composition dependence of the activity coefficients. A more effective approach is to use simplified one-parameter forms of the local composition models through the use of reasonable physical assumptions (Reid *et al.*, 1987).

For the Wilson equation, if it is assumed that ($\lambda_{ij} = \lambda_{ji}$) the following is obtained:

$$\lambda_{ii} = -\beta(\Delta H_{v,i} - RT) \qquad (3.159)$$

In Equation (3.159), β is a proportionality constant and $\Delta H_{v,i}$ is the enthalpy of vapourization of pure component i at the temperature, T. An analogous expression can be obtained for λ_{jj} and with β being fixed, there is only one adjustable parameter *i.e.* λ_{ij}. The value of β can be an arbitrary one such as (β = 1), as used by Tassios (1971) or if theoretical considerations are employed, the following is obtained:

$$\beta = \frac{z}{2} \tag{3.160}$$

where z is the coordination number, as described previously. This more successful approach was employed by both Wong and Eckert (1971) and Schreiber and Eckert (1971). There were other researchers such as Hiranuma and Honma (1975) who correlated λ_{ij} with intermolecular dispersive interactions and dipole-dipole forces.

For molecules with considerable or large size discrepancies, Lauderelli *et al.*(1975) proposed that Equation (3.159) be used for the molecule with the smaller molar volume (molecule 2) and that for the molecule for the larger molar volume (molecule1), the following be used:

$$\beta = \frac{z}{2}\left(\frac{V_2^L}{V_1^L}\right) \tag{3.161}$$

where V_1^L and V_2^L are the liquid molar volumes of molecules 1 and 2, respectively. The parameters $\lambda_{ij}, \lambda_{jj}$ and λ_{ii} are considered as purely being interaction energies per unit segment and not per molecule and in this case, the unit segment is that corresponding to one molecule of component 2.

For the NRTL equation, Bruin and Prausnitz (1971) formulated an expression analogous to that for the Wilson equation in Equation (3.159), where g_{ii} was substituted for λ_{ii} and a fixed value for α_{ij} was used.

A one-parameter form for the UNIQUAC equation was also obtained by Abrams and Prausnitz (1975) by representing the energetic parameters, with the following:

$$u_{ii} = -\frac{\Delta U_i}{q_i} \tag{3.162}$$

The expression for the cross-interaction energy term is shown in Equation (3.163).

$$u_{ij} = u_{ji} = \left(u_{ii} u_{jj}\right)^{0.5} \left(1 - c_{ij}\right) \tag{3.163}$$

where

$$\Delta U_i \approx \Delta H_{vi} - RT \tag{3.164}$$

The approximation in Equation (3.164) is only applicable for conditions that are far away from the critical region. The only adjustable parameter is c_{ij}, which is positive and much smaller than unity for mixtures of nonpolar fluids. For mixtures where there are associations between unlike molecules which are stronger than that for like molecules, c_{ij} may be negative.

Activity Coefficients at Infinite Dilution from the G^E Models

Limiting activity coefficients or activity coefficients at infinite dilution $\left(\gamma_i^\infty\right)$ can be readily evaluated from the reduction of the various activity coefficient models that have been presented above (since $\gamma_i \rightarrow \gamma_i^\infty$ as $x_i \rightarrow 0$). These values are indispensable for the accurate design of separation equipment operating in the dilute region and also of considerable interest from a theoretical standpoint for the development and validation of correlative and predictive liquid phase behaviour models. The various expressions for γ_i^∞ that are obtained from a selection of the G^E models for binary mixtures are shown in Table 3.2.

Due to difficulties in obtaining accurate experimental data in the dilute regions and limitations associated with the mathematical treatment of experimental data, the use of activity coefficient model parameters has to be used with caution for the determination of γ_i^∞ values.

Table 3.2. Expressions for binary activity coefficient correlations at infinite dilution.

Model	Expression
Margules (2-suffix)	$\ln\gamma_i^{\infty} = A$
Margules (3 & 4-suffix)	$\ln\gamma_i^{\infty} = A_{ij}$
van Laar	$\ln\gamma_i^{\infty} = A_{ij}$
Wilson	$\ln\gamma_i^{\infty} = -\ln\Lambda_{ij} + 1 - \Lambda_{ji}$
NRTL	$\ln\gamma_i^{\infty} = \tau_{ij}\exp\left(-\alpha_{ij}\tau_{ij}\right) + \tau_{ji}$
UNIQUAC	$\ln\gamma_i^{\infty} = m + q_i - q_i\left(\tau_{ij} + \ln\tau_{ji}\right)$ where $m = \ln\left(\frac{r_i}{r_j}\right) + \frac{z}{2}q_i\left(\frac{q_i r_j}{q_j r_i}\right)$

In general, the determination of γ_i^{∞} values through the extrapolation of VLE data obtained at finite concentrations either through the use of G^E model parameters or graphical techniques is not advocated for accurate measurements (Raal and Muhlbauer, 1998). There are much more effective extrapolative techniques as those devised by Gatreaux and Coates (1955) and Ellis and Jonah (1962), as modified by Maher and Smith (1979a). These are discussed in Appendix B.

Comparison of the G^E Models

Due to the almost limitless combinations of diverse chemical components for phase equilibrium investigations coupled with a limited database of reliable phase equilibrium data for systems of interest over a wide pressure and temperature range, a conclusive evaluation of the efficiency and applicability of the models described above is yet to be determined.

Preference of one model over another is not only dictated by the fit of the experimental data to the model but is also in practical terms influenced by the computational and mathematical aspects of the implementation of the model. In general, the models contain two or three adjustable parameters and an increase in the number of parameters gives a better fit to the data.

However, at the same time, the taxing requirement that the VLE data set incorporated into the fitting procedure is both sufficiently large and accurate is necessitated to justify the use of more

constants. The performance of one model over the other is often not predictable and is often obtained through a "trial and error" approach in terms of the criteria defined above.

Many researchers have attempted to compare the correlating efficiency of the more popular activity coefficient models, as observed in the works of Walas (1985), Reid *et al.* (1987), Gess *et al.* (1991) and Malanowski and Anderko (1992).

Some of the findings can be summarized below as follows:

(a) The empirical models in the form of *the Margules, van Laar and related equations* have the advantage of simplicity in their algebraic form and ease of computational and mathematical evaluation of the adjustable parameters from the experimental data. In addition, these models often surprisingly exhibit excellent correlations of experimental data obtained for fairly non-ideal mixtures (including partially miscible systems), which are comparable or superior to semi-theoretical models. An example of the latter can be found in the work of Chamorro *et al.* (2004), where those systems exhibiting moderate positive deviations were investigated. The inherent disadvantages of this approach, as mentioned previously, are that the evaluated parameters have no theoretical significance or a temperature dependence (which is crucial for the simultaneous description of G^E and H^E) and are limited to binary systems (except for the Wohl expansion). In terms of the computational implementation of the models, the Margules and van Laar expressions are fairly well-behaved and convergence is achieved without the need for a large number of iterations, with only the van Laar equation being slightly sensitive to the initial parameter estimates (Gess *et al.*, 1991).

(b) The original "local composition" model *i.e. the Wilson equation* is able to correlate the vapour-liquid equilibrium of binary and multicomponent homogenous mixtures with great accuracy with only binary parameters. With its greater simplicity when compared to the NRTL and UNIQUAC equations, it is quite clearly the most favourable amongst the local composition models for the above application. It is indeed highly recommended for strongly nonideal binary mixtures such as alcohol + hydrocarbon mixtures (Reid *et al.*, 1987; Palmer, 1987). For the treatment of partially miscible systems, the use of the empirically-modified Wilson equation, shown in Equation (3.124) is undesirable. The third term (C) is simply a constant multiple of the expression for G^E, and as such, serves to introduce a strong inter-correlation between the parameters. In terms of the computational implementation, this results in convergence problems as obtaining a unique set of parameter values is difficult with this approach. This is as a result of a wide range of parameter combinations being made possible as a result of the parameters being highly correlated. This expression is also not suitable for representing multicomponent data. The T-K Wilson equation is more suitable for handing systems that exhibit partial miscibility,

although not being directly applicable to liquid-liquid equilibria and not being widely tested as the other multicomponent models. Models such as those by Huang and Lee (1994) are directly applicable to ternary liquid-liquid equilibria but have also not been widely tested for flexibility.

(c) The *NRTL equation* is recommended in many instances for the representation of vapour-liquid and liquid-liquid equilibria and in particular, is frequently superior to the other equations in representing aqueous systems. It is simpler in algebraic form than the UNIQUAC equation, however, it is a three-parameter model suffering from an increased interdependence of the three parameters. The arbitrary assignment of values to the non-randomness parameter can present many problems and can indeed affect the accuracy of the correlation.

(d) The *UNIQUAC equation* is applicable to multicomponent vapour-liquid and liquid-liquid equilibria, as for the NRTL equation; however, the model uses only two parameters per binary interaction. It is particularly recommended for molecules with widely differing sizes and for highly nonideal systems since it incorporates actual molecular parameters such as molecular surface areas and volumes in its formulation. The UNIQUAC equation has also shown to be more readily applicable to mixtures with macromolecules such as polymers since the surface areas available for interaction *i.e.* surface fraction (as opposed to mole fractions) are the primary concentration variable (Reid *et al.*, 1987). It is undoubtedly the most complex commonly encountered G^E equation and it is surprisingly outperformed on some occasions by some of the simpler empirical and semi-theoretical models when treating moderately nonideal systems.
In the correlations of the liquid phase nonidealities in this study with the γ_i - ϕ_i approach, the Wilson, T-K Wilson, NRTL, UNIQUAC and modified UNIQUAC equations were employed.

3.5.2.4 Computational aspects of the γ_i - ϕ_i approach

The key criterion for a successful correlation with a G^E model is to find the values of the adjustable parameters (usually two or three) that best fit the experimental data set by satisfying the γ_i - ϕ_i approach for satisfying the isofugacity criterion *i.e.* Equation (3.58). Since the number of points in an experimental VLE data set exceeds the number of adjustable parameters to be estimated, an exact solution of Equation (3.58) for several data sets is not possible. An exact fit for the data within the empirical or semi-theoretical framework of the model is not achievable due to random and systematic errors and shortcomings of the model (Prausnitz *et al.*, 1980). Consequently, the concept of a best fit is introduced and the optimum parameters must be obtained to best represent the constraints imposed by Equation (3.58) to allow for accurate interpolations and extrapolations.

As mentioned before, the statistical approach employed in the actual data fitting procedure is an important factor in determining the success of the correlation. In this regard two approaches have been traditionally employed within the field of phase equilibrium thermodynamics in the form of the least squares regression and the maximum likelihood regression approaches. Both methods have been compared and discussed at length by many researchers (Van Ness *et al.*, 1978; Prausnitz *et al.*, 1980; Palmer, 1987; Gess *et al.*, 1991). Despite the popularity of the maximum likelihood method, which accounts for all the errors in the experimental variables in the fitting procedure, it is intolerant of the presence of systematic errors in the data set (Skjold-Jorgensen, 1983). It has also been shown that despite the increased statistical complexity of the maximum likelihood method; it offers no real advantages over a least squares approach (Van Ness *et al.*, 1978). Consequently, the statistical approach employed for the reduction of VLE data with the γ_i - ϕ_i approach in this study has been the latter. Interested readers are referred to the works of Sutton and Macgregor (1977a, 1977b), Kemeny and Manczinger (1978), Van Ness *et al.*(1978), Neau and Peneloux (1981), Silverman and Tassios (1984) and Gess *et al.* (1991) for a discussion of the critical evaluations of the different computational approaches for the reduction of VLE data with the γ_i - ϕ_i approach.

In terms of the experimental thermodynamic variables, although it is desirable to obtain a full data set of P-T-x-y measurements, there are some equipment types that provide T-x isothermal or P-x isobaric data (Raal and Muhlbauer, 1998). The measurement of a full data set is also seen as an "overdetermination" of the system as the measurement of any three variables allows for the computation of any remaining variable with the Gibbs-Duhem equation. In general, if only two of the four experimental variables are known, the remaining two can be computed through the use of phase equilibrium calculations (Malanowski and Anderko, 1992), shown in Table 3.3. Of course, in accordance with the Phase Rule, only two of the four variables for a binary VLE data set are independent, with the other two being dependent. Van Ness *et al.* (1973) advocated such an approach for the vapour phase composition, which was viewed as being subject to an appreciable measurement uncertainty; necessitating computation. It is proposed that a greater expenditure of efforts be directed towards the accurate measurement of P-x data for isothermal data than obtaining vapour phase compositions. Consequently, where uncertainty exists in the measurement of a thermodynamic variable, the computation of the variable is favoured. The computations in Table 3.3, which serve as the framework for the data regression procedure can be used as a check of the consistency of the data (in the availability of P-T-x-y data) or for the computation of remaining thermodynamic variables in an incomplete data set. For the purposes of this work, the first two computations in Table 3.3 *i.e.* a BUBL P and a BUBL T calculation, as borrowed from the nomenclature of Prausnitz *et al.* (1967) are applicable.

Table 3.3. Phase equilibrium computations.

Computation	Independent variable	Dependent variable
Bubble-point (isothermal)	T, x	P, y
Bubble-point (isobaric)	P, x	T, y
Dew-point (isothermal)	T, y	P, x
Dew-point (isobaric)	P, y	T, x
P - T flash	P, T, q [a]	x, y

[a] Feed composition.

In the actual implementation of the least squares method, an objective function is formulated as the sum of squares of the errors between one or more experimental values and the calculated values. The objective is to obtain a set of parameter estimates (incorporated into the expression for the calculated quantity) which minimize the sum of the squares of the errors between the experimental and calculated values in the objective function. There is considerable flexibility and controversy in the formulation of an objective function to control the regression (Van Ness *et al.*, 1978; Silverman and Tassios, 1984). In a full data set (P-T-x-y), the errors in any of these four or in any combination of two of the four can be used as part of the objective function. In this work, the two objective functions (OF) used for the isothermal and isobaric bubble-point calculations are shown in Equations (3.165) and (3.166), respectively.

$$OF = \sum_{i=1}^{n} \left(P^{exp} - P^{calc} \right)_i^2 \tag{3.165}$$

where P^{exp} is the experimental pressure and P^{calc} is the calculated pressure.

$$OF = \sum_{i=1}^{n} \left(T^{exp} - T^{calc} \right)_i^2 \tag{3.166}$$

where T^{exp} is the experimental temperature and T^{calc} is the calculated temperature.

The algorithms for the actual implementation of the two regressions are shown in Figures (3.2) and (3.3), respectively. The above algorithms have been modified from the original forms, presented in the texts of Smith *et al.* (2001) and Gess *et al.* (1991) so as to allow for incorporation into the computational framework of a technical computing software package with an inbuilt regression function as in MATLAB® (version 7.0.1), where the Levenberg-Marquardt algorithm was employed in the regression to obtain the best values for the parameter estimates.

A brief description of the implementation of the above algorithms is provided below.

(a) BUBL P Calculation

The algorithm for this method is shown in Figure 3.2 and as will be shown for the BUBL T calculation, the regression consists of two loops *i.e.* an inner and outer loop; each with different constraints for the exit condition. In the BUBL P version, the outer loop is for pressure (P) and the inner for the vapour phase composition (y_i). The initialization of the outer loop proceeds with an input of the experimental temperatures $\{T\}$, experimental pressures $\{P^{exp}\}$, liquid phase compositions $\{x_i\}$ and an estimate of the model parameters. All the fugacity coefficients $\{\varphi_i\}$ are initialized to a value of unity. The vapour pressures of the pure components $\{P_i^{sat}\}$ are then computed with a suitable vapour correlation and an expression for the calculated values of the activity coefficients $\{\gamma_i\}$ is then obtained with the initial parameter estimates.

In the method used for the BUBL P regression, which is that of Barker (1953), the objective function for the regression, shown in Equation (3.165) requires an expression for the calculated pressure (P^{calc}). This can be derived from Equations (3.58) and (3.59) and is shown below as follows:

$$P^{calc} = \sum_{i=1}^{n} \frac{x_i \gamma_i P_i^{sat}}{\Phi_i} \tag{3.167}$$

Of course, for a binary mixture, n = 2.

A suitable regression technique (Levenberg-Marquardt, Nelder-Mead Simplex, *etc.*) can then minimize the OF to find the best fit for the parameters. One of the exit conditions for the outer loop is that convergence of the calculated pressure values be attained as specified by some pre-

determined tolerance (ε) *i.e.* $\Delta P = \frac{1}{n}\sum_{i=1}^{m}\left|P_2^{calc} - P_i^{calc}\right|_i$, where P_{calc}^2 is from the most recent minimization and P_1^{calc} from the preceding iteration.

The γ_i values are recalculated from the newly optimized activity coefficient model parameters and the calculation of the $\{y_i\}$ values is then achieved with the following:

$$y_i^a = \frac{x_i \gamma_i P_i^{sat}}{\Phi_i P} \tag{3.168}$$

where P and γ_i are the calculated values. The superscript "a" signifies that the y_i value is from the initial computation of y_i the inner loop.

The values of ϕ_i^{sat} and ϕ_i^v can then be computed with Equations (3.71) and (3.72) together with a suitable second virial coefficient estimation method such as that by Hayden and O'Connell (1975). Due to the interdependence of the y_i and ϕ_i^v values *i.e.* Equations (3.168) and (3.72), an iterational sequence in the form a second loop is necessitated to obtain internal consistency with regards to the above two quantities. In the first iteration, the values of y_i are normalized *i.e.* $y_i = \frac{y_i}{\sum_{i=1}^{n} y_i}$. This initial normalization serves to ensure that the set of y_i values used for the calculation of φ_i^v values do sum to unity and it facilitates the convergence of y_i values for subsequent iterations. The superscript "b" signifies that the y_i value is actually from the final computation of y_i in the inner loop. This step is omitted for all subsequent iterations as an exit condition with normalized y_i values (although summing up to unity) will not be consistent with the current pressure estimates.

The exit condition for the inner loop is a convergence of the y_i values upon recalculation from the ϕ_i^v values *i.e.* $\Delta y < \varepsilon$, as for the pressure. In addition to the convergence of the pressure, another constraint in the outer loop ensures that the y_i values calculated in the inner loop sum to unity. The parameter values from the previous iteration are used as the initial guesses for the next iteration sequence.

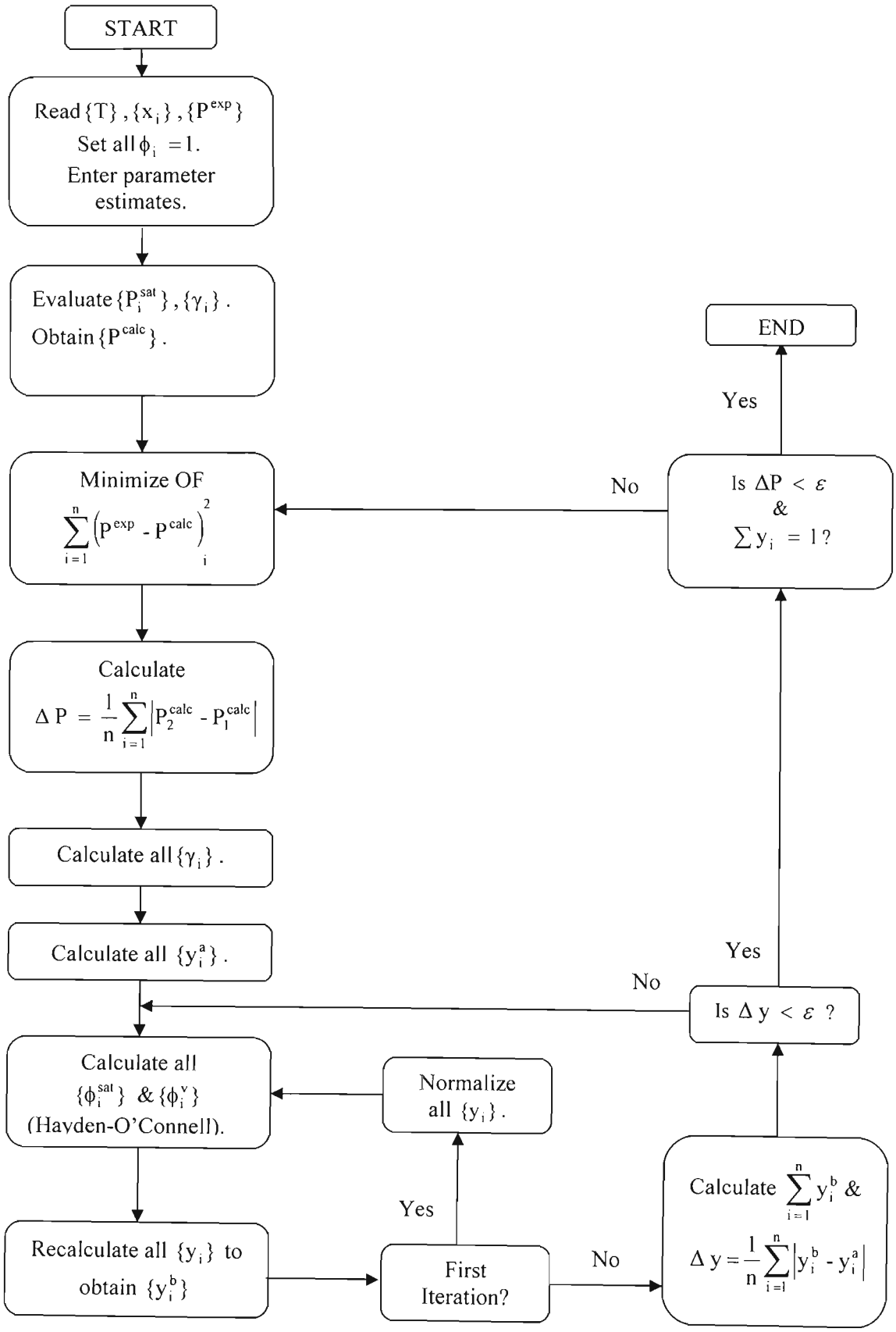

Figure 3.2. Algorithm for a LPVLE γ_i - ϕ_i BUBL P calculation.

When the constraints for both the inner and outer loop exit conditions have been satisfied, the iteration sequence terminates and the optimized parameter values, together with the calculated experimental variables, are obtained

(b) BUBL T Calculation

This computation, shown in Figure 3.3., is inherently more difficult than a BUBL P calculation as there is no explicit temperature dependence of the equilibrium condition in the γ_i - ϕ_i relation as shown in Equation (3.58). Consequently this necessitates an indirect route for the formulation of an expression for the calculated temperature in the objective function and this is quite often achieved through the pure component vapour pressure, where the latter is an explicit function of temperature.

In this approach, one of the components *i.e.* j is arbitrarily chosen as the key component, whose vapour pressure (P_j^{sat}) can be incorporated into an expression for the equilibrium temperature.

The practical implementation of this method involves the use of ratios of the vapour pressures of two components (i and j) in a binary mixture *i.e.* $\left(\frac{P_j^{sat}}{P_i^{sat}}\right)$, which, as opposed to the individual vapour pressures, are weaker functions of temperature (Smith *et al.*, 2001).

Multiplying both sides of Equation (3.167) by P_j^{sat} and rearranging, yields the following:

$$P_j^{sat} = P\sum_{i=1}^{n}\frac{\Phi_i}{x_i\gamma_i}\left(\frac{P_j^{sat}}{P_i^{sat}}\right) \qquad (3.169)$$

An expression for the equilibrium temperature can then be obtained by substituting the above in a suitable vapour pressure correlation (*e.g.* Antoine equation) with constants (A_j, B_j and C_j) that have been obtained from a reliable source. Rearranging the expression for the Antoine equation to solve for T as a function of P_j^{sat} yields the following:

$$T = \frac{B_j}{A_j - \ln P_j^{sat}} - C_j \qquad (3.170)$$

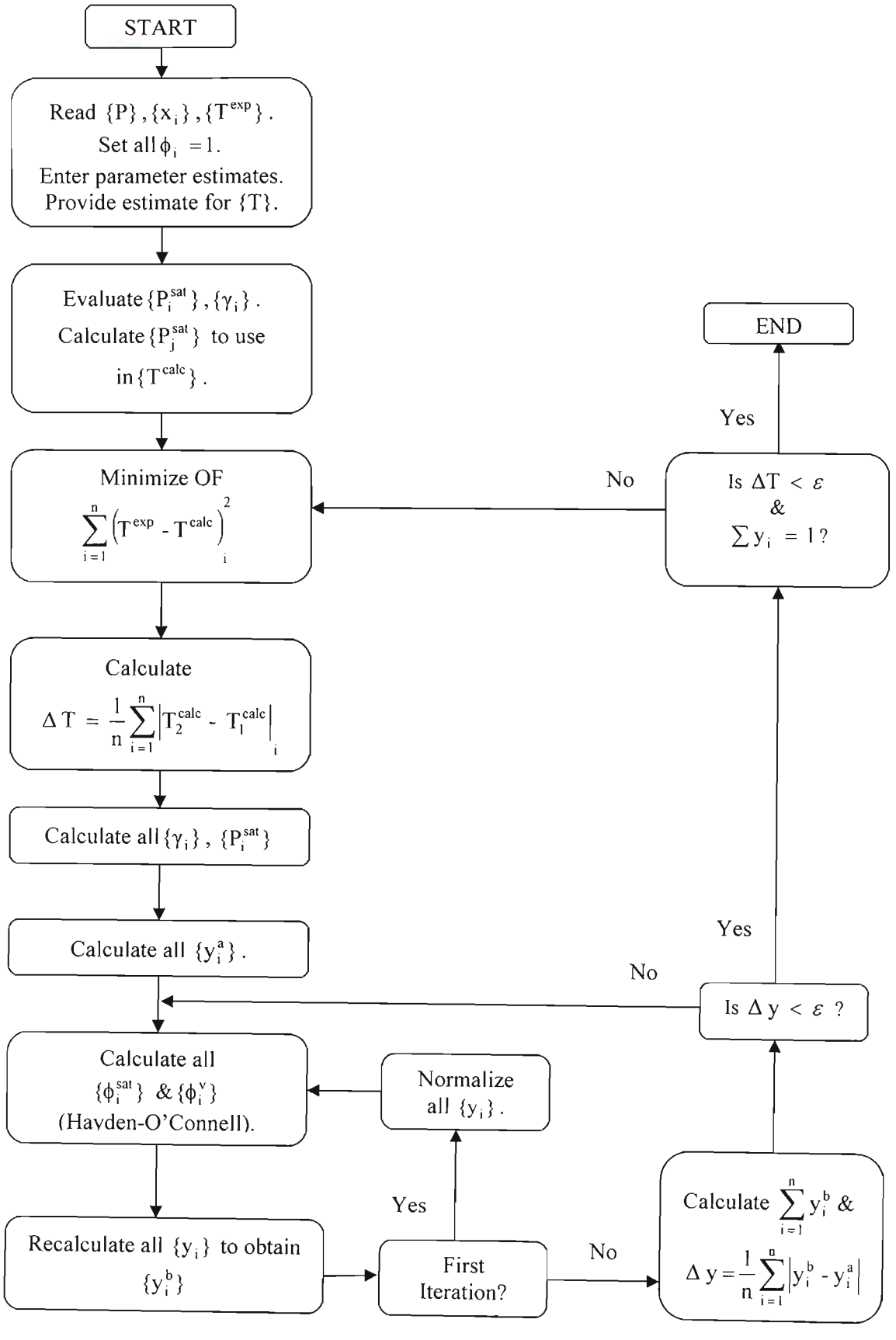

Figure 3.3. Algorithm for a LPVLE γ_i - ϕ_i BUBL T calculation.

Substituting the appropriate quantities and relations into Equation (3.169) and substituting this expression for into Equation (3.170), allows for an expression for the calculated temperature *i.e.* T^{calc}, to be obtained.

With regards to the initialization of the iteration sequence in Figure 3.3, a temperature estimate is required for the calculation of $\left(\frac{P_j^{sat}}{P_i^{sat}}\right)$ and Φ_i. Smith *et al.* (2001) propose a weighted average boiling point approach as follows:

$$T^{calc} = \sum_{i=1}^{m} x_i T_i^{sat} \tag{3.171}$$

Thereafter the algorithm is controlled by temperature values generated in the outer loop *i.e.* from the minimization of the objective function, which are used as the initial estimates for subsequent iterations.

The remaining aspects of the regression procedure, shown in Figure 3.3, can be grasped intuitively from the discussion of the procedure for a BUBL P calculation and from the theoretical framework for the method as established in Section (3.5.2).

The treatment of HPVLE with the γ_i - ϕ_i method involves the consideration of the different thermodynamic behaviour of the system (especially the vapour phase) at higher pressures and the formulation of alternative algorithms to those used in the low to moderate-pressure case. Two notable developments have been the Chao-Seader (1961) and the Prausnitz and Chueh (1968) combined methods, where the latter was employed for mixtures containing supercritical components. A discussion of the above two methods is provided in the text of Raal and Muhlbauer (1998).

3.5.3 The Phi-Phi (ϕ_i - ϕ_i) Method

3.5.3.1 Overview

As opposed to the γ_i - ϕ_i approach, the ϕ_i - ϕ_i approach, also known as the direct method, allows for the use of the same auxiliary function in the form of ϕ_i for the representation of the real thermodynamic behaviour of both the liquid and vapour phases in a mixture through the use of an equation of state with reliable mixing rules. In addition to calculating fugacities, equations

of state can perform a myriad of tasks such as the calculation of vapour pressures, critical properties, densities, enthalpies, heat capacities, entropies and excess free energies as a function of pressure, temperature and composition. The origins of this approach were largely as a result of a need to overcome the limitations of the γ_i - ϕ_i method in the treatment of supercritical components (where a standard-state fugacity would be required for the supercritical liquid) and to effectively maximize the advantages of a unified approach in facilitating phase equilibrium computations.

In the ϕ_i - ϕ_i approach, the expression for the liquid phase fugacity (f_i^L) is as follows:

$$f_i^L = x_i \phi_i^L P \tag{3.172}$$

Applying the isofugacity criterion in Equation (3.47) and substituting Equations (3.48) and (3.171), allows for an expression for the equilibrium condition in the ϕ_i - ϕ_i approach to be obtained:

$$y_i \varphi_i^V = x_i \phi_i^L \tag{3.173}$$

where the pressure term (P) on either side has been cancelled out. In addition to a knowledge of the experimental variables of the liquid and vapour phase compositions, the calculation of the fugacity coefficients for the liquid (ϕ_i^L) and vapour (ϕ_i^V) phases is required for the solution of Equation (3.172). The latter can obtained from exact pressure-explicit expressions of ϕ_i^L and ϕ_i^V for component i in a mixture:

$$\ln \phi_i^L = \left(\frac{1}{RT}\right) \int_{V^L}^{\text{infinity}} \left[\left(\frac{\partial P}{\partial n_i}\right)_{T,V,n_j} - \left(\frac{RT}{V^L}\right) \right] dV - \ln\left[\frac{PV^L}{n_T RT}\right] \tag{3.174}$$

$$\ln \phi_i^V = \left(\frac{1}{RT}\right) \int_{V^V}^{\text{infinity}} \left[\left(\frac{\partial P}{\partial n_i}\right)_{T,V,n_j} - \left(\frac{RT}{V^V}\right) \right] dV - \ln\left[\frac{PV^V}{n_T RT}\right] \tag{3.175}$$

For the solution of Equations (3.174) and (3.175), an accurate equation of state with appropriate mixing rules is required to represent the volumetric behaviour of the system for all the system components and their interactions over the entire vapour and liquid density range.

Despite the considerable advantages offered by the equation of state approach in the correlation and especially in the prediction of phase equilibria, the traditional limitations of this method have stemmed from the empirical nature of the mixing rules (Wicterle, 1978) and inaccurate representation of the volumetric properties of the liquid phase. This has resulted in noticeable deficiencies of the method for the representation of liquid phase densities and the phase equilibria of highly nonideal systems with polar, associating or highly asymmetric components. This has stimulated the development of novel mixing rules in a contemporary approach *i.e.* the "modern direct method", as coined by Raal and Muhlbauer (1998), to allow for the advantages of the γ_i - ϕ_i and ϕ_i - ϕ_i approaches to be combined in a hybrid method that would allow for the treatment of both condensable and noncondensable highly nonideal mixtures over a wide temperature and pressure range. The formulation of this method has tremendous repercussions for the development of a truly predictive unified approach that would allow for the use of existing parameters from previous correlations or excess free energy information in existing databanks or tables for the computation of industrially-significant phase equilibria (VLE, VLLE and LLE).

3.5.3.2 Equations of State (EOS)

As with the different approaches that were proposed for the correlation of the liquid phase composition dependence of the G^E function in Section (3.5.2.3), there have been many equations of state (Walas, 1985) have been proposed to represent the PVT behaviour for pure substances and mixtures (with suitable mixing rules). A slightly modified grouping of equations of state approaches into categories, as that presented by Raal and Muhlbauer (1998), can be presented as follows:

(a) Statistical mechanical n-parameter virial equation of state.
(b) Complex virial equations of state.
(c) Statistical thermodynamic perturbation theory equations of state
(d) Traditional cubic equations of state/ Classical mixing rules
(e) Traditional cubic equations of state/Novel mixing rules.

A detailed classification scheme of the EOS approach, together with a pertinent review of the contemporary state of cubic EOS models and mixing rules is provided by Valderrama (2003).
The two-parameter and the three-parameter *truncated virial equations of state* have been discussed within the framework of the applicability of the latter in the gamma-phi method. Despite its sound theoretical basis *i.e.* its statistical-mechanical correctness, it has not been

widely used otherwise. This can be attributed to the lack of information on virial coefficients for non-simple fluids and absence of third virial coefficient data (Sandler *et al.*, 1994). More importantly, due to its inability to represent the co-existence of the vapour and liquid phases, even with its flexibility in truncation (Walas, 1985) it is not applicable to the ϕ_i - ϕ_i method.

Unlike the virial equation of state, its empirical extensions in the form of *complex-type virial equations* such as the Benedict-Webb-Rubin relation (Benedict *et al.*, 1940), also known as the BWR equation of state, allow for the computation of the vapour-liquid equilibrium condition. The original BWR equation of state had eight parameters, which were obtained from empirical correlations of liquid fugacity and volumetric data (Palmer, 1987). However, due to the many deficiencies in the original formulation of the BWR equation of state (Sandler *et al*, 1994), there have been many modifications that have been proposed to improve the model. Of these, the most recommended and popular is the 11-parameter Benedict-Webb-Rubin-Starling (BWRS) equation of state which was proposed by Starling and Powers (1970). The form of this equation and the associated mixing rules for the treatment of mixtures is shown in Appendix B. Due to its algebraic complexity, its purely empirical form, inter-correlation of the parameters and the difficulty in determining roots for liquid and vapour densities, BWR-based equations are extremely unattractive and are the subject of very little attention in research circles (Palmer, 1987). A fairly comprehensive review of complex virial equations of state, in particular the BWR and its modifications, is provided by Sandler *et al.* (1994).

Perturbation theory equations of state have been formulated purely through the use of a statistical thermodynamic approach *i.e.* a molecular viewpoint, where bulk or macroscopic system properties are related to occurrences at the molecular level (Prausnitz *et al.*, 1979). Despite the relative simplicity of the theoretical framework of perturbation theory, it results in statistical mechanical equations of state that have complex forms. These equations, as opposed to classical thermodynamic models do not inherently incorporate a binary interaction parameter (*i.e.* k_{ij} for equations of state) and this is indeed important for the development of the predictive capability of an equation (which is obtained with $k_{ij} = 0$). These equations of state have been the subject of numerous efforts to develop equations that characterize specific interactions in groups of molecules with similar structures. The principal drawbacks of these methods are the computational complexity and the empirical nature of the models. Consequently, these methods have infrequently been employed in practical applications such as the calculation of mechanical properties of pure substances and mixtures and in the computation of phase equilibria.

Cubic equations of state are classified as PVT relations that are explicit in pressure and third-order in volume. The popularity of this family of equations stems from their algebraic simplicity in form, ease of computation with reliable solution algorithms, accuracy in thermodynamic representation and flexibility in describing wide-ranging phase behaviour (Raal and Muhlbauer, 1998). The great value of the cubic equation approach is that the values of the parameters of the equation can be obtained from pure component properties, making the method more amenable to the development of predictive methods. The success of this approach is most appropriately exemplified in the form of the Soave-Redlich-Kwong and Peng-Robinson equations of state being hailed as real success stories of applied chemical thermodynamics (Ghosh, 1999). The recognition that classical mixing rules were inapplicable to complex, highly nonideal mixtures and for the treatment of liquid phase fugacities necessitated the development of an alternative technique in the formulation of mixing rules for equations of state. In this approach, the use of novel mixing rules allows for an interrelation of information from traditionally low-pressure excess free energy models (A^E or G^E) and the interaction parameters of the equation of state via the mixing rules. In this way, the advantages of the combined method in LPVLE (in treating complex mixtures and the liquid phase) and the direct method (wide pressure range) can be combined in a single approach *i.e.* the modern direct method.

Discussion will be limited to cubic equations of state and the associated use of traditional and novel mixing rules, which comprise the field of interest of the author. An in-depth discussion of the remaining methods is beyond the scope of this study and interested readers are referred to the works of Wichterle (1978), Sandler *et al.* (1994), Raal and Mulbauer (1995, 1998), Sarry (1999), Wei and Sadus (2000) and Eliezer *et al.* (2002). The discussion of the cubic equations of state will initially be limited to a treatment of the pure fluid case only as a discussion of the approach as applied to mixtures will be deferred to the discussion on mixing rules, due to the complexity and importance of the latter.

Cubic Equations of State

The current body of literature on cubic equations of state is so vast that many researchers (Zabaloy and Vera, 1998; Sandler *et al.*, 1994) acknowledge the difficulty in providing a representative synopsis of the field in a generalized discussion of this approach. The extension and modification of cubic equations of state have been an active area of research ever since van der Waals published his prototype equation in 1873 (van der Waals, 1873). Since then, the more successful forms of the cubic equations of state have been responsible for wide applicability of the equation of state approach in the computer-aided design of industrial processes (process

simulators) and in the petroleum industry for gas, oil and condensate fluids (Stamataki and Tassios, 1998).

Out of the evolutionary process from the van der Waals equation of state, the Soave-Redlich-Kwong (Soave, 1972) and the Peng-Robinson (Peng and Robinson, 1976) equations of state have indeed been the most popular and successfully applied models for the representation of thermodynamic and phase equilibrium properties of pure components and mixtures (Twu *et al.*, 1998a; Ghosh, 1999; Valderrama, 2003). The SRK and PR EOS models are the most widely used cubic EOS employed in computer simulation packages, research and optimizations for thermodynamic and phase equilibrium properties (Valderrama, 2003). The original forms of the above equations and their modifications will be presented together with commentary on their applicability in the representation of the thermodynamic properties of pure substances and mixtures.

van der Waals Equation of State (1873) and the Generalized Cubic Equation of State

It was realized during early times that the application of the ideal gas equation was highly limited and hence inadequate for satisfying the demands of science and industry. In order to quantitatively account for the shortcomings of the above in the representation of the volumetric behaviour of fluids, van der Waals proposed the following PVT functional relationship:

$$P = \frac{RT}{V - b} - \frac{a}{V^2} \tag{3.176}$$

where P is the pressure, V is the molar volume, R is the universal gas constant, a is the attraction parameter and b is the repulsive parameter.

The a and b parameters serve to effectively characterize the forces between the molecules (considered as hard spheres) in a fluid as being either repulsive or attractive. The parameter a is actually a measure of the intermolecular attractive forces, which are dominant over relatively large separations of the molecular centres *i.e.* long-range interactions. The b parameter, also known as the effective molecular volume (Walas, 1985) or covolume term, serves to take into account the finite volumes possessed by molecules that gives rise to repulsive interactions when the molecules are in contact *i.e.* short-range interactions. It is a rough measure of the size of the hard sphere fluid molecules. Consequently the fluid pressure can be viewed as being due to a combination of two types of contributions, as quantified by an attractive and a repulsive term.

An examination of the form of Equation (3.176) for the hard sphere van der Waals equation of state (vdW Eos) reveals that these two terms are as follows:

$$P_{repulsive} = \left(\frac{RT}{V - b}\right) \tag{3.177}$$

$$P_{attractive} = -\left(\frac{a}{V^2}\right) \tag{3.178}$$

As can be inferred from the above, the effect of the $P_{repulsive}$ term is to actually increase the pressure relative to that predicted for an ideal gas at the same temperature. Conversely, the effect of the $P_{attractive}$ term is to decrease the system pressure below that predicted for an ideal gas. The $P_{attractive}$ term can be generalized to the following form:

$$P_{attractive} = \left(\frac{a}{g(V)}\right) \tag{3.179}$$

where $g(v)$ expresses the dependence of the attractive term on the molar volume.

On the basis of the above, the generalized form of a cubic equation of state derived from the original form of the vdW equation (Cisternass, 1988) can be represented as follows:

$$P = \frac{RT}{v - b} - \frac{a}{g(V)} \tag{3.180}$$

The values of the a and b parameters can be found by one of two methods. The first is by the fitting of the parameters to experimental or literature pure component properties (vapour pressures, phase densities). The second involves using thermodynamic constraints imposed by critical point conditions to obtain the parameters. With the former approach, the general temperature dependency of the parameters can be captured. At the critical point, the first and second derivatives of pressure with respect to volume at constant temperature are zero *i.e.* $\left(\frac{\partial P}{\partial V}\right)_T = \left(\frac{\partial^2 P}{\partial V^2}\right)_T = 0$. Performing these differentiations with the equation of state provides two simultaneous equations, whose solution yields expressions of the critical parameters *i.e.* a_c and b_c. The values of the a and b parameters, obtained through the application of the critical approach *i.e.* a_c and b_c, in the different cubic equations are shown in Table. 3.4.

Table 3.4. Values of the a_c and b_c parameters for cubic EOS.

Equation	a_c	b_c
van der Waals (1873)	$\frac{27R^2T_c^2}{64P_c}$	$\frac{RT_c}{8P_c}$
Redlich-Kwong(1949)	$\frac{0.42748\,R^2T_c^{2.5}}{P_c}$	$\frac{0.08664RT_c}{P_c}$
Soave-Redlich-Kwong (1972)	$\frac{0.42747\,R^2T_c^2}{P_c}$	$\frac{0.08664RT_c}{P_c}$
Peng-Robinson (1976)	$\frac{0.45724\,R^2T_c^2}{P_c}$	$\frac{0.07780RT_c}{P_c}$

In the original vdW EOS, the values of the parameters for a particular fluid were constants (as a function of the critical temperature and pressure), however, in the modifications to be discussed later (except the RK EOS), usually the value of at least one of the parameters is expressed in a temperature-dependent form. The use of critical constraints in the formulation of analytical expressions for the parameters of cubic EOS is a very useful and unique feature of the cubic EOS model. For other non-cubic EOS models which are complex, obtaining a suitable analytic representation of the parameters is almost impossible (Twu *et al*, 2006).

Of course to apply these relations to phase equilibrium computations, an expression of the pressure or volume-explicit equation of state in terms of fugacities of the mixture components is required (to apply the isofugacity crierion). This is conveniently achieved by expressing the equation of state in terms of a cubic form of the compressibility factor (Z), as shown in Equation (3.60), and then substituting into Equations (3.174) and (3.175). The forms of the cubic equations in terms of Z, together with expressions for the pure fluid fugacity coefficient (ϕ) are shown in Table. 3.5. The expressions for the mixture component fugacities are dependent upon the mixing rule employed for the cubic EOS and as such will be presented in the separate treatment of mixing rules to follow.

Due to the simple analytical forms of the cubic equations of state, the mathematical solution of these forms is fairly straightforward. Although analytical formulae can be employed for the solution of cubic EOS, numerical methods are frequently employed, where in the latter one or more iterative sequences or loops are necessitated.

Table 3.5. Expressions for cubic EOS in terms of Z and ϕ.

Equation	Z and ϕ Expressions	Equation no.
vdW (1873)	$Z^3 - Z^2(1+B) - ZA - AB = 0$	(3.181)
	where $A = \frac{aP}{R^2T^2}$ and $B = \frac{bP}{RT}$.	
	$\ln\phi = Z - 1 - \frac{A}{Z} - \ln(Z-B)$	(3.182)
RK (1949)	$Z^3 - Z^2 - Z(A-B-B^2) - AB = 0$	(3.183)
	where $A = \frac{aP}{R^2T^{2.5}}$ and $B = \frac{bP}{RT}$.	
	$\ln\phi = Z - 1 - \ln(Z-B) - \frac{A}{B}\ln\left(\frac{Z+B}{Z}\right)$	(3.184)
SRK (1972)	$Z^3 - Z^2 - Z(A-B-B^2) - AB = 0$	(3.185)
	where $A = \frac{aP}{R^2T^2}$ and $B = \frac{bP}{RT}$.	
	$\ln\phi = Z - 1 - \ln(Z-B) - \frac{A}{B}\ln\left(\frac{Z+B}{Z}\right)$	(3.186)
PR (1976)	$Z^3 - Z^2(1-B) - Z(A-3B^2-2B) - (AB-B^2-B^3) = 0$	(3.187)
	where $A = \frac{aP}{R^2T^2}$ and $B = \frac{bP}{RT}$.	
	$\ln\phi = Z - 1 - \ln(Z-B) - \frac{A}{2B\sqrt{2}}\ln\left(\frac{Z(1+\sqrt{2})B}{Z(1-\sqrt{2})B}\right)$	(3.188)

For any given system (as specified by a_m and b_m) below the critical temperature, there exists two possible scenarios for the numerical solution of a cubic EOS *i.e.* one real root or three real roots for the solution of the compressibility factor of a cubic EOS. In the latter case, the largest root corresponds to the vapour phase, the smallest to the liquid phase and the intermediate root has no physical significance as it thermodynamically unstable since its solution corresponds to $\left(\frac{\partial P}{\partial V}\right)_T > 0$, which actually violates thermodynamic principles. Interested readers are referred to the text of Elliot and Lira (1999) for a discussion on stable roots and the implementation of

numerical solutions for cubic EOS. From the latter, it can be inferred that not all the "real roots" obtained are physically real and all the values of V that are less than b indeed have no physical significance. Of course, at the critical point all three roots converge to the same value.

The simplicity of the theoretical approach inherent in the vdW EOS approach in its treatment of molecular interactions, the absence of temperature dependency for the energy parameter and the inability of the model to treat polar or nonideal mixtures (with classical mixing rules) has effectively excluded the use of this equation for use in accurate phase equilibrium computations. It has typically been employed for the computation of vapour phase thermodynamic properties. The vdW EOS has, however, been of significant value to contemporary researchers as being applied to perturbation theory equations of state and a modern direct approach known as the UNIWAALS EOS (Gupte *et al.*, 1986a, 1986b). Of course, an irrefutable contribution of this equation has been its inspiration of highly successful cubic equations of state in the form of the Soave-Redlich-Kwong and the Peng-Robinson equations of state.

Redich-Kwong (1949) and Soave-Redlich-Kwong Equations of State (1972)

In accordance with the statement by Prausnitz (1985) in his article on the contributions of Otto Redlich to chemical thermodynamics, "Redlich's great contribution was to revive the spirit of van der Waals". The introduction of the Redlich-Kwong (RK) equation of state in 1949 was a significant milestone and it represented a considerable improvement over both the complex virial-type and other equations of considerably simpler forms for use in applications such as distillation column process simulators (Palmer, 1987). Interestingly enough Otto Redlich, one of the chief architects of the equation, mentioned in his book (1978) that the basis for the development of the model as a modification of the vdW EOS had no formal theoretical basis and as such was described as an "inspired empirical" formulation. The key attribute of the equation was the inclusion of the size parameter (b) and an expression for the temperature dependency of the energy parameter term (a) in the denominator of the attractive term, as shown in Equation (3.188) The latter was not regarded as a novel feature as soon after the publication of the vdW EOS, the temperature dependence of the a term was acknowledged by many (Walas, 1985).

$$P = \frac{RT}{V - b} - \frac{a}{T^{0.5}V(V + b)} \qquad (3.188)$$

The above modifications served to improve the accuracy of the generic cubic EOS model and the greatest success of the RK EOS model has been in successfully computing second virial coefficient curves of simple fluids at low pressures (Palmer, 1987). However, the RK EOS suffers from limited accuracy (for vapour pressures and liquid densities) and applicability (to only to nearly ideal systems or simple fluids). In addition, the RK EOS is not suitable for the liquid phase representation (not a single application of the EOS to liquids can be found in the original RK EOS article) and hence cannot be used in VLE computations. However, the RK EOS has found some applicability in the γ_i - ϕ_i approach, as in the method of Chao and Seader (1961) for the computation of the vapour phase nonideal behaviour, where its advantage over the B-truncated virial equation of state lies chiefly in its simpler algebraic form.

In general, the accuracy of the RK equation diminishes as the molecules increase in size or complexity which can be attributed to the RK EOS containing only two corresponding state parameters (T_C, P_C) in with no consideration of size-shape effects, which was discussed in Section (3.5.2.2). In response to this, Wilson (1964) proposed the introduction of the acentric factor (ω) into an expression for one of the parameters to account for size-shape effects, as shown in Sandler *et al.* (1994). Although the equation was inappropriate for regions above the critical, the idea facilitated the work of Soave in producing the most successful modification of the R-K equation, of which there were about 150 (Valderrama, 2003) in the form of the Soave-Redlich-Kwong (SRK) EOS in 1972, as shown below:

$$P = \frac{RT}{V - b} - \frac{a(T,\omega)}{V(V + b)} \tag{3.189}$$

where the temperature-dependent term in the RK equation was replaced by a more effective function *i.e.* $a(T,\omega)$.In the latter, the a parameter was expressed as a function of the acentric factor(ω) and temperature(T). The $a(T,\omega)$ functional relationship, shown in Equation (3.190) was obtained through the use of a multiplicative temperature-dependent term in the form of an $\alpha(T)$parameter. The latter allowed for the temperature dependence of the energy term to be related to the expressions for the parameters at the critical point *i.e.* a_c, as shown in Table 3.4.

$$a(T,\omega) = a_c\alpha(T,\omega) \tag{3.190}$$

As can be deduced from the above, the$\alpha(T,\omega)$ parameter has a value of unity at the critical point. An expression for$\alpha(T,\omega)$, also known as the cohesion energy parameter (Ghosh, 1999),

was expressed in the form of a linear relationship between the square root of α and the square root of the reduced temperature (T_r).

The form of this expression proposed by the original researchers can be represented as follows [a]:

$$\alpha = \left[1 + \kappa\left(1 - T_r^{0.5}\right)\right]^2 \tag{3.191}$$

where κ was related to ω in a quadratic way through the following:

$$\kappa = 0.480 + 1.574\omega - 0.176\omega^2 \tag{3.192}$$

The coefficients of Equation (3.192) were obtained by obtaining values for κ which had corresponded to the vapour pressures of hydrocarbons at $T_r = 0.7$ *i.e.* corresponding to the acentric factor.

The above correlation was modified by Graboski and Daubert (1978), who had used different pure component parameters (vapour pressures) in their regression to obtain the following:

$$\kappa = 0.48508 + 1.55171\omega - 0.15613\omega^2 \tag{3.193}$$

There have been many correlations that have been proposed for representing the temperature dependency of the attractive term in cubic equations of state with $\alpha(T_r, \omega)$, where the T term has been replaced by the T_r term, to more accurately represent the functional form of the term. These different forms are presented in Table 3.6.

Although the SRK equation allowed for significant improvements with regards to the RK EOS for the treatment of VLE of nonpolar and weakly polar substances, as with the latter approach the principal respectable feature of the method is its acceptable representation of the PVT properties (vapour pressures) of the vapour phase (Raal and Muhlbauer, 1998). In terms of the liquid phase densities, poor representation was observed especially with the use of the SRK approach towards the critical region. As mentioned, the RK and SRK equations were developed within the theoretical framework of representing the PVT behaviour of light hydrocarbons and both methods give a poor representation of the vapour pressures of polar substances.

[a] Where the original expression has been squared on both sides, as for the expressions in Table 3.6.

Table 3.6. Correlations for the $\alpha(T_r,\omega)$ term in cubic EOS.

Method	Correlation [a]	Eq. no.
Soave (1972)	$\alpha = \left[1+\kappa\left(1-T_r^{0.5}\right)\right]^2$	(3.191)
	$\kappa = 0.480+1.574\omega+0.176\omega^2$	(3.192)
Peng and Robinson (1976)	$\alpha = \left[1+\kappa\left(1-T_r^{0.5}\right)\right]^2$	(3.191)
	$\kappa = 0.37464+1.54226\omega-0.26992\omega^2$	(3.194)
Graboski and Daubert (1978)	$\alpha = \left[1+\kappa\left(1-T_r^{0.5}\right)\right]^2$	(3.191)
	$\kappa = 0.48508+1.55171\omega-0.15613\omega^2$	(3.193)
Soave (1979)	$\alpha = 1+\left(1-T_r\right)\left(C_1++\frac{C_2}{T_r}\right)$	(3.195)
Harmens and Knapp (1980)	$\alpha = \left[1+C_1\left(1-T_r^{0.5}\right)+C_2\left(T_r^{-1}-1\right)\right]^2$	(3.196)
	$\alpha = \left[1+C_1\ln T_r+C_2(\ln T_r)^2\right]^2 \quad (T_r>1)$	(3.197)
Heyen (1980)	$\alpha = \exp\left[C_1\left(1-T_r^n\right)\right]$	(3.198)
Mathias (1980)	$\alpha = \left[1+\kappa\left(1-T_r^{0.5}\right)-P\left(1-T_r\right)\left(0.7-T_r\right)\right]^2$	(3.199)
	$\kappa = 0.485+1.551\omega-0.156\omega^2$	(3.200)
Mathias and Copeman (1983)	$\alpha = \left[1+C_1\left(1-T_r^{0.5}\right)+C_2\left(1-T_r^{0.5}\right)^2+C_3\left(1-T_r^{0.5}\right)^3\right]^2$	(3.201)
Adachi and Lu (1984)	$\alpha = 10^{C_1[1-T_r]}$	(3.202)
Soave (1984)	$\alpha = 1+C_1\left(1-T_r\right)+C_2\left(T_r^{-1}-1\right)$	(3.203)
Stryjek and Vera (1986a,1986b)	$\alpha = \left[1+\kappa\left(1-T_r^{0.5}\right)\right]^2$	(3.204)
PRSV(1986a)[b]	$\kappa = \kappa_0+\kappa_1\left(1+T_r^{0.5}\right)\left(0.7-T_r\right)$	(3.205)
	$\kappa_0 = 0.378893+1.4897153\omega-0.1731848\omega^2+0.0196554\omega^3$	(3.206)
PRSV2(1986b)[b]	$\kappa = \kappa_0+\left[\kappa_1+\kappa_2\left(\kappa_3-T_r\right)\left(1-T_r^{0.5}\right)\right]\left(1+T_r^{0.5}\right)\left(0.7-T_r\right)$	(3.207)

Table 3.6. Correlations for the $\alpha(T_r,\omega)$ term in cubic EOS (cont).

Method	Correlation [a]	Eq. no.
Carrier *et al.* (1987)	$\alpha = 1+C_1\left(1-T_r^{0.5}\right)+C_2\left(1-T_r\right)$	(3.208)
Yu and Lu (1987)	$\alpha = 10^{\left[C_1\left(A_0+A_1T_r+A_2T_r^2\right)\left(1-T_r\right)\right]}$	(3.209)
Androulakis *et al.* (1989)	$\alpha = 1+C_1\left(1-T_r^{2/3}\right)+C_2\left(1-T_r^{2/3}\right)+C_3\left(1-T_r^{2/3}\right)$	(3.210)
Melhem *et al.* (1989)	$\alpha = \exp\left[C_1\left(1-T_r^{0.5}\right)+C_2\left(1-T_r^{0.5}\right)^2\right]$	(3.211)
Twu *et al.* (1991)	$\alpha = T_r^{C_3(C_2-1)}\exp\left[C_1\left(1-T_r^{C_2C_3}\right)\right]$	(3.212)
Twu *et al.* (1995a, 1995b)	$\alpha = \alpha^{(0)}+\omega\left(\alpha^{(1)}-\alpha^{(0)}\right)$	(3.213)
	$\alpha^{(0)} = \left(T_r^{-0.201158}\right)\left(e^{0.141599\left[1-T_r^{2.63165}\right]}\right)$	(3.214)
	$\alpha^{(1)} = \left(T_r^{-0.660145}\right)\left(e^{0.500315\left[1-T_r^{2.63165}\right]}\right)$	(3.215)
Zabaloy and Vera (1996)	$\alpha = 1+C_1T_r\ln T_r+C_2\left(T_r-1\right)+C_3\left(T_r^2-1\right)$	(3.216)

[a] Where A_0, A_1, A_2, C_1, C_2 and C_3 are coefficients that are specific to pure substances.

[b] As applied to the PR EOS.

Also, the requirement of a binary interaction parameter to characterise the hydrocarbon-hydrocarbon interactions was not as crucial as that for polar or non-hydrocarbon mixtures, to which the equations were not applied. Consequently, the deficiency of the SRK approach to incorporate a binary interaction parameter with a theoretical basis (*i.e.* related to molecular parameters in the model), results in quite poor or distressing results for the representation of VLE for polar mixtures (Palmer, 1987).

Peng-Robinson Equation of State (1976)

The novel cubic EOS presented by Peng and Robinson in 1976 served to effectively extend the ideas presented by Soave (1972) and was developed along the lines of addressing the flaws of the preceding approaches (Walas, 1985) through the attainment of several goals. Most notably,

an improved representation of the liquid phase density was desired as this would enhance the suitability of the cubic EOS approach for the phase equilibrium calculations. Additionally, for the treatment of mixtures, the introduction of a single binary interaction parameter (independent of pressure, temperature and composition) in the mixing rules was deemed as necessary in this approach.

As in the SRK EOS, the repulsive term of the vdW EOS was unchanged and the temperature dependence of the attractive contribution was incorporated into the energy term (where the $\alpha(T_r,\omega)$ term was recalculated). However, the form used was a more complex expression of volume and the covolume (b) parameter for the volume dependency in the denominator of the attractive term as follows:

$$P = \frac{RT}{V-b} - \frac{a(T,\omega)}{V(V+b)+b(V-b)} \tag{3.217}$$

where the relationship between $a(T,\omega)$ and $\alpha(T_r,\omega)$ remains unchanged from Equation (3.190) and the critical state constants are shown in Table 3.4.

The functional form of the correlation for $\alpha(T_r,\omega)$ with κ was changed, as shown in Table 3.6, due to the different approach of the authors in obtaining the coefficients. The PR EOS has been tested thoroughly on a wide range of different systems and finds great applicability in industry for gas processing and reservoir process simulators. It also shows promise in applicability to a few polar systems with the fitting of binary interaction parameters to the data. It has also been acknowledged that improvements in the liquid phase densities have been obtained; however, the density predictions for some substances are still quite inaccurate. As for the SRK EOS, the PR EOS also suffers from inaccuracy in the critical region, the poor representation of the phase equilibrium of heavy hydrocarbons and highly polar, associating fluids (water, alkanols) and the correlated generalized parameters for non-hydrocarbons cannot be used for extrapolation or representation of a wide range of substances. The review articles by Martin (1979) and Abbot (1979) highlight the shortcomings of traditional forms of cubic EOS models.

Modifications of Cubic Equations of State

Modifications of the original forms and parameter correlations for the SRK and the PR EOS models were necessitated to address two crucial flaws inherent in the traditional cubic EOS approach. The first relates to the poor representation of the vapour pressures of polar, polar-

associating and heavy fluids over a wide range of pressures and temperatures. The second deals with representation of the volumetric properties of dense phases *i.e.* the liquid phase, especially near the critical region. The opportunities for proposing modifications of cubic EOS arise in both the numerator and the denominator of attractive term of the model. Traditionally, there has been an aversion to changing the repulsive term of the cubic EOS form as this would make the cubic EOS higher-order (*e.g.* quartic) or transcendental. The numerical solution of both of these forms is indeed much more complex. Consequently, modifications of the repulsive term have been more popular for the statistical-mechanical modifications of the vdW EOS in the form of the non-cubic Carnahan-Starling (1969, 1972) and Guggenheim (1965) expressions as reviewed by Wei and Sadus (2000).

(a) Modifications to the numerator of the attractive term in cubic equations of state

The accuracy of a cubic EOS in correlating phase equilibria, in addition to the functional form of the mixing rule (Djordjevic *et al.*, 2001), is strongly dependent on the efficiency of the cubic EOS in reproducing correct saturated pure component vapour pressures (Vidal, 1983; Van Ness and Abbott, 1982; Twu *et al.*, 1991). To help improve the pure component vapour pressure representation by cubic EOS models, more effective correlations for the α term, as shown in Table 3.6, was proposed by many researchers. As mentioned above, discrepancies in the α correlations for Soave (1972), Peng and Robinson (1976) and Graboski and Daubert (1978) are attributed to the use of different approaches; these discrepancies have resulted in some models be more successful than others as will be discussed below. However, the limitations of many of these correlations is that they were developed for representing the vapour pressure data of particular compounds or groups of compounds as opposed to being applicable to a wide range of chemical groups (especially non-hydrocarbon or polar fluids).The modifications as pertinent to the development of the PR EOS will feature prominently in the discussion as these are regarded as being of the greatest significance.

A universal relationship between between α at $T_r = 0.7$ and ω, can be shown from the work of Soave (1986), where for the van der Waals, RK and PR EOS models a fundamental relationship for the ratio $\left(\frac{\alpha}{T_r}\right)$ exists:

$$\left(\frac{\alpha}{T_r}\right) = \xi\left(\frac{P_r}{T_r}\right) \tag{3.218}$$

where ξ is a universal function that depends on the EOS chosen.

Substituting the definition of the acentric factor from Equation (3.74) into the above yields:

$$\alpha(\text{at } T_r = 0.7) = 0.7\,\xi\left(\frac{10^{-(\omega+1)}}{0.7}\right) \tag{3.219}$$

For a generic cubic EOS, a value of κ is obtained which reproduces exactly the vapour pressure at $T_r = 0.7$ to give the value of ω. On the other hand, a set of ω values allow for the generation of κ values for the EOS, without the requirement of experimental data.

The most important step in the work of Soave (1972) was the manner in which the κ value was correlated with the acentric factor (ω). Soave ensured that the universal relation between α at $T_r = 0.7$ and ω, shown in Equation (3.219), was not violated. Consequently, the early approach of Soave (1972) still remains a credible correlation (Ghosh, 1999) for $\alpha(T_r, \omega)$. The Soave correlation has been described by Ghosh (1999) and Valderrama (2003) as being the most popular. However, it was found that the $\alpha(T_r, \omega)$ correlation of Soave (1972) does accurately represent calculated vapour pressures at low temperatures and the supercritical condition as it does not monotonically increase with temperature and (Twu *et al.*, 2006).

In what appears to be the most controversial aspect of the approach in the original formulation of the PR EOS, is the method used to obtain the (ω, κ) pairs to evaluate the $\alpha(T_r, \omega)$ function. Peng and Robinson (1976) optimized the PR EOS for the representation of saturated vapour pressures from the normal boiling point to the critical point for a large number of compounds. This of course violated the relationship in Equation (3.219) although it allowed for more vapour pressure data to be used for the correlation. The lack of applicability of the PR EOS to polar compounds is seen as the sacrificial lamb of the above approach in the original PR EOS. Soave (1979) later on proposed a different correlation for strongly polar substances such as water and alkanols. The correlation of Melhem (1989) is of a similar form to those devised by Mathias and Copeman (1989) but is inferior in its prediction of vapour pressures when compared to other correlations in Table 3.6.

Mathias and Copeman (1983) presented the first significant modification of the PR EOS, termed the first-generation PR EOS modification by Zabaloy and Vera (1998). It was a different $\alpha(T_r, \omega)$ expansion, as shown in Equation (3.201), but still retained the original form of the correlation for κ, as used by Peng and Robinson. Of interest is the fact that in an earlier attempt at a $\alpha(T_r, \omega)$ correlation, Mathias (1980) used Equation (3.119) which vanishes at $T_R = 0.7$ for the SRK EOS. For the PR modification of Mathias and Copeman (1983), this is clearly not the case, which once again alludes to the importance of adherence to Equation (3.219). Both

functions of Mathias (1980) and Mathias and Copeman (1983) exhibit extrema at the critical region and to overcome this, a different $\alpha(T_r,\omega)$ correlation for temperatures higher than the critical is consequently necessitated. However, in the use of the latter relation, a discontinuity at the critical point and significant errors in the predicted thermodynamic properties (most notably enthalpies) are observed.

In the second-generation PR EOS modification, Stryjek and Vera (1986a, 1986b) devised empirical correlations for $\alpha(T_r,\omega)$, as shown in Table 3.6 using experimental data for many substances and found that for the PR EOS with α values at $T_r = 0.7$, the values of ω were independent of the chemical nature of the molecule (polarity and degree of association). The correlations, shown in Equations (3.205) - (3.207), obtained in this way satisfied the universal relation. With $\kappa_2 = 0$, the PRSV2 form reverted to the PRSV form. The equations of Stryjek and Vera (1986a, 1986b) have indeed proven to be quite popular amongst contemporary researchers and are highly recommended by Sandler *et al.* (1994).

A generalized $\alpha(T_R,\omega)$ function was developed by Twu *et al* (1995a, 1995b) to allow for the proper representation of the hydrocarbon vapour pressures from the triple point to the critical point. The form of the relation as applied to the SRK EOS is shown as Equations (3.213)-(3.215) in Table 3.6. The authors claim that it provides an accurate representation of both light and heavy hydrocarbons vapour pressures that is superior to the original correlation of Soave (1972).

In a very recent development, in what is seen as the third-generation PR EOS modification, Zabaloy and Vera (1996) proposed the relation shown in Equation (3.216) known as the ZVPR correlation. The development of this approach for the $\alpha(T_r,\omega)$ function involved the use of Equation (3.218) together with a polynomial expansion in terms of T_r for the difference in the heat capacities (C_P) of the saturated phases. The simplest form of this correlation is shown as Equation (3.216) in Table 3.6.

In a comparative study of several EOS models and $\alpha(T_r,\omega)$ functions with nonpolar, polar and associating compounds, Zabaloy and Vera (1998) concluded that the ZVPR and the PRSV2 approaches successfully represented the pure component vapour pressures from the triple point to the critical point and this was independent of the generic form of the EOS used. As was to be expected, there was indeed a bias in the accuracy of the representation of vapour and liquid phase saturated volumes in favour of the former. In the study, the calculation of the saturated phase molar volumes (by forcing the EOS to fit the pure component vapour pressures exactly),

revealed the real limit of the structural form of the EOS. The PR equation was clearly shown to be superior to the vdW, the RK and the statistical-mechanical modified Carnahan-Starling (Vera and Prausnitz, 1972) EOS models.

(b) Modifications to the denominator of the attractive term in cubic equations of state

A general criticism of the cubic EOS approach is that the critical compressibility factor (Z_C) becomes a constant, regardless of the chemical identity of the substance *i.e.* $Z_C = 0.375, 0.333$ and 0.307 for the vdW, PR and SRK EOS models, respectively (Valderrama, 2003). For real substances, the value of Z_C, obtained from experiment is generally lower than that predicted from the EOS (Twu *et al.*, 2006). As a result, the representation of the PVT properties of real fluids such as liquid densities by cubic EOS is frequently inaccurate. The modification of the volume dependency term in the denominator of the cubic EOS has been the usual approach for improving the representation of liquid phase densities. This is achieved through the introduction of a temperature dependency for the covolume term as was performed by Xu and Sandler (1987). However, the polynomial terms used by Xu and Sandler (1987) were very fluid-specific.

Another approach (apart from volume translation, to be discussed below) has been in the introduction of temperature dependencies into the $g(V)$ term to obtain a multi-parameter EOS. It was generally observed that three-parameter EOS models gave much better representation of the volumetric properties of the system such as compressibility factors and densities than two-parameter EOS models. The various three or four-parameter EOS modifications are shown in Table 3.7. A noteworthy modification was that by Schmidt and Wenzel (1980) in Equation (3.225) where the acentric factor (ω) has been incorporated into the expression. The Patel-Teja Equation in (3.227) has been described as the most popular model of the three-parameter EOS approach (Sandler *et al.*, 1994). A modified form of this equation, known as the generalized Patel-Teja EOS, has shown to be successful in correlating VLE for mixtures (Valderrama, 2003).

With an additional parameter, the EOS modified by the $g(V)$ terms discussed have been able to improve vapour pressure and liquid molar volume predictions and with a judicious approach to parameter selection, can be used for polar substances as well (Sandler *et al.*, 1994). However, the three-parameter cubic EOS models have not demonstrated success over the two-parameter cubic SRK and PR EOS in the critical region (Raal and Muhlbauer, 1998) since a generic cubic EOS must overestimate the critical compressibility in order to ensure accuracy for predictions in other regions.

Table 3.7. Modifications of the $g(V)$ term in cubic EOS.

Method	$g(V)$ Expression [a]	Eq. no.
Claussius (1880)	$V^2 + 2cV + c^2$	(3.220)
Fuller (1976)	$V + cb$	(3.221)
Usdin and McAuliffe (1976)	$V^2 + cV$	(3.222)
Heyen (1980)	$V^2 + cV + bV - bc$	(3.223)
Harmens and Knapp (1980)	$V^2 + cbV - cb^2 + b^2$	(3.224)
Schmidt and Wenzel (1980)	$V^2 + (1+3\omega)bV - 3b^2\omega$	(3.225)
Kubic (1982)	$(V+c)^2$	(3.226)
Patel and Teja(1982)	$[V(V+b)+c(V-b)]$	(3.227)
Toghiani and Viswanath (1986)	$V^2 + cbV + bV - cb^2$	(3.228)
Trebble and Bishnoi (1987)	$[V^2 + V(b+c) - (bc+d^2)]$	(3.229)
Schwartzentruber and Renon (1989)	$[(V+c)(V+2c+b)]$	(3.230)

[a] Where b and c are coefficients that are specific to pure substances.

A blatant shortcoming of the three-parameter EOS is in the use of a third parameter; where the evaluation of which requires the input of more pure component data and an additional mixing rule for the extension of the approach to mixtures for the third parameter.

(c) Volume-translated forms of Cubic Equations of State

In many of the approaches presented in **(a)** and **(b)**, a strategy of the "forced-fitting" of cubic EOS models to pure component vapour pressures or saturated liquid molar volumes was necessitated to obtain a better representation of PVT behaviour by these equations. This also results in the cubic EOS not being able to satisfy the proper critical constraints, overestimating critical constants (T_C, P_c) and for real fluids not being able to obtain accurate representation of the equilibrium constants (K values) for the phase equilibrium computations. However, a unique feature of cubic EOS models allows for the liquid phase density correlations to be improved by the method of volume translation without affecting the computed phase equilibrium constants.

The original translation concept of Martin (1979) was shown to significantly improve the liquid phase densities obtained from cubic EOS models and was later developed by Peneloux *et al.* (1982) who formally applied the volume translation concept in the form of a consistent volume correction to the SRK EOS. The latter approach serves to minimize the errors in the predicted saturated liquid molar volumes whilst leaving the vapour pressures and equilibrium constants unaffected. In the volume translation procedure, a small fluid-specific molar volume correction factor (c) is incorporated into the expression for volume *i.e.* $V^* = V + c$ .The application of the volume translation to the SRK EOS yields the VT-SRK EOS:

$$P = \frac{RT}{V + c - b} - \frac{a(T,\omega)}{(V + c)(V + c - b)} \tag{3.231}$$

The volume translation parameter (c) is evaluated by ensuring that the correct saturated liquid molar volume is obtained at some reference temperature *i.e.* at $T_R = 0.7$ (Sandler *et al.*, 1994). The volume correction proposed by Peneloux *et al.* (1980) for the SRK EOS used the Rackett compressibility factor (Z_{RA}) from Spencer and Danner's Modified Rackett equation (1972) for saturated liquid volumes:

$$c = \left(\frac{RT_c}{P_c}\right)(0.120025 - 0.40768Z_{RA}) \tag{3.232}$$

The c parameter can be in the form of a constant or in a temperature-dependent form. However, Twu *et al.* (2006) commented that the calculation of the volume correction for temperatures greater than the critical should exclude any temperature dependency to avoid any anomalies in the calculation of heat capacities at supercritical conditions. Twu *et al.* (2006) comment upon the disadvantages of the Peneloux volume translation approach and in a comparative approach with the former, present their own universal volume translation method for light and heavy hydrocarbons, which was shown to be superior to the Peneloux *et al.* (1982) method across the temperature range.

Tsai and Chen (1998) developed a volume-translated PR EOS known as the VTPR EOS. The temperature dependence of the EOS parameter was obtained through the regression of a relation that provides improved correlations of pure fluid vapour pressures. Stamaki and Tassios (1998) employed the use of a translated and modified PR EOS, known as the (t-mPR) EOS (Magoulas and Tassios, 1990) in the evaluation of cubic EOS at high through the use of correlation and prediction results for hydrocarbon mixtures. It was shown that a generalized correlation for volume translation was effective for pressures up to 200 MPa.

The volume-translated cubic EOS approach leads to a tremendous improvement for the liquid phase molar volumes. The method is highly recommended for the computation of the phase equilibria and PVT properties of hydrocarbon mixtures and reservoir fluids. However, despite the volume-translation approach being a very promising method with apparent advantages, it has not proven to be popular from a practical point of view (Valderrama, 2003). It has also been noted that volume-translations of cubic EOS can produce problems at high pressures such as negative volumes and isochoric heat capacities (Zielke and Lempe, 1997).

3.5.3.3 Mixing Rules for Cubic Equations of State

The greatest utility of cubic EOS is arguably their use for treatment of the fluid phase equilibria of binary and multicomponent mixtures. To extend cubic EOS models for the treatment of mixtures, the same form of the cubic EOS can be retained provided that an effective method of obtaining the mixture parameters can be employed. This is most commonly achieved through the use of mixing and combining rules which relate the pure component properties to that of the mixture. An alternative method, described in the text of Walas (1985), involves the calculation of mixture pseudocritical properties through the use of suitable combining rules, from which the EOS mixture parameters can be obtained. The latter approach has usually not been employed in phase equilibrium computations and will not feature in this review. The use of mixing rules in cubic EOS is probably the most controversial aspect of this approach and the importance of this subject has warranted its deferment to a separate treatment as it undoubtedly constitutes the largest area of contemporary research for cubic EOS.

The traditional cubic EOS approach has been shown to be particularly efficient in the treatment of the vapour phase of nonpolar substances for pressures up to the critical; whereas for the treatment of the liquid phase of highly nonideal, polar or associating compounds, this has traditionally been the preserve of low-pressure liquid phase excess free energy correlations. Consequently, a unified cubic EOS/ (A^E or G^E) approach for the correlation and prediction of the phase equilibrium properties of a diverse group of substances across wide pressure and temperature ranges would indeed be a powerful tool. The latter has served as the fundamental development criterion for the majority of the developments of non-classical or modern mixing rules since the idea was first proposed in the pioneering work of Vidal (1978).

A contemporary classification scheme for cubic EOS mixing rules, as presented by Raal and Muhlbauer (1995) is shown in Figure 3.4.

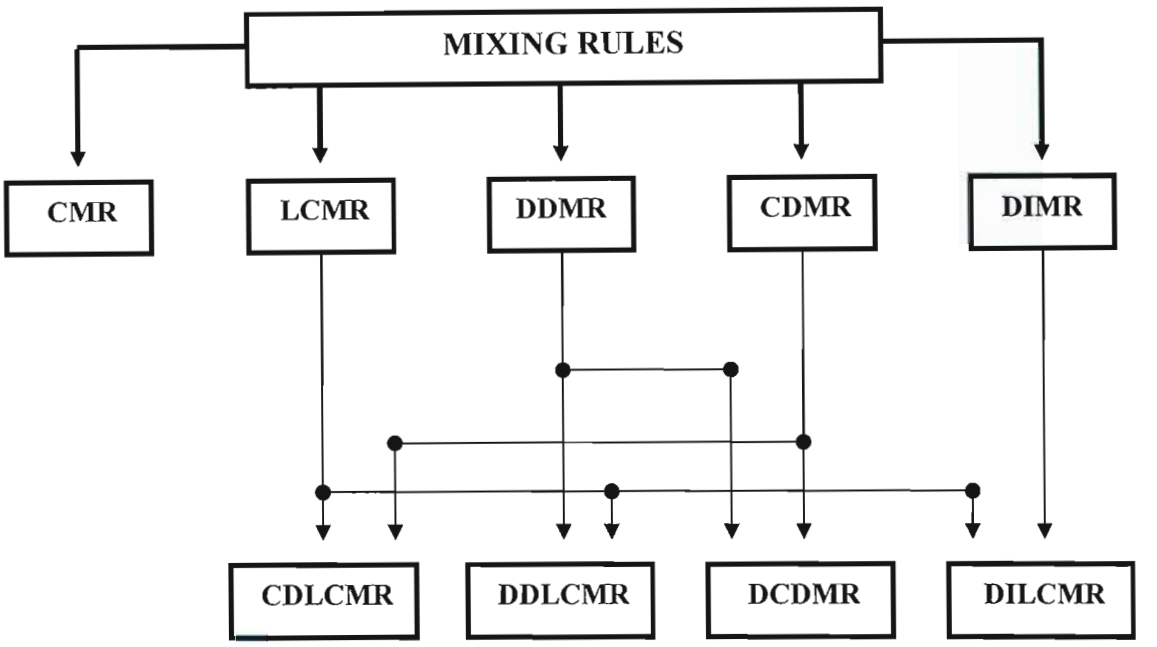

Figure 3.4. Classification scheme for cubic EOS mixing rules (MR): **CMR**, Classical; **LCMR**, Local Composition; **DDMR**, Density-Dependent; **CDMR**, Composition and Density-Dependent; **DIMR**, Density-Independent; **CDLCMR**, Composition-Dependent Local Composition; **DILCMR**, Density-Independent Local Composition; **DCDMR**, Density and Composition-Dependent; **DDLCMR**, Density-Dependent Local Composition.

A large majority of the contemporary EOS mixing rules can be classified as belonging to one of five principal groupings in the form of the classical mixing rules (CMR), local composition mixing rules (LCMR), density-dependent mixing rules (DDMR), composition-dependent mixing rules (CDMR) and density-independent mixing rules (DIMR) or to the hybrid methods that constitute the lower hierarchy of Figure 3.4. These hybrid methods can be grouped as being composition-dependent local composition mixing rules (CDLCMR), density-dependent local composition mixing rules (DDLCMR), density and composition-dependent mixing rules (DCDMR) and density-independent local composition mixing rules (DILCMR).

A description of the origins, implementation and applicability of these methods to cubic EOS will be dealt with later; with greater emphasis being accorded to those mixing rules of greater contemporary relevance in the research arena and those used in this study. It should be also acknowledged that since the presentation of this classification scheme by Raal and Muhlbauer (1998), there have been novel developments such as those by Brandani and Brandani (2004) and Barragan-Aroche and Bazua-Rueda (2005) within the context of the mixing rule classification scheme presented above. However, since these methods are beyond the scope of this study and are largely unexplored, they have not been represented in Figure 3.4.

In a comparative study of the applicability of mixing rules to optimize the predictive capability of the PRSV EOS for the treatment of multicomponent VLE, Solorzano-Zavala (1996) provided a synopsis of the critical requirements of a successful mixing rule or MR, which can be described as follows:

(a) The MR should be have a *simple algebraic form* to facilitate the practical implementation of the mixing rule into the cubic EOS and subsequent computations.

(b) The MR should *not contain too many parameters* as this would result in an increased input of information for parameter evaluation/fitting and so as to make the method less amenable for the development of predictive capability.

(c) In the application of the MR to multicomponent systems, the parameters of the MR should be *invariant to the sub-division* of a component into identical subcomponents *i.e.* not exhibit the Michelsen-Kistenmacher syndrome (Michelsen and Kistenmacher, 1990). If a mixture of A,B and C in a ternary system is formed where there are equimolar amounts of B and C, then the parameters for the ternary system (with zero mole % A) should be the same as that obtained for the corresponding B + C binary system. However, if this is not adhered to, then the mixture parameters are not suitable for a system with more than two components. The testing of a model for the Michelsen-Kistenmacher syndrome can be checked by examining the forms of the algebraic expansions for the a_m term in a binary A-B binary mixture and analogous A-B parameter value in a ternary A-B-C expression (where all the C terms are changed into B terms and B-B interactions are removed). If the above two expressions are not identical, then the MR suffers from the Michelsen-Kistenmacher syndrome.

(d) The statistical-mechanical constraint in the form of the *quadratic composition dependence* of the second virial coefficient at low densities *i.e.* Equation (3.66) should be satisfied. This is easily seen through the expansion of the arrangement of a cubic EOS model as a power series in density to arrive at an expression that approximately equivalent to that of the second virial coefficient, where it can be shown that a_m and b_m have to satisfy the following statistical-mechanical relation:

$$B_{mix} = \sum_i^n \sum_j^n y_i y_j B_{ij} = \sum_i^n \sum_j^n y_i y_j \left(b - \frac{a}{RT} \right)_{ij} = b_m - \frac{a_m}{RT} \qquad (3.233)$$

where $\left(b - \frac{a}{RT} \right)_{ij}$ is the cross second virial coefficient of the EOS.

To check for adherence to the quadratic second virial coefficient or (QSVC) condition, the expression for a_m is divided by RT and subtracted from the expression for b_m. If the condition shown in Equation (3.233) is not reproduced, then the QSVC condition has been violated for the mixing rule. Adherence of MR to the above boundary condition gives the cubic EOS/MR approach the credibility of being theoretically-correct.

(e) The MR should exhibit the *same accuracy in modelling/predicting* both binary and multi-component phase equilibria.

(f) The MR should have *universal applicability* for nonpolar, polar, associating and asymmetric mixtures. Asymmetry with regards to mixing rules relates to the system components *i.e.* those systems with components which have large differences in size or a large ratio of covolume parameters (Coutsikos *et al.*, 1995) or in terms of excess Gibbs free energy behaviour *i.e.* large discrepancies in the relative magnitudes of activity coefficients at infinite dilution (Twu and Coon, 1996).

(g) The *known parameters* regressed from a previous application of the γ_i - ϕ_i method to the mixture of interest should be readily incorporated into the MR.

(h) The MR should allow for the *prediction* of other thermodynamic quantities of interest (*e.g.* enthalpy, entropy).

(i) The MR should be able to allow for the treatment of *liquid-liquid* and *vapour-liquid-liquid* equilibria.

(j) The MR should reduce to the *classical one fluid vdW mixing rules* for the treatment of ideal or nonpolar mixtures as one of its boundary conditions.

The reasoning behind the above criteria will be apparent with the perusal of the review of mixing rules to follow. The satisfaction of **(a)** - **(j)** represents an idealized scenario for the formulation of a mixing rule. However, the identification of the above criteria for a successful MR has assisted in focussing efforts in the development of more successful MR approaches from the original one fluid classical mixing rule of van der Waals, a discussion of which serves as an appropriate starting point for the discussion of mixing rules.

(a) Classical Mixing Rules

The most commonly used mixing rules are the classical or van der Waals one-fluid mixing rules, which can be represented as quadratic functions as follows:

$$a_m = \sum_{i=1}^{n}\sum_{j=1}^{n} z_i z_j a_{ij} = z_i^2 a_{ii} + z_j^2 a_{jj} + 2 z_i z_j a_{ij} \tag{3.234}$$

$$b_m = \sum_{i=1}^{n}\sum_{j=1}^{n} z_i z_j b_{ij} \tag{3.235}$$

where a_m and b_m are the EOS parameters for the mixture. The use of z_i and z_j indicate the use of the expression with either the liquid (x_i) or vapour phase compositions (y_i). The terms of a_{ij} and b_{ij} are the cross parameters for the a_m and b_m terms, respectively, that take into account the unlike (i-j) interactions in a binary mixture. These can be obtained from a set of combining rules incorporating interaction parameters as follows:

$$a_{ij} = (a_i a_j)^{0.5}(1 - k_{ij}) \tag{3.236}$$

$$b_{ij} = \left(\frac{b_i + b_j}{2}\right)(1 - d_{ij}) \tag{3.237}$$

where a_n and b_n $(n = i, j)$ are the constants of the relations for pure components i and j. As for Equations (3.234) and (3.235), the equations above retain the quadratic form. The terms k_{ij} and d_{ij} are the concentration-independent binary interaction parameters, which are strictly empirical and hence different for each binary system Generally, d_{ij} is set equal to zero, resulting in a linear form for the mixture covolume term, as shown in Equation (3.238). However, it should be noted that in certain instances, the use of the second interaction parameter allows for a more accurate correlation (Shibata and Sandler, 1989a).

$$b_m = \sum_{i}^{n} z_i b_i \tag{3.238}$$

The distinction between mixing rules and combining rules can clearly be seen at this juncture, as the latter are used to obtain binary parameters that characterize unlike interactions, as in Equations (3.236) and (3.237). Mixing rules inherently involve the judicious selection of a composition-dependent expression for the a_m and b_m parameters. The expressions for mixture component fugacities (ϕ_i) for the SRK and PR EOS with the incorporation of the classical mixing rules are shown below as Equations (3.239) and (3.240), respectively:

$$\ln\phi_i = \frac{b_i}{b_m}(Z-1) - \ln(Z-B_m) - \frac{A_m^a}{B_m}\left[\frac{2\sum_{i=1}^{n} z_j a_{ij}}{a_m} - \frac{b_i}{b_m}\right]\ln\left(\frac{Z+B_m}{Z}\right) \qquad (3.239)$$

$$\ln\phi_i = \frac{b_i}{b_m}(Z-1) - \ln(Z-B_m) - \frac{A_m}{2\sqrt{2}B_m}\left[\frac{2\sum_{i=1}^{n} z_j a_{ij}}{a_m} - \frac{b_i}{b_m}\right]\ln\left(\frac{Z+(1+\sqrt{2})B_m}{Z+(1+\sqrt{2})B_m}\right) \qquad (3.240)$$

The determination of the binary interaction coeffficients *i.e.* k_{ij} and d_{ij} has also traditionally been an area of much debate (Solorzano-Zavala *et al.*, 1996; Ghosh, 1999). It should be noted that in the classical mixing rules these parameters are symmetric *i.e.* $k_{ij} = k_{ji}$ and $d_{ij} = d_{ji}$, which can be regarded as too simple a treatment for highly nonideal mixtures. These are usually obtained by the regression of experimental phase equilibrium data for each pair of components, however, some predictive methods have been developed for their computation.

In the regression analysis, the EOS is used to calculate a particular system property (VLE or density data) and a suitable objective function (Paunovich *et al.*, 1980) is employed to minimize the differences between the experimental and predicted values. The interaction parameters are then obtained as values that best fit the experimental data to the predicted EOS values. Correlative or predictive schemes have also been developed to obtain the binary interaction parameters from pure component properties. Chueh and Prasunitz (1967) developed a relation of the binary interaction parameter of the RK EOS to the pure component critical volumes. Graboski and Daubert (1978) employed the use of the difference in the solubility parameter between hydrocarbon and non-hydrocarbon mixture components to develop a correlation for the binary interaction parameter.

[a] Where the terms A and B for the respective EOS have been defined in Table 3.5, however in these terms, the mixture parameters *i.e.* a_m and b_m replace the pure component energy and covolume terms.

Other attempts include those by Arai and Nishiumi (1987), Gao *et al.* (1992) and Coutinho *et al.* (1994). A common downfall of the above approaches has been a lack of universal or general applicability of these correlations for the binary interaction parameter. Additionally these approaches require the input of data in addition to that for the cubic EOS *i.e.* critical properties and acentric factors. Consequently, the regression analysis with phase equilibrium data has been the preferred method, however, concerns over the accuracy of the experimental data now come to the fore. Caution must also be exercised for complex systems where multiple interaction parameters could be obtained as a result of widely differing interactions. Also, concerns are expressed over the consideration of the pressure, temperature and composition dependency of the binary interaction parameters in VLE computations for nonideal systems (Mohammed and Holder, 1987; Voros and Tassios, 1993). Indeed the development of reliable generalized correlations for k_{ij} has indeed been the major impediment for the development of the predictive capability of cubic EOS for multicomponent mixtures (Stamataki and Tassios, 1998).

A fairly recent development that deserves mention is that by Jaubert and Mutelet (2004) who proposed a group contribution method for the calculation of k_{ij} for use in the PR EOS. The work was inspired from the earlier attempts of Peneloux and co-workers (1986, 1989, 1991), who were able to propose the first successful bridge between classical mixing rules and cubic EOS/ (A^E or G^E) models through a predictive approach for k_{ij}. The significance of the work of Jaubert and Muletet (2004) was that it was an attempt to remedy the fairly empirical nature of the k_{ij} correlations, which require too many inputs. Although the binary systems studied by the authors were alkane-alkane systems, the k_{ij} values obtained were indeed highly accurate and sometimes superior to those obtained by cubic EOS/(A^E or G^E) models.

The classical mixing rules were inspired by the statistically-mechanically sound mixing rule for the second virial coefficient, as shown in Equation (3.66) *i.e.* to ensure that the cubic EOS has a quadratic low-density composition dependence. Despite the presence of thermodynamic rigour, the simple form of classical mixing rules with just one symmetric binary interaction parameter are only adequate for representing the VLE of binary mixtures of nonpolar or slightly polar molecules (Peng and Robinson, 1976; Han *et al.*, 1988) which are similar (with regards to size or chemical nature) such as hydrocarbons and inert gases. With regards to polar and associating fluids or systems with molecules with large relative size discrepancies (Wei and Sadus, 2000), reasonable phase equilibrium computations cannot be achieved. Also, the liquid phase densities obtained with the CMR approach for pure fluids and mixtures are significantly erroneous.

Modifications of the vdW MR

There have been many proposed modifications of the classical mixing rules to allow for an improved treatment of highly nonideal systems. The approaches of Deiters and Schneider (1986), McHugh and Krukonis (1986) and Tsonopoulos and Heidman (1986), as discussed in Raal and Muhlbauer (1998) involve the incorporation of an interaction parameter into the expression for the van der Waals mixture covolume (b_m).

A noteworthy modification by Twu *et al.* (1991) of the classical mixing rules was the use of an asymmetric k_{ij} *i.e.* $k_{ij} \neq k_{ji}$ for the a_m parameter in the treatment of polar/polar and polar/non-polar systems which are highly nonideal and asymmetric:

$$a_m = \sum_{i=1}^{n}\sum_{j=1}^{n} z_i z_j \left(a_i a_j\right)^{0.5}\left(1 - k_{ij}\right) + \sum_{i=1}^{n} z_i \left[\sum_{j=1}^{n} z_j \left(a_i a_j\right)^{1/6}\left(k_{ji} - k_{ij}\right)^{1/3}\right]^{1/3} \qquad (3.241)$$

where k_{ij} and k_{ji} are the binary interaction parameter and usually $k_{ij} \neq k_{ji}$.

The use of the asymmetric binary interaction parameters resemble those used in the NRTL equation *i.e.* Equation (3.132). The motivation for the use of two different interaction parameters is to take into account unlike interactions in strongly asymmetric systems. In the case of $k_{ij} = k_{ji}$, the original form of the van der Waals can be recovered. This relation has been shown to provide excellent correlation of highly nonideal mixtures, comparable to that achieved by activity coefficient models for the liquid phase (Twu *et al.*, 2006). However, due to the form of the equation, the asymmetric vdW MR violates the theoretical boundary condition.

As mentioned above, there are two major shortcomings of the generalized CMR approach *i.e.* the representation of saturated liquid densities and the representation of mixtures that exhibit large discrepancies in the chemical nature and relative sizes of the components (asymmetric, polar, associating, heavy mixture components, *etc.*). To address the first of these deficiencies, the use of volume-translated cubic EOS forms as discussed before, the use of fluid-specific parameters in the mixing rules (binary interaction parameters) or the asymmetric approach of Twu *et al.* (1991), as shown above, can certainly help matters. Of even greater concern is the second shortcoming of the CMR approach, which is more fundamental in nature than the first and not easily rectified with a simple modification of the original approach as the geometric form of the vdW mixing rules is inapplicable for representing composition variations and highly

nonideal or complex mixtures. Consequently, this has necessitated the formulation of alternative mixing rules with a non-traditional compositional dependence to incorporate a flexible thermodynamic framework for the representation of highly nonideal solution behaviour such as the excess energy (A^E or G^E) models traditionally used to correlate low to moderate-pressure VLE data in the dense liquid phase.

(b) Local Composition Mixing Rules

Huron-Vidal mixing rule

The genesis of the extension of the local composition concept to the EOS mixing rules can be attributed to the efforts of Heyen (1981) and the more consequential efforts of Vidal (1978) and that of Huron and Vidal (1979) in their search for novel mixing rules. Huron and Vidal (1979) proposed that local excess free energy models could be introduced into EOS mixing rules by expressing the excess Gibbs free energy $\left(G^E\right)$ in terms of the pure component (ϕ) and mixture component (ϕ_i) fugacity coefficients as follows:

$$G^E = RT\left[\ln\phi - \sum_{i=1}^{n} x_i \ln\phi_i\right] \tag{3.242}$$

An examination of Equation (3.242) immediately reveals its significance for phase equilibrium computations, as it allows for an EOS with an expression for ϕ and ϕ_i on the right-hand side to be related to the activity coefficient (γ_i) term on the left-hand side through the substitution of a suitable G^E model.

There were three assumptions inherent in the above approach of the Huron and Vidal mixing rule (HVMR). Firstly, the value of G^E calculated from an EOS at infinite pressure equals the value calculated from a liquid phase G^E model (which is taken to be independent of pressure) *i.e.* $G^E_{EOS}(T, P \rightarrow \infty, x_i) = G^E_{\gamma}(T, P \rightarrow \infty, x_i)$. The use of infinite pressure ensures that the liquid root of the EOS was used. Secondly, the covolume parameter b is equal to the molecular volume in the limit of infinite pressure, as the infinite pressure limit of an EOS is derived on the basis that in a liquid solution, the molecules are so closely packed that there is no free volume *i.e.* $\left(\lim_{P \rightarrow \infty} V = b\right)$.

The last relates to that of the excess volume, which is taken to be zero at infinite pressure. The latter two assumptions can be explained in terms of the following:

$$G^E = A^E + PV^E \tag{3.243}$$

where A^E is the excess Helmholtz free energy and V^E is the excess volume. To ensure that the G^E term remains finite in the limit of infinite pressure, V^E must evaluate to zero.

Through the use of a generic cubic EOS and the linear mixing rule for the mixture covolume parameter in Equation (3.238) with Equation (3.242), the following expression for the mixture energy parameter is obtained:

$$a_m = b_m\left[\sum_{i=1}^{n} z_i \frac{a_i}{b_i} + \frac{G_\infty^E}{\sigma}\right] \tag{3.244}$$

where G_∞^E is the excess Gibbs free energy from an activity coefficient model taken in the limit of infinite pressure *i.e.* where $G_\gamma^E(T, P \to \infty, x_i)$ and σ is a numerical constant whose value is dependent upon the cubic EOS used *i.e.* for the SRK EOS, $\sigma = -\ln 2$ and for the PR EOS, $\sigma = \frac{1}{\sqrt{2}}\ln\left(\sqrt{2}-1\right)$.

In general, as with the remaining excess free energy mixing rules, any activity coefficient model can indeed be used (Van Laar, Redlich-Kister, *etc.*), however, the semi-theoretical framework of the local composition models (Wilson, T-K Wilson, NRTL and UNIQUAC) have been very been very successful and popular for the representation of nonideal mixtures. The incorporation of the latter affords the mixing rule with status of a local composition mixing rule (LCMR). The use of a group contribution approach (*e.g.* UNIFAC) for excess free energy expression allows for the development of arguably the most powerful tool in applied chemical thermodynamics in the form of a completely predictive cubic EOS/(A^E or G^E) approach. A lengthy discussion of the past and present developments of such predictive approaches has not been included in this review due the use of the direct method for phase equilibrium correlation being of primary consideration.

At this juncture, the author considers it a necessary exercise to present a generalization of the approach for the formulation of EOS/ (A^E or G^E) mixing rules, as it is would serve to facilitate

an understanding of the remaining material in this review. In this approach, a mixing rule for the energy parameter *i.e.* a_m is obtained by equating the excess free energy equation obtained from the cubic EOS with that of a traditional low-pressure liquid phase activity coefficient model *i.e.* $\frac{G^E_{EOS}}{RT} = \frac{G^E_\gamma}{RT} (\text{at } P = P^{ref})$, where the activity coefficient model (G^E_γ) is typically regarded as pressure-independent since it is parameterized typically at low pressures. However, due to the inherent pressure dependency of the excess molar Gibbs free energy from a cubic EOS (G^E_{EOS}) approach, the equality shown above is specified at a specific reference pressure. The choice of the latter has principally given rise to three approaches for the formulation of cubic EOS/ (A^E or G^E) mixing rules.

The first is the infinite-reference pressure (IRP) approach of Huron and Vidal (1979), Wong and Sandler (1992) and Twu and Coon (1996). The second is the zero-reference pressure (ZRP) approach of Michelsen (1990a, 1990b), Dahl and Michelsen (1990), Twu *et al.* (1997) and Twu *et al.* (1998a, 1998b). The third is the no-reference pressure (NRP) method seen in the LCVM approach of Boukouvalas *et al.* (1994) and the approach of Twu *et al.* (1999). The fundamental difference in these approaches lies in the assumptions that are necessitated. In the IRP approach, the assumption of a constant excess Helmholtz energy applies. The ZRP and NRP approaches assume that there is either a constant reduced liquid volume or the same volume as that of van der Waals applies.

The G^E_∞ expression used by Huron and Vidal (1979) was a modified form of the classical NRTL equation (1969) as shown in Equation (3.130).The only modification in the use of the infinite pressure condition has been the introduction of the pure component covolume term (b_j) in the NRTL equation through the G_{ij} term, as shown in Equation (3.245).

$$G^*_{ij} = b_j \exp\left(-\alpha_{ji}\tau_{ji}\right) \tag{3.245}$$

where G^*_{ij} is the modified term from the classical NRTL equation and the remaining terms have been described in the discussion on the NRTL approach in Section (3.5.2.3).

Incorporating the modified NRTL equation into the HVMR for a_m results in the following:

$$a_m = b_m\left[\sum_{i=1}^{n} z_i \frac{a_i}{b_i} - \frac{1}{\sigma}\left(\frac{\sum_{j=1}^{n} x_j G^*_{ji}\tau_{ji}}{\sum_{k=1}^{n} x_k G^*_{ki}}\right)\right] \tag{3.246}$$

From Equation (3.245) it can be seen that if $\alpha = 0$, then the HVMR reduces to the vdW one-fluid CMR. The expressions for a mixture component (ϕ_i) in the application of the HVMR to the SRK and PR EOS models is shown below as Equations (3.247) and (3.248), respectively:

$$\ln\phi_i = \frac{b_i}{b_m}(Z-1) - \ln(Z-B_m) - \left[\frac{a_i}{RTb_i} - \frac{\ln\gamma^{a}_{i,\infty}}{\ln 2}\right]\ln\left(\frac{Z+B_m}{Z}\right) \tag{3.247}$$

$$\ln\phi_i = \frac{b_i}{b_m}(Z-1) - \ln(Z-B_m) - \frac{1}{2\sqrt{2}}\left[\frac{a_i}{RTb_i} - \frac{\ln\gamma_{i,\infty}}{\ln 2}\right]\ln\left(\frac{Z+\left(1+2\sqrt{2}\right)B_m}{Z+\left(1-2\sqrt{2}\right)B_m}\right) \tag{3.248}$$

It was shown by Huron and Vidal (1979) that the HVMR can be used to correlate the VLE data for strongly nonideal systems with good accuracy.

The mixing rule has been applied to variety of polar and asymmetric systems (Adachi and Sugie, 1985; Gupte and Daubert, 1986; Heidemann and Rizvi, 1986). There have been a number of studies (Djordjevic *et al.*, 2001) where the validity of the Huron-Vidal MR with a variety of cubic EOS models (vdW, RK, SRK and PRSV) and also activity coefficient models (van Laar, Redlich-Kister, NRTL, UNIQUAC and ASOG) has been established. In particular, the studies by Tochigi *et al.* (1990) and Soave *et al.* (1994) involved the use of a SRK group contribution method with the HVMR to predict HPVLE and the infinite-pressure activity coefficient, respectively.

The principal shortcomings of the HVMR approach can be described as both theoretical and computational. Tsonopoulos and Heidman (1986) pointed out the computational difficulties of the method in terms of the investment of computational time, which in the HVMR method is proportional to the cube of the number of components in the mixture as opposed to the square for the CMR approach.

[a] $\gamma_{i,\infty}$ is the infinite-pressure activity coefficient.

Sandler *et al.* (1994) comment upon the inapplicability of this method for the treatment of non-polar fluids in mixtures, which have traditionally been the domain of the traditional cubic EOS and the van der Waals CMR approach, since the HVMR does not reduce to the classical mixing rules. Consequently, this method is indeed mixture component-specific and is not efficient for representing nonpolar + non-polar and polar + nonpolar mixtures as the same mixing rule parameters have to be used to describe all the components. An inflexible model which cannot account for widely-differing molecular behaviours is indeed ineffective for the treatment of diverse multicomponent mixtures. It should be noted, however, that there have been recent studies such by Seo *et al.* (2000) and Ioannidis and Knox (2001) which have demonstrated the suitability of the Huron-Vidal mixing rules for the treatment of highly nonideal mixtures. The use of the SRK EOS and the HVMR produced good correlation of a pentane + ethanol system studied at near critical temperatures in the study of Seo *et al.* (2000). An additional theoretical inconsistency of this method is that the low-density limit boundary condition of adherence of the mixing rules to the quadratic composition dependence of the second virial coefficient is not adhered to.

The use of the infinite-pressure limit has also introduced many inconsistencies as the value of the excess Gibbs energy used in the EOS *i.e.* G^{E}_{∞} differs from that at finite pressures, especially near atmospheric or low pressures. This results in the parameters obtained with this model not being the same as those which are obtained when LPVLE data is correlated directly with the activity coefficient model. This is as a result of ignoring the pressure dependency of the excess Gibbs free energy from liquid phase models (which are principally applied at low pressures) when applying the infinite-pressure limit. Consequently, from a predictive point of view, the activity coefficient model parameters that have been regressed from LPVLE data, as provided in databases, cannot be used in the G^{E} part of the MR model. This necessitates the expenditure of additional effort in having to recorrelate experimental data. Also, the temperature dependencies of the parameters obtained from this model are too high to allow any predictive capability for the model.

Modifications of the HVMR

To address the deficiencies that are present in the original HVMR approach, there has been a considerable expenditure of effort in adjusting the stringency of the infinite-pressure limit by numerous researchers (Mollerup, 1986; Gupte *et al.*, 1986a, 1986b; Gani *et al*, 1989; Michelsen, 1990a, 1990b; Dahl and Michelsen, 1990; Heideman and Kokal, 1990, Lermite and Vidal, 1992; Soave *et al.*, 1994; Novenario *et.al*, 1996).

The initial proposition by Mollerup (1986) to obtain the parameters directly from an expression for the zero-pressure excess Gibbs free energy was elaborated upon and implemented by Michelsen (1990a, 1990b). Through the use of the SRK EOS and the application of a reference pressure of zero to the HVMR, Michelsen (1990b) obtained the modified Huron-Vidal first order (MHV1) mixing rule in the following form:

$$\alpha_m = \sum_{i=1}^{n} z_i \alpha_i + \frac{1}{q_1}\left[\frac{G_\gamma^E(T, P \to 0, x_i)}{RT} + \sum_{i=1}^{n} z_i \ln\left(\frac{b_m}{b_i}\right)\right] \tag{3.249}$$

where

$$\alpha_m = \frac{a_m}{b_m RT} \tag{3.250}$$

$$\alpha_i = \frac{a_i}{b_i RT} \tag{3.251}$$

with $q_1 = -0.593$ and $q_1 = -0.530$ being recommended by Michelsen (1990b) for the SRK EOS and PR EOS, respectively. $G_\gamma^E(T, P \to 0, x_i)$ is the liquid phase excess free energy correlation with a zero-pressure standard-state. The correlation used for the mixture covolume (b_m) is the linear vdW MR.

In a second formulation by Dahl and Michelsen (1990) for improving the accuracy of the MR, the modified Huron-Vidal second order (MHV2) mixing rule was proposed as follows:

$$q_1\left(\alpha_m - \sum_{i=1}^{n} z_i \alpha_i\right) + q_2\left(\alpha_m^2 - \sum_{i=1}^{n} z_i \alpha_i^2\right) = \frac{G_\gamma^E(T, P \to 0, x_i)}{RT} + \sum_{i=1}^{n} z_i \ln\left(\frac{b_m}{b_i}\right) \tag{3.252}$$

with $q_1 = -0.478$ and $q_2 = -0.0047$ being recommended by Dahl and Michelsen (1990) for the SRK EOS. Huang and Sandler (1993) propose values of $q_1 = -0.4347$ and $q_2 = -0.003654$ for the PR EOS. When $q_2 = 0$, the MHV1 form is recovered. Due to the quadratic form of Equation (3.252), an analytical solution is necessitated to obtain α_m, where the larger root is selected for a_m (Dahl and Michelsen, 1990).

The fugacity for a component i in a mixture with the modified Huron-Vidal mixing rules, as applied to the SRK and PR EOS are shown in Equations (3.253) and (3.254), respectively.

$$\ln \phi_i = \ln\left(\frac{1}{Z - B_m}\right) + \left[\frac{P}{RT(Z - B_m)} - \frac{P\alpha}{RT(Z + B_m)}\right] b_i - \bar{\alpha}_i \ln\left(\frac{Z + B_m}{Z}\right) \qquad (3.253)$$

$$\ln \phi_i = \frac{b_i}{b_m}(Z - 1) - \ln(Z - B_m) - \frac{\bar{\alpha}_i}{2\sqrt{2}} \ln\left(\frac{Z + (1 - \sqrt{2})B_m}{Z + (1 - \sqrt{2})B_m}\right) \qquad (3.254)$$

where for the MHV1 form:

$$\bar{\alpha}_i = \left(\frac{1}{q_1}\right)\left[q_1\alpha_i + \ln\gamma^{a}_{i,0} + \ln\left(\frac{b_m}{b_i}\right) + \left(\frac{b_i}{b_m}\right) - 1\right] \qquad (3.255)$$

and for the MHV2 form:

$$\bar{\alpha}_i = \frac{1}{q_1 + 2q_2\alpha_m}\left[q_1\alpha_i + q_2(\alpha_m^2 + \alpha_i^2) + \ln\gamma^{\infty}_{i,0} + \ln\frac{b_m}{b_i} + \frac{b_i}{b_m} - 1\right] \qquad (3.256)$$

The MHV1 and MHV2 mixing rules have been applied to the correlations and predictions a host of thermodynamic properties (VLE, LLE, VLLE, gas solubility, excess enthalpy, excess heat capacity, *etc.*). In terms of a comparison of the two, the MHV2 approach is the most popular and is only slightly more complex than the original HVMR model (as it requires a solution of the quadratic expression for α_m), however, it allow for the direct use of information available in low-pressure G^E correlations databases and tables without recorrelation of model parameters.

Indeed, the group contribution approach known as the as the MHV2-UNIFAC, as reviewed by Fredenslund and Sorensen (1994), has been quite a promising predictive method. Hence with incorporation of a suitable group contribution method in these modified approaches, predictions of phase equilibria are now possible. One of the most important potential applications of the MHV1 and MHV2 approaches is in extending the predictive capability of group contribution methods to supercritical mixtures (Heidemann, 1996). However, the use of these methods for asymmetric systems of gases and hydrocarbons is debatable (Ghosh, 1999).

[a] Where $\gamma_{i,0}$ is the zero-pressure activity coefficient.

There have been many modifications of the MHV1 and MHV2 approaches as in the works of Boukouvalas *et al.* (1994) *i.e.* the LCVM, Tochigi *et al.* (1995), Michelsen (1996) and Zhong and Matsuoka (1999).

As with the original HVMR, the MHV1 and MHV2 forms do not satisfy the second virial coefficient boundary condition and they do not readily reduce to the classical mixing rules. However, next to the Wong-Sandler mixing rules, the MHV1 and MHV2 mixing rules are the most popular for correlation and prediction of phase equilibria in the contemporary research arena.

The other significant modifications of the Huron-Vidal approach include the Kurihara-Tochigi-Kojima model of Kurihara *et al.* (1987), the Huron-Vidal-Orbey-Sandler (HVOS) approach of Orbey and Sandler (1995b) and the coupling of infinite dilution activity coefficient (γ_i^∞) with the HVMR in the HVID model of Feroiu and Geana (1996). In the latter model, an attempt at developing a predictive capability for the Huron-Vidal approach was made by Feroiu and Geana (1996) who proposed the use of low-pressure γ_i^∞ values in the HVMR. However, despite a study by the authors showing the applicability of the HVID approach for the prediction of VLE over a wide range of pressures and temperatures for quite nonideal systems, there has not been a great deal of interest in this approach.

(c) Density-Dependent Mixing Rules

The satisfaction of the boundary conditions for cubic EOS necessitated that at low densities the quadratic composition dependence of the second virial coefficient should be reproduced and that at high or liquid-like densities, the G^E behaviour of the system should be in accordance with that obtained from traditional low-pressure liquid phase G^E correlations. A common notion was that the incorporation of a density-dependence into the mixing or combining rules would allow for the adherence of the above and for better representation of both dense and non-dense phases in doing so. Initial attempts in this regard were by Mollerup (1981) and Whiting and Prausnitz (1982) and later on by Lee and Sandler (1987), Mohamed and Holder (1987) and Shibata and Sandler (1989b). The latter three approaches are discussed in great detail in the text of Raal and Muhlbauer (1998).

The traditional density-dependent mixing rules (DDMR) will not be discussed in any detail here as it has not proven popular due to significant drawbacks associated with its use. The form of the EOS that is obtained with incorporation of the DDMR into cubic EOS approaches is non-cubic (with regards to density or volume) and in general the order of the EOS changes with the

number of components in the mixture. This is of course in direct violation of the one-fluid van der Waals model. Also, due to the complex form of the EOS incorporating DDMR equations, the investment in computational times for numerical computations is highly unattractive.

Mixing Rules of Twu and co-workers

The research efforts of Twu and co-workers (1996, 1997, 1999, 2001) have seen numerous modifications and extensions of mixing rules for developments of cubic EOS/A^E models to allow for adherence to the van der Waals and second virial coefficient constraints successfully applied to asymmetric and highly nonideal systems. Their work has both covered and extended the spectrum of methods for developing cubic EOS/A^E models. The most recent work of Twu and co-workers has culminated in the formulation of both zero-reference pressure (ZRP) and no- reference pressure (NRP) DDMR that have been shown to be quite promising and of theoretical significance. These methods will be described qualitatively as an in-depth discussion of the approach is beyond the scope of this work.

The Twu, Coon and Bluck (TCB) mixing rule (Twu *et. al.*, 1997) was essentially an extension of the Twu-Coon (TC) mixing rule (Twu and Coon, 1996) from that of infinite pressure to zero pressure to develop a ZRP mixing rule. This was to address the inability of the TC mixing rule to accurately represent the incorporated activity coefficients of the liquid phase despite the use of binary interaction parameters to correct for the assumption of a constant excess Helmholtz energy. Excellent agreement between the experimental data and VLE predictions by the model over wide temperature and pressure ranges was obtained using only the information from the activity coefficient model. Interestingly enough, Twu *et al.* (1997) showed that there was no significant difference in the results were obtained with or without (using a linear mixing rule for the covolume) the observance of the second virial coefficient condition in the mixing rule.
The development of a no-reference pressure (NRP) approach by Twu *et al.* (1999) was to eliminate the difficulties associated with the ZRP approach of Twu *et al.* (1997). In the latter, G^E parameters had to be applied close to zero pressure and the range of the liquid volume obtained from the EOS at zero pressure was limited to a reduced temperature of 0.7. With the NRP approach, the liquid volume range was extended to the critical point and since the pressure limit is removed, the application of a suitable excess free energy correlation at the system conditions to the mixing rule was achieved without the creation of any problems with the incorporation of the model. Further changes were introduced into the NRP mixing rule by Chung and Twu (2001) in a later effort to simplify the phase equilibrium calculations and facilitate the incorporation of the method into process design applications. Both methods

discussed above have a density-dependence in an explicit form and this allows the model to reproduce the liquid phase activity coefficient model behaviour with great success. Both models provide excellent agreement between experimental VLE data and predictions over a wide range of pressures and temperatures with published activity coefficient model parameters.

(d) Density-Dependent Local Composition Mixing Rules

In general, the cubic EOS/G^E approaches that have been dealt with so far and to be discussed later are not predictive since the binary interaction parameter (k_{ij}) used in the mixing rules for the incorporated G^E model must be adjusted through a suitable correlative procedure with the experimental data, to validate the approximation of equating the low-pressure excess free energy from activity coefficient models and the cubic EOS excess free energy at some reference pressure. Of course, for those mixing rules which are incompatible with the current body of available excess free energy information, any enforced reparameterization of the mixing rule model excludes the model from predictive capability.

The density-dependent local composition mixing rules (DDLCMR) are an important part of the development of a predictive framework or group contribution equations of state (GC EOS) for incorporating predictive local composition excess free energy models into density-dependent EOS mixing rules. This approach serves to embody the ultimate objective of the modern direct method of Raal and Muhlbauer (1998) to allow for a purely predictive approach with a unified thermodynamic cubic EOS/$(A^E$ or $G^E)$ approach for the treatment of both vapour and liquid phases of highly nonideal or polar mixtures, whereby the parameters of the former could be interrelated and obtained in a predictive manner from available information (databases, tables, previous correlations) on the latter. Two DDLCMR methods, as discussed and evaluated by Raal and Muhlbauer (1998), are the GC EOS of Skjold-Jorgensen (1984, 1988) and also the UNIWAALS EOS of Gupte *et al.* (1986a, 1986b). Orbey and Sandler (1995b) are highly critical of the UNIWAALS approach and its subsequent modification by Gani *et al.* (1989) who state that although the use of the above affords a predictive method, its use leaves much to be desired with regards to accuracy.

Despite the traditional exclusion of other cubic EOS/ (A^E or G^E) approaches from the modern direct method classification, the incorporation of group contribution methods such as UNIFAC or ASOG for the excess free energy model parameters and for the binary interaction parameter (Jaubert and Mutelet, 2004), allows for other mixing rules to be used as predictive methods.

(e) Density-Independent and Density-Independent Local Composition Mixing Rules

This class of mixing rule models is a fairly recent addition and is a significant break-though for obtaining theoretically correct mixing rules. As its title implies, it is independent of the densities of the mixture components hence does not introduce the principal drawbacks of traditionally density-dependent terms in the EOS which are computationally complex and violate the cubic form of traditional cubic EOS.

Wong-Sandler Mixing Rule (1992)

Wong and Sandler proposed a novel mixing rule to satisfy the correct theoretical behaviour of the EOS at both low and high densities in the absence of any density dependence and to allow for the incorporation of existing literature G^E information without the need for recorrelation. The formulation of this approach was a result of two key observations. The first was that whilst the vdW one fluid mixing rules for a_m and b_m were sufficient conditions to ensure adherence with the proper quadratic composition dependence of the second virial coefficient in the low-density boundary condition, they are not necessary conditions. As shown in Equation (3.233), the vdW mixing rule places constraints on a_m and b_m to satisfy the quadratic second virial coefficient (QSVC) condition. In the Wong-Sandler (WS) mixing rule, use is made of the last equality in Equation (3.233) *i.e.* $\left(b - \frac{a}{RT}\right)_{ij}$, the cross second virial coefficient of the EOS, as one of the constraints for the EOS mixture parameters in the linear combining rules as follows:

$$\left(b - \frac{a}{RT}\right)_{ij} = 0.5\left[\left(b_i - \frac{a_i}{RT}\right) + \left(b_j - \frac{a_j}{RT}\right)\right]\left(1 - k_{ij}\right) \qquad (3.257)$$

where k_{ij} is the second virial coefficient binary interaction parameter, whose importance in this approach will be discussed later.

The second key consideration is that the excess Helmholtz free energy on mixing is much less pressure-dependent $\left(A^E\right)$ than the corresponding excess Gibbs free energy $\left(G^E\right)$. This can be seen from:

$$G^E\left(T, P = \text{low}, x_i\right) = A^E\left(T, P = \text{low}, x_i\right) = A^E\left(T, P = \infty, x_i\right) \qquad (3.258)$$

The first of the equalities stems from Equation (3.243) for the condition at low-pressures and the second, from the inherent pressure independence of A^E, which can be shown as follows:

$$A^E_{EOS}(T, P=\infty, x_i) = A^E_\gamma(T, P=\infty, x_i) = A^E_\gamma(T, \text{low } P, x_i) = G^E_\gamma(T, \text{low } P, x_i) \quad (3.259)$$

where A^E_{EOS} refers to the excess Helmholtz free energy obtained from the EOS and A^E_γ and G^E_γ refer to the excess free energies from an activity coefficient model.

With a local composition G^E model being substituted for the A^E_{EOS} term, this method becomes a density-independent local composition mixing rule (DILCMR). Through the combination of the above expressions in (3.257)-(3.259) with that of the HV LCMR approach in Equation (3.244), yields the following:

$$a_m = b_m\left[\sum_{i=1}^{n} z_i\left(\frac{a_i}{b_i}\right) - \frac{G^E_\gamma(T, \text{low } P, x_i)}{\sigma}\right] \quad (3.260)$$

$$b_m = \left[\frac{\sum_{i=1}^{n}\sum_{j=1}^{n} z_i z_j\left(b - \frac{a}{RT}\right)_{ij}}{1 + \frac{G^E_\gamma(T, \text{low } P, x_i)}{RT} - \sum_{i=1}^{n} z_i\left(\frac{a_i}{b_i RT}\right)}\right] \quad (3.261)$$

where σ is a constant that is dependent upon the cubic EOS used, as for Equation (3.244).

To simplify the above, the following terms are used:

$$\frac{a_m}{RT} = \frac{QD}{1-D} \quad (3.262)$$

$$b_m = \frac{Q}{1-D} \quad (3.263)$$

$$Q = \sum_{i=1}^{n}\sum_{j=1}^{n} z_i z_j\left(b - \frac{a}{RT}\right)_{ij} \quad (3.264)$$

$$D = \frac{G_{\gamma}^{E}(T, \text{low } P, x_i)}{\sigma RT} + \sum_{i=1}^{n} z_i \left(\frac{a_i}{b_i RT} \right) \tag{3.265}$$

The fugacity for a component i in a mixture with the WS mixing rules as applied to the SRK and PR EOS is shown in Equations (3.266) and (3.267), respectively.

$$\ln \phi_i = -\ln(Z - B_m) + \beta \left(\frac{1}{b_m} \right)(Z-1) + \left(\frac{a_m}{b_m RT} \right) \left[\chi \left(\frac{1}{a_m} \right) - \beta \left(\frac{1}{b_m} \right) \right] \ln \left(\frac{Z}{Z + B_m} \right) \tag{3.266}$$

$$\ln \phi_i = \beta \left(\frac{1}{b_m} \right)(Z-1) + \frac{1}{2\sqrt{2}} \left(\frac{a_m}{b_m RT} \right) \left[\chi \left(\frac{1}{a_m} \right) - \beta \left(\frac{1}{b_m} \right) \right] \ln \left(\frac{Z + \left(1 - \sqrt{2}\right) B_m}{Z + \left(1 + \sqrt{2}\right) B_m} \right) - \ln(Z - B_m) \tag{3.267}$$

where

$$\beta = \left[\left(\frac{1}{1-D} \right) \left(2 \sum_{i=1}^{n} z_j \left(b - \frac{a}{RT} \right)_{ij} \right) - \left(\frac{Q}{(1-D)^2} \right) \left(1 - \left(\frac{a_i}{b_i RT} + \frac{\ln \gamma_{i,\infty}}{\sigma} \right) \right) \right] \tag{3.268}$$

$$\chi = DRT \left[\left(\frac{1}{1-D} \right) \left(2 \sum_{i=1}^{n} z_j \left(b - \frac{a}{RT} \right)_{ij} \right) - \left(\frac{Q}{(1-D)^2} \right) \left(1 - \left(\frac{a_i}{b_i RT} + \frac{\ln \gamma_{i,\infty}}{\sigma} \right) \right) \right] + b_m RT \left[\frac{a_i}{b_i RT} + \frac{\ln \gamma_{i,\infty}}{\sigma} \right] \tag{3.269}$$

The above cubic EOS + WSMR combination satisfies the boundary condition of the quadratic composition dependence of the second virial coefficient and the high-density constraint that excess free energy expression in the EOS MR behave like that for a traditionally low-pressure liquid phase G^E model *i.e.* to allow for the incorporation of excess free energy information from low-pressure G^E models. The latter feature has a great deal of significance for the development of predictive methods for EOS methods using information from predictive or correlative low-pressure G^E models *i.e.* making HPVLE predictions using low-pressure data. This allows for existing databanks of low-pressure G^E data (Wong *et al.*, 1992) and parameters obtained by the $\gamma_i - \phi_i$ approach to be readily employed for use in the WSMR approach. Additionally due to the

inherent temperature dependence of the EOS approach, the parameters in the excess free energy terms used in the WSMR exhibited much lower temperature dependence than those for the corresponding excess free energy models used directly. Consequently, the repercussions of this for data correlation are significant as wider temperature and pressure extrapolation procedures can be achieved with greater confidence. The study of Wong *et al.* (1992) showed that the WSMR can be employed to make predictions at conditions that were hundreds of bars and Kelvins above the conditions at which the parameters for the experimental data were regressed.

In a study of the WSMR by Wong and Sandler (1992), the mixing rule was combined with the PRSV EOS and excellent VLE, LLE and VLLE correlations were obtained when compared to those that were obtainable when the activity coefficient models had been used directly. Consequently, the WSMR has extended the applicability of cubic EOS models to the realm of applicability of activity coefficient models. Huang and Sandler (1993) conducted a comparative study of the WSMR and MHV2 mixing rules with the SRK and PR EOS models for binary and ternary systems. Both methods were seen to be effective in obtaining HPVLE predictions from low-pressure data. The WSMR was found to be superior to the MHV2 mixing rule as the errors in the latter were at least half those of the former. There were many other studies that have also demonstrated the applicability of the WSMR to wide pressure and temperature ranges and to polar, associating or moderately asymmetric fluid mixtures (Ghosh, 1999). The WSMR has been employed in many comparative studies, especially with Huron-Vidal based approaches (Orbey and Sandler, 1996; Solorzano-Zavala *et al.*, 1996; Wang *et al.*; 1996).

The use of the binary interaction parameter (k_{ij}) in the WSMR approach has probably been the most controversial aspect of the WSMR formulation (apart from the difficulty in reduction to the vdW one fluid form) and this stems from the fact that the equality in Equation (3.259) is an approximation *i.e.* it is not exact. Consequently, the k_{ij} value in the WSMR approach has the important function of ensuring that the excess Helmholtz free energy at infinite pressure (from the cubic EOS) is equivalent to the excess Gibbs free energy at low pressures (from an activity coefficient model). This value of k_{ij} has to be adjusted or fitted to the data set, hence with the WSMR some reparameterization is necessitated to ensure accurate correlations. Consequently, the k_{ij} quantity is not a freely adjustable or independent parameter (Djordjevic *et al.*, 2001).

Modifications of the WSMR

In a study of the attributes and limitations of the WSMR, Coutsikos *et al.* (1995), discovered that the WSMR binary interaction parameter (k_{ij}), as shown in Equation (3.255), was actually composition-dependent and that this composition-dependence increased as the asymmetry of the system increased. It was found that for highly extreme situations of system asymmetry, the composition dependence of k_{ij} results in a violation of the quadratic composition dependency of the second virial coefficient. It was also shown by Coutsikos *et al.* (1995) that as the system asymmetry increases together especially at high system pressures, the condition represented in Equation (3.258) breaks down as follows:

$$G^E(T, P = \text{low}, x_i) = A^E(T, P = \text{low}, x_i) \neq A^E(T, P = \infty, x_i) \tag{3.270}$$

Consequently, it can be inferred from the study of Coutsikos *et al.* (1995) that for relatively symmetric systems (similar values of infinite dilution activity coefficients), there is reasonable representation of the activity coefficient behaviour of the system over the entire composition range is observed. However, with highly asymmetric systems, poor representation of the activity coefficients is frequently observed.

Orbey and Sandler (1995a) revisited the WSMR approach to address inconsistencies primarily related to the binary interaction parameter (as discussed before) and the reduction of their model to the classical vdW MR. The latter is as result of the proven applicability of vdW MR working very well for nonpolar systems, consequently it is desirable that proposed novel mixing rules reduce to the classical mixing rules. It was shown in a comparative study by Voros and Tassios (1993) of several mixing rules, including the original WSMR, that the one fluid vdW mixing rules gave the best results for nonpolar systems with inorganic gases.

It was pointed out by Orbey and Sandler (1995b) that the condition shown in Equation (3.257) does not hold for any arbitrary value of k_{ij}. Therefore it was suggested that the value of k_{ij} should be chosen so that A^E_{EOS} is virtually independent of pressure or that its value is chosen so as to reproduce the experimental G^E curve at the pressure measurements. From the above, it can be seen that the k_{ij} parameter contains no additional information as that already contained in the existing G^E information and it was suggested that $k_{ij} = 0$ could be used in the reformulated approach. To facilitate a smooth transition from activity coefficient-like behaviour to vdW MR,

Orbey and Sandler (1995a) changed the representation of the cross second virial coefficient term, as follows:

$$\left(b - \frac{a}{RT}\right)_{ij} = \frac{\left(b_i + b_j\right)}{RT} + \frac{\sqrt{a_i a_j}}{RT}\left(1 - k_{ij}\right) \tag{3.271}$$

With the above form, the decomposition of the reformulated WSMR (henceforth known as the WSMR2 model, where WSMR1 will refer to the original model) to the classical mixing rules is facilitated. Orbey and Sandler then used the form of the modified NRTL equation as that used by Huron and Vidal (1979) and by setting $\alpha_{ij} = 0$ in the latter, the following is obtained:

$$\frac{A^E}{RT} = \frac{x_1 x_2 \left(b_1 \tau_{12} + b_2 \tau_{21}\right)}{x_1 b_1 + x_2 b_2} \tag{3.272}$$

Applying the classical mixing rules for a_m *i.e.* Equation (3.235), gives the following:

$$k_{12} = 1 - \frac{1}{2\sqrt{a_1 a_2}}\left[a_1 \frac{b_2}{b_1} + a_2 \frac{b_1}{b_2} + \frac{RT}{C}\left(b_1 \tau_{12} + b_2 \tau_{21}\right)\right] \tag{3.273}$$

In the experimental data reduction procedure, the authors propose two types of procedures; the choice of which is dictated by the nature of the mixture under study *i.e.* ideal mixtures versus nonideal mixtures. With regards to the former, "mode 1" was applied, where $\alpha_{ij} = 0$, as in Equation (3.271), and determined the value of $\left(b_1 \tau_{12} + b_2 \tau_{21}\right)$ or chose to force it to reproduce the known value of the binary interaction parameter $\left(k_{ij}\right)$ using Equation (3.273). In the mode for nonideal mixtures *i.e.* "mode 2", the value of k_{ij} was set equal to zero and a suitable value for α_{ij} was empirically determined to be 0.1. In this mode, there were two adjustable parameters *i.e.* τ_{12} and τ_{21}. These could be obtained as follows:

$$\tau_{ij} = \ln \gamma_i^{\infty} - \tau_{ij}\left(\frac{b_i}{b_j}\right)\exp\left(-\alpha_{ij}\tau_{ij}\right) \tag{3.274}$$

where the γ_i^{∞} values could be obtained experimentally or from that of predictive liquid phase G^E models.

The τ_{12} and τ_{21} parameters can be obtained through correlation of experimental VLE data. Orbey and Sandler tested this equation on five nonideal binary systems and one ternary system, where it was discovered that the WSMR2 model was indeed capable of both correlating and for predicting VLE data of complex systems over wide temperature and pressure ranges. The use of the modified NRTL equation and the UNIFAC method was particularly recommended for data correlation and prediction, respectively. An important point to note about the WSMR2 approach is that only through the use of the modified NRTL equation or Wohl expansion (with optimal parameter values) can the reduction of the WSMR2 model to the classical or vdW mixing rules be achieved. It was argued later by Twu *et al.* (2001) that even with the reformulated WSMR2 approach, since a modified form of the NRTL was used for the excess free energy expression, the VLE parameters regressed from experimental VLE data with the classical form of the NRTL equation were not readily applicable to WSMR2, since the G_{ij} term has a different form.

Mixing rules of Twu and Coon (1996)

In an infinite-reference pressure (IRP) approach, Twu and Coon (1996) attempted to address the problems associated with the Wong and Sandler IRP mixing rules to formulate a mixing rule that would readily reduce to the van der Waals one-fluid theory. Twu and Coon recognized that the use of the ideal solution as the reference state *i.e.* $\Delta A_{\text{ideal solution}}$ in the cubic EOS/A^E mixing rule does not result in the mixing rules readily decomposing into the classical mixing rule form, which was the case for the approach of Wong and Sandler (1992), where:

$$A^E_{WS} = \Delta A - \Delta A_{\text{ideal solution}} \tag{3.275}$$

where A^E_{WS} is the excess Helmholtz free energy used by Wong and Sandler (1992) and ΔA is the quantity calculated by from the cubic EOS. Twu and Coon used the van der Waals fluid as the reference state to ensure that the classical mixing rules are readily recoverable from the novel mixing rule, as follows:

$$A^E_{nr} = \Delta A - \Delta A_{vdW} \tag{3.276}$$

where A^E_{nr} is a non-random portion of the excess Helmholtz free energy to account for the non-central force contribution, which can be included when a non-random liquid theory based on the local composition concept is used.

The form of the Twu-Coon (TC) equations for the mixture parameters, a_m and b_m, as used by Twu and Coon at infinite pressure is as follows:

$$a_m^* = b_m^* \left[\frac{a_{m,vdW}^*}{b_{m,vdW}^*} + \frac{1}{\sigma}\left(\frac{A_{nR}^E}{RT} \right) \right] \tag{3.277}$$

$$b_m^* = \left[\frac{b_{m,vdw}^* - a_{m,vdW}^*}{1 - \left(\frac{a_{m,vdW}^*}{b_{m,vdW}^*} + \frac{1}{\sigma}\left(\frac{A_{nR}^E}{RT} \right) \right)} \right] \tag{3.278}$$

where $a_{m,vdW}^*$ and $b_{m,vdW}^*$ are the van der Waals mixture parameters that are obtained from the asymmetric van der Waals MR *i.e.* Equation (3.238) and the linear mixing rule *i.e.* Equation (3.236), respectively. The quantity σ is a constant whose value depends on the EOS used (as shown previously).

As opposed to the WSMR1 and WSMR2 IRP approaches, the enforcement of the quadratic combining rule for the b_{ij} parameter as in Equation (3.237) is applied in this approach. This serves to address one of the flaws of the WSMR1 and WSMR2 approaches with only one binary interaction term for treating highly asymmetric systems. Twu and Coon (1996) argue that the use of two binary interaction coefficients *i.e.* k_{ij} and d_{ij}, allows for both limiting activity coefficients (γ_i^∞) to be represented in a highly asymmetric system. This allows for accurate representation of the G^E model across the composition range.

The fugacity for a component i in a mixture with the TC mixing rules as applied to the SRK and PR EOS is shown in Equations (3.279) and (3.280), respectively.

$$\ln \phi_i = -\ln\left(Z - b_m^*\right) + \beta(Z-1) + \left(\frac{a_m^*}{b_m^*} \right)[\beta - \chi] \ln\left(\frac{Z}{Z + B_m} \right) \tag{3.279}$$

$$\ln \varphi_i = -\ln\left(Z - b_m^*\right) + \beta(Z-1) - \frac{1}{2\sqrt{2}}\left(\frac{a_m^*}{b_m^*} \right)[\beta - \chi] \ln\left(\frac{Z + \left(1 - \sqrt{2}\right)B_m}{Z + \left(1 + \sqrt{2}\right)B_m} \right) \tag{3.280}$$

The terms in Equations (3.279) and (3.280) are defined as follows:

$$\beta = -\left(\frac{1}{1-D}\right)\left(1-\left(\frac{a^{*}_{m,vdW}}{b^{*}_{m,vdW}}\left(\left(\frac{2\sum_{j=1}^{n} z_j a_{ij}}{a^{*}_{m,vdW}}\right)-\left(\frac{2\sum_{j=1}^{n} z_j b_{ij}}{b_{m,vdW}}-1\right)\right)+\frac{\ln\gamma_{i,nr}}{\sigma}\right)\right)$$
$$+\frac{1}{Q}\left(\frac{2\sum_{j=1}^{n} z_j\left(b^{*}-a^{*}\right)_{ij}}{\sum_{i=1}^{n}\sum_{j=1}^{n} z_i z_j\left(b^{*}-a^{*}\right)_{ij}}\right) \qquad (3.281)$$

$$\chi = \beta+\left(\frac{1}{D}\right)\left(\frac{a^{*}_{m,vdW}}{b^{*}_{m,vdW}}\left(\left(\frac{2\sum_{j=1}^{n} z_j a_{ij}}{a^{*}_{m,vdW}}\right)-\left(\frac{2\sum_{j=1}^{n} z_j b_{ij}}{b_{m,vdW}}-1\right)\right)+\frac{\ln\gamma_{i,nr}}{\sigma}\right) \qquad (3.282)$$

where

$$D = \frac{a^{*}_{m,vdW}}{b^{*}_{m,vdW}} + \frac{A^{E}_{nr}}{\sigma RT} \qquad (3.283)$$

$$Q = b_{m,vdW} - \frac{a_{m,vdW}}{RT} \qquad (3.284)$$

As can be readily inferred from the form of the above that when $A^{E}_{nr} = 0$ (for simple or non-polar mixtures), the TC mixing rule (as opposed to the WSMR1 and WSMR2 approach) reverts to the vdW MR form. Twu and Coon (1996) asserted that due to the presence of the k_{ij} and l_{ij} parameters in their mixing rule and the reduction of their mixture rules to that of the vdW classical mixing rules, the TC method would be effective for the representation of highly asymmetric systems and mixtures of nonpolar substances and light gases, respectively. Twu and Coon (1996) demonstrated the ability of their model to provide accurate correlations and predictions for highly nonideal mixtures such as hydrocarbon + alcohol and water + alcohol mixtures, where a slightly superior performance of the TCMR over the WSMR1 and WSMR2 models was observed.

(f) Composition-Dependent, Composition-Dependent Local Composition and Density and Composition-Dependent Mixing Rules

Composition-dependent mixing rules have probably received the least attention of all the above-mentioned approaches and are in general are not considered as being effective (Orbey and Sandler, 1995b). The CDMR of Panagiotopoulos and Reid *et al.* (1987) is in the form of an empirical adjustment of the van der Waals combining rule for a_{ij} *i.e.* Equation (3.236). In this approach, a composition-dependent term for the binary interaction parameter and an additional parameter were introduced as follows:

$$a_{ij} = \left(a_{ii} a_{jj}\right)^{0.5} \left(1 - \delta_{ij}\right) \tag{3.285}$$

where

$$\delta_{ij} = k_{ij} - \left(k_{ij} - k_{ji}\right) z_1 \tag{3.286}$$

where the asymmetric convention for the binary interaction coefficient *i.e.* $\left(k_{ij} \neq k_{ji}\right)$ has been used. If $\left(k_{ij} = k_{ji}\right)$, then the form of the vdW MR is recovered. The linear mixing rule, as shown in Equation (3.238), is used for b_m.

Additional CDMR approaches similar to the one above have been proposed by Adachi and Sugie (1986), Sandoval *et al* (1986), and Schwartzentruber and Renon (1989a, 1989b). Surprisingly, these models have been shown to provide good correlations of complex and highly nonideal binary mixtures that could only be properly treated by the liquid phase G^E models (Sandler *et al.*, 1994). In a hybrid approach, a composition-dependent local composition mixing rule (CDLCMR) has been proposed by Schwartzentruber and Renon (1989a, 1989b). The actual formulation of this approach was similar to that of the UNIWAALS of Gupte *et al.* (1986a, 1986b) in that a predictive liquid phase excess energy model was employed together with a traditional cubic EOS to obtain the mixture parameters. Interested readers are referred to work of Schartzentruber and Renon (1989a, 1989b) for more details on the complete formulation and applicability of the method.

The CDMR approach is subject to numerous theoretical and fundamental flaws. The most blatant is the non-quadratic composition dependence of the second virial coefficient obtainable from the mixing rule expression. The second problem is these methods apparently suffer from

the Michelsen-Kistenmacher syndrome, as described before. Thirdly, in what is described as the dilution effect, the added composition-dependent term depends explicitly on mole fractions as opposed to mole ratios. When the number of components increases, the composition terms in the mixing rule diminish to a great extent (Sandler *et al.*, 1994).

Schwartzentruber and Renon (1991) formulated a new density and composition-dependent mixing rule (DCDMR) to address the inconsistencies of the CDMR approach and still retain the flexibility and the efficiency associated with use of the latter. The a_m term was expressed as the sum of a quadratic and non-quadratic term, where suitable algebraic manipulation of the latter allowed for the dilution and Michelsen-Kistenmacher syndrome to be avoided. To ensure that the quadratic composition dependency of the second virial coefficient in the mixing rule was adhered to, Schwartzentruber and Renon developed a five-parameter cubic EOS that retained the form of a traditional cubic EOS. However, the composition dependency for the third virial coefficient was violated in the above approach. In a comparative study by Schwartzentruber and Renon (1991) of the DCDMR and the previous approach of Schwartzentruber and Renon (1998a,1998b), it was concluded that the former addresses the inconsistencies of the latter but does not yield any significant improvement over the latter with regards to phase equilibrium computations.

Recommendations for the use of cubic EOS/$\left(A^E \text{ or } G^E\right)$ models

Critical commentary and comparative studies of the applicability of mixing rules in cubic EOS have been provided by quite a few researchers (Knudsen *et al.*, 1993; Sandler *et al.*, 1994; Coutsikos *et al.*, 1995; Kalospiros *et al.*, 1995; Orbey and Sandler, 1995; Voutsas *et al.*, 1995; Heidemann, 1996; Michelsen, ,1996; Michelsen and Heidemann, 1996; Ohta, 1996; Orbey and Sandler, 1996; Solorzano-Zavala, 1996; Voutsas *et al.*, 1996; Wang *et al.*, 1996; Orbey and Sandler, 1997; Ghosh, 1999; Kontogeorgis and Vlamos, 2000; Djordjevic *et al.*, 2001; Valderrama, 2003). Unfortunately the above treatments have lacked the sort of consensus or conclusive recommendations which would greatly facilitate the task of selecting the most effective cubic EOS/MR combination for a particular task. Consequently, the above studies of this highly complex subject matter have to be subject to a great deal of scrutiny and an attempt at a reasonable synopsis of the above is presented below with relevance to the cubic EOS/MR approaches employed in this study and of comtemporary significance.

There have been many comparative studies of cubic EOS/$\left(A^E \text{ or } G^E\right)$ mixing rules that have centred on the relative efficiencies of models in representing highly asymmetric systems *i.e.*

mixtures that contain a combination of supercritical and subcritical or condensable compounds. These are of great interest to the gas processing, supercritical extraction technology and petroleum refinery sectors. In particular, studies by Kalospiros (1995), Voutsas *et al.* (1996), Orbey and Sandler (1997), Kontogeorgis and Vlamos (2000) have presented findings in this regard. Kalospiros *et al.* (1995) noted that there are inconsistencies with the zero-pressure Huron-Vidal modifications in the form of MHV1 and MHV2 as these mixing rules were not able to reproduce the G^E model in the entire α_m range; where the latter has been quantified in Equation (3.250). The above fallacy was particularly prominent for asymmetric systems *i.e.* those systems with components with widely differing α_{ii} values; where the latter is quantified in Equation (3.251). In a study by Voutsas *et al.* (1996) with a variety of models, the MHV2 model was observed to behave relatively poorly for highly asymmetric systems (supercritical fluid mixtures, synthetic gas condensate, asymmetric hydrocarbon mixtures, *etc.*).

Orbey and Sandler (1997) investigated the reason as to why the zero-reference pressure models such as the MHV1 and MHV2 models performed poorly with asymmetric mixtures, especially supercritical mixtures. This was explained in terms of the use of the zero-pressure standard state, where in order to use the mixing rule for a mixture and its components, real roots for the liquid densities of the mixture components have to be obtained at the solution temperature and zero pressure. To accommodate components that do not exist as liquids under these conditions, these mixing rules incorporate an empirical extrapolation for the liquid volume, which can be inaccurate when highly supercritical components are used. They also accounted for the infinite-reference pressure WSMR1 being unsuitable for such mixtures as there was no account of the free energy change in going from pure compressed supercritical component to the hypothetical pure liquid. Consequently, on the basis of the above, these types of mixing rules in their original forms are not recommended for highly asymmetric mixtures or those containing a supercritical component. However, it should be noted that a great deal of controversy and lack of consensus exists amongst researchers with regards to the validity of the above generalization. Valderrama and Alvarez (2004) strongly assert that in several research works coupled their own findings the accuracy and flexibility of the WSMR models to correlate high-pressure phase equilibrium with supercritical fluids. Indeed, the success of the works of Kolar and Kojima (1994), Yang *et al.*(1997), Brandani *et al.* (1998) certainly support the above argument.

The WSMR1 and Huron-Vidal-type mixing rules, together with other models, have often been the subject of many comparative studies or critical commentaries such as those by Orbey and Sandler (1995), Solorzano-Zavala *et al.* (1996), Wang *et al.* (1996). In the study of Wang *et al.* (1996), the relative efficiencies of the WSMR1, MHV2 and TC mixing rules with the SRK EOS

and a host of G^E models (van Laar, Wilson, NRTL and UNIQUAC) in the treatment of non-polar + nonpolar, polar + nonpolar and polar + polar binary mixtures was tested. In general, all of the three mixing rules allowed for good accuracy in the correlations. However, from the three models the WSMR1 performed the best for the three types of mixtures in combination with the UNIQUAC model. Similar results were obtained by Solorzano-Zavala *et al.* (1996) who studied a host of mixing rules and activity coefficient models for the treatment of highly nonideal polar associating mixtures. The WSMR1 approach was shown to have the advantage over the HVMR approach for almost all the binary mixtures, however, for multicomponent mixtures no clear advantage was observed. The Wilson model was highly recommended as the G^E model to use in the mixing rule as opposed to the van Laar model, which was completely unsuccessful.

In summary, the principal flaws of the Huron-Vidal and the modified Huron-Vidal (MHV1 and MHV2) and Wong-Sandler approaches, as discerned by many researchers have been the lack of applicability to asymmetric systems, inability to readily reduce to the vdW mixing rules and lack of adherence to the second virial coefficient quadratic composition dependency (for the MHV1 and MHV2). The IRP, ZRP and NRP approaches of Twu and co-workers (1996, 1997, 1999) were specifically designed to address the flaws of the WSMR1 and WSMR2 approaches and criticism of the method of Twu and Coon (1996) can only be related to the necessity of the inclusion of an additional parameter *i.e.* d_{ij}. Despite the theoretical correctness of the ZRP and NRP approaches of Twu and co-workers, the WSMR and the HV-based forms still persist as favourites amongst contemporary researchers, who clearly demonstrate the applicability of these models for a spectrum of mixture types and operating ranges. Consequently, the theoretical flaws of the HV-based approaches are yet to be translated into a form that is both conclusive and quantitative for the practical representation and computation of the equilibrium condition (Palmer, 1987; Sandler *et al.*, 1994; Solorzano-Zavala, 1996).

With regards to the choice of cubic EOS in the direct method, the SRK and PR EOS clearly emerge as favourites as they have been widely studied and their efficiency in the correlation and prediction of phase equilibria has been demonstrated on countless occasions. As mentioned before, the success of a VLE correlation hinges upon the judicious selection of the mixing rule (discussed above) and the $\alpha(T_r, \omega)$ correlation; where the latter ensures that there is accurate representation of the saturation vapour pressure of the pure components. The PRSV cubic EOS form has been the most popular and highly recommended by an overwhelming majority of contemporary researchers (Sandler *et al.*, 1994; Zabaloy and Vera, 1998; Oh *et al.*, 2004; Giner, 2005). In this work, the HV, MHV1 and MHV2 mixing rules together with the PRSV EOS and

the Wilson G^E model were employed in the application of the cubic EOS/$\left(A^E \text{ or } G^E\right)$ approach for selected systems under investigation.

3.5.3.4 Computational aspects of the ϕ_i - ϕ_i approach

In the discussion of the γ_i - ϕ_i approach earlier on, it was shown that different mathematical and statistical routines have been formulated to allow for both computational economy and correlating efficiency in the reduction of VLE data. Interested readers are referred to the works of Paunovic *et al.* (1981), Elliot and Daubert (1985), Mohammed *et al.* (1987), Engelzos *et al.* (1989), Niesen and Yesavage (1989), Engelzos *et al.* (1990), Engelzos *et al.* (1993), Teh and Rangaiah (2002) and most recently that Lopez *et al.* (2006) for discussion of the limitations and merits associated with the variety of different statistical methods, objective function forms, algorithm formulations, *etc.* As mentioned before, the least squares method is the most popular amongst contemporary researchers (Lopez *et al.*, 2006) for the correlation of VLE data and has been applied in the direct method computations for the systems investigated in this work.

As with the γ_i - ϕ_i approach, a suitable form for the objective function (OF) is required for the least squares implementation of the nonlinear model parameter estimation method. From an examination of the isofugacity criterion for the ϕ_i - ϕ_i approach, as in Equation (3.173), it can immediately be seen that the pressure dependence for the equilibrium condition is not explicitly represented (it cancels out). Consequently, an analogous approach to the γ_i - ϕ_i method for the OF in the BUBL P computation cannot be employed as pressure cannot be solved for directly. Consequently, the use of an OF with the bubble-point pressure in the ϕ_i - ϕ_i method involves very tedious and computational expensive (memory, time) additional iterative procedures (Melhem, 1989; Lopez *et al.*, 2006). It was also shown that the bubble-point pressure OF was highly sensitive to variations in the binary interaction parameter $\left(k_{ij}\right)$ of the RK EOS when compared to other minimization criteria (Ashour, 1986). Elliot and Daubert (1985) also advise that caution should be exercised when using the normalized bubble-point pressure OF as it can perform poorly due to the presence of inaccurate data in the low composition ranges.

Alternative objective functions have also been proposed (Paunovich *et al.*, 1981; Elliot and Daubert, 1985; Gess *et al.*, 1991; Lopez *et al.*, 2006) and these include those based on the minimization of the errors (differences between the experimental and calculated values) in the vapour phase composition, relative volatility, phase equilibrium constants(K values), the Gibbs energies of the cubic EOS and the activity coefficient model (Coutsikos *et al.*, 1995; Giner *et*

al., 2005). The study by Lopez *et al.* (2006) on the relative efficiencies of several objective functions based on bubble pressures, vapour compositions and equilibrium constants. On the basis of their findings, the optimal OF for VLE correlations and predictions is the following:

$$OF = \sum_{i=1}^{n}\left(y_1^{exp} - K_1^{calc}\, x_1^{exp}\right)_i^2 + \sum_{i=1}^{n}\left(y_2^{exp} - K_2^{calc}\, x_2^{exp}\right)_i^2 \tag{3.287}$$

where

$$K_i^{calc} = \left[\frac{\phi_i^L}{\phi_i^V}\right]^{calc} \tag{3.288}$$

The OF based on Equation (3.287) has been shown to offer the greatest "computational value" as it was both computationally inexpensive and provided excellent representation of highly asymmetric systems at elevated temperatures and pressures through the use of the correlated parameters form of the OF. Additionally, the authors investigated the statistical-mechanical correctness of the k_{ij} value obtained from the VLE computation and found that its value did not violate the quadratic composition dependence of the second virial coefficient. Consequently, the OF shown above was employed for the BUBL P computations with the ϕ_i - ϕ_i method.

In the data reduction procedure for the cubic EOS/(A^E or G^E) approach, use can be made of the existing literature G^E information or the model parameters from previous correlations with the γ_i - ϕ_i approach. However, in the absence of such data for novel systems, reparameterization of the G^E model (usually two parameters) in the cubic EOS mixing rule together with the fitting the binary interaction parameter (k_{ij}) for the relevant mixing rules is a necessary exercise.

For the models that were studied here i.e the Huron-Vidal, MHV1 and MHV2 mixing rules with the Wilson model, there were two G^E model parameters that had to be determined through the minimization of the OF.

The algorithm for the implementation of the correlation strategy is shown in Figure 3.5. All numerical computations were implemented in the MATLAB® (version 7.0.1) workspace. Unless otherwise shown, reference should be made to Sections (3.5.3.2) and (3.5.3.3) for the calculation of the thermodynamic quantities employed in the computational procedure.

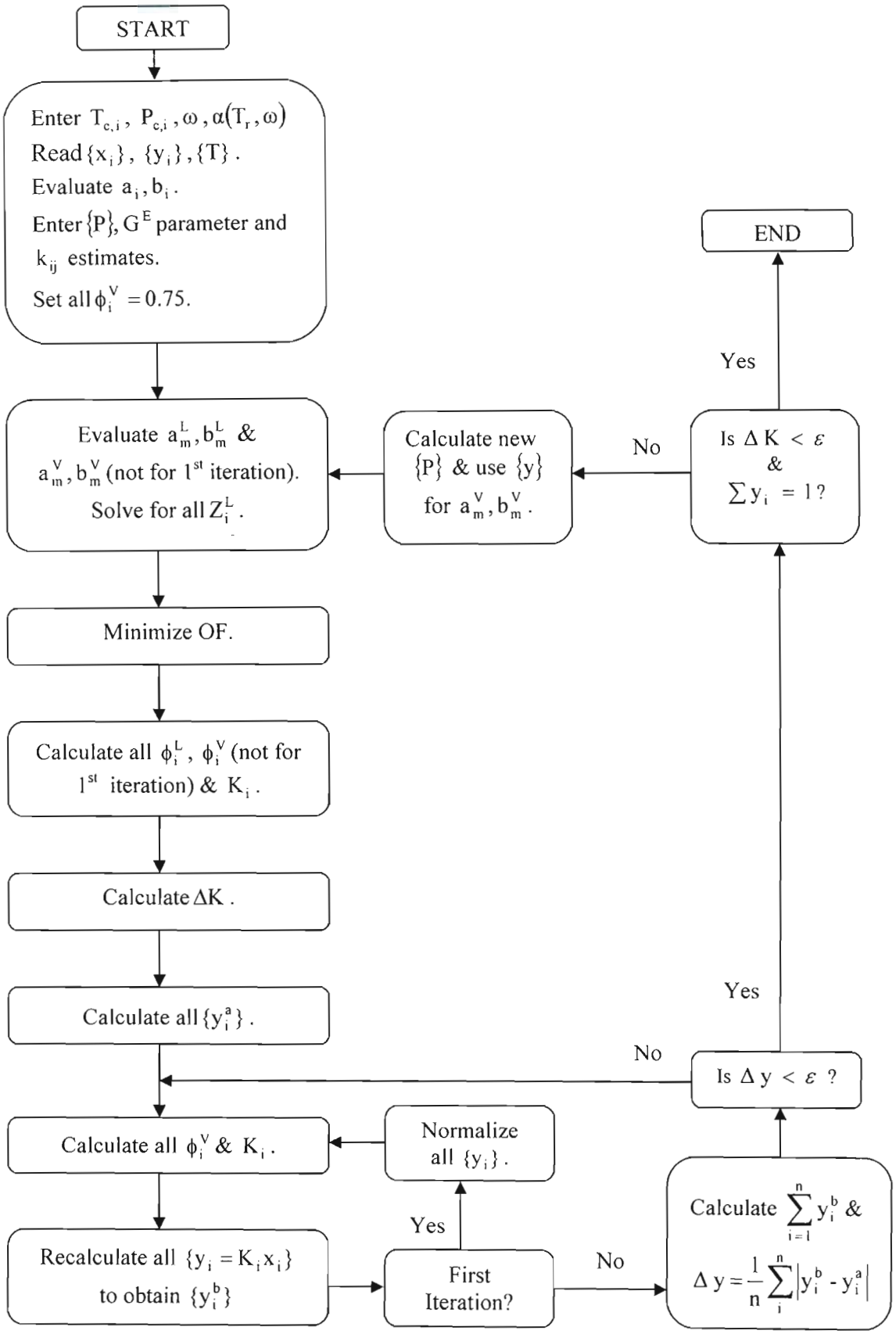

Figure 3.5. Algorithm for a ϕ_i - ϕ_i BUBL P calculation.

As explained above, in the BUBL P calculation for the ϕ_i - ϕ_i method an expression for the calculated pressure in the OF cannot be formulated explicitly in terms of a calculated system pressure. Consequently, in the outer loop, the iteration begins with an estimate of system pressure values. Together with the optimized adjustable parameters from the OF minimization routine, the pressure estimate is then tested through the computation of the vapour composition values $\left(y_i = \sum K_i x_i\right)$ generated in the inner loop. The failure of $\left(y_i = \sum K_i x_i\right)$ to sum to unity necessitates the adjustment of the current pressure estimate through a suitable procedure (as discussed below).

The implementation of the BUBL P ϕ_i - ϕ_i method begins with the input of the required pure component critical properties in the form of $T_{c,i}$ and $P_{c,i}$ and also the acentric factor (ω) together with the $\alpha(T_r, \omega)$ correlation used for the calculation of the pure component energy and covolume parameters $(a_i$ and $b_i)$. The $\alpha(T_r, \omega)$ correlation used in this work is that of Stryjek and Vera (1986a) in the form of the PRSV EOS (as applied to the PR EOS) and is shown in Table 3.6. An examination of the expressions for the PRSV EOS in Equations (3.204) - (3.206), reveals the incorporation of an adjustable parameter in the form of κ_1, which is specific for each compound. The latter can be obtained either through the regression of experimental or literature data or from the tabulation of Stryjek and Vera (1986a) of κ_1 values for over ninety compounds of industrial interest.

A convenient feature in the initialization of a BUBL P calculation for the vapour phase fugacity is to set $\phi_i^V = 0.75$. In this way, with suitable estimates for the system pressure (P), G^E liquid model parameters for the cubic EOS/(A^E or G^E) mixing rules and also the binary interaction parameter (k_{ij}), only the liquid phase mixture energy $\left(a_m^L\right)$ and covolume $\left(b_m^L\right)$ parameters need to be calculated in the initialization of the outer loop. An expression can then be obtained for the cubic EOS in terms of the compressibility factor (Z), from which the liquid phase root $\left(Z^L\right)$ can be obtained as the smallest real root. Subsequent iterations incorporate the above procedure for the vapour phase, when the first set of calculated vapour compositions is generated in the inner loop. The cubic EOS roots were obtained numerically with inbuilt MATLAB® (version 7.0.1) functions for root solving.

The solution of the the cubic EOS roots allows for the the computation of the liquid $\left(\phi_i^L\right)$ and vapour phase (except for the first round where $\phi_i^V = 0.75$) fugacity coefficients. The OF is

formulated for all the data points and the sum of squares is minimized using the Nelder-Mead Simplex method to obtain the best values for the parameter estimates. With the newly optimized parameters, new values for the ϕ_i^L and ϕ_i^V (except for the first round) can be obtained.

The ΔK is calculated as the absolute average of the difference in the values across the data set:

$$\Delta K = \frac{1}{n}\sum_{i=1}^{n}\left(\left|K_1^2 - K_1^1\right| + \left|K_2^2 - K_2^1\right|\right) \tag{3.289}$$

where the superscripts "1" and "2" refer to the calculated K values from the previous iteration round and current iteration, respectively. The exit condition (Elliot and Lira, 1999) for the outer loop is usually the convergence of the sum of the vapour compositions to a value of unity (as discussed below) and $\Delta K < \varepsilon$ (where ε is some predefined deviation tolerance) for the exit condition can be excluded. All values of K used in the algorithm are calculated from Equation (3.288), hence no superscript or subscript is used in this section to designate otherwise.

The values of the vapour composition can then be calculated from the following:

$$y_i^a = K_i x_i \tag{3.290}$$

The values of all the ϕ_i^V and K_i terms can now be calculated from the above. The superscript "a" signifies that the y_i value is from the initial computation of y_i the inner loop.

Due to the interdependence of the y_i, ϕ_i^V and K_i terms, internal consistency or convergence of the calculated y_i values has to be checked for. Consequently, the values of y_i are recalculated from the ϕ_i^V and K_i values in the form of y_i^b. Since the sum of the y_i values is of course not of constrained to sum to unity at this juncture and more than one iteration round is required for a solution, normalization is conducted for the first iteration, as shown below for a binary mixture:

$$y_i^b = \frac{K_1 x_1}{K_1 x_1 + K_2 x_2} \tag{3.291}$$

where $y_2^b = \left(1 - y_1^b\right)$.

The superscript "b" signifies that the y_i value is from the final computation of y_i the inner loop. This step is omitted for all subsequent iterations as an exit condition with the normalized

y_i values (although summing up to unity) will not be consistent with the current pressure estimates. The difference between the calculated y_i and the y_i^* values *i.e.* Δy is then computed to check for an internal consistency of the vapour composition values in the inner loop. If the values exceed the predefined tolerance (ε), the iteration is continued within the inner loop until such time, the exit condition is satisfied. The y_i^b values in the loop serve as the initial values *i.e.* y_i^a when the exit condition is not satisfied in the inner loop.

The following step is to check for the exit condition in the outer loop *i.e.* whether the y_i values sum to unity and whether $\Delta K < \varepsilon$ (as discussed above). If the exit condition is not satisfied, a new pressure estimate is formulated on the basis of whether the $\sum y_i > 1$ or $\sum y_i < 1$. For the former case, the current pressure estimate is too low and must be increased; the converse applies to the latter case. The new pressure estimate can be obtained from a variety of schemes as discussed by Anderson and Prausnitz (1980a, 1980b) and Gerald and Wheatley (1999). In this work, the new pressure estimate (P_{new}) was calculated with the following:

$$P_{new} = S(P_{old}) \tag{3.292}$$

where P_{old} is the pressure estimate from the iteration that has just terminated as a result of the sum of vapour compositions *i.e.* S, not summing up to unity in the inner loop.

$$S = \sum_{i=1}^{n} y_i^b \tag{3.293}$$

This value of S can be used to generate an improved estimate for pressure in accordance with the line of reasoning from above. Since the deviation of the sum of y_i values is incorporated into the value of S, it can effectively provide a measure of the deviation of the pressure estimate from the thermodynamically consistent value for the data set. The optimized values of the parameters from the previous iteration are used as the initial estimates for the subsequent iterational sequence. As mentioned above, with the generation of the first set of y_i values from the execution of the first iteration, values of ϕ_i^V are determined in the initialization of the OF. When the constraints for the inner and outer loop exit conditions have been satisfied, the iteration sequence terminates and the optimized parameter values, together with the calculated experimental variables, are obtained.

3.5.4 Comparison of the γ_i - ϕ_i and ϕ_i - ϕ_i approaches in the treatment of Vapour-Liquid Equilibria.

A qualitative comparative analysis of the two methods discussed can be most aptly presented on the basis of a few predefined criteria in a tabular form in Table 3.8. For an in-depth rating-based analysis of the suitability of the methods, the text of Raal and Muhlbauer (1998) can be consulted. As can be deduced from Table 3.8, the apparent weight of the arguments in favour of the modern direct method, it is indeed justifiably one of the most promising and active areas in contemporary applied chemical thermodynamics.

3.6. Thermodynamic Consistency Testing of Vapour-Liquid Equilibrium data

3.6.1 Overview

An appropriate starting point for a discussion of this crucial aspect of VLE treatment would be the comment of Palmer (1987), "VLE data are deceptively easy to measure but extraordinarily difficult to measure correctly". As such there is currently a large body of published VLE data (Goral, 2001), especially from older sources, that violate the rigourous and "bureaucratic" framework (Prausnitz, 1979) of phase equilibrium thermodynamics. Accurate phase equilibrium data are the key ingredient for the successful design of industrial separation processes, which for most chemical and petrochemical plants, constitutes the most important and most costly aspect of the entire plant's operations. The graphical consistency of VLE data *i.e.* points on a smooth curve can in many instances be misleading as to the quality of the data, as systematic errors can easily be masked. Consequently, the employment of a judicious approach in evaluating the quality of the data is a worthwhile exercise and is most effectively achieved through ensuring the adherence or consistency of the experimental data with regards to the well-established framework of thermodynamics.

As mentioned before thermodynamic consistency testing is only applicable for P-T-x-y data sets, consequently in the absence of the above, no proper thermodynamic consistency can be performed (Jackson and Wilsak, 1995) with the experimental data. However, the inapplicability of thermodynamic consistency testing to P-T-x data sets should not be seen as a deficiency as it merely serves to complement the measurement of the P-T-x-y data. It is much more advisable to compute any variables subject to uncertainties, than to employ thermodynamic consistency for a full data set where uncertainty exists in one of the variables.

Table 3.8. Comparison of the γ_i - ϕ_i and ϕ_i - ϕ_i approaches.

Criterion	γ_i - ϕ_i	ϕ_i - ϕ_i
Temperature dependence of parameters	The liquid-phase G^E models are primarily correlated on the basis of composition dependence and as such do not have an explicit temperature-dependence. This results in a rather strong temperature dependence for the parameters.	Since an EOS is inherently a PVT relation, the cubic EOS has an explicit temperature dependence; hence the parameters have a weak temperature-dependency.
Conditions of applicability.	Restricted to conditions far away from the critical; usually below 1 MPa. This is due to limitations in the treatment of the vapour phase and components above their critical point.	Can be used for quite a wide range of pressures and temperatures up to the critical region.
Physical state of components	Usually only used for subcritical or condensable components. Difficulty is experienced in defining a liquid phase standard state for a supercritical component (even with the asymmetric convention).	Can be used for both supercritical and subcritical mixtures.
Chemical nature	Provides very good correlation for a diverse range of chemical mixtures (nonpolar, polar, associating, *etc.*).	Excellent treatment of nonpolar or slightly-polar substances. Although treatment of polar and associating fluids has been poor, with the advent of cubic EOS/ (G^E or A^E) models, the reproduction of the G^E model behaviour can be achieved for these types of mixtures.
Extrapolation and Interpolation	Caution required when extrapolating or interpolating with the parameters obtained with this method (due to the strong temperature dependency).	Accurate extrapolations over large temperature and pressure ranges (weak temperature dependency of parameters). Good interpolations.

Table 3.8. Comparison of the γ_i - ϕ_i and ϕ_i - ϕ_i approaches (cont).

Criterion	γ_i - ϕ_i	ϕ_i - ϕ_i
Ease of use.	Requires two different auxiliary functions to represent the phases in separate treatments. Often greater controversy in the vapour phase treatment.	It is a unified approach with the same auxiliary function to describe all the equilibrium phases. This facilitates the development of a thermodynamic framework needed for the correlation, prediction and interpretation of phase equilibria.
Predictive capability	Currently not significantly explored for predictive capability due to the use of the two separate departure functions and reservations about using traditional cubic EOS in this approach for the vapour phase.	Excellent predictive capability with the modern direct method through the incorporation of group contribution methods (GC-EOS) or the infinite dilution activity coefficients (HVID) with EOS/ (A^E or G^E) mixing rules.
Treatment of dense and non-dense phases	There is fairly good treatment of both phases through two separate focussed methods for a limited pressure range.	Treatment of the liquid phase has traditionally been a weak point of this method, however, with the volume-translated cubic EOS models and the no-reference pressure (NRP) novel mixing rules, good representation of liquid phase can be achieved.
Complementary ability	Since this method is for the most part inflexible and has no predictive capability, parameters from other types of computational methods are not usable.	Information from γ_i - ϕ_i method can be readily incorporated into cubic EOS/(A^E or G^E) approach for ZRP or NRP mixing rules
Physical significance of the parameters	Parameters in the local composition G^E models have a semi-theoretical basis.	The binary interaction parameter (k_{ij}) is purely empirical.

The satisfaction of the Gibbs-Duhem equation, shown in Equation (3.82), has traditionally served as one of the most important thermodynamic relations employed for validating the thermodynamic consistency of a VLE data set. Different mathematical and thermodynamic manipulations of the basic Gibbs-Duhem relation allow for the formulation of a variety of thermodynamic consistency (TC) tests that can be used to verify the consistency of a data set. These tests have usually taken the form of the slope test, integral test, the differential test and the tangent-intercept test (Prausnitz, 1969; Van Ness and Abbott, 1982; Smith *et al.*, 2001). Additional tests have been proposed in recent times to complement the use of older approaches. These include the Van Ness-Byer-Gibbs test (Van Ness *et al*, 1973), the infinite dilution test of Kojima and co-workers (1990, 1991) and the Direct Test of Van Ness (1995). The systematic application of the different TC tests (Jackson and Wilsak, 1995) provides a very simple yet powerful tool to allow for a holistic perspective on the quality of VLE data set to be achieved.

A critical underlying consideration in the use of TC tests is that although a data set may be considered as being consistent by satisfying the criteria of the thermodynamic tests that it is subjected to, this does not guarantee its correctness (Jackson and Wilsak, 1995; Valderrama and Alvarez, 2004). In fact, a data set can pass a TC test and still be erroneous (Jackson and Wilsak, 1995). Conversely, a more costly outcome is when an accurate data set fails a TC test and is deemed inconsistent. Jackson and Wilsak (1995) have attributed this to the incorporation of questionable assumptions in the formulation of the applied TC test such that the TC tests are themselves subject to uncertainties (Van Ness *et al.*, 1973).

Traditional division of thermodynamic consistency testing for VLE data sets, as with other theoretical VLE treatments has been based on the pressure region of operation *i.e.* low-pressure and high-pressure VLE thermodynamic consistency tests. HPVLE measurements have not been made in this study and HPVLE consistency testing is consequently not reviewed. A detailed treatment of this subject matter can be found in the works of Chueh *et al.* (1965), Won and Prausnitz (1973), Christiansen and Fredenslund (1975), Raal and Muhlbauer (1998) and more recently Valderrama and Alvarez (2004). A fairly informal and convenient contemporary classification scheme for LPVLE TC tests involves the assignment of a method as an area test, slope test, an infinite dilution test or modelling test.

3.6.2 Area Test

The area or integral test is probably the most popular and widely applied of all TC tests due to its simplicity as a practical means to test the thermodynamic consistency of a data set. The classical area test was established through the independent efforts of Herington (1947) and

Redlich and Kister (1948a). It is based on an integration of the Gibbs-Duhem equation and its derivation is shown below.

For a binary mixture, the Gibbs-Duhem equation, shown in Equation (3.82) divided by dx_1 can be represented as follows:

$$\frac{d\ln\gamma_1 x_1}{dx_1} + \frac{d\ln\gamma_2 x_2}{dx_1} - \varepsilon_T - \varepsilon_p = 0 \tag{3.294}$$

where

$$\varepsilon_T = -\left[\frac{H^E}{RT^2}\right]\frac{dT}{dx_1} \tag{3.295}$$

$$\varepsilon_P = \left[\frac{V^E}{RT}\right]\frac{dP}{dx_1} \tag{3.296}$$

For the isothermal or isobaric case, $\varepsilon_T = 0$ or $\varepsilon_P = 0$, respectively. For a general case, which is applicable to either isothermal or isobaric data, $\varepsilon = \varepsilon_P$ or ε_T and Equation (3.294) reduces to:

$$\frac{d\ln\gamma_1 x_1}{dx_1} + \frac{d\ln\gamma_2 x_2}{dx_1} - \varepsilon = 0 \tag{3.297}$$

However, the following substitution can be used:

$$\left[\frac{d}{dx_1}(x_1\ln\gamma_1) - \ln\gamma_1\right] + \left[\frac{d}{dx_1}(x_2\ln\gamma_2) + \ln\gamma_2\right] = 0 \tag{3.298}$$

To allow for the following to be obtained:

$$\frac{d}{dx_1}(x_1\ln\gamma_1 + x_2\ln\gamma_2) - \varepsilon = \ln\gamma_1 - \ln\gamma_2 = \ln\frac{\gamma_1}{\gamma_2} \tag{3.299}$$

Since the quantity in parenthesis in Equation (3.299) is recognisable as $\left(\frac{G^E}{RT}\right)$:

$$\frac{d}{dx_1}\left(\frac{G^E}{RT}\right) = \ln\frac{\gamma_1}{\gamma_2} + \varepsilon \tag{3.300}$$

Integrating the above from $x_1 = 0$ to $x_1 = 1$:

$$\int_0^1 \frac{d\left(G^E/RT\right)}{dx_1} dx_1 = \int_0^1 \left(\ln\frac{\gamma_1}{\gamma_2} + \varepsilon\right) dx_1 \tag{3.301}$$

Since the term on the left-hand side of Equation (3.301) evaluates to zero, the basis for the area test is the following:

$$\int_0^1 \left(\ln\frac{\gamma_1}{\gamma_2}\right) dx_1 + \int_0^1 \varepsilon\, dx_1 = 0 \tag{3.302}$$

To evaluate the ε term, two separate cases have to be considered *i.e.* isothermal and isobaric.

For the isothermal case, $\varepsilon_T = 0$ and it is often justifiable to assume that pressure dependence of the γ_i values at low pressures is negligible (Van Ness, 1995), so that $\varepsilon_P = 0$ and the following is obtained:

$$\int_0^1 \left(\ln\frac{\gamma_1}{\gamma_2}\right) dx_1 = 0 \tag{3.303}$$

Of course, the above relation is not applicable for HPVLE TC testing as the assumption with regards to ε_P does not hold.

For the isobaric case, $\varepsilon_P = 0$ and the temperature dependency of γ_i through the enthalpy term cannot be ignored so that the following form is obtained:

$$\int_0^1 \left(\ln\frac{\gamma_1}{\gamma_2}\right) dx_1 - \int \frac{H^E}{RT^2} dT = 0 \tag{3.305}$$

The application of the area TC test involves the use of experimental data to calculate $\ln\gamma_1$ and $\ln\gamma_2$ and then subtracting these values to obtain $\left(\ln\frac{\gamma_1}{\gamma_2}\right)$, which is then added to the ε term and plotted against x_1 for each datum point. A numerical integration procedure is then employed to integrate the resulting graph from $x_1 = 0$ to $x_1 = 1$. The latter is frequently achieved through the use of a smoothing or polynomial function. The criterion for the data set to be considered as thermodynamically consistent by this TC test is for the result of the integration *i.e.* the net area, to be zero. However, a nearly ideal system will quite often produce a net value irrespective of the consistency status of the data set (Jackson and Wilsak, 1995). Smith (1984) employed the use of the area ratio (of the area above the abscissa to that below or its reciprocal) as a measure of the consistency of the data. Smith devised five catergories for the assessment of the data on the basis of the outcome of the test *i.e.* for 0 - 0.6, data was totally unacceptable; for 0.6 - 0.8, data was marginal; for 0.8 - 0.9, data was fair; 0.9 - 0.95, data was good and for 0.95 - 1.0, the data was excellent. In general, the designation of an allowed tolerance for the area TC test has been quite controversial and given rise to the formulation of different tests and alternative criteria (Palmer, 1987; Barnicki, 2002). The isobaric case has been the focus of much attention, due to the limited availability of heat of mixing $\left(H^E\right)$ data required for the isobaric area TC test. Interested readers are referred to the recent works of Jelic (2000) and Barnicki (2002) on a few significant early developments in the realm of TC area tests. More recent developments in the field of TC area tests include those by Kojima-Moon-Ochi TC test (Kojima *et al.*, 1990) and the commendable rigour of the approach of Wisniak (1993, 1994).

The limitations of the area TC test have been well-documented by many researchers (Palmer, 1987; Van Ness, 1995; Raal and Muhlbauer). Due to the integral nature of this TC test, the possibility of compensatory effects in error propagation causing inconsistent data sets to pass the test cannot be ruled out. The above can be complemented by the unjustified neglect of terms in the TC area test expression. This is most often exemplified in the treatment of the isobaric case for the TC area test, where the lack of availability of H^E has quite often resulted in many researchers ignoring the contribution of this term. It should be noted that Herington (1951) attempted to provide a correlation for the H^E data, however this method is rather empirical and its usefulness not been properly assessed (Barnicki, 2002).

The greatest criticism of the method is probably due to its apparent limitations in the treatment of isothermal data as it does not identify problems in pressure measurement as it is more suited to assessing problems in phase composition measurement. From Equation (3.58), it can easily

be seen that for a binary mixture the ratio of the activity coefficients *i.e.* $\left(\frac{\gamma_1}{\gamma_2}\right)$, the key expression in the TC area test, the pressure cancels out as shown below:

$$\frac{\gamma_1}{\gamma_2} = \frac{y_1 \Phi_1 x_2 P_2^{sat}}{y_2 \Phi_2 x_1 P_1^{sat}} \tag{3.305}$$

At low pressures, it can be taken to assess only the consistency of the x - y data set at the given temperature. However, the greatest error is seen in the measurement of the vapour composition (which favours the computation of this variable *i.e.* in a P - T - x data set) and secondarily in the liquid phase composition (Palmer, 1987). Consequently, many P - T - x data sets which are consistent may fail the area test due to errors in the y values.

The satisfaction of the integral test is deemed as a necessary condition for thermodynamic consistency, but it is not a sufficient guarantor of the thermodynamic consistency of a data set. Consequently, it is recommended that the test is always used in conjunction with other more rigourous or sound TC tests, whose outcomes offer greater assurance on the quality of a data set.

3.6.3 Slope Test

The slope test or differential test is derived from the LPVLE isothermal expression for TC area tests, shown in Equation (3.303). Simple mathematical manipulation of Equation (3.303) yields the following:

$$-x_1 \frac{d \ln \gamma_1}{dx_1} = x_2 \frac{d \ln \gamma_2 x_2}{dx_1} \tag{3.306}$$

The expression above serves to relate the slopes of the activity coefficient curves to one another. In the application of this test, the experimental data is used to calculate the values of $\ln \gamma_1$ and that of $\ln \gamma_2$ for each value of x_1 and x_2, respectively. Separate plots of x_1 vs $\ln \gamma_1$ and x_2 vs $\ln \gamma_2$ are prepared and smoothing functions are fitted to both plots. Since the plots are actually independent of one another, the two smoothing functions are differentiated and substituted into (3.306). A comparison of the slopes at various points can then performed to assess the quality of the data across the composition range.

A suitable criterion to ascertain whether the TC test represented by (3.306) is satisified is achieved by using the following relation:

$$I = \frac{(A - B)^2}{AB} \tag{3.307}$$

where A is the left-hand side and B is the right-hand side of Equation (3.306). This quanitity can be computed at any point in the data set for which the fit is valid and not only for those values at which data points lie. The value of I can vary anywhere from positive to negative infinity. A value of zero provides an assurance of perfectly consistent data and a negative value indicates the presence of thermodynamic inconsistencies in the data set (slopes with opposite signs). There is a tolerance for positive values; however, with the occurrence of increasing positive values of I, the thermodynamic consistency of the data set diminishes.

The slope test is seemingly a very simple test to implement; however, researchers are plagued by inexperience in effectively interpreting the results from this test. It is usually not considered as useful unless there are gross or quite large errors in the data set *i.e.* negative values for I, and is consequently not very popular or widely used. It should also be mentioned that the method is not recommended for systems that undergo phenomena such as self or cross-association at some part of the composition range and method is inapplicable across the entire composition range in this instance (Jackson and Wilson, 1995).

3.6.4 Infinite Dilution Test

This novel contemporary approach was pioneered by Kojima *et al.* (1990) in the form of an extrapolation to the limiting condition of infinite dilution. As for the integral test, a smoothing function is fitted to the $\left(\ln \frac{\gamma_1}{\gamma_2} \right)$ quanitity as a function of the liquid phase composition (x_1). The function is then extrapolated to $x_1 = 0$ and $x_1 = 1$ to obtain values for the activity coefficients at infinite dilution *i.e.* γ_1^∞ and γ_2^∞. The next step involves modelling the relationship of $\frac{G^E}{RTx_1x_2}$ vs x_1, where the G^E value is computed from experimental data. The function is extrapolated to $x_1 = 0$ and $x_1 = 1$ and the values that are obtained for the γ_1^∞ and γ_2^∞ values are compared with those from the previous approach. Kojima *et al.* (1990) defined the criterion for acceptable discrepancies between the two as being within 30 %.

Jackson and Wilsak (1995) modified the approach of Kojima *et al.*(1990) adopting the same approach as for the differential test *i.e.* preparing separate plots of $\ln \gamma_1$ versus x_1 and $\ln \gamma_2$ versus x_2 and fitting smoothing functions to the plots. The γ_1^∞ and γ_2^∞ values can be obtained from the required extrapolations from the respective plots. As mentioned, in general, the extrapolations for obtaining γ_i^∞ values from finite concentration VLE data is generally not recommended when performed directly.

3.6.5 Modelling Test

A quick memory jog of the BUBL P and BUBL T procedure employed in the γ_i - ϕ_i approach reveals that thermodynamic consistency tests and the Gibbs-Duhem equation are an implicit part of the computational procedure based on the method of Barker (1953). In the isothermal case *i.e.* a BUBL P calculation, the pressure and vapour phase composition are calculated and for the isobaric case *i.e.* a BUBL T calculation, temperature and the vapour phase composition were the computed variables. In the latter, both the calculated quantities were computed through the use of an activity coefficient model for the liquid phase and the truncated virial coefficient equation of state for the vapour phase. Analogously, the modelling TC test of Van Ness-Byer-Gibbs (1973) involves the use of the use of the equilibrium condition to compute experimental variables from incompete experimental data sets (usually P-T-x) and the selection of a suitable thermodynamically consistent model to fit the data set. A comparison of the experimental and calculated variables yields a set of residuals *e.g.* $\Delta y_1 = \left| y_1^{exp} - y_1^{calc} \right|$. A quanititative criterion can be established for assessing the consistency of the data set with regards to the relative magnitude of the residuals. Gmehling and Onken (1977) suggest that if the average value for $\Delta y_1 > 0.01$, the data set can be considered as being inconsistent. However, the satisfaction of this TC test does not exclude the data set from being considered as inconsistent (Gess *et al.*, 1991) as sometimes the error can be attributed to the model not fitting the data well *i.e.* the test is not invariant to model selection (Palmer, 1987).

A more effective way to analyze residuals is through the use of a graphical inspection of the "scatter plot tests" of the residuals in the Van Ness-Byer-Gibbs approach (1973). Interpreting the results from this test is most effectively achieved through the use of three plots (Jackson and Wilsak, 1995) to graphically observe the existence of any bias in the data set. In the isothermal case, the first plot is that of the pressure that is calculated from the model $\left(P^{calc}\right)$ versus the experimental liquid phase composition $\left(x_1\right)$. The second and third plots are of the pressure

residuals (ΔP) versus x_1 and the vapour phase composition residuals (Δy) versus x_1. The purpose of the first two plots is to ensure that an adequate fit of the P^{calc} - x data has been achieved with the activity coefficient model. Of course if a good fit is not obtained with an appropriate thermodynamic model, then it is highly likely that the P - x data set may be erroneous.The P^{calc} versus x_1 plot allows for a perspective to be achived with regards to the ΔP versus x_1 scatter plot. If a good fit of the P^{calc} - x data has been achieved, the experimenter can proceed to a Δy versus x_1 scatter plot. A thermodynamically consistent data set has a random scattering of the Δy residuals about zero. If non-random scattering occurs, the y values are inconsistent with P - x data at the given temperature. Application of the above arguments involves merely replacing all references to pressure by the system temperature. This test is highly sensitive and extremely effective for detecting subtle thermodynamic inconsistencies if applied properly.

Jackson and Wilsak provide an extensive critical commentary on the limitations of the use of the Van Ness-Byer-Gibbs test (1973). The first relates to the *a priori* selection of a suitable thermodynamic model to represent the liquid phase. Improper selection of a model will undoubtedly appear as a poor fit of the P - x data, as discussed above. This can indeed be misleading, especially for inexperienced researchers who will terminate the test at this point and consider the data set as being inconsistent. Since this method is highly model-dependent, if a suitable model cannot be found, this excludes the test from use in the TC testing of a data set.

Secondly, in fitting a data set to an overly flexible model (*e.g.* polynomial with higher-order terms), the improper spread of data points across the composition range can create problems. This is as a result of the model not properly representing the system behaviour in those regions where there is a considerable void in the data. This is why the viewing of the P^{calc} versus x_1 plot is justified as an anomalous behaviour of the model in specific composition regions can be detected.

Jackson and Wilsak also consider the design of the TC test for the use of Barker's least squares method for the data regression as being highly limiting. They feel that the use of alternative statistical techniques with different assumptions such as the maximum likelihood method might be more effective in obtaining a better model fit in certain instances. A rather insignificant variation of a measured experimental variable in a highly sensitive composition region can produce bias in that region. With the maximum likelihood method, errors in all of the measured variables are assumed and incorporated into the model fitting procedure as opposed to the least squares approach where two of the four variables are regarded as being independent. Problems

with convergence for some systems may also be experienced with regressions with Barker's method and for those systems where the model parameters exceed the data points, the model cannot be used. Problems with interpretation of poor results may also be experienced with this method. If there are inconsistencies observed for a system where the assumptions of the model or method are questionable, the poor results may be due to bad data, improper model selection or a combination of both.

A more effective TC test was proposed by Van Ness (1995) and was derived in an analogous fashion as for the area test in Section (3.6.2), where the residual quantity can be directly related to the Gibbs-Duhem equation as follows:

$$\Delta\left(\ln\frac{\gamma_1}{\gamma_2}\right) = \frac{d\ln\gamma_1 x_1}{dx_1} + \frac{d\ln\gamma_2 x_2}{dx_1} - \varepsilon \tag{3.308}$$

The significance of the above approach is that it represents a simple and direct means to test the thermodynamic consistency of each point in a data set by through the use of a residual related directly to the Gibbs-Duhem equation itself. Van Ness (1995) proposed the use of an alternative objective function, shown in Equation (3.309), to fit the data so as to complement the residual quantity by causing the latter to scatter about the abscissa.

$$OF = \sum_{i=1}^{n}\left[\left(\ln\frac{\gamma_1}{\gamma_2}\right)^{exp} - \left(\ln\frac{\gamma_1}{\gamma_2}\right)^{calc}\right]_i^2 \tag{3.309}$$

Consequently, in the application of the Direct TC test, a plot of the residuals obtained from the above OF *i.e.* $\Delta\left(\ln\frac{\gamma_1}{\gamma_2}\right)$ versus x_1, is made. Van Ness devised a quantitative criterion in the form of a consistency index to assess the thermodynamic consistency of the data on the basis of the relative magnitude of the root mean square deviation (RMSD) values of the $\left(\ln\frac{\gamma_1}{\gamma_2}\right)$ quantity in the model fitting procedure. This index was in the form of a scale to rate the quality of the data on the basis of its deviation from thermodynamic consistency. It has been reproduced from the original article of Van Ness in Appendix B.

As can be seen from above, TC testing is a useful but somewhat subjective theoretical treatment that requires a very insightful and systematic approach to effectively assessing the quality or the

thermodynamic consistency of a VLE data set. A judicious approach is often necessitated in effectively combining complementary TC tests to obtain a multi-dimensional perspective on the quality of the data set and hence capitalizing on the wealth of information that the unique TC tests in this approach affords the researcher. In the Van Ness-Byer-Gibbs TC test as applied by Jackson and Wilsak (1995) to three model systems, the influence of model selection for both the liquid and vapour phase nonidealities was observed to quite worringly greatly influence the outcome of the TC test, especially with regards to the the use of the average Δy as a criterion for thermodynamic consistency. Consequently, the subjective nature of this test results in the thermodynamic consistency of a data set hinging upon the judicious selection of models, in addition to the actual quality of the data (which should be the primary criterion).

Van Ness (1995) suggested that the Direct Test would dampen the uncertainties associated with the application of a modelling TC test in terms of model selection, objective function and fit. Consequently, this TC test in conjunction with consistency index presented in Appendix B was chosen for the thermodynamic validation of the P-T-x-y data sets obtained in this study.

3.7 Predictive Vapour-Liquid Equilibrium methods

The development of predictive methods for the computation of VLE for a fairly diverse group of compounds and for a wide range of pressures and temperatures is an active and prominent sphere of research in contemporary thermodynamics as the rewards of success in this arena are unquantifiable. It would effectively end the uneviable plight of those thermodynamicists having to experimentally acquire VLE data and the constant dilemma faced by process engineers for the optimal design of operations where phase equilibrium data is required.

In the midst of other approaches (not discussed here), the success of predictive VLE methods in recent times arguably hails from the hybridization of the γ_i - ϕ_i and ϕ_i - ϕ_i methods, which has seen the successful emergence of the cubic EOS/$\left(A^E \text{ or } G^E\right)$ approach. In the latter approach, the tremendous flexibility of excess free energy models for the treatment of highly nonideal or complex mixtures is coupled with the applicability of the EOS approach at higher temperatures and pressures (especially for the treatment of supercritical components). With the incorporation of a group contribution method for the G^E model, an extremely powerful predictive approach emerges. A few group contribution EOS or GC EOS methods that have been proposed in recent times includes that of the UNIWAALS approach (Gupte, 1986a, 1986b), the GC EOS of Skjold-Jorgensen (1984, 1988), the MHV2-UNIFAC (Fredenslund and Sorensen, 1994), and also the Predictive Soave-Redlich-Kwong or PSRK EOS suggested by Holderbaum and Gmehling (1991).

The fundamental assumption of group contribution methods used for the prediction of activity coefficients is that a mixture may be viewed as a solution of the structural units from which the molecules are formed *i.e.* as functional groups as opposed to a solution of the molecules themselves. In this way, the advantage of group contribution methods is that the number of functional groups is smaller than the possible number of molecules. The UNIFAC model (Fredenslund *et al.*, 1977) has in particular gained widespread popularity and has been subject to several modifications in the last 20 years to extend its range of applicability (temperatures, pressures, mixture components, *etc.*). A discussion of the UNIFAC method together with its application in the highly promising PSRK EOS is presented in this shortened review section to highlight the invaluable contribution of group contribution methods in the field of applied thermodynamics. A review of alternative predictive VLE methods can be found in the texts of Walas (1985) and Raal and Muhlbauer (1998).

3.7.1 UNIFAC Method

The UNIQUAC Functional-group Activity Coefficients (UNIFAC) method, as its name implies, is based on the UNIQUAC local composition activity coefficient model, discussed in Section (3.5.2.3). In the original UNIFAC method, proposed by Fredenslund *et al.* (1977), a molecule can be decomposed into functional groups or subgroups. The representation of a molecule as a collection of these functional groups allows for the surface areas, volumes and other parameters (required by the UNIQUAC method) of thousands of molecules to be obtained from a relatively smaller number of sub groups. Despite a similar approach existing for the ASOG method (Wilson and Deal, 1962), the UNIFAC method has found more widespread application and has been subject to a continual development and revision (Raal and Muhlbauer, 1998).

In the application of the UNIFAC method, as in the UNIQUAC method, the activity coefficient is considered as consisting of a combinatorial (athermal) and a residual contribution, as shown in Equation (3.149). Unless otherwise stated, the same notation as for the UNIQUAC equation is used.

$$\ln \gamma_i = \ln \gamma_i^C + \ln \gamma_i^R \qquad (3.149)$$

The combinatorial contribution retains the same form as in the original UNIQUAC equation *i.e.* Equations (3.150) and (3.151) since only the pure component size and surface area parameters are required.

For the summations over all the functional groups of type k , the following applies:

$$r_i = \sum_{k=1}^{p} v_{ki} R_k \tag{3.310}$$

$$q_i = \sum_{k=1}^{p} v_{ki} Q_k \tag{3.311}$$

where R_k is the size parameter for group k, Q_k is the surface area parameter for group k, v_{ki} is the number of groups of type k in molecule i.

The residual contribution is somewhat more challenging to evaluate and has been changed so as to incorporate the solution-of-groups concept for the summation over all the groups as follows:

$$\ln \gamma_i^R = \sum_{k=1}^{p} v_{ki} \left(\ln \Gamma_k - \Gamma_k^{(i)} \right) \tag{3.312}$$

In Equation (3.312), it is assumed that the residual contribution is proportional to the difference between the contributions from each of the solute groups in the liquid mixture (Γ_k) and that for the groups as pure components $\left(\Gamma_k^{(i)}\right)$. It should also be noted that for $(x_i = 1)$, the symmetric normalization of the activity coefficient is adhered to *i.e.* $\gamma_i^R = 1$.

The (Γ_k) and $\left(\Gamma_k^{(i)}\right)$ terms are evaluated from the following:

$$\ln \Gamma_k = Q_k \left[1 - \ln \left(\sum_{m=1}^{p} \theta_m \psi_{mk} \right) - \sum_{m=1}^{p} \frac{\theta_m \psi_{km}}{\sum_{n=1}^{r} \theta_n \psi_{nm}} \right] \tag{3.313}$$

There is undoubtedly some confusion that might arise with respect to the $\left(\Gamma_k^{(i)}\right)$ term but it should be remembered that this term is merely the contribution of group k in a reference solution containing only molecules of type i and it is calculated separately for each component in the mixture, as opposed to the (Γ_k) quantity which involves all the solute groups.

The area fraction of group m (θ_m) is calculated as follows:

$$\theta_m = \frac{Q_m X_m}{\sum_{n=1}^{r} Q_n X_n} \tag{3.314}$$

where

$$X_m = \frac{\sum_{j=1}^{t} v_{mj} x_i}{\sum_{j=1}^{t}\sum_{n=1}^{r} v_n x_j} \tag{3.315}$$

The group interaction parameter term (ψ_{nm}) is obtained from the group interaction parameter between groups m and n *i.e.* a_{mn} as follows:

$$\psi_{mn} = \exp\left(-\frac{a_{mn}}{T}\right) \tag{3.316}$$

The use of the UNIFAC method and sample calculations are provided by Raal and Muhlbauer (1998) and Elliot and Lira (1999), from where the R_k, Q_k and a_{mn} terms *i.e.* the principal user inputs have also been tabulated. Gmehling (2003) reported that the status of the parameter matrix *i.e.* available parameters was up to 77 main groups.

The principal weaknesses of the original UNIFAC method, as discussed by Fredenslund and Sorensen (1994), can be summarized as follows:

(a) The method *cannot distinguish* between the differences in the thermophysical properties of isomers due to the empirical nature of the "solution-of-groups" concept.

(b) The *original prescription* for the use of the $\gamma_i - \phi_i$ approach (in the symmetric normalization convention) limits the use of the method in the low to moderate-pressure region and hence excludes the treatment of supercritical components

(c) The *temperature range* for the use of the method is limited to 275 - 425 K.

(d) The method does not include predictive capability for *electrolytes or polymers*.

(e) The UNIFAC parameters based on VLE data *cannot be extended* to the reliable prediction of LLE hence necessitating a separate UNIFAC-LLE approach (Magnussen *et al.*, 1981), where different parameters are used in the latter.

(f) Erroneous results are obtained as a result of *proximity effects* due to the relative positioning of strongly polar groups *e.g.* whether the groups are adjacent or on the same central molecule (an alcohol versus a glycol).

(g) The values for *activity coefficients* at infinite dilution $\left(\gamma_i^{\infty}\right)$ and the *enthalpy of mixing* $\left(H_i^E\right)$ terms obtained by the UNIFAC method have been unsatisfactory.

The last deficiency of the UNIFAC method in **(g)** is not surprising as it can be attributed to the limitations of the VLE data sets used to obtain the group interaction parameters, where there has been limited information from the highly-dilute region or from the temperature dependence of the activity coefficients have been incorporated. Raal and Muhlbauer (1998) recommend that a cautious approach to the use of the UNIFAC method should be employed as in some cases the results are in considerable error.

To improve the original UNIFAC model, two similar independent modifications of the original UNIFAC method have been developed in the form of the modified UNIFAC (Dortmund) by Weidlich and Gmehling (1986) and the modified UNIFAC (Lyngby) by Larsen *et al.* (1987). Common to both methods are modifications to the combinatorial and residual contributions, where a temperature-dependency has been incoporated into both terms and the combinatorial term has been empirically modified. Interested readers are referred to the review article of Fredenslund and Sorensen (1994) for an in-depth discussion of the modified UNIFAC (Lyngby) method and to the review article by Kojima (1997) for a discussion on both of the modified approaches. Gmehling (2003) demonstrates the success of the modified UNIFAC (Dortmund) over the original UNIFAC through a comparison of the predictions by both methods for 2200 consistent data sets. In the original UNIFAC approach, the computation of the vapour phase for the data sets resulted in a mean deviation with a value of 0.0141 and for the modified UNIFAC (Dortmund), a mean deviation of 0.0088 was obtained (compared to the 0.0058 obtained in the UNIQUAC correlation).

Analogously, improvements were also obtained for predictions of VLE temperatures, pressures, excess enthalpies and activity coefficients at infinite dilution. However, since UNIFAC is a G^E

model, its usefulness is limited to low to moderate-pressures and also for subcritical mixture components. Consequently, through the incorporation of a cubic EOS with UNIFAC as in the cubic EOS/$\left(A^E \text{ or } G^E\right)$ approach, the predictive modified UNIFAC (Dortmund) method can be extended to the treatment of supercritical mixtures and higher temperatures and pressures.

The Predictive Soave-Redlich-Kwong (PSRK) EOS is a predictive cubic EOS/$\left(A^E \text{ or } G^E\right)$ approach and was originally developed by Holderbaum and Gmehling in 1991, who combined the SRK cubic EOS with the UNIFAC model. Fischer and Gmehling (1995) then derived the PSRK EOS in a theoretical approach by incorporating the excess Helmholtz energy into the expression. The PSRK mixing rules (Chen *et al.*, 2002) for the mixture parameters has the following form:

$$\frac{a_m}{b_m RT} = \sum_{i=1}^{n} z_i \frac{a_i}{b_i RT} + \frac{1}{A}\left(\frac{G_\gamma^E}{RT} + \sum_{i=1}^{n} z_i \ln \frac{b_m}{b_i}\right) \tag{3.317}$$

where $A = -0.64663$ and the G_γ^E quantity is calcuated from the UNIFAC model. The classical linear mixing rule was used for the b_m parameter, as shown in Equation (3.238). The remaining terms have been described in the review on EOS mixing rules. A comparison between the MHV1 mixing rule in Equation (3.249) and the PRSK form shown above yields that the only difference between the two is in the value of the q_1 or A, respectively. However, there is a more implicit difference between the two in the form of the choice of the reference pressures. Whereas the MHV1 approach is a zero-reference pressure mixing rule, the PSRK model has atmospheric pressure as its reference pressure. This is of course most convenient as it facilitates the use of UNIFAC group interaction parameters, which are most obtained from regressions of VLE data at or near atmospheric pressure. Besides the use of UNIFAC, the parameters from any model can be used in the PSRK model with recourse to any changes of the form of the mixing rules (Fischer and Gmehling, 1995).

In a comparison of the PSRK EOS method (Holderbaum and Gmehling, 1991; Fischer and Gmehling, 1996) with other group contribution EOS methods such as the MHV2, LCMV, UNIWAALS and the GC EOS of Skjold-Jorgensen (1984, 1988), the PSRK EOS method was shown to have some important advantages over these methods. Firstly, the PSRK approach has a well-defined reference state in the form of the liquid mixture at atmospheric pressure, where the constant(A) is obtained through the use of quasi-liquid volumes of many substances at atmospheric pressure. Secondly, the PRSK model was shown to give good results for VLE and

gas solubility predictions for a wide range of pressures and temperatures. The last advantage of the PSRK method is that it has greater applicability than other methods due to its much larger parameter matrix.

However, despite the promise that this method has shown, a few significant limitations were identified in the use of this method (Fischer and Gmehling, 1995). It has been shown to share the same deficiency with the UNIFAC approach in the poor representation of alkane + water systems. Also, predictive capability of the method for highly asymmetric systems *i.e.* for those systems with large relative molecular size discrepancies (from ratios of 15 - 20) is severely lacking especially with regards to bubble-point pressure predictions. Consequently, the PSRK approach has been subject to numerous revisions and extensions over the years to improve its applicability to asymmetric systems (Gmehling *et al.*, 1997; Li *et al.*, 1998; Yang and Zhong, 2001; Chen *et al.*, 2002) and electrolytes (Yan *et al.*, 1999). A recent modification (Ahlers, 2003) of the PSRK EOS approach has been in the form of the development of a universal group contribution EOS, where a volume-translated PR EOS was used in place of the SRK EOS to improve the predictions of the liquid densities of pure components and those of mixtures.

3.8 Conclusion

The theoretical framework for the interpretation, modelling and verification of experimental vapour pressure and VLE data has been most effectively achieved through a review of favoured or traditional approaches coupled with a survey of the most recent methods and developments in the field. Despite its deferment to the penultimate section of this review chapter, thermodynamic consistency testing, where applicable *i.e.* for P-T-x-y data sets, is an integral part of ensuring the success of the practical use of the experimental data in VLE-related industrial applications. The debate over the relative efficiencies of the γ_i - ϕ_i and ϕ_i - ϕ_i approaches is at the heart of the controversy surrounding VLE computations. For the lower pressure range, the γ_i - ϕ_i method still persists amongst researchers and for elevated pressures and temperatures, the ϕ_i - ϕ_i method remains a favoured approach.

As mentioned earlier, the ϕ_i - ϕ_i method has a stronger predictive capability as it is a unified approach with computational input requirements that can easily be related to pure component properties. Consequently, an examination of the current state or active developments in the field of theoretical VLE reveals that is an active hub of research due to the great promise of this method in providing the "holy grail" of vapour-liquid equilibrium computations *i.e.* a universal method for the representation of the thermodynamic properties of diverse chemical mixtures (nonpolar, polar, polar associating, asymmetric, supercritical, *etc.*) over a wide temperature and pressure range in the absence of any experimental data.

CHAPTER 4

THE DESIGN AND DEVELOPMENT OF A NOVEL VLE MEASUREMENT APPARATUS

4.1 Introduction

The successful design, development and operation of an experimental phase equilibrium apparatus hinges upon effectively incorporating or translating the theoretical considerations for the acquisition of accurate VLE data into the practical aspects for the equipment design and operation. This is often dependent upon the judicious selection of suitable principal and auxiliary construction materials, sealing methods and materials, optimal sizing and design of the critical sections of the apparatus (equilibrium chamber, sampling sections, *etc.*), ensuring that well-defined operating limits (pressure and temperature) for the apparatus have been established and that there are inbuilt safety measures to prevent accidents.

The review of the historically-significant VLE equipment designs spanning the last 100 years (presented in Chapter 2) provided invaluable insight into the important practical aspects required for the successful design of such equipment. The development of an "intuitive reasoning" from scrutiny of past VLE equipment designs coupled with a contemporary approach served as the platform for the conception and the execution of ideas for the design of the novel apparatus presented in this work.

The history of VLE equipment in the Thermodynamics Research Unit at the University of KwaZulu-Natal has seen considerable variation in the types of equipment designs that have been constructed and numerous modifications to these original designs over the past 20 years. A review of the HPVLE vapour phase recirculation, LPVLE dynamic recirculation and HPVLE static measurements in our laboratories has been provided by Moodley (2003), Harris (2004) and Naidoo (2004), respectively. The predecessor to the equipment design presented in this study in the Thermodynamics Research Unit was the apparatus of Harris (2004). The purpose of the design of Harris (2004) was to address an identified deficiency in the experimental VLE data acquisition capabilities of our laboratories. The objectives which were formulated for the design of the equipment of Harris were, however, too ambitious for the operational principles for the VLE measurement method *i.e.* the traditional low-pressure dynamic vapour condensate

and liquid recirculating method. Consequently, the operation of the equipment proved quite problematic resulting in the quality of VLE data obtained being comprised.
An integral part of the successful design of the new apparatus was the preliminary investigation of the shortcomings of the equipment of Harris, which was conducted in the predesign stage to ensure that a repetition of the flaws in the design of the novel apparatus would not occur.

4.2. Apparatus of Harris (2004)

An appropriate starting point in the predesign stage for an experimental apparatus, in addition to the identification of the requirements of the apparatus *i.e.* operating limits (to be discussed later), is the assessment of the imperfections of previous designs and the proposal of feasible solutions to address those flaws. The fundamental design problems experienced in the design and operation of past VLE still designs has been acquired through the comprehensive review in Chapter 2 and as a result, all that remains is a systematic approach to assessing the shortcomings of the previous design in our laboratories *i.e.* the equipment of Harris (2004).

The primary objective in the design of the equipment of Harris (2004) was to develop a versatile VLE apparatus with the following capabilities:

(a) The operating range with respect to temperature would be 300 - 700 K.

(b) The operating range with respect to pressure would be 1 kPa - 30 MPa.

(c) The apparatus would allow for a dual mode of operation *i.e.* both isothermal and isobaric.

(d) The time taken to reach equilibrium would be relatively short.

(e) The apparatus would be designed such that there were provisions for the sampling of both the vapour and liquid phases.

The design and construction of the novel apparatus was initiated in 2001 in the workshop of the School of Chemical Engineering. The design of the equipment of Harris was based, for the most part, on the highly successful glass still design of Raal (Raal and Muhlbauer, 1998), which was of the dynamic liquid and vapour condensate recirculating type; where the latter was discussed in Chapter 2.

4.2.1 Selection of construction materials

Due to the intended operating limits for the novel apparatus well exceeding atmospheric pressure, the selection of a suitable material of construction was a key initial consideration in the design of the apparatus. The key factors affecting the selection of a suitable material of construction are the following:

(a) *Mechanical and physical properties* such as the tensile strength, compressive strength, yield strength, hardness, creep and density.

(b) *Thermophysical properties* such as thermal expansion coefficients, thermal conductivity and thermally-induced strength loss.

(c) Favourable *machineability and weldability* characteristics of the material in the construction of the respective sections.

(d) *Corrosion resistance* and relative inertness of the material to a host of aqueous and non-aqueous environments.

(e) The *cost and availability* of the material relative to other suitable or available materials.

A suitable material that possesses the desirable characteristics in accordance with the above criteria is the austenitic 316 grade stainless steel. The attributes of 316 stainless steel (316 SS) make this grade one of the most commonly used stainless steels in the fabrication of products in the industrial, architectural and transportation sectors. The 316 SS material has a tensile strength of 515 MPa and a yield strength of 205 MPa (Atlas Steels, 2006). To complement the static mechanical strength properties of 316 SS, the alloy is able to retain its strength properties for fairly long time periods at extremely high or low temperatures; as discussed by Sinnot (1999). In addition to this, 316 SS has excellent welding and machining properties, where the latter allows for relatively higher machining rates and lower tool wear in the fabrication process.

Arguably, one of the most attractive features of this material is its corrosion resistance due to the incorporation of chromium, nickel and other alloying elements in the formulation of the alloy. As a result, excellent corrosion resistance is exhibited by 316 SS in a range of atmospheric environments and corrosive media due to the formation of a protective chromium oxide surface layer. Despite its pitting and crevice corrosion in warm chloride environments, it

is considered as being quite safe for laboratory applications as it is used in the construction of suitable containers for the storage and the transportation of chemicals (Atlas Steels, 2006).
In terms of the costing of 316 SS, it is regarded as a medium-cost material (Lancaster, 1971) with cast iron and carbon steels at one extreme (low-cost) and titanium and platinum at the other extreme (high-cost). The 316 SS grade offers great economic value as a result of its excellent strength and hardness (certainly higher than other materials in its cost bracket).

Consequently, 316 SS was chosen in the study by Harris and in this work as the principal material of construction. The equipment of Harris was machined from a 316 SS monobloc and there was minimal welding in the construction of the apparatus to facilitate the in-house construction of the apparatus (due to the requirement of specialized welding tools and procedures). The wall thickness or dimensions were calculated on the basis of the intended operating pressure range in accordance with the guidelines of Sinnot (1999).

4.2.2 Design of the apparatus of Harris (2004)

The general design and operational principles of a dynamic recirculating LPVLE apparatus, as discussed in Section 2.6.2 in Chapter 2, encompasses the incorporation of several principal and auxiliary sections. The principal sections are the reboiler, the Cottrell tube, the equilibrium chamber and the sample traps. Auxiliary sections include the pressure stabilization setup, condensing and cooling systems, direct or indirect drive magnetically coupled stirrers, thermal lagging, design of the return line and the electronic systems and hardware for data logging and pressure/temperature control.

The general layout of the apparatus of Harris, as reproduced from the thesis of Harris (2004) is shown in Figure 4.1. For a more effective discussion of the apparatus, descriptions of the principal and auxiliary sections will be conducted in separate focused treatments to assess the flaws of the apparatus in a more systematic manner. Emphasis will be placed on identifying and assessing the impact of key considerations for the optimal design of the apparatus as opposed to reproducing details on the fundamental operational principles of the key sections, which were dealt with at length in Chapter 2.

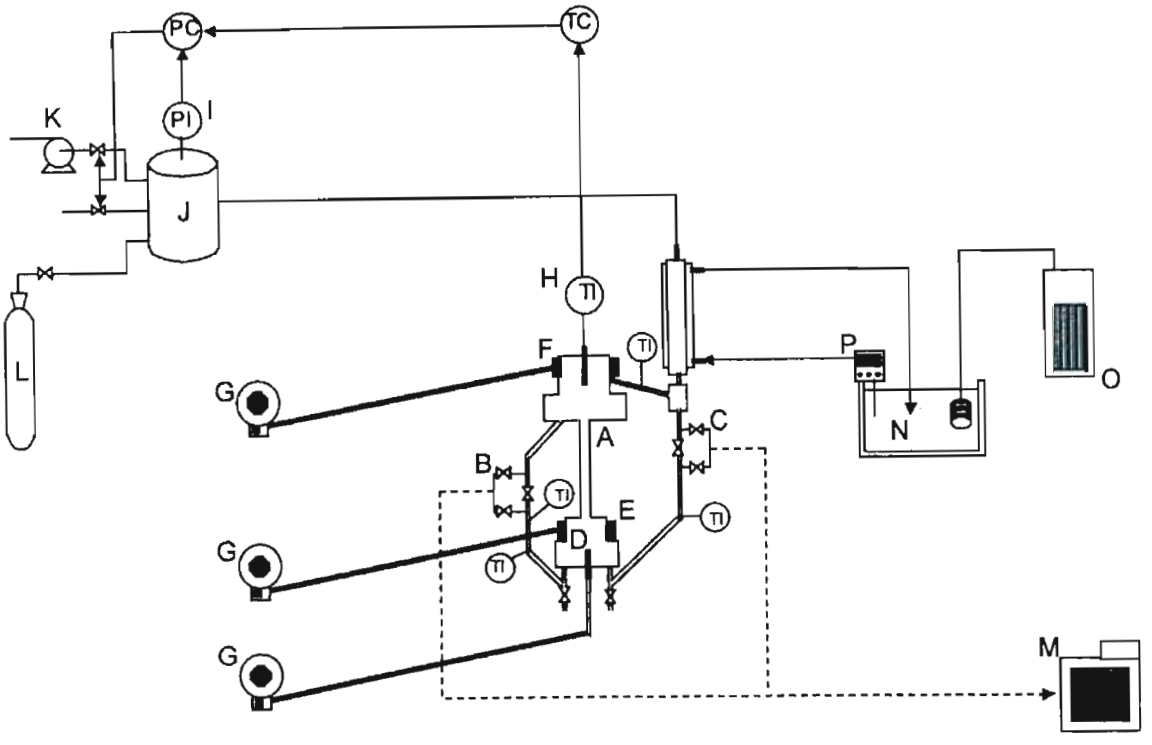

A: Equilibrium still; B: liquid sampling loop; C: vapour sampling loop; D: cartridge heater; E: reboiler band heater; F: equilibrium band heater; G: variable-voltage power supply; H: main temperature sensor; I: pressure transducer; J: pressure ballast; K: vacuum pump; L: inert high-pressure gas; M: GC; N: coolant for condenser; O: cold finger; P: coolant circulation pump

Figure 4.1. Schematic layout of the apparatus of Harris (2004).

4.2.2.1 The Reboiler

As one of the major operational sections of the apparatus, the optimal design of the reboiler is quite crucial for ensuring that an efficient and steady approach to the equilibrium condition is attainable. The technical and schematic diagrams of the final design of the reboiler of Harris (2004) are shown in Figures (4.2) and (4.3), respectively. The reboiler was machined from a 316 SS monobloc and as can be seen from Figure 4.2, the use of bolted flanges and gasket sealing were employed in the design. The latter is the most favourable approach from a practical point of view as it facilitates the disassembly of the apparatus for servicing and for implementing any design modifications. The custom-made Supergraf® gasket was used for the sealing purposes and six 6 mm high tensile bolts were used to hold the flanges together. The use of the graphite-based material as a sealing or insulating material is highly advantageous due to its chemical inertness, non-flammability, high compressibility, temperature limit of 773.15 K (Harris, 2004) and availability at moderate cost.

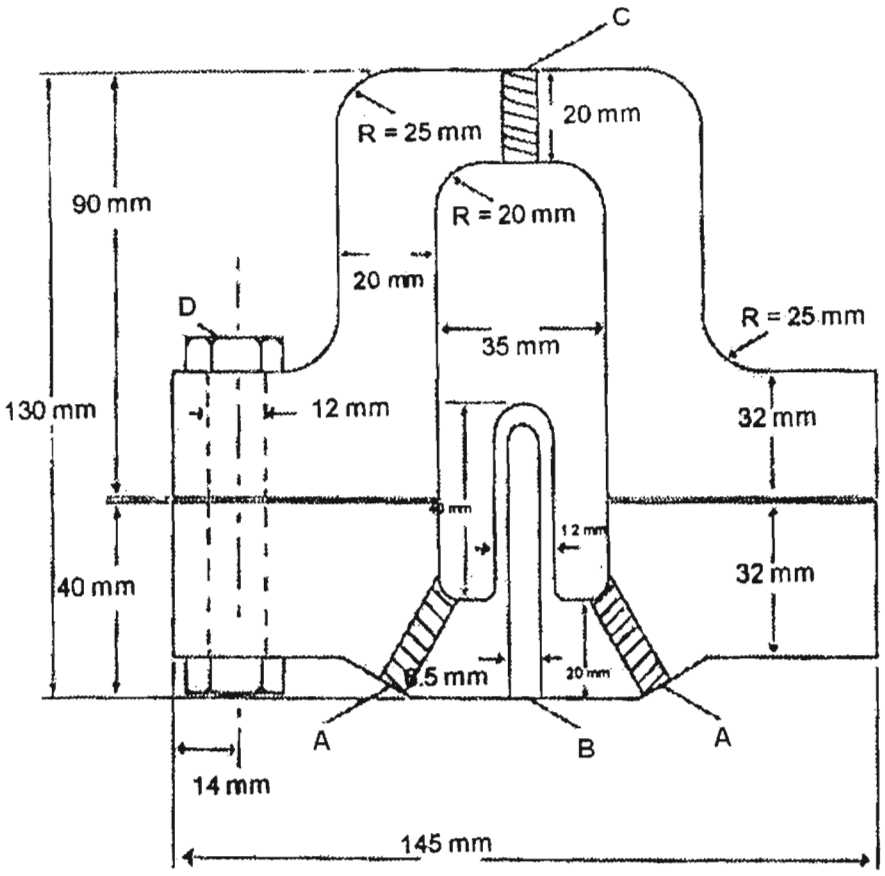

Figure 4.2. Technical diagram of the reboiler of Harris (2004): **A**, vapour condensate and liquid return inlets; **B**, heater cartridge cavity; **C**, Cottrell tube inlet; **D**, high tensile nut and bolt.

The edges of the reboiler were rounded to reduce any thermally-induced stresses in the operation of the equipment at elevated temperatures. The reboiler serves to provide sufficient heat input so as to initiate and sustain rapid, smooth and controlled boiling of the liquid mixture charged to the still. This is most efficiently achieved through the use of two separately-controlled heating circuits in the reboiler *i.e.* internal and external heating. A few of the early researchers who realized the value of this approach were Brown (1952), Ellis (1952), Dvorak and Boublik (1963) and Yerazunis *et al.* (1964).The use of the external heater is to negate the effect of the external environment (heat losses) on the boiling operations of the reboiler *i.e.* to maintain the contents of the reboiler at the boiling temperature. The internal heater should ideally be in intimate thermal contact with the contents of the reboiler to allow for an efficient dissipation of heat to enable a very precise control of the rate and nature of boiling of the mixture and to monitor the equilibrium temperature as a function of heat input into the reboiler.

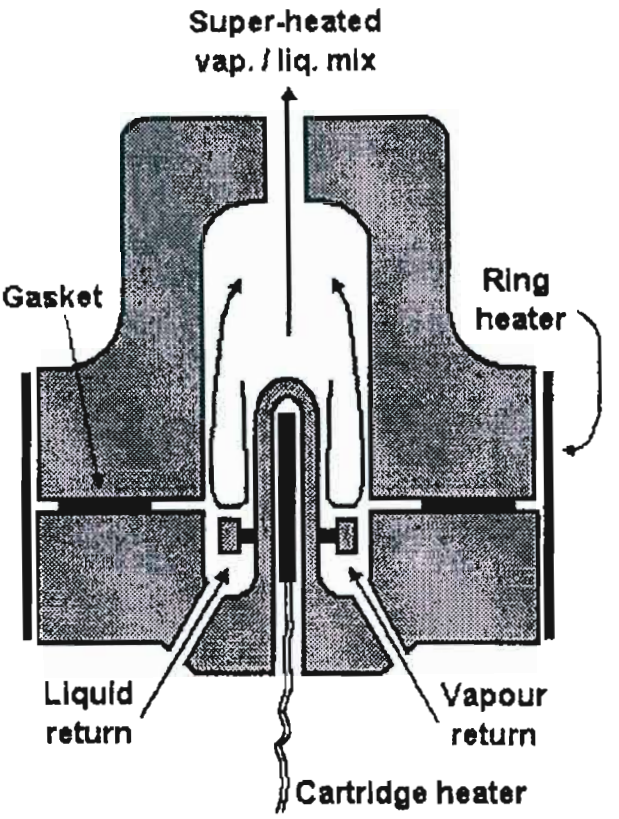

Figure 4.3. Schematic of the reboiler operation in the apparatus of Harris (2004).

The reboiler of Harris was designed with provisions to accommodate both an external and internal heater. The former, in the form a 500 W split band heater, was fitted around the upper flange of the reboiler. The heat from the external heater would be conducted through the metal walls to heat the equipment and the reboiler contents. The internal heater was a standard 250 W cartridge heater that was fitted into a specially machined thin-walled cavity in a central position in the lower flange of the reboiler, as in the glass still design of Hiaki *et al.* (1994). Harris felt that the thinner walls would be sufficient to ensure that the heat response of the system to increments in energy input would be rapid.

The inlet for the Cottrell tube was a large and smooth opening at the top of the reboiler in the upper flange. The inlet points for the return of the liquid and vapour condensate streams were located at the base of the reboiler in the lower flange and unlike the Cottrell tube, were small and constricted.

Immediate criticism of the reboiler design would stem from three principal design shortcomings *i.e.* the absence of any stirring in the reboiler, the size and wall thickness of the reboiler and the design and positioning of the vapour condensate and liquid phase inlets.

Perhaps the greatest flaw in the design, apart from an over-sizing of the apparatus, was the absence of any mechanical agitation in the reboiler. The effects of the lack of incorporation of the latter in the boiling chamber of the earliest designs of VLE apparatus has been well documented by many researchers (Raal and Muhlbauer, 1998) In the absence of any agitation or mixing of the cooler returning streams with the reboiler contents, the occurrence of non-equilibrium vapourization or flashing adversely affects the attainment of a proper equilibrium condition and the correct phase compositions in the sample traps.
The above effect is exacerbated for systems that have a high relative volatility (large differences in boiling points). The exclusion of stirring in the reboiler could probably be attributed to the considerable difficulties in incorporating magnetically coupled stirring in stainless steel designs (as will be discussed later), however, this is merely supposition as any discussion on this aspect of the design was absent from the thesis of Harris (2004).

The most noticeable aspect in Figure 4.2 is probably the size and wall thickness of the reboiler. The latter would pose potential problems in the operation of the apparatus as a huge mass of stainless steel with a low thermal conductivity is not ideal for a rapid "thermal response" of the apparatus. Indeed, it is acknowledged by Harris (2004) that this was one of the principal problems of the VLE apparatus at elevated temperatures. In the vapour-liquid equilibrium measurements, the determination of the attainment of equilibrium is achieved qualitatively by determining the "plateau region", as was discussed before. This is achieved by noting the response of the system to increased heat input into the system via the boiling mixture in the reboiler; with a large mass of stainless steel with a low thermal conductivity as in the design of Harris, the thermal response of the system would not be optimal. In a broader context, for the proper vapour-liquid equilibrium condition, where thermal, mechanical and material equilibrium is required, the attainment of a thermal equilibrium with this design would be the limiting factor, especially at higher temperatures.

Another key oversight in the design was the positioning and the design of the vapour condensate and liquid phase return lines. The base of the reboiler is not the optimal choice for a position for the re-entry of the streams as the combined effect of the hydrostatic head and the constricted openings would severely dampen the flow dynamics of the returning phases (a function which should only be fulfilled by the constricted openings so as to allow for a smooth return flow). Ideally, the point of re-entry should be on the side, as in the design of Raal (Raal and Muhlbauer, 1998), to ensure a balance between a restricted return (with a capillary insert) and sufficient return flow for rapid recirculation. Another feature in the design of Raal and that of many early researchers (Gillespie, 1946; Brown, 1952; Dvorak and Boublik, 1963) in the field that should have been adopted is the union of the vapour condensate and liquid streams into a

single entry point into the reboiler. This allows for sufficient premixing of the streams, which together with stirring in the reboiler, assists in negating the occurrence of flashing.

4.2.2.2 The Cottrell tube

The importance of the Cottrell tube in the design of dynamic VLE stills is frequently overlooked and as such, the optimal performance of the equipment is not achieved. The insulation, dimensions (inner diameter), length, shape and positioning of the Cottrell tube with respect to the equilibrium chamber are the key factors influencing its design and operation.

The Cottrell tube was a standard 316 SS 1/4 inch outer diameter tube that was vacuum-jacketed at the top section that protruded into the equilibrium chamber. This served to minimize the transfer of any superheat from the vapour-liquid mixture in the Cottrell tube to the equilibrium mixture. The vacuum-jacket was formed by welding a larger a larger concentric tube around the 1/4 inch tube after firstly evacuating the annular space between the two tubes.
The disadvantage in the design of the Cottrell tube was that with no transparent sections in the latter, there was no observation of the fluid flow characteristics of the systems. This is crucial, especially at the base of the reboiler, as the optimal heat input in the operation of the still must be determined (by observation) to ensure the continuous and efficient generation and transport of slugs of vapour and liquid through the Cottrell tube. In fact, the observation of the fluid flow characteristics of the mixture is frequently used as one of the criteria for judging the attainment of the equilibrium condition (Maia de Oliveira *et al.*, 2002).

4.2.2.3 The Equilibrium chamber

The equilibrium chamber can be considered as the heart of the VLE apparatus as its serves to provide a suitable environment for the undisturbed and optimal contacting of the phases for the attainment of the true equilibrium condition. The key thermodynamic variable measured in the equilibrium chamber is the equilibrium temperature and this necessitates the incorporation of provisions for the insertion of a temperature sensor in the equilibrium section. Of course for an analytical apparatus, the equilibrium process must immediately be followed by an efficient and rapid disengagement of the phases to allow for sampling. Consequently, the proper design of the equilibrium chamber is crucial and is often the limiting factor for the acquisition of accurate VLE data (Yerazunis *et al.*, 1964).

The design of the equilibrium chamber of Harris (2004), as with the reboiler and the Cottrell tube, was based on the glass still design of Raal (Raal and Muhlbauer, 1998). The advantageous aspects of the design of the equilibrium chamber of Raal were disclosed in great detail in Chapter 2 and also apply in principle to the design of Harris (2004), especially with regards to the design of the packed section and the packing material. The technical and schematic diagrams of the final design of the equilibrium chamber of Harris (2004) are shown in Figures (4.4) and (4.5), respectively. As for the reboiler, the equilibrium chamber consisted of two separate flanges and was sealed with a custom-made Supergraf® gasket.

The most important novel features of the design were related to the thermal lagging of the stainless steel interior of the packed section of the equilibrium chamber and also the use of external heating for the equilibrium chamber. In addition to the desirable sealing properties of graphite for use as a gasket in the equilibrium chamber, graphite is also an excellent insulating material and coupled with its chemical inertness, it is suitable for use in the interior of the equilibrium chamber.

As can be observed from Figure 4.5, the vapour-liquid mixture that was transported up the Cottrell was discharged onto a thin 316 SS plate, which is backed by a Supergraf® layer. In this way, any thermal influence of the main body of the equilibrium chamber (which can be subject to significant thermal fluctuations) does not manifest in any disturbances of the equilibrium process in the packed section. The vapour and liquid mixture then equilibrates in the packed section, which is packed with 3 mm rolled SS wire mesh cylinders, and the phases are subsequently disengaged. Supergraf® insulation was also used as a backing layer for the thin-walled 316 SS tube that was concentric around the packed section.

The use of the concentric sections for the exit path of the vapour was analogous to the glass VLE still design of Raal to ensure that the vapour fulfills its "thermal lagging" function (Rose and Williams, 1955) and to negate the effect of any entrainment of liquid in the vapour phase. The use of thin walls for the concentric 316 SS tube ensured that a uniform and rapid heat response is obtained (in heating the concentric tube to the equilibrium temperature) to facilitate the proper attainment of equilibrium and the rapid disengagement of the vapour phase. The exit paths for the disengaged vapour and liquid phases from the equilibrium chamber are shown more clearly in Figure 4.5.

The use of external heating for the equilibrium chamber was necessitated due to the need for an initial heating of the main block or body to facilitate the attainment of a thermal equilibrium within this crucial section of the apparatus.

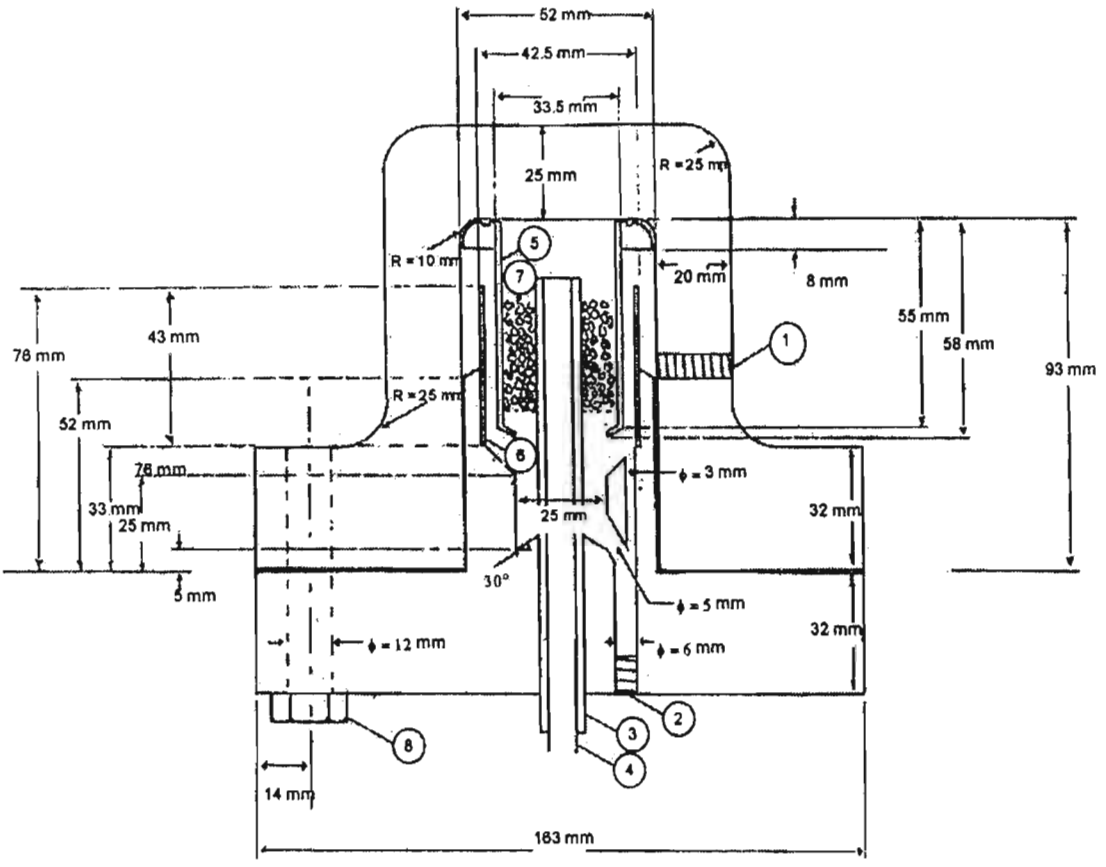

1: Vapour exit; 2: liquid exit; 3: Cottrell tube jacket; 4: Cottrell tube; 5: thin walled SS tubing; 6: thin walled SS tubing; 7: SS packing; 8: high tensile nut and bolt (x6);

Figure 4.4. Technical diagram of the equilibrium chamber of Harris (2004).

To prevent any superfluous heating of the equilibrium chamber and any transfer of this heat to the packed section, the heating was turned off after an initial heating period. A custom-made 600 W split band heater was fitted around the upper flange to fulfill this function. The use of split band heater was necessitated due to the protrusion of the take-off or exit tubes from the equilibrium chamber.

As in the design of the reboiler, the same argument with regards to the large wall thickness applies to the design of the equilibrium chamber. However, for the latter, the thermal response of the equilibrium chamber to increments in energy input (through the split band heater) is inapplicable, provided that the packed section is quite well-insulated.

The use of the external heating in the initial heating period for the apparatus to facilitate thermal equilibrium was inefficiently conducted as the temperature of the main body could not be monitored as a function of energy input from the variable-voltage transformer.

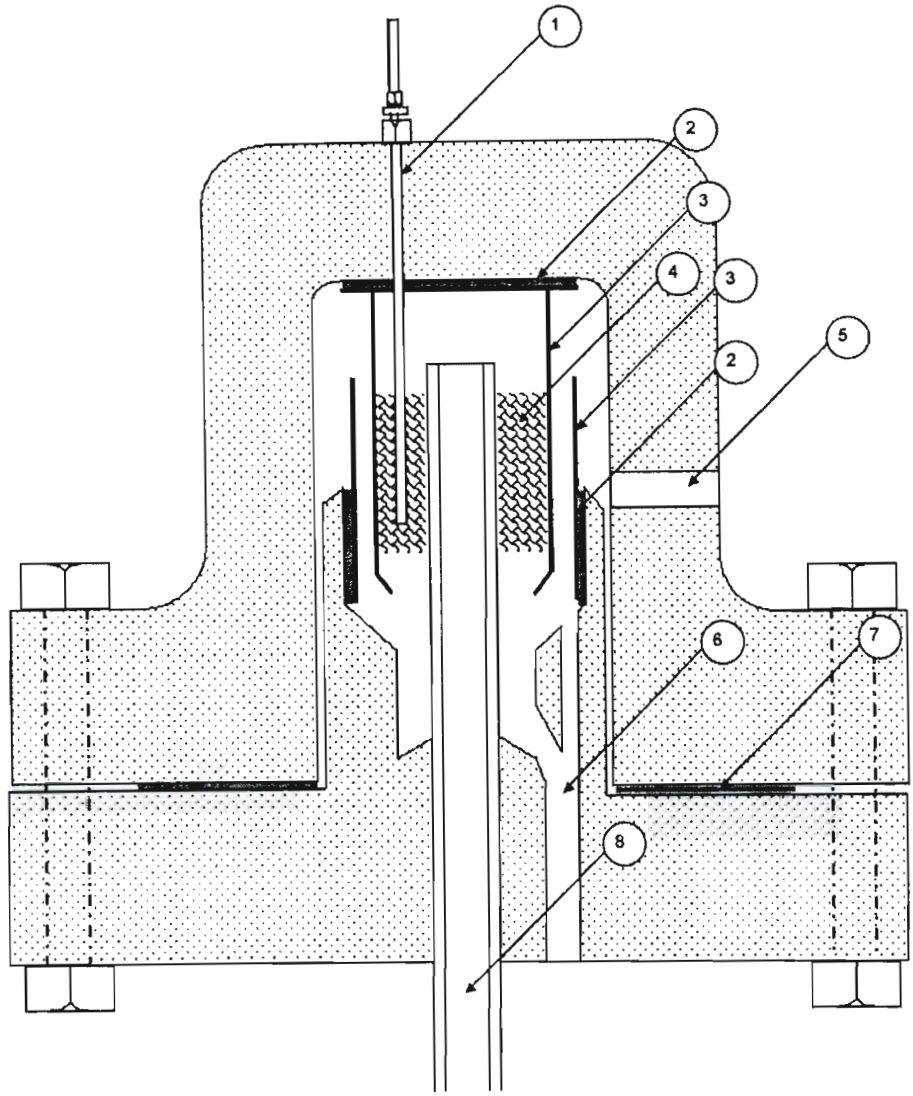

1: Temperature probe 2: Supergraf use as thermal insulation; 3: thin walled 316 SS tubing; 4: SS packing; 5: vapour return; 6: liquid return; 7: Supergraf gaskett; 8: Cottrell tube;

Figure 4.5. Schematic of the equilibrium chamber of Harris (2004).

A much more effective strategy would have been to incorporate a suitable temperature sensor in an appropriate position within the main body to ensure that the equilibrium chamber was controlled at a suitable temperature.

The aspects of the temperature probe selection and the measurement of the equilibrium temperature in the packed section will be commented upon at a later stage.

4.2.2.4 Liquid and vapour condensate sampling provisions

In addition to the attainment of a true equilibrium condition and efficient phase disengagement in the equilibrium chamber, representative sampling of the liquid and vapour condensate has traditionally been a major source of error in most dynamic LPVLE still designs.

The measurement of the vapour phase is quite often considered as being the least accurate of all the measure variables in a P-T-x-y VLE data set (Palmer, 1987), as was revealed by the theoretical treatment of VLE data from LPVLE recirculating stills by Van Ness *et al.*(1973). As opposed to the sections discussed above, the design of the liquid and vapour condensate sampling provisions in the design of Harris (2004) was not based on the glass still design of Raal (Raal and Muhlbauer, 1998). Despite claims of two separate sampling strategies and associated designs for $P < 100\,kPa$ and $P > 100\,kPa$, an inspection of the original apparatus of Harris (2004) (coupled with the fact no VLE measurements for $P > 100\,kPa$ were presented) failed to substantiate the credibility of the above statements made by Harris (2004). The design for the sampling arrangement of the phases for $P < 100\,kPa$, where the latter was a verifiable feature of the apparatus of Harris, is shown in Figure 4.6.

The sampling arrangement consisted of a sample loop with three Swagelok® control valves and a static sampling port with a septum. During the operation of the equipment in the non-sampling mode, valve 2 and valve 3 were closed and valve 1 (which directly intervened in the circulation of the two phases in the apparatus) was left open to allow for the continuous operation of the apparatus. When equilibrium had been attained and the phases were to be sampled, valve 1 was closed and valves 2 and 3 were opened. The sample loop was then flushed for a certain time period, after which valves 2 and 3 were closed and a small volume of the sample was trapped in the respective sample loop. A sample could then be withdrawn from the sampling loop through the insertion of gas-tight syringe in the septum of the sample port and the phase composition determined by gas chromatographic analysis.

Harris (2004) discussed initial problems that were experienced with the positioning of the sampling points with regards to the optimal height of the sample loops vertically above the top of the reboiler. Due to the constant recirculation of the liquid and vapour condensate phases, fluctuations of the liquid levels in the vapour condensate and liquid return lines occurred. There was also considerable mixing of both phases and the reboiler contents in the respective return lines at the base of the reboiler. Due to the above, the occurrence of any backflow into the sample traps would serve to compromise the accuracy of the phase composition determinations. There were no details that were divulged by Harris with regards to the procedure that was employed in the optimization of the positioning of the sampling traps above the reboiler for the acquisition of accurate VLE data. The undesirable sampling arrangement in Figure 4.6, as with the exclusion of mechanical agitation in the reboiler, can probably be attributed to the search for a convenient as opposed to an optimal design. Indeed, the design of a sample trap with a transparent section to be suitable for operating pressures of up to 30 MPa (the upper pressure limit set for the apparatus of Harris) would be quite a challenging task.

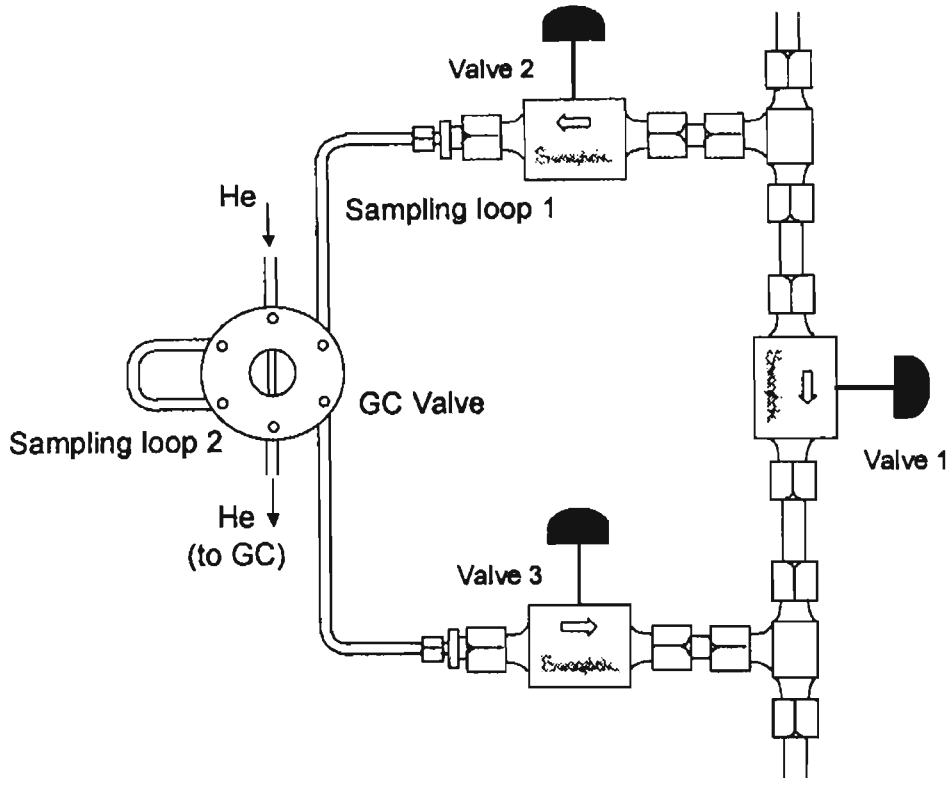

Figure 4.6. Sampling arrangement of Harris (2004) for P < 100 kPa.

As discussed in Chapter 2, an important feature that should be incorporated in the design of sample traps is that of mechanical agitation, a feature that was included in the VLE still designs of Dvorak and Boublik (1963), Yerazunis *et al.* (1964), Raal *et al.* (1972) and Raal (Raal and Muhlbauer, 1998). The vertical positioning of the sample loops coupled with the existence of temperature gradients due to the absence of any stirring create the possibility for a concentration profile as a function of the length of immersion of the syringe needle into the sample loop *i.e.* a non-uniform sampling profile.

As with the Cottrell tube, there should ideally be some transparency in the sample devices as the fluid flow behaviour or rate of circulation of the phases in the traps *i.e.* the drop count, as discussed in Chapter 2, is an important indicator of the approach of the system to equilibrium (Rogalski and Malanowski, 1980; Maia de Oliveira *et al.*, 2002) Also transparency in the sample traps affords an effective check on the possible occurrence of any backflow in the sample trap.

The use of cooling systems (water jackets, cooling coils, *etc.*) in the sample traps is a fairly useful feature that was used in the sampling system designs of Brown (1952), Dvorak and Boublik (1963) and Yerazunis *et al.* (1964), especially for studies on high-temperature systems (for which the equipment of Harris was designed) as a cooling of the sample does not effect the

equilibrium composition and a cooler sample facilitates handling of the sample and a representative subsequent analysis (negates any loss of volatile mixture components).

4.2.2.5 Pressure stabilization system

The favoured approach in an overwhelming majority of dynamic LPVLE still designs has been to connect the pressure stabilization system to the VLE apparatus through the top of the condenser. This arrangement offers the greatest convenience and ensures that no loss of material (as vapour) from any part of the apparatus occurs (provided that the condensing system is efficient and there are no leaks in any other part of the apparatus). The basic arrangement for the pressure stabilization system of Harris (2004) is shown in upper left hand corner in Figure 4.1. As can be seen from the diagram, the pressure connections were also made via the top of the condenser.

An important feature of the pressure stabilization system is the size or volume of the ballast vessel that is employed in the pressure stabilization strategy for the system. Harris (2004) stated that a 25 liter ballast was used, however, an examination of the final state of the apparatus of Harris revealed that the ballast vessel used was actually a ~3 liter 316 SS vessel. A pressure sensor was attached to the top of the ballast vessel for low-pressure measurements. The pressure stabilization setup for low-pressure measurements *i.e.* $P < 100\,kPa$ incorporated the use of two electromagnetic valves in the form of Clippard solenoid valves (to be discussed in greater detail later). One of these valves was connected to a high-pressure source *i.e.* atmospheric and the other to a low-pressure source *i.e.* a vacuum pump. In this fashion, for $P < 100\,kPa$, the actuation of the solenoid valves through a personal computer (pc) linkup (to be discussed in greater detail later) would allow for control of a setpoint pressure (in isobaric mode) or temperature (in isothermal mode).

For high-pressure measurements, the pressure stabilization scheme of Harris is shown in Figure 4.7. In the high-pressure measurements, nitrogen was used as the pressurizing medium for the system and the gas was introduced directly into the system with no intermediate ballast. The system pressure was controlled by setting the desired pressure on the second-stage regulator on the nitrogen cylinder and then having a constant bleed to the atmosphere through a common manifold at the top of the condenser. Harris did not divulge any details with regards to the incorporation of safety measures in conjunction with the operation at elevated pressures and details were also not furnished as to efficiency of the rather crude pressure control strategy that was employed for the latter.

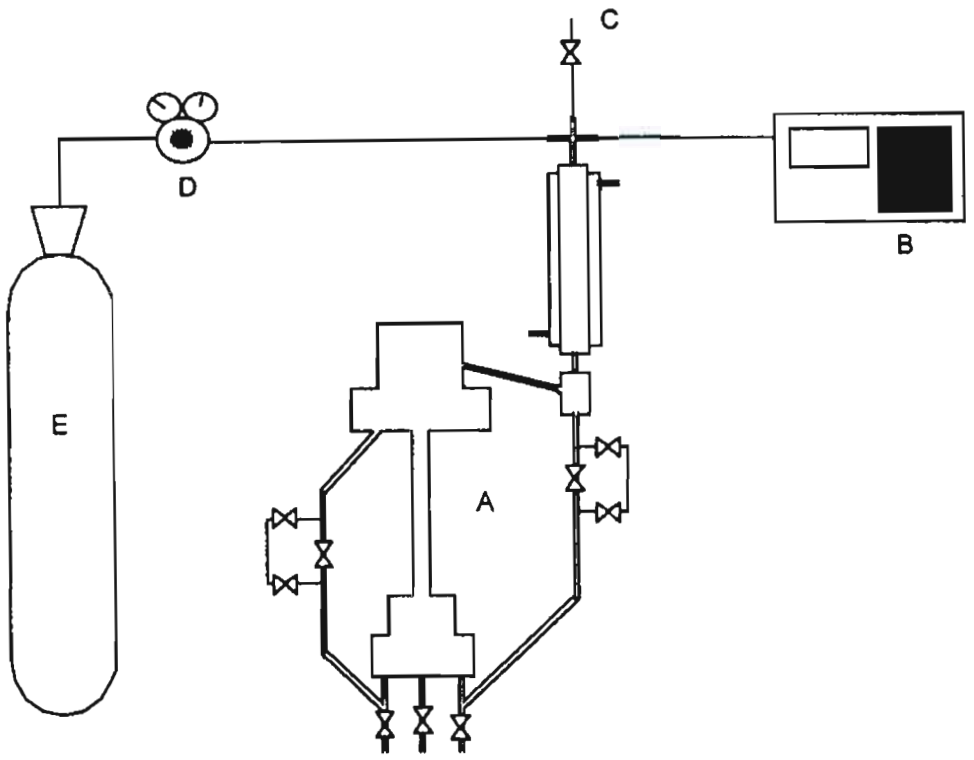

A: VLE still; B: high pressure module; C: constant bleed to atmosphere; D: pressure regulator; E: Nitrogen cyclinder.

Figure 4.7. High-pressure stabilization arrangement of Harris (2004).

The actual ballast volume of ~3 liters used by Harris (2004) was insufficient to smooth out the pressure fluctuations in a dynamic LPVLE apparatus, where pressure fluctuations due to nature of the method *i.e.* constant boiling and recirculation of a vapour-liquid mixture, are to be dampened. Ideally, the ballast volume should be much larger than that of the entire apparatus and a ballast vessel should be available for both high and low pressures (not just low pressures as used by Harris). In fact, a ballast vessel would be more of a necessity at higher pressures, where the latter also serves as a safety measure to prevent overpressurization of the system by being a large volume vessel intermediate between the high-pressure gas cylinder and the VLE apparatus. In all honesty, for operation at higher pressures, safety features such as safety relief valves should be incorporated in the appropriate pressure lines.

4.2.2.6 The Condensing system

The effective design of a condensing system hinges upon the availability of a large surface area for heat exchange and a large temperature difference between the boiling point of the mixture being condensed and the temperature of the coolant fluid used in the condenser. An inefficient

condenser would have disastrous consequences for the attainment of equilibrium as with a constant loss of material through the condenser, the attainment of a material equilibrium for the system is severely compromised.

The final design of the condenser used in the work was a fairly efficient design as it was a "double effect" condenser, as shown in Figure 4.8. The condenser was machined out of 316 SS and consisted of both an outer condensing jacket and an internal heat exchange coil of 1/8 inch stainless steel tubing. The use of an internal thin-walled coil allows for a marked increase in surface area for heat exchange and an increase in the efficiency of the heat exchange as it is intimate contact with the vapour phase.

The design and operation of the condensing system proved to be inadequate for the systems and the conditions investigated by Harris. This was ascertained through a discovery that quite considerable amounts of (d,l)-menthol and isomenthol (chemical systems that were studied by Harris) had escaped through the condenser and accumulated in the cooler environment of the stainless steel ballast and more worryingly on the SS diaphragm of the pressure transducer. This is attributed in most likelihood to the use of only the outer cooling jackets, as observed in a visual inspection of the final arrangement of the condensing system of Harris. Without the use of the highly effective internal coil, material loss, especially for difficult systems, should be anticipated.

A key oversight in the design of the condenser of Harris (2004) was that for measurements of those systems that contain components that are solids at or above ambient conditions in the form of heavy components, as with the (d, l)-menthol and l-isomenthol systems that were measured in the study, and with differing volatilities, special considerations are necessitated with regards to the design and operation of the condensing system (Haynes and Van Winkle, 1954).
This was exemplified in the works of Coon *et al.* (1989) and Gupta *et al.* (1991) who described in detail the difficulties in the measurement of VLE of polynuclear aromatic compounds with the dynamic LPVLE method. If the temperature of the coolant was too low, the heavy component was observed to solidify. Conversely, if the temperature was too high, the less volatile component was lost.
The author considers that the most effective design of condensing system for a system with heavy and less volatile components would be employ the use of two separately controlled condensing systems in series.

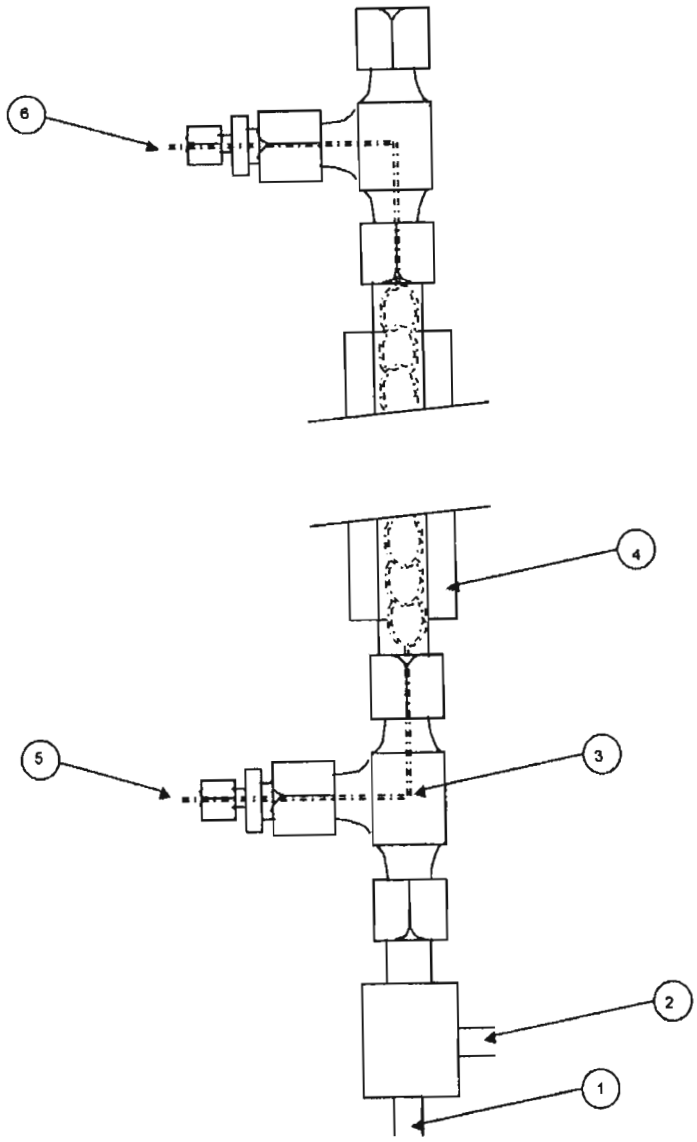

1: Condensed vapour outlet; 2: vapour inlet; 3: internal heat exchanger; 4: jacketted vessel; 5: cooling fluid inlet; 6: cooling fluid outlet

Figure 4.8. The Condenser of Harris (2004).

The first condensing system would have the coolant fluid at a temperature lower than the boiling point of the heavy component but higher than its melting point so that the heavier component would condense without solidifying. The second condenser, which would be located higher up, would have a lower-temperature coolant fluid for the less volatile components, which do not condense in the first condenser due to the temperature being too high for sufficient condensation. In this way, a system consisting of heavy components and light components can be properly condensed and then returned to the recirculation train with minimal material loss through the condenser.

4.2.2.7 Thermal lagging

The proper insulation of the entire VLE apparatus serves to ensure that heat losses from the key operational sections of the apparatus are minimized and that a proper internal equilibrium is attained within the apparatus. In terms of the reboiler, adequate insulation ensures that there is efficient utilization of energy and consequently, less heating duties for the external and internal heaters in the boiling of the reboiler contents. For the equilibrium chamber, ideally an adiabatic condition should be maintained so as to negate any disturbance of the approach of the phases to a true equilibrium.

Preliminary tests were conducted by Harris on the effect of the amount of insulating material placed around the reboiler and the equilibrium chamber. The insulating material used was glass wool fibre. It was shown that a significant improvement of the thermal stability of the apparatus was achieved with insulation. However, the data (presented graphically as shown in Figure 4.9) was difficult to interpret conclusively as a plot of temperature (as a function of heat loss for the apparatus) versus time, with and without insulation, did not have units for the time scale, as shown in the thesis of Harris (2004).

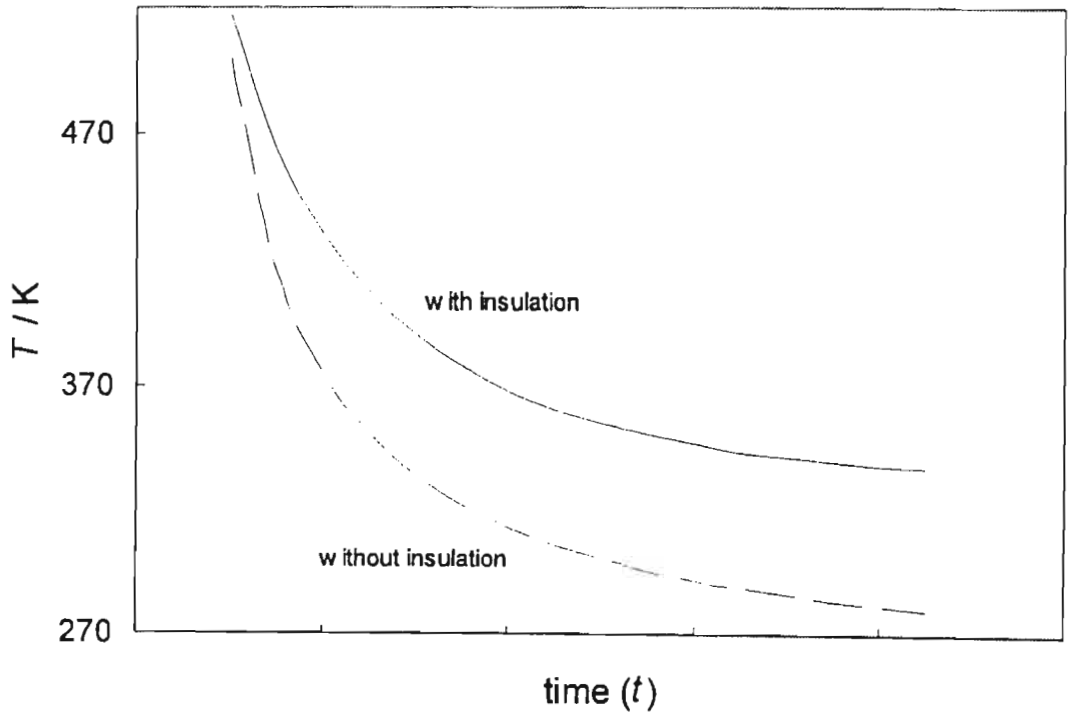

Figure 4.9. Heat loss profile of the apparatus of Harris (2004) with and without insulation.

4.2.2.8 The Return line

The importance of the design of the return line is frequently overlooked by many experimenters. The return of the liquid and vapour streams to the reboiler after being sampled in the sample traps can be achieved in variety of ways. Many researchers have opted for combining these two streams as early as possible in the descent to the base of the reboiler (Rose and Williams, 1955). In more effective VLE still designs (Dvorak and Boublik, 1963; Yerazunis *et al.*, 1964; Rogalski and Malanowski, 1980), static mixing sections have been used, which also serve as buffers for any back-surges or backflow, in addition to promoting good premixing of the vapour condensate and liquid streams *en route* to the reboiler. As mentioned before, the use of separate return lines for the two phases with no premixing of the phases prior to re-entry into the reboiler was not optimal due to the above.

Another major flaw in the design was the injudicious use of a Swagelok® check valve (Model: SS-53S4) in the return line of the vapour condensate phase near the base of the reboiler. The internal mechanism of the check valve was a metal poppet which did not allow any reverse flow. After consultation with Swagelok® technical and sales representatives, it was ascertained that the horizontally-mounted valve needed a considerable forward flow to be activated *i.e.* raise the poppet for forward flow. Further testing of the valve confirmed that the flow of the liquid streams into the reboiler (especially the vapour condensate stream) was not sufficient to activate the valve on any appreciable continual basis. Since the operation of a dynamic LPVLE apparatus is essentially based on a continuous circulation of the respective phases, the use of this check valve probably adversely effected the operation of the apparatus by diminishing the return flow of the vapour condensate stream into the reboiler.

A solitary commendable feature of the return line design was the use of controlled heating for the latter. The use of return line heating, in conjunction with heating of all the lines in the apparatus, was to circumvent the difficulties associated with measurements with compounds that are solids at or above ambient temperatures.

The preheating of the return lines not only reduces the heating duties of the reboiler heaters, but also serves to minimize the occurrence of flashing as the difference in temperature between the reboiler contents and the return line mixture entering the reboiler is decreased. However, even with the use of the latter, there is no substitute for mechanical agitation in the reboiler and caution should be exercised when heating the return lines as excessive heating promotes backflow.

4.2.2.9 Pressure and temperature measurement, data logging and control

The system pressure and temperature are arguably the most important thermodynamic variables in the data set and the measurement of which are considered as being associated with arguably the least uncertainty in the P-T-x-y data set (Palmer, 1987). Consequently, the assumed accuracy of either one or both of these two variables forms the basis for many thermodynamic treatments of the raw data. This is exemplified in the VLE computations discussed in Chapter 3, as in the method of Barker (1953) and the Van Ness-Byer-Gibbs TC test (1973). Accordingly, the measurement and the control of system pressure and temperature, which also form the principal basis for the attainment of the equilibrium condition, have to be conducted with the greatest of accuracy.

For the measurement of the equilibrium temperature, provisions were made in the equilibrium chamber, as shown in Figure 4.5, in the form of the insertion of a temperature probe into a 1/8 inch outer diameter thermowell tube. The positioning of the thermowell tube ensured that it would be in intimate contact with the equilibrium phases at the equilibrium temperature. The original sensor that was used was a Pt-100 platinum resistance thermometer; however, difficulties were experienced in the use of the Pt-100 sensor used by Harris (2004). The Pt-100 sensor was claimed to be irreparably damaged when employed for measurements at $T > 400\,K$. Thereafter, a type K thermocouple was employed for the measurements at elevated temperatures. The output of the temperature sensor (resistance for the Pt-100 and voltage for the thermocouple) was read off an Agilent 6.5 digit multimeter (Model: 34401A).

The pressure was measured with a Sensotec Super TJE pressure transducer (Model: 1833-02), which was rated for a pressure of 25 psi, and was displayed on a DPM LCD display (Model: 5004). For high-pressure measurements, a Cole Palmer pressure standard (Model: P-68037-05) was connected to the top of the condenser.

Platinum resistance thermometers are inherently more linear across their range of operation than other temperatures sensors and do not require the measurement of a cold junction temperature or a cold junction compensation in the measurement of an absolute temperature (as for a thermocouple). The commercial availability of Pt-100's for temperatures up to 750 K is well established and has made these sensors quite popular for a variety of applications in the research, industrial, pharmaceutical and food technology fields. It was even acknowledged by Harris (2004) that the Pt-100 sensor that was used originally was more accurate than the type K thermocouple.

The computer-aided control strategy for pressure and temperature in the VLE apparatus of Raal (Raal and Muhlbauer, 1998) and Harris (2004) is similar to that of Hiaki *et al.* (1994). The system temperature and pressure, as displayed on the Agilent multimeter and the DPM pressure display, respectively, were logged into a Microsoft Visual Basic® software interface program, VALVECON, via RS-232 serial port communication with a pc.

The data logging interface is shown in Figure 4.10. This allowed for the real time monitoring of the system variables from the respective sensors, which would allow for the VALVECON program to execute its control of temperature or pressure from the feedback system. The hardware for the control of the system pressure was in the form of a pulse-width modulation control strategy of two 12V DC Clippard "on-off" solenoid valves (Model: ETO-3-24) with a power supply to activate the valves (which are normally in a closed position) to control the pressure. As mentioned above, each solenoid valve can open to either a high or low-pressure source, relative to the setpoint or desired pressure.

In the control of the system pressure *i.e.* in isobaric mode, a setpoint pressure (P_{set}) is entered in the VALVECON PROGRAM interface, as shown in Figure 4.10. In response to the pressure values logged into the program, control is executed over the system pressure by activating the appropriate solenoid valve and respective pressure source to correct the system pressure (P_{system}). For the subatmospheric operations *i.e.* for $P_{set} < 100\,kPa$, if $P_{system} < P_{set}$, the solenoid valve connected to atmospheric pressure is activated to open and conversely if $P_{system} > P_{set}$, the solenoid valve connected to the vacuum pump line is activated. The algorithm, as implemented in Microsoft Visual Basic®, is shown in Figure 4.13, where system refers to the VALVECON program.

The dead-band input (in pressure units), shown in Figure 4.11, is the allowed deviation or tolerance for the system pressure before the solenoid valves are activated to control system pressure in terms of the opening or closing of the solenoid valves. Provisions have also been made in the formulation of the VALVECON program to exercise control over the sampling rate through the control option in the program, shown in Figure 4.12. In this way, the latency in the data logging and subsequent execution of the pressure control by the VALVECON program could be controlled *i.e.* it controls the amount of logged pressure inputs that are used to formulate an average pressure value, to which the VALVECON program can respond to execute the necessary control strategy for the system pressure. The VALVECON program, in conjunction with the pressure stabilization setup, was able to control the system pressure in isobaric mode to ± 0.03 kPa.

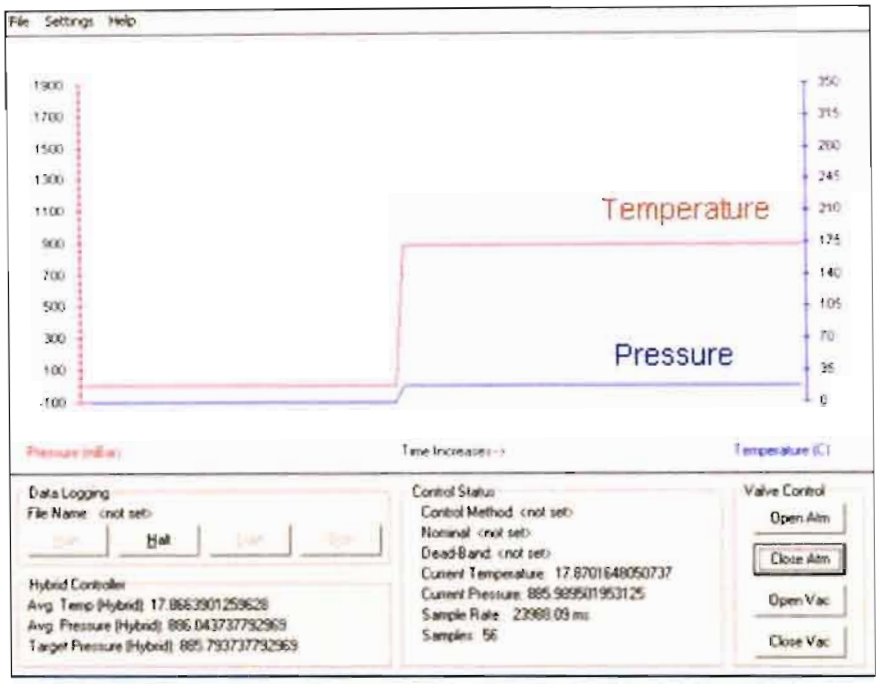

Figure 4.10. Data logging interface of the VALVECON program.

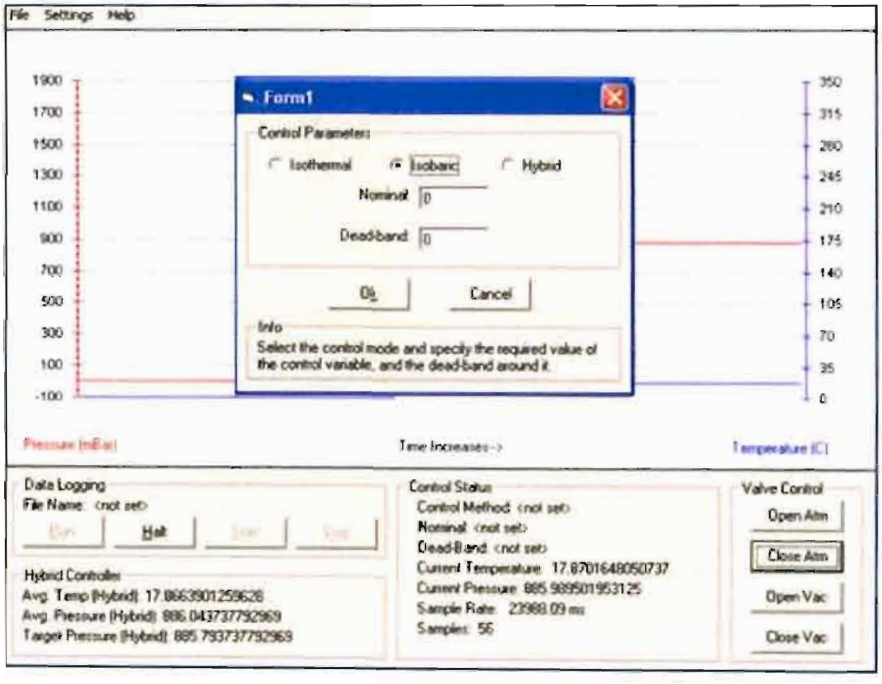

Figure 4.11. Initialization of the isobaric mode of operation with the VALVECON program.

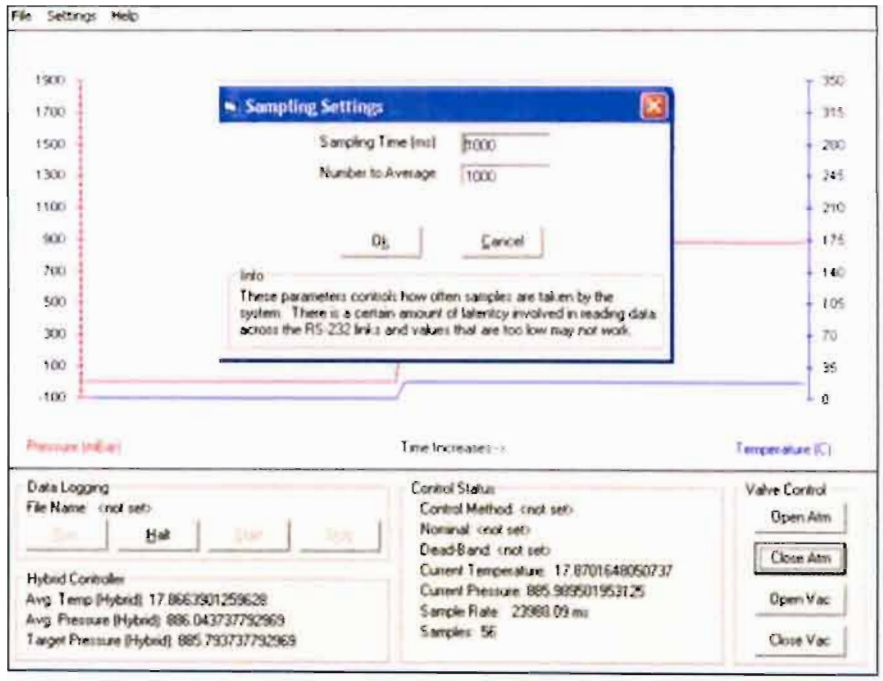

Figure 4.12. Sampling rate control in the VALVECON program.

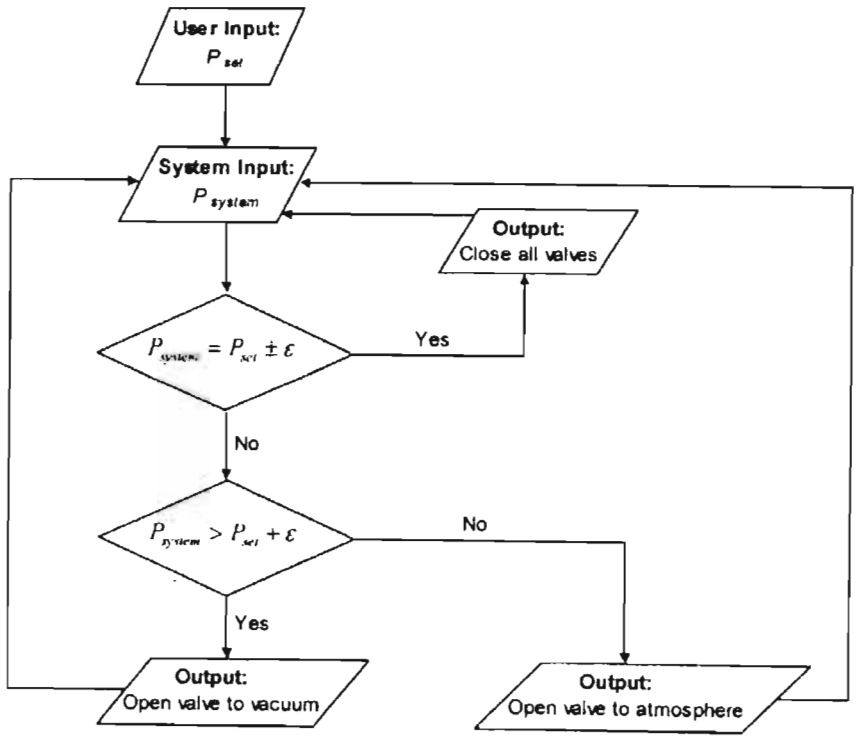

ε = tolerance, typically 0.015 kPa

Figure 4.13. Algorithm for isobaric control with the VALVECON program.

For the isothermal control mode, the setpoint temperature is entered into the VALVECON control interface as for the pressure in the isobaric control mode. Provisions are made to enter calibration parameters (gradient and offset) for the temperature sensor, assuming that a linear response of the temperature as a function of resistance exists (as for a Pt-100 sensor), as shown in Figure 4.14.

In the isothermal control mode, whose algorithm is shown in Figure 4.15, the system pressure is employed to control the temperature. After the entry of the setpoint temperature (T_{set}) by the user, the VALVECON program employs the use of the system pressure (P_{system}) as the setpoint pressure (P_{set}), upon which to base the control of the system temperature (T_{system}). The program monitors the temperature over a time period and then averages it to obtain the average system temperature or $T_{system(average)}$. If $T_{system(average)} < T_{set}$, P_{system} is increased by 0.03 kPa and if $T_{system(average)} > T_{set}$, P_{system} is decreased by 0.03 kPa. The procedure described above is continued until $T_{system} = T_{set}$. Harris described difficulties with the temperature control system especially at elevated temperatures, where increasing instability of the temperature control strategy was observed.

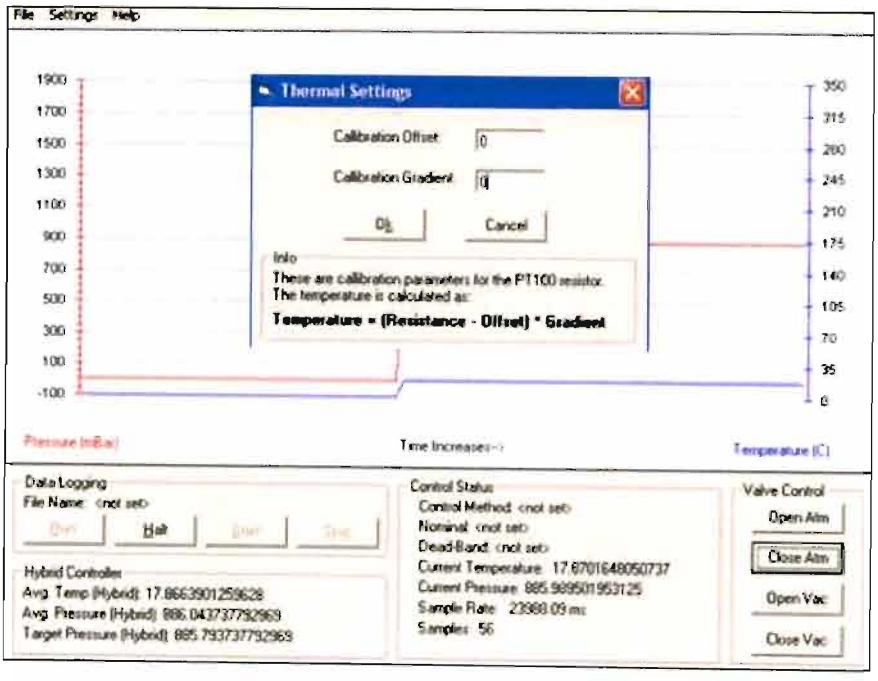

Figure 4.14. Initialization of the isothermal mode of operation for the temperature sensor in the VALVECON program.

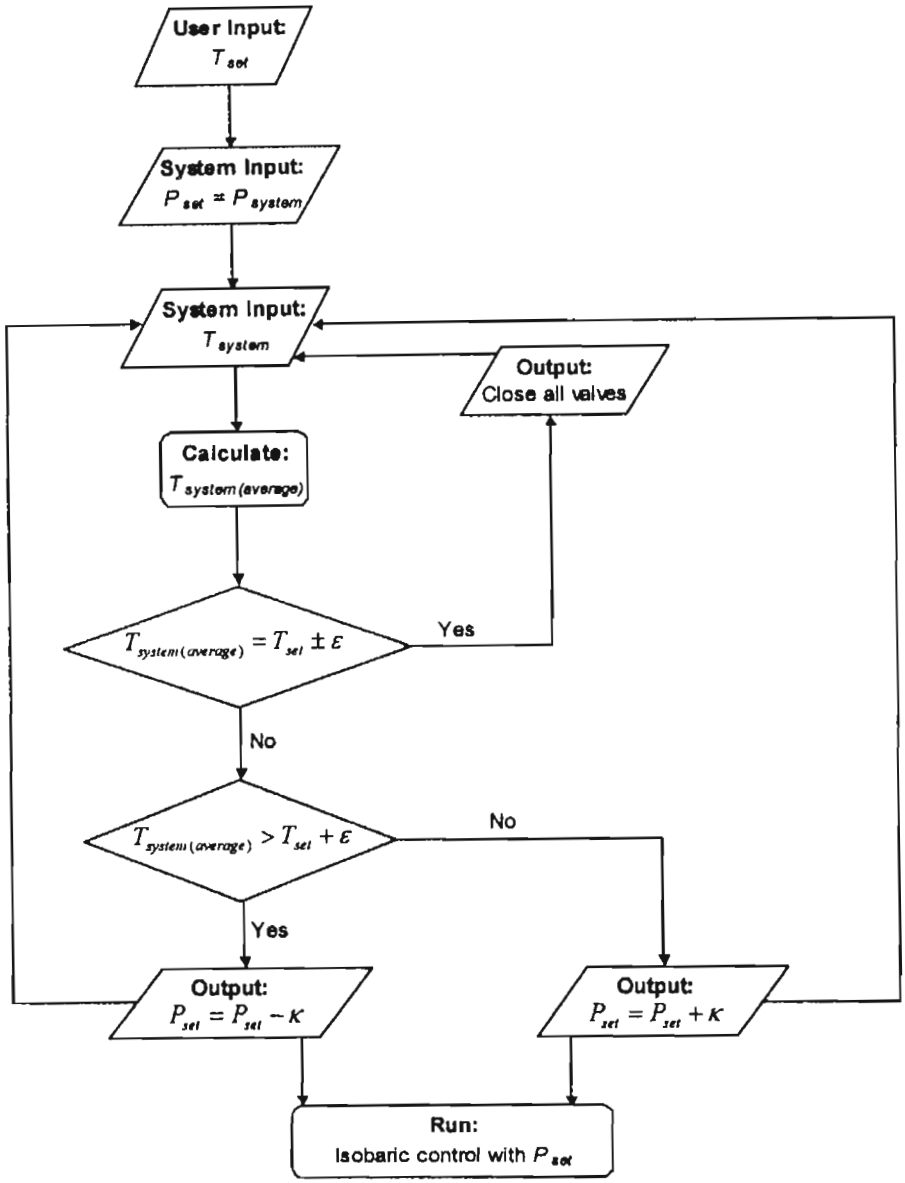

ε = tolerance, typically 0.1 kPa
κ = slight change in pressure, typically 0.03 kPa

Figure 4.15. Algorithm for isothermal control with the VALVECON program.

4.2.3 Experimental measurements of Harris (2004)

The investigations undertaken by Harris on the dynamic VLE apparatus that was developed were in the form of vapour pressure measurements and binary vapour-liquid equilibrium measurements. The vapour pressure measurements undertaken were that for n-heptane, n-decane, n-dodecane, n-hexadecane, 1-octadecene, 1-hexadecanol and (d, l)-menthol in the low-pressure region and that for acetone for pressures up to 1 MPa.

The vapour-liquid equilibrium measurements were for the cyclohexane + ethanol system at 40 kPa, the (d, l)-menthol + l-isomethol system at 448.15 K and the n-dodecane + 1-octadecene system at 3.00 kPa and 26.66 kPa.

The initial testing of the apparatus was conducted with vapour pressure measurements for both saturated and unsaturated hydrocarbons for an overall temperature range between 308.33 K and 583.90 K. The experimental vapour pressure data was regressed with the Antoine equation and compared to the literature vapour pressure data to obtain temperature deviations. The absolute average deviations of the experimental vapour pressures from the literature values (ΔT) revealed that good agreement was observed for n-heptane $(\Delta T = 0.15)$, n-decane $(\Delta T = 0.56)$ and n-hexadecane $(\Delta T = 0.20)$. There was fairly acceptable agreement observed for 1-hexadecanol $(\Delta T = 1.95)$ and (d, l)-menthol $(\Delta T = 1.55)$, however, poor agreement was observed for the dodecane $(\Delta T = 4.55)$ and 1-octadecene $(\Delta T = 2.99)$ compounds.

Harris did not provide any ΔT values for the acetone vapour pressure measurements, however, from a graphical inspection of a comparative plot of the literature and experimental vapour pressure values, reasonably good agreement was observed. Harris segmented the vapour pressure measurements into three distinct temperature regions in the form of $T < 373.15\,K$, $373.15\,K < T < 473.15\,K$ and $T > 473.15\,K$ to obtain a better perspective on the scatter of the data points as a function of temperature. From the trends in the data, Harris concluded that with an increase in temperature, an increase in the data scatter was observed.

The use of the highly nonideal cyclohexane + ethanol system has been well established as a test system in our laboratories (Joseph, 2001) and was studied by Harris at a pressure of $40\,kPa$. Although data reduction was performed for the isobaric VLE measurements, the lack of any thermodynamic consistency (TC) testing for the P-T-x-y data meant that an assessment of the quality of the latter was not obtained in the study. However, from a graphical inspection of the data plots *i.e.* T - x -y and x-y curves and the fit of the data to the thermodynamic models, some idea of the quality of the data could be gauged. Graphically, the data was not very smooth and did not compare quite well to that of Joseph (2001). From the γ_i - ϕ_i correlation of the data to the G^E thermodynamic models (Wilson and NRTL), with the B-truncated virial EOS for the vapour phase, it was observed that the regressed model parameters were not able to effectively reproduce the experimental data over the entire composition range.

Harris then proceeded with the measurement of VLE for a high-temperature test system in the form of n-dodecane + 1-octadecene at $P = 26.66$ kPa with literature data from the study of Jordan and Van Winkle (1951). In addition to the temperature fluctuations for the investigations at elevated temperatures, the onset of the second major shortcoming of the design in the form of unreliable vapour composition measurements at elevated temperatures came to the fore. It was observed by Harris that the composition of the vapour phase would not remain constant, even with the attainment of an "equilibrium condition" and would tend to become equivalent to that of the liquid phase composition over time.

Harris measured a P-T-x data set with the values of the vapour compositions being computed, as discussed in the γ_i - ϕ_i BUBL P calculations in Chapter 3. The data was regressed with the γ_i - ϕ_i and ϕ_i - ϕ_i methods and Harris presented a plot of Δy_1 versus x_1, where the residual was calculated as the difference between the literature and the experimental value. The residuals did not scatter evenly or randomly about zero and in all probability there were systematic errors present in the data set.

Harris then measured novel VLE data for the n-dodecane + 1-octadecene system at 3.00 kPa and for the (d,l)-menthol + l-isomenthol system at 448.15 K. As with the previous VLE study, the values for the vapour phase compositions for the n-dodecane + 1-octadecene system were computed. However, for the (d,l)-menthol + l-isomenthol system, the vapour phase composition was measured as the system had a lower relative volatility and was measured for a shorter time span. As for the cyclohexane + ethanol P-T-x-y data set, no TC testing of the data was conducted for the menthol systems. The fitting of the isobaric n-dodecane + 1-octadecene VLE data to thermodynamic models was particularly poor and it was acknowledged by Harris that the problem could not be attributed to inadequacies of the thermodynamic models in providing a fit to the data.

The study of the (d,l)-menthol + l-isomenthol system was a very inappropriate choice and probably one of convenience, so as to prevent the manifestation of problems that had been associated with the measurement of the vapour phase compositions. Due to the very low volatility of the system, the vapour phase composition was roughly equivalent to the liquid phase composition across the entire composition range in the x-y diagram of the system. However, the P-x-y curve obtained by Harris was irregular in shape. Since the experimenter failed to perform any TC testing for the P-T-x-y data sets that had been obtained, Harris failed to capitalize on any information that the results of the TC tests might have revealed about the nature of the erroneous measurements.

Harris attempted to address the two persistent and crippling problems in the measurement of vapour pressure and VLE measurements with the equipment in the form of the temperature fluctuations and erroneous vapour phase measurements. Harris identified the potential causes for the above and then attempted different remedies to alleviate the above. With regards to the temperature fluctuations, Harris attributed this outcome to three possible scenarios, as discussed below:

The first was that the volume of the material in the reboiler was insufficient to sustain the constant recirculation train of the dynamic system resulting in an irregular or discontinuous boiling of the mixture. Consequently, the measured temperature would fluctuate upon the momentary termination of the recirculation train and the halt in the generation of a vapour-liquid mixture up the Cottrell tube to contact the temperature sensor. Harris investigated this uncertainty by observing the system behaviour as a function the volume of material charged to the reboiler (from 90 ml - 200 ml). The effect of this on the diminution of the temperature fluctuations was negligible.

Secondly, it was felt that the temperature difference between the vapour condensate (richer in the lower-boiling material) and the reboiler contents was contributing to a "disruption" of the reboiler operation. This "disruption" would of course relate to the flashing or non-equilibrium vapourization of the reboiler contents. To investigate the possibility of the above, Harris insulated and heated the vapour condensate return line. The results of the investigation revealed that a small improvement in temperature stability was observed.

Thirdly, it was felt that there was too much heat being lost from the system and Harris attempted to use more insulating material in the form of "thick cladding" around the entire apparatus. Although significant improvements were noted, the temperature fluctuations were still evident in the operation of the apparatus.

Harris concluded that the temperature fluctuations could be attributed to the large bulk of stainless steel (approximately 50 kg) used for the design of the apparatus. With the large heat capacity of a large mass of stainless steel, a large amount of energy is required to heat up the equipment and conversely, a large amount of energy is given off when the equipment cools down. Consequently, the attainment of a thermal equilibrium between the chemical contents of the still (with a much smaller heat capacity) and the 316 SS main body is adversely affected by the large difference in heat capacity.

Problems with the vapour phase measurement were particularly evident for the n-dodecane + 1-octadecene system. In addition to the first possibility identified for the temperature fluctuations *i.e.* insufficient material in the reboiler, Harris identified three additional causes for erroneous vapour phase compositions.

The first potential cause for erroneous vapour phase measurements was that this was due to considerable backflow of boiled mixture up the vapour return line from the reboiler *i.e.* there was no confidence in the effectiveness of the restricted opening for the vapour return line inlet. This resulted in the sampled vapour phase not being representative of the equilibrium composition. It was at this stage that Harris inappropriately employed the use of a check valve to arrest any backflow. The use of the check valve did not yield any improvement in the results that were obtained.

Secondly, it was felt that the superheat from the Cottrell tube was being conducted into the base of the equilibrium chamber, as shown in Figure 4.16. From this, one can infer that there was very little confidence in the effectiveness of the vacuum jacket around the Cottrell tube. In the event of any superheating of the base of the equilibrium chamber, Harris postulated that the flashing of the liquid phase would occur, resulting in the vapour phase containing more of the less volatile material than its true equilibrium composition. The base of the equilibrium chamber was cooled with compressed air to investigate the above but no effect was observed. There were no details furnished with regards to the manner in which this was achieved *i.e.* extent of cooling and cooling mechanism.

Thirdly, a converse scenario with regards to that proposed for the temperature fluctuations was considered in the form of the equipment retaining too much heat, however, this possibility was not investigated properly as acknowledged by Harris.

In the recommendations for an improvement of the design, Harris mentioned that the following could be attempted for an improved future design:

(a) The overall wall thickness and the bulk of stainless steel used for the construction of the various sections of the apparatus should be reduced in accordance with a reduced pressure capacity for the apparatus. For the design of the reboiler and the equilibrium chamber, a design was suggested to incorporate two pieces that screw into each other, as shown in Figure 4.17 to eradicate the need for the use of flanges in the reboiler and the equilibrium chamber.

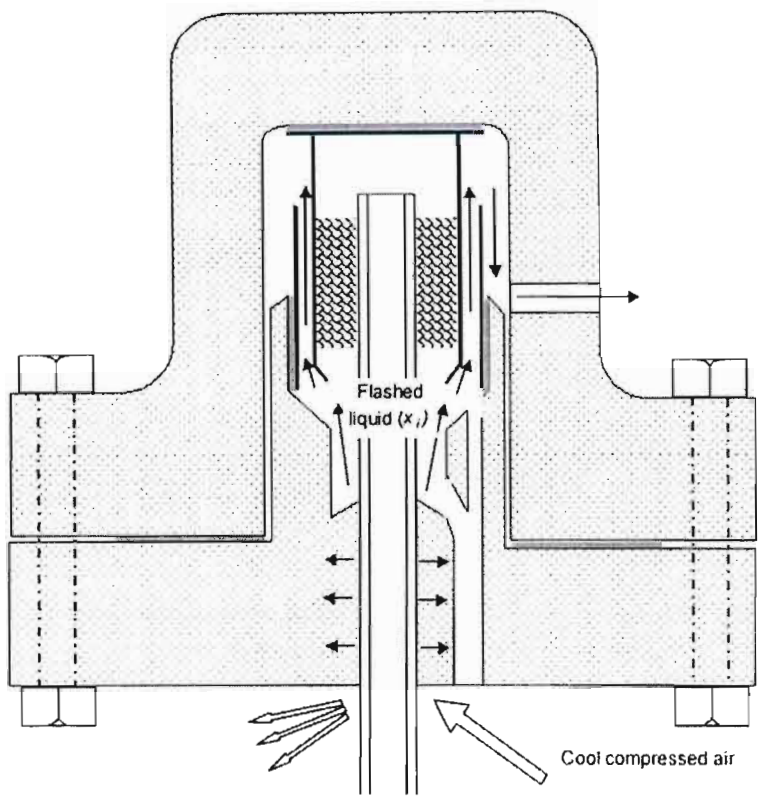

Figure 4.16. Possible scenario of the superheating of the equilibrium chamber and the attempt by Harris (2004) to remedy the situation.

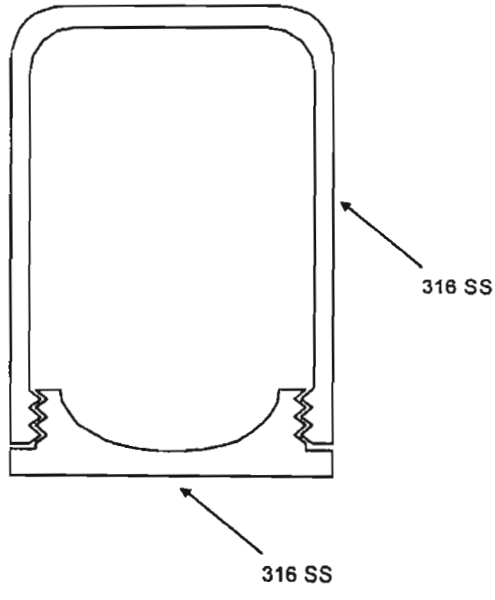

Figure 4.17. Proposed design for the reboiler and the equilibrium chamber.

(b) It was also suggested that the Cottrell tube should be designed such that a sideways entry of the vapour-liquid mixture occurs, as in the Rogalski and Malanowski (1980) still that was shown in Chapter 2. It was felt that this would serve to eliminate the conduction of superheat from the Cottrell tube to the equilibrium mixture.

(c) The last suggestion was that a view glass (possibly sapphire) can be incorporated into the design of the equilibrium chamber. There were no reasons provided as to what the advantages of such an arrangement would be.

Apart from the suggestion of a reduction of the wall thickness of the sections of the apparatus and corresponding diminution of the operating pressure limit, the remaining recommendations are of little value. The design of the "screw-type" reboiler and equilibrium chamber is impractical and is difficult to machine precisely to achieve proper sealing. The suggestion of the sideways entry violates the principles that have been established in our laboratories for the design of dynamic LPVLE stills, as a centrally positioned Cottrell tube allows for a uniform and angularly symmetric concentration profile in the packed section of the equilibrium chamber. Consequently, from the above, it can be concluded that there were more fundamental and blatant flaws in the design of the apparatus than was realized by Harris (2004).

4.2.4 Preliminary testing of the apparatus of Harris (2004)

To investigate any other potential shortcomings of the apparatus of Harris (2004), a short qualitative preliminary investigation of the apparatus was deemed as a prerequisite for the design of the novel apparatus. As a result of time constraints for the completion of this study, only vapour pressures were measured with the apparatus to investigate the temperature fluctuations experienced by Harris. Consequently, no VLE measurements were undertaken to investigate the nature of the erroneous vapour composition measurements obtained with the apparatus. Since the preliminary study is a purely qualitative one, the experimental procedure and measurements will not be described in any great detail, as they serve to merely augment the criticisms of the apparatus of Harris (2004) in the search for more effective design considerations for the novel apparatus in this study.

The general operation of the apparatus proved to be somewhat challenging and tedious. Firstly, the determination of an optimal amount of the pure component to charge into the apparatus was subject to great uncertainty and, as was the case for the original experimenter, this was achieved rather tentatively. Long time delays (~3 hours) were incurred in the start-up procedure for the apparatus *i.e.* the preheating stage, which was necessitated before the initiation of any

appreciable boiling of the reboiler contents could be observed. The discernment of the latter proved quite difficult as there was no temperature monitoring in the reboiler or any transparency in the apparatus to observe the fluid flow characteristics. The original temperature sensor used was replaced by a more accurate class A Pt-100 sensor supplied by Kaytherm and for the pressure measurements, the Sensotec Super TJE pressure transducer was used. The pressure transducer was thoroughly serviced prior to use as a result of material that had accumulated and fouled the stainless steel diaphragm of the sensor during the studies of Harris. Vapour pressures were measured for acetone, n-heptane, n-decane and n-dodecane for the low-pressure $(P < 100\,kPa)$ region for an overall temperature range of 314.63 - 446.74 K. The results were compared with that from the Dortmund Data Bank (1999) and the deviations (ΔT) were calculated for each experimental point as the difference between the experimental and literature values. The deviation plots for the vapour pressure measurements of the respective compounds are shown in Figures (4.18) - (4.21).

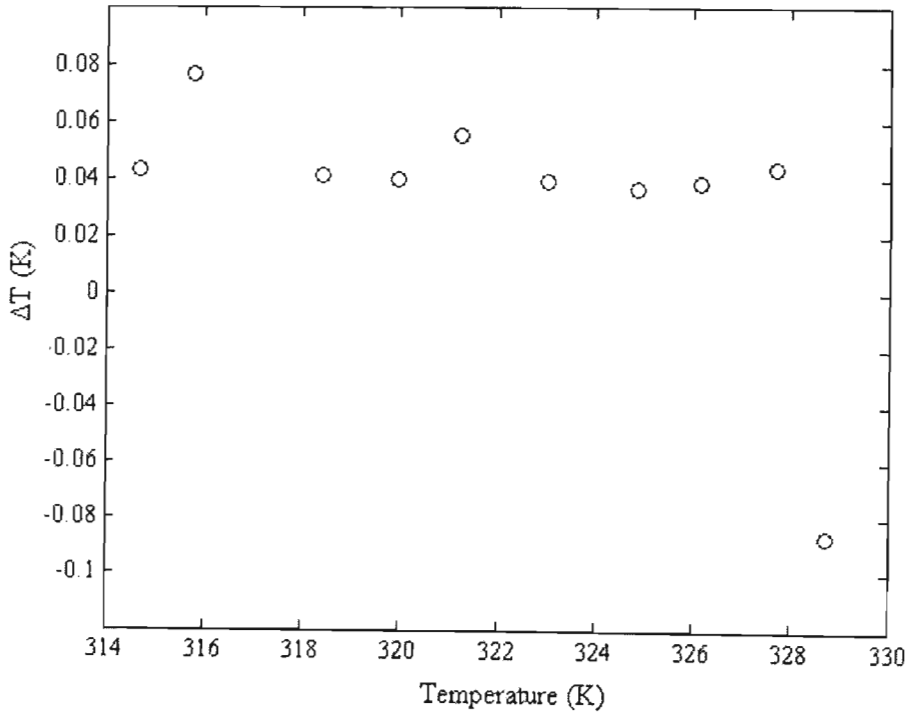

Figure 4.18. Deviation plot for the vapour pressures of acetone.

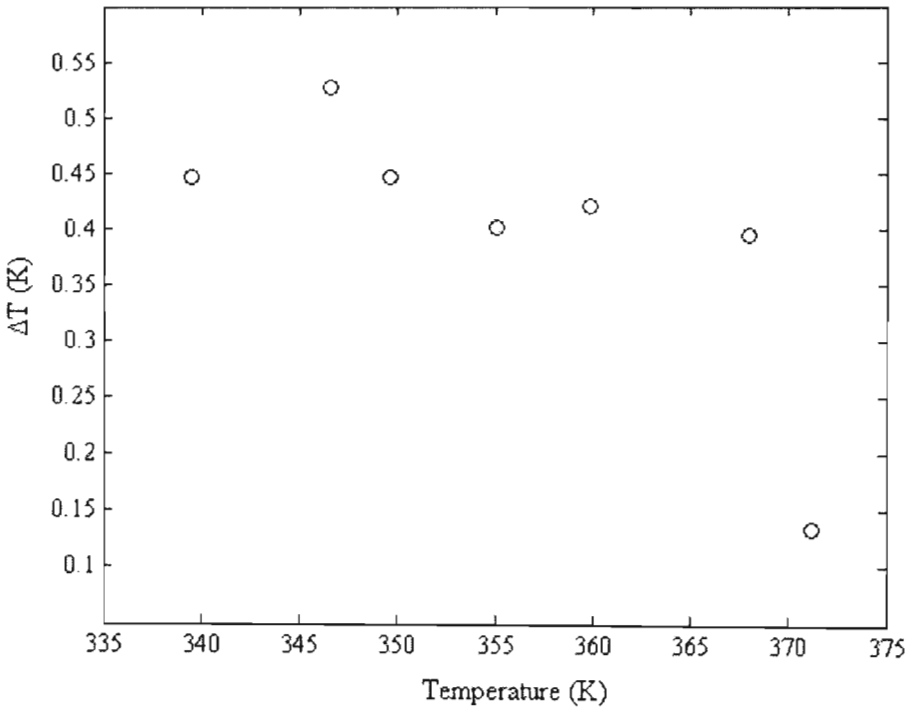

Figure 4.19. Deviation plot for the vapour pressures of n-heptane.

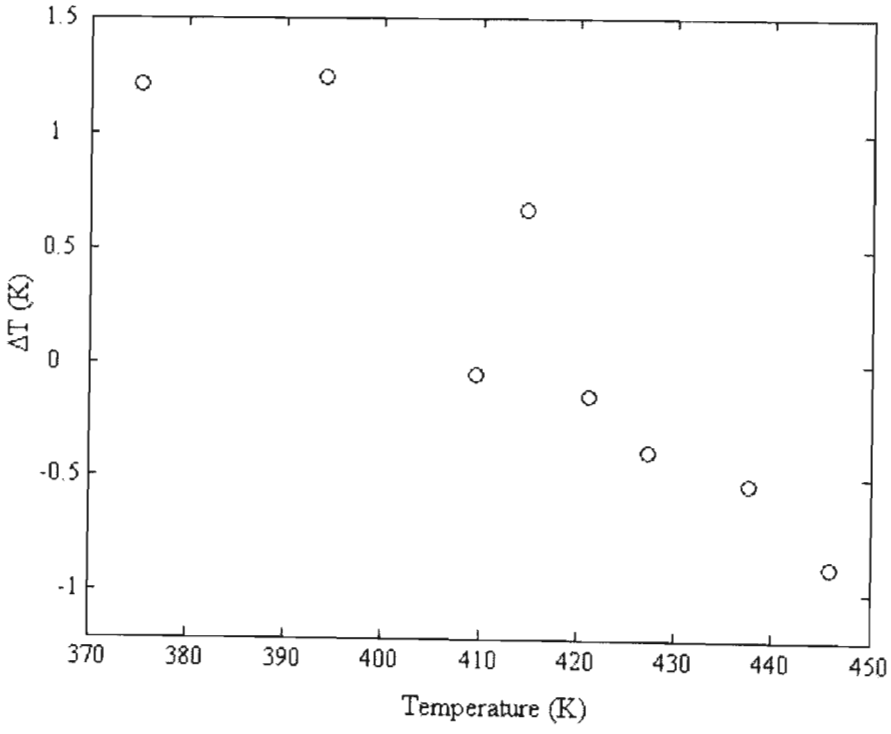

Figure 4.20. Deviation plot for the vapour pressures of n-decane.

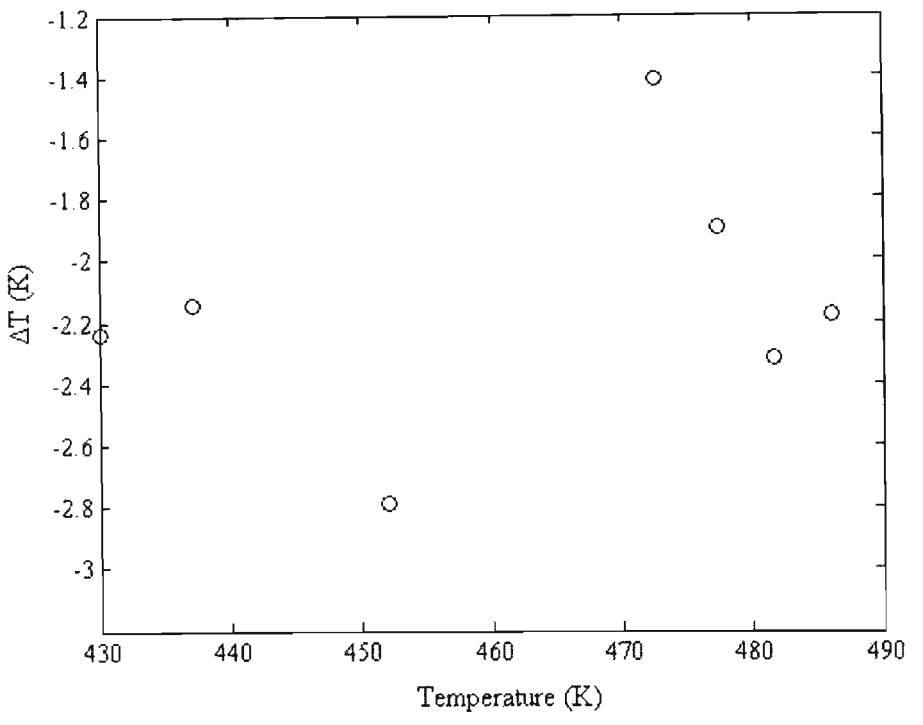

Figure 4.21. Deviation plot for the vapour pressures of n-dodecane.

From the plots in Figures (4.18) - (4.21), it can clearly be observed that with for the higher-boiling compounds *i.e.* n-decane and n-dodecane, there is a considerable increase in the size of the temperature deviations. This observation is in agreement with the experimental observations of Harris. With regards to operation at relatively low temperatures, the temperature stability of the apparatus was fairly well-behaved. However, at elevated temperatures *i.e.* for temperatures greater than 423.15 K, there was appreciable instability observed in the equilibrium temperature measurements for the pure component vapour pressures measured in the apparatus. As reported by Harris, these fluctuations were sinusoidal in nature (fluctuating above and below an average value).

The preliminary investigation of the apparatus of Harris (2004) served to corroborate the claims made by Harris with regards to the difficulties encountered in the operation of the apparatus and the effect of this on compromising the quality of the acquired data. Coupled with the critical dissection of the contents of the thesis of Harris (2004), dealt with in the previous sections, a very powerful body of knowledge had been accumulated that would subsequently be applied to the design of the novel apparatus presented in this study.

4.3 Apparatus of Reddy (2006)

The initial considerations for the novel design were based on addressing the principal flaws of the equipment of Harris (2004) and the incorporation of innovative features that would result in a more efficient design. A synopsis of the assessment of the principal limitations and oversights by Harris coupled with the initial proposals that were formulated is shown below as follows:

(a) The solitary valid recommendation by Harris (2004) was that of constructing a similar apparatus with *much thinner walls* coupled with the diminution of the *operating pressure limit*. As discussed above, the large heat capacity of the large bulk of stainless steel adversely affects the attainment of an internal thermal equilibrium, produces a very poor thermal response of the VLE apparatus as a function of heat input (in determining the "plateau region") and makes the general operation of the apparatus a very time-consuming procedure (start-up procedures, equilibrium times, *etc.*). After an examination of trends in the field of VLE measurement for subcritical components coupled with the VLE requirements of industrial concerns, the feasible maximum operating pressure and temperature limits for the apparatus was considered as being 1 MPa and 600 K, respectively.

The idea of Harris to use the "screw-type" design for the reboiler and equilibrium chamber designs was not feasible, as was discussed above. The use of flanges and gaskets, especially with the optimal sealing properties and resilience of graphite-based gaskets, was considered as the optimal choice. The latter arrangement would facilitate the servicing (disassembly) of the equipment, as for an apparatus in its tentative developmental stages, frequent disassembly and reassembly of the apparatus should be anticipated in the modifying of the apparatus to obtain an optimal performance

(b) The exclusion of any *mechanically agitation* in the design of the VLE apparatus of Harris severely compromised the quality of the data acquired due to the probable occurrence of non-equilibrium vapourization or flashing due to improper mixing of the phases in the reboiler. This of course had manifested in the temperature fluctuations (which were also contributed to by the quite large heat capacity of the large mass of 316 SS) and the erroneous vapour phase compositions.

It is quite inexplicable that no consideration was given to the above in the design stage or in the later stages of the operation and troubleshooting of the VLE apparatus. As alluded to earlier, the incorporation of a magnetically coupled stirrer in the apparatus would have proven to be quite a difficult task due to the impermeability of a magnetic flux through such a large thickness of stainless steel and due to the design of the housing for the cartridge heater insert in the reboiler,

as shown in Figure 4.3. Although the latter arrangement is probably the most optimal in this type of design (as would be reproduced in the novel apparatus), the protrusion of the cartridge heater wires from the base of the reboiler further increases the difficulty of incorporating any magnetic coupling in close proximity to the base of the reboiler. The use of a direct drive stirrer in a sealed vessel is not feasible due the concerns over leaks. However, despite the above, the incorporation of a magnetically coupled stirrer was deemed as an indispensable addition to the novel apparatus and initial considerations for the incorporation of the stirrer revolved around the incorporation of a stirring mechanism on a stainless steel ball bearing or ceramic bush around the heater cartridge "finger-like" cavity in the reboiler.

(c) The incorporation of *transparent sections* in key strategic positions in a VLE apparatus facilitates the operation and monitoring of the establishment of equilibrium in the apparatus. The complete lack of any transparency in the apparatus of Harris created a great deal of uncertainty with regards to the optimal amount of material to be charged to the still to sustain the recirculation train, the efficiency and continuity of the vapour-liquid mixture transported up the Cottrell tube as a function of temperature, the occurrence of any backflow in the return lines (and into the sample traps) and the general fluid flow characteristics of the system as an approach to the equilibrium condition (rate of circulation or drop count). With the necessity of the incorporation of transparent sections to aid with the above, especially for the Cottrell tube and re-designed sample traps, it was anticipated the operating pressure limit of the apparatus would be reduced.

(d) In the design of the *sample traps*, provisions should be made to ensure that observation of the nature of the flow of the phases (drop count, backflow into the traps, *etc.*) is possible coupled with magnetic stirring and appropriate sampling provisions (a septum nut and a septum). In the design of Harris (2004), the use of the sampling loops did not allow for the above and were unsatisfactory. An overflow weir-type design as for the glass still of Raal (Raal and Muhlbauer, 1998) ensures that a small amount of the material is contained (in a dynamic state) in the sample trap and is mixed constantly to dissipate any concentration gradients. However, unlike the VLE design of Raal, this design would be duplicated for the both the liquid and vapour phases. In the design of the traps for elevated pressure, a stainless steel flanged body with a glass housing insert would have to be used, wherein a Teflon® stirrer bar would be contained. Teflon® discs and Viton® o-rings would be used to seal the entire unit. The latter would be coupled to an external magnetic field. As in the design of Raal, pressure equalization would be incorporated across the traps to ensure that fluid pressure buildup did not occur in the sample trap. The use of Teflon® and Viton® necessitated the monitoring of the temperature of the sample traps and provisions were made for this.

(e) The use of *temperature sensors* in the key sections of the apparatus, in addition to the equilibrium temperature obtained from the packed section, should be employed to ensure that the thermal profile of the operational areas can be effectively monitored. The use of a temperature sensor in the reboiler would have allowed for the effective monitoring of the temperature of the reboiler contents as a function of the energy input into the internal and external heaters from the variable-voltage transformers. In this way, the onset of boiling of the mixture and hence the optimal amount of energy input to sustain boiling can be determined by monitoring the temperature of the reboiler. In this way, for an apparatus with a poor thermal response to energy input, monitoring of the reboiler temperature ensures that too much heat is not added to early to prevent the superheating of the mixture.

Also, for the equilibrium chamber, where an external heater is required for the pre-heating of the main body, the use of a temperature sensor in the latter would be most advantageous to ensure that no excessive heating of the equilibrium chamber occurs. A strategy that has been used frequently has been to maintain the equilibrium chamber a few Kelvins above the equilibrium temperature. Pt-100 temperature sensors of the appropriate dimensions would be incorporated in the above-mentioned sections in the novel VLE apparatus to provide the advantages mentioned above. Temperature sensors would also be used in the return line, as providing feedback to the temperature controller unit, as discussed in **(f)**.

(f) The design of the *return lines* in the apparatus of Harris was another serious design flaw. The vapour condensate and liquid lines should be combined into a single line a fair distance away from re-entry into the reboiler to allow for some premixing of the phases to occur.

The return line was temperature-controlled in the original design of Harris with a CN-40 digital temperature controller unit and this was incorporated into the new design, however, the design of the temperature control system would have to be to be altered. Ideally there should be no heating of the return line near the vicinity of the sample traps, as this promotes backflow, which is also caused by excessive heating of the return lines.

(g) The cooling of *liquid and vapour condensate streams* would be a necessary feature due to the sealing materials used in the sample traps *i.e.* Teflon® and Viton®. The sections of the liquid and vapour condensate return lines before the sample traps would be jacketed to allow for the flow of the coolant fluid.

(h) The *pressure stabilization system* would have to be improved together with the implementation of the necessary *safety measures*. As mentioned previously, the insufficient volume of the ~ 3 liter 316 SS ballast vessel used by Harris (2004) is quite ineffective for smoothing or dampening inherent pressure fluctuations for a dynamic VLE still.

A much larger vessel (to be used at higher pressures) with a ballast volume of at least 50 liters would be effective. Safety measures are necessary in the event of the overpressurization of the apparatus, which would be connected to a high-pressure gas cylinder for superatmospheric operations.

4.3.1 Design and construction of the apparatus of Reddy

A schematic of the final design of the vapour-liquid equilibrium still is shown in Figure 4.22; for clarity the data acquisition/control, pressure stabilization and cooling/condensing systems have been shown separately as the auxiliary features in Figure 4.23. A detailed presentation of the features of the principal sections of the apparatus has been deferred to a later separate discussion on the respective section.
As in the treatment of the apparatus of Harris (2004), the discussion of the novel apparatus will feature individual treatments for the principal and auxiliary sections of the apparatus.

4.3.1.1 The Reboiler

The design of the reboiler was principally guided by the objectives of boiling of the reboiler contents in the recirculation train both smoothly and rapidly in a very controlled fashion with minimal superheating of the vapour-liquid mixture. In addition to the optimal design of the main body of the reboiler, the incorporation of novel features would be necessitated to achieve this.

A comparison of the reboiler developed in this study with the design of Harris (2004), shown in Photograph 4.1, immediately reveals the considerable diminution of the bulk of 316 SS in the design of the former, in terms of the thinner walls and flanges, together with the overall size of the reboiler. Of course, the reduced wall thickness results in a reduced pressure capacity and the dimensions of the reboiler constructed in this study were rated for a safe working pressure of 1 MPa.

The detailed schematic diagram of the design of the reboiler is shown in Figure 4.24. The bolts have been omitted for clarity in favour of the more important aspects of the design. The reboiler was machined from 316 SS monobloc in the form of an upper and lower flanged section. The sealing of the upper and lower flanges of the reboiler was achieved with eight 6 mm bolts and the 316 SS reinforced graphite gasket, where the rigidity of the 316 SS would complement the excellent sealing properties of the graphite (resilience, compressibility, *etc.*).

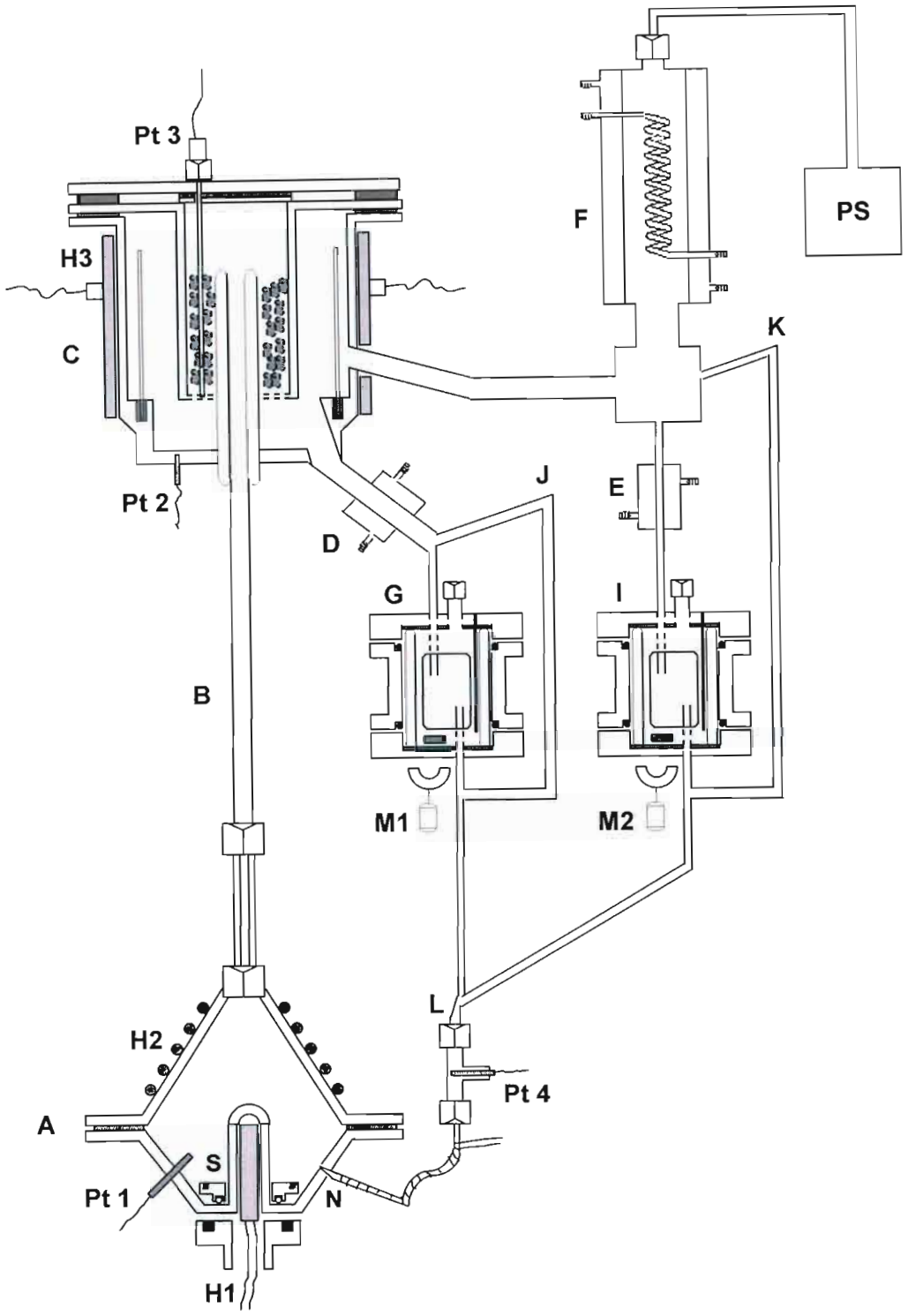

Figure 4.22. The VLE apparatus of Reddy: **A**, reboiler; **B**, Cottrell tube; **C**, equilibrium chamber; **D**, liquid cooler; **E**, vapour condensate cooler; **F**, condenser; **G**, liquid sample trap; **H1**, **H2**, **H3**; heaters; **I**, vapour condensate sample trap; **J**, liquid trap pressure equalizer tube; **K**, vapour condensate sample trap equalizer tube; **L**, return line union; **N**, capillary; **M1**,**M2**, motor-shaft mounted magnets; **PS**, pressure stabilization system; **Pt1**, **Pt2**, **Pt3**, **Pt4**, platinum temperature resistors; **S**, reboiler stirrer.

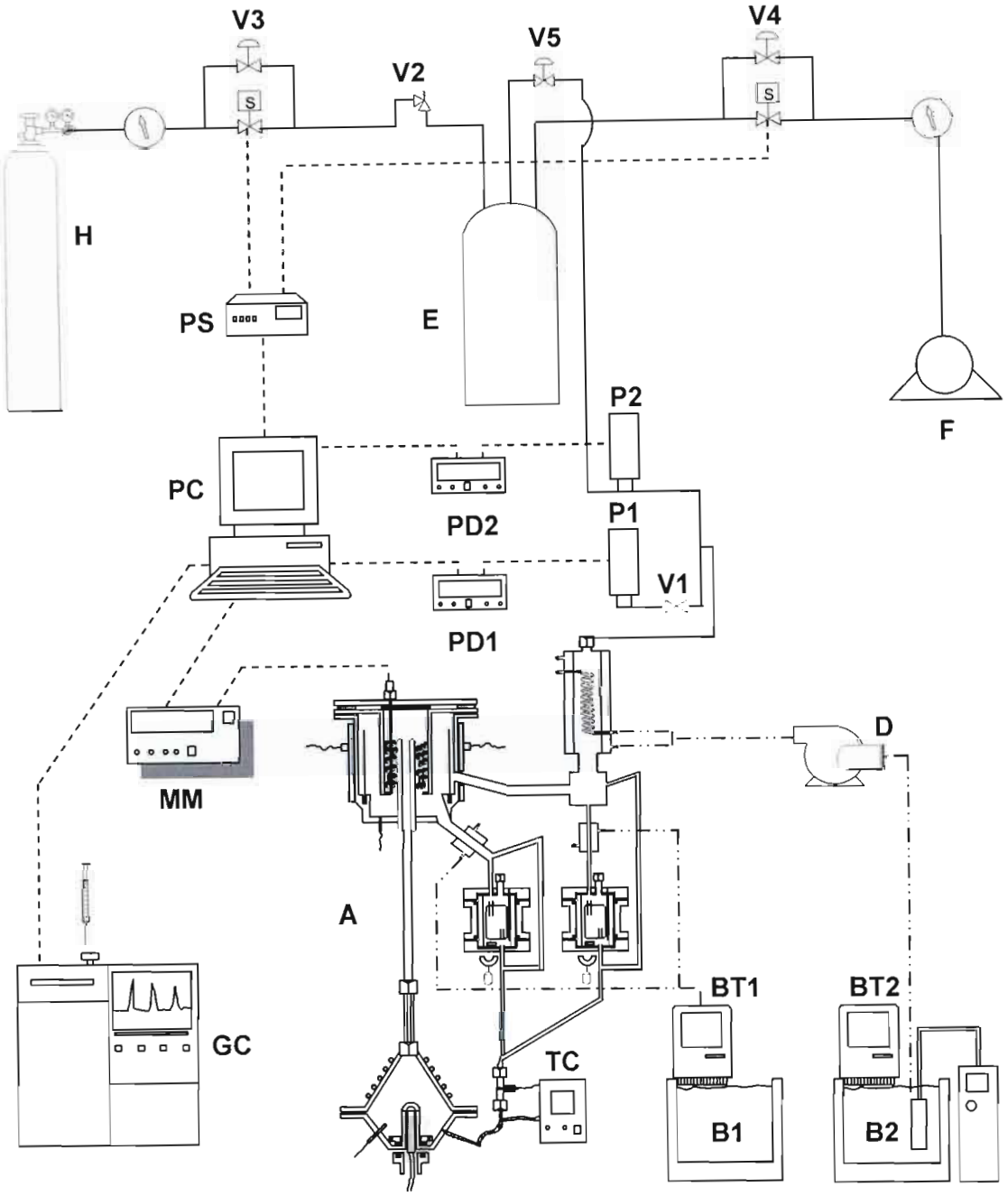

Figure 4.23. Auxiliary features of the apparatus of Reddy: **A**, VLE still; **B1,B2**, water baths; **BT1**, **BT2**, thermostats/circulator pumps; **C**, refrigeration apparatus; **D**, coolant fluid pump; **E**, ballast tank; **F**, vacuum pump; **GC**, gas chromatograph; **H**, gas cylinder; **MM**, multimeter; **P1**, pressure transmitter (Wika); **P2**, pressure transducer (Sensotec); **PC**, personal computer; **PD1**, **PD2**, pressure displays; **PS**, power supply unit; **TC**, temperature controller; **V1**, shut-off valve; **V2**, safety relief valve; **V3,V4,V5**, control valves; .....electronic lines; _ . . _ . .water lines; _____ pneumatic lines.

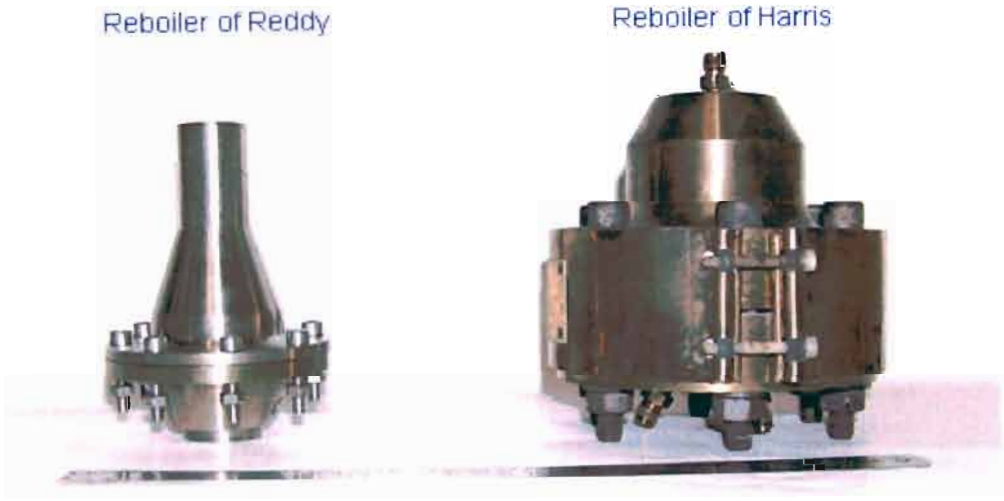

Photograph 4.1. Comparison of the reboilers of Reddy (2006) and Harris (2004).

The custom-made graphite gasket was supplied by James Walker SA. The SS tubing of various dimensions (1/8 inch, 3/16 inch , 1/4 inch and 3/8 inch OD) used for the pressure lines in the apparatus and auxiliary sections were supplied by East Coast Instrumentation. Swagelok® 316 SS tube fittings were used with the latter and were supplied by Johannesburg Valve and Fitting Co.

Special considerations were necessitated for the machining of the interior of the reboiler to allow for a smooth and edge-free interior, as shown for the upper flange in Photograph 4.2. This would serve to facilitate the smooth boiling and uninterrupted flow of the reboiler contents (by negating any eddies or turbulent flow patterns) through the upper flange of the reboiler and into the Cottrell tube. In this way, the excellent flow dynamics within the reboiler would minimize the adverse effects of turbulent boiling on pressure and temperature control and would also serve to facilitate the attainment of equilibrium.

The lower flange of the reboiler, as with the upper flange, was machined with great care to ensure that a smooth interior would be obtained. The critical features in the construction of the lower flange were the machining of the heater cartridge insert, the design of the inlets for the drain/fill valve and the return line, the provisions for the incorporation of a temperature sensor and the design of the reboiler stirrer and associated drive system.

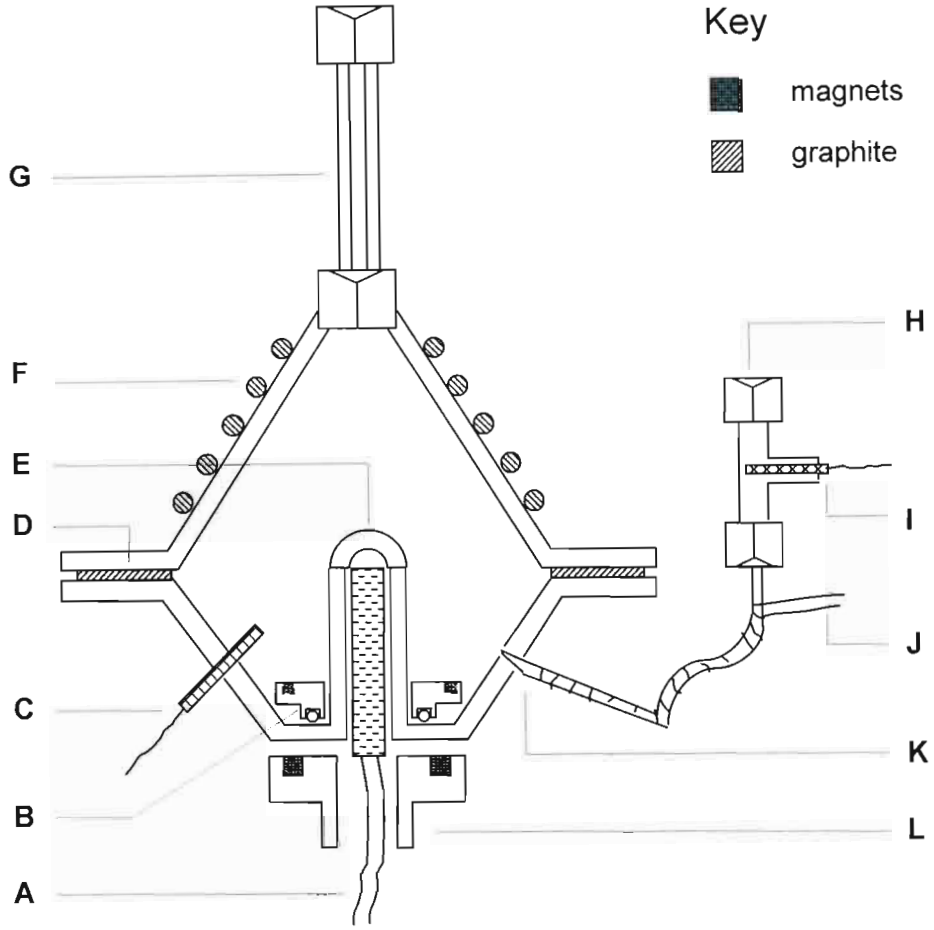

Figure 4.24. Schematic of the reboiler of Reddy: **A**, heater cartridge internal heater; **B**, reboiler stirrer; **C**, reboiler Pt-100; **D**, graphite gasket; **E**, heater cartridge cavity; **F**, Supernozzle external heater; **G**, glass insert in Cottrell tube; **H**, return line union; **I**, return line Pt-100; **J**, return line heating; **K**, capillary; **L**, indirect drive pulley system.

The design of the heater cartridge cavity to achieve a central position in the reboiler is an effective design and was borrowed from the VLE still designs of Brown (1952), Ellis (1952), Rogalski and Malanowski (1980), Wiesniewska *et al.* (1993), Hiaki *et al.* (1994) and Harris (2004). In this design, the transfer of heat to the bulk of the fluid is achieved quite rapidly and efficiently from the internal heater. To facilitate the creation of nucleation sites for steady boiling, the surface of the reboiler heater cartridge cavity was roughened or "activated" to disrupt the surface energy of the molecules *i.e.* surface tension. This is of course, analogous to the strategy of early researchers such as Swietolawski (1945) who employed the use of sintered powdered glass to achieve this effect. The roughened surface of the cavity is shown in Photograph 4.3 and was achieved by recessing grooves or threading the exterior of the heater cartridge cavity.

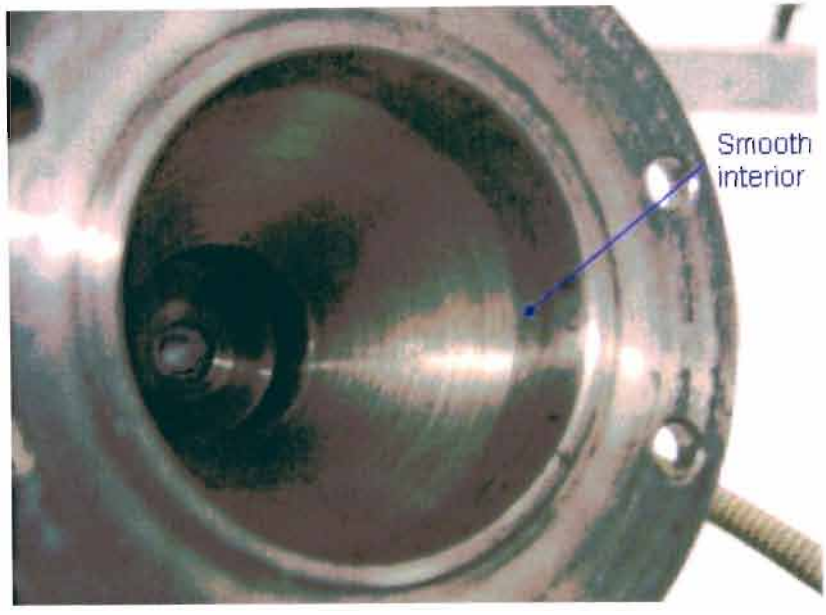

Photograph 4.2. The smooth interior of the reboiler upper flange.

The heater cartridge cavity was machined in accordance with a fixed wall thickness (1.5 mm) and the safe dimensions for a 250 W standard cartridge heater *i.e.* 12 mm x 60 mm (OD x length), as supplied by Kaytherm. The heater cartridge was fitted into the cavity in the lower flange of the reboiler, as shown in Photograph 4.4, to give a tight fit.

A combination drain/fill valve was used in the design to avoid the incorporation of any redundant features in a very compact reboiler design and the inlet for the latter was positioned at the side of the base of the reboiler lower flange (see Photograph 4.4). This was chosen as an optimal position for the latter to minimize the effects of dead volume or any stagnant concentration spaces in the operation of the apparatus. Due to the high temperatures that are usually generated in the reboiler, a suitable valve had to be chosen to withstand elevated temperatures and also for resistance to any form of chemical attack. A Nupro® severe service screwed bonnet needle valve (Model: SS-2JBR-HT-BG) was selected as the valve consisted of a Grafoil® packing material and had a temperature rating of 588 K.

The design of the return line inlet ensured that the returning phases in the return line would enter at the side as opposed to entry at the base, as for the design of Harris (2004) which was discussed previously. A capillary section (with the ID of a 3/16 inch standard tube) was machined in the return line tube for the re-entry of the phases into the reboiler to minimize any backflow and to smooth the return flow of the mixed streams back into the reboiler *i.e.* to avoid turbulence, which would contribute to uneven boiling. Preliminary tests were conducted in the

workshop prior to the final assembly of the apparatus to ensure that the sizing of the inlet was optimal and did not hinder the return flow into the reboiler to an extent that was much too large.

The incorporation of a temperature sensor in the reboiler is an extremely useful addition as it allows for the thermal response of the system to be monitored as a function of the energy input from the variable-voltage resistors. For this purpose, a class A Pt-100, as supplied by Temperature Controls, was fitted in the side of the lower flange of the reboiler. The termination head of the Pt-100 sensor was insulated with glass wool tape around a layer of a graphite winding. The relative positions of these inlets are shown in Photographs 4.4 and 4.5.

Perhaps the most innovative feature of the design of the reboiler has been that of the stirrer. The apparent difficulties in the incorporation of mechanical agitation were as a result of the design of the heater cartridge cavity, protrusion of the heater cartridge wires from the base of the reboiler and the relative impermeability of an external magnetic field through stainless steel. From an inspection of the design of the reboiler lower flange, the most apparent option for a stirrer is to employ a bush or ball bearing around the heater cartridge, around which the stirrer body can be fixed. However, after consultation with both local and national suppliers, ball bearings of suitable dimensions or temperature capabilities could not be sourced. Secondly, the use of a bush made from a suitable material such as a ceramic material was considered, however, difficulties in sourcing a bush of the correct dimensions and cutting the ceramic materials were experienced. A more feasible option than the first two was to use an open race of 316 SS 3 mm balls, sourced from Bearing Man, upon which a machined 316 SS stirrer could spin. This is shown in Photograph 4.6 and the 316 SS machined ball race is shown in Photograph 4.3.

The problem of a weak magnetic field available to a magnetic section in the stirrer body with conventional ferromagnetic materials such as soft-iron cores, for magnetically coupled stirring had to be addressed prior to the design and the machining of the stirrer body. The use of alternative and stronger magnetizing materials had to be investigated. The commercial availability of rare-earth magnets, which can have a magnetic force field that has an attractive power 1000 times their weight, has seen the use of these magnets in a variety of applications (Lee Valley Tools, 2006). In particular, the neodymium-iron-boron (NdFeB) rare-earth magnets have indeed found widespread popularity and were used in this study. The use of the rare-earth magnets was an integral part of the success of the magnetically coupled stirring system.

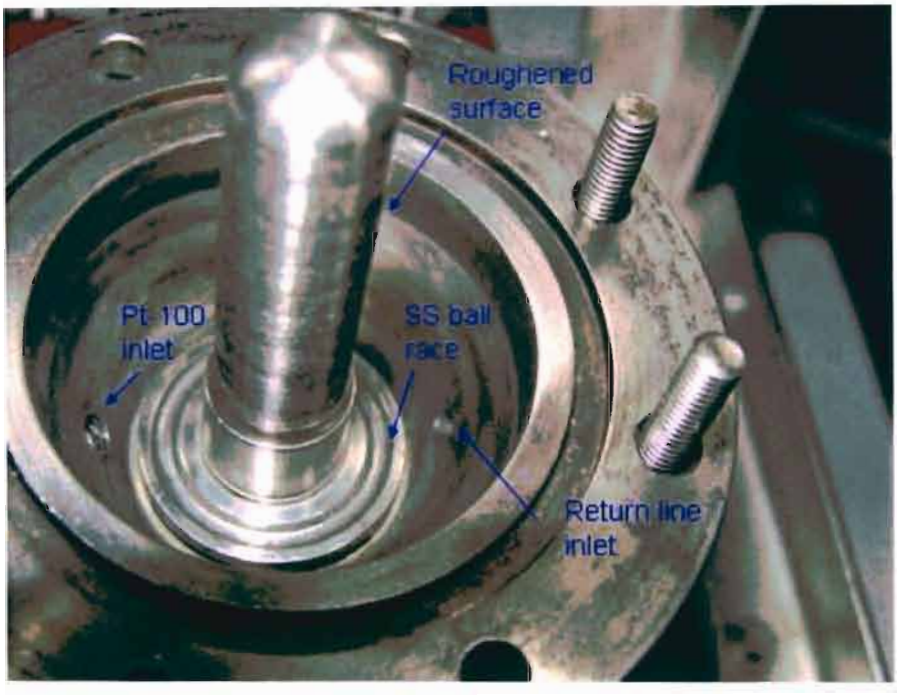

Photograph 4.3.The roughened surface of the reboiler heater cartridge cavity.

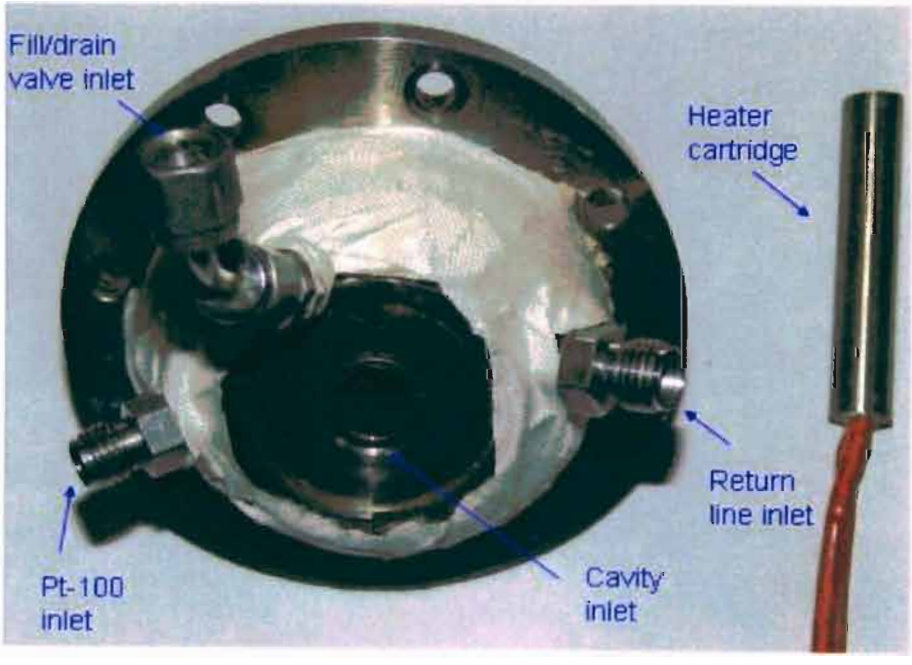

Photograph 4.4.The heater cartridge and cavity inlet in the lower flange of the reboiler.

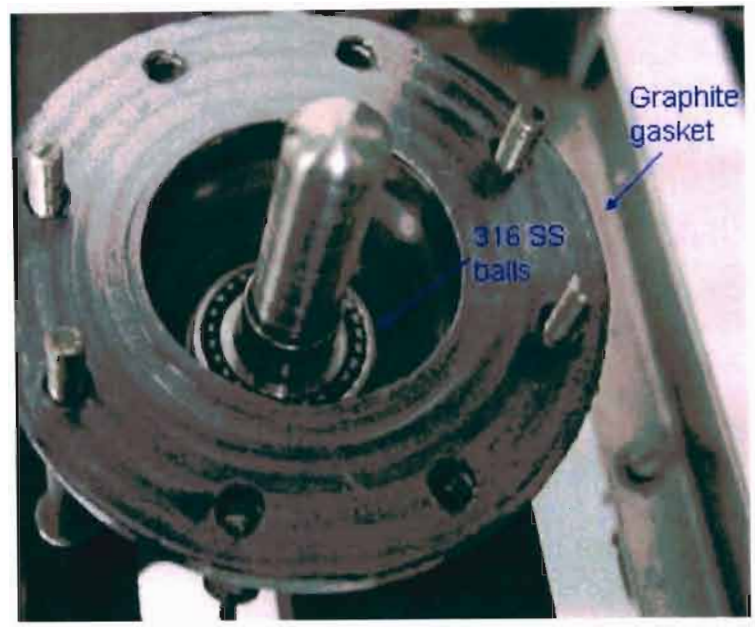

Photograph 4.5. The 316 SS open ball race for the reboiler stirrer.

The stirrer body was machined from 316 SS and is shown in Figure 4.6. It has been altered from an earlier design, where the use of large impellers had resulted in an improper operation of the reboiler. This was due to irregular mechanical agitation, even at low motor speeds, which resulted in large vortices being created and the reboiler contents being pushed away from the central internal heater, which produced thermal gradients and uneven boiling.

The design of the stirrer was optimized to ensure that adequate mixing of the reboiler contents occurred. Grooves were recessed into the body of the stirrer to allow for effective mixing together with the impellers, in which rare-earth magnets were encapsulated. With the bipolar arrangement of the magnets, a more effective magnetic coupling of the stirrer would be achieved. A 316 SS race was machined in the base of the stirrer body, analogous to the SS ball race in Photograph 4.3, to improve the smoothness of the stirring motion. The dimensions of the 316 SS stirrer were critical to ensure that there was no contact between any part of the stirrer body and the Pt-100 sensor that was fitted in the side of the lower flange, as shown in Photograph 4.7. The next problem to be addressed was how to couple the magnetized stirrer body to an external rotating magnetic field. Due to the protrusion of the heater cartridge wires directly below the reboiler cavity, a magnet mounted on a motor shaft could not be directly placed underneath the reboiler. Consequently, an indirect drive pulley system had to be designed. The first component sourced was that of a MAXON 12V DC geared motor, as supplied by Accutech Automation.

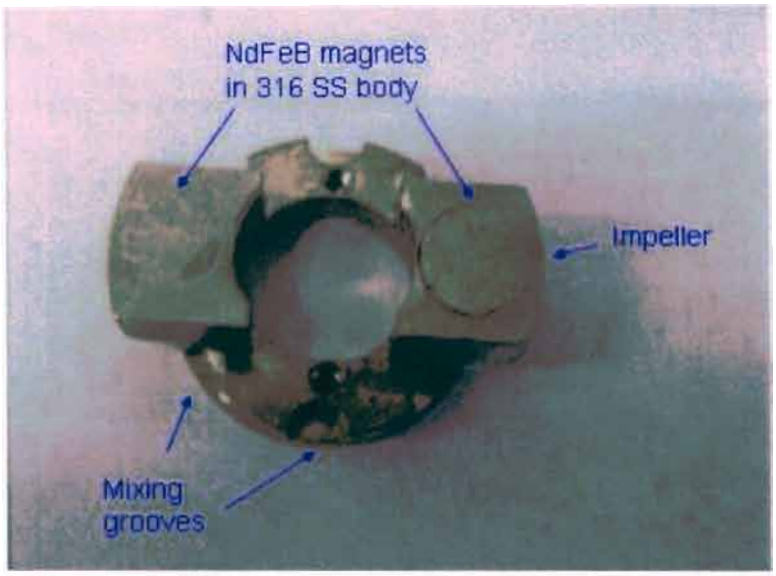

Photograph 4.6. The final design of the reboiler internal stirrer.

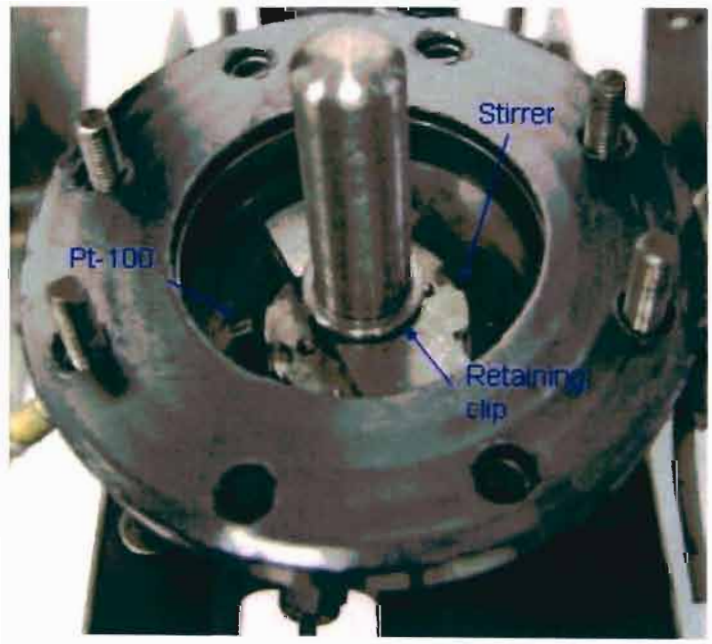

Photograph 4.7. The fitting of the reboiler internal stirrer.

The use of a geared motor ensures that high torque is achievable in a very controlled fashion, which is crucial for steady stirring of the reboiler contents to avoid any bumping or turbulence. The body of the stirring base and the shaft was fabricated from Bakelite®, a material that has shown to exhibit good insulating properties, a consideration that was necessitated in the event of high-temperature operation and the transfer of heat from the reboiler (by convection) to the pulley system body.

The shaft was encapsulated with the rare-earth magnets in a bipolar arrangement, as for the internal stirrer and was hollow to allow for the passage of the heater cartridge wires so that the rotational motion of the shaft was unhindered. The shaft was attached to a ball bearing to allow for the free movement of the shaft in the pulley body. The above features of the indirect drive pulley system are shown in Photograph 4.8. As a result of the bipolar arrangement of both the internal magnetic stirrer and the magnetically coupled shaft, the disturbance of the open ball race by magnetic repulsion effects (any temporary alignment of poles possibly during start-up) had to be negated. This was achieved by press-fitting a retaining clip just above the top of the stirrer (shown in Photograph 4.7) to ensure that any magnetic repulsion did not manifest in a significant disturbance of the stirrer and ball race.

The pulley on the motor shaft was machined from aluminum to ensure lightness in construction for easier movement and was coupled to the base of the Bakelite® pulley shaft by a 65 mm o-ring band. A 12 V DC power supply (Model: GP 30-5) was used to drive the MAXON motor. The above features are shown in the underside of the pulley system in Photograph 4.9.

The final aspect of the design of the reboiler was the external heater. The upper flanged section of the reboiler would serve as a suitable mounting for an external heater as there was no available space on an already crowded lower flange (return line, Pt-100 sensor, heater cartridge, drain/fill valve, *etc.*). Additionally, the cone shape of the upper flange would be suitable for accommodating a heating coil. A 900 W Supernozzle heater was custom-made by Resistohm for the apparatus since the use of nichrome windings around a cone shape at high input voltages is not a safe practice.

The Supernozzle heater was encased with refractory cement, shown in Photograph 4.10, to negate heat losses from the reboiler and for more efficiency in energy utilization. To negate the loss of heat from the lower flange, this section was insulated with a layer of graphite and a wrapping of glass wool tape, as shown on the exterior of the lower flange in Photograph 4.4.

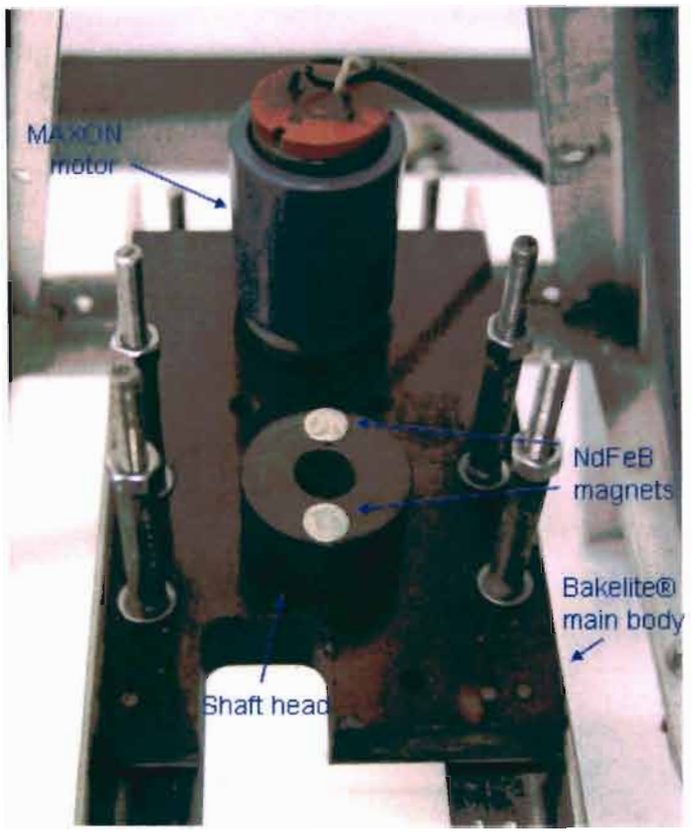

Photograph 4.8. The top section of the indirect drive pulley system.

Photograph 4.9. The bottom section of the indirect drive pulley system.

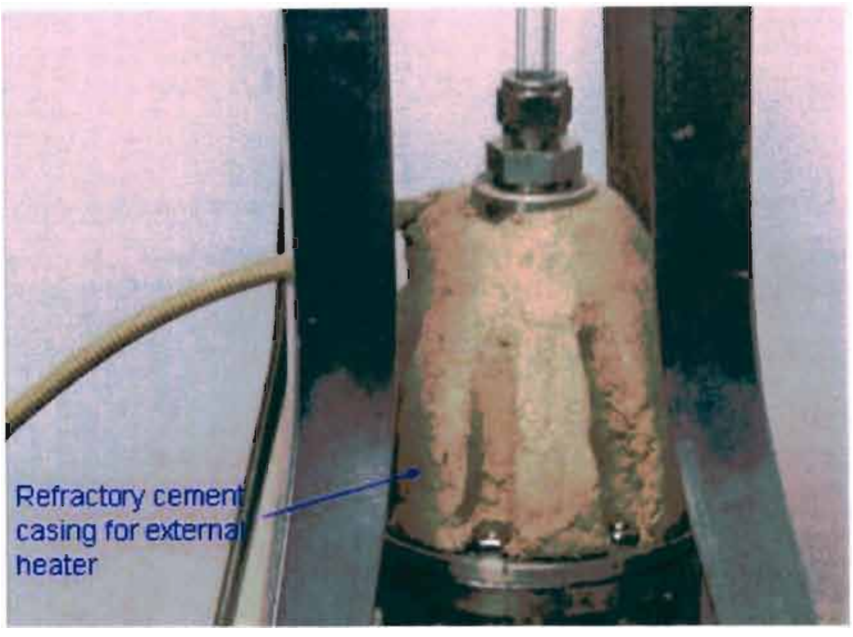

Photograph 4.10. Refractory cement casing for the external heater.

The design of the reboiler ensured that the heating duties of the internal and external heaters could be optimized by monitoring the temperature in the reboiler. In this way, slow heating of the reboiler contents by introducing small increments of energy input into the heaters ensured that minimal superheating of the system occurred. In addition, the incorporation of the magnetically coupled stirrer ensured the dissipation of any concentration gradients to minimize flashing and superheating, together with the use of a capillary section and the roughened surface of the internal heater cavity. With the above innovative features in the reboiler design, the many criticisms of the operation of a dynamic recirculating apparatus with regards to reboiler-related effects were hoped to have been addressed.

4.3.1.2 The Cottrell tube

The lack of transparency of the fluid flow behaviour in a VLE apparatus, especially in key sections, can render the operation of the still as being quite a challenging task. This was evident in the equipment of Harris, where numerous uncertainties relating to the optimal amount of liquid to charge to the still and with regards to the proper or continuous operation of the still had plagued the researcher. The Cottrell tube serves as a transport interface for the boiled mixture by the vapour-lift principle and the behaviour of the mixture in this section is an important indicator of the proper operation of the still.

To endow the Cottrell tube with transparency, a Pyrex® borosilicate glass insert was used in conjunction with a section of 316 SS 1/4 inch tube. The glass insert was supplied by a local glassblower and was annealed to reduce vulnerability of the insert to shock or strain-induced breakages. The suitable dimensions of the glass insert were calculated on the basis of the intended pressure range through the use of a formula obtained from the Corning Glass Works technical data on Pyrex® glass, as shown below:

$$P = \frac{13790t}{D} \tag{4.1}$$

where P is the safe working pressure in kPa, t is the wall thickness and D is the outside diameter (same units as t). For a glass insert with a 2.2 mm wall thickness and a 10 mm OD, the safe working pressure is well over 1 MPa.

The use of a glass insert in an otherwise stainless steel tube necessitated special considerations with regards to the selection of suitable fittings and seals for the glass-to-metal coupling. Metric-to-fractional Swagelok® tube fittings had to be used due to the metric dimensions of the glass of the fractional inch dimensions of the tubing. Of greater concern was the sealing of the glass insert in the union fitting; conventional 316 SS ferrules could not be used as these were too rigid and would break the glass upon the tightening and sealing of the fitting.
As for most of the sealing applications in this work, the sealing properties of graphite were utilized in preparing custom-made graphite ferrules. The combination of the softness and the sealing properties of graphite made the material suitable for this purpose.

Initially the glass insert was coupled to a rigid section of 316 SS tubing, however, the occurrence of frequent breakages of the glass insert were experienced due the slightest mechanical shock or misalignment of the rigid 1/4 inch stainless steel tubing and the glass insert. To address the above, a Swagelok® 1/4 inch SS flexible hose tube fitting (Model: 321-4-X-2-B2) was sourced from Johannesburg Valve and Fitting Co to endow some flexibility to the tube by buffering any mechanical disturbance of the glass insert. This is shown in Photograph 4.11. Unfortunately, the maximum pressure rating of the flexible hose fitting was 750 kPa, which meant a reduction of the pressure capacity of the equipment from an initial working pressure limit of 1 MPa.
For the safe operation of the equipment at elevated pressures, Plexiglass® shields (not shown) were used around the open sections of Cottrell tube in the event of a glass breakage under pressure.

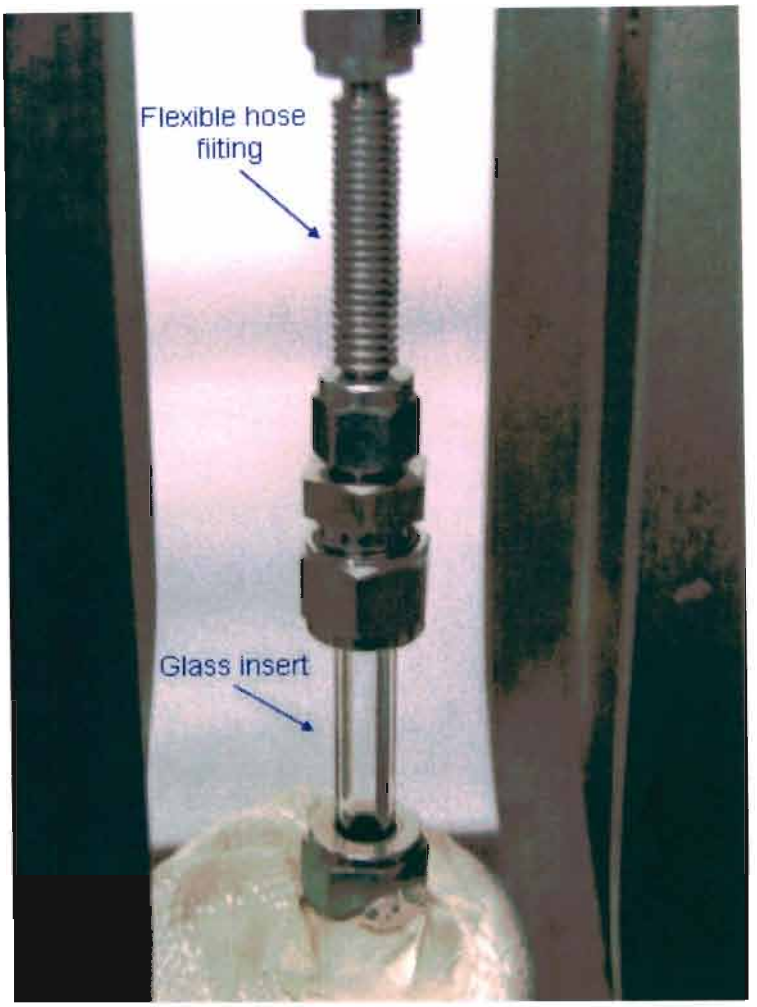

Photograph 4.11. The Cottrell tube.

4.3.1.3 The Equilibrium chamber

There were less novel modifications necessitated in the design of the equilibrium chamber when compared to the considerable expenditure of effort for the design of the reboiler. However, there are many crucial design factors inherent in the general design of an equilibrium chamber such as the external heating of the equilibrium chamber, the design and insulation of the packed section and the location and fitting of the temperature sensor/s. A common starting point, as for the discussion of the reboiler, is the comparison of the equilibrium chamber in this study with that of Harris (2004), as shown in Photograph 4.12. Analogous conclusions can be drawn from the comparison of the reboilers *i.e.* the diminution of the overall size and bulk of the respective section.

Photograph 4.12. Comparison of the equilibrium chambers of Reddy (2006) and Harris (2004).

The schematic diagram for the equilibrium chamber of Reddy is shown in Figure 4.25. The bolts have been omitted in favour of the more important aspects of the design. The equilibrium chamber consisted of three flanged sections which were sealed with custom-made graphite gaskets and held together by eight 6 mm bolts. The flanged sections are shown in Photograph 4.13. The top flange contains the main Pt-100 sensor for the measurement of the equilibrium temperature, the middle flange is the housing for the packed section and the outermost flange is the main body. The middle flange housed the packed section (where equilibrium occurs) and it was packed with 3 mm rolled 316 SS wire mesh cylinders to a level that was just below the top of discharge point of the Cottrell tube. The advantages of using this type of packing have been described in Chapter 2.

As recommended by Raal and Muhlbauer (1998), the temperature sensor was positioned at the base of the packed section, to ensure that the most reliable equilibrium temperature was measured. To assist with proper equilibrium temperature measurements, the temperature sensor was sealed in the Swagelok® fitting in the upper flange with a graphite ferrule instead of a 316 SS ferrule to negate the effect of the temperature of the main body on the temperature sensor. Since graphite is an excellent insulating material, there was minimal thermal contact between the main body and the sensor (as affecting temperature measurements) through the ferrule in the fitting. The use of the softer graphite ferrule would also serve to minimize any damage to the temperature sensor.

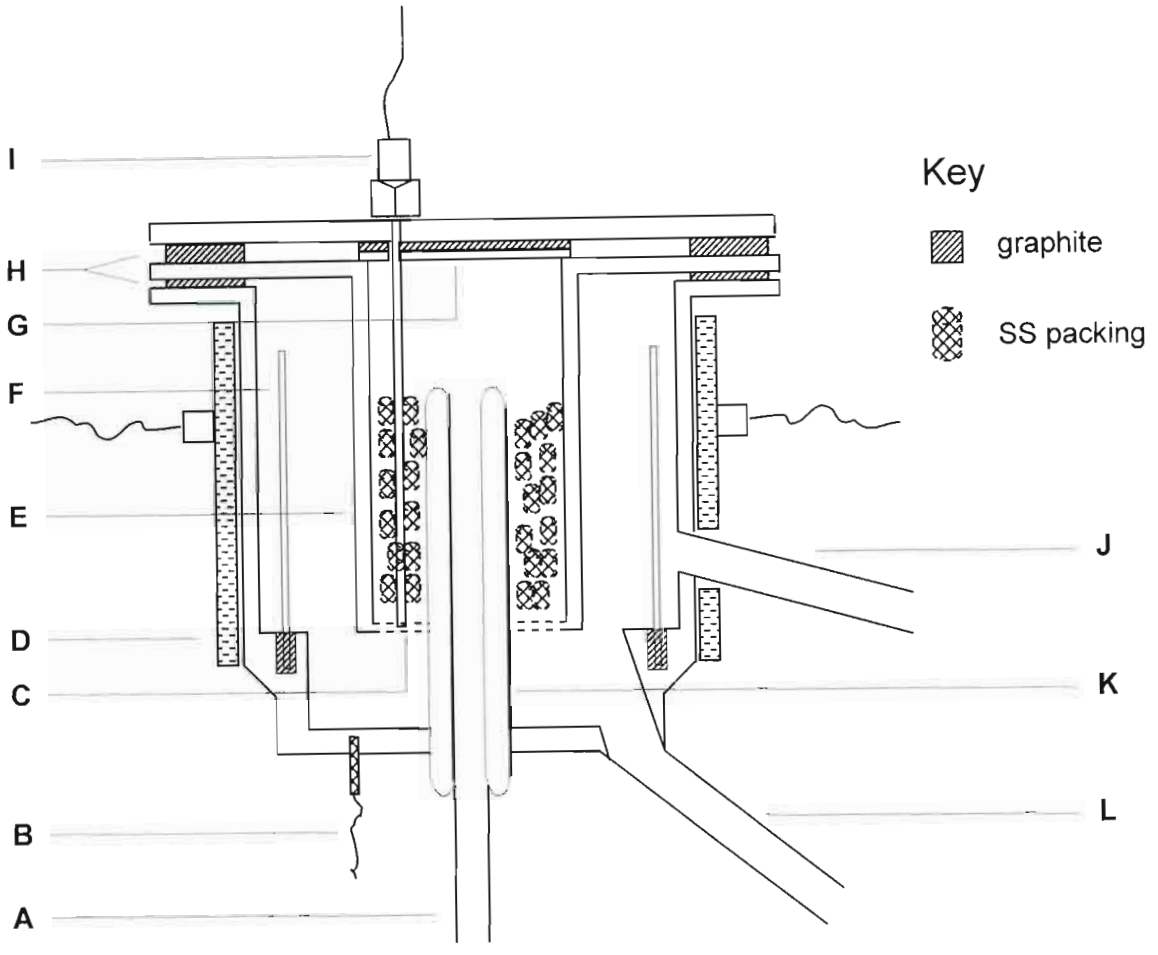

Figure 4.25. Schematic diagram of the equilibrium chamber of Reddy: **A**, Cottrell tube; **B**, main body Pt-100; **C**, drain holes; **D**, split band external heater; **E**, packed section housing; **F**, thin-walled 316 SS concentric tube; **G**, graphite-backed 316 SS disc; **H**, graphite gaskets; **I**, packed section Pt-100 sensor; **J**, vapour take-off tube; **K**, Cottrell tube vacuum jacket; **L**, liquid take-off tube.

The temperature sensor used was a 4-wire 1/10 DIN Pt-100 sensor, supplied by Wika Instruments. The sensor was mineral-insulated and encased in a 1/8 inch 316 SS sheath and the lead wires were insulated with high-temperature fiberglass /SS over-braided flex hose.

The interior of the packed section was insulated with a graphite-layer backing around a press-fitted stainless steel thin-walled tubing and there was also insulation at the top of the packed section in the form of a graphite layer above a 316 SS disc, as shown in Figure 4.25. This arrangement ensured that there was minimal thermal influence of the external environment on the occurrences within the equilibrium section. A uniform distribution of radially-symmetric exit or drain holes (1.5 mm OD) were machined at the base of the packed section for the exit of the phases through the perforations.

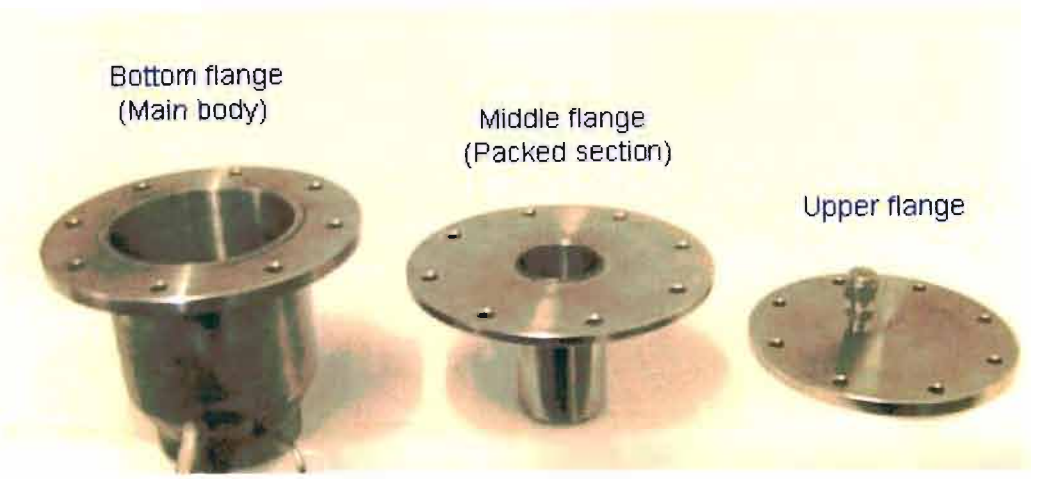

Photograph 4.13. The three flanged sections of the equilibrium chamber.

The main body of the equilibrium chamber was machined to allow for minimal dead volume and the rapid disengagement of the phases upon the attainment of equilibrium. As with the design of Harris, a concentric thin-walled (1 mm) 316 SS tube was used around the packed section so as to minimize liquid drop entrainment in the vapour phase and to ensure that the vapour phase fulfills its thermal lagging function. To isolate the 316 SS tube from thermal contact with the main body, the concentric tube was press-fitted into graphite packing in the main body, as shown in Figure 4.25. For the exit of the phases from the equilibrium chamber, the OD of the exit tubes for the vapour and liquid phases was 3/8 inch (as compared to the 1/4 inch inlet of the Cottrell tube), to minimize any internal pressure gradients due to fluid buildup and for the rapid exit of the phases from the equilibrium chamber.

The external heating of the equilibrium chamber serves to ensure that there are no temperature gradients between the interior of the equilibrium chamber and the external environment and to facilitate the attainment of an internal thermal equilibrium in the main body of the equilibrium chamber. This is important for those cases where insulation material is insufficient or for operation at elevated temperatures. The external heater used in this study was a split band mica heater, where each half had a rating of 500 W. The latter was supplied by Kaytherm. The use of two separate halves was necessitated as a result of the protrusion of the vapour take-off tube in the exterior of the main body (shown in Photograph 4.13). The base of the equilibrium chamber was also insulated from the rest of the apparatus by using a graphite layer as an intermediate between the equilibrium chamber main body and the supporting 316 SS frame, as shown in Photograph 4.14.

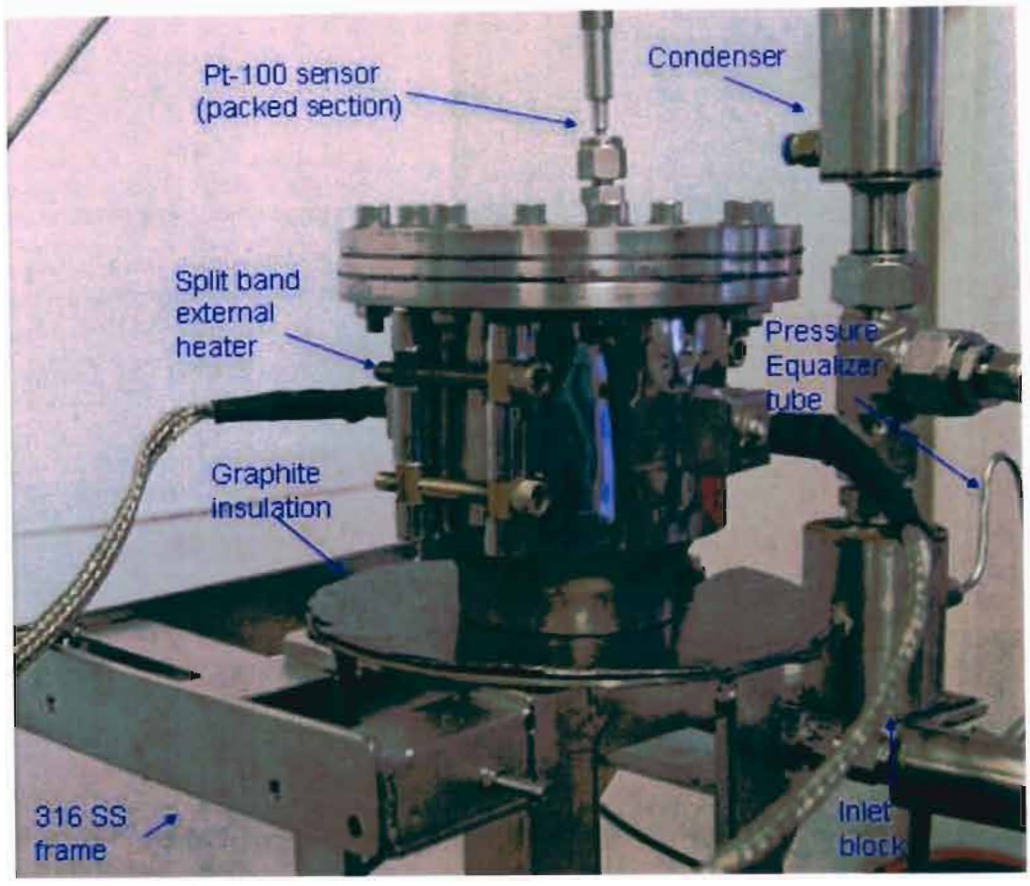

Photograph 4.14. Heating arrangement and external features of the equilibrium chamber.

Judicious control of the heating of the equilibrium chamber is important to ensure proper operation and this necessitates the inclusion of a temperature sensor. In this study, a hole was drilled at the base of the main body of the equilibrium chamber and a class A Pt-100, supplied by Temperature Controls, was press-fitted into the drilled cavity.

4.3.1.4 The Sample traps

In the design of the sample traps, the desirable features of the vapour condensate sample trap of the glass still of Raal (Raal and Muhlbauer, 1998) would be retained in a design that would be suitable for elevated pressures but still retain some transparency. Unlike the design of the glass VLE apparatus of Raal, the same design would be used for the vapour condensate and the liquid sample traps to allow for the advantages of the magnetically stirred overflow-type sample trap design for the sampling of both equilibrium phases.

The design favoured for the sample trap body was that of two outer flanged sections and a middle body, which would serve as the supporting frame for a sight glass section of suitable dimensions. The schematic diagram for the design of the sample traps is shown in Figure 4.26. The drain valve and bolts have been omitted from the diagram in favour of other more important aspects of the design.

The determination of suitable dimensions for the sight glass was the initial step that preceded the design of the 316 SS housing. The formula used in the sizing of the Cottrell tube insert was applied to the sizing of the Pyrex® sight glasses, which were then acquired from a local glassblower. The top flange was fitted with provisions for the inlet of the cooled streams, a sample nut fitting for the sample septum and a thin-walled thermowell, into which Pt-100's could be inserted to monitor the liquid temperature. As can be observed from Figure 4.26, the Pt-100 thermowell was designed such that the sensor would be resident in the liquid sample trapped below the overflow tube to obtain correct temperatures.

The bottom flange featured provisions for a drain valve to drain the sample trap and an exit tube that was welded into the base. These arrangements are shown in Photograph 4.15. The height of this welded tube above the base of the lower flange determined the height and volume of liquid that would remain in a dynamic state in the sample trap. This was a crucial design factor as any excessive holdup of material in any part of the still is undesirable and has to be minimized as this slows down the approach to equilibrium, especially for measurements in the dilute regions. The height of the exit or overflow tube was determined by the length of the syringe needle used for the phase sampling through the sample septum. The contents of both stirrers were stirred with magnetically coupled Teflon® stirrer bars being used in the sample traps.

Pressure equalization was employed across the traps to ensure that there was minimal holdup of the phases exiting the sample traps. As can be observed from Figure 4.22, the pressure equalizer tubes were elevated from the horizontal axis to ensure that no material could enter and possibly block the equalizing tube, as this would result in a pressure drop across the sample trap.
Transverse rectangular windows with smooth edges were cut into the middle flange body to allow for the observation of the fluid flow characteristics in the respective traps.

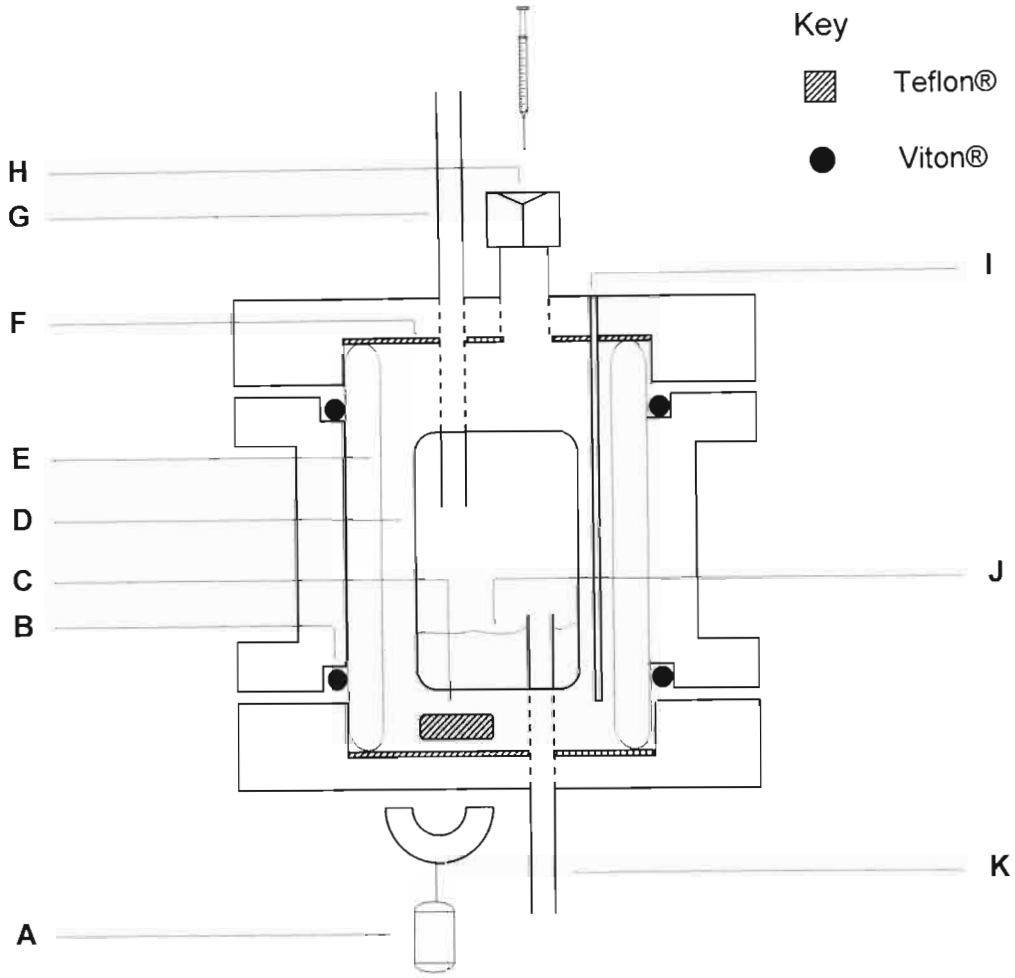

Figure 4.26. Schematic diagram of the sample trap design: **A**, motor-shaft mounted magnet; **B**, o-ring sealing gasket; **C**, stirrer bar; **D**, window; **E**, sight glass insert; **F**; cushioning gasket; **G**, inlet feed tube; **H**, sample septum nut; **I**, Pt-100 thermowell inlet; **J**, "trapped" liquid contents; **K**, exit tube for the overflow.

The sealing of the glass insert in the 316 SS body was another challenging area that required some ingenuity. Firstly, the edges of the glass housing were requested to be fire-polished to ensure a smooth finish, which would ensure better sealing of the sight glass. Thereafter, it was decided to use a cushioning/sealing gasket together with a sealing gasket for the glass insert, where the sealing mechanism would be implemented in the two outer flanges. The cushioning/sealing gasket, used was in the form of Teflon® discs that were embedded in a recessed groove in the upper and lower flanges. The proper sealing of the glass inserts was achieved through the use of Viton® o-rings around the edges of the inserts. The sealing arrangement described above is shown in Photograph 4.16, where the top flange has been removed.

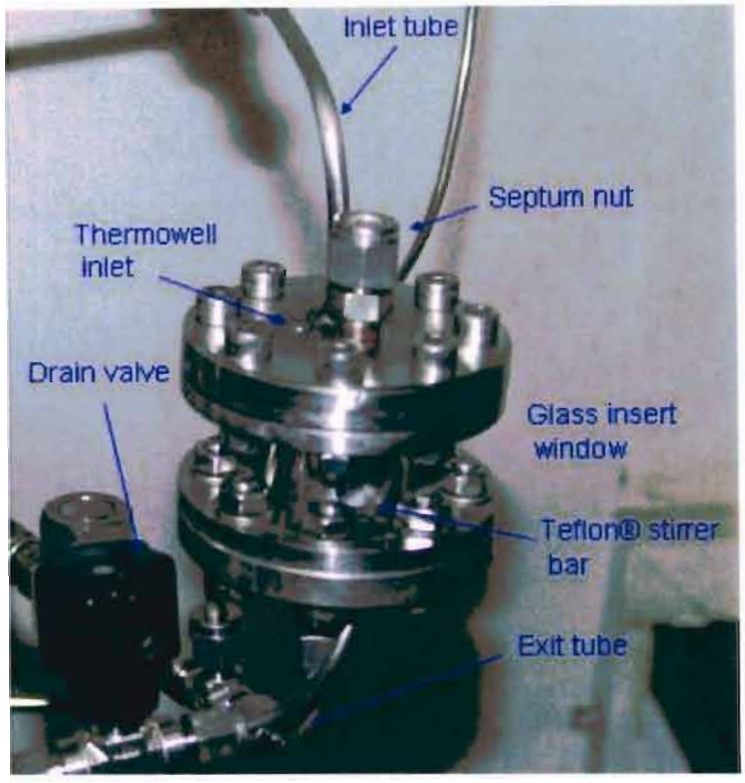

Photograph 4.15. External features of the sample trap design.

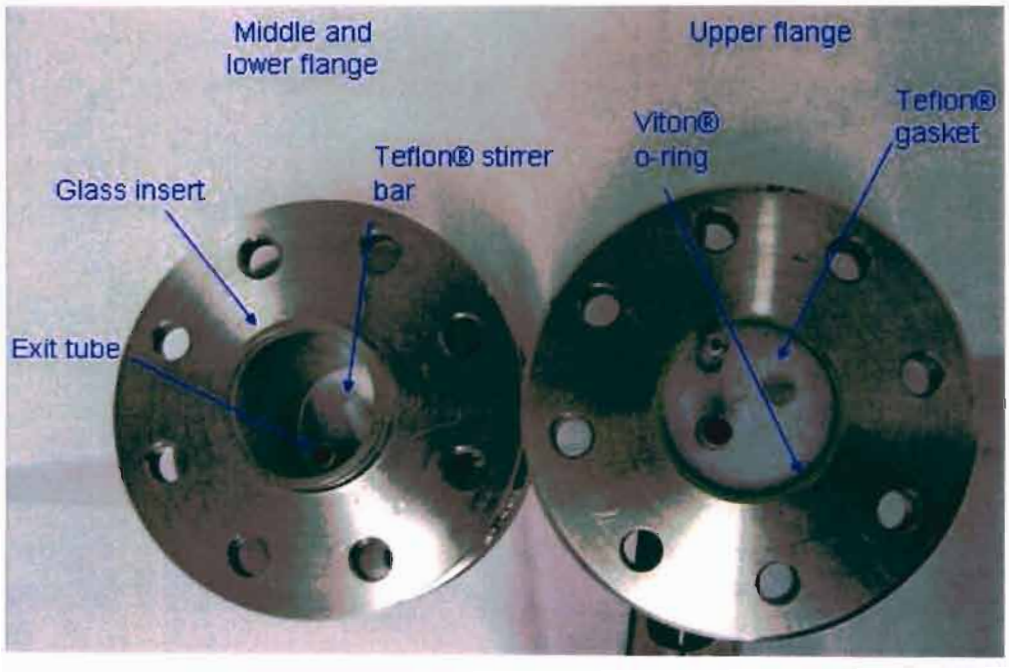

Photograph 4.16. Sealing arrangements for the sight glass in the sample trap.

The flanges were held together by eight 6 mm bolts, where great care had to be exercised in the tightening procedure for the bolts and nuts to ensure proper sealing (sufficient gasket pressure) without any leaks. The traps were essentially the same design except for the pressure equalization arrangements and the drain valves used. The high-temperature Nupro® severe service screwed bonnet needle valve (Model: SS-2JBR-HT-BG) used for the reboiler, was also used for the liquid sample trap. To minimize the costs associated with valve sourcing and since the temperature of the vapour phase is lower than that of the liquid, a lower temperature-rated valve could be used for the vapour condensate sample trap. A Whitey® non-rotating stem valve (Model: SS-ODPS2), with a temperature rating of 493.15 K was sourced from Johannesburg Valve and Fitting Co for this purpose.

The sealing arrangement of the sample traps proved to be remarkable as no leaks were detected in the latter throughout the course of this study. The incorporation of additional features (stirring, temperature monitoring and pressure equalization) also served to improve confidence in obtaining a sample that was representative of the equilibrium composition.

4.3.1.5 The Return line

An effective design for the overall return line is to ensure that the union of the liquid and vapour condensate return lines occurs at a junction which is fair distance away from the entry point for the combined phases into the reboiler. This ensures that there is sufficient premixing of the streams, which in some cases have vastly different compositions, to negate the occurrence of flashing in the reboiler. Ideally the return line should terminate as a capillary section at the entry point in the reboiler to minimize any backflow due to liquid level fluctuations or surges. Novel features that can be incorporated include the use of a temperature-controlled section to preheat the returning streams.

The design of the return line is shown in Photograph 4.17. As can be seen from the diagram, the vapour condensate and liquid return lines are combined into a single line prior to re-entry into the reboiler. After the union of the return lines, entry of the combined stream occurs via the return line entry tube into the reboiler. A temperature control strategy was employed for this section of the return line through the use of a CN-40 temperature controller, supplied by Temperature Controls. The heating of the line was achieved with nichrome wire windings in glass cloth tubing around the respective section (not shown in the diagram).

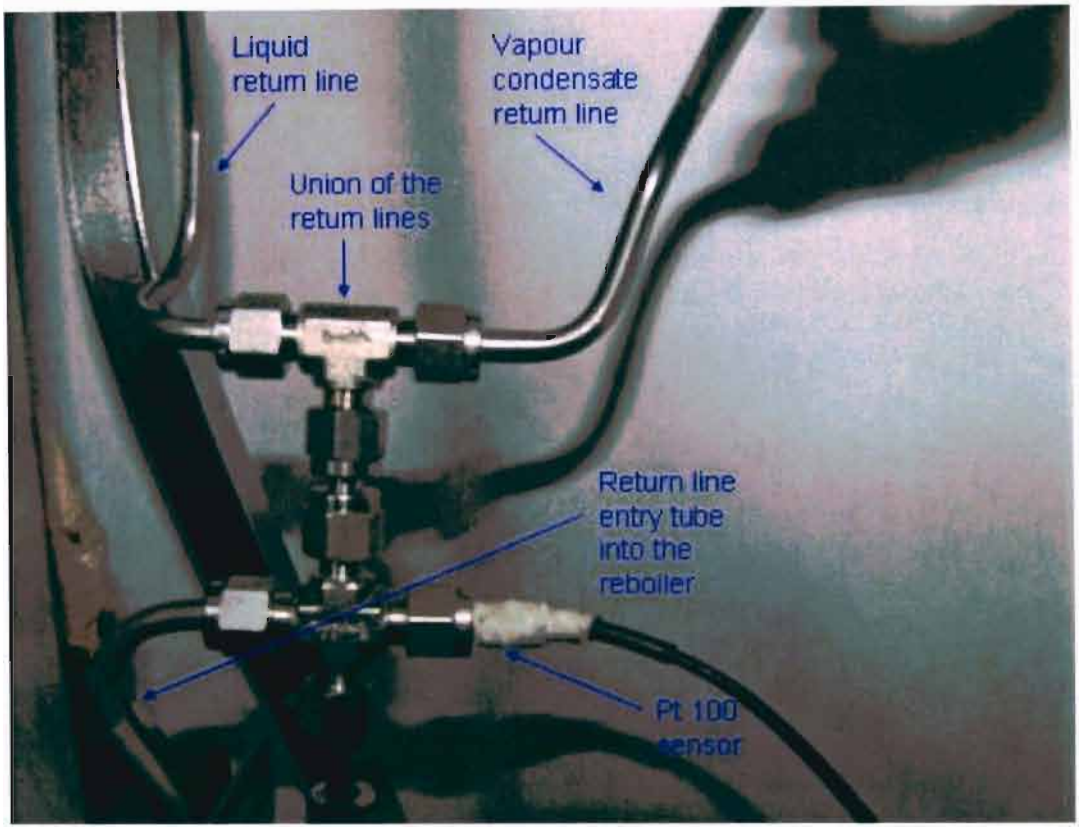

Photograph 4.17. The union of the liquid and vapour condensate return lines.

The setpoint temperature was controlled in conjunction with feedback from a class A Pt-100 sensor which was sourced from Temperature Controls and incorporated into the return line, as shown in Photograph 4.17. As with the reboiler Pt-100 sensor, the termination head of the sensor was insulated with glass wool tape and graphite. The return line entry tube into the reboiler was the most feasible section for which to employ the heating of the return line due to its proximity to the reboiler.

In the operation of the apparatus, the return line design was observed to function quite well with no backflow being observed. However, as mentioned before, this is quite dependent on the heating of the return line, as excessive heating can result in a backflow into the sample traps together with a superheating of the mixture.

4.3.1.6 Cooling and condensing systems

There were no special considerations that were necessitated in the design of the condensing system, as no difficult mixtures with regards to the design of the condensing system (*e.g.* for chemicals that are solid at ambient conditions) were to be studied during the course of the study. Consequently, the same condenser design, as used by Harris (2004), shown in Figure 4.8 was retained. However, it was decided that liquid and vapour condensate cooling jackets would be incorporated in the respective return lines in the likelihood of any future high-temperature studies, which would compromise the integrity of the sample trap sealing materials.

The general layout of the operational features of the cooling and condensing system was presented in Figure 2.23. The coolant feed systems for the cooling and condensing systems were designed to operate independently of one another due to the much colder coolant temperatures required for the latter. Two 22 liter water baths, fitted with Grant thermostats with inbuilt circulator pumps (Model: GD 120) as acquired from Polychem Supplies, were used for this purpose.

For the cooling jackets on the return lines, the circulator pump of the Grant thermostat was used to circulate the coolant fluid (50 % water : 50 % ethylene glycol) at ambient temperatures. However, for the "double effect" condenser, the use of narrow 1/8 inch tubing in the internal coil heat exchanger coupled with the vertical elevation of the condenser above the pump location necessitated a large pump head or capacity to overcome the large pressure drop in the narrow bore tube. The Grant circulator pump proved insufficient in this regard to sustain any appreciable flow of the coolant fluid through the coil. A more powerful Elepon seal-less pump (Model: SL-25S) was sourced from auxiliary equipment of a previous equipment design in our laboratories for this purpose. Since much lower temperatures than ambient were required for the efficient condensation of the vapour phase in the condenser, a Julabo cold finger refrigeration apparatus (Model: FT 200) was employed to lower the temperature of the circulated coolant fluid (20 % water : 80 % ethylene glycol) in the inner coil and the external jacket heat exchanger.

4.3.1.7 Pressure stabilization system

The general layout of the pressure stabilization system was shown in Figure 4.23. The basic design configuration of Harris (2004) has been retained; however, a few significant modifications have been made for an improved control of system pressure and for the safe operation of the apparatus at elevated pressures.

A second pressure sensor was required in addition to the Sensotec Super TJE pressure transmitter of Harris (which was rated at 25 psi) for operation at elevated pressures. A Wika P-10 pressure transmitter, as supplied by Wika Instruments, with a pressure range of 0 - 1 MPa was used for this purpose. The optimal inline positioning for these pressure sensors was in an intermediate position between the ballast tank and the VLE apparatus. This would place the sensor in an optimal position to provide feedback to the data acquisition and control system for the effective control of system pressure. The positioning the sensors after the condenser would ensure that with an efficient condensing system, no deposition of chemical vapours would occur on the SS diaphragms of the pressure sensors, resulting in unstable pressure readings. A Swagelok ball valve (Model: SS-42S4) was used to isolate the Sensotec pressure sensor for operation at elevated pressure $(P > 150\,kPa)$ where the Wika pressure sensor would be used for pressure logging and control. In conjunction with the incorporation of the second pressure transmitter, the VALVECON program was modified to allow for the logging of pressures from the Wika pressure sensor for pressure control at elevated pressures. The interface for this modified program is shown in Figure 4.27. Another valve was used further along the pressure line to isolate the VLE apparatus in the event of an emergency shut-down.

To improve the pressure stability of the system, a 113.4 liter ballast tank was employed as the pressure reservoir. On either side of the VLE system inlet tube into the ballast, the pressure lines with inline Clippard solenoid valves (from the apparatus of Harris) were connected to a high and low-pressure source on either side. The pressure rating of the Clippard solenoid valves was 105 psi, consequently, the valves could be employed for pressure control for subatmospheric pressure ranges as well as for elevated pressures below the valve pressure rating. The different control strategies for subatmospheric and superatmospheric studies are discussed in Chapter 6. Polyflow tubing, obtained from East Coast Instrumentation, with a pressure rating of 1 MPa was used with quick-connect fittings between the termination points of the by-pass loop and the respective pressure sources to allow for quick disconnection (in changing the nitrogen cylinder or bleeding the ballast, *etc.*). The normally-closed solenoid valves were arranged in a by-pass loop configuration in conjunction with larger needle valves that facilitated the faster pressurization or evacuation of the ballast with the opening of the latter. This is shown in Figure 4.28, as magnified from Figure 4.23, where the same arrangement is used for the valves for both the high and low-pressure sources. The small admittance of flow through the solenoid valve makes it suitable for fine-pressure control, however, unsuitable for effecting large changes in system pressure in a short time. The high-pressure source for superatmospheric operation was compressed nitrogen delivered from a high-pressure cylinder.

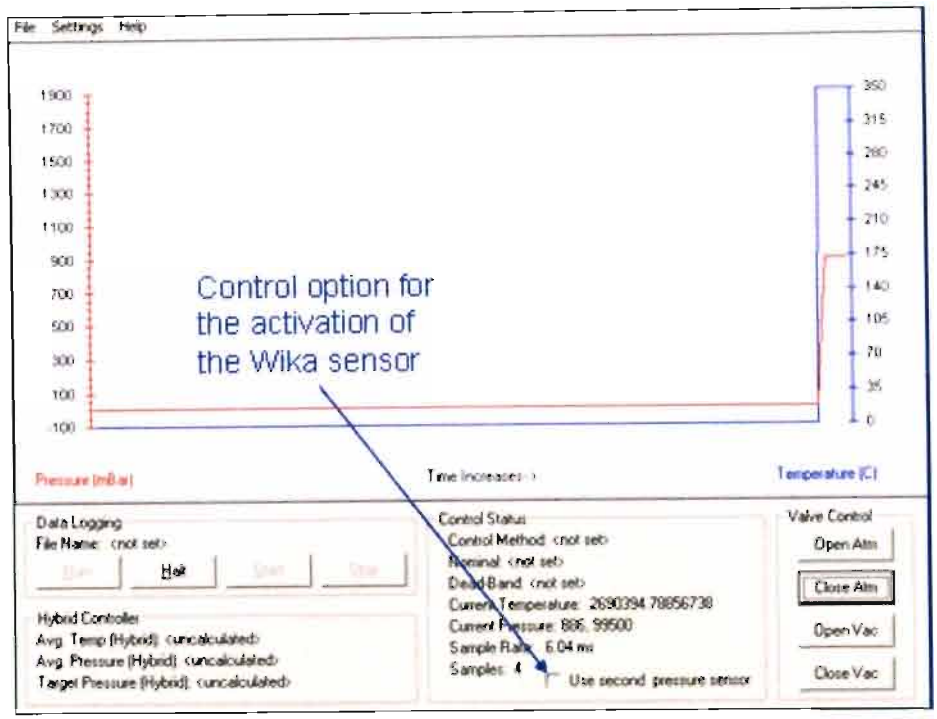

Figure 4.27. Modified VALVECON program data logging interface.

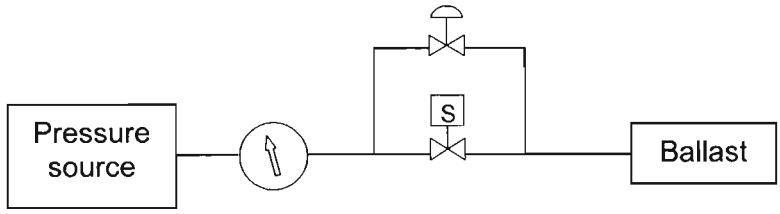

Figure 4.28. The by-pass loop configuration for the pressure stabilization system.

As a safety measure, a safety relief valve was fitted on the inlet line from the nitrogen cylinder to the ballast tank. The low-pressure source was supplied by an Edwards Speedivac vacuum pump.

The use of the pressure stabilization system allowed for a stable pressure profile for the system pressure, which is crucial for obtaining reliable VLE data and for the steady-state operation of the dynamic LPVLE apparatus. Of course, with the use of safety features coupled with the large ballast, the occurrence of accidents such as system overpressurization could safely be negotiated.

4.4 Conclusion

The design of the equipment of Reddy has been achieved through a very systematic and effective process. After a comprehensive review of the history of dynamic LPVLE recirculation designs over the course of the last hundred years, an invaluable insight was gained into the general difficulties in the design and the operation of VLE stills. Thereafter, an assessment of the VLE equipment of Harris (2004) was conducted initially to ascertain what the principal difficulties with the equipment were. To investigate how these design flaws translated into difficulties in the operation of the apparatus and the acquisition of reliable data, preliminary testing of the apparatus was conducted. The combination of the above exercises allowed for the accumulation of a body of theoretical and practical knowledge that was required for the design of the apparatus which has been presented in this study.

CHAPTER 5

SELECTION OF CHEMICAL SYSTEMS

5.1 Introduction

A judicious approach is often required in the selection of a chemical system to be investigated in a specific type of VLE apparatus. The nature of chemical systems to be studied is arguably of equal importance as the designation of the intended pressure and temperature range as a determinant of aspects of the design of the apparatus. The diversity of the thermophysical and chemical properties of a burgeoning pool of laboratory and research chemicals produces a rather large array of chemical mixture combinations, often necessitating the incorporation of specialized features to accurately measure VLE for a specific type of mixture as in corrosive acetic acid + water mixtures at elevated temperatures (Freeman and Wilson, 1985), high relative volatility mixtures (Dvorak and Boublik, 1963) or those systems with solids at ambient conditions (Coon *et al.*, 1989). This attests to the difficulty in the design of a "universal VLE apparatus", which is applicable to all mixture types.

In this study, the systems of interest would be chosen on the basis that the systems would be theoretically and industrially relevant, as well as being suitable to fully test the capabilities of the equipment. Mixtures of hydrocarbons and alkanols have been an active area of research over the past 50 years or so and represent a class of highly nonideal systems that satisfy the above criteria.

5.2 Systems chosen for experimental studies

Apart from aromatic hydrocarbons, aliphatic hydrocarbons (alkanes, cycloalkanes, *etc.*) and alkanols are two of the most widely investigated classes of organic compounds in phase equilibrium studies (Li *et al.*, 2000; Goral, 2001; Peleitero *et al.*, 2001). This is attributed to their significance from both an industrial and theoretical perspective. Industrially, the separation of hydrocarbon + alkanol and alkanol + alkanol mixtures is necessitated to purify the product streams of large-scale industrial processes such as the SASOL Fischer-Tropsch processes and also for the alcohol synthesis industry (Li *et al.*, 2000).

Theoretically, vapour-liquid equilibrium studies on these mixtures can be used derive information on the nature of the molecular interactions on the components. Alkanol + alkanol and alkane + alkane mixtures frequently exhibit nearly ideal thermodynamic behaviour (small or negligible G^E values), however, alkane + alkanol mixtures exhibit strong departures from ideality *i.e.* large G^E values (Gess *et al.*, 1991) and in some cases, azeotropic behaviour. This is of course attributed to the significant differences in the nature of interactions between the two compounds.

Saturated hydrocarbons are nonpolar and exhibit weak van der Waals forces between the molecules. Alkanols, on the hand, are strongly polar and are associating due to their hydrogen-bonding capability. As a result of their associating nature, an alcohol solution forms chain associates and mixing alkanols with alkanes or cyloalkanes results in a degradation of these chain associates giving rise to the observed nonidealities (Browarzik, 2004).

Traditionally, studies on mixtures of hydrocarbons and alkanols have presented challenges for accurate measurement of such data as evident in the studies of published alkanol + alkane VLE data by Moon *et al.* (1991) and Goral (2001). The majority of published data on these types of mixtures have been available at low pressures with very few data sets at elevated pressures and /or temperatures (de Loos *et al.*, 1988; Sauerman *et al.*, 1995; Van Nhu *et al.*, 1998; Oh *et al.*, 2004).

In this study, three types of systems were to be studied *i.e.* an azeotropic cycloalkane + alkanol mixture, an alkanol + alkanol mixture and high relative volatility alkanol + alkane mixtures. To demonstrate the versatility and capabilities of the experimental apparatus, both isobaric and isothermal VLE data sets would be obtained for the respective systems investigated. All three types of systems, especially the latter, would provide a severe test of the VLE measurement capability of the apparatus (as will be discussed later).

5.2.1 Vapour Pressure measurements

The measurement of pure component vapour pressures for alkanols (N'Giumbi *et al.*, 1999) and saturated hydrocarbons (Chirico *et al.*, 1989; Morgan and Kobayashi, 1994; Bourasseau *et al.*, 2004) is also of considerable interest. In particular, interest in the accurate measurement of the vapour pressures of n-alkanes stems from their use as reliable standards (Chirico *et al.*, 1989) for evaluating enthalpies of vapourization and the development of correlative schemes for higher n-alkanes, whose thermophysical properties are problematic to measure. In particular, n-heptane and n-decane have been investigated for use in this regard (Chirico *et al.*, 1989).

Accurate vapour pressures are an integral part of the successful correlation or prediction of VLE data, as was discussed in Chapter 3. In this study, vapour pressure data would be measured for cyclohexane, n-heptane and n-octane in the low-pressure range and for ethanol and 1-propanol at higher pressures. The superatmospheric measurements would demonstrate the capability of the apparatus for thermophysical measurements over an extended pressure range. The measured vapour pressure data can then be regressed to obtain parameters of various vapour pressure correlating equations.

5.2.2 Vapour-Liquid Equilibrium measurements

5.2.2.1 The cyclohexane + ethanol system

The test system chosen for this study was that of the cyclohexane + ethanol binary system. The cyclohexane + ethanol system is strongly nonideal and exhibits the existence of an azeotrope in its VLE composition range. The applicability of the cyclohexane + ethanol mixture as a test system has clearly been demonstrated by previous studies in our laboratories (Harris, 2001; Joseph, 2001; Sewnarain, 2001). A literature review of isobaric studies on the cyclohexane + ethanol system is shown in Table 5.1; the literature data used in this study were those of Joseph (2001).

In addition to the use of the cyclohexane + ethanol mixture as a suitable test system at a pressure of 40 kPa, additional isobars would be obtained, including one above atmospheric pressure. The latter would serve as novel measurements for this type of system on this VLE apparatus and for the cyclohexane + ethanol system, where most of the data has been in the low-pressure region. Although the data sets of Grafahrend (1988), as reported in the Dortmund Data Bank (1999), had been measured at elevated pressures, it should be mentioned that these were obtained for an extremely narrow composition range *i.e.* for a mole fraction range of between 0.9900 - 1.0000.

5.2.2.2 The 1-propanol + 2-butanol system

The study of alkanol + alkanol systems is theoretically of great interest as a result of the study of the formation of cross isomers in the variety of chain associate structures. As a result of the fairly small difference in the boiling points and similar molecular interactions for both these compounds, fairly ideal behaviour could be expected. No literature data was available for VLE measurements on this system in the intended operating range of the author.

Table 5.1. Survey of isobaric measurements for the cyclohexane + ethanol system.

Author/s	System pressure (kPa)	Temperature range (K)	Number of experimental points
Morachevsky and Zharov (1963)	40.0	314.60 - 329.65	7
Morachevsky and Zharov (1963)	100.0	338.00 - 353.94	7
Yuan *et al.* (1963)	100.0	337.92 - 347.14	32
De Alfonso *et al.* (1988)	100.0	337.85 - 350.30	39
Grafahrend (1988)	100.8	350.52 - 351.31	9
Grafahrend (1988)	750.0	412.41 - 412.86	7
Grafahrend (1988)	1000	423.15 - 423.97	7
Joseph (2001)	40.0	314.56 - 329.59	30

5.2.2.3 The 1-propanol + n-dodecane and the 2-butanol + n-dodecane systems

The study of the alkanol + n-dodecane systems would represent an extreme test of the VLE measurement capabilities of the apparatus. Due to the large difference in the boiling points of the n-alkane and the respective alkanols, the system has a very high relative volatility, coupled with the nonideal nature of the alkanol + alkane system. The above types of systems have traditionally been difficult to measure with conventional dynamic recirculating VLE stills (Maia de Oliveira, 2002). As for the 1-propanol + 2-butanol system, no literature data were found for this system for the intended operating range of the author and all measurements would constitute novel data.

5.3 Conclusion

The selection of chemical components for phase equilibrium studies have been presented in the form of alkanols and saturated hydrocarbons (n-alkanes and cyclohexane). These serve to not only satisfy contemporary areas of focus for industrially-relevant and theoretical research areas

but also to clearly demonstrate the efficacy or possible shortcomings of the design in the measurement of vapour pressure or VLE data.

CHAPTER 6

EXPERIMENTAL PROCEDURE

6.1 Introduction

The proper execution of an experimental procedure in the acquisition of phase equilibrium data is as crucial as the optimal design of the VLE apparatus itself. Experimental thermodynamicists have been confronted with an abundance of experimental difficulties and uncertainties. This was exemplified in the uncertainties that characterized the operating procedure for the vapour condensate recirculating apparatus of Jones and Colburn (1943), where a slight incorrect input of energy in the nichrome windings around the crucial sections of the apparatus had compromised the operational efficiency of the apparatus and the quality of data acquired. Consequently, a systematic and judicious approach is necessitated for the successful design of a phase equilibrium determination, where the experimental procedure includes everything from the procurement of the chemical systems from a supplier to the actual measurements conducted in the laboratory.

The successful design of an analytical VLE experiment requires, in addition to the identification of the key system variables, a formulation of strategies to address existing or potential challenges that might be experienced during the course of the experiment. The relative difficulty in the design of VLE experiments, in addition to phenomenological occurrences such as azeotropic behaviour, chemical association in the vapour phase, phase splitting, thermally-induced polymerization and decomposition, is dependent upon the operating conditions (temperature, pressure), nature of the chemical systems under study, measurements to be undertaken (P-T-x-y), number of components in the system (binary or multicomponent) and the composition range to studied (dilute or finite composition ranges).

The difficulties in the design of equipment for the extremes of pressure and temperature have been discussed throughout the course of this work. Key considerations in this regard are preserving the integrity of the system components that are prone to thermal and/or mechanical degradation. These typically include elastomeric seals, packing glands, o-rings, sample septa, stopcocks, glass inserts, *etc.* In addition to the above, the chemical compatibility of these materials has to be thoroughly investigated especially for elevated temperatures, where chemicals can aggressively attack the system components or even the main body itself. This was

experienced by Freeman and Wilson (1985), where investigations of acetic acid and water mixtures at elevated temperature (above 394.3 K) resulted in corrosion of the stainless steel body of the apparatus.

The nature of the chemical components to be studied should be investigated thoroughly beforehand from both a safety and practical standpoint. The former is to ensure that threats to the health and the safety of the experimenter and to those in the immediate environment are minimized. Material and safety data sheets (MSDS) are an important source of information on the potentials hazards in the handling of chemicals with regards to acute and chronic toxicity, corrosiveness, flammability and permissible exposure limits to laboratory and research chemicals, *etc.* In terms of the actual measurement procedure for chemicals, the thermal sensitivity, hygroscopic nature, photostability, oxidative stability, *etc.* of the chemical components can compromise the accuracy of the VLE measurements. Measurements on n-alkanes (Morgan and Kobayashi, 1994), alkenes (Joyce *et al.*, 1999), polynuclear aromatic hydrocarbons (Sivaraman and Kobayashi, 1982; Gupta *et al.*, 1991) and chemically associating oxygenates such as carboxylic acids (Prausnitz *et al.*, 1980; Gess *et al.*, 1991), together with the highly nonideal alkane + alkanol mixtures (Oh *et al.*, 2004) have traditionally been classes of compounds for which difficulty has been experienced in obtaining reliable phase equilibrium data. Measurements on the high molecular weight aliphatic and aromatic compounds have been plagued by thermal decomposition and polymerization and those of oxygenated organic compounds by hydrogen-bonding and association in the vapour phase.

The measurement of multicomponent VLE is complicated by the large number of experimental variables that have to be determined, consequently investigations of ternary or binary phase equilibria are more frequently conducted. It is more convenient to predict the multicomponent phase equilibria from suitable binary VLE measurements (Prausnitz *et al.*, 1980) through the use of binary interaction parameters from thermodynamic models (as in the γ_i - ϕ_i method).

Traditionally the measurement of the majority of LPVLE data has been between 5 and 95 mole % for the composition range of the mixture studied (Gmehling, 2003) and this attests to the difficulty in the accurate measurement of VLE in the extremely dilute range with conventional LPVLE stills. Usually, measurement of infinite dilution activity coefficients with VLE methods has been achieved with differential ebulliometry, semi-micro static cells or differential static methods (Raal and Muhlbauer, 1998).

Each VLE measurement technique has its own unique experimental challenges and uncertainties. For the static method, tedious degassing procedures are necessitated to evacuate

the charged mixtures together with the difficulties in obtaining representative vapour samples. The HPVLE dynamic dual phase recirculation method suffers from uncertainties due to the use of pumps to effect phase recirculation *i.e.* contamination in the pump body, internal pressure fluctuations, *etc*.

The greatest limitations in the operation of LPVLE dynamic recirculating apparatus have been the following:

(a) The attainment of a *true equilibrium* (Marsh, 1989).

(b) The *partial condensation* of the vapour phase in the equilibrium chamber.

(c) The inability to achieve *smooth boiling* and an equilibrium state with minimal fluctuations in pressure and temperature.

(d) Accurate *measurement and control* of pressure.

(e) The *superheating* of the mixture.

(f) The determination of the *true values* of the equilibrium temperatures and vapour compositions (Abbott, 1986).

Consequently, in this study an operating procedure was formulated to attempt to circumvent the above and the description of the experimental procedure conducted in this study will focus on the preparation of the experimental apparatus, the start-up procedure for an experimental run and the data acquisition system

6.2 Preparation of the experimental apparatus and the chemical systems

The preparation of the apparatus for vapour pressure or VLE measurements is a crucial exercise to ensure the efficient operation of the VLE still during the experimental run, upon which the accuracy of the measured thermodynamic variables for the system hinges. A traditional source of frustration for many experimental thermodynamicists has been difficulties in ensuring the complete absence of leaks from the various sections of the apparatus. The adverse effects of leaks do not extend only to uncertainties in the measured temperatures and pressures; however,

the loss of material from the system through a leak (especially in the equilibrium chamber or sample traps) can adversely affect the phase composition measurements.
Consequently, the leak testing of a VLE apparatus has to be conducted thoroughly and is a routine procedure in the preparation of a VLE apparatus for an experimental run. However, leak testing was preceded by the need to address another key area of concern *i.e.* contamination of the equilibrium mixture.

The preparation of the chemical systems for study is equally important as leak testing, especially for substances that are hygroscopic or prone to degradation (thermal, photochemical, oxidative, *etc.*). The latter necessitates special procedures in the preparation of these types of systems for phase equilibrium measurements. The presence of residues from materials of construction, gaskets, o-rings, welding fluxes or from chemicals from previous runs, *etc.* can compromise the quality of the VLE data obtained in the determination of the equilibrium phase compositions. Contaminants are most effectively removed by running a low-boiling solvent such as pentane through the system for a certain time period. Acetone is a commonly used solvent, however, the concerns over the incompatibility of acetone and the Viton® o-rings in the sample traps precluded the use of this solvent in the system. It decided to use the more volatile of the components under study in the binary VLE mixture as the "cleaning" solvent. After the solvent is circulated throughout the apparatus for approximately 10 hours, the still is drained to remove most of the effluent. The VLE apparatus is then evacuated to about 0.1 kPa, heated slightly (~ 323.15 K) and left overnight to remove trace amounts of the solvent.

In the leak-testing procedure, the apparatus is pressurized (up to about 0.6 MPa) and a surfactant-based liquid leak detector, such as the commercially available formulation, Snoop®, is applied to the various tube fittings, gaskets and other seals in the apparatus. The existence of a leak can be easily detected in the form of the bubbling of the surfactant as a result of a leak in the fitting.

The greatest challenges with regards to the occurrence of leaks in the apparatus were to be found in the glass-to-metal couplings in the Cottrell tube, where graphite ferrules were used. The graphite ferrule packing was easily disturbed especially for elevated pressures and temperatures and had to be frequently repacked with more graphite material for a leak-proof seal. The apparatus was also leak tested under pressure and under vacuum, where the system is pressurized or evacuated and the pressure decrease or increase, respectively, is monitored as a function of time. In these leak tests, the VLE apparatus was isolated from the ballast to ensure that the large ballast did not hinder the rapid detection of leaks in the system.

The chemical systems under study in this work were saturated aliphatic compounds (cyclohexane, n-heptane, n-octane and n-dodecane) and the alkanols (ethanol, 1-propanol and 2-butanol). The purities of the compounds were firstly analyzed by gas chromatographic analysis to ensure that the purity was in accordance with that stated by the supplier. In the event that the substance was not obtainable in sufficient purity or found to contain significant impurities, purification procedures were necessitated.

The stated and tested purities (after the purification of the chemicals) of the chemicals used in this study together with the suppliers are shown in Table 6.1. The alkanes and higher alkanols were fractionally distilled in a 1.5 m glass distillation column packed with glass Raschig rings. The initial fraction was discarded in favour of the medium-boiling cut (Riddick *et al.*, 1986). As opposed to alkanes, which pick up moisture in trace amounts through surface adsorption, alkanols (especially lower alkanols) are very hygroscopic due to their hydrogen-bonding nature. The ethanol used in this study was purified through the use of a reaction of the ethanol with magnesium turnings activated with iodine, as described by Riddick *et al.* (1986). The ethanol was then refluxed and distilled to obtain "super-dry ethanol". The higher alkanols were distilled at their normal boiling points and as for the alkanes, the middle fraction was collected. All the chemicals that were distilled in this study were stored over 0.3 nm molecular sieves to remove any traces of water.
The compressed gases used for the operation of the gas chromatograph (helium, hydrogen and air) and also for the pressurization of the system (nitrogen) were UHP grade as sourced from Afrox Scientific.

With the removal of the trace amounts of contaminants and the elimination of system leaks, the apparatus was then deemed fit to be employed for the measurement of vapour pressures or vapour-liquid equilibria. The validation of the purity of the chemicals and the necessity of the purification steps ensured that erroneous phase equilibrium measurements would not be obtained as result of questionable purities of the substances investigated for the experimental determinations in this study.

6.3 Calibration of the pressure and temperature sensors

The accurate measurement of the system pressure and temperature is of unparalleled importance for the successful measurement and subsequent treatment of a VLE data set, where the presumed accuracy in the measurement of pressure and/or temperature (in most treatments) most often forms the basis for the thermodynamic computation of the equilibrium condition.

Table 6.1. Purities and the suppliers of the chemicals used in this study.

Chemical	Supplier	Stated purity [a]	Tested purity [a,b]
Cyclohexane	BDH Chemicals	≥ 99.90	99.99
n-Heptane	Saarchem	≥ 99.50	99.99
n-Octane	Merck	≥ 99	99.93
n-Dodecane	Merck	≥ 99	99.99
Ethanol	Shalom	99.9	99.95
1-Propanol	Riedel-de Haen	≥ 99.5	99.99
2-Butanol	Fluka	≥ 99.5	99.99

[a] Purity in mole fraction %.

[b] With gas-liquid chromatography after purification.

Improper calibration of the pressure and temperature sensors can severely hamper the quality of the data set through the introduction of systematic errors, and if left undetected, can lead to speculation and misdiagnosis of the source of error. Consequently, in the testing of novel phase equilibrium equipment, there should be no uncertainty (within the limits of the accuracy of the sensor or data acquisition/control system) with regards to the measurement of temperature and pressure.

The trends in the choice of sensors for the measurement of pressure and temperature were discussed at length in Chapter 2 and Appendix A. In general, the mechanical pressure gauges and manometers have been displaced by electronic pressure sensors such as strain gauge-based pressure transducers and pressure transmitters. The latter can be readily integrated into data acquisition systems to allow for real time data logging and automated pressure and temperature control strategies.

In general, electronic pressure sensors are calibrated by comparing the pressure readings from a reference pressure sensor with that of the sensor to be calibrated. This is achieved by connecting both sensors to a common pressure manifold in a leak-free system and varying the system pressure until calibration has been achieved for the desired pressure range through a comparison of the two readings. The pressure sensors *i.e.* the Sensotec Super TJE pressure transducer and the Wika P-10 transmitter used in this study were calibrated by Wika Instruments for the respective pressure ranges.

The calibration of temperature sensors can be achieved through a variety of methods such as using the fixed thermophysical properties of standard substances *e.g.* melting points, boiling points and triple points. Alternatively, a stable isothermal fluid environment can be used to compare the sensor with a reference temperature sensor (another Pt-100 or quartz thermometer). The equilibrium chamber Pt-100 temperature sensor was custom-made by Wika Instruments and subsequently calibrated by the company (upon request) after the manufacture of the sensor. Standard charts of the temperature versus resistance relationship for a Pt-100 sensor were used for the calibration of the remaining temperature sensors in the apparatus since these were qualitative measurements.

6.4 Start-up procedure

In the start-up procedure, the ballast was isolated from the high-pressure source and the vacuum pump was switched on. The control valve on the by-pass loop on the vacuum line was then opened to allow for the rapid evacuation of the ballast and the VLE still. The pressure control system was not employed so the "normally closed" solenoid valves had not been activated as yet. After the evacuation of the ballast had been achieved by monitoring the pressure readings from the respective displays, the vacuum line was isolated from the ballast.
Nitrogen was then slowly fed from the nitrogen cylinder, through the use of the by-pass loop control valve, into the VLE still via the ballast. The nitrogen supply was turned off once the desired subatmospheric pressure value had been reached, in the form of a sufficient vacuum to draw the liquid mixture into the still via the drain/fill valve on the reboiler. It is important that the vacuum used be higher than the vapour pressure of the components at the temperature of the still to prevent the occurrence of flashing during the introduction of the material into the still.

The capacity of the VLE still is approximately 170 - 180 ml and this is slightly variable with regards to the pressure and temperature range (as affecting the density of the vapour phase), the thermophysical properties of the chemical components (thermal expansivities, volatilities, *etc.*) and the circulation rate as controlled by the heat input into the still. The material was fed slowly into the reboiler until the liquid level was just above the glass insert in the Cottrell tube, as shown in Chapter 4. After the liquid mixture had been charged to the still, the power supply for the stirrer was switched on and a suitable current input determined an optimal stirring rate for the reboiler contents. The heaters for the internal and external heater of the reboiler and the external heater of the equilibrium chamber were then turned on and initial heating was at a low voltage input (usually 20 V) from the respective Chuan Hsin (Model: SRV-10) variable-voltage transformers (0 - 240 V) or variacs. Thereafter the desired pressure was manually set with the

by-pass loop control valves on both the low-pressure and the high-pressure input sides. With a crude setting of the system pressure, the VALVECON program described in Chapter 4, could be activated and the setpoint temperature (isothermal) or pressure (isobaric) was entered for fine pressure control with the two solenoid valves. Two operational modes with regards to the pressure range were formulated for the system based on the pressure ratings of the pressure sensors *i.e.* $P \leq 150\,kPa$ and $150\,kPa < P < 750\,kPa$. For the former, the Sensotec pressure transducer was used to log data into the VALVECON program for the control of pressure. For operation at elevated pressures, the Sensotec pressure transducer was isolated from the system with a shut-off or ball valve. The intended system pressure was first manually set and the modified VALVECON program was then activated to control a setpoint pressure or temperature, as for the low-pressure operation. At high pressures, the vacuum pump was disconnected from the low-pressure side and atmospheric pressure was used to correct the system pressure fluctuations by serving as a vent. The pressure and temperature control that was achievable with the pressure stabilization system in conjunction with the data acquisition and control program was ± 0.01 kPa and ± 0.01 K, respectively.

With the activation of the VALVECON program to control the system pressure, the temperature of the contents of the reboiler and the boiling characteristics of the mixture were monitored as a function of heat input in the form of small (~ 5 V) energy increments into the VLE still heaters from the variable-voltage resistors. The Pt-100 sensor in the reboiler was used to monitor the temperature and was read off a RKC temperature controller display (Model: CB-40) sourced from Temperature Controls. At the same time, the temperature of the equilibrium chamber was monitored of the same display as the reboiler temperature sensor to ensure it was not heated too rapidly. A switching between the sensors was made possible with a multi-channel TCL Pt-100 selector switch box, as supplied by Temperature Controls. When continuous boiling of the mixture was observed in the Cottrell tube, coupled with a steady flow of the liquid and vapour condensate phases in the respective traps, the heat input was not increased and the system was left to stabilize.

6.5 Determination of equilibrium

In judging the approach of the system to the equilibrium condition, the simultaneous monitoring of several system variables is necessitated. These include the variables from the thermodynamic data set *i.e.* the P-T-x or P-T-x-y variables (where applicable) together with other qualitative aids such as the observation of the system behaviour with regards to the nature of the fluid flow

characteristics of the phases in certain sections of the apparatus (Cottrell tube, sample traps, *etc.*).

The most frequently used criterion for judging the equilibrium condition is that of stability of the equilibrium temperature (in isobaric operation) or system pressure (in isothermal operation) as a function of time and heat input. The attainment of a "plateau region" corresponds to that drop rate (Rogalski and Malanowski, 1980) or heat input (Kneisl *et al.*, 1989) which results in the flattening of the curve of the variation of the pressure or temperature of the system as a function of heat input into the reboiler. The use of the drop rate as a qualitative criterion for the determination of equilibrium was discussed in Chapter 2.

The typical system behaviour for the VLE of a mixture as a function of temperature in an isobaric determination is shown in Figure 6.1, where the region A-B corresponds to the "plateau region". Of course, the sensitivity of the sensors and the analytical technique is crucial in ascertaining the "plateau region". The accuracy of both the Sensotec pressure transducer and that of the Wika pressure transmitter was 0.05 % for the full span of the range of operation. The Wika Pt-100 had an accuracy of ± 0.005 K. Even with highly accurate sensors, the limiting factor is actually the accuracy of the pressure and temperature control system, which as mentioned before was ± 0.01kPa and ± 0.01 K, respectively.

The determination of the equilibrium condition in this study was based on the satisfaction of three criteria in the form of the following:

(a) The *attainment of a plateau region* for the system temperature (isobaric mode) or pressure (isothermal mode) as a function of small voltage increments (~ 5 V) from the variac into the reboiler internal heater. With each voltage increment, the system was allowed a response time of 10 - 15 minutes before the next voltage increment was administered. When a stable pressure or temperature reading was recorded as a function of energy input for a satisfactory time or voltage increment period, the first of the two principal criteria for the determination of the equilibrium condition was satisfied.

(b) The *phase composition stability* as measured by a suitable analytical technique. Samples of the liquid phase and vapour condensate were withdrawn from the sample traps at regular intervals and analyzed by gas-liquid chromatography. For P-T-x measurements, only the liquid phase was sampled. In conjunction with uncertainties in the detection limit of the analytical apparatus and uncertainties in the calibration procedure, a deviation of ± 0.002 mole fraction was considered as an acceptable criterion for composition stability.

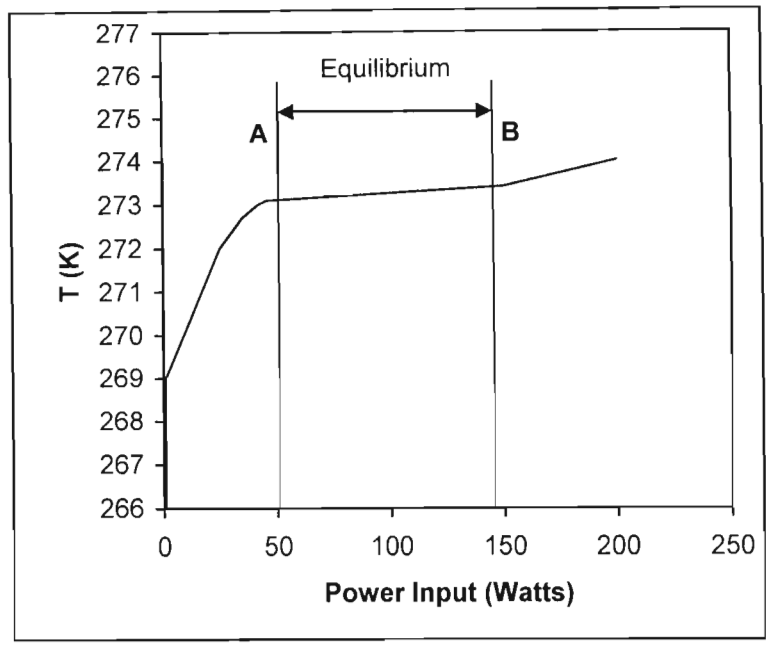

Figure 6.1. Approach of the system to the plateau region.

(c) The observation of the *fluid flow characteristics* of the system. As mentioned before, in this study, this was used as a purely qualitative criterion. With the initiation of steady state boiling, the fluid flow dynamics of the phases in the Cottrell tube and the sample traps was observed as a function of energy input into the still. The Cottrell tube was observed to ensure that there was a continuous and steady "pumping" of slugs of vapour and liquid up the Cottrell tube. The drop rate and flow patterns of the equilibrium phases were monitored. It is imperative that the equilibrium temperature be independent of the circulation rate (as a function of heat input) for internal consistency in the apparatus (Yerazunis *et al.*, 1964). This was constantly monitored for throughout the run.

With the satisfaction of the above three criteria, the system was deemed to be at equilibrium and the pressure and temperature were recorded. For the determination of the vapour pressure measurements for the pure components, only **(a)** and **(c)** apply. Equilibrium times of around 20 - 30 minutes were typically achieved for the operation of the apparatus.

6.6 Analytical technique for the phase composition determinations

Gas-liquid and gas-solid chromatography are currently the most popular analytical methods for the quantification of gaseous and volatile liquid mixtures and in addition to routine laboratory analyses, these have found widespread applicability in many diverse fields such as forensic

science, refinery gas analysis and in the formulation of cosmetics and perfumes. The inherent advantages of this method include small sample sizes (0 - 5 μL), excellent detection limits (10^{-12} $g.s^{-1}$ with an FID detector, 10^{-6} $g.cm^{-3}$ with a TCD detector), excellent reproducibility, ease of automation in the data acquisition and control of the analysis, simple operating procedure and the fairly moderate cost of commercially available gas chromatographs.

Commonly used gas chromatographic detectors are the thermal conductivity detector (TCD) and the flame ionization detector (FID). A TCD detector is a concentration-dependent ($g.cm^{-3}$) detector and it is therefore highly sensitive to fluctuations in the carrier gas flow rate. The FID detector on the other hand, is a mass-flow dependent detector ($g.s^{-1}$) and is not largely affected by the carrier gas flow fluctuations. However, the FID detector cannot be used in determinations with chemical species that are non-carbonaceous (*e.g.* water). Since only organic mixtures would be studied here, coupled with the superior detection limit, insensitivity to fluctuations in carrier gas flow and the larger linear response range, a gas chromatograph with a FID detector was considered as being most suitable for the quantitative analyses of the vapour condensate and the liquid phase compositions in the VLE measurements.

The analysis of the phases was performed with a Shimadzu GC-14 gas chromatograph which was equipped with dual packed column injection ports and dual flame ionization detectors. The data acquisition and control of the gas chromatograph parameters were achieved with a Shimadzu GCsolution® software interface on an Acer personal computer. This was linked up to the inbuilt communications bus module in the Shimadzu gas chromatograph via serial port communication. The software interface is shown in Figure 6.2. The use of the interface allowed for the development of methods by programming the injector, column and detector temperatures, setting the column flow rate, setting experimental run times, *etc.* The data acquisition system allowed for the real time logging of the data, which could be stored as an output file for post-run analysis, as shown in Figure 6.3.

The packed columns used in this study were a Poropak® Q column and a SE-30 column. The Porapak® Q column was supplied by Langet Labs and was employed for the alkanol + alkanol and the cycloalkane + alkanol VLE studies. Since Porapak® Q is an adsorbent column, the use of this column renders this analysis as technically a gas-solid chromatographic determination. The SE-30 column was provided by the Separations for use in the alkane + alkanol VLE phase determinations. The specifications of the columns used in this study are shown in Table 6.2. The columns were fitted with custom-made graphite ferrules instead of 316 SS ferrules to prevent any damage to the stationary phase material in the column when it was tightened in the injector and detector inlet ends.

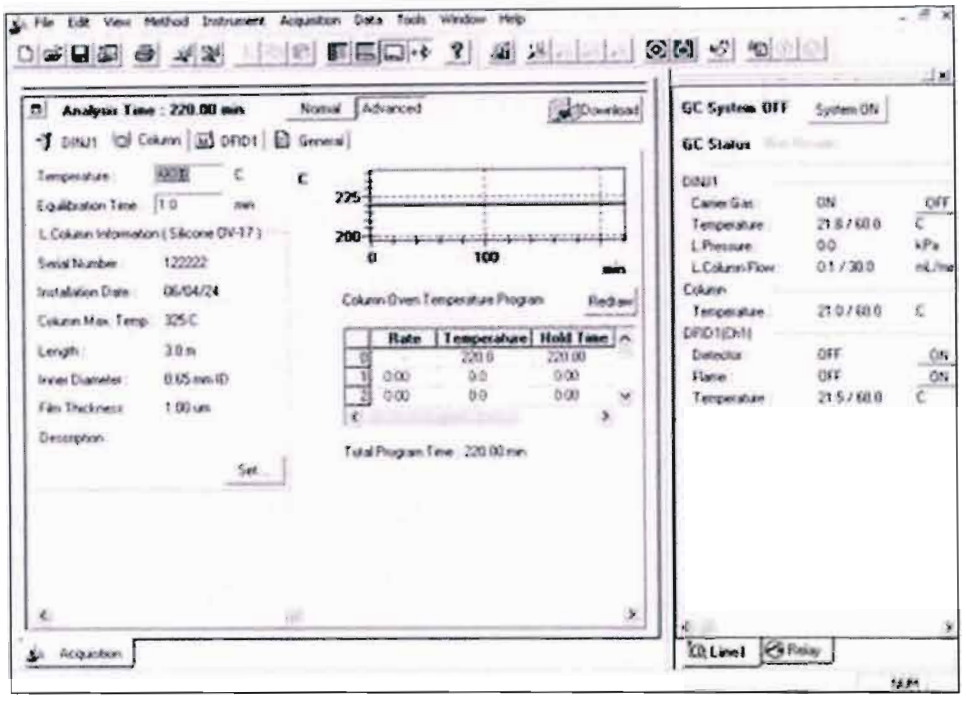

Figure 6.2. Control interface for the Shimadzu GCsolution® software.

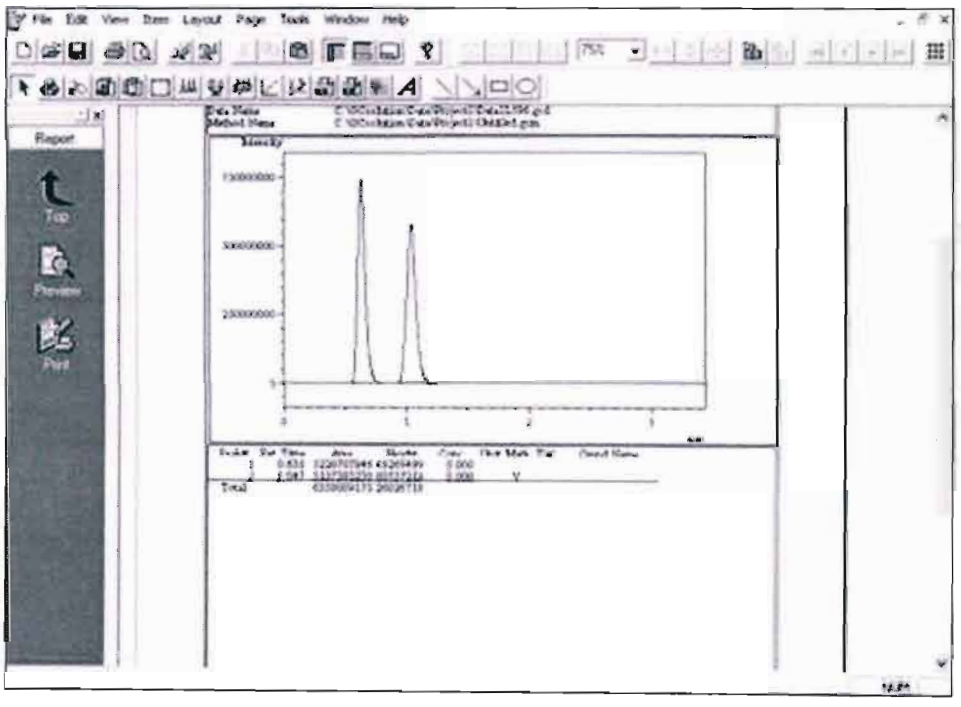

Figure 6.3. Post-run analysis of the chromatograms.

Table 6.2. Specifications of the gas chromatograph columns.

Column	Porapak® Q	SE-30
Tubing	316 SS	316 SS
Outer diameter (mm)	3.2	3.2
Inner diameter (mm)	2.2	2.2
Column length (m)	2	2
Phase loading	–	10% on Chromosorb W-HP
Mesh range	80/100	80/100
Temperature limit (K)	523.50	573.15

Both columns were preconditioned prior to use to remove any traces of solvents or any other contaminants (from the preparation of the columns) as the latter can contribute to "ghost peaks" appearing in the chromatograms and affect the column performance. The presence of "ghost peaks" can adversely affect the quantitative of analysis, especially when these peaks overlap with those for solutes that that are to be determined. The conditioning procedure was conducted by heating the column at a temperature 20 K below that of the column maximum temperature for approximately 10 - 15 hours with a steady flow of helium gas flowing through the column. The outlet of the detector was disconnected from the column and capped during this procedure to prevent the contamination of the detector.

The calibration procedure used for the gas chromatographic detector was the chromatogram area ratio method described by Raal and Muhlbauer (1998). The method describes the use of area ratios as opposed to absolute areas for the determination of the response factors, which can then be used for a quantitative analysis.

The response factor is the proportionality constant for the relationship between the number of moles or mole fractions of a component injected in the column and the corresponding response of the detector in the form of an area on a chromatogram.

For a binary mixture, the response factor can be represented as follows:

$$\frac{n_1}{n_2} = \left(\frac{A_1}{A_2}\right)\left(\frac{F_1}{F_2}\right) = \frac{x_1}{x_2} \qquad (6.1)$$

From Equation (6.1), it can be seen that the absolute areas depend upon the individual amounts of the components injected; which is generally not reproducible with conventional gas chromatograph syringes. Consequently, it is more effective to use area ratios together with the detector response factor to determine the respective mole fractions of the components. In this method, binary mixtures of the components are gravimetrically prepared across the entire composition range and the phase compositions are analyzed by the gas chromatographic method. The area ratios $\left(\frac{A_i}{Aj}\right)$ of the two components obtained from chromatogram are then plotted against the corresponding mole fraction ratios $\left(\frac{x_i}{x_j}\right)$ in the form of two inverse plots *i.e.* $\left(\frac{A_1}{A_2}\right)$ versus $\left(\frac{x_1}{x_2}\right)$ and $\left(\frac{A_2}{A_1}\right)$ versus $\left(\frac{x_2}{x_1}\right)$ for components 1 and 2. The slopes of the plots, as extrapolated to zero, should roughly be in agreement with each other.

The calibrations of the FID detector for the binary VLE measurements conducted in this study, together with the operating conditions for the Shimadzu GC-14 gas chromatograph, are shown in Appendix C. In the analysis of the phase equilibrium samples, the samples were withdrawn from the respective sample traps with a 1 μL gas chromatography liquid syringe, as supplied by DLD Scientific. The syringe was flushed several times successively with the sample before a sample was subsequently withdrawn for analysis. The injection sizes were approximately 0.5 μL and the sample was quantified in triplicate to ensure reproducibility. The uncertainty for the measurement of the phase compositions in the calibration procedure and the vapour-liquid equilibrium experiments was ± 0.001 mole fraction. This was determined by preparing mixtures of known compositions, analyzing the mixtures by gas chromatography and then quantifying the sample through the use of the area ratio method. The results were then compared with the actual known compositions of the test mixtures to ascertain the uncertainty in the measurements.

In the shut-down procedure for the Shimadzu GC-14 gas chromatograph unit, the injector, column and detector were cooled to ~ 303.15 K with a constant flow of the helium carrier gas. The gas flows from the respective cylinders were turned off, the GCsolution® program was closed and the gas chromatograph was turned off.

6.7 Shut-down procedure

To ensure the safe shut-down of the VLE apparatus and the auxiliary equipment, strict procedures were necessitated to ensure that this was achieved in a very systematic manner. The

VALVECON control program was halted and the system was maintained at the current pressure value whilst the mixture was cooled. This was achieved by terminating the heat input into the still by switching the variacs off. For subatmospheric operation, the polyflow tubing was removed from the quick connect fitting on the vacuum side. The vacuum pump was turned off after being opened to atmosphere to prevent a buildup of an internal vacuum in the pump causing the pump oil to be sucked into the gauge.

After sufficient cooling of the reboiler and the equilibrium chamber had occurred, (from the temperature readings of the respective Pt-100 sensors), the VLE apparatus was then depressurized (if $P_{sys} > 150\,kPa$) or pressurized (if $P_{sys} < 90\,kPa$). For the former, this was achieved through bleeding through one of the by-pass loop control valves from the ballast. In the case of the latter, nitrogen gas was supplied to equalize the pressure with that of atmospheric pressure. The contents of the still was then drained through the drain/fill valve of the reboiler and safely disposed off in designated waste bottles.

6.8 Maintenance of the VLE apparatus and auxiliary equipment

The inevitable wear and tear and finite lifetimes of materials used in the construction of the VLE apparatus necessitated that frequent checks on the integrity of these sections had to be performed.

With regards to the graphite-based gaskets, the robustness and durability of these gaskets ensured that the gasket did not have to be changed as a result of the continuous operation of the apparatus, which did not seem to induce wearing of the gasket. Changes were only necessitated when the respective graphite-sealed sections were opened and the gasket was disturbed or damaged. As mentioned before, the sealing arrangement for the sample traps *i.e.* the Teflon® discs and Viton® o-rings did not present any sealing problems throughout the course of this study. In terms of the seals, the only sections of the apparatus that needed attention were the graphite ferrules in the glass-to-metal couplings in the Cottrell tube. The ferrule had to be repacked and sometimes replaced to obtain proper sealing.

The sample septa used in the traps were Teflon®-backed silicon septa (Model Autosep T) with a temperature rating of 523.15 K. These were changed on the basis of the condition of the septa in terms of the syringe needle perforation damage (usually after 20-30 sample withdrawals).

With regards to the auxiliary equipment, the gas chromatograph, vacuum pump and coolant pump deserve special mention. The gas chromatograph column and detector were conditioned every three months to ensure that any accumulated volatile contaminants in the system were removed. The Edwards vacuum pump was serviced once during the course of the study, where the oil had to be changed due to dilution by chemical vapours. The coolant pump was removed from the condensing system and water was run through the pump to ensure that any fouling of the pump from the coolant fluid mixture was removed.

6.9 Conclusion

The general operating procedure for the operation of the VLE apparatus and the associated auxiliary equipment has been described in considerable detail. Additionally, the considerations inherent in the proper operation of the gas chromatograph have been described. Although the operating procedure mentioned has been optimized for the nature and scope of the systems and conditions investigated in this study, there must a reasonable amount of room for flexibility in the operating procedure in the event that changes are necessary to extend the apparatus for operation under different physical conditions.

CHAPTER 7

EXPERIMENTAL RESULTS

7.1 Introduction

The experimental procedure and associated purification procedures for the chemical systems investigated in this study have been described in great detail in Chapter 6. The experimental results that were obtained from the systematic application of the above-mentioned experimental procedure to the measurements involving alkanols and saturated hydrocarbons will be presented here. The experimental investigations undertaken in this study constituted the measurement of vapour pressures and binary vapour-liquid equilibria. Five vapour pressure curves and thirteen vapour-liquid equilibrium data (P-T-x-y and P-T-x) sets have been obtained.

The measurement of pure component thermophysical properties such as vapour pressures can be viewed as the most appropriate starting point for the preliminary testing of an analytical phase equilibrium apparatus and serves as a suitable test of the most basic aspects of the equipment design. Vapour pressures have been measured for cyclohexane, n-heptane and n-octane in the low-pressure or subatmospheric range and for ethanol and 1-propanol for pressures higher than atmospheric.

The measurement of vapour-liquid equilibrium data involves consideration of a host of factors, which have been exhaustively dealt with in Chapters 2 and 4, when compared to the scope of vapour pressure measurements. The systems of interest in this study *i.e.* hydrocarbon + alkanol and alkanol + alkanol mixtures were chosen on the basis of theoretical and industrial interest as well as to fully test the capabilities of the equipment. VLE data sets in the form of P-T-x-y data have been measured for the systems of cyclohexane + ethanol and 1-butanol + 2-butanol and P-T-x measurements have been obtained for the 1-propanol + n-dodecane and 2-butanol + n-dodecane systems.

7.2 Vapour Pressure measurements

The results of the vapour pressure measurements for the compounds under study are presented in Table 7.1 for $10\,kPa < P < 100\,kPa$ and in Table 7.2 for $10\,kPa < P < 600\,kPa$.

Table 7.1. Experimental vapour pressure measurements for 10 kPa < P < 100 kPa.

P (kPa)	T (K)	P (kPa)	T (K)
	Cyclohexane		
24.08	312.78	69.06	341.67
30.70	318.96	77.87	345.37
38.72	325.07	85.44	348.28
46.85	330.32	91.68	350.53
55.20	335.01	101.32	353.78
61.52	338.21		
	n-Heptane		
16.91	320.43	74.44	361.37
23.50	328.58	79.37	363.45
35.39	339.42	86.51	366.31
56.16	352.66	100.11	371.21
67.57	358.24		
	n-Octane		
22.77	352.83	66.65	384.36
29.84	360.22	75.26	388.38
37.76	366.89	82.77	391.59
44.73	371.89	89.59	394.32
52.75	376.93	99.12	397.87
59.82	380.87		

The experimental vapour pressures were compared with those obtained from the literature vapour pressures computed with Antoine coefficients obtained from the Dortmund Data Bank or DDB (1999) and from Riddick *et al.* (1986). Graphical plots of the comparison between experimental and literature vapour pressure values data are shown in Figures (7.1) - (7.5).

Table 7.2. Experimental vapour pressure measurements for 10 kPa < P < 600 kPa .

P (kPa)	T (K)	P (kPa)	T (K)
	Ethanol		
30.24	323.82	100.79	351.28
40.31	329.92	110.86	353.68
50.39	334.84	120.93	355.92
70.33	342.49	180.00	366.77
80.63	345.77	190.00	368.31
85.67	347.26	200.00	369.75
98.45	350.68		
	1-Propanol		
69.79	360.86	260.00	397.13
74.92	362.60	290.00	400.57
79.60	364.11	310.00	402.71
84.80	365.70	330.00	404.74
89.78	367.14	350.00	406.69
94.77	368.52	380.00	409.43
99.70	369.82	400.00	411.18
105.14	371.30	420.00	412.84
110.10	372.42	450.00	415.23
113.19	373.15	480.00	417.52
120.75	374.88	500.00	418.96
130.10	376.91	520.00	420.37
171.00	384.57	530.00	421.06
199.90	389.14	550.00	422.41
228.50	393.15	561.50	423.16
229.90	393.34		

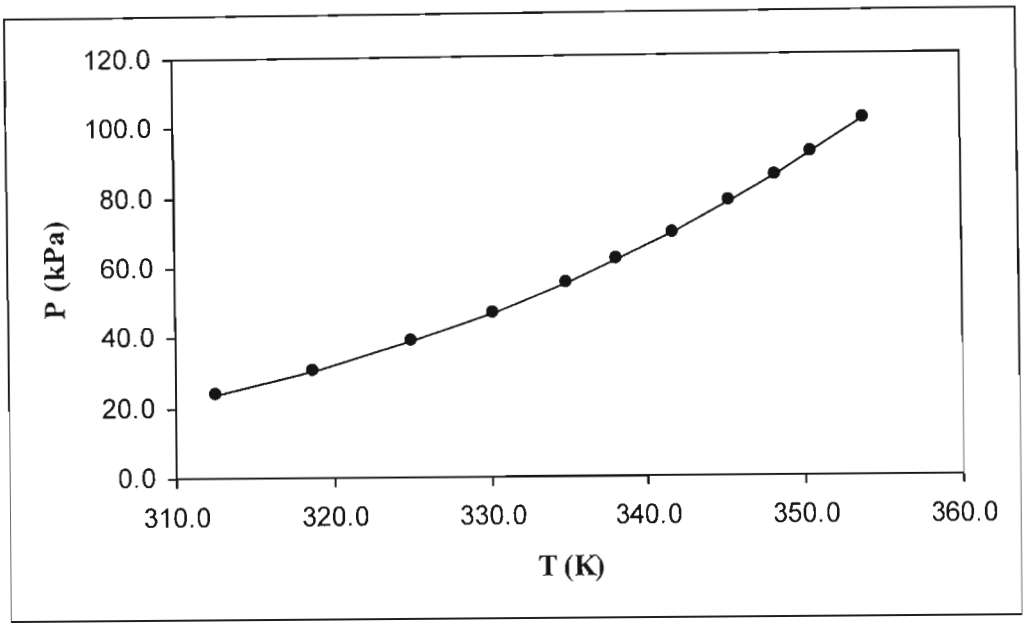

Figure 7.1. Graphical plot of the comparison of the experimental and literature vapour pressures of cyclohexane: • experimental values; _____ literature values (DDB, 1999).

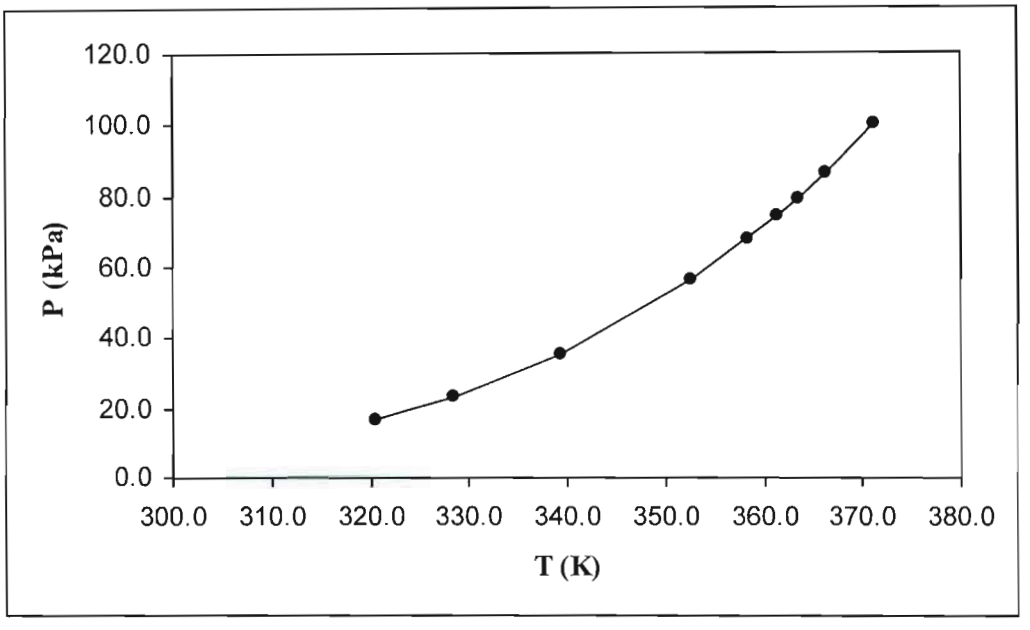

Figure 7.2. Graphical plot of the comparison of the experimental and literature vapour pressures of n-heptane: • experimental values; _____ literature values (DDB, 1999).

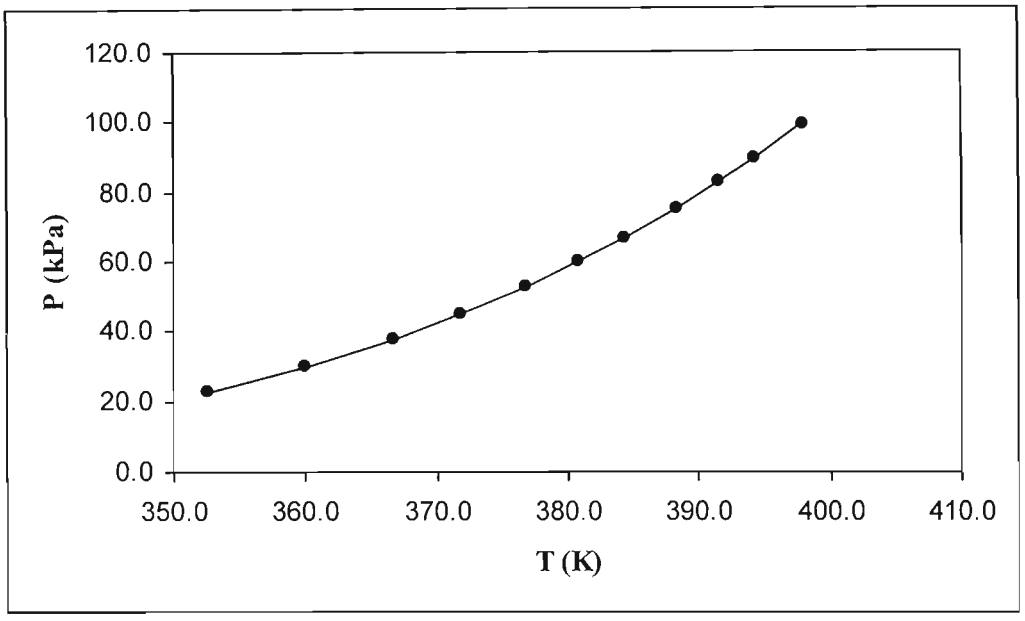

Figure 7.3. Graphical plot of the comparison of the experimental and literature vapour pressures of n-octane: • experimental values; ——— literature values (DDB, 1999).

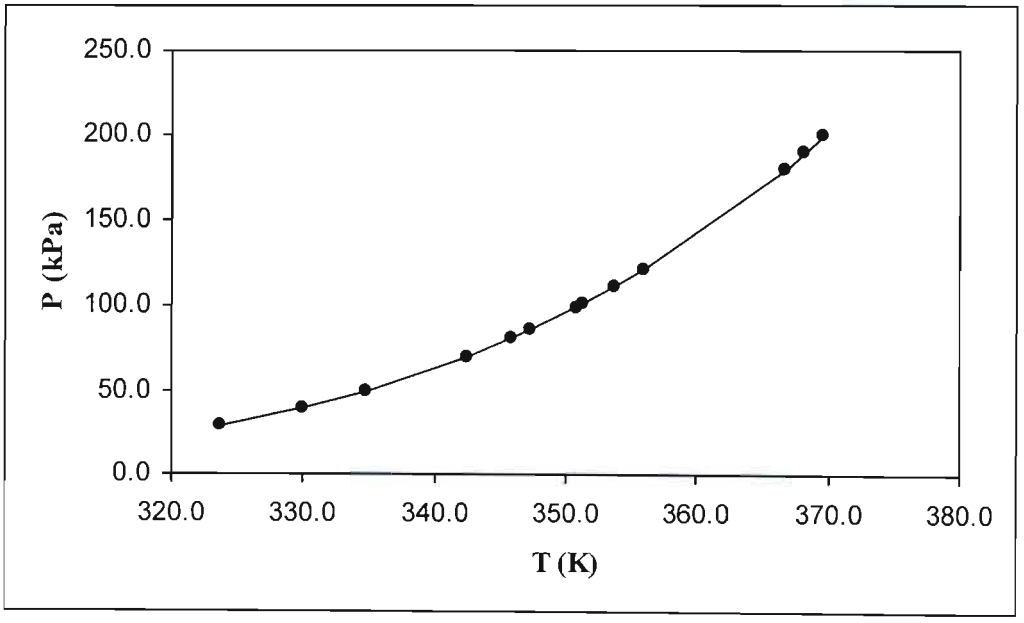

Figure 7.4. Graphical plot of the comparison of the experimental and literature vapour pressures of ethanol: • experimental values; ——— literature values (DDB, 1999).

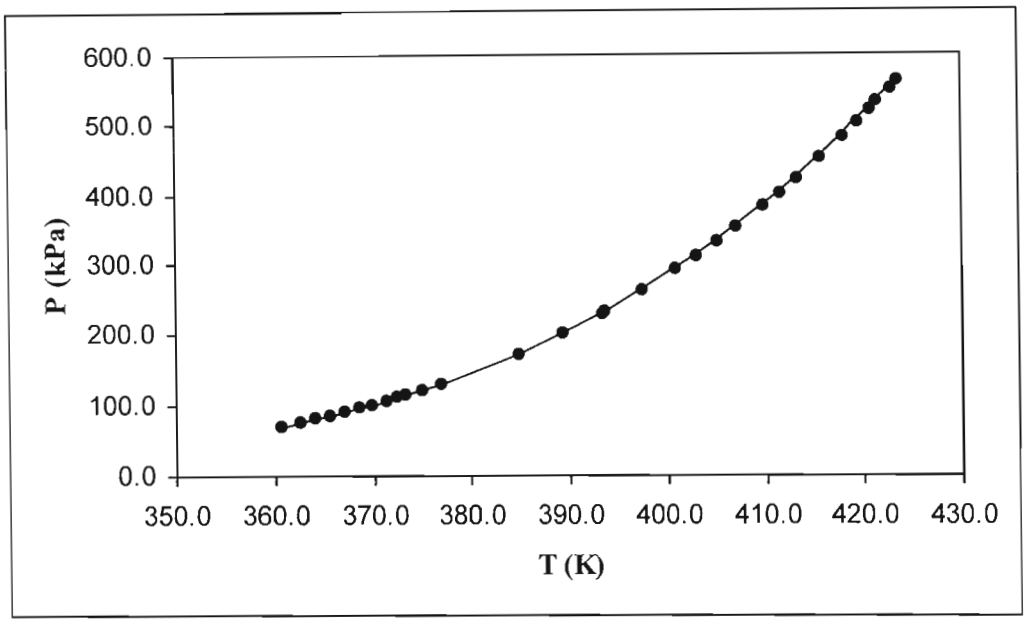

Figure 7.5. Graphical plot of the comparison of the experimental and literature vapour pressures of 1-propanol: • experimental values; ——— literature values (Riddick *et al.*, 1986)

7.3 Vapour-Liquid Equilibrium measurements

Vapour-liquid equilibrium measurements in the form of isotherms and isobars have been obtained for four binary systems in the form of cyclohexane + ethanol, 1-propanol + 2-butanol, 1-propanol + n-dodecane and 2-butanol + n-dodecane. The VLE data sets for the cyclohexane + ethanol systems were the only P-T-x-y isobaric measurements obtained in this study. Isothermal measurements were obtained for the remaining VLE data sets *i.e.* the P-T-x-y data for the 1-propanol + 2-butanol systems and the P-T-x data for the alkanol + n-dodecane systems.

7.3.1 The cyclohexane + ethanol system

For the cyclohexane (1) + ethanol (2) system, four isobaric data sets were measured at pressures of 40 kPa, 69.8 kPa, 97.7 kPa and 150 kPa; the data for these measurements are presented in Tables (7.3) - (7.6), respectively. The T-x_1-y_1 plots and the corresponding x_1-y_1 plots are shown in Figures (7.6) - (7.9) and Figures (7.10) - (7.13), respectively.

The T-x_1-y_1 measurements at 40 kPa constituted a test system and were compared to the data obtained by Joseph (2001), as shown in Figure 7.6.

Table 7.3. Vapour-liquid equilibrium data for cyclohexane (1) + ethanol (2) at 40 kPa.

T (K)	x_1	y_1
329.76	0.0000	0.0000
327.21	0.0130	0.1095
318.50	0.1172	0.4647
316.88	0.1742	0.5323
315.97	0.2414	0.5766
314.80	0.5077	0.6236
314.68	0.5602	0.6247
314.70	0.7045	0.6368
314.82	0.7427	0.6416
314.81	0.7878	0.6502
315.51	0.8965	0.6626
316.30	0.9458	0.6938
317.58	0.9715	0.7352
318.71	0.9802	0.7685
325.96	1.000	1.000

Table 7.4. Vapour-liquid equilibrium data for cyclohexane (1) + ethanol (2) at 69.8 kPa.

T (K)	x_1	y_1
342.30	0.0000	0.0000
340.04	0.0148	0.0991
335.05	0.0640	0.3085
331.87	0.1283	0.4119
330.31	0.1858	0.4815
329.39	0.2508	0.5233
328.66	0.4236	0.5727
328.53	0.5043	0.5816
328.52	0.5663	0.5843
328.60	0.7148	0.5995
328.59	0.7526	0.6032
328.67	0.7916	0.6055
329.04	0.8598	0.6185
329.70	0.9108	0.6384
330.67	0.9389	0.6652
332.49	0.9657	0.7289
337.70	0.9894	0.8787
341.99	1.0000	1.0000

Table 7.5. Vapour-liquid equilibrium data for cyclohexane (1) + ethanol (2) at 97.7 kPa.

T (K)	x_1	y_1
350.50	0.0000	0.0000
343.56	0.0638	0.2742
340.46	0.1256	0.3872
338.99	0.1868	0.4527
337.57	0.3630	0.5270
337.37	0.4298	0.5460
337.28	0.5689	0.5601
337.42	0.7190	0.5789
337.43	0.7569	0.5803
337.46	0.7742	0.5805
338.06	0.8512	0.5978
338.78	0.9025	0.6189
340.73	0.9434	0.6644
348.82	0.9589	0.7387
348.82	0.9907	0.8965
352.60	1.0000	1.0000

Table 7.6. Vapour-liquid equilibrium data for cyclohexane (1) + ethanol (2) at 150 kPa.

T (K)	x_1	y_1
367.66	0.0000	0.0000
355.17	0.0679	0.2416
352.24	0.1314	0.3562
350.75	0.1945	0.4131
350.02	0.2439	0.4549
349.44	0.3635	0.4921
349.21	0.5163	0.5224
349.23	0.5715	0.5286
349.51	0.7192	0.5542
350.54	0.7993	0.5931
354.91	0.9168	0.6750
361.71	1.0000	1.0000

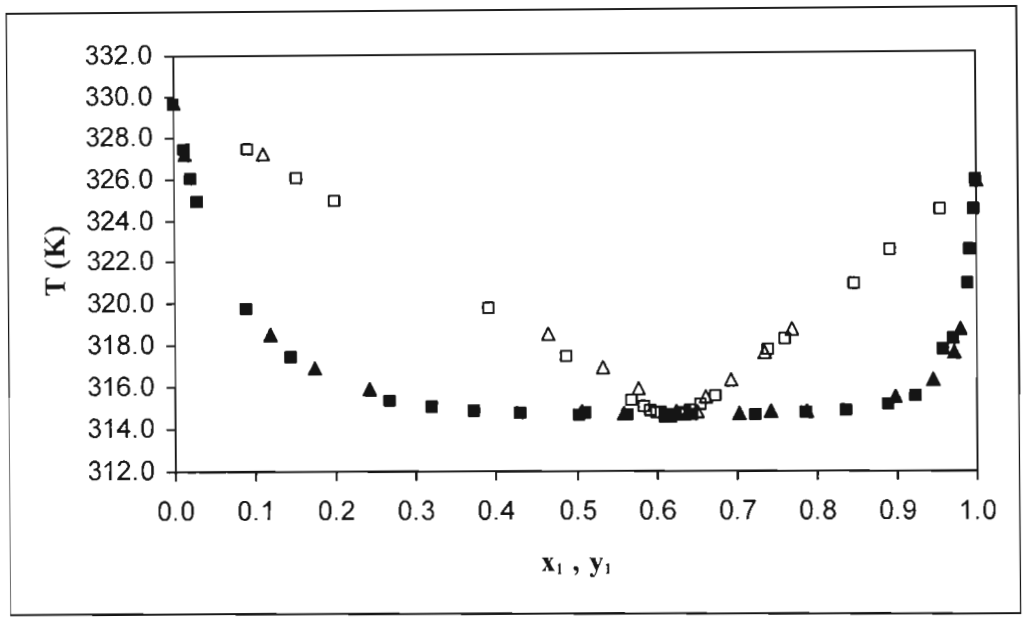

Figure 7.6. T-x_1-y_1 plot for cyclohexane (1) + ethanol (2) at 40.0 kPa: ▲ experimental T-x_1 values; △ experimental T-y_1 values; ■ T-x_1; □ T-y_1 (Joseph, 2001).

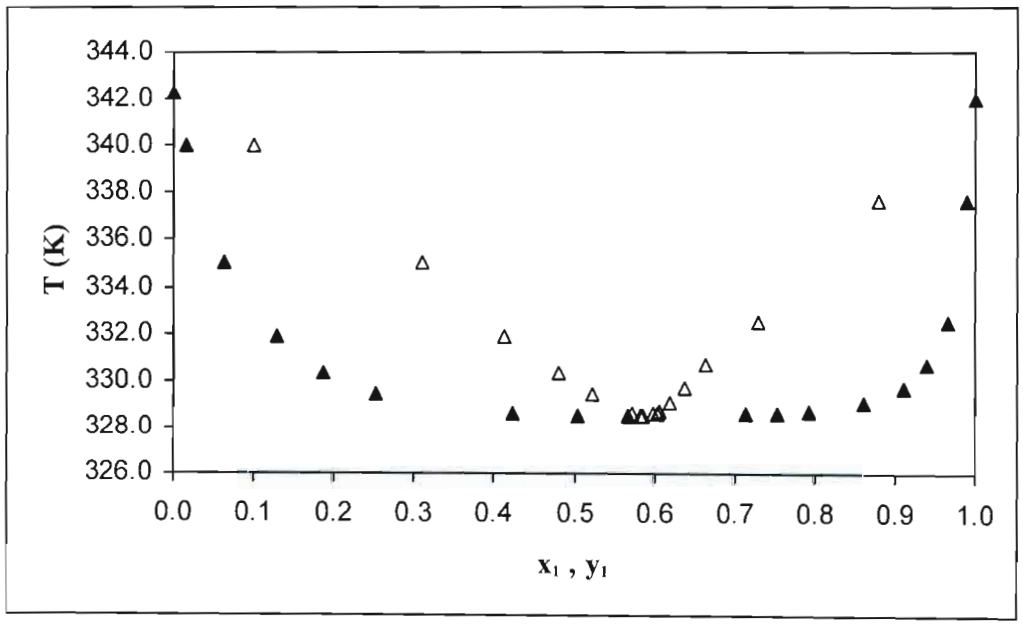

Figure 7.7. T-x_1-y_1 plot for cyclohexane (1) + ethanol (2) at 69.8 kPa: ▲ experimental T-x_1 values; △ experimental T-y_1 values.

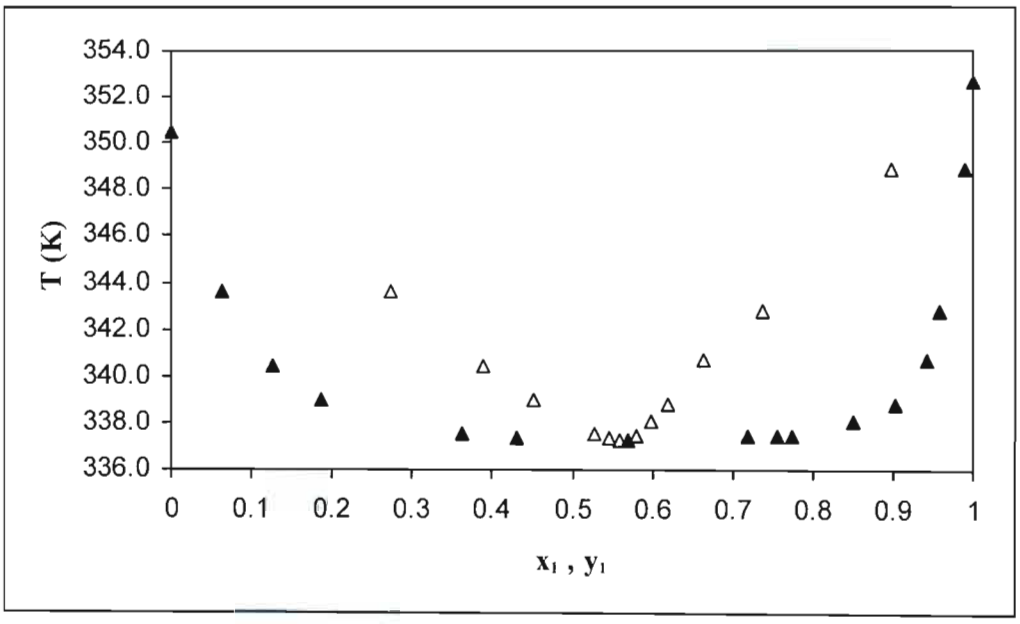

Figure 7.8. T-x_1-y_1 plot for cyclohexane (1) + ethanol (2) at 97.7 kPa: ▲ experimental T-x_1 values; △ experimental T-y_1 values.

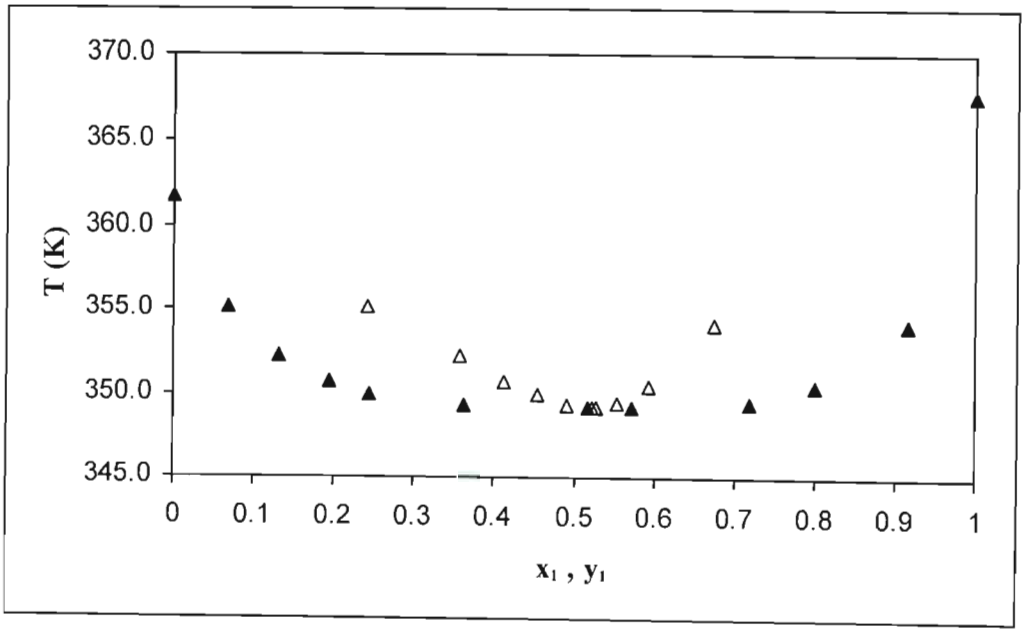

Figure 7.9. T-x_1-y_1 plot for cyclohexane (1) + ethanol (2) at 150 kPa: ▲ experimental T-x_1 values; △ experimental T-y_1 values.

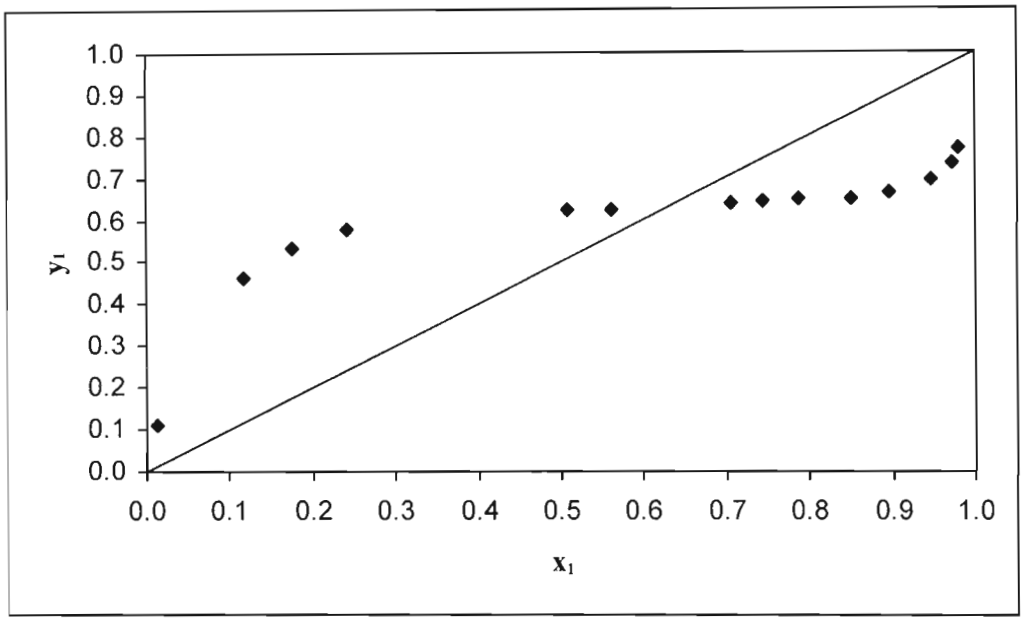

Figure 7.10. Experimental x_1-y_1 plot for cyclohexane (1) + ethanol (2) at 40 kPa.

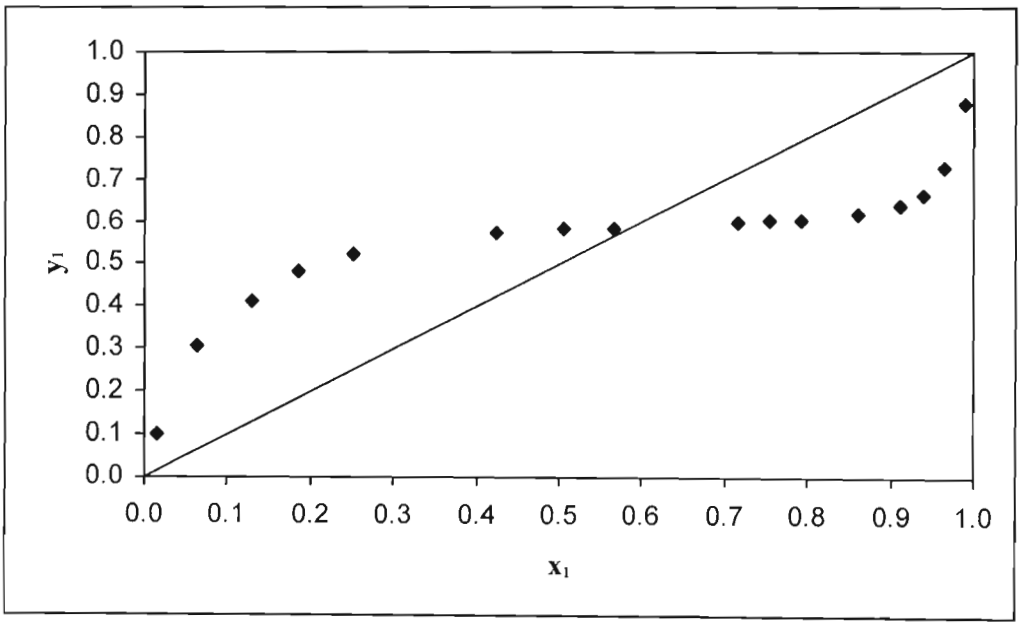

Figure 7.11. Experimental x_1-y_1 plot for cyclohexane (1) + ethanol (2) at 69.8 kPa.

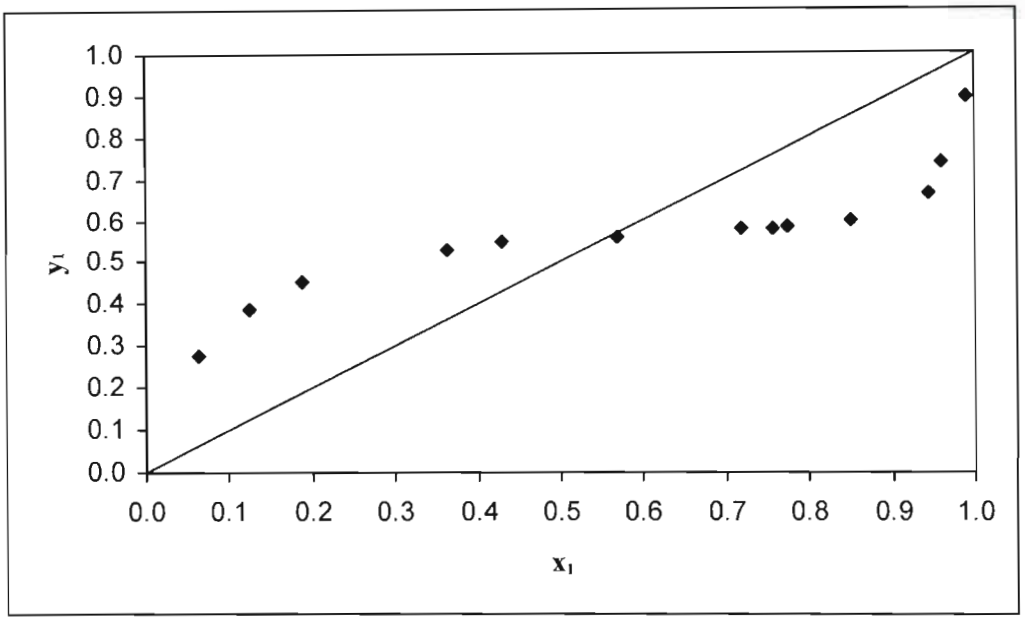

Figure 7.12. Experimental x_1-y_1 plot for cyclohexane (1) + ethanol (2) at 97.7 kPa.

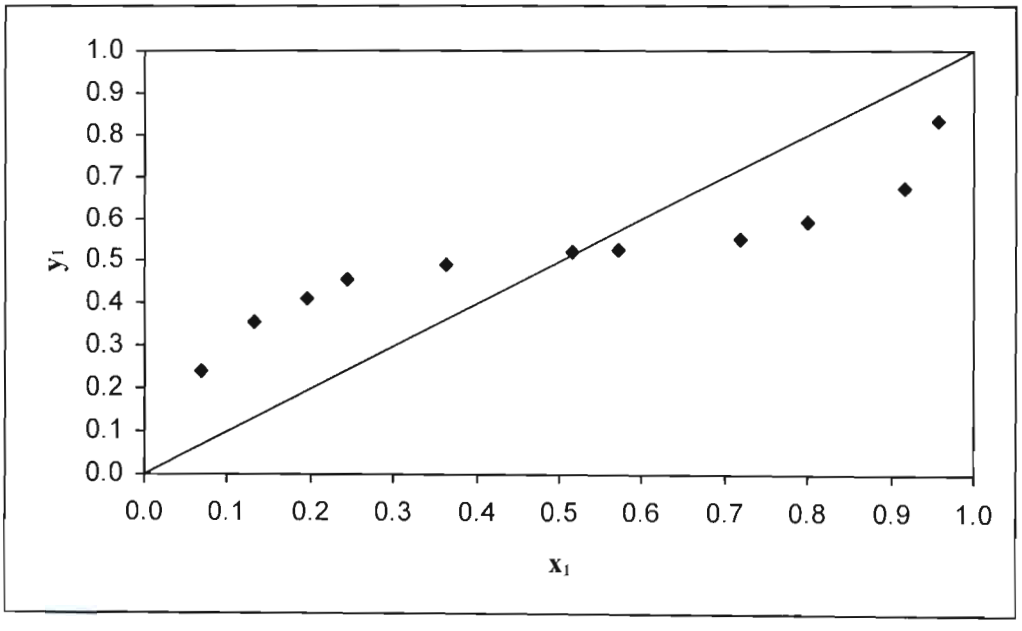

Figure 7.13. Experimental x_1-y_1 plot for cyclohexane (1) + ethanol (2) at 150 kPa.

7.3.2 The 1-propanol + 2-butanol system

For the 1-propanol (1) + 2-butanol (2) system, three isotherms were measured at temperatures of 373.15 K, 393.15 K and 423.15 K; the data for these measurements are presented in Tables (7.7) - (7.9), respectively. The P-x_1-y_1 plots and the corresponding x_1-y_1 plots are shown in Figures (7.14) - (7.16) and Figures (7.17) - (7.19), respectively. All the isotherms for this system constituted novel measurements since there were no literature data sets to compare the data with.

Table 7.7. Vapour-liquid equilibrium data for 1-propanol (1) + 2-butanol (2) at 373.15 K.

P (kPa)	x_1	y_1
103.7	0.0000	0.0000
103.9	0.0224	0.0235
105.3	0.1315	0.1405
106.8	0.2642	0.2788
107.8	0.3810	0.4010
108.8	0.5103	0.5326
110.0	0.6371	0.6599
111.2	0.7928	0.8072
111.9	0.8686	0.8793
113.2	1.0000	1.0000

Table 7.8. Vapour-liquid equilibrium data for 1-propanol (1) + 2-butanol (2) at 393.15 K.

P (kPa)	x_1	y_1
209.6	0.0000	0.0000
211.9	0.1307	0.1420
215.1	0.2653	0.2811
218.3	0.4246	0.4379
219.5	0.4784	0.5007
222.2	0.6300	0.6483
223.3	0.6975	0.7103
224.9	0.7927	0.8080
226.1	0.8684	0.8782
228.5	1.0000	1.0000

Table 7.9. Vapour-liquid equilibrium data for 1-propanol (1) + 2-butanol (2) at 423.15 K.

P (kPa)	x_1	y_1
491.9	0.0000	0.0000
502.0	0.0237	0.0253
513.2	0.1314	0.1441
523.0	0.2674	0.2809
532.2	0.4212	0.4316
535.9	0.4850	0.4981
546.8	0.6957	0.7122
551.1	0.7933	0.8067
554.70	0.8671	0.8750
559.5	0.9651	0.9669
561.3	1.0000	1.0000

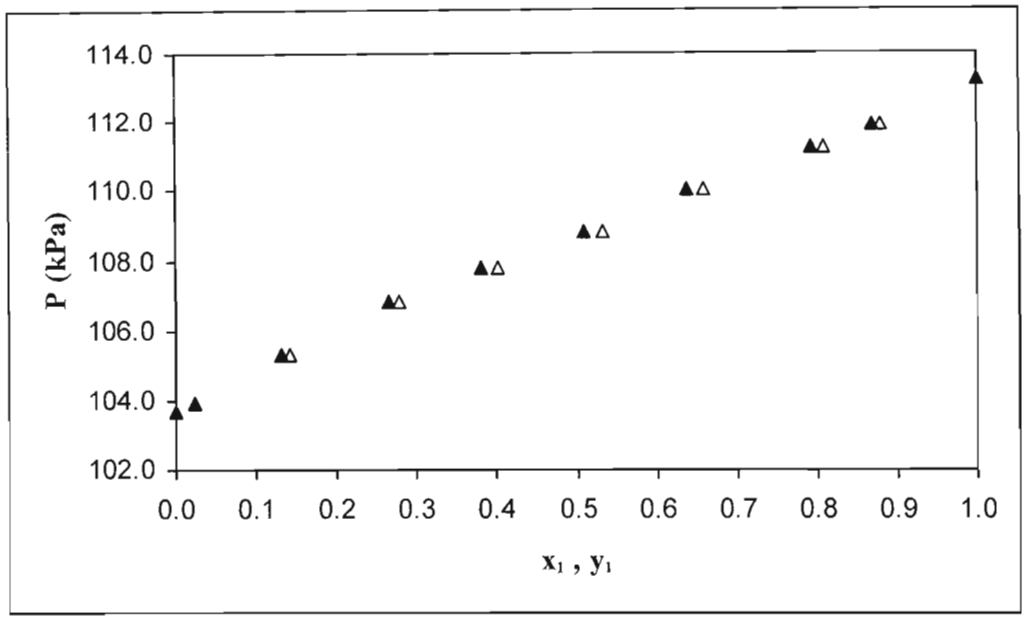

Figure 7.14. P-x_1-y_1 plot for 1-propanol (1) + 2-butanol (2) at 373.15 K: ▲ experimental P-x_1 values; △ experimental P-y_1 values.

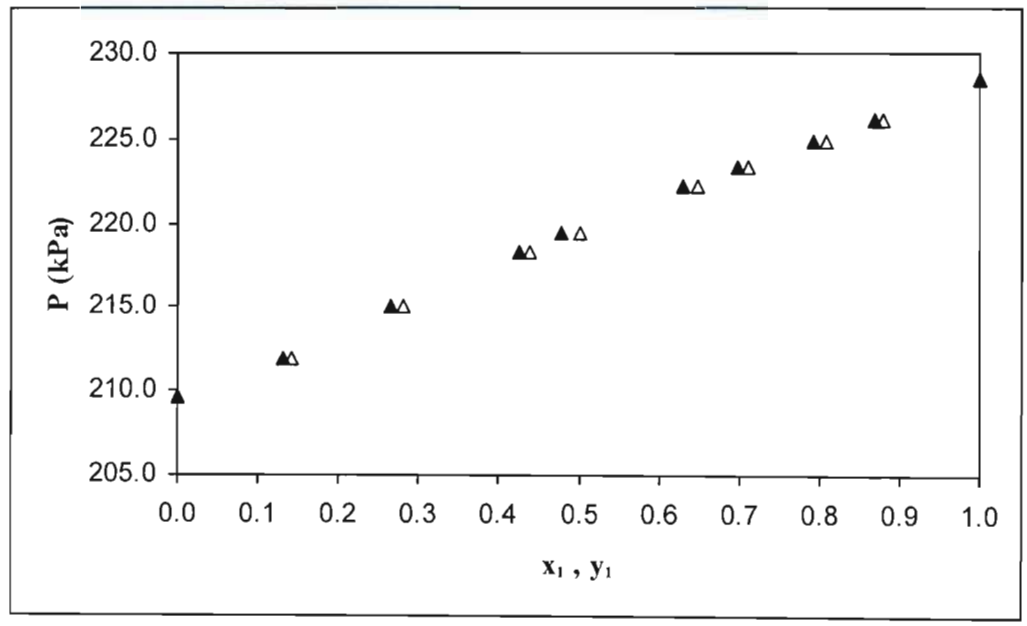

Figure 7.15. P-x_1-y_1 plot for 1-propanol (1) + 2-butanol (2) at 393.15 K: ▲ experimental P-x_1 values; △ experimental P-y_1 values.

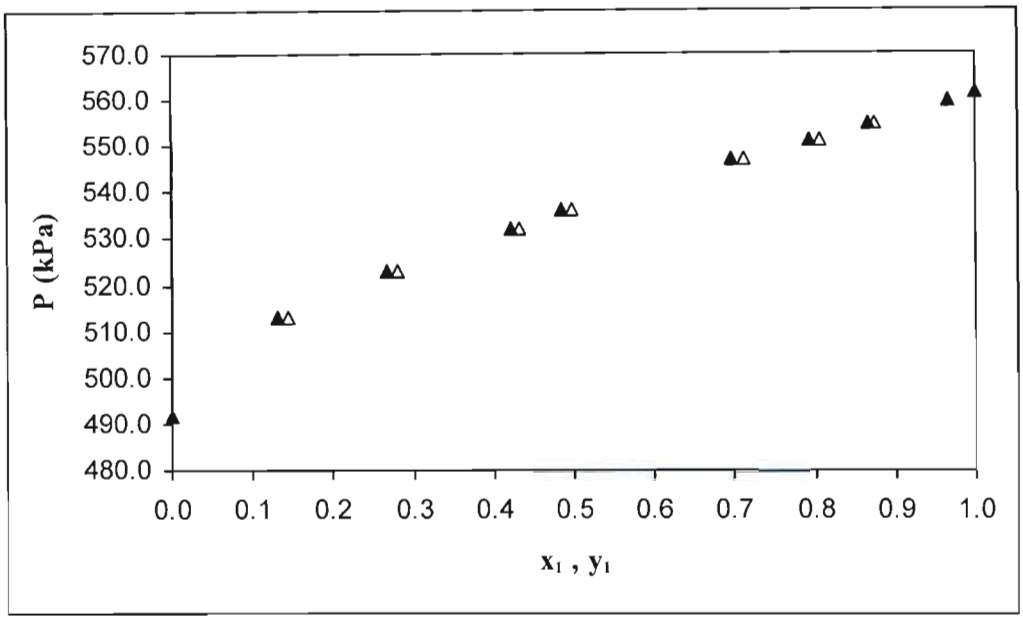

Figure 7.16. P-x_1-y_1 plot for 1-propanol (1) + 2-butanol (2) at 423.15 K: ▲ experimental P-x_1 values; △ experimental P-y_1 values.

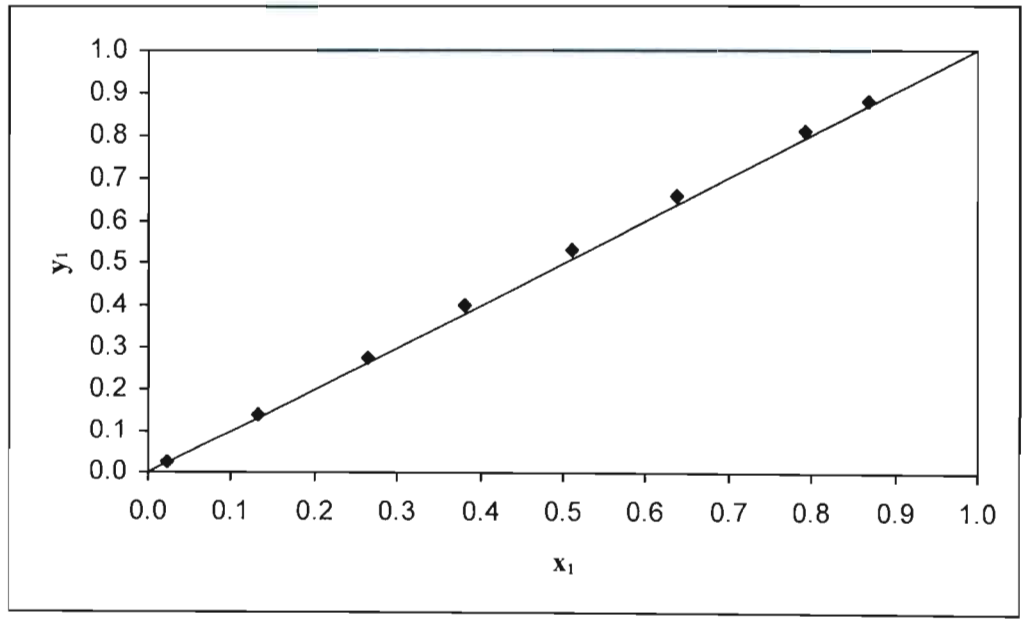

Figure 7.17. Experimental x_1-y_1 plot for 1-propanol (1) + 2-butanol (2) at 373.15 K.

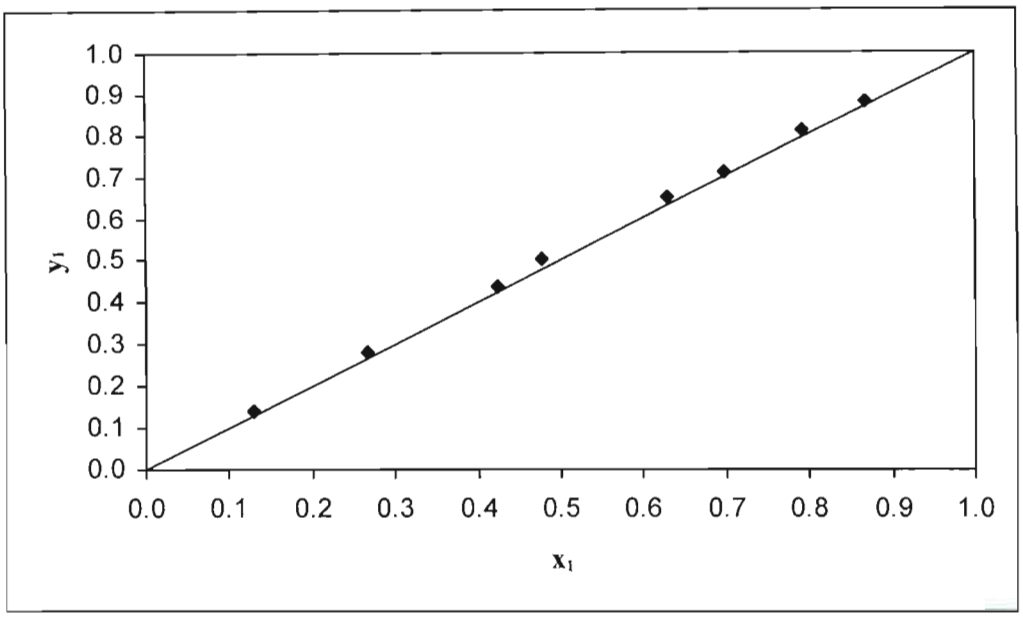

Figure 7.18. Experimental x_1-y_1 plot for 1-propanol (1) + 2-butanol (2) at 393.15 K.

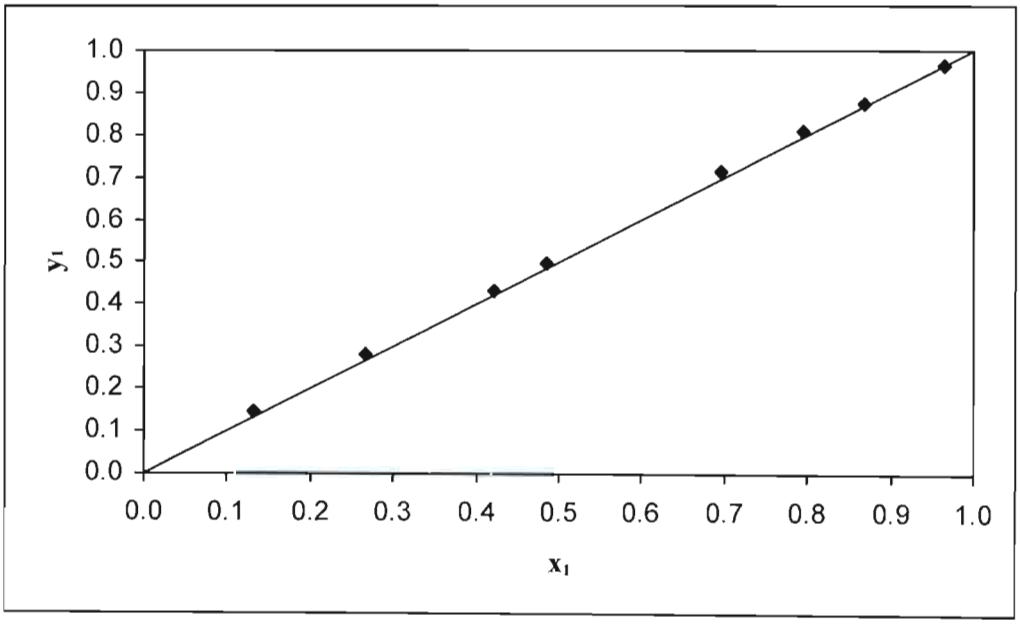

Figure 7.19. Experimental x_1-y_1 plot for 1-propanol (1) + 2-butanol (2) at 423.15 K.

7.3.3 The 1-propanol + n-dodecane system

For the 1-propanol (1) + n-dodecane (2) system, three isothermal P-x_1 sets were measured at the temperatures of 373.15 K, 393.15 K and 423.15 K. The vapour phase composition (y_1) was computed, as discussed in Chapter 8; the experimental P-x data and calculated y_1 values for these measurements are presented in Tables (7.10) - (7.12), respectively. The P-x_1-y_1 plots and the corresponding x_1-y_1 plots are shown in Figures (7.20) - (7.22) and Figures (7.23) - (7.25), respectively. All the isothermal data sets measured for this system constituted novel measurements since there were no literature data sets to compare the data with.

Table 7.10. Vapour-liquid equilibrium data for 1-propanol (1) + n-dodecane (2) at 373.15 K.

P (kPa)	x_1	y_1^{calc}
2.04	0.0000	0.0000
93.3	0.0611	0.9771
97.1	0.1104	0.9795
102.9	0.2058	0.9806
105.1	0.2668	0.9809
107.5	0.3637	0.9811
109.3	0.4860	0.9812
110.2	0.5512	0.9813
110.8	0.6250	0.9815
110.9	0.6407	0.9815
111.6	0.7277	0.9818
112.3	0.8275	0.9826
113.2	1.0000	1.0000

Table 7.11. Vapour-liquid equilibrium data for 1-propanol (1) + n-dodecane (2) at 393.15 K.

P (kPa)	x_1	y_1^{calc}
4.95	0.0000	0.0000
180.9	0.0629	0.9703
189.0	0.0980	0.9734
200.3	0.1459	0.9750
205.4	0.1905	0.9757
211.4	0.2679	0.9763
215.4	0.3351	0.9765
217.7	0.4025	0.9767
219.9	0.4569	0.9768
222.8	0.5474	0.9769
223.9	0.6223	0.9770
224.8	0.7070	0.9772
226.5	0.8519	0.9781
228.5	1.0000	1.0000

7.3.4 The 2-butanol + n-dodecane system

Three isothermal P-x_1 data sets were obtained at temperatures of 373.15 K, 393.15 K and 423.15 K for the 2-butanol + n-dodecane system. The vapour phase compositions (y_1) were computed, as discussed in Chapter 8; the experimental P-x_1 data and calculated y_1 values for these measurements are presented in Tables (7.13) - (7.15), respectively. The P-x_1-y_1 plots and the corresponding x_1-y_1 plots are shown in Figures (7.26) - (7.28) and Figures (7.29) - (7.31), respectively. All the isothermal data sets measured for this system constituted novel measurements since there were no literature data sets to compare the data with.

Table 7.12. Vapour-liquid equilibrium data for 1-propanol (1) + n-dodecane (2) at 423.15K.

P (kPa)	x_1	y_1^{calc}
15.32	0.0000	0.0000
478.5	0.1436	0.9648
493.5	0.1865	0.9667
514.2	0.2602	0.9684
526.0	0.3364	0.9692
532.5	0.3946	0.9696
541.2	0.4885	0.9700
547.9	0.5989	0.9704
551.7	0.7286	0.9707
557.8	0.8987	0.9723
561.3	1.0000	1.0000

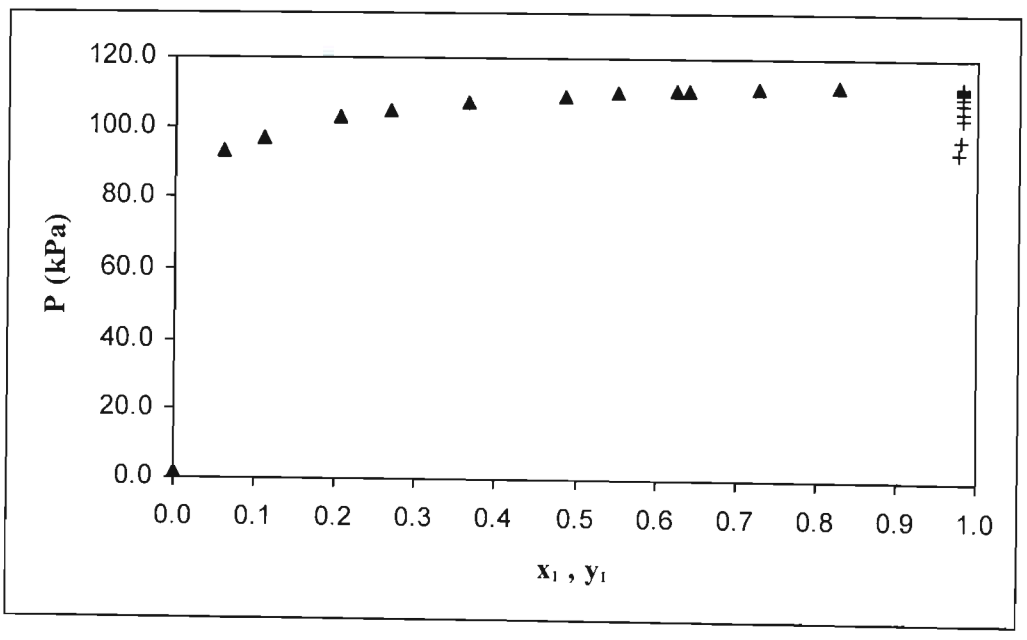

Figure 7.20. P-x_1-y_1 plot for 1-propanol (1) + n-dodecane (2) at 373.15 K: ▲ experimental P-x_1 values; + calculated P-y_1 values.

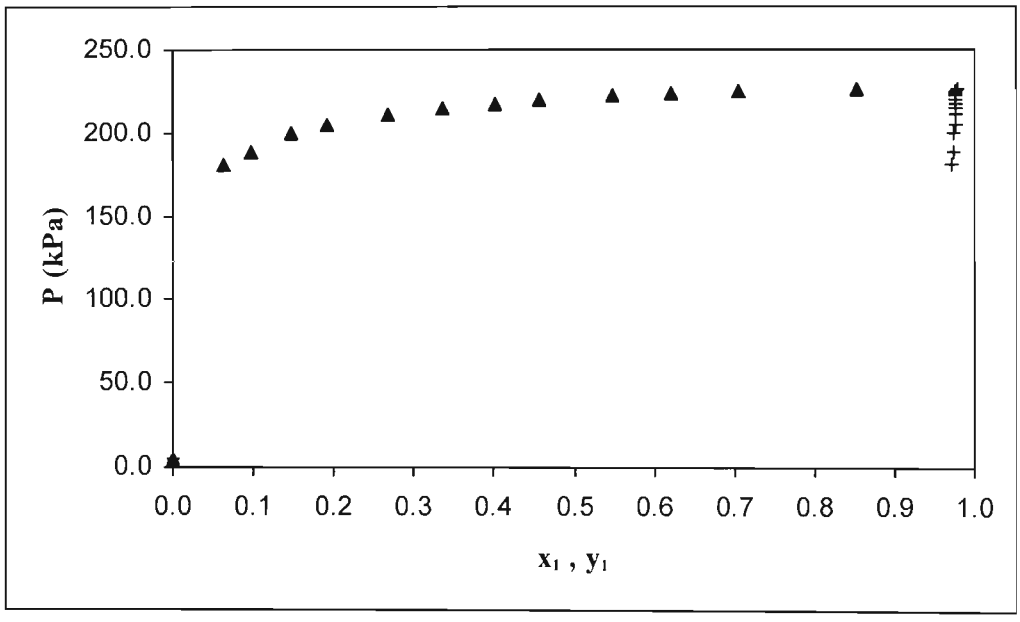

Figure 7.21. P-x_1-y_1 plot for 1-propanol (1) + n-dodecane (2) at 393.15 K: ▲ experimental P-x_1 values; + calculated P-y_1 values.

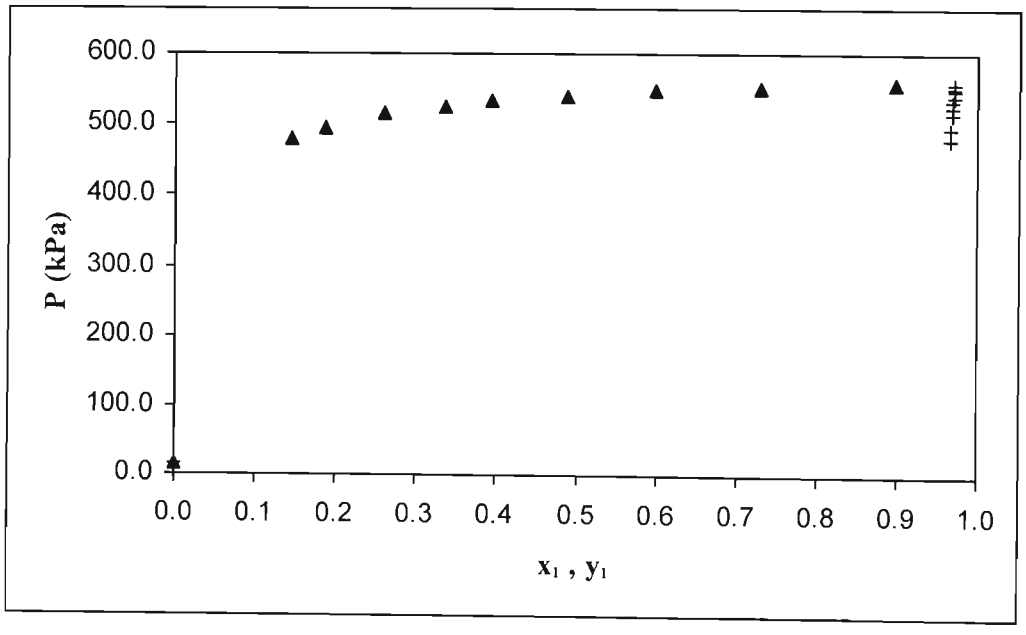

Figure 7.22. P-x_1-y_1 plot for 1-propanol (1) + n-dodecane (2) at 423.15 K: ▲ experimental P-x_1 values; + calculated P-y_1 values.

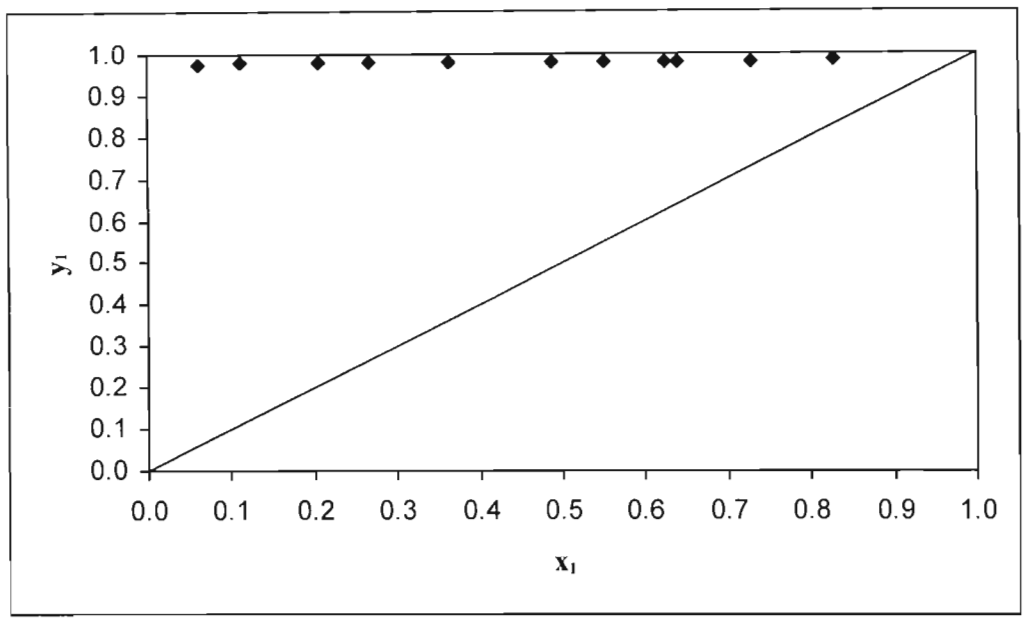

Figure 7.23. x_1-y_1 plot for 1-propanol (1) + n-dodecane (2) at 373.15 K.

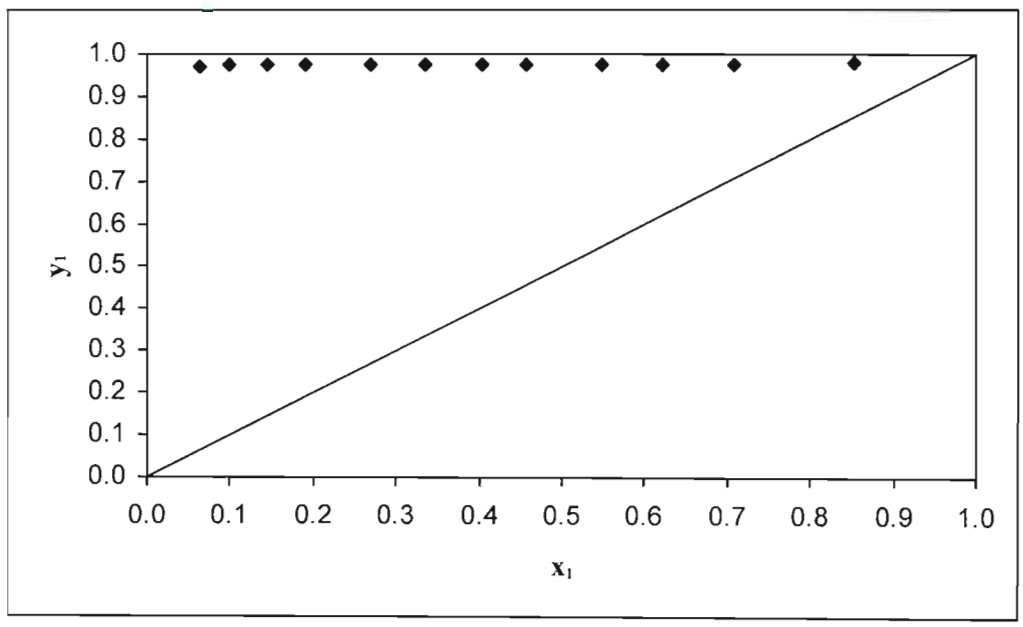

Figure 7.24. x_1-y_1 plot for 1-propanol (1) + n-dodecane (2) at 393.15 K.

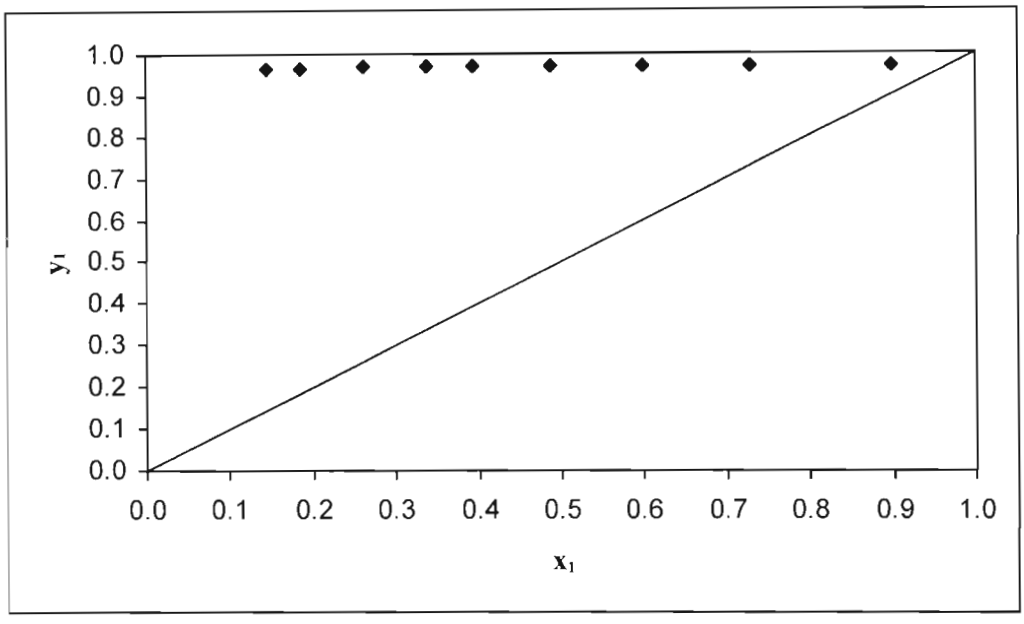

Figure 7.25. x_1-y_1 plot for 1-propanol (1) + n-dodecane (2) at 423.15 K.

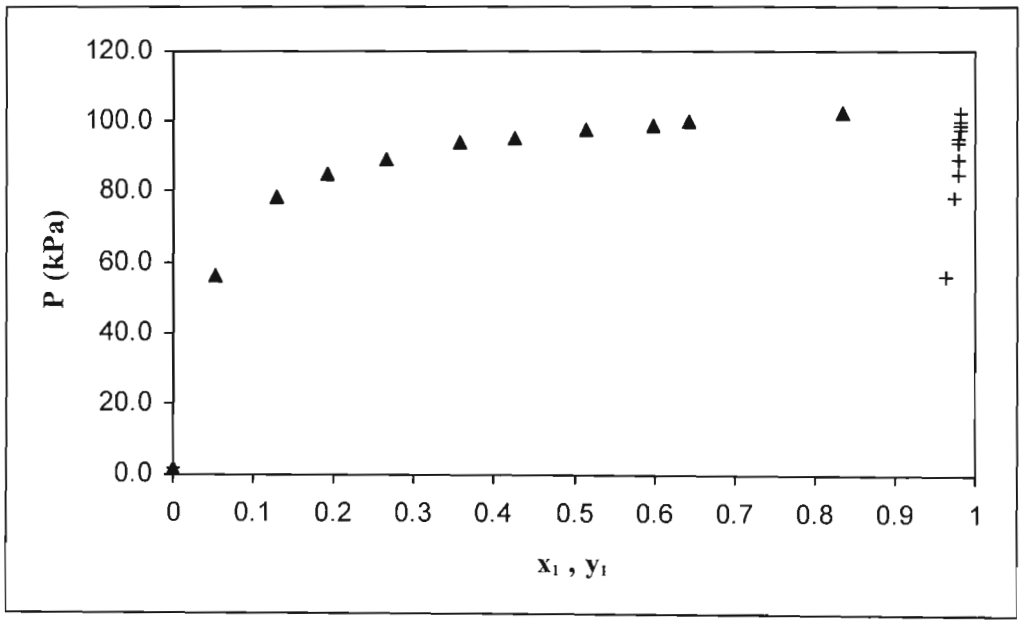

Figure 7.26. P-x_1-y_1 plot for 2-butanol (1) + n-dodecane (2) at 373.15 K: ▲ experimental P-x_1 values; + calculated P-y_1 values.

Table 7.13. Vapour-liquid equilibrium data for 2-butanol (1) + n-dodecane (2) at 373.15 K.

P (kPa)	x_1	y_1^{calc}
2.04	0.0000	0.0000
56.3	0.0522	0.9624
78.4	0.1288	0.9750
85.3	0.1924	0.9777
89.5	0.2641	0.9790
93.8	0.3577	0.9799
95.5	0.4243	0.9802
97.8	0.5157	0.9806
99.0	0.5989	0.9809
99.8	0.6427	0.9810
102.3	0.8340	0.9822
103.7	1.0000	1.0000

Table 7.14. Vapour-liquid equilibrium data for 2-butanol (1) + n-dodecane (2) at 393.15 K.

P (kPa)	x_1	y_1^{calc}
4.95	0.0000	0.0000
105.0	0.0498	0.9494
154.0	0.1344	0.9686
173.4	0.2277	0.9729
180.3	0.2739	0.9739
187.9	0.3685	0.9751
191.8	0.4332	0.9755
199.2	0.6092	0.9764
203.1	0.7317	0.9771
205.8	0.8212	0.9780
208.2	0.9073	0.9804
209.6	1.0000	1.0000

Table 7.15. Vapour-liquid equilibrium data for 2-butanol (1) + n-dodecane (2) at 423.15 K.

P (kPa)	x_1	y_1^{calc}
15.32	0.0000	0.0000
221.5	0.0828	0.9373
356.0	0.1362	0.9524
409.8	0.2268	0.9617
450.0	0.3721	0.9670
458.4	0.4561	0.9684
477.8	0.6832	0.9704
482.5	0.7301	0.9707
491.9	1.0000	1.0000

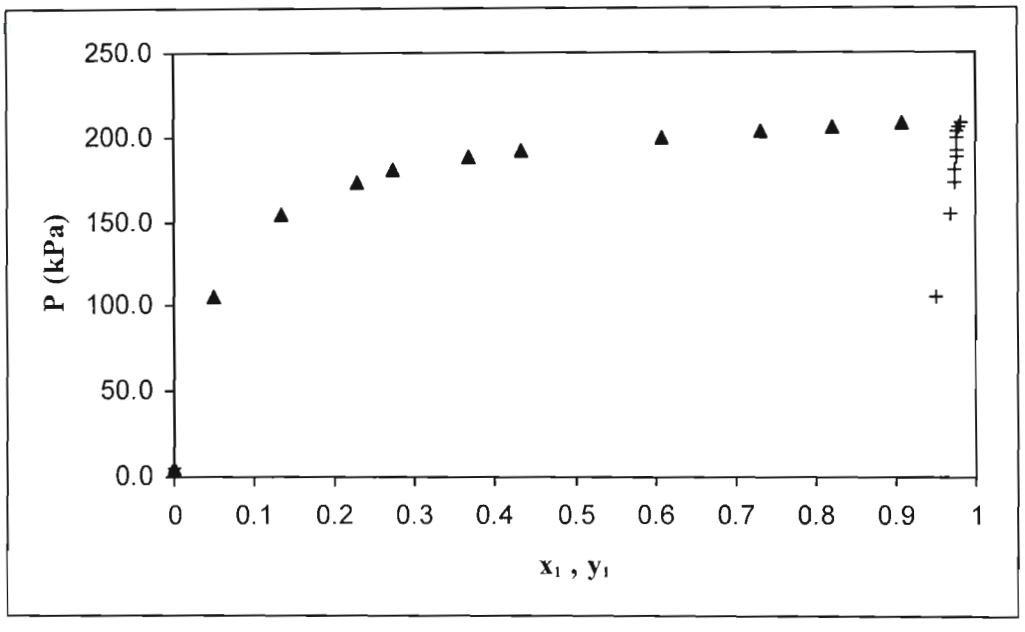

Figure 7.27. P-x_1-y_1 plot for 2-butanol (1) + n-dodecane (2) at 393.15 K: ▲ experimental P-x_1 values; + calculated P-y_1 values.

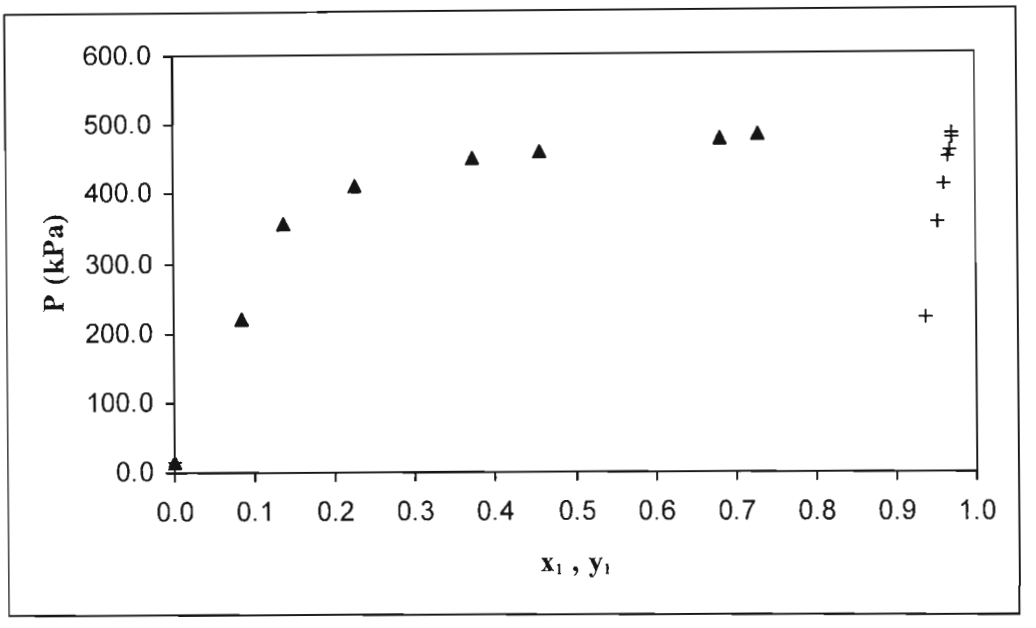

Figure 7.28. P-x_1-y_1 plot for 2-butanol (1) + n-dodecane (2) at 423.15 K: ▲ experimental P-x_1 values; + calculated P-y_1 values.

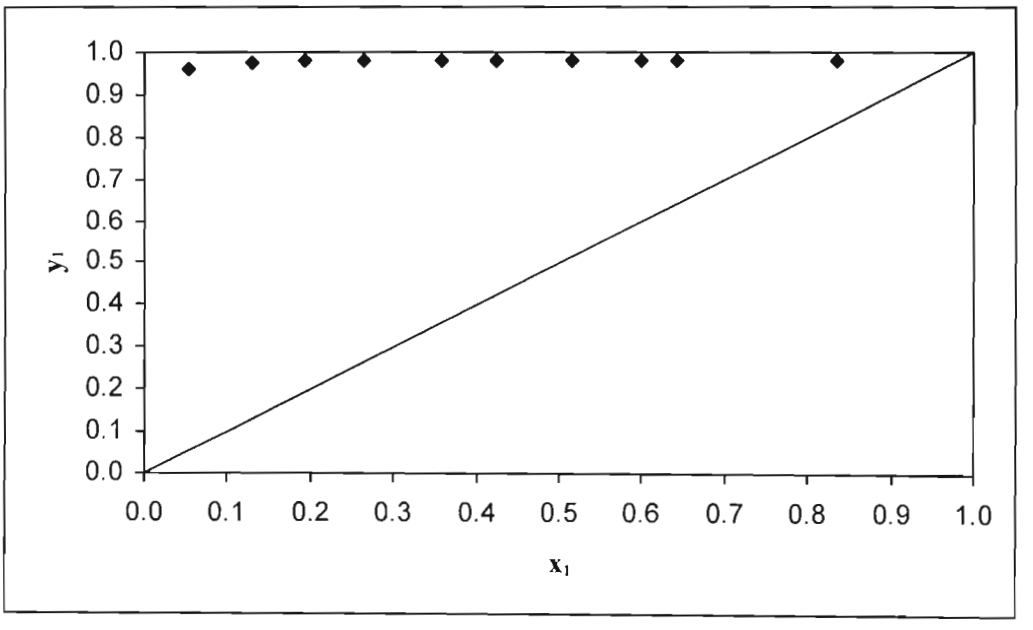

Figure 7.29. x_1-y_1 plot for 2-butanol (1) + n-dodecane (2) at 373.15 K.

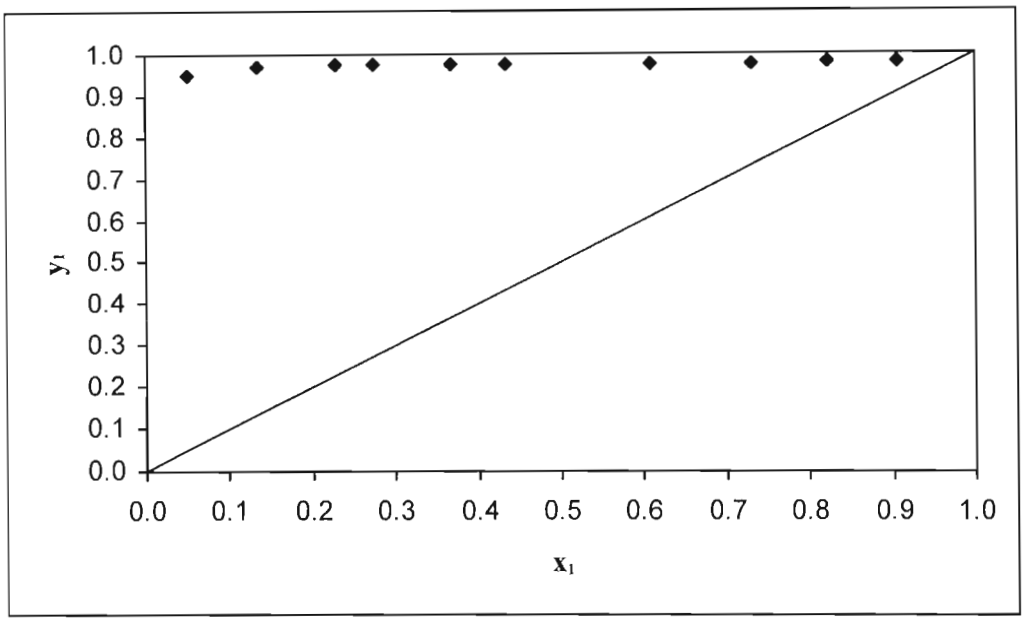

Figure 7.30. x_1-y_1 plot for 2-butanol (1) + n-dodecane (2) at 393.15 K.

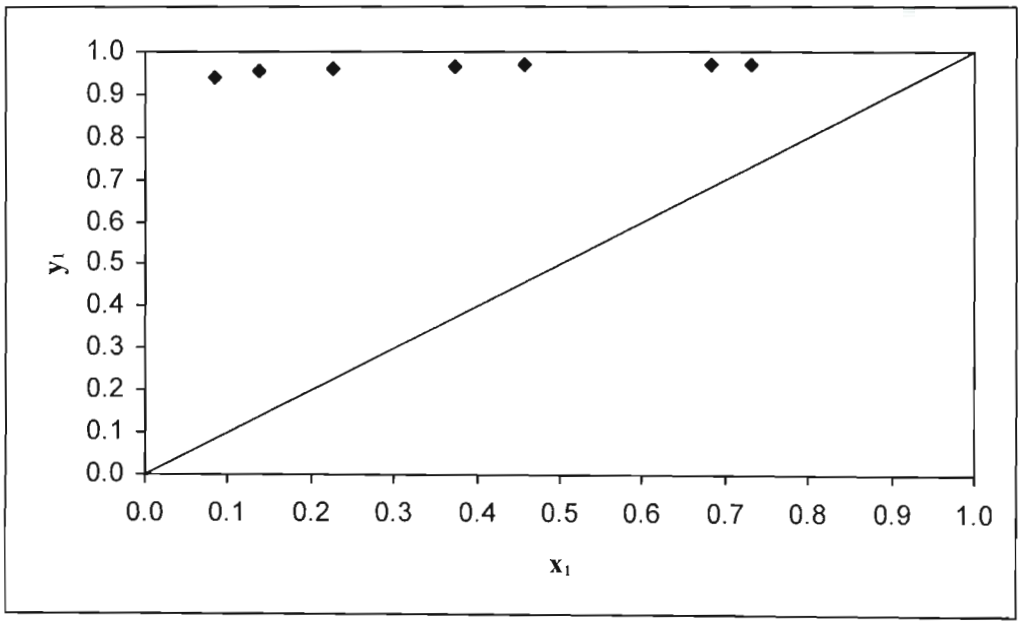

Figure 7.31. x_1-y_1 plot for 2-butanol (1) + n-dodecane (2) at 423.15 K.

7.4 Conclusion

The results for the pure component vapour pressure and the binary vapour-liquid equilibrium data measurements have been presented. The raw experimental results will be subjected to rigorous data fitting procedures to correlate and validate the various data sets with a variety of thermodynamic models in Chapter 8.

CHAPTER 8

DISCUSSION

8.1 Introduction

An effective interpretation and analysis of the data presented in Chapter 7 is achieved through the judicious employment of the rigourous thermodynamic framework for both the correlation of the experimental data with thermodynamic models and the testing of the quality of the data with thermodynamic consistency tests. The procedures for the above have been discussed at great length in Chapter 3 and the results of the application of these procedures, together with critical analyses of the results, are presented in this Chapter.

The treatment of vapour pressure measurements is inherently less complex than that for binary or multicomponent phase equilibria since it is a pure component thermodynamic property. In the regression of the vapour pressure data, a variety of vapour pressure correlating equations in the form of the Antoine, Cox, Wagner, Frost-Kalkwarf and modified Frost-Kalkwarf relations were employed for this purpose. The thermodynamic consistency testing of the vapour pressure data comprised the graphical treatment of the DIPPR Compilation Project (Daubert and Jones, 1990) in which the data set was examined for thermally-induced decomposition or polymerization.

The treatment of binary vapour-liquid equilibrium data, which comprises the bulk of this chapter, was achieved through a variety of thermodynamic models in the form of G^E correlating equations, equations of state and associated mixing rules. Correlation of the data was achieved through the use of both the gamma-phi $(\gamma_i - \phi_i)$ and phi-phi $(\phi_i - \phi_i)$ computations of the equilibrium condition for the relevant systems.

In the $\gamma_i - \phi_i$ approach, the B-truncated virial equation of state was used for the treatment of the vapour phase and the local composition G^E correlating equations (Wilson, T-K Wilson, NRTL, UNIQUAC and modified UNIQUAC equations) were used for the representation of the liquid phase nonideal behaviour. The Wilson equation was employed for the computation of the vapour phase composition and the simultaneous regression of the P-T-x data for the alkanol + n-dodecane systems.

In the $\phi_i - \phi_i$ computations, the cubic EOS/$\left(A^E \text{ or } G^E\right)$ approach was used where the Peng-Robinson-Stryjek-Vera or PRSV equation of state was combined with the Huron-Vidal, MHV1 and MHV2 mixing rules and the Wilson G^E model for the treatment of selected isothermal measurements. The correlating efficiency of the various G^E equations and local composition mixing rules could then be effectively assessed for the representation of the relevant systems in the $\gamma_i - \phi_i$ and $\phi_i - \phi_i$ approaches, respectively.

In a broader context, the results from the $\gamma_i - \phi_i$ and $\phi_i - \phi_i$ correlations could be employed for comparing the relative efficiencies of the $\gamma_i - \phi_i$ and $\phi_i - \phi_i$ approaches on the basis of the fit of the experimental data to the thermodynamic models in both approaches. Thermodynamic consistency testing of P-T-x-y data is an invaluable exercise that provides a wealth of information on the quality of the data set that cannot be provided by other theoretical treatments. The thermodynamic consistency testing of the P-T-x-y data measured in this study was performed with the Direct TC Test of Van Ness (1995).

The details of the computational procedures for the data treatment were disseminated in great detail in Chapter 3 and as such, will not be reproduced here. The technical computing software package MATLAB® (version 7.0.1) was employed for all the computations. These were undertaken on a Sahara desktop computer with a 2.40 GHz Intel Celeron® processor and 224MB of DDR RAM. The inbuilt MATLAB® (version 7.0.1) optimization routines and associated algorithms in the form of the Nelder-Mead Simplex or Levenberg-Marquardt methods were employed for the minimization routines on the basis of computational and correlative efficiency.

8.2 Vapour Pressure measurements

8.2.1 Comparison of experimental and literature Vapour Pressure data

The experimental vapour pressures of cyclohexane, n-heptane, n-octane, ethanol and 1-propanol have been presented in Chapter 7, together with the comparative plots with the literature values which were obtained from the Dortmund Data Bank (1999) for all the compounds except for 1-propanol, where the literature data was extracted from Riddick *et al.* (1986). The deviations plots for the comparison of the experimental and literature vapour pressure data sets are shown in Figures (8.1) - (8.5).

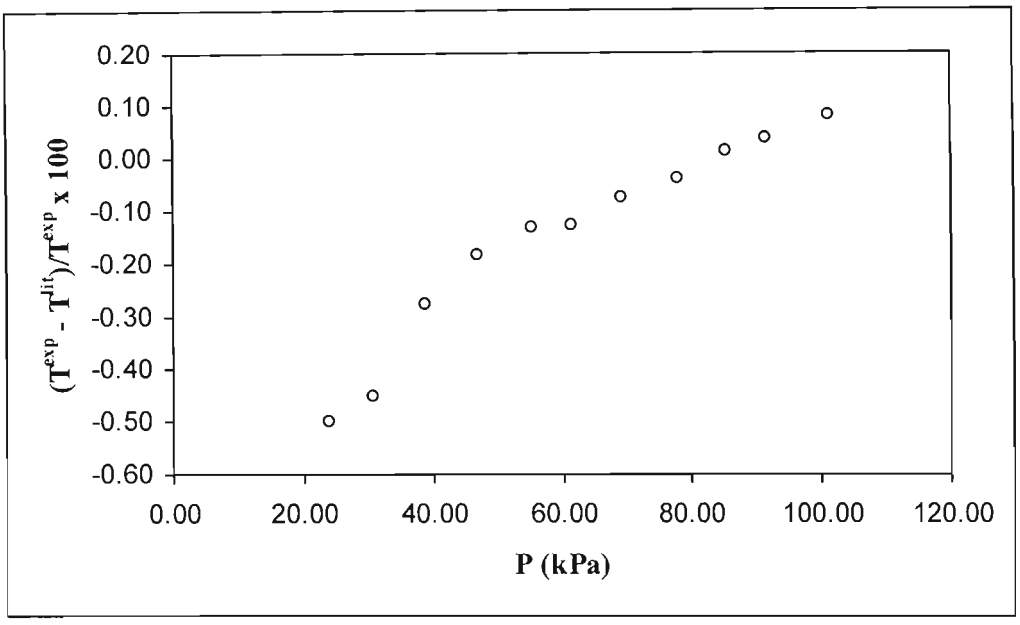

Figure 8.1. Deviation plot for the comparison of the experimental and literature vapour pressures for cyclohexane.

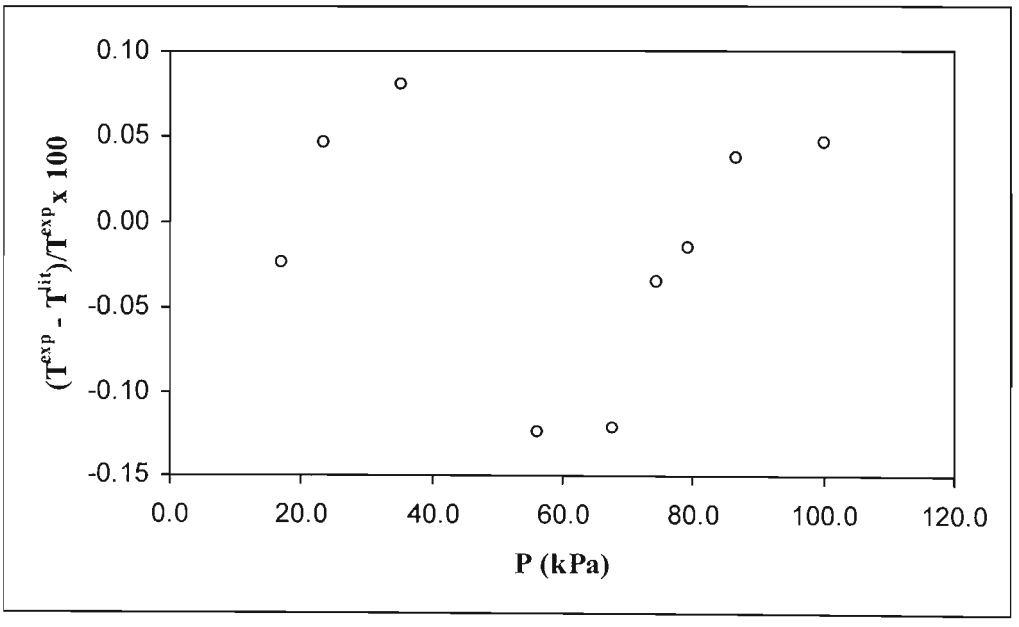

Figure 8.2. Deviation plot for the comparison of the experimental and literature vapour pressures for n-heptane.

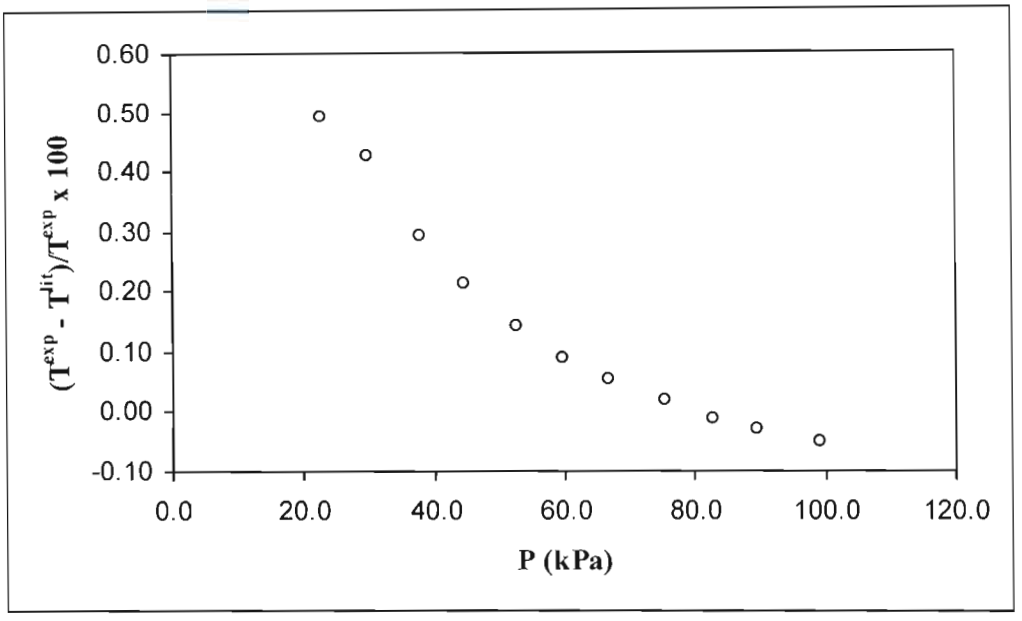

Figure 8.3. Deviation plot for the comparison of the experimental and literature vapour pressures for n-octane.

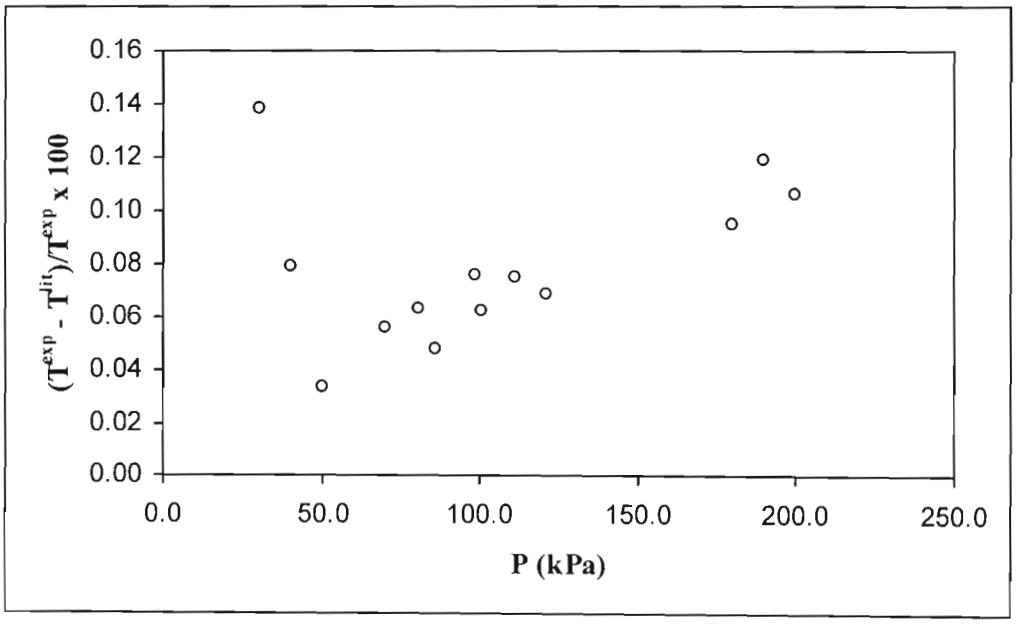

Figure 8.4. Deviation plot for the comparison of the experimental and literature vapour pressures for ethanol.

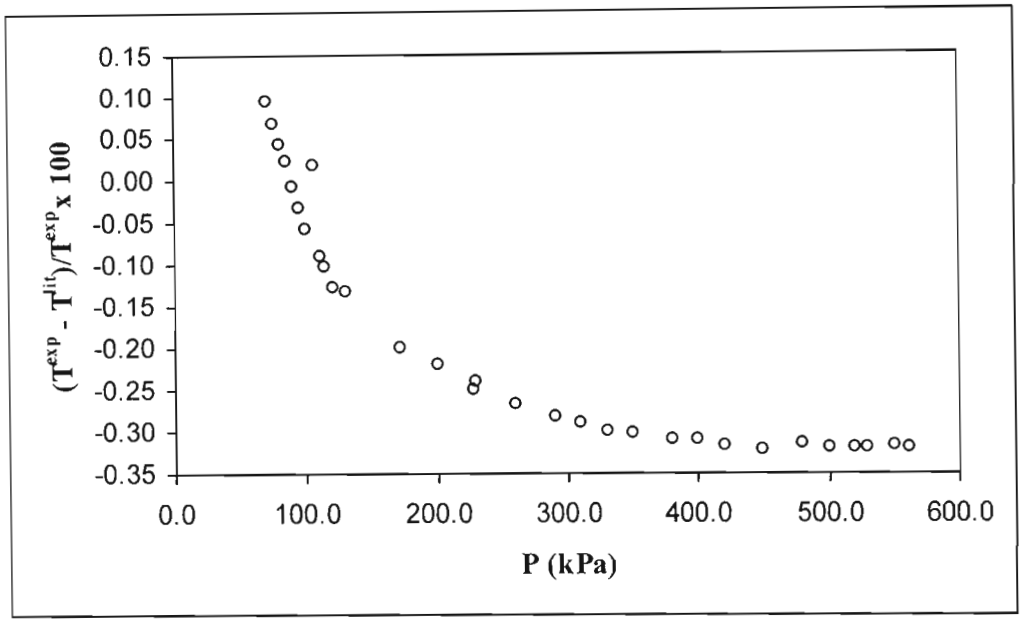

Figure 8.5. Deviation plot for the comparison of the experimental and literature vapour pressures for 1-propanol.

Inevitably, the existence of scatter observed in the deviation plots is to be expected since the Antoine coefficients in literature sources have in most instances been obtained from the regression of experimental measurements for a limited data range or from extrapolative procedures (Malanowski and Anderko, 1992). Also, the inefficiencies of the model and the statistical method employed for the correlation of the data contribute to differences between the experimental and literature values.Consequently, as mentioned in Chapter 2, one has to exercise caution when using vapour pressure correlations with coefficients that have been obtained for a limited experimental data range and which have to be used across a wider range.

The Dortmund Data Bank (Gmehling, 2003) is one of the world's largest databases for pure component thermophysical properties and mixture phase equilibria (VLE, LLE, *etc.*) and serves universities, research institutes and the relevant industries. Consequently, many researchers can confidently advocate the use of thermophysical property data from the databank as literature data with which to compare one's experimental measurements. However, for the literature vapour pressure correlation constants of 1-propanol, considerable discrepancies were observed between the experimental vapour pressure data measured in this study and that predicted by the Antoine constants obtained from the Dortmund Data Bank (1999) and this was indeed quite prominent at higher pressures. Alternative literature sources were then consulted (Hirata *et al.*, 1975; Riddick *et al.*, 1986; Reid *et al.*, 1987) and it was quite surprising to find a great deal of scatter being exhibited in vapour pressure predictions for the 1-propanol vapour pressures for

the range measured in this study with the correlation constants from the various literature sources. The data of Riddick *et al.* (1986) was selected for comparative purposes only and it was decided that the validation of the correctness of the data set would rather be achieved through consistency testing and the fit of the data to the models, as to be dealt with in the sections to follow.

The absolute average deviations (AAD) for a comparison of experimental and literature quantities can be represented as follows:

$$AAD = \left(\frac{1}{n} \sum_{i=1}^{n} |\Delta T| \right) \tag{8.1}$$

where n is the number of data points and ΔT is the difference between the experimental and the literature values for the boiling point temperature. The AAD values for the boiling point temperatures measured in this study are shown in Table 8.1.

From the AAD values and the visual inspection of the deviation plots in Figures (8.1) - (8.5), there is excellent comparison of the experimental results with the literature values. However, in the curves for n-octane and 1-propanol, it does seem that there is some systematic deviation of the measured vapour pressure curve from that of the predicted curve. It is unlikely that this is as a result of the experimental apparatus or the procedure as the curves for n-heptane and ethanol confirm this. In the event of the existence of a systematic error in the experimental procedure (which was unchanged for all the vapour pressure measurements) this would have been observed for all the measurements. In fact, such non-random scattering is evident in vapour pressure determinations conducted by other researchers (Chirico *et al.*, 1989; Morgan and Kobayashi, 1994; Mokbel *et al.*, 2000). The above can probably be attributed to the fitting procedure and the inherent mathematical limitations of the vapour correlating equations in displaying a bias when attempting to correctly reproduce the shape of the vapour pressure curve.

In a comparison of the deviation plots above for the vapour pressures that have been measured with this VLE apparatus with those measured with the apparatus of Harris (2004), as shown in Chapter 4, it can clearly be observed that for analogous temperature and pressure ranges, a great improvement in the results were obtained in this study. This was complemented by the excellent and rapid approach of the system to the "plateau region" for the pure component vapour pressure measurements. As opposed to vapour pressure measurements with the apparatus of Harris, the system behaviour with the novel apparatus presented here was largely unaffected for operation at elevated temperatures.

Table 8.1. Absolute average deviations (AAD) for the boiling point temperatures.

Compound	AAD (K)	Temperature range(K)
Cyclohexane	0.17	312.78 - 353.78
n-Heptane	0.06	320.43 - 371.21
n-Octane	0.17	352.83 - 397.87
Ethanol	0.08	323.82 - 369.75
1-Propanol	0.27	360.86 - 423.16

8.2.2. Correlation of Vapour Pressure data

The fitting of the experimental data to a variety of thermodynamic models is a very fruitful exercise (especially with accurate vapour pressure data) as it allows for comparison of the correlating efficiency of the models. As mentioned, the models employed for the data correlation were the Antoine, Cox, Wagner, Frost-Kalkwarf and modified Frost-Kalkwarf or Frost-Kalkwarf (mod) relations. The applicability of these models in representing the vapour pressures of pure components was discussed in Chapter 2. In the fitting procedures of the experimental measurements with the various correlations, the units used for pressure and temperature were kilopascals (kPa) and Kelvins (K), respectively. The fits of the data to the various models, which were discussed at length in Chapter 3, are shown in Tables (8.2) - (8.6).

The percentage standard deviation (s_r) is a measure of the success of the overall fit of the data to the model (Ruzicka *et al.*, 1998) and is obtained as follows:

$$s_r = 100\sqrt{\left(\sum_{i=1}^{n}\left[\frac{\left(P^{exp} - P^{lit}\right)}{P^{exp}}\right]_i^2\right)\left(\frac{1}{n-m}\right)} \qquad (8.2)$$

where P^{exp} is the experimental vapour pressure value, P^{lit} is the value that is predicted by the model, n is the number of experimental values in the data set and m is the number of adjustable parameters in the correlating model. Discussion of the relative correlative and computational efficiencies of the models is presented in Appendix D.

Table 8.2. Model parameters and % standard deviation (s_r) values for cyclohexane vapour pressures.

	Vapour Pressure correlation model				
	Antoine	**Cox**	**Frost-Kalkwarf**	**Frost-Kalkwarf (mod)**	**Wagner**
A	14.0323	2.55462	76.0210	143.728	-4.203655
B	2914.80	-5.13332×10^{-4}	6668.88	8733.90	-4.973066
C	-44.1604	-2.16821×10^{-6}	-8.97231	-20.0177	5.87342
D	-	-	127.586	2.44148×10^{-5}	-18.9153
s_r	0.15	0.21	0.12	0.13	0.14

Table 8.3. Model parameters and % standard deviation (s_r) values for n-heptane vapour pressures.

	Vapour Pressure correlation model				
	Antoine	**Cox**	**Frost-Kalkwarf**	**Frost-Kalkwarf (mod)**	**Wagner**
A	13.2147	2.66105	54.6982	115.482	-12.5936
B	2548.15	-7.57716×10^{-4}	6154.01	8439.76	13.4137
C	-75.2090	1.04807×10^{-7}	-5.66142	-15.1694	-23.7458
D	-	-	-23.0439	1.17068×10^{-5}	49.5170
s_r	0.74	0.82	0.70	0.74	0.71

Table 8.4. Model parameters and % standard deviation (s_r) values for n-octane vapour pressures.

	Vapour Pressure correlation model				
	Antoine	**Cox**	**Frost-Kalkwarf**	**Frost-Kalkwarf (mod)**	**Wagner**
A	13.7901	2.80160	29.8702	104.075	-9.87613
B	2999.09	-1.01810×10^{-3}	5449.90	8618.60	6.61180
C	-71.6584	-3.52912×10^{-7}	-1.92301	-13.2320	-14.7592
D	-	-	-103.585	8.79009×10^{-6}	-32.8455
s_r	0.16	1.23	0.12	0.16	0.12

Table 8.5. Model parameters and % standard deviation (s_r) values for ethanol vapour pressures.

	Vapour Pressure correlation model				
	Antoine	**Cox**	**Frost-Kalkwarf**	**Frost-Kalkwarf (mod)**	**Wagner**
A	15.4389	2.93175	47.8661	119.284	-12.7830
B	2961.81	-8.54440×10^{-5}	6948.48	9384.48	11.2544
C	-77.6891	-7.58522×10^{-5}	-4.21789	-15.2102	-26.6361
D	-	-	-36.5759	9.72231×10^{-6}	76.5171
s_r	0.56	0.53	0.51	0.54	0.49

Table 8.6. Model parameters and % standard deviation (s_r) values for 1-propanol vapour pressures.

	Vapour Pressure correlation model				
	Antoine	**Cox**	**Frost-Kalkwarf**	**Frost-Kalkwarf (mod)**	**Wagner**
A	15.5289	2.90243	79.9898	120.340	-6.15356
B	3100.82	-6.73404×10^{-5}	8504.16	10015.1	-4.65526
C	-86.0541	-3.99627×10^{-5}	-8.86185	-15.1917	0.910400
D	-	-	10.1231	8.56478×10^{-6}	-28.9584
s_r	0.34	0.61	0.33	0.33	0.34

In general, the correlations performed quite well for the hydrocarbons in the $P \leq 100$ kPa pressure range, with very little discrepancies in the relative fits of the experimental data for all the models except the Cox equation, which was outperformed by the other models on all occasions. Modelling of the alkanols in the form of ethanol and 1-propanol from Tables (8.5) and (8.6) revealed the relative efficiencies of these models in representing polar associating compounds for $P > 100$ kPa. As discussed in Chapter 2, the three-parameter correlating equations in the form of the Antoine, Cox and Miller relations were considered as generally not being applicable at elevated pressures for the latter.

In addition, the range of applicability of these equations for the correlation of associating organic compounds such as alkanols had been recommended to be diminished when compared to that for hydrocarbons *i.e.* 0 - 200 kPa versus 5 - 80 kPa, as was recommended for the Antoine equation (Malanowski and Anderko, 1992). The above generalizations are clearly not observed in the results for the percent deviations in the fits of the equations to the ethanol and 1-propanol vapour pressure data in Tables (8.5) and (8.6).These results serve to create doubt concerning the generalization that the Antoine equation is quite unsuitable for representing associating organic compounds at elevated pressures, as it is only marginally outperformed by the Wagner equation in terms of the fit of the data. However, it should be noted that comprehensive further testing of the Antoine equation at elevated pressures and with a diverse array of polar associating compounds (beyond the scope of this study) is necessary before any assertions can be made.

Surprisingly, the Cox equation which had performed poorly for the saturated hydrocarbons provided an acceptable fit. In many of the above correlations, the four-parameter equations such as the much fancied Wagner equation shows marginal advantages over the other methods with the Frost-Kalkwarf and modified Frost-Kalwarf relation also performing quite well. However, as mentioned in Chapter 3, the Frost-Kalkwarf equation cannot be solved explicitly for pressure and involves iterative calculations and the modified Frost Kalkwarf equation, as discussed in Appendix D, is not the most computationally efficient method and its success is highly dependent upon the input of suitable initial estimates for the adjustable parameters.

Consequently, the general performance of the Antoine equation and unexpected accuracy in the representation of 1-propanol demonstrates why this correlation remains a popular choice amongst researchers for correlating vapour pressures at low to moderate pressures.

8.2.3. Thermodynamic Consistency testing of the Vapour Pressure data

A qualitative thermodynamic consistency test of experimental data was recommended by researchers in the DIPPR Compilation Project (Daubert and Jones, 1990) and was described in Chapter 2. In this test, the experimental data are represented in the form of a $\ln P$ versus $\frac{1}{T}$ plot. This test allows for a visual means for detecting the occurrence of decomposition or polymerization with an increase in temperature. If the slope of the plot is observed to increase significantly with an increase in temperature, thermal decomposition is indicated. Conversely, a decrease in the slope indicates polymerization.

This test is quite pertinent to both alkanes and alkanols. The tendency for alkanes (especially higher alkanes) to undergo thermally-induced decomposition is well documented by many researchers (*e.g.* Morgan and Kobayashi, 1994). Alcohols, on the other hand, exhibit the propensity for thermally-induced polymerization (Joyce *et al.*, 1999) due to their hydrogen-bonding capability facilitating the formation of chain associates. One has to be careful in employing the use of these plots as they can sometimes be misleading as random scattering can create false conclusions therefore it is advisable to use this test over an extended pressure range to allow for a proper assessment. Consequently, in this work, the 1-propanol vapour pressures were chosen for this qualitative thermodynamic consistency test. The appropriate plot is shown in Figure 8.6.

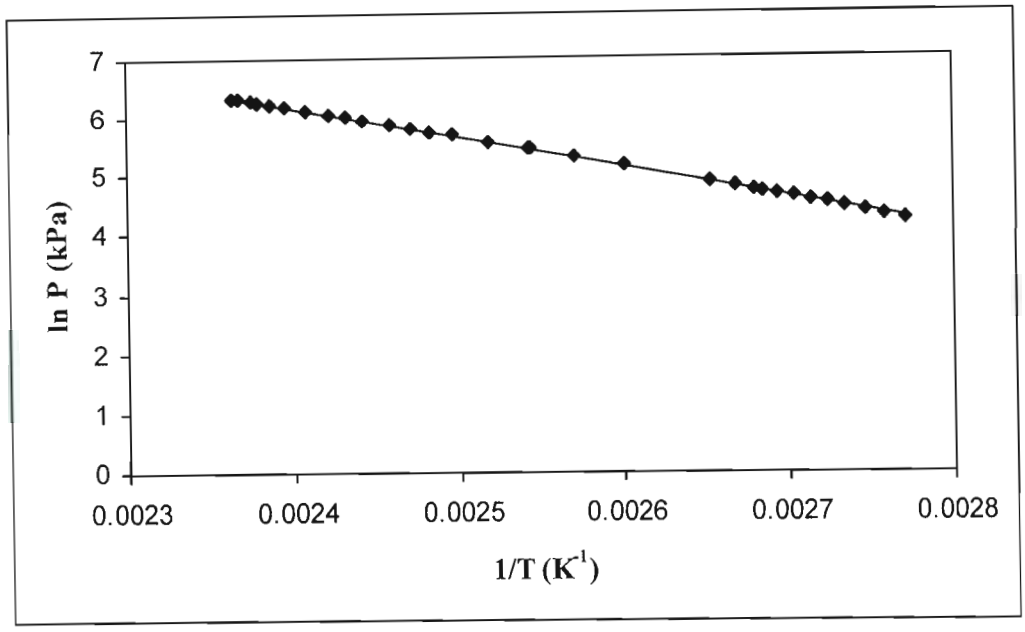

Figure 8.6. Plot of ln P versus inverse temperature (1/T) for the experimental vapour pressures of 1-propanol.

It can clearly be observed from the plot that the slope is quite linear across the entire pressure range hence it is highly unlikely that thermally-induced decomposition or polymerization could have occurred for 1-propanol. This indicates the ability of the apparatus to accurately measure pure component vapour pressures over an extended pressure and temperature range.

The measurement of vapour pressures over extended pressure ranges is an invaluable exercise as the regression of the experimental P-T data yields correlation constants that can be used with much greater confidence than those obtained by mathematical treatments such as extrapolations. This was clearly observed in the case of the available vapour pressure literature correlation constants for 1-propanol versus the experimental measurements obtained in this study. For the latter, the excellent fit of the data to the models and the thermodynamic consistency of the data serve as validation of the accuracy of the measurements. It is therefore important for contemporary researchers to ensure that experimental measurements are obtained for extensive pressure and temperature ranges so that experimentally-derived vapour correlation constants can be obtained as the latter are an integral part of a successful vapour-liquid equilibrium correlation in both the γ_i - ϕ_i and ϕ_i - ϕ_i computations of the equilibrium condition.

The investigation of vapour pressures is an integral prerequisite in the use of the apparatus for the measurement of mixture phase equilibrium. It serves to test the efficiency of the dynamic recirculating LPVLE apparatus in key or fundamental aspects of its operation such as the

operation of the reboiler (boiling of the mixture), Cottrell tube (continuity of the pumping action), the internal flow patterns of the phases in the still (sample traps and return lines), temperature and pressure control as well as the calibrations of the sensors. Once confidence has been established with the above, the researcher can then proceed onto the measurement of mixture VLE data and to be confronted by a spectrum of new potential challenges.

8.3 Vapour-Liquid Equilibrium measurements

8.3.1 Comparison of experimental and literature VLE data

The most pragmatic starting point in the measurement of phase equilibrium data with a novel apparatus is to proceed with the study of an appropriate test system. In this regard, the selection of cyclohexane + ethanol as a test system was considered as being suitable since VLE measurements would primarily be obtained for alkanol + hydrocarbon systems.

The experimental and literature data sets are presented on the same set of axes in Figure 7.6. In the comparison of the experimental results with those of Joseph (2001), good agreement between the two data sets was observed. However, in the cyclohexane-rich region, there are slight differences between the two data sets for the T-x_1 points in this region, where the data obtained in this study was observed to provide a smoother T-x_1 curve. With regards to the credibility of the data source, it should be mentioned that the data set was successfully screened for thermodynamic consistency by the author (Joseph, 2001). The remaining data sets measured in this study constituted novel measurements and consequently could not be compared against literature measurements to assess the accuracy of the measured data; for which thermodynamic consistency testing could be employed for the P-T-x-y data sets.

8.3.2 Correlation and computation of VLE data

The experimental VLE data sets in this study were fitted to thermodynamic models through the use of both the gamma-phi $(\gamma_i - \phi_i)$ and phi-phi $(\phi_i - \phi_i)$computations of the equilibrium condition. Both these methods were discussed in great detail in Chapter 3; together with the fitting procedure employed for the determination of the optimal adjustable parameters for the models quantifying the phase nonidealities. The $\gamma_i - \phi_i$ and $\phi_i - \phi_i$ computations will be dealt with separately due to the inherent differences between the methods and to also facilitate a comparison of the two methods. Due to difficulties and perhaps apparatus limitations in measurement of reliable vapour phase compositions (y), only P-T-x measurements were

obtained for the very high relative volatility 1-propanol + n-dodecane and 2-butanol + n-dodecane systems, where the γ_i - ϕ_i method was used to compute the vapour phase. The ϕ_i - ϕ_i method with the cubic EOS (A^E or G^E) approach was used for correlating selected isothermal measurements for the alkanol + alkanol and the alkanol + n-dodecane systems.

8.3.2.1 The Gamma-Phi (γ_i - ϕ_i) Method

The γ_i - ϕ_i method with the B-truncated virial EOS is applicable to the computation and the modelling of the vapour-liquid equilibria of subcritical components for low to moderate pressures. Consequently, this approach was suitable for the treatment of all the VLE measurements conducted in this study. The most distinct attribute of this method is its excellent representation of highly non-ideal mixtures consisting of polar and polar associating components through the flexible framework of empirical or semi-theoretical G^E models, which explicitly express the compositional dependence of the liquid phase nonidealities.

In this study, only local composition semi-theoretical G^E models were chosen for the representation of the liquid phase in the form of the Wilson, T-K Wilson, NRTL and modified UNIQUAC or UNIQUAC (mod) models. These models have demonstrated great success in the correlation of the liquid phase nonideal behaviour and due to the semi-theoretical nature of the model, the parameters have physical significance beyond the data set for which they are obtained and these can be used for the prediction of multicomponent phase equilibrium. In the treatment of the vapour phase, the B-truncated virial equation of state was employed for the computation of the pure component and mixture fugacity coefficients. The virial coefficients were obtained through the method of Hayden and O'Connell (1975), as described by Prausnitz *et al.* (1980).

There were two types of computations employed for the treatment of the data *i.e.* BUBL P and BUBL T calculations. For the isothermal measurements of 1-propanol + 2-butanol, the BUBL P computation was applicable, where the reduction of the data set was achieved with a simultaneous calculation of the predicted equilibrium pressures and vapour phase compositions. For the 1-propanol + n-dodecane and the 2-butanol + n-dodecane systems, the vapour phase was computed in the BUBL P procedure with the Wilson equation. In the BUBL T approach, the isobaric data sets *i.e.* the cyclohexane + ethanol systems were reduced to model parameters and the equilibrium temperatures and vapour phase compositions were calculated. The pure component properties, methods for the computation of input parameters for the BUBL P and BUBL T computations and the respective data sources are shown in Table 8.7.

Table 8.7. Input parameters and data sources for the γ_i - ϕ_i BUBL P and BUBL T methods.

Input parameter	Method	Source
Vapour pressure	Antoine equation	This work [b]
Liquid molar volume	Modified Rackett	Reid *et al.* (1987)
Virial coefficients	Hayden and O'Connell	Prausnitz *et al.* (1980)
Size and area parameters [a]	-	Prausnitz *et al.* (1980)
Critical constants	-	Reid *et al.* (1987)

[a] As required for the UNIQUAC and UNIQUAC (mod) equations.

[b] Antoine constants were regressed from the experimental vapour pressure data measured in this work.

Computation of Activity Coefficients (γ_i) and the excess molar Gibbs energy (G^E)

With the availability of a full P-T-x-y data set, a significant attribute of the γ_i - ϕ_i approach is that it allows for a direct computation of the experimental activity coefficients (γ_i) and hence the excess molar Gibbs energy (G^E), as was discussed in Chapter 3. The latter serve to quantify the departure of the thermodynamic behaviour of the individual system components and the system, respectively, from that of an ideal solution (for which $G^E = 0$). An examination of the curves of the activity coefficient and the G^E behaviour across the composition range (as a function of x_1) provides invaluable information about the behaviour of the system and a variety of shapes can be obtained in this regard (Walas, 1985).

The activity coefficients (γ_i) and excess molar Gibbs energies (G^E) computed from the experimental data are presented in Tables (8.8) and (8.9) for the cyclohexane + ethanol and 1-butanol + 2-butanol systems, respectively. The activity coefficients (γ_i) and excess molar Gibbs energies (G^E) that have been computed from the experimental P-T-x data and the calculated vapour phase compositions are presented in Tables (8.10) and (8.11) for the 1-propanol + n-dodecane and the 2-butanol + n-dodecane systems, respectively.

Table 8.8. Experimental activity coefficients (γ_i) and excess molar Gibbs energies (G^E) for cyclohexane (1) + ethanol (2).

T (K)	x_1	y_1	γ_1	γ_2	G^E (J.mol^{-1})
		P = 40 kPa			
327.21	0.0130	0.1095	8.1865	1.0150	114.3
318.50	0.1172	0.4647	5.2586	1.0445	617.0
316.88	0.1742	0.5323	4.3050	1.0607	798.3
315.97	0.2414	0.5766	3.4821	1.0965	974.9
314.80	0.5077	0.6236	1.8723	1.5980	1437.4
314.68	0.5602	0.6247	1.7078	1.7948	1457.5
314.70	0.7045	0.6368	1.3829	2.5835	1331.4
314.82	0.7427	0.6416	1.3153	2.9101	1252.2
314.81	0.7878	0.6502	1.2569	3.4467	1158.8
315.51	0.8965	0.6626	1.0951	6.5761	724.9
316.30	0.9458	0.6938	1.0535	10.9540	470.9
317.24	0.9657	0.7252	1.0397	14.8217	343.1
317.58	0.9715	0.7352	1.0341	16.9003	298.7
318.71	0.9802	0.7685	1.0258	20.1104	223.5
		P = 69.8 kPa			
340.04	0.0148	0.0991	7.2909	1.0044	95.4
335.05	0.0640	0.3085	6.1333	1.0065	340.4
331.87	0.1283	0.4119	4.5331	1.0601	675.6
330.31	0.1858	0.4815	3.8523	1.0757	851.4
329.39	0.2508	0.5233	3.1983	1.1223	1035.3
328.66	0.4236	0.5727	2.1228	1.3546	1349.4
328.53	0.5043	0.5816	1.8186	1.5522	1419.2
328.52	0.5663	0.5843	1.6275	1.7636	1425.5

Table 8.8. Experimental activity coefficients (γ_i) and excess molar Gibbs energies (G^E) for cyclohexane (1) + ethanol (2) (cont).

T (K)	x_1	y_1	γ_1	γ_2	G^E (J.mol^{-1})
		P = 69.8 kPa			
328.60	0.7148	0.5995	1.3186	2.5759	1277.5
328.59	0.7526	0.6032	1.2605	2.9439	1205.7
328.67	0.7916	0.6055	1.1995	3.4621	1100.7
329.04	0.8598	0.6185	1.1131	4.8954	861.3
329.70	0.9108	0.6384	1.0594	7.0818	622.7
330.67	0.9389	0.6652	1.0347	9.1698	460.4
332.49	0.9657	0.7289	1.0343	12.2211	327.4
337.70	0.9894	0.8787	1.0207	14.1830	135.8
		P = 97.7 kPa			
343.56	0.0638	0.2742	5.8764	1.0419	432.4
340.46	0.1256	0.3872	4.6271	1.0727	718.3
338.99	0.1868	0.4527	3.8034	1.0978	917.3
337.57	0.3630	0.5270	2.3793	1.2901	1338.6
337.37	0.4298	0.5460	2.0942	1.3964	1425.2
337.28	0.5689	0.5601	1.6269	1.7977	1485.5
337.42	0.7190	0.5789	1.3235	2.6267	1326.7
337.43	0.7569	0.5803	1.2598	3.0250	1245.4
337.46	0.7742	0.5805	1.2309	3.2511	1198.1
338.06	0.8512	0.5978	1.1298	4.6145	931.5
338.78	0.9025	0.6189	1.0769	6.4790	701.5
340.73	0.9434	0.6644	1.0372	9.0767	451.3
342.82	0.9589	0.7387	1.0599	8.9618	416.0
348.82	0.9907	0.8965	1.0328	12.4399	160.6

Table 8.8. Experimental activity coefficients (γ_i) and excess molar Gibbs energies (G^E) for cyclohexane (1) + ethanol (2) (cont).

T (K)	x_1	y_1	γ_1	γ_2	G^E (J.mol^{-1})
		P = 150 kPa			
355.17	0.0679	0.2416	5.0904	1.0313	411.1
352.24	0.1314	0.3562	4.1944	1.0511	678.5
350.75	0.1945	0.4131	3.4233	1.0956	912.6
350.02	0.2439	0.4549	3.0653	1.1168	1038.1
349.44	0.3635	0.4921	2.260	1.2662	1297.4
349.21	0.5163	0.5224	1.6979	1.5833	1438.9
349.23	0.5715	0.5286	1.5507	1.7633	1433.7
349.51	0.7192	0.5542	1.2796	2.5207	1269.7
350.54	0.7993	0.5931	1.1929	3.1007	1072.9
354.19	0.9168	0.6750	1.0605	5.2289	564.0

In the computation of the γ_i values at higher pressures for the isothermal data sets of the alkanol + alkanol and alkanol + n-dodecane systems, it should be noted that the pressure dependency of the γ_i term is traditionally ignored, consequently it was proposed by Prausnitz *et al.* (1980) that a pressure adjusted γ_i be used (see Chapter 3). However, for the pressure range measured in this study *i.e.* low to moderate pressures, the measured γ_i values can be largely considered independent of pressure (Raal and Muhlbauer, 1998).

A discussion of the experimental thermodynamic behaviour of the systems that have been measured within the framework of the γ_i - ϕ_i approach is an appropriate precursor to a discussion on the fitting of the data to the semi-theoretical G^E models. The systems will be treated on the basis of the latter together with a qualitative discussion on the activity coefficient and G^E behaviour and additional considerations such as relative volatility and azeotropic points for the relevant systems.

Table 8.9. Experimental activity coefficients (γ_i) and excess molar Gibbs energies (G^E) for 1-propanol (1) + 2-butanol (2).

P (kPa)	x_1	y_1	γ_1	γ_2	G^E (J.mol^{-1})
		T = 373.15 K			
103.9	0.0224	0.0235	0.9670	1.0007	-0.2
105.3	0.1315	0.1405	0.9974	1.0042	10.3
106.8	0.2642	0.2788	0.9984	1.0082	17.3
107.8	0.3810	0.4010	1.0046	1.0043	13.7
108.8	0.5103	0.5326	1.0049	0.9995	7.0
110.0	0.6371	0.6599	1.0078	0.9919	6.1
111.2	0.7928	0.8072	1.0009	0.9953	-0.8
111.9	0.8686	0.8793	1.0012	0.9885	-1.5
		T = 393.15 K			
211.9	0.1307	0.1420	1.0129	0.9971	-2.8
215.1	0.2653	0.2811	1.0016	1.002	7.2
218.3	0.4246	0.4379	0.9883	1.015	11.2
219.5	0.4784	0.5007	1.0081	0.9994	11.7
222.2	0.6300	0.6483	1.0025	1.004	9.8
223.3	0.6975	0.7103	0.9966	1.016	8.2
224.9	0.7927	0.8080	1.0042	0.9894	3.7
226.1	0.8684	0.8782	1.0012	0.9937	0.8
		T = 423.15 K			
513.2	0.1314	0.1441	1.0152	1.0230	76.6
523.0	0.2674	0.2809	0.9883	1.0364	81.1
532.2	0.4212	0.4316	0.9785	1.0534	73.6
535.9	0.4850	0.4981	0.9865	1.0520	68.6

Table 8.9. Experimental activity coefficients (γ_i) and excess molar Gibbs energies (G^E) for 1-propanol (1) + 2-butanol (2) (cont).

P (kPa)	x_1	y_1	γ_1	γ_2	G^E (J.mol^{-1})
		T = 423.15 K			
546.8	0.6957	0.7122	1.0005	1.0402	43.4
551.1	0.7933	0.8067	1.0006	1.0363	27.5
554.7	0.8671	0.8750	0.9986	1.0487	18.0
559.5	0.9651	0.9669	0.9990	1.0663	4.5

(a) The cyclohexane + ethanol system

The cyclohexane + ethanol system is highly nonideal as a result of the large disparity in the nature of the energies of the intermolecular forces that characterise the liquid phase interactions for the cycloalkane and alkanol mixture components. The alkanol is a strongly associating polar compound that exhibits hydrogen-bonding whereas the cycloalkane is a nonpolar compound with a dipole moment of 0.3 Debyes (Reid *et al.*, 1987). This is reflected in the relative magnitudes of the γ_i values in Table 8.8, where for systems with strongly associating compounds, positive deviations from ideal solution behaviour *i.e.* $\gamma_i >> 1$ are observed (Letcher and Battino, 2001).

In general, the γ_i values decrease with increasing temperature, which is consistent with the values in Table 8.8. Highly nonideal systems are also characterized by large changes upon mixing for the G^E value, which is confirmed by an inspection of the G^E values for the system in Table 8.8. The $\ln\gamma_i$ versus x_1 and G^E versus x_1 plots for the cyclohexane + ethanol system at 69.8 kPa are shown in Figures (8.7) and (8.8), respectively, to illustrate the nature of the nonideal behaviour of the mixture components and the system, respectively, as a function of composition.

Table 8.10. Activity coefficients (γ_i) and excess molar Gibbs energies (G^E) for 1-propanol (1) + n-dodecane (2).

P (kPa)	x_1	y_1^{calc}	γ_1	γ_2	G^E (J.mol^{-1})
		T = 373.15 K			
93.3	0.0611	0.9771	13.2695	1.0424	611.1
97.1	0.1104	0.9795	7.6520	1.0228	759.2
102.9	0.2058	0.9806	4.3465	1.1443	1270.3
105.1	0.2668	0.9809	3.4229	1.2444	1516.0
107.5	0.3637	0.9811	2.5668	1.4488	1795.5
109.3	0.4860	0.9812	1.9520	1.8114	1956.0
110.2	0.5512	0.9813	1.7350	2.0792	1961.5
110.8	0.6250	0.9815	1.5384	2.4742	1889.3
110.9	0.6407	0.9815	1.5034	2.5866	1869.8
111.6	0.7277	0.9818	1.3309	3.3747	1672.9
112.3	0.8275	0.9826	1.1784	5.1238	1295.9
		T = 393.15 K			
180.9	0.0629	0.9703	12.3710	1.0355	623.9
189.0	0.0980	0.9734	8.3040	1.0027	685.9
200.3	0.1459	0.9750	5.9031	1.0477	976.8
205.4	0.1905	0.9757	4.6332	1.0985	1203.4
211.4	0.2679	0.9763	3.3875	1.2149	1534.2
215.4	0.3351	0.9765	2.7570	1.3481	1760.0
217.7	0.4025	0.9767	2.3189	1.5012	1900.1
219.9	0.4569	0.9768	2.0625	1.6588	1979.6
222.8	0.5474	0.9769	1.7430	2.0043	2022.9
223.9	0.6223	0.9770	1.5405	2.4016	1960.7
224.8	0.7070	0.9772	1.3614	3.0798	1790.3
226.5	0.8519	0.9781	1.1386	5.8922	1220.2

Table 8.10. Activity coefficients (γ_i) and excess molar Gibbs energies (G^E) for 1-propanol (1) + n-dodecane (2) (cont).

P (kPa)	x_1	y_1^{calc}	γ_1	γ_2	G^E (J.mol^{-1})
		T = 423.15 K			
478.5	0.1436	0.9648	5.8259	1.0149	934.9
493.5	0.1865	0.9667	4.6215	1.0358	1105.0
514.2	0.2602	0.9684	3.4432	1.1155	1416.4
526.0	0.3364	0.9692	2.7202	1.2331	1673.6
532.5	0.3946	0.9696	2.3455	1.3465	1817.2
541.2	0.4885	0.9700	1.9231	1.5917	1960.3
547.9	0.5989	0.9704	1.5865	2.0211	1965.5
551.7	0.7286	0.9707	1.3126	2.9722	1737.3
557.8	0.8987	0.9723	1.0763	7.5989	955.3

The general trends for the magnitudes of the γ_i values as a function of x_1 can be observed from an inspection of Figure 8.7. The highest γ_i values are obtained in the very dilute region for the component as this region corresponds to infinitely dilute conditions, where maximum nonideal thermodynamic behaviour is obtained for a system component. The γ_i values for finite concentrations (0.05 - 0.95 mole fraction) are much smaller and tend to a value of unity as the pure component limit is reached.

Together with the relative magnitudes of the γ_i values, the relative asymmetry of the γ_i - x_1 behaviour for the two systems is an indication of the nonideality of the system. This is confirmed in Figure 8.8, where a slight asymmetry of the G^E - x_1 curve is observed for the cyclohexane-rich end. This can be explained in terms of the formation of hydrogen-bonds even in the cycloalkane-rich region (Peleitero *et al.*, 2001) for the strongly associating alkanol component molecules. The positive G^E value indicates that mixing interactions between the two components are unfavourable.

Table 8.11. Activity coefficients (γ_i) and excess molar Gibbs energies (G^E) for 2-butanol (1) + n-dodecane (2).

P (kPa)	x_1	y_1^{calc}	γ_1	γ_2	G^E (J.mol^{-1})
		T = 373.15 K			
56.3	0.0522	0.9624	10.2160	1.0470	511.5
78.4	0.1288	0.9750	5.7858	1.0378	801.6
85.3	0.1924	0.9777	4.2133	1.081	1053.7
89.5	0.2641	0.9790	3.2190	1.1686	1313.6
93.8	0.3577	0.9799	2.4886	1.3387	1593.1
95.5	0.4243	0.9802	2.1351	1.4960	1717.9
97.8	0.5157	0.9806	1.7980	1.7812	1806.0
99.0	0.5989	0.9809	1.5669	2.1415	1782.0
99.8	0.6427	0.9810	1.4715	2.4093	1745.0
102.3	0.8340	0.9822	1.1626	4.9718	1215.7
		T = 393.15 K			
105.0	0.0498	0.9494	9.8879	1.0511	527.7
154.0	0.1344	0.9686	5.3939	1.0183	791.6
173.4	0.2277	0.9729	3.5777	1.0955	1179.0
180.3	0.2739	0.9739	3.0887	1.1616	1365.3
187.9	0.3685	0.9751	2.3895	1.3214	1624.6
191.8	0.4332	0.9755	2.0730	1.4749	1752.2
199.2	0.6092	0.9764	1.5287	2.1297	1810.9
203.1	0.7317	0.9771	1.2969	3.0616	1603.2
205.8	0.8212	0.9780	1.1710	4.4658	1298.3
208.2	0.9073	0.9804	1.0740	7.7600	832.5

Table 8.11. Activity coefficients (γ_i) and excess molar Gibbs energies (G^E) for 2-butanol (1) + n-dodecane (2) (cont).

P (kPa)	x_1	y_1^{calc}	γ_1	γ_2	G^E (J.mol^{-1})
		T = 423.15 K			
221.5	0.0828	0.9373	5.4369	0.8813	85.7
356.0	0.1362	0.9524	5.2296	1.055	956.6
409.8	0.2268	0.9617	3.6040	1.0611	1184.4
450.0	0.3721	0.9670	2.4023	1.2117	1571.5
458.4	0.4561	0.9684	1.9955	1.3549	1689.9
477.8	0.6832	0.9704	1.3852	2.2410	1682.6
482.5	0.7301	0.9707	1.3078	2.6315	1608.0

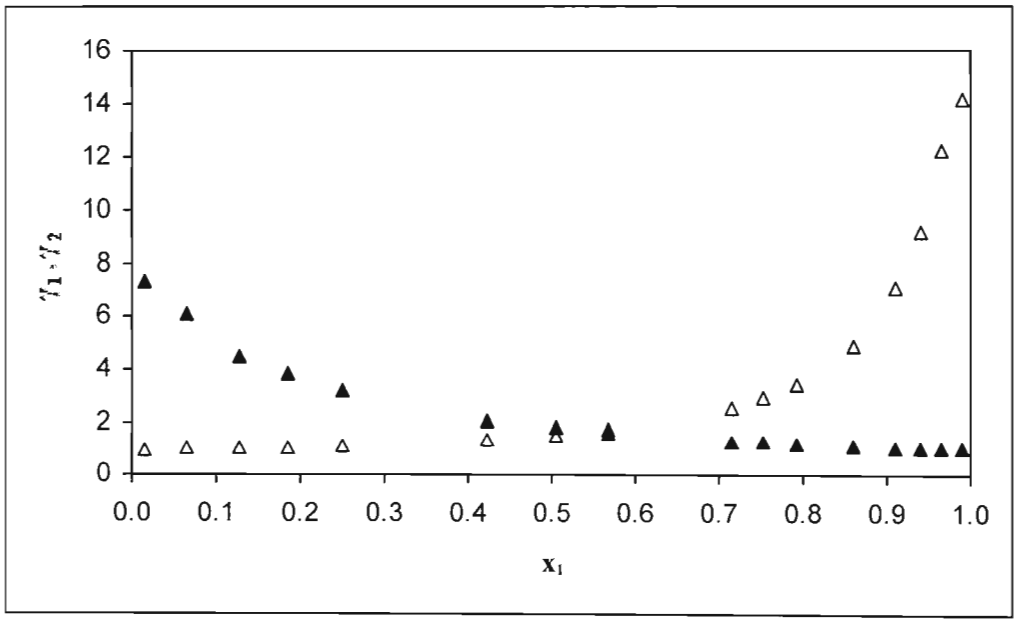

Figure 8.7. Plot of $\ln\gamma_i$ (i = 1,2) versus x_1 for cyclohexane (1) + ethanol (2) at 69.8 kPa: ▲ γ_1 - x_1 values; △ γ_2 - x_1 values.

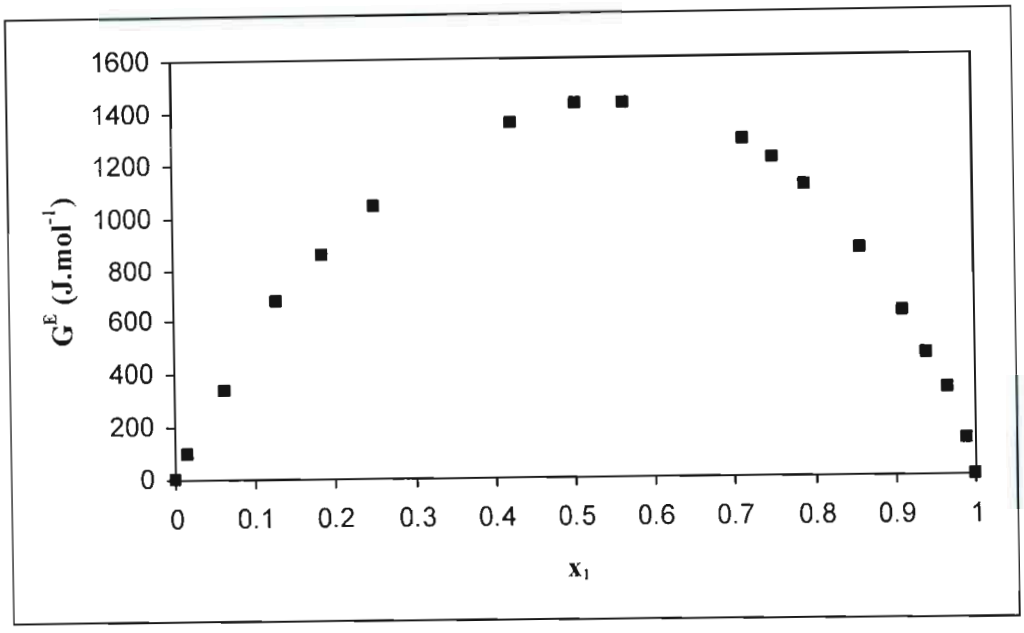

Figure 8.8. Plot of G^E versus x_1 for cyclohexane (1) + ethanol (2) at 69.8 kPa.

An observation of the T-x_1-y_1 plots in Chapter 7 for the cyclohexane (1) + ethanol (2) system reveal the existence of a minimum boiling point azeotrope for the system, where the boiling point for the azeotropic composition is lower than that of either of the pure component boiling points. The azeotropic behaviour corresponds to a condition of highly nonideal behaviour where the mixture is destabilized relative to that of an ideal solution (Atkins, 1999). It is characterised by the equilibrium liquid and vapour phases having the same composition; hence no separation is achieved.

(b) The 1-propanol + 2-butanol system

As mentioned before, alkane + alkane and alkanol + alkanol mixtures frequently exhibit ideal behaviour, as opposed to alkane + alkanol mixtures, however, the study of alkanol + alkanol interactions is quite interesting due to the nature of the hydrogen-bonding interactions between the two components. In particular, the study of interactions between n-alkanols and isomeric alkanols have been of particular interest (Darwish *et al.*, 1997; Mara *et al.*, 1997; Li *et al.*, 2000; Rhodes *et al.*, 2001) to understand the effects of isomer structure on the thermodynamics as related to the structures of the hydrogen-bonded chain associate complexes (Browarzik, 2004). In this study, the 1-propanol + 2-butanol system had a relative volatility (α_{12}) close to unity due to the closeness of the boiling points of the two compounds and the similar nature of the intermolecular interactions. The γ_i and G^E values have been presented in Table 8.9. The ideal nature of the system is reflected in the sizes of the latter quantities.

However, it should be observed that in some regions of the composition range, the values of γ_i and G^E are slightly less than unity. This is characteristic for systems where the components are strongly associated and exhibit negative deviations from ideal solution behaviour (Letcher and Battino, 2001). The values appear slightly scattered due to the liquid and vapour compositions being quite similar in value, which tests the limits of the estimated uncertainties in the quantification of the phases *i.e.* in the phase sampling, gas chromatographic calibration procedure and sample analysis, *etc.* It was also commented upon by Ellis (1952) that accurate VLE measurements for low-activity coefficient and close-boiling systems are challenging as the slightest error in pressure or temperature measurement or in the quantification of the phases can cause scatter in the γ_i and G^E values obtained.

(c) The 1-propanol + n-dodecane and 2-butanol + n-dodecane systems

In addition to the use of the γ_i - ϕ_i method for the data reduction process, the method was also employed to compute the vapour phase composition for the 1-propanol + n-dodecane and the 2-butanol + n-dodecane systems. This was necessitated due to irregularities in the measurement of the vapour phase compositions for the above two systems as discussed below.

The 1-propanol + n-dodecane and 2-butanol + n-dodecane systems have a very high relative volatility and it was anticipated beforehand that the above two types of systems could indeed prove to be quite challenging for the acquisition of accurate P-T-x-y VLE data. As mentioned before, the study of the VLE of very high relative volatility systems has traditionally proven to be quite difficult to achieve with conventional dynamic recirculating VLE stills (Maia de Oliveira, 2002) and can be attributed to a combination of poor experimental procedure, equipment design limitation and the limitations associated with the inherent or fundamental operational principles of the method.

In terms of the objectives of this study, it was felt that only the first two of the above potential shortcomings for the measurements of high relative volatility systems could be addressed as the apparatus was optimized within the context of the conventional dynamic liquid and vapour condensate recirculation method. The optimized and efficient experimental procedure for the VLE measurements has been described in Chapter 6 and the development of the novel apparatus has been discussed in Chapter 4. In terms of the latter, novel and innovative features were incorporated into the design of the VLE apparatus such as an improved return line design, the use of return line heating and efficient stirring in the reboiler, *etc.*

In the actual operation of the apparatus for the VLE measurements on the alkanol + n-dodecane systems, there were no apparent difficulties or anomalies detected in the approach of the system to equilibrium in the composition range measured and the systems were observed to attain a proper equilibrium state on the basis of the criteria defined in Chapter 6 *i.e.* stable and continuous fluid flows together with unchanging values for the thermodynamic variables (within the experimental uncertainties) at the "plateau region".

In the graphical presentation of the data, both the P-x_1 and P-y_1 data points were observed to produce a smooth curve, as shown in Figure 8.9 for the 1-propanol + n-dodecane system at 373.15 K. However, the computation of the experimental activity coefficients yielded quite startling results as the γ_i values for the n-dodecane component did not adhere to the fundamental pure component limits for the γ_i auxiliary departure function *i.e.* the symmetric normalization of the γ_i value in the γ_i - ϕ_i approach (discussed in Chapter 3) as shown below:

$$\gamma_i \rightarrow 1 \text{ as } x_i \rightarrow 1 \tag{3.51}$$

The γ_i values for the n-dodecane component in its pure component limit did not exhibit the above behaviour and were much too high (values of ~10). The computation of the experimental γ_i values in the γ_i - ϕ_i method is achieved through the following rearrangement of Equation (3.58):

$$\gamma_i = \frac{y_i P \Phi_i}{x_i P_i^{sat}} \tag{8.3}$$

The terms in Equation (8.3) have been defined in Chapter 3. Of significance in the above, are the directly measured experimental thermodynamic variables in the form of the pressure (P), liquid phase composition (x_i) and the vapour phase composition (y_i). Since the Φ_i term is merely a correction term that for the most part at low pressures is close to unity and the accuracy of the system pressure measurement was confirmed with the vapour pressure measurements, the relative values of x_i and y_i were quite significant for the computation of the γ_i value. This can be explained in terms of the saturation vapour pressure of n-dodecane $\left(P_i^{sat}\right)$ being much lower than that of the system pressure (P) for the composition range measured, as an observation of the data in Chapter 7 reveals.

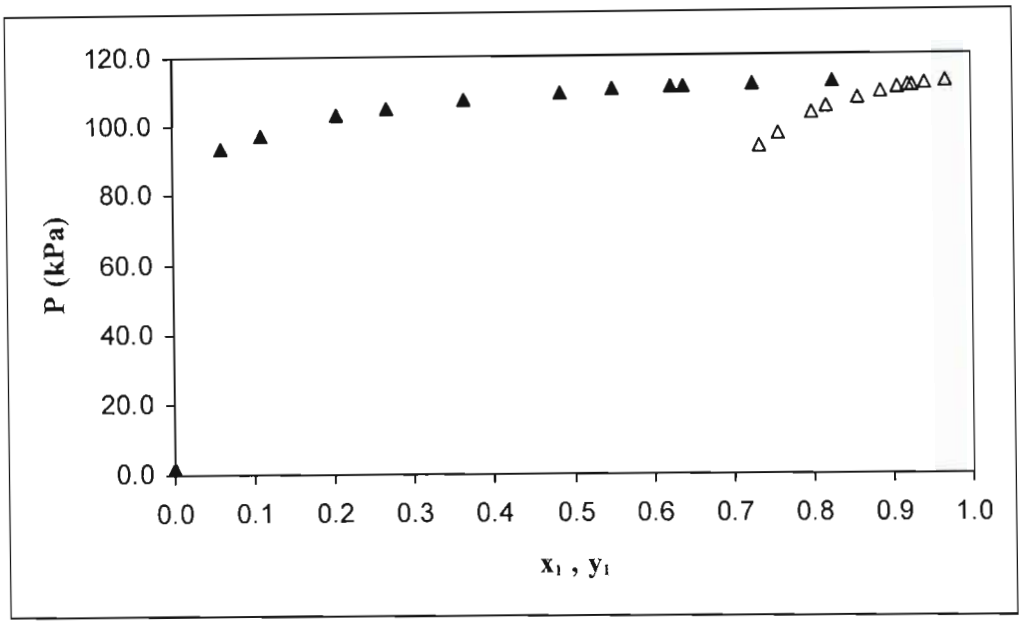

Figure 8.9. P-x_1-y_1 plot for 1-propanol (1) + n-dodecane (2) at 373.15 K: ▲ experimental P-x_1 values; △ experimental P-y_1 values.

Consequently, with the $\left(\frac{P\Phi_i}{P_i^{sat}}\right)$ term being quite large (a much smaller denominator value) in Equation (8.3) for the alkanol + n-dodecane systems, the ratio of $\left(\frac{y_i}{x_i}\right)$ must decrease quite dramatically *i.e.* a large discrepancy between the two phase composition values must exist at the pure component limit for n-dodecane. At this point, it was suspected that the vapour phase measurements were in error since a large positive deviation of the latter from the true equilibrium values can produce γ_i values that are too high and do not obey the symmetric convention.

In trying to establish conclusive reasons for the erroneous P-T-x-y measurements, as manifested in the high γ_i values in the n-dodecane-rich region, a search for similar types of high relative volatility systems was conducted (since the measurements in this study represented novel data) to observe the trends in the VLE behaviour of such systems. The only similar high relative volatility alkanol + n-alkane system found in open literature (Hirata *et al.*, 1975) was that of the 1-butanol (1) + n-decane (1) system at T = 373.15 K, as measured by Lee and Scheller (1967). The P-x_1-y_1 curve for this system is shown in Figure 8.10. Of course, this system has a lower relative volatility than the alkanol + n-dodecane systems studied here.

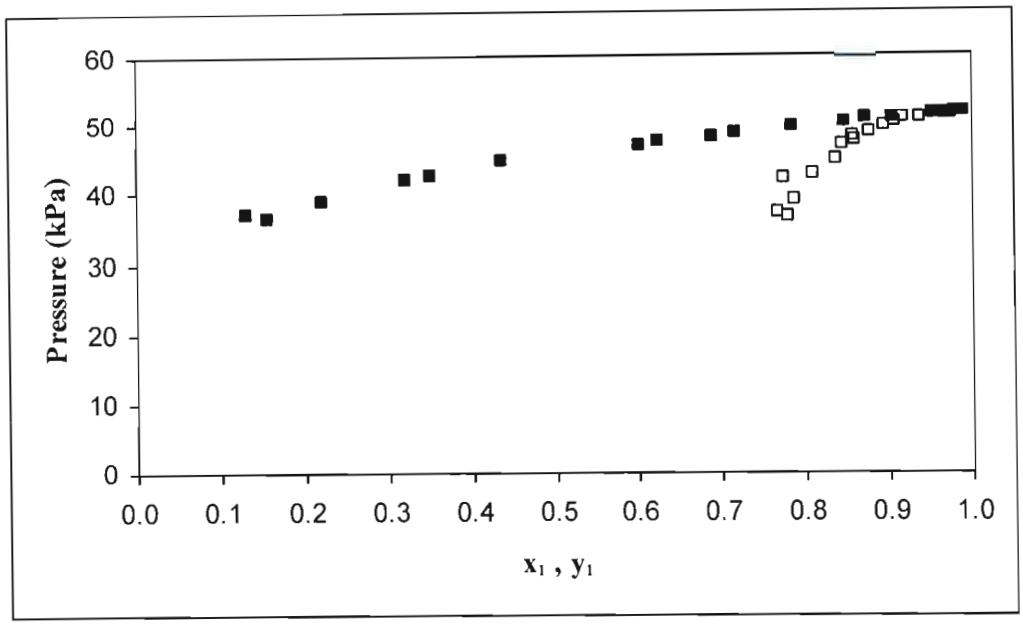

Figure 8.10. P-x_1-y_1 plot for 1-butanol (1) + n-decane (2) at 373.15 K: ■ P-x_1; □ P-y_1 (Lee and Scheller, 1967).

Unfortunately, time constraints and the lack of availability of chemicals did not permit VLE measurements with the apparatus for the 1-butanol + n-decane system. As observed from Figure 8.10, there is a great deal of scatter in the data set, attesting to the difficulties in the measurement of this type of system. As for the data set of the author, the majority of the measurements are in the alkanol-rich end. The lack of data in the alkane-rich region exemplifies the difficulty for "finite concentration" VLE stills to obtain data for these types of difficult systems. This was observed in the operation of the VLE apparatus in this study, where attempted measurements in the n-dodecane-rich region by the author severely compromised the approach of the system to a proper equilibrium condition. This task would be better suited for an ebulliometric apparatus (Rogalski and Malanowski, 1980) or static micro-cell (Raal and Muhlbauer, 1998).

An examination of the liquid and vapour composition values for the n-decane component yielded that it was quite similar to the experimentally measured values for the n-dodecane component in the alkanol + n-dodecane systems studied here. Since the alkanol + n-dodecane systems had a much higher relative volatility (the difference in the normal boiling points of decane and dodecane is roughly 50 K), it is expected that in comparison to the 1-butanol + n-decane system, the vapour pressure composition for the dodecane component for a given P-x_1 value, should be much lower. This was then confirmed by the incompatibility of the data with

the predictions from the G^E models, which predicted much lower vapour phase compositions for the isothermal P-x_1 data.

The above is in accordance with the studies of Van Ness *et al.* (1973), where it was concluded that the greatest uncertainty with the VLE recirculation stills is to be found in the vapour phase composition measurement. In accordance with the recommendations of Van Ness *et al.* (1973), it was therefore decided to compute the vapour phase. This is most effectively achieved by the BUBL P calculation, discussed in Chapter 3, with the least squares statistical criterion. In the computation of the equilibrium vapour phase composition, the representation of the vapour phase and liquid phase nonidealities are important.

As for the correlative procedures, the highly recommended method of Hayden and O'Connell (Prausnitz *et al.*, 1980; Gess *et al*, 1991; Raal and Muhlbauer, 1998) was employed for calculating the virial coefficients in the B-truncated virial EOS. The liquid-phase thermodynamic model employed was that of the Wilson equation. The efficacy of the Wilson equation in representing VLE data for the systems studied here will be discussed later in the correlation procedures.

The calculated vapour composition values have been presented together with the experimental P-T-x data in Tables (8.10) and (8.11) for the 1-propanol + n-dodecane and 2-butanol + n-dodecane systems, respectively. A comparative plot of the experimental and computed vapour composition measurements is shown in Figure 8.11. An examination of the relative magnitudes for the experimental and computed vapour compositions yields that there are significant discrepancies between the two sets of values. This attests to the difficulty in the accurate measurement of the vapour phase compositions for this type of system. The improper mixing of the two components in the reboiler can produce non-equilibrium vapourization (even with the innovation in incorporating efficient stirring in the reboiler of the stainless steel apparatus developed here) which gives rise to unreliable vapour compositions as shown above. It was observed in this study that variations in the circulation rate, rate of heat input and the extent of magnetic stirring had no effect on the results that were obtained with regards to the vapour composition measurements, consequently it is not recommended that this type of system be studied with dynamic recirculating VLE stills (even with the modifications in this study). As mentioned before, in the course of the study, it was deemed that the operating procedure and the design of the apparatus was optimized for the acquisition of VLE measurements (as demonstrated for the other systems measured) and that the erroneous measurements of VLE for high relative volatility systems could serve to present a case for the fallibility of this method for VLE measurements of such systems as the latter are "a most severe test" (Ellis, 1952) of the dynamic recirculating method traditionally employed for LPVLE studies

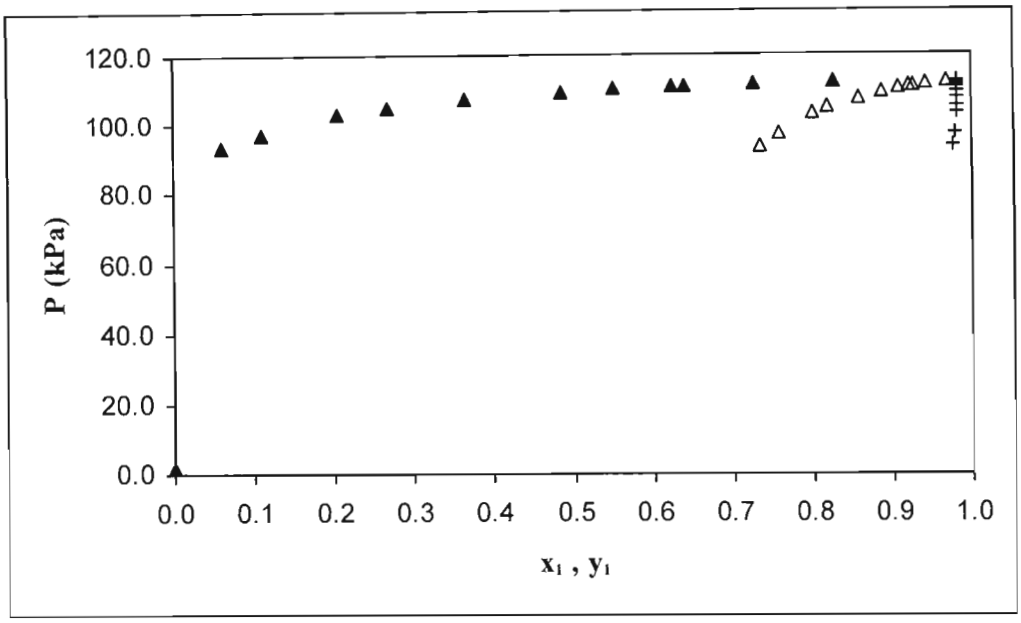

Figure 8.11 Comparison of the experimental and calculated vapour compositions for 1-propanol + n-dodecane at 373.15 K: ▲ experimental P-x_1 values; △ experimental P-y_1 values; + calculated P-y_1 values.

Indeed, similar conclusions were reached by Ellis (1952) in comparative investigations of his novel dynamic equilibrium still with other types of dynamic VLE stills such as the Gillespie design (Gillespie, 1946) in a preliminary investigation of high relative volatility systems such as the ethanol + nitrobenzene and benzene + nitrobenzene mixtures. The latter were found to be "difficult to boil" and it was observed that different equilibrium stills gave different T-x_1-y_1 curves for the isobaric data sets. Unfortunately, no further details were provided with regards to the nature of the discrepancies observed for these measurements. Ellis (1952) also mentioned that his still was used for investigations of the ethanol + decane high relative volatility system but did not provide any results or a discussion of the above in his original journal publication.

The γ_i and G^E values have been computed from the experimental P-T-x data and are shown with the calculated vapour phase compositions in Tables (8.10) and (8.11) for the 1-propanol + n-dodecane and 2-butanol + n-dodecane systems, respectively. The $\ln\gamma_i$ versus x_1 plots for the 1-propanol + n-dodecane and 2-butanol + n-dodecane systems at 373.15 K are shown in Figures (8.12) and (8.13), respectively, and the corresponding G^E versus x_1 plots are shown in Figures (8.14) and (8.15), respectively. The noticeable absence of γ_i values in the alkane-rich side was attributed to difficulties in obtaining measurements in this region, as discussed before.

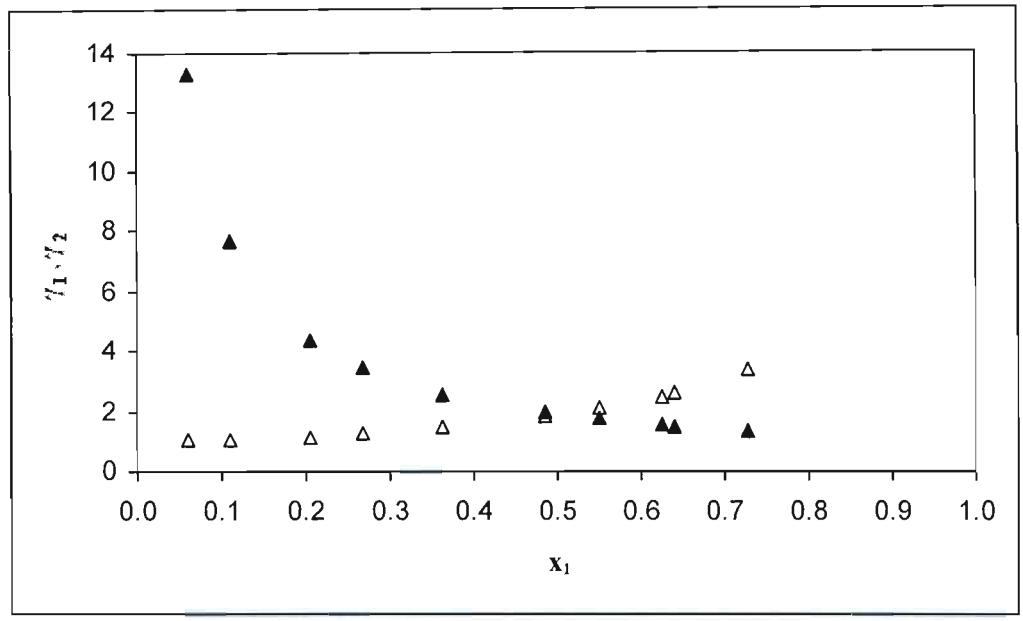

Figure 8.12. Plot of $\ln\gamma_i$ (i = 1,2) versus x_1 for 1-propanol (1) + n-dodecane (2) at 373.15 K:

▲ γ_1 - x_1 values; △ γ_2 - x_1 values.

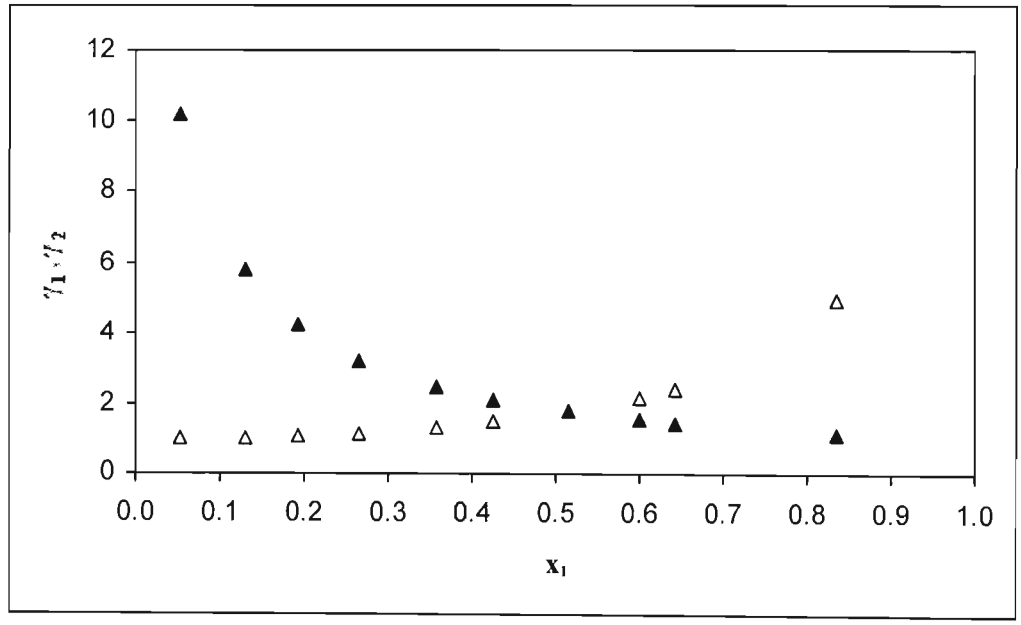

Figure 8.13. Plot of $\ln\gamma_i$ (i = 1,2) versus x_1 for 2-butanol (1) + n-dodecane (2) at 373.15 K:

▲ γ_1 - x_1 values; △ γ_2 - x_1 values.

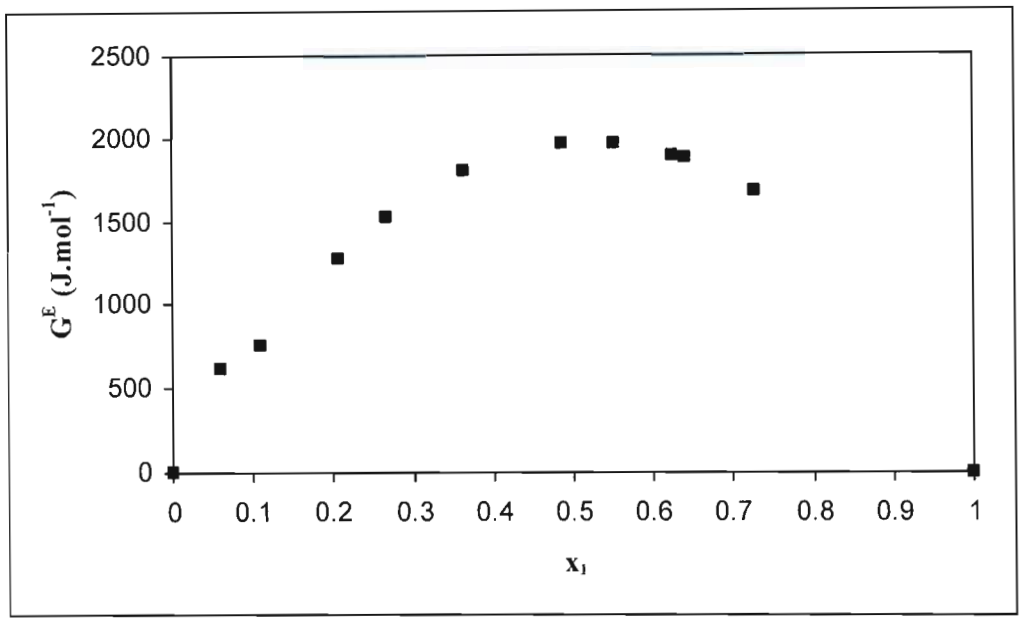

Figure 8.14. Plot of G^E versus x_1 for 1-propanol (1) + n-dodecane (2) at 373.15 K.

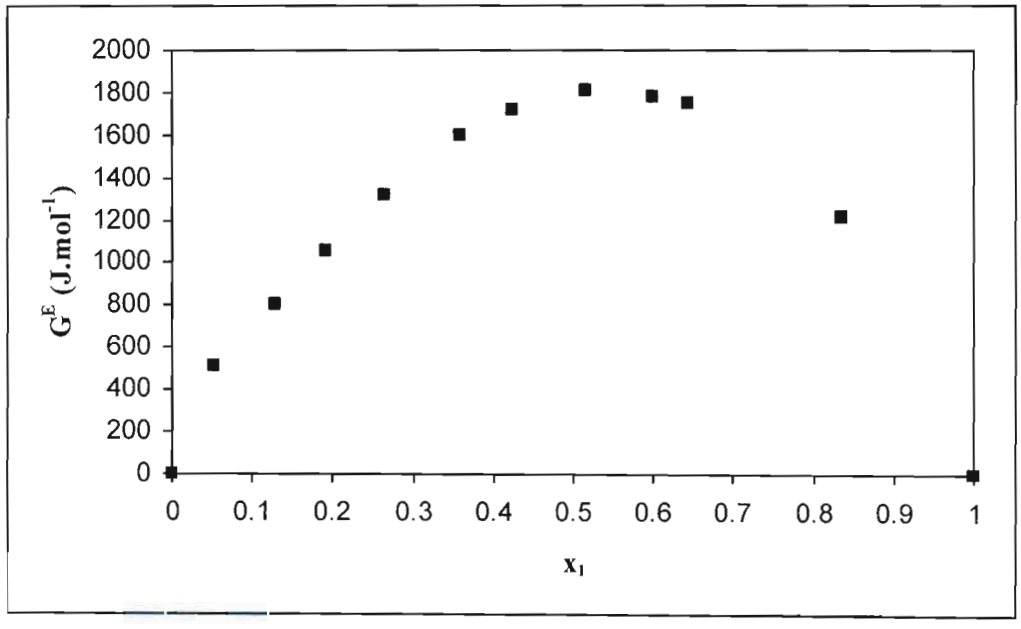

Figure 8.15. Plot of G^E versus x_1 for 2-butanol (1) + n-dodecane (2) at 373.15 K.

As observed for the cyclohexane + ethanol system, the γ_i values are much greater than unity as the dilute region is approached. The curves exhibit similar behaviour to that of the cyclohexane + ethanol system, where the asymmetry of the compositional dependence of the G^E values indicates the nonideal nature of the system. There is very little difference between the relative values of G^E and γ_i for the two systems as the values for the 1-propanol component in the alkanol + n-dodecane mixtures are slightly higher than that for the 2-butanol component in the analogous system.

Both the alkanol + n-dodecane systems were described as high relative volatility systems, as a result of the discrepancies in the boiling points of the two components. The relative volatility (α_{12}) of a binary mixture can be formally defined as follows:

$$\alpha_{12} = \frac{\gamma_1 P_1^{sat}}{\gamma_2 P_2^{sat}} \tag{8.4}$$

In the above, the effects of the vapour phase nonideality and the Poynting correction have been ignored, as this quantity is being employed for purely qualitative purposes here. A few values of α_{12} computed for selected regions of the composition range are presented in Table 8.12 for the 1-propanol + n-dodecane system at 373.15 K.

Table 8.12 Values of the relative volatility (α_{12}) for the 1-propanol (1) + n-dodecane (2) system at 373.15 K.

x_1	γ_1	γ_2	α_{12}
0.0611	13.2695	1.0424	588
0.4860	1.9520	1.8114	50
0.8275	1.1784	5.1238	11

Table 8.12 clearly reveals the trends in α_{12} as a function of composition and an explanation as to why greater difficulty is experienced in general for measurements in the alkane-rich region (Lee and Scheller, 1967) for VLE measurements for an already challenging high relative volatility alkanol + n-alkane mixture, where the n-alkane is the heavy component.

Correlation of the Vapour-Liquid Equilibrium data

The experimental VLE data were regressed with MATLAB® (version 7.0.1) through the use of the Levenberg-Marquardt algorithm, as was discussed in Chapter 3. The optimal adjustable parameters for the models, together with the deviations for the calculated quantities are shown in Tables (8.13) - (8.16) for the cyclohexane + ethanol, 1-propanol + 2-butanol, 1-propanol + n-dodecane and 2-butanol + n-dodecane systems, respectively. Discussion of the correlative and computational efficiencies of the models is presented in Appendix D.

The absolute average deviation (AAD) for a calculated quantity is defined as follows:

$$AAD = \left(\frac{1}{n} \sum_{i=1}^{n} |\Delta Q| \right) \tag{8.5}$$

where n is the number of data points and ΔQ is the difference between the experimental and calculated values for the equilibrium relation *i.e.* temperature (T), pressure (P) or vapour phase compositions (y). The AAD values for the relevant computed thermodynamic variables are shown in Tables (8.13) - (8.16) for the cyclohexane + ethanol, 1-propanol + 2-butanol, 1-propanol + n-dodecane and 2-butanol + n-dodecane systems, respectively.

The superiority of the Wilson equation for the representation of the majority of the systems studied is apparent from Tables (8.13) - (8.16). The correlation efficiency of the Wilson equation was complemented by an excellent computational efficiency (see Appendix D). This is accordance with the findings of a large majority of researchers employing G^E correlations in the γ_i - ϕ_i method for the representation of the liquid phase (Rice and El-Nikheli, 1995; Joseph *et al.*, 2002; Kim *et al.*, 2004).

Surprisingly, the Wilson equation was outperformed by the other models in the representation of the fairly ideal 1-propanol + 2-butanol system. The T-K Wilson equation, which was formulated for the treatment of partially miscible systems, was outperformed by the Wilson equation even for those systems with components with large differences in molar volumes as for the alkanol + n-dodecane systems, with regards to the pressure residuals.

The NRTL equation gave a good overall representation of the systems as for the Wilson equation. In the NRTL model, the non-randomness parameter (α_{ij}) can be used as a third parameter but was fixed at a predetermined value, as recommended by Gess *et al.* (1991), to

avoid convergence problems. The constant value for the non-randomness parameter was set at 0.47, as proposed by Bruin and Prausnitz (1971).

The complex UNIQUAC and UNIQUAC (mod) equations performed the worst of all the models in the overall representation of the data. The modified UNIQUAC equation (Prausnitz *et al.*, 1980) was in fact formulated to treat associating hydrogen-bonded fluids such as alcohols with a modified area parameter (q') and did not display any superiority in this regard for these types of mixtures over the other equations. In the application of the UNIQUAC (mod) equation, there was no distinction between the available surface area for interaction (q') for straight chain and isomeric alcohols (such as n-butanol versus 2-butanol); hence the use of generalized parameters might not be optimal in this regard. The UNIQUAC and UNIQUAC (mod) models were also computationally the least efficient (due to their algebraic forms) in the regression procedure.

The modelling of the high relative volatility alkanol + n-dodecane systems proved quite problematic for a few models, as manifested in the regression procedure and the regressed parameters. The UNIQUAC and UNIQUAC (mod) equations were greatly affected in this regard, where the models converged very slowly to a solution and inconsistencies in the parameters were also observed, as shown in Tables (8.15) and (8.16).

In general the BUBL P computations for the isothermal data were much faster than the BUBL T computations for the isobaric data. The accuracy of the BUBL T computation was also found to be quite dependent upon the vapour pressure correlation constants employed for the calculated temperature (see Chapter 3). Consequently, any errors in the vapour pressure representation of the designated component in the formulation of an objective function for the calculated temperature (see Chapter 3) would severely compromise the accuracy of the results obtained.

The VLE curves calculated using the various models are presented in Figures (8.16) - (8.19) and Figures (8.20) - (8.22), for the cyclohexane + ethanol and 1-propanol + 2-butanol systems, respectively. For the alkanol + n-dodecane systems, the vapour phase was computed with the Wilson equation, as discussed before. From the plots shown in Figures (8.16) - (8.19), the excellent fit of the data to the Wilson equation is observed. However, the model was observed to slightly overpredict the cyclohexane vapour phase composition on the cyclohexane-rich side of the azeotrope. The superiority of the NRTL equation over the Wilson equation in representing the 1-propanol + 2-butanol system is observed for all the isotherms shown in Figures (8.20) - (8.22).

Table 8.13. Model parameters (A_{12} and A_{21}) [a] and absolute average deviation (AAD) values for the cyclohexane (1) + ethanol (2) VLE data.

Model	A_{12} (J.mol^{-1})	A_{21} (J.mol^{-1})	ΔT (K)	Δy_1
		P = 40 kPa		
Wilson	1812.88	9029.81	0.10	0.0141
T-K Wilson	947.17	8748.01	0.19	0.0139
NRTL ($\alpha_{12} = 0.47$)	6681.98	3910.63	0.22	0.0151
UNIQUAC	4799.03	-653.60	0.70	0.0230
UNIQUAC (mod)	11862.50	-2009.33	0.20	0.0156
		P = 69.8 kPa		
Wilson	1724.77	8271.85	0.08	0.0102
T-K Wilson	905.08	7981.35	0.15	0.0099
NRTL ($\alpha_{12} = 0.47$)	6084.20	3678.80	0.16	0.0103
UNIQUAC	4445.14	-596.69	0.55	0.0141
UNIQUAC (mod)	10901.93	-2143.06	0.33	0.0153
		P = 97.7 kPa		
Wilson	1882.64	7696.92	0.12	0.0115
T-K Wilson	1052.67	7404.01	0.15	0.0109
NRTL ($\alpha_{12} = 0.47$)	5646.92	3756.47	0.12	0.0111
UNIQUAC	4199.03	-522.65	0.47	0.0148
UNIQUAC (mod)	10188.91	-2182.68	0.35	0.0158
		P = 150 kPa		
Wilson	2168.03	6602.17	0.23	0.0218
T-K Wilson	1407.80	6194.11	0.16	0.0220
NRTL ($\alpha_{12} = 0.47$)	4659.40	3961.46	0.20	0.0223
UNIQUAC	3323.29	-187.37	0.11	0.0220
UNIQUAC (mod)	9121.91	-2259.45	0.40	0.0242

[a] Wilson and T-K Wilson : $A_{12} = \lambda_{12} - \lambda_{22}$ and $A_{21} = \lambda_{21} - \lambda_{11}$; NRTL : $A_{12} = g_{12} - g_{22}$ and $A_{21} = g_{21} - g_{11}$; UNIQUAC and UNIQUAC (mod) : $A_{12} = u_{12} - u_{22}$ and $A_{21} = u_{21} - u_{11}$.

Table 8.14. Model parameters (A_{12} and A_{21}) [a] and absolute average deviation (AAD) values for the 1-propanol (1) + 2-butanol (2) VLE data.

Model	A_{12} (J.mol^{-1})	A_{21} (J.mol^{-1})	ΔP (kPa)	Δy_1
		T = 373.15 K		
Wilson	3162.03	-2155.12	0.3	0.0042
T-K Wilson	3232.67	-2235.36	0.07	0.0033
NRTL ($\alpha_{12} = 0.47$)	-1776.00	2416.65	0.07	0.0035
UNIQUAC	-1380.30	1851.80	0.09	0.0036
UNIQUAC (mod)	1201.93	-1201.92	0.3	0.0028
		T = 393.15 K		
Wilson	1370.99	-882.68	1.3	0.0079
T-K Wilson	1525.71	-1102.72	0.73	0.0061
NRTL ($\alpha_{12} = 0.47$)	-541.12	920.13	0.73	0.0061
UNIQUAC	-732.16	976.28	0.73	0.0061
UNIQUAC (mod)	-2074.69	3100.14	0.68	0.0059
		T = 423.15 K		
Wilson	4679.83	-2591.87	6.3	0.0087
T-K Wilson	4942.67	-2879.87	1.2	0.0056
NRTL ($\alpha_{12} = 0.47$)	-2137.28	3607.69	1.5	0.0062
UNIQUAC	-1906.65	2840.912	1.6	0.0063
UNIQUAC (mod)	506.94	-506.94	3.3	0.0086

[a] Wilson and T-K Wilson : $A_{12} = \lambda_{12} - \lambda_{22}$ and $A_{21} = \lambda_{21} - \lambda_{11}$; NRTL : $A_{12} = g_{12} - g_{22}$ and $A_{21} = g_{21} - g_{11}$; UNIQUAC and UNIQUAC (mod) : $A_{12} = u_{12} - u_{22}$ and $A_{21} = u_{21} - u_{11}$.

Table 8.15. Model parameters (A_{12} and A_{21}) [a] and the absolute average deviation (AAD) values for the 1-propanol (1) + n-dodecane (2) VLE data.

Model	A_{12} (J.mol^{-1})	A_{21} (J.mol^{-1})	Δ P (bar)
	T = 373.15 K		
Wilson	12082.29	4173.61	0.018
T-K Wilson	10854.45	-642.71	0.047
NRTL ($\alpha_{12} = 0.47$)	8116.83	8354.41	0.044
UNIQUAC	-1259.37	5399.64	0.098
UNIQUAC (mod)	686.57	-4990.73	0.11
	T = 393.15 K		
Wilson	11905.20	5727.39	0.039
T-K Wilson	10677.71	-270.49	0.092
NRTL ($\alpha_{12} = 0.47$)	8723.72	8495.90	0.14
UNIQUAC	1514.68	-5684.34	0.44
UNIQUAC (mod)	1514.6767	-5684.34	0.44
	T = 423.15 K		
Wilson	10819.92	7318.30	0.073
T-K Wilson	8998.43	584.52	0.15
NRTL ($\alpha_{12} = 0.47$)	9380.71	7980.05	0.24
UNIQUAC	-1083.0	5027.92	0.24
UNIQUAC (mod)	-852.3914	-4294.1759	0.76

[a] Wilson and T-K Wilson : $A_{12} = \lambda_{12} - \lambda_{22}$ and $A_{21} = \lambda_{21} - \lambda_{11}$; NRTL : $A_{12} = g_{12} - g_{22}$ and $A_{21} = g_{21} - g_{11}$; UNIQUAC and UNIQUAC (mod) : $A_{12} = u_{12} - u_{22}$ and $A_{21} = u_{21} - u_{11}$.

Table 8.16. Model parameters (A_{12} and A_{21}) [a] and the absolute average deviation (AAD) value for the 2-butanol (1) + n-dodecane (2) VLE data.

Model	A_{12} (J.mol^{-1})	A_{21} (J.mol^{-1})	ΔP (bar)
	T = 373.15 K		
Wilson	8855.63	4833.55	0.02
T-K Wilson	7924.69	704.30	0.04
NRTL ($\alpha_{12} = 0.47$)	8449.70	6636.18	0.01
UNIQUAC	-995.51	3805.75	0.06
UNIQUAC (mod)	12882.74	-12884.49	0.20
	T = 393.15 K		
Wilson	8923.79	4953.29	0.04
T-K Wilson	8196.85	533.06	0.08
NRTL ($\alpha_{12} = 0.47$)	8625.77	6587.49	0.02
UNIQUAC	-1070.05	3980.75	0.12
UNIQUAC (mod)	214.11	-10862.14	0.42
	T = 423.15 K		
Wilson	7794.93	8719.48	0.14
T-K Wilson	6730.85	2480.60	0.14
NRTL ($\alpha_{12} = 0.47$)	9047.31	5554.90	0.14
UNIQUAC	-764.84	3493.40	0.20
UNIQUAC (mod)	-4687.62	-3913.49	0.48

[a] Wilson and T-K Wilson : $A_{12} = \lambda_{12} - \lambda_{22}$ and $A_{21} = \lambda_{21} - \lambda_{11}$; NRTL : $A_{12} = g_{12} - g_{22}$ and $A_{21} = g_{21} - g_{11}$; UNIQUAC and UNIQUAC (mod) : $A_{12} = u_{12} - u_{22}$ and $A_{21} = u_{21} - u_{11}$.

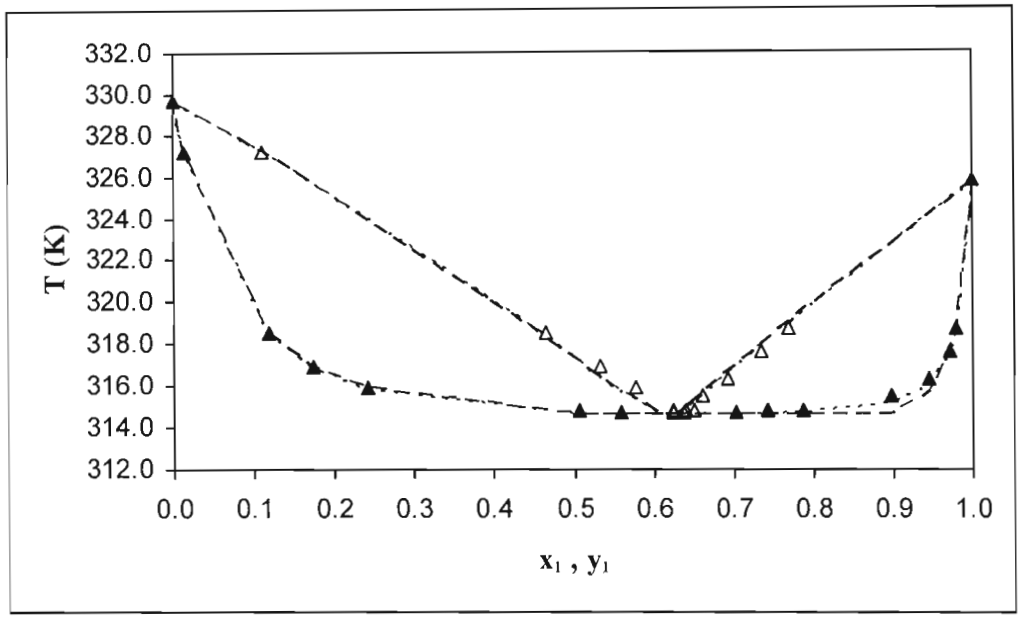

Figure 8.16. Experimental and calculated T-x_1-y_1 data for cyclohexane (1) + ethanol (2) at 40 kPa: ▲ experimental T-x_1 values; △ experimental T-y_1 values; - - - - - Wilson model; —— —— NRTL model.

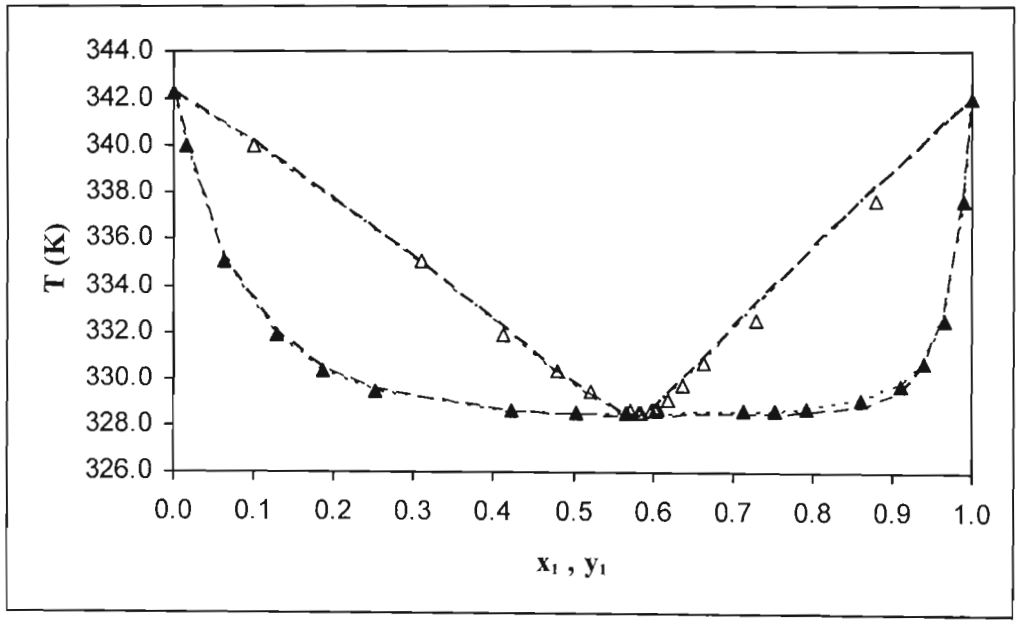

Figure 8.17. Experimental and calculated T-x_1-y_1 data for cyclohexane (1) + ethanol (2) at 69.8 kPa: ▲ experimental T-x_1 values; △ experimental T-y_1 values; - - - - - Wilson model; —— —— NRTL model.

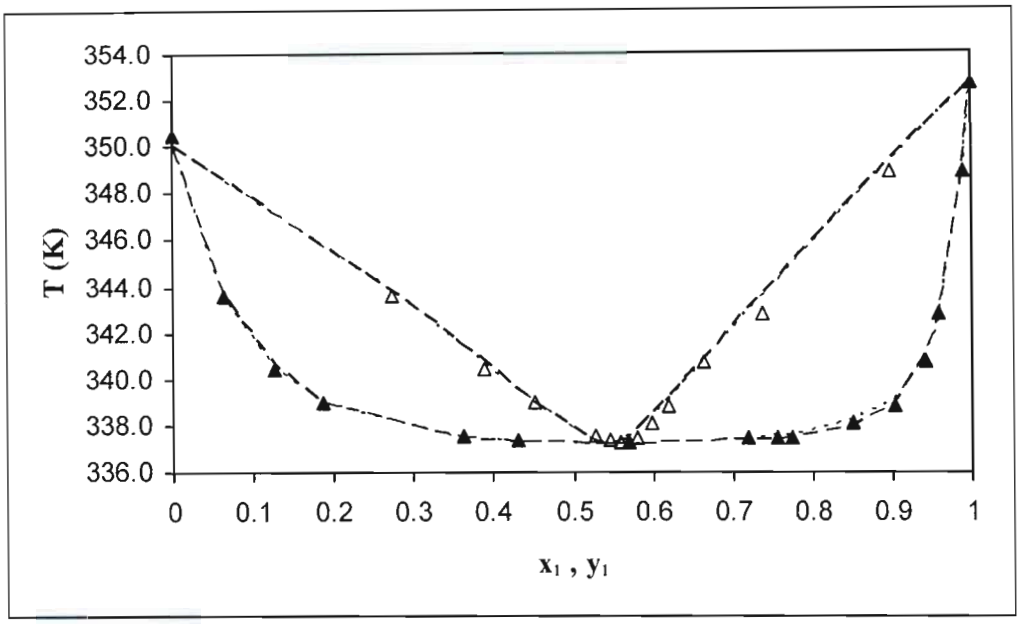

Figure 8.18. Experimental and calculated T-x_1-y_1 data for cyclohexane (1) + ethanol (2) at 97.7 kPa: ▲ experimental T-x_1 values; △ experimental T-y_1 values; - - - - - Wilson model; —— —— NRTL model.

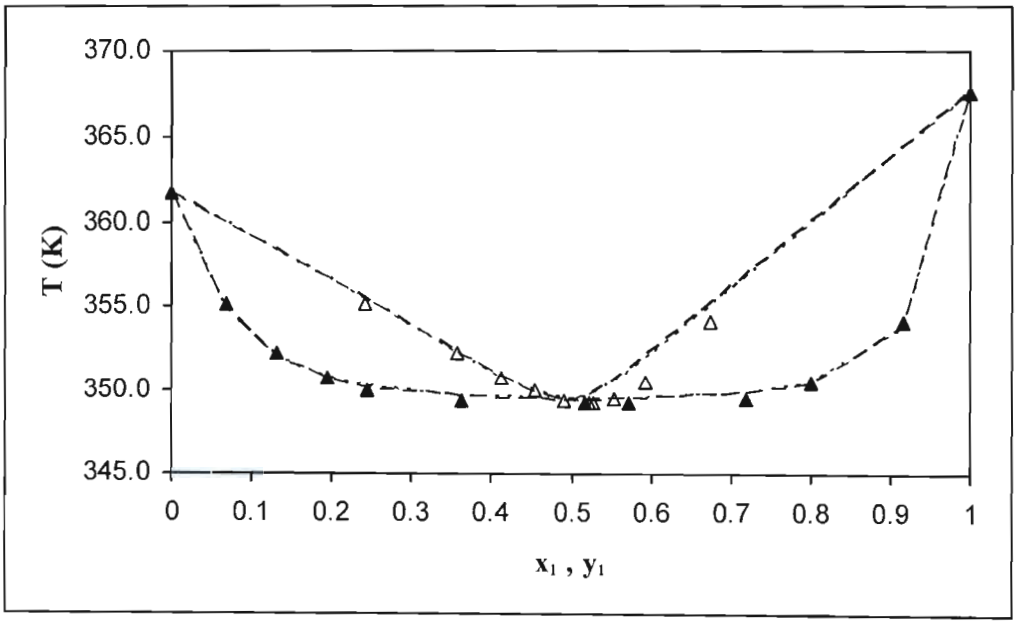

Figure 8.19. Experimental and calculated T-x_1-y_1 data for cyclohexane (1) + ethanol (2) at 150 kPa: ▲ experimental T-x_1 values; △ experimental T-y_1 values; - - - - - Wilson model; —— —— NRTL model.

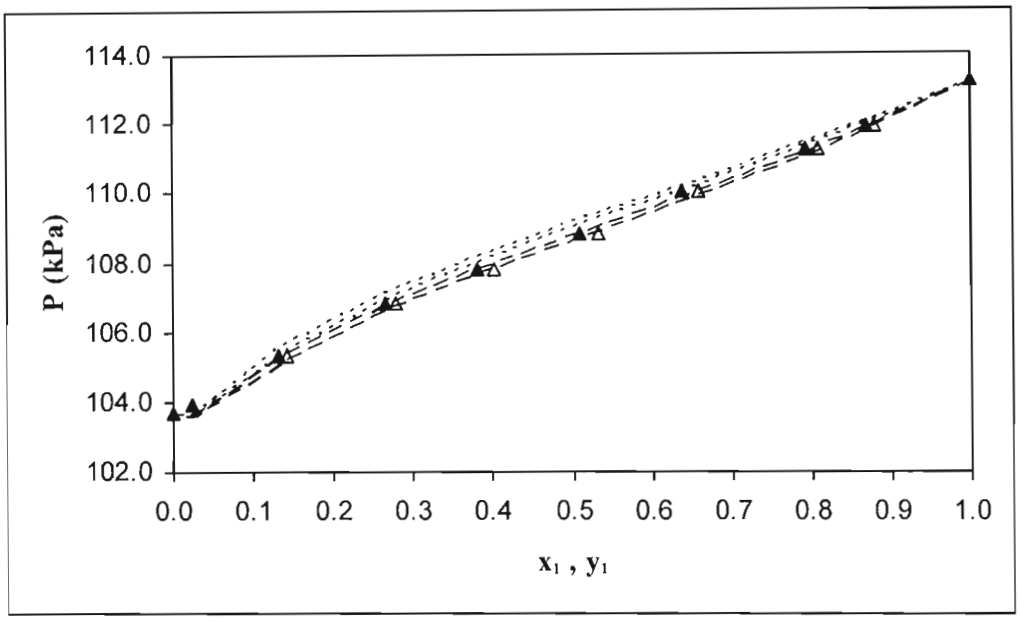

Figure 8.20. Experimental and calculated P-x_1-y_1 data for 1-propanol (1) + 2-butanol (2) at 373.15 K: ▲ experimental P-x_1 values; △ experimental P-y_1 values; - - - - - Wilson model; —— —— NRTL model.

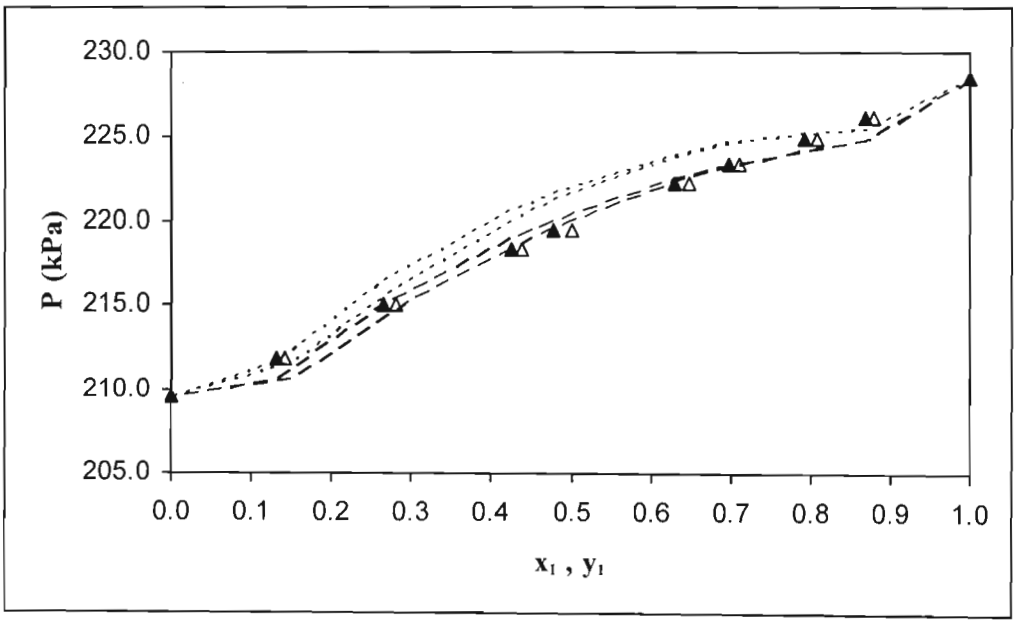

Figure 8.21. Experimental and calculated P-x_1-y_1 data for 1-propanol (1) + 2-butanol (2) at 393.15 K: ▲ experimental P-x_1 values; △ experimental P-y_1 values; - - - - - Wilson model; —— —— NRTL model.

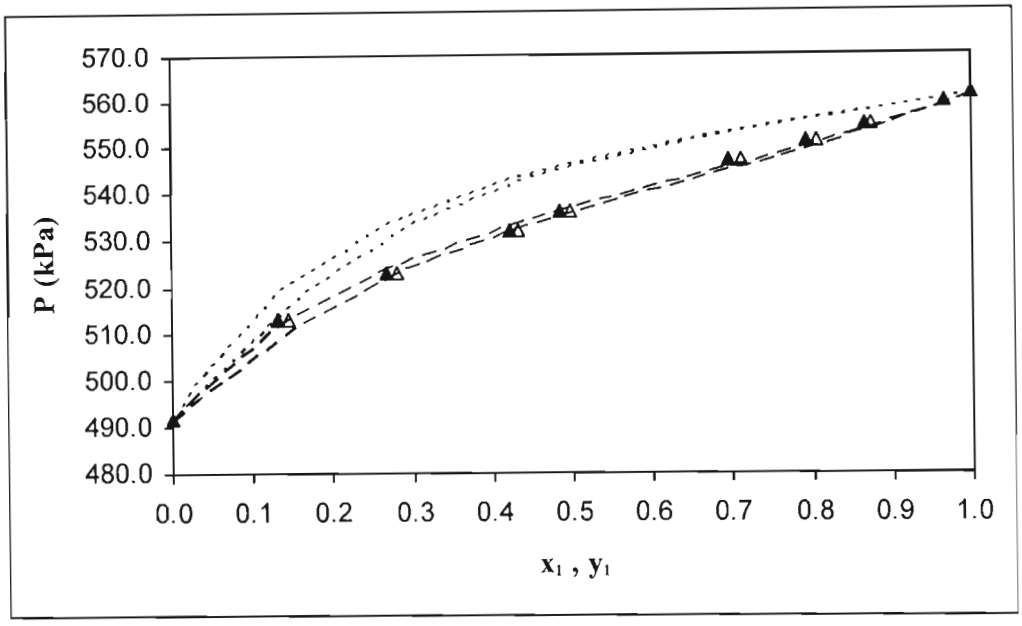

Figure 8.22. Experimental and calculated P-x_1-y_1 data for 1-propanol (1) + 2-butanol (2) at 423.15 K: ▲ experimental P-x_1 values; △ experimental P-y_1 values; - - - - - Wilson model; —— —— NRTL model.

8.3.2.2 The Phi-Phi (ϕ_i - ϕ_i) Method

The considerable utility and potential of the cubic EOS/ (A^E or G^E) approach in the framework of the ϕ_i - ϕ_i method for phase equilibrium correlations and computations was discussed at length in Chapter 3. The most important advantages of this approach are in terms of the wide applicability of the approach with regards to an extensive pressure and temperature range (up to the critical point) coupled with the unified treatment of both phases (through the fugacity coefficient). The only significant potential drawbacks of this approach are with regards to uncertainties in the treatment of highly nonideal polar or associating subcritical systems and highly asymmetric systems with a supercritical and heavy component. Since the latter were not measured in this study, the only initial concerns were with regards to the former in terms of the alkanol + alkanol and the alkanol + n-dodecane systems studied.

The modelling of the isothermal data with the ϕ_i - ϕ_i method has greater practical significance (Raal and Muhlbauer, 1998) than for isobaric data, consequently, only selected isothermal data sets were modelled with this method.

The highly recommended PRSV EOS was employed as the cubic EOS model together with the Huron-Vidal, MHV1 and MHV2 models as the corresponding mixing rules. The applicability of

the MHV1 approach for strongly nonideal mixtures at high and low pressures was demonstrated in the studies by Ohta (1996) and Ohta *et al.* (2002), where in the latter study the MHV1 model was shown to be superior to the Wong-Sandler mixing rule. The Wilson equation has been less popular than the NRTL equation in the cubic EOS/ (A^E or G^E) approach (Elizalde-Solis *et al.*, 2003; Giner *et al.*, 2005; Lopez *et al.*, 2006) but was chosen in this study to allow for a direct comparison of the relative efficiency of the equation in the cubic EOS/ (A^E or G^E) approach versus the traditional use of the Wilson equation in the γ_i - ϕ_i method. The use of the Wilson equation would also allow for a direct comparison of the vapour composition values predicted from the γ_i - ϕ_i approach versus those computed in the cubic EOS/(A^E or G^E) approach for the alkanol + n-dodecane systems.

Correlation of the Vapour-Liquid Equilibrium data

The systems modelled in the ϕ_i - ϕ_i method were for the isothermal measurements for the alkanol + alkanol and alkanol + n-dodecane systems in a BUBL P calculation, as described in Chapter 3. The required inputs for the BUBL P calculations are shown in Table 8.17.

The experimental VLE data were regressed with MATLAB® (version 7.0.1) with the Nelder-Mead Simplex method algorithm described in Chapter 3. The optimal adjustable parameters, together with the deviations for the calculated quantities for the Wilson model with the Huron-Vidal, MHV1 and MHV2 mixing rules, are shown in Table 8.18 for the 1-propanol + 2-butanol system.

For the 1-propanol + n-dodecane and 2-butanol + n-dodecane systems, for which experimental P-T-x data was obtained and the vapour phase composition (y) was computed, the residual in y *i.e.* Δy_1 was expressed as the difference between the value computed in the γ_i - ϕ_i method and that predicted by the ϕ_i - ϕ_i method. The optimal adjustable parameters, together with the deviations for the calculated quantities for the Wilson model with the MHV1 and MHV2 mixing rules, are shown in Tables (8.19) and (8.20) for the 1-propanol + n-dodecane and 2-butanol + n-dodecane systems, respectively. A synopsis of the relative correlative and computational efficiencies of the models is presented in Appendix D.

The comparative plots showing the experimental P-T-x-y data for the 1-propanol + 2- butanol system, as compared with the predictions from the HV and MHV1 models, is shown in Figure 8.23.

Table 8.17. Input parameters and data sources for the $\phi_i - \phi_i$ BUBL P computations.

Input parameter	Method	Source
$\alpha(T_r, \omega)$ correlation	PRSV	Stryjek and Vera (1986a)
Liquid molar volume	Modified Rackett	Reid *et al.* (1987)
Critical constants	-	Reid *et al.* (1987)
MHV1 [a] constants	-	Michelsen (1990b)
MHV2 [b] constants		Huang and Sandler (1993)

[a] q_i.

[b] q_1 and q_2.

The Huron-Vidal mixing rule could not be employed for the alkanol + n-dodecane systems as the model failed to converge to a proper solution in the minimization routine. Instability was primarily observed in the n-dodecane-rich region. This can probably be attributed to the poor representation of the dense n-dodecane liquid phase in the n-dodecane-rich region, which has been a traditional limitation of the use of cubic EOS models with the classical mixing rules. The effect of the initial guess on the performance of the model was investigated but did not yield any significant results. In general, the mixing rule model was the least efficient from a computational perspective, as discussed in Appendix D. However, excellent results were obtained for the model in the fitting of the 1-propanol + 2-butanol systems. The method was clearly superior with regards to the size of the pressure residuals and the overall fit of the data to the model when compared to the modified Huron-Vidal mixing rules, as shown in Table 8.18 and Figure 8.21.

From Table 8.18, it can be seen that the MHV1 mixing rule provided a satisfactory representation of the 1-propanol + 2-butanol data and provided the best fit for the experimental P-y_1 values. Although in the original formulation of the MHV2 model by Dahl and Michelsen (1990), the SRK EOS was employed for the demonstration of the usefulness of the model, the MHV2 mixing rule was observed to be much more efficient when employed with the PRSV EOS than the SRK EOS in a preliminary investigation with the two EOS models this study.

Table 8.18. Model parameters (A_{12} and A_{21}) [a] and absolute average deviation (AAD) values for the 1-propanol (1) + 2-butanol (2) VLE data.

Model	A_{12} (J.mol^{-1})	A_{21} (J.mol^{-1})	ΔP (kPa)	Δy_1
		T = 373.15 K		
HV-Wilson	1630.17	-1225.78	0.39	0.0042
MHV1-Wilson	820.1034	-820.1035	0.89	0.0007
MHV2-Wilson	2922.85	-1925.46	0.90	0.0066

[a] $A_{12} = \lambda_{12} - \lambda_{22}$ and $A_{21} = \lambda_{21} - \lambda_{11}$.

Table 8.19. Model parameters (A_{12} and A_{21}) [a] and absolute average deviation (AAD) values for the 1-propanol (1) + n-dodecane (2) VLE data.

Model	A_{12} (J.mol^{-1})	A_{21} (J.mol^{-1})	ΔP (kPa)	Δy_1 [b]
		T = 373.15 K		
MHV1-Wilson	9967.16	5151.73	4.1	0.0007
MHV2-Wilson	12312.28	6034.16	2.3	0.0003
		T = 393.15 K		
MHV1-Wilson	10151.09	7735.55	7.3	0.0005
MHV2-Wilson	11720.88	7191.40	5.4	0.0009

[a] $A_{12} = \lambda_{12} - \lambda_{22}$ and $A_{21} = \lambda_{21} - \lambda_{11}$.

[b] Where y_{exp} is the value computed in the $\gamma_i - \phi_i$ method.

Table 8.20. Model parameters (A_{12} and A_{21}) [a] and absolute average deviation (AAD) values for the 2-butanol (1) + n-dodecane (2) VLE data.

Model	A_{12} (J.mol^{-1})	A_{21} (J.mol^{-1})	ΔP (kPa)	Δy_1 [b]
		T = 373.15 K		
MHV1-Wilson	7927.97	4444.88	3.1	0.0005
MHV2-Wilson	9204.30	4918.45	2.2	0.0004
		T = 393.15 K		
MHV1-Wilson	8110.31	6236.67	6.7	0.0005
MHV2-Wilson	9102.23	5823.35	5.6	0.0011

[a] $A_{12} = \lambda_{12} - \lambda_{22}$ and $A_{21} = \lambda_{21} - \lambda_{11}$.

[b] Where y_{exp} is the value computed in the $\gamma_i - \phi_i$ method.

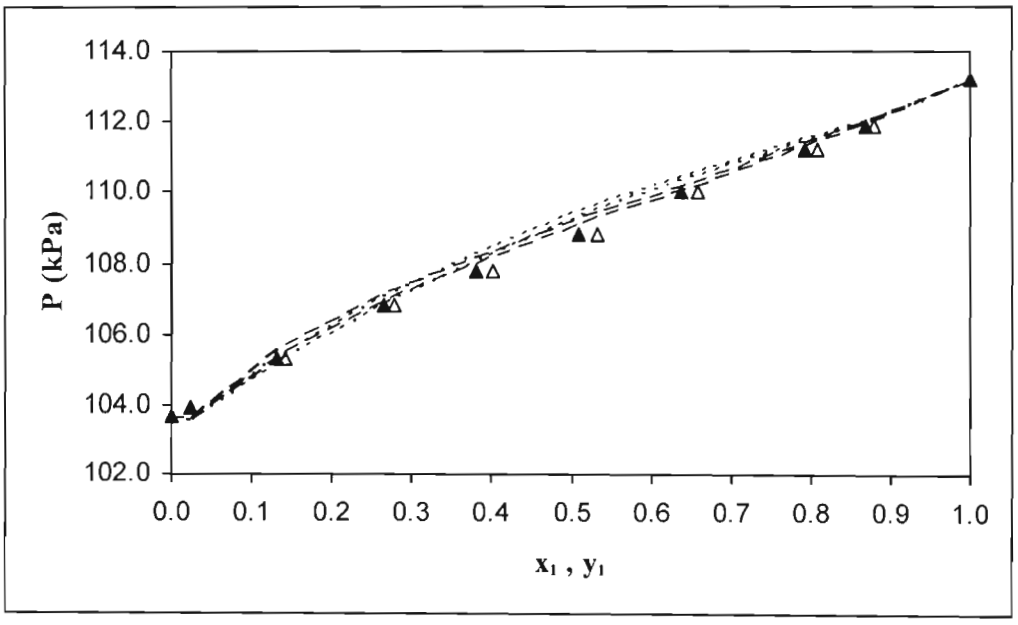

Figure 8.23. Experimental and calculated P-x_1-y_1 data for 1-propanol (1) + 2-butanol (2) at 373.15 K: ▲ experimental P-x_1 values; △ experimental P-y_1 values; - - - - - HV model; —— —— MHV1 model.

Despite being the most algebraically complex of all the mixing rules investigated here, the MHV2 model proved to be the most successful in terms of computational efficiency, however, the worst in terms of correlative efficiency for the 1-propanol + 2-butanol system, as shown in Table 8.18.

In the representation of the alkanol + n-dodecane systems, the small Δy residuals clearly indicate the excellent compatibility of the zero-reference pressure (ZRP) MHV1 and MHV2 mixing rules with the computed thermodynamic variables from the γ_i - ϕ_i approach (where the vapour composition was computed from the Wilson model for the P-T-x data sets). In terms of the fit of the P-T-x data by the models through an examination of the pressure residuals, a better representation of the data was achieved with the MHV2 mixing rules. Indeed the MHV1 and MHV2 mixing rules seem to complement one another with regards to vapour phase composition and pressure residuals, respectively.

The promising results in the fitting of the data sets above clearly affirms the tremendous potential of the cubic EOS/(A^E or G^E) approach and shows that the theoretical deficiencies of the HV-based approaches might not affect the computation of the phase equilibrium condition as adversely as postulated by some researchers.

8.3.3 Comparison of the Gamma-Phi (γ_i - ϕ_i) and Phi-Phi (ϕ_i - ϕ_i) Methods

The use of both the γ_i - ϕ_i and ϕ_i - ϕ_i methods in the treatment of the alkanol + alkanol and alkanol + n-dodecane systems allows for direct comparisons between the two approaches. With regards to the former, representation of the 1-propanol + 2-butanol system by the Wilson equation in both approaches is presented in Figure 8.24. As can be observed from the comparative plot, the use of the Wilson equation in the cubic EOS/ (A^E or G^E) with the HV mixing rule is only slightly inferior to that for the use of the model in the traditional γ_i - ϕ_i method. Quite clearly the use of the Wilson equation is reproduced quite well in the cubic EOS/ (A^E or G^E) approach for the conditions of the 1-propanol + 2-butanol system studied here.

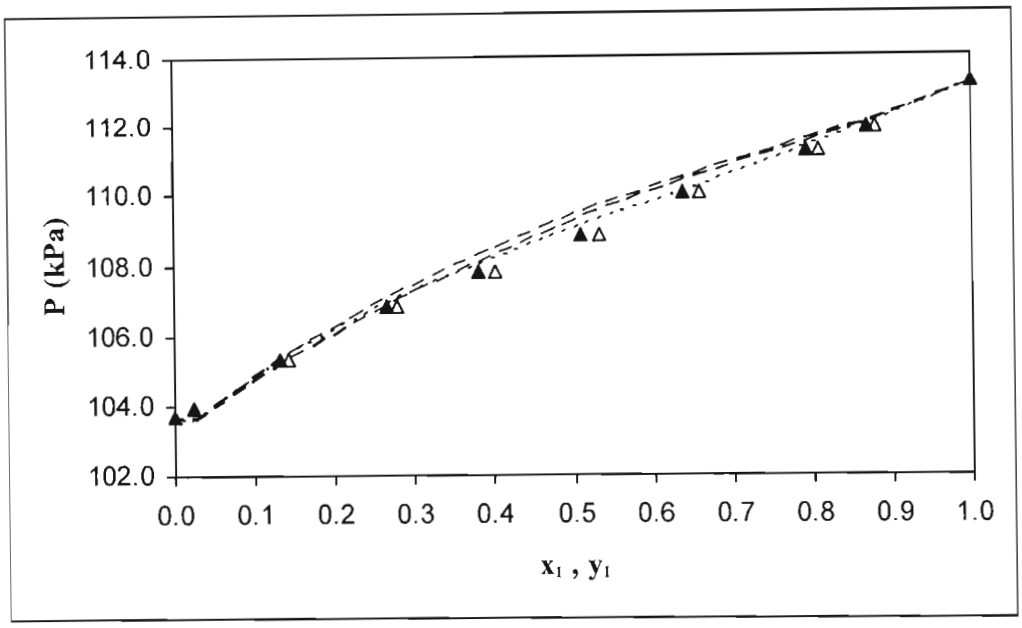

Figure 8.24. Comparison of the gamma-phi and phi-phi methods for the representation of 1-propanol (1) + 2-butanol (2) at 373.15 K with the Wilson equation: ▲ experimental P-x_1 values; △ experimental P-y_1 values; - - - - - Wilson model (γ_i - ϕ_i); —— —— HV-Wilson model (ϕ_i - ϕ_i).

As mentioned above, the small Δy residuals for the very high relative volatility alkanol + n-dodecane systems shown in Tables (8.19) and (8.20) clearly demonstrate good compatibility between the ZRP mixing rule models and the low-pressure Wilson G^E model, from which the vapour phase computations were computed in the γ_i - ϕ_i method.

The relative fits of the P-T-x data in the two methods is judged by the ΔP residuals in Tables (8.15) and (8.16) for the γ_i - ϕ_i method and Tables (8.21) and (8.20) for the ϕ_i - ϕ_i method. It can be observed that the Wilson model in the former approach provides a slightly better overall fit to the data than that for the latter.

8.3.4 Thermodynamic Consistency testing of the VLE data

The validation of a P-T-x-y VLE data set through thermodynamic consistency testing is an integral part of the theoretical treatment of the data. Thermodynamic consistency testing can be achieved through the any of or a combination of approaches discussed in Chapter 3; however, the Direct Test proposed by Van Ness (1995) for thermodynamic consistency testing is an effective means to assess the quality of a data set in a fairly unambiguous way and was consequently employed in this study.

In the application of the Direct TC test, which is inherently a modelling test, for the selection of an objective function (OF) and thermodynamic model, Van Ness (1995) proposed the following OF:

$$OF = \sum_{i=1}^{n} \left[\left(\ln \frac{\gamma_1}{\gamma_2} \right)^{exp} - \left(\ln \frac{\gamma_1}{\gamma_2} \right)^{calc} \right]_i^2 \qquad (3.310)$$

where γ_1 and γ_2 are the activity coefficients of components 1 and 2, the superscripts "exp" and "calc" designate the experimental and calculated quantities, respectively and n is the number of data points.

In the application of the Direct TC Test, Van Ness (1995) suggested the use of the 3-parameter Margules equation. However, as mentioned before, only semi-theoretical local composition G^E models would be employed for the representation of the liquid phase nonidealities in this study. In this regard, the Wilson equation proved adequate for the purposes of the Direct Test of Van Ness (1995). The minimization of the OF in Equation (3.306) produced a set of residuals in the form of root mean square deviation values (rmsd) as defined in Equation (8.6), the value of which served as the basis for the assessment of the data set in conjunction with the consistency index defined by Van Ness (presented in Appendix B). In this fashion, the data can be rated on a scale of 1-10, where high quality data would be in the vicinity of 1-3, satisfactory data would be around 4-5 and data of increasingly poor quality would be found from 5 onwards.

$$\delta \ln\left(\frac{\gamma_1}{\gamma_2}\right) = \sqrt{\left(\frac{1}{n}\right)\sum_{i=1}^{n}\left(\ln\left(\frac{\gamma_1}{\gamma_2}\right)^{exp} - \ln\left(\frac{\gamma_1}{\gamma_2}\right)^{calc} \right)^2} \qquad (8.6)$$

The results for the application of the Direct TC test to the P-T-x-y data sets measured in this study *i.e.* the cyclohexane + ethanol and the 1-propanol + 2-butanol systems are shown in Tables (8.21) and (8.22), respectively, in the form of the residuals and the associated consistency indices. The low values for the residuals for both sets of P-T-x-y measurements serve to validate the quality of the VLE data measured in this study. In addition, the consistently low values of the residual and consistency index for the cyclohexane + ethanol system demonstrate the excellent reproducibility in the accuracy of the experimental procedure and the apparatus through the systematic approach employed by the experimenter in acquiring VLE data.

Table 8.21. Results for the Direct TC Test on the cyclohexane (1) + ethanol (2) isobaric VLE data sets.

System pressure (kPa)	$\delta \ln\left(\frac{\gamma_1}{\gamma_2}\right)$	Index
40	0.049	2
69.8	0.048	2
97.7	0.044	2
150	0.062	3

Table 8.22 Results for the Direct TC Test on the 1-propanol (1) + 2-butanol (2) isothermal VLE data sets.

System temperature (K)	$\delta \ln\left(\frac{\gamma_1}{\gamma_2}\right)$	Index
373.15	0.008	1
393.15	0.026	2
423.15	0.050	2

For comparative purposes, the values obtained by other researchers such as Ku and Tu (2005) ranged from a consistency index of 4 to 8 for the isobaric VLE studies on acetone, ethanol and 2,2,4-trimethylpentane.

In the application of the Direct TC test, it was found that the test results are also model-dependent as it depends on the ability of the model to represent the activity coefficient behaviour of the system. Consequently, this test is not exempt from some of the deficiencies plaguing modelling TC tests in general *i.e.* considerations of the fit of the model in assessing that the quality of the P-T-x-y data.

8.4 Conclusion

The extensive theoretical framework of phase equilibrium thermodynamics disseminated in Chapter 3 has been put into practice for the experimental vapour pressure and VLE data acquired in this work, as shown in the contents of this Chapter. An excellent fit of the vapour pressure data to the correlating equations was achieved and the thermodynamic consistency testing validated the data for the 1-propanol pure component. The data for the vapour-liquid equilibrium measurements were fitted to the thermodynamic models in the gamma-phi and phi-phi models with varying degrees of success. In the case of the alkanol + n-dodecane systems, the value of the theoretical methods in indicating otherwise-undetectable erroneous data was clearly displayed.

A comparison of the correlating efficiencies of the gamma-phi and phi-phi methods was achieved through the modelling of the alkanol + alkanol and the alkanol + n-dodecane systems. There have been no significant differences between the two methods in terms of the representation of the systems that have been studied in both approaches. The latter, coupled with the applicability of the phi-phi method at elevated pressures and temperatures, exemplifies the tremendous promise of the cubic EOS/ (A^E or G^E) approach for the treatment of the VLE of highly nonideal subcritical components, which has traditionally been the domain of the gamma-phi method. The application of thermodynamic consistency testing to the experimental P-T-x-y data sets did not reveal the existence of any inconsistencies in the data sets.

CHAPTER 9

CONCLUSIONS

The project undertaken in this study encompassed the design and the development of a novel VLE apparatus through a systematic and informed manner so as to negate the traditional difficulties and limitations associated with past designs such as that of Harris (2004). A host of novel features were incorporated into the apparatus to further enhance the operational efficiency and the accuracy of vapour pressure and VLE measurements obtainable with the apparatus. The experimental vapour pressure and VLE data that were measured were subjected to theoretical treatment to assess the consistency of the data (where applicable) and to fully demonstrate the capabilities of the semi-theoretical framework of phase equilibrium thermodynamics in the representation of the nonideal VLE behaviour of the experimental systems that have been studied here.

9.1 Construction of a novel apparatus

The design of the novel VLE apparatus was based on the highly successful contemporary dynamic glass VLE still of Raal (Raal and Muhlbauer, 1998) that had been developed and tested in our laboratories. It was desirable to retain the excellent VLE measurement capabilities of this design but to extend the pressure and the temperature range of operation with a 316 SS VLE still design with Pyrex® glass inserts in strategic positions. For the final design of the apparatus, the maximum pressure and temperature limits for safe operation were 750 kPa and 600 K, respectively.

A great deal of innovation was employed in the incorporation of novel features for the design of the crucial sections of the apparatus. The use of the glass inserts in the Cottrell tube and the sample traps proved invaluable for monitoring and ensuring a proper approach of the measured systems to equilibrium by allowing for stable and continuous fluid flows to be maintained in the respective sections (as a function of heat input) and also, in general, facilitated the operation of the apparatus by the user. However, minor difficulties were experienced in the sealing of the glass-to-metal coupling fittings in the Cottrell tube design as the graphite ferrules that were used had to frequently be changed or re-packed to prevent any leaks in the system.

In addition to the use of graphite-based gaskets for the sealing of the reboiler and the equilibrium chamber flanged sections, the excellent sealing properties and chemical inertness of graphite was exploited for use in the design of an effective insulation scheme in the equilibrium chamber to further ensure that the packed section was maintained in an adiabatic state.

The design of the magnetically coupled stirrer with an indirect drive pulley system in the reboiler proved quite challenging in both the conception and execution of the final design. However, the latter was seen as being indispensable for the novel apparatus, as a study of past VLE designs, including that of Harris (2004), had demonstrated the dire consequences of the exclusion of mechanical agitation in the reboiler.

A great deal of attention had also been accorded to the design of the return line, where the respective phase return lines were combined before the re-entry of the mixed stream into the reboiler, where the common entry point was at the side of the reboiler and not directly underneath as in the design of Harris (2004).

The design of the apparatus with the novel features served to improve the approach of the apparatus to equilibrium for reliable VLE measurements (as indicated by a stable "plateau region") and to also facilitate the general operation of the apparatus. The versatility of the apparatus was demonstrated in the acquisition of vapour pressure and VLE data for subatmospheric and superatmospheric pressure ranges, as well as the acquisition of both isobaric and isothermal data sets for the VLE measurements.

9.2 Vapour Pressure measurements

The initial or preliminary testing of the most basic functioning of the apparatus was achieved by measuring pure component vapour pressures. The measurement of the pure component vapour pressures of 1-propanol for an extended pressure range was appropriate for demonstrating the capabilities of the apparatus. The accuracy of the measurements for the latter was validated through the use of vapour pressure correlating equations and qualitative thermodynamic consistency testing. The measurements also served to highlight the need for accurate experimental measurements of vapour pressures for extended pressure and temperature ranges, as for the 1-propanol measurements in this study. Considerable scatter amongst a variety of credible literature sources was observed for the literature vapour pressure predictions for 1-propanol with the correlation constants provided in various sources. Consequently great caution

must be exercised when employing the use of vapour pressure correlation constants from literature sources, especially for the use of the latter in phase equilibrium computations.

9.3 Vapour-Liquid Equilibrium measurements

The design of the apparatus was principally for the acquisition of VLE data for organic compounds at low to moderate pressures. These were undertaken for mixtures of alkanols and hydrocarbons in the form of the cyclohexane + ethanol isobaric data and the isothermal measurements for the 1-propanol + 2-butanol, 1-propanol + n-dodecane and 2-butanol + n-dodecane systems.

The test system selected was that of the highly nonideal cyclohexane + ethanol system at a pressure of 40 kPa. Good agreement between the experimental data and that for the literature data set of Joseph (2001) was obtained. Thereafter novel isobaric measurements were obtained for the cyclohexane + ethanol system at 69.8 kPa, 97.7 kPa and 150 kPa.

The alkanol + alkanol system investigated was the low relative volatility 1-propanol + 2-butanol system at 373.15 K, 393.16 K and 423.15 K. The latter constituted novel VLE measurements. Due to the ideal nature of the system, activity coefficients close to unity were obtained throughout the composition range.

The investigation of the very high relative volatility 1-propanol + n-dodecane and 2-butanol + n-dodecane systems represented a truly severe test of the performance and capability of the novel VLE apparatus. These measurements constituted novel data and as for the 1-propanol + 2-butanol system, isothermal data sets were measured at 373.15 K, 393.15 K and 423.15 K. In terms of the operation of the apparatus for the measurement of VLE of the alkanol + n-dodecane systems, there were no anomalies detected in the approach of the system to the equilibrium condition. However, in the computation of activity coefficients for the system, it was noticed that the latter did not obey the fundamental pure component limits for activity coefficient behaviour i.e. the symmetric normalization condition, especially for the n-dodecane component. Suspicions of the irregular activity coefficient values being due to the erroneous vapour phase measurements were aided by an observation of the excellent fit of the P-T-x data to the thermodynamic models and the predicted vapour phase compositions being higher than the corresponding experimentally measured values.
Consequently, even with the incorporation of innovative and novel features in the design and construction of the apparatus to measure "difficult" systems, the acquisition of a full P-T-x-y

data set for the alkanol + n-dodecane systems could not be achieved. The above findings serve to provide insight as why there has been an aversion to the measurement of VLE data for the high relative volatility and highly nonideal alkanol + n-alkane systems, especially with conventional dynamic recirculating VLE stills.

9.4 Theoretical treatment of the data

The theoretical treatment of the experimental data in the form of correlation and thermodynamic consistency testing allows for both maximizing the usefulness of the data and validating the data set. The gamma-phi $(\gamma_i - \phi_i)$ and phi-phi $(\phi_i - \phi_i)$ methods were employed in the correlation of the P-T-x-y and P-T-x data sets for the selected systems to allow for a comparison of the representation of the equilibrium condition through the two very different approaches.

In the $\gamma_i - \phi_i$ method, a variety of G^E thermodynamic models in the form of the Wilson, T-K Wilson, NRTL, UNIQUAC and modified UNIQUAC equations were employed together with the B-truncated virial equation of state to represent the liquid and vapour phases, respectively. The P-T-x-y experimental data sets for the cyclohexane + ethanol and 1-propanol + 2-butanol systems were regressed to the thermodynamic models to allow for the optimized model parameters and the appropriate calculated thermodynamic variables to be simultaneously obtained in the BUBL T and BUBL P methods, respectively. For the P-T-x data sets of the alkanol + n-dodecane systems, the application of the BUBL P procedure with the Wilson equation allowed for the computation of the vapour phase to complete the data set. Good fits of the experimental data to the flexible frameworks of the G^E models were observed with the Wilson equation providing the best overall fit to the systems studied.

In the $\phi_i - \phi_i$ computations, the highly promising cubic EOS/ (A^E or G^E) method was investigated with the Wilson G^E model and the Huron-Vidal-based approaches in the form of the original Huron-Vidal model and the modified Huron-Vidal models *i.e.* MHV1 and MHV2 coupled with the PRSV equation of state. Selected isotherms of the 1-propanol + 2-butanol and the alkanol + n-dodecane systems were modelled in this approach and the results were compared with those obtained in the $\gamma_i - \phi_i$ method. Direct comparison between the two methods revealed the great potential of the cubic EOS/ (A^E or G^E) method for representing the VLE behaviour of highly nonideal subcritical components in the form of the systems and conditions investigated in this study.

The contribution of this work to the body of contemporary phase equilibrium thermodynamics has been two-fold *i.e.* in terms of the practical aspects inherent in the design and operation of dynamic recirculation VLE measurement equipment and in an examination of the relative efficiencies of the theoretical frameworks of the γ_i - ϕ_i and ϕ_i - ϕ_i approaches in the treatment of the VLE of the systems measured in this study. With regards to the former, the challenges encountered here confirm and highlight the limitations of the conventional dynamic recirculating equipment for the measurement of "difficult' systems such as those exhibiting high relative volatilities and identify the need for alternative means or greater innovation for the measurement of such systems. The latter is a less likely avenue that can be explored in this regard. It was with great confidence that the highly effective novel features that were incorporated into this design were considered as allowing for a design which could be quite close to the optimal design of an apparatus which could allow for good efficiency with the dynamic liquid and vapour condensate recirculating method for the measurement of difficult systems.

The novel VLE data that have been obtained in this study are of considerable value for the development and validation of the predictive frameworks of approaches such as the predictive cubic EOS/ (A^E or G^E) method in the representation of VLE for a diversity of systems over different pressure and temperature ranges. From the conclusions obtained in this study with regards to the comparison of the γ_i - ϕ_i and ϕ_i - ϕ_i methods coupled with the inherent advantages of the latter, the cubic EOS/ (A^E or G^E) method approach is arguably one of the most promising areas of research in the field of contemporary phase equilibrium thermodynamics.

CHAPTER 10

RECOMMENDATIONS

The overall performance of the equipment has been quite satisfactory as evident in the results that have been obtained for the vapour pressure and vapour-liquid equilibrium measurements for both subatmospheric and superatmospheric measurements, with the exception of the isothermal VLE data sets for the very high relative volatility alkanol + n-dodecane systems. The erroneous vapour phase compositions that were obtained for the latter can probably be attributed to the inherent limitations of the operational principles of the dynamic recirculating method and to a lesser extent, the design of the equipment.

It was shown in this study that even with the incorporation of efficient stirring in the reboiler coupled with an optimized return line for the liquid and vapour condensate phases in the design of a dynamic recirculating VLE apparatus, the occurrence of non-equilibrium vapourization could not be negated for all the systems under study. This is favoured with an increase in the relative volatility of a system, had not been prevented for the measurements of the VLE behaviour of alkanol + n-dodecane systems. The latter constitute measurements for a very high relative volatility system, which are a class of VLE mixtures that have traditionally been difficult to accurately measure with dynamic liquid and vapour condensate recirculating method (Ellis, 1952; Maia de Oliveira, 2002).

It is therefore recommended that for measurements for these types of systems, alternative methods be used so that the problems incurred due to the boiling (reboiler), disengagement (equilibrium chamber) and mixing (return lines, reboiler) of the separated phases, which are the fundamental operational aspects of the dynamic recirculation VLE design, can be avoided. Indeed the measurements for such systems have been demonstrated in equipment designs where the phases are not recirculated but rather contained in a "stationary state" with efficient mechanical agitation as in the static equipment designs that have been presented in the studies by Fischer and Gmehling.(1996) and Motchelaho (2006).

10.1 Equipment design

In terms of the design of the equipment, potential improvements with regards to the operational efficiency of the apparatus can be achieved by modifying key functional areas such as the sample traps and the return lines.

10.1.1 The Sample traps

The holdup of the recirculated phases for sampling purposes in the static sampling traps is of increasing significance as the composition range approaches the dilute region for either of the pure components ends in a binary mixture. The sizing of the sample traps in this study were largely determined by the availability of cylindrical glass inserts for the intended pressure range of operation, where the latter meant that the sample traps were slightly over-sized relative to the vapour condensate sampling trap in the glass still design of Raal (Raal and Muhlbauer, 1998).
A diminution of the size of the sample trap would allow for less holdup in the sample trap to improve the approach of the system to equilibrium in the dilute regions. From the formula for determining the optimal dimensions of a Pyrex® glass insert under pressure, as shown in Chapter 4, the use of thicker-walled glass inserts for a given outer diameter would result in a decrease in the volume of liquid that is held up in the sampling trap.

10.1.2 The Return lines

As for the sample traps, the design of the return lines (including the exit tube from the equilibrium chamber) should ensure that there is minimal holdup or convolution in the return of the phases to the reboiler. Consequently, the length and the orientation of the return lines should maximize the effects of gravity *i.e.* hydrostatic head to allow for a fast flow for returning the phases as a combined stream to the reboiler. The design of the return lines in the apparatus did not allow for the fastest achievable flow rates for the phases due to the necessity of having to incorporate cooling sections (external cooling jackets) and also having ensuring that there was sufficient holdup of the phases for the latter to be effective (as discussed in Chapter 4). Consequently, the return lines can be shortened and the orientation of the latter can be changed to be at an acute angle to the vertical as opposed to horizontal to allow for faster flow patterns. To reduce the length of the return lines and still retain the effective cooling of the streams, an internal cooling coil can be incorporated in favour of the external cooling jackets in a shortened version of the return line cooling sections to that ensure efficient cooling of the faster flow of the phases is achieved.

10.2 Theoretical treatment of the data

Recommendations for theoretical treatment of the data would for be researchers who are active in the field of LPVLE measurement to demonstrate a greater willingness to examine the relative efficiencies of the γ_i - ϕ_i and ϕ_i - ϕ_i computations in the treatment of experimental VLE data,

as conducted in this study, to hasten unification of the γ_i - ϕ_i and ϕ_i - ϕ_i approaches into a more powerful thermodynamic framework *i.e.* the cubic EOS/ (A^E or G^E) method, for the correlation and computation of VLE data.

REFERENCES

An explanation of the formats used for the citations of the various reference sources and the contractions used for the journal publication names is give in Appendix E.

Abbott, M.M., *AIChE.J.* **19** (1973) 596.

Abbott, MM. and H.C. Van Ness, *AIChE.J.* **21(1)** (1975) 62-71.

Abbott, M.M., "Measurement of vapour-liquid equilibrium", in: T.S. Storvick and S.I. Sandler (Eds.), Phase Equilibria and Fluid Properties in the Chemical Industry, *Am.Chem.Soc.Symp.Ser.* 60, New York, 1978, pp. 87-98.

Abbott, M.M., *Adv.Chem.Ser.* **182** (1979) 47-70.

Abbott, M.M., *Fluid Phase Equilib.* **29** (1986) 193-207.

Abdoul, W., E. Rauzy and A. Peneloux, *Fluid Phase Equilib.* **68** (1991) 47-102.

Abrams, D.S., H.A. Massaldi and J.M. Prausnitz, *Ind.Eng.Chem.Fundam.* **13(3)** (1974) 259-262.

Abrams, D.S. and J.M. Prausnitz, *AIChE.J.* **21** (1975) 116-128.

Adachi, Y. and B. Lu, *AIChE.J.* **30** (1984) 991.

Adachi, Y. and H. Sugie, *Fluid Phase Equilib.* **28** (1986) 103-118.

Adachi, Y., *Fluid Phase Equilib.* **35** (1987) 309-312.

Adams, W.R., J.A. Zollweg, W.B. Streett and S.S. Rizvi, *AIChE.J.* **34(8)** (1988) 1378-1391.

Ahlers, J., PhD Thesis, University of Oldenburg, Oldenburg, Germany, 2003.

Altsheler, W.B., E.D. Unger and P. Kolachov, *Ind.Eng.Chem.* **43** (1951) 2559.

Anderson, T.F. and J.M. Prausnitz, *Ind.Eng.Chem.Proc.Des.Dev.* **17** (1978) 552.

Anderson, T.F. and J.M. Prausnitz, *Ind.Eng.Chem.Proc.Des.Dev.* **19** (1980a) 1-8.

Anderson, T.F. and J.M. Prausnitz, *Ind.Eng.Chem.Proc.Des.Dev.* **19** (1980b) 9-14.

Androulakis, I., N. Kalospiros and D.P. Tassios, *Fluid Phase Equilib.* **45** (1989) 135.

Antoine, C. *Compt.Rend.* **107** (1888a) 681.

Antoine, C. *Compt.Rend.* **107** (1888b) 836.

Arai, T. and H. Nishiumi, *Bull.Coll.Eng.Hosei Univ.* **20** (1987) 1.

Aroyan, H.J. and D.L. Katz, *Ind.Eng.Chem.* **43** (1951) 185.

Ashour, I., "PAREST - a computer program for the estimation of binary interaction parameters for equations of state", presented at Report LUTKDH/ (TKKA-7006)/1-24, Department of Chemical Engineering, Lund University, Sweden, 1986.

Atkins, P.W., Physical Chemistry, fourth ed., Oxford University Press, New York, 1999, pp. 200.

Atlas Steels, "Stainless Steel -Grade 316-Properties, Fabrication and Applications". Available online from: http://www.atlas-steels.com.au/technical-info.html.

Baba-Ahmed, A., P. Guilbot and D. Richon, *Fluid Phase Equilib.* **166** (1999) 225-236.

Bae, H., K. Nagahama and M. Hirata, *J.Chem.Eng.Japan.* **14** (1981) 1.

Barker, J.A., *Austr.J.Chem.* **6** (1953) 207.

Barnicki, S.D., "How Good Are Your Data?", June 2002. Available online from: http://www.cepmagazine.org.

Barragan-Aroche, J.F. and E.R. Bazua, *Fluid Phase Equilib.* **227** (2005) 97-112.

Behrens, P.K. and S.I. Sandler, *J. Chem.Eng.Data.* **28(1)** (1983) 52-56.

Bell, T.N., E.L. Cussler, K.R. Harris, C.N. Pepela and P.J. Dunlop, *J.Phys.Chem.* **72** (1968) 4693-4695.

Benedict, M., G. Webb and L. Rubin, *J.Chem.Phys.* **8** (1940) 334.

Berro, C., M. Rogalski and A. Peneloux, *Fluid Phase Equilib.* **8** (1982) 55-73.

Besserer, G.J. and G.J. Robinson, *Can.J.Chem.Eng.* **49** (1971) 651-656.

Bobbo, S., R. Stryjek, N. Elvassore and A. Bertucco, *Fluid Phase Equilib.* **150-151** (1998) 343-352.

Bondi, A., Physical Properties of Molecular Crystals, Liquids and Glasses, Wiley, New York, 1968.

Boukouvalas, C., N. Spiliotis, P. Coutsikos, N. Tzouvaras and D.P. Tassios, *Fluid Phase Equilib.* **92** (1994) 75.

Bourasseau, E., T. Sawaya, I. Mokbel, J. Jose and P. Ungerer, *Fluid Phase Equilib.* **225** (2004) 49-57.

Brandani, F., S. Brandani and V. Brandani, *Chem.Eng.Sci.* **53(4)** (1998) 853-856.

Brandani, S. and V. Brandani, *J.Chem.Therm.* **36** (2004) 1041-1047.

Briones , J.A., J.C. Millins, M.C. Thies and B.U. Kim, *Fluid Phase Equilib.* **36** (1987) 235-246.

Brown, I., *Austr.J.Sci.Res., Ser A: Phys.Sci.* **5** (1952) 530.

Bruin, S. and J.M. Prausnitz, *Ind.Eng.Chem.Proc.Des.Dev.* **10** (1971) 562.

Cailletet, L., *C.R. Acad.Sci.(Paris)*, **85**, (1877) 851-852.

Carnahan, N.F. and K.E. Starling, *J.Chem.Phys.* **51** (1969) 635.

Carnahan, N.F. and K.E. Starling, *AIChE.J.* **18** (1972) 1184.

Carrier, B., M. Rogalski and A. Peneloux, *Ind.Eng.Chem.Res.* **27** (1988) 1714.

Carveth, H.R., *Int.J.Phys.Chem.* **3** (1899) 193-213.

Chai, J.C. and Y.P Chen, *Fluid Phase Equilib.* **145** (1998) 193.

Chamorro, C.R., M.C. Martin, M.A. Villamanan and J.J. Segovia, *Fluid.Phase.Equilib.* **220** (2004) 105-112.

Chang, S.D. and B.C.Y. Lu, *Chem.Eng.Progr.Symp.Ser.* **63** (1967) 18-27.

Chao, K and J. Seader, *AIChE.J.* **7** (1961) 598.

Chen, C.C., S. Watanasiri, P. Mathias and V.V. de Leeuw, "Industry Perspective on the Economic Value of Applied Thermodynamics and the Unmet Needs of AspenTech Clients" in: T.M. Letcher (Ed.) , Chemical Thermodynamics for Industry, The Royal Society of Chemistry, Cambridge, 2004, Chapter 15, pp. 173.

Chen, J., K. Fischer and J. Gmehling, *Fluid Phase Equilib.* **200** (2002) 411-429.

Chilton, T.H., 4th Symposium on Chem.Eng. Education, Wilmington, Delaware, USA, 1935, pp. 64-71.

Chirico, R.D., A. Nguyen, W.V. Steele, M.M. Strube and C. Tsonopoulos, *J.Chem.Eng.Data.* **34** (1989) 149-156.

Chou, C., R. Forbert and J.M. Prausnitz, *J.Chem.Eng.Data.* **35** (1990) 26.

Christiansen, L.J. and Aa. Fredenslund, *AIChE.J.* **21** (1975) 49.

Christov, M. and R. Dohrn, *Fluid Phase Equilib.* **202** (2002) 173-174.

Chueh, P.L., N.K. Muirbrook and J.M. Prausnitz, *AIChE.J.* **11** (1965) 1097.

Chueh, P.L. and J.M. Prausnitz, *Ind.Eng.Chem.Fundam.* **6** (1967) 492.

Chung, T.H. and C.H. Twu, *Fluid Phase Equilibria.* **191** (2001) 1-14.

Cisternass, L.A., *Fluid Phase Equilib.* **39** (1988) 75-87.

Clausius, R., *Ann.Phys.Chem.* **9** (1880) 337.

Coon, J.E., J.E. Auwaerter and E. McLaughlin, *Fluid Phase Equilib.* **44** (1989) 305-345.

Corning Glass Works U.S.A, Technical Sales Department of Corning Limited, Laboratory Division, Technical Data on Pyrex® borosilicate glass.

Cottrell, F.G., *J.Am.Chem.Soc.* **41** (1919) 721-728.

Coutinho, J., G. Kontogeorgis and E. Stenby, *Fluid Phase Equilib.* **102** (1994) 31.

Coutsikos, P., N.S. Kalospiros and D.P. Tassios, *Fluid Phase Equilib.* **108** (1995) 59-78.

Dahl, S. and M.L. Michelsen, *AIChE.J.* **36** (1990) 1829.

Darwish, N.A. and Z.A. Al-Anber, *Fluid Phase Equilib.* **131** (1997) 287.

Daubert, T.E. and D.K. Jones, "Project 821: Pure Component Liquid Vapor Pressure Measurements" in: T.B. Selover (Ed.), Design Institute for Physical Property Data: Ten Years of Accomplishment, AIChE Symposium Series No.275, 1990, Volume 86, pp.29-39.

Daubert, T.E., "Vapor Pressures of 13 Pure Industrial Chemicals" in: J. Cunningham and D.K. Jones (Eds.), Experimental Results for Phase Equilibria and Pure Components, DIPPR Data Series, 1991, Volume 1, pp. 81-95.

Deiters, U.K. and G.M. Schneider, *Fluid Phase Equilib.* **29** (1986) 145-160.

Deiters, U.K. and G.M. Schneider, *Ber.Bunsenges.Phys.Chem.* **12** (1986) 1316.

Deiters, U.K., M. Hloucha and K. Leonard, "Experiments?-No Thank You!" in: T.M. Letcher (Ed.), Chemical Thermodynamics: A Chemistry for the 21st Century, Blackwell Science, Oxford, 1999, Chapter 15, pp. 187-195.

De Alfonso, C., A.A. Canovas and S.B. Llana, *An.Quim.Ser.A.* **82** (1988) 320, as retrieved from the Dortmund Data Bank, DDBST Software and Separation Technology GmbH, DDB Software Package Version 1999, Oldenburg, 1999.

de Loos, T.W., H.J. van der Kooi and P.L. Ott, *J.Chem.Eng.Data.* **31** (1986) 166-168.

de Loos, T.W., W. Poot and J. De Swaan Arons, *Fluid Phase Equilib.* **42** (1988) 209-227.

DiAndreth, J.R., J.M. Ritter and M.E. Paulaitis, *Ind.Eng.Chem.Res.* **26** (1987) 337-343.

Dohrn, R. and G. Brunner, *Fluid Phase Equilib.* **106** (1995) 214.

Dorau, W., H. Kremer and H. Knapp, *Fluid Phase Equilib.* **11** (1983) 83.

Dortmund Data Bank, DDBST Software and Separation Technology GmbH, DDB Software Package Version 1999, Oldenburg, 1999.

Douslin, D.R. and A.G. Osborn, *J.Sci.Instrum.* **42** (1965) 369.

D'Souza, R., J.R. Patrick and A.S. Teja, *Can.J.Chem.Eng.* **66** (1988) 319-323.

D'Souza, R. and A.S. Teja, *Fluid Phase Equilib.* **39** (1988) 211-224.

Dvorak, K. and T. Boublik, *Collect.Czech.Chem.Commun.* **28** (1963) 1249-1255.

Dymond, J.H. and E.B. Smith, The Virial Coefficients of Pure Gases and Mixtures: A Critical Compilation, Clarendon Press, Oxford, 1980.

Eliezer, S., A. Ghatak and H. Hora, Fundamentals of Equations of State, World Scientific Publishing Company, Singapore, 2002.

Elizalde-Solis, O., L.A. Galicia-Luna, S.I. Sandler and J.G. Sampayo-Hernandez, *Fluid Phase Equilib.* **210** (2003) 215-227.

Elliot, J.R. and T.E Daubert, *Ind.Eng.Chem.Proc.Des.Dev.* **24** (1985) 743.

Elliot, J.R. and C.T. Lira, Introductory Chemical Engineering Thermodynamics, Prentice-Hall, Upper Saddle River, New Jersey, 1999.

Ellis, S.R.M., *Trans.IChemE.* **30** (1952) 58-64.

Ellis, S.R.M. and D.A. Jonah, *Chem.Eng.Sci.* **17** (1962) 971-976.

Englezos, P., N. Kalogerakis and P.R. Bishnoi, *Fluid Phase Equilib.* **53** (1989) 81-88.

Englezos, P., N. Kalogerakis, M.A. Trebble and P.R. Bishnoi, *Fluid Phase Equilib.* **58** (1990) 117-132.

Englezos, P., N. Kalogerakis and P.R. Bishnoi, *Can.J.Chem.Eng.* **71** (1993) 322-326.

Eubank, P.T., B.G. Lamonte and J.F. Javier Alvarado, *J.Chem.Eng.Data.* **45** (2000) 1040-1048.

Feroiu, V. and D. Geana, *Fluid Phase Equilib.* **120** (1996) 1-10.

Figuiere, P., J.F. Hom, S. Laugier, H.L. Renon, D. Richon and H. Szwarc, *AIChE.J.* **26(5)** (1980) 872-875.

Fink, S.D. and H.C. Hershey, *Ind.Eng.Chem.Res.* **29** (1990) 295-306.

Fischer, K. and J. Gmehling, *J.Chem.Eng.Data.* **39** (1994) 309-315.

Fischer, K. and J. Gmehling, *Fluid Phase Equilib.* **112** (1995) 1-22.

Fischer, K., and J. Gmehling, *Fluid Phase Equilib.* **119** (1996) 113-130.

Fischer, K., *Fluid Phase Equilib.* **121** (1996) 185-206.

Fischer, K. and M. Wilken, *J.Chem.Thermodyn.* **33** (2001) 1285-1308.

Flory, P.J., Principles of Polymer Chemistry, Cornell University Press, Ithaca, New York, 1953.

Fontalba, F. D. Richon and H.L. Renon, *Rev.Sci.Instrum.* **55** (1984) 944-951.

Fornari, R., P. Alessi and I. Kikic, *Fluid Phase Equilib.* **57** (1990) 1-33.

Fredenslund, Aa., J. Mollerup and L. Christensen, *Cryogenics.* **13** (1973) 414.

Fredenslund, Aa., J. Gmehling and P. Rasmussen, Vapor-Liquid Equilibria Using UNIFAC, Elsevier, Amsterdam, 1977.

Fredenslund, Aa and J.M. Sorensen, "Group Contribution Estimation Methods" in S.I. Sandler (Ed.), Models for Thermodynamic and Phase Equilibria Calculations, Marcel Dekker, New York, 1994, Chapter 4, pp.287-362.

Freeman, J.R. and G.M. Wilson, "High Temperature Vapour-Liquid Equilibrium Measurements on Acetic Acid/Water Mixtures" in: M.S. Benson and D. Zudkevitch (Eds.), Experimental Results from the Design Institute for Physical Property Data I: Phase Equilibria, AIChE Symposium Series No.244, 1985, Volume 81, pp.14.

Freitag, N.P. and D.B. Robinson, *Fluid Phase Equilib.* **31(1)** 1986 183-201.

Fuller, G.G., *Ind.Eng.Chem.Fundam.* **15** (1976) 254.

Gani, R., N. Tzouvaras, P. Rasmussen and Aa. Fredenslund, *Fluid Phase Equilib.* **47** (1989) 133.

Gao, G., J.L. Dadiron, H. Saint-Guirons, P. Xans and F. Montel, *Fluid Phase Equilib.* **74** (1992) 85.

Garber, J.D. and W.T Ziegler, *J.Chem.Eng.Data.* **24** (1979) 330-338.

Gatreaux, M.F. and J. Coates, *AIChE.J.* **1** (1955) 496-500.

Gelus, E., S. Marple, Jr and M.E. Miller, *Ind.Eng.Chem.* **41(8)** (1939) 1757-1761.

Gerald, C.F. and P.O. Wheatley, Applied Numerical Analysis, sixth ed., Addison-Wesley, Reading, Massachusetts, 1999.

Gess, M.A., R.P. Danner and M. Nagvekar, Thermodynamic Analysis of Vapour-Liquid Equilibria: Recommended Models and a Standard Database, Design Institute for Physical Property Data, American Institute of Chemical Engineers, 1991.

Ghosh, P., *Chem.Eng.Technol.* **22(5)** (1999) 379-399.

Gibbs, R.E. and H.C. Van Ness, *Ind.Eng.Chem.Fundam.* **11(3)** (1972) 410-413.

Gillespie, D.T.C., *Ind.Eng.Chem.Anal.Ed.* **18** (1946) 575

Giner, B., M.C. Lopez, P. Cea, C. Lafuente and F.M. Royo. *Fluid Phase Equilib.* **232** (2005) 50-56.

Gmehling, J. and U. Onken, Vapour Liquid Equilibrium Data Collection, DECHEMA Chemistry Data Series, Volumes 1-8, Frankfurt, 1977.

Gmehling, J., J. Li and K. Fischer, *Fluid Phase Equilib.* **141** (1997) 113-127.

Gmehling, J., "The Basis for the Synthesis, Design and Optimization of Thermal Separation Processes" in: T.M. Letcher (Ed.), Chemical Thermodynamics: A Chemistry for the 21st Century, Blackwell Science, Oxford, 1999, Chapter 1, pp. 1-13.

Gmehling, J. *Pure Appl. Chem.* **75(7)** (2003) 875-888.

Goral, M., *Fluid Phase Equilib.* **178** (2001) 153.

Graboski, M.S. and T.E Daubert, *Ind.Eng.Chem.Proc.Des.Dev.* **17** (1978) 441-443.

Grafahrend, W., PhD Thesis, Berlin, 1988, as retrieved from the Dortmund Data Bank, DDBST Software and Separation Technology GmbH, DDB Software Package Version 1999, Oldenburg, 1999.

Griswold, J., D. Andres and V.A. Klein, *Petrol.Ref.* **22(6)** (1943) 99-108.

Guggenheim, E.A., Mixtures: the theory of the equilibrium properties of some simple classes of mixtures, solutions and alloys, Oxford University Press, Oxford, 1952.

Guggenheim, E.A., *Mol.Phys.* **9** (1965) 199.

Guillevic, J., D. Richon and H.L. Renon, *Ind.Eng.Chem.Fundam.* **22** (1983) 495.

Gupta, A., S. Gupta, F.R. Groves, Jr and E. McLaughlin, *Fluid Phase Equilib.* **65** (1991) 305-326.

Gupte, P.A., P. Rasmussen and Aa. Fredenslund, *Ind.End.Chem.Fundam.* **25** (1986a) 636.

Gupte, P.A., P. Rasmussen and Aa. Fredenslund, *Fluid Phase Equiib.* **29** (1986b) 485.

Gupte, P.A. and T.E. Daubert, *Fluid Phase Equilib.* **28** (1986) 155.

Hala, E., J. Pick, V. Fried and O. Vilim, Vapour-Liquid Equilibrium, second ed., Pergamon Press, Oxford, 1967.

Han, S.J., H.M. Lin and K.C. Chao, *Chem.Eng.Sci.* **43** (1988) 2327.

Harmens, A. and H. Knapp, *Ind.Eng.Chem.Fundam.* **19** (1980) 291-294.

Harris, R.A., MSc Dissertation, University of Natal , Durban, South Africa, 2001.

Harris, R.A., PhD Thesis, University of KwaZulu-Natal, Durban, South Africa, 2004.

Hayden, J.G. and J.P. O'Connell, *Ind.Eng.Chem.Proc.Des.Dev.* **14(3)** (1975) 209-216.

Haynes, S. and M. Van Winkle, *Ind.Eng.Chem.* **46(2)** (1954) 334-335.

Heertjes, P.M., *Chem.Proc.Eng.* **41** (1960) 385-386.

Heidemann, R.A. and S.S.H. Rizvi, *Fluid Phase Equilib.* **29** (1986) 439.

Heidemann, R.A. and S.L. Kokal, *Fluid Phase Equilib.* **56** (1990) 17-37.

Heidemann, R.A., *Fluid Phase Equilib.* **116** (1996) 454-464.

Heintz, A. and W.B. Streett, *Ber.Bunsenges.Phys.Chem.* **87** (1983) 298-303.

Herington, E.F.G., *Nature* **160** (1947) 610.

Herington, E.F.G., *J.Inst.Petrol.* **37** (1951) 457.

Heyen, G., "Liquid and vapour properties from a cubic equation of state" in: H. Knapp and S.I. Sandler (Eds.), Proceedings of the Second International Conference on Phase Equilibria and Fluid Properties in the Chemical Industry, DECHEMA, Frankfurt/Main, Germany, 1980.

Heyen, G., "A Cubic Equation of State with Extended Range of Application", presented at the Second World Congress on Chemical Engineering, Montreal, Canada, 1981.

Hiaki, T., K. Yamato, H. Miyazawa and K. Kojima, *Can.J.Chem.Eng.* **72** (1994) 142-147.

Hildebrand, J. and S.E. Wood, *J.Chem.Phys.* **1** (1933) 817.

Hildebrand, J.H. and R.L. Scott, The Solubility of Non-electrolytes, Dover, 1964.

Hipkin, H. and H.S. Meyers, *Ind. Eng.Chem.* **41(12)** 2524-2528.

Hiranuma, M. and K. Honma, *Ind.Eng.Chem.Proc.Des.Dev.* **14** (1975) 221.

Hirata, M., S. Ohe and K. Nagahama, Computer Aided Data Book of Vapor-Liquid Equilibria, Elsevier, New York, 1975.

Hochgeschurtz, T., K.W. Hutchinson and J.R. Roebers, G.Z. Liu, J.C. Mullins and M.C. Thies, "Production of Mesophase Pitch by Supercritical Fluid Extraction" in: E. Kiran and J.F. Brennecke(Eds.), Supercritical Fluid Engineering Science, Washington D.C., 1993, pp. 347-362.

Holderbaum, T. and J. Gmehling, *Fluid Phase Equilib.* **70** (1991) 251.

Hsu, J.J.C., N. Nagaranjan and R.L. Robinson, *J.Chem.Eng.Data.* **30** (1985) 485-491.

Huang, A., S. Leu, H. Ng and D. Robinson, *Fluid Phase Equilib.* **19** (1985) 21.

Huang, H. and S.I. Sandler, *Ind.Eng.Chem.Res.* **32** (1993) 1498.

Huang, J.F. and L.S. Lee, *Fluid Phase Equilib.* **101** (1994) 27-51.

Huang, J.F. and L.S. Lee, *Fluid Phase Equilib.* **121** (1996) 27-43.

Huron, M. and J.Vidal, *Fluid Phase Equilib.* **49** (1979) 255.

Inglis, J.KH., *Philos.Mag.* **11**(1906) 640-658.

Inomata, H., K. Tuchiya, K. Arai and S. Saito, *J.Chem.Eng.Japan.* **19** (1986) 386.

Inomata, H., N. Ihawa, K. Arai and S. Saito, *J.Chem.Eng.Data.* **33** (1988) 26-29.

Jackson, P.L. and R.A. Wilsak, *Fluid Phase Equilib.* **103** (1995) 155-197.

Japas, M. and E. Frank, *Ber.Bunsenges.Phys.Chem.* **89** (1985) 793.

Jaubert, J.N. and F. Muletet, *Fluid Phase Equilib.* **224** (2004) 285-304.

Jelic, J.M., A.Z. Tasic, B.D. Djordjevic and S.P. Serbanovic, *J.Serb.Chem.Soc.* **65(12)** (2000) 877-889.

Jennings, D.W. and A.S. Teja, *J.Chem.Eng.Data.* **34** (1989) 305-309.

Jin, Z.L., K.Y. Liu and W.W. Sheng, *J.Chem.Eng.Data.* **38** (1993) 353-355.

Jones, C.A., E.M. Schoenborn and A.P. Colburn, *Ind.Eng.Chem.* **35** (1943) 666-672.

Jordan, B.T. and M. Van Winkle, *Ind.Eng.Chem.* **43(12)** (1951) 2908-2912.

Joseph, M.A., MSc Dissertation, University of Natal, Durban, South Africa, 2001.

Joseph, M.A., J.D. Raal and D. Ramjugernath, *Fluid Phase Equilib.* **182** (2001) 157-176.

Joseph, M.A., D. Ramjugernath and J.D. Raal, *Dev.Chem.Eng.Min.Proc.* **10(5/6)** 2002 615-637.

Joyce, P.C., B.E. Leggett and M.C. Thies, *Fluid Phase Equilib.* **158-160** (1999) 723-731.

Kaiser, T., C. Volmerbaumer and G. Schweiger, *Ber.Bunsenges.Phys.Chem.* **96** (1992) 976-980.

Kalospiros, N.S., N. Tzouvaras, P. Coutsikos and D.P. Tassios, *AIChE.J.* **41(4)** (1995) 928-937.

Kalra, H. and D. Robinson, *Cryogenics*. **15** (1975) 409.

Kalra, H., H. Kubota, D.B. Robinson and H.J. Ng, *J.Chem.Eng.Data.* **23(4)** (1978) 317-321.

Katayama, T., K. Ohgaki, G. Maekawa, M. Goto and T. Nagano, *J.Chem.Eng.Japan.* **8(2)** (1975) 89-92.

Kato, R. and J. Gmehling, *J.Chem.Thermodyn.* **37** (2005) 609.

Kay, W.B., *Ind.Eng.Chem.* **28** (1936) 1014-1019.

Kemeny, S. and J. Manczinger, *Chem.Eng.Sci.* **33** (1978) 71-76.

Kim, C., A. Clark, P. Vimalchand and M. Donohue, *J.Chem.Eng.Data.* **34** (1989) 391.

Kim, Y., P. Uusi-Kyyny, J.P. Pokki, M. Pakkanen, R. Multala, L.M. Westerlund and J. Aittamaa, *Fluid Phase Equilib.* **226** (2004) 173-181.

King, M.B. and D.A. Alderson, F.H. Fallah, K.M. Kassim, J.R. Sheldon and R.S. Mahmud, "Some Vapour-Liquid and Vapour-Solid Equilibrium Measurements of Relevance for Supercritical Extraction Operations and their Correlation." in: M.E. Paulaitis, J.M.L. Penninger, R.D. Gray and P. Davidson (Eds.), Chemical Engineering at Supercritical Fluid Conditions, Ann Arbor: The Butterworth Group, Michigan, USA, 1983, pp 31-80.

Kneisl, P., J.W. Zondlo, W.B. Whiting and M. Bedell, *Fluid Phase Equilib.* **46** (1989) 85-94.

Knudsen, K., E.H. Stenby and Aa. Fredenslund, *Fluid Phase Equilib.* **82** (1993) 361-368.

Kobayashi, R.S. and D.L. Katz, *Ind.Eng.Chem.* **45(2)** (1953) 440-457.

Kogan, V.B., Heterogenous Equilibria, *Izdatelstvo Khimiya*, Leningrad, 1968.

Kojima, K., H.M. Moon and K. Ochi, *Fluid Phase Equilib.* **56** (1990) 269-284.

Kojima, K., *Fluid Phase Equilib.* **136** (1997) 63-77.

Kolar, P. and K. Kojima, *J.Chem.Eng. Japan.* **27(4)** (1994) 460-465.

Kolbe, B. and J. Gmehling, *Fluid Phase Equilib.* **23** (1985) 213-226.

Konrad, R., I. Swaid and G.M. Schneider, *Fluid Phase Equilib.* **10** (1983) 307.

Kontogeorgis, G.M. and P.M. Vlamos, *Chem.Eng.Sci.* **55** (2000) 2351-2358.

Krumins, A.E., A.K. Rastogi, M.E. Rusak and D.P. Tassios, *Can.J.Chem.Eng.* **58** (1980) 663-669.

Ku, H.C. and C.H. Tu, *Fluid Phase Equilib.* **213** (2005) 99-108

Kubota, H., H. Inotome, Y. Tanaka and T. Makita, *J.Chem.Eng.Japan.* **16** (1983) 99.

Kuenen, J.P, *Philos.Mag.* **40** (1895) 176-194.

Kurihara, K. and T. Tochigi, K. Kojima, *J.Chem.Eng.Japan.* **20** (1987) 227-231.

Ladurelli, A.J., C.H. Eon and G. Guiochon, *Ind.Eng.Chem.Fundam.* **14** (1975) 191.

Lancaster, J.F., "Material Selection" in R.W. Nichols (Ed.), Pressure Vessel Engineering Technology, Applied Science Publishers, London, 1971, Chapter 5, pp. 235.

Larsen, B.L., P. Rasmussen and Aa. Fredenslund, *Ind.Eng.Chem.Res.* **26** (1987) 2274-2286.

Laugier, S., D. Richon and H.L. Renon, *Fluid Phase Equilib.* **54** (1990) 19-34.

Lauret, A., D. Richon and H.L. Renon, *Int.J.Energy.Research.* **18** (1994) 267-275.

Lee, L.L. and W.A. Scheller, *J.Chem.Eng.Data.* **12(4)** (1967) 497-499, as reported by M. Hirata, S. Ohe and K. Nagahama, Computer Aided Data Book of Vapor-Liquid Equilibria, Elsevier, New York, 1975.

Lee, S.C., *J.Phys.Chem.* **35** (1931) 3558-3582.

Lee Valley & Veritas, Lee Valley Tools, "About Rare-Earth Magnets", 2006. Available online from: http://www.leevalley.com.

Legret, D., D. Richon and H.L. Renon, *AIChE.J.* **27(2)** (1981) 203-207.

Lermite, C., and J. Vidal, *Fluid Phase Equilib.* **72** (1992) 111.

Leslie, R.T. and E.C. Kuehner, "Ebulliometry" in: L.M. Kolthoff, P.J. Elving and E.B. Sandel (Eds.), Treatise on Analytical Chemistry, Wiley, New York, 1968, Volume 8, Chapter 89, pp. 5085-5107.

Letcher, T.M. and R. Battino, *J.Chem.Ed.* **78(1)** (2001) 103-111.

Li, J., K. Fischer and J. Gmehling, *Fluid Phase Equilib.* **143** (1998) 71-82.

Li, J, C. Chen and J. Wang, *Fluid Phase Equilib.* **169** (2000) 75-84.

Lin, H., H. Kim, W. Leet and K. Chao, *Ind.Eng.Chem.Fundam.* **24** (1985) 260.

Liphard, K.G. and G.M. Schneider, *J.Chem.Thermodyn.* **7** (1975) 805-814.

Lopez, J.A., V.M. Trejos and C.A. Cardona, *Fluid Phase Equilib.* **248** (2006) 147-157.

Magnussen, T., R. Rasmussen and Aa. Fredenslund, *Ind.Eng.Chem.Proc.Des.Dev.* **20** (1981) 331-339.

Magoulas, K. and D.P. Tassios, *Fluid Phase Equilib.* **56** (1990) 119-140.

Maher, P.J. and B.D. Smith, *Ind.Eng.Chem.Fundam.* **18(4)** (1979a) 354-357.

Maher, P.J. and B.D. Smith, *J.Chem.Eng.Data.* **24** (1979b) 16-22.

Maia de Oliveira, H.N., F.W. Bezerra Lopes, A.A. dantas Neto, O. Chiavone-Filho, *J.Chem.Eng.Data.* **47** (2002) 1384-1387.

Malanowski, S., "Selection of experimental methods for determination of low pressure vapour-liquid equilibrium", Microfilm F 3.5, presented at the CHISA-75 Congress, Prague, 1975.

Malanowski, S., *Fluid Phase Equilib.* **8** (1982a) 197-219.

Malanowski, S., *Fluid Phase Equilib.* **9** (1982b) 311-317.

Malanowski, S. and A. Anderko, Modelling Phase Equilibria: Thermodynamic Background and Practical Tools, John Wiley, New York, 1992.

Marek, J., *Coll.Czech.Chem.Comm.* **20** (1955) 1490.

Margules, M., *S.B.Akad.Wiss.Wien., Math.Naturw.Kl. II*, **104** (1895) 1243.

Marina, J.M. and D.P. Tassios, *Ind.Eng.Chem.Proc.Des.Dev.* **12** (1973) 67-71.

Marsh, K.N., "The Measurement of Thermodynamic Excess Functions of Binary Liquid Mixtures" in: M.L. McGlashan (Ed.), Chemical Thermodynamics (A Specialist Periodical Report), The Chemical Society, London, 1978, Volume 2, Chapter 1, pp. 1-45.

Marsh, K.N., *Fluid Phase Equilib.* **52** (1989) 169-184.

Martin, J.J., *Ind.Eng.Chem.Fundam.* **18** (1979) 81-97.

Mathias, P., *Ind.Eng.Chem.Proc.Des.Dev.* **22** (1983) 385.

Mathias, P. and T. Copeman, *Fluid Phase Equilib.* **13** (1983) 91.

MATLAB® (version 7.0.1) Optimization Toolbox technical support. Available online from: http://www.mathworks.com/access/helpdesk/help/toolbox/.

Matzik, I. and G.M. Schneider, *Ber.Bunsenges.Phys.Chem.* **89** (1985) 551.

Maurer, G. and J.M. Prausnitz, *Fluid Phase Equilib.* **2(2)** (1978) 91-99.

McGarry, J., *Ind.Eng.Chem.Proc.Des.Dev.* **22** (1983) 313-322.

McHugh, M. and V. Krukonis, Supercritical Fluid Extraction Principles and Practice, Butterworths, Stoneham, Massachusetts, 1986.

Meister, K.H., *Linde Reports on Science and Technology*. **39** (1985) 23.

Melhem, G., R. Saini and B. Goodwin, *Fluid Phase Equilib.* **47** (1989) 189.

Meng, L., Y.Y. Duan and L. Li, *Fluid Phase Equilib.* **226** (2004) 109.

Meskel-Lesavre, M., D. Richon and H.L. Renon, *Ind.Eng.Chem.Fundam.* **20** (1981) 284-289.

Michelsen, M. and H. Kistenmacher, *Fluid Phase Equilib.* **58** (1990) 229-230.

Michelsen, M.L., *Fluid Phase Equilib.* **60** (1990a) 47-85.

Michelsen, M.L., *Fluid Phase Equilib.* **60** (1990b) 213-219

Michelsen, M.L. and R.A. Heidemann, *Ind.Eng.Chem.Res.* **35(1)** (1996) 278-287.

Michelsen, M.L., *Fluid Phase Equilib.* **121** (1996) 15-26.

Miller, P. and B.F. Dodge, *Ind.Eng.Chem.* **32** (1940) 434.

Miller, D.G, *Ind.Eng.Chem.Fundam.* **2** (1963) 78-79.

Miller, D.G., *J.Phys.Chem.* **68** (1964) 1399.

Moelwyn-Hughes, E.A., "Physical Chemistry", second ed., Pergamon Press, Oxford, 1961, pp 709.

Mohammed, R.S. and G.D. Holder, *Fluid Phase Equilib.* **32** (1987) 295-317.

Mohammed, R.S., P.G. Bendale, R.M. Enick and G.E. Holder, "Empirical Two-Parameter Combining Rules for Cubic Equations of State", presented at the AIChE Annual Meeting, New York, USA, 1987.

Mokbel, I., K. Ruzicka, V. Majer, V. Ruzicka, M. Ribeiro, J. Jose and M. Zabransky, *Fluid Phase Equilib.* **169** (2000) 191-207.

Mollerup, J., *Fluid Phase Equilib.* **7** (1981) 121.

Mollerup, J., *Fluid Phase Equilib.* **25** (1986) 323-327.

Moodley, K., PhD Thesis, University of Natal, Durban, South Africa, 2003.

Moon, H.M., K. Ochi and K. Kojima, *Fluid Phase Equilib.* **62** (1991) 29-40.

Morachevsky, A.G. and V.T. Zharov, *Zhurnal Prikladnoi Khimii* **36** (1963) 2771, as reported by J. Gmehling and U. Onken, Vapour Liquid Equilibrium Data Collection, Organic Hydroxy compounds: Alcohols, DECHEMA Data Series, Frankfurt, 1977, Volume 1, Part 2a, pp. 429.

Morgan, D.L. and R. Kobayashi, *Fluid Phase Equilib.* **97** (1994) 211-242.

Morris, W.O. and M.D. Donohue, *J.Chem.Eng.Data.* **30** (1985) 259-263.

Motchelaho, A.M., Personal communication, 2006.

Muhlbauer, A.L. and J.D. Raal. *Chem.Eng.J.* **60** (1995) 1-29.

Muirbrook, N.K. and J.M. Prausnitz, *AIChE.J.* **11** (1965) 1092.

Myers, H.S. and M.R. Fenske, *Ind.Eng.Chem.* **47(8)** (1955) 1653.

Nagahama, K. and M. Hirata, *Bull.Japan.Petrol.Inst.* **18** (1976) 79.

Nagahama, K., *Fluid Phase Equilib.* **116** (1996) 364-365.

Naidoo, P., PhD Thesis, University of KwaZulu-Natal, Durban, South Africa, 2004.

Nakayama, T., H. Sagara, K. Arai and S. Saito, *Fluid Phase Equilib.* **38** (1987) 109.

Nannoolal, Y., D. Ramjugernath and J. Rarey "Prediction of the Vapor Pressure of Non-Electrolyte Organic Compounds via Group Contributions and Group Interactions", presented at the 19th International Conference on Chemical Thermodynamics, Boulder, USA, 2006.

Nasir, P., J. Martin and R. Kobayashi, *Fluid Phase Equilib.* **5(1)** (1980/1981) 279-288.

Neau, E. and A. Peneloux, *Fluid Phase Equilib.* **6** (1981) 1-19.

Ng, H.J. and D.B. Robinson, *J.Chem.Eng.Data.* **23** (1978) 325.

Ng, H.J. and D.B. Robinson, *Fluid Phase Equilib.* **2** (1979) 273-282.

N'Giumbi, J., C. Berro, I. Mokbel, E. Rauzy and J. Jose, *Fluid Phase Equilib.* **162** (1999) 143-158.

Niesen, V., A. Palavra, A.J. Kidnay and V.F. Yesavage, *Fluid Phase Equilib.* **31(3)** (1986) 283-298.

Niesen, V.G. and V.F. Yesavage, *Fluid Phase Equilib.* **50** (1989) 249-266.

Nothnagel, K.H., D.S. Abrams and J.M. Prausnitz, *Ind.Eng.Chem.Proc.Des.Dev.* **12** (1973) 25.

Novenario, C.R., J.M. Caruthers and K.C. Chao, *Ind.Eng.Chem.Res.* **35** (1996) 269.

Null, H.R., Phase Equilibrium in Process Design, Robert E. Krieger, New York, 1980.

Occhiogrosso, R.N., J.T. Igel and M.A. McHugh, *Fluid Phase Equilib.* **26** (1986) 165-179.

Oh, B.C., Y. Kim, H.Y. Shin and H. Kim, *Fluid Phase Equilib.* **220** (2004) 41-46.

Ohta, T., *Chem.Eng.J.* **61** (1996) 27-33.

Ohta, T., M. Takemura and T. Yamada, *J.Chem.Thermodyn.* **34** (2002) 711-716.

Olson, J.D., *Fluid Phase Equilib.* **52** (1989) 209-218.

Orbey, H and S.I. Sandler, *AIChE.J.* **41** (1995a) 683.

Orbey, H. and S.I. Sandler, *Fluid Phase Equilib.* **111** (1995b) 53-70.

Orbey, H. and S.I. Sandler, *Fluid Phase Equilib.* **121** (1996) 67-83.

Orbey, H. and S.I.Sandler, *Fluid Phase Equilib.* **132** (1997) 1-14.

Osborn, A.G. and D.W. Scott, *J. Chem.Thermodyn.* **10** (1978) 619.

Othmer, D.F., *Ind.Eng.Chem.* **20** (1928) 743-746.

Othmer, D.F. and F.R. Morely, *Ind.Eng.Chem.* **38(7)** (1946) 751-757.

Othmer, D.F. *Ind.Eng.Chem.Anal.Ed.* **20** (1948) 763.

Palmer, D.A., Handbook of Applied Thermodynamics, CRC Press, Boca Raton, 1987.

Park, S.D., C.H. Kim and C.S. Choi, *J.Chem.Eng.Data.* **36** (1991) 80-84.

Patel, N.C. and A.S. Teja, *Chem.Eng.Sci.* **37** (1982) 463.

Paunovic, R., S. Jovanivic and A. Mihajlov, *Fluid Phase Equilib.* **6** (1981) 141.

Peleteiro, J., D. Gonzalez-Salgado, C.A. Cerdeirina, J.L. Valencia and L. Romani, *Fluid Phase Equilib.* **191** (2001) 83-97.

Peneloux, A., E. Rauzy and R. Freze, *Fluid Phase Equilib.* **8** (1982) 7-23.

Peneloux, A., W. Abdoul and E. Rauzy, *Fluid Phase Equilib.* **47(2-3)** (1989) 115-132.

Peng, D. and D.B. Robinson, *Ind.Eng.Chem.Fundam.* **15(1)** (1976) 59-64.

Pitzer, K.S. and R.F. Curl, *J.Am.Chem.Soc.* **79** (1957) 2369.

Pividal, K.A., A. Britigh and S.I. Sandler, *J.Chem.Eng.Data.* **37** (1992) 484-487.

Pozo de Fernandez, M.E. and W.B. Streett, *J. Chem.Eng.Data.* **29(3)** (1984) 324-329.

Prausnitz, J.M, C.A. Eckert, R.V. Orye and J.P. O'Connell, Computer Calculations for Multi-component Vapour-liquid Equilibria, Prentice-Hall, Englewood Cliffs, New Jersey, 1967.

Prausnitz, J.M. and P. Chueh, Computer Calculation for High-Pressure Vapor-Liquid Equilibria, Prentice-Hall, Englewood Cliffs, New Jersey, 1968.

Prausnitz, J.M., Molecular Thermodynamics of Fluid Phase Equilibria, Prentice-Hall, Englewood Clifffs, New Jersey, 1969.

Prausnitz, J.M., *Science.* **205** (1979) 759.

Prausnitz, J.M., T.F. Anderson, E.A. Grens, C.A. Eckert, R. Hsieh and J.P. O'Connell, Computer Calculations for Multicomponent Vapor-Liquid and Liquid-Liquid Equilibria, Prentice-Hall, Englewood Cliffs, New Jersey, 1980.

Prausnitz, J.M, *Fluid Phase Equilib.* **24** (1985) 63.

Raal, J.D., R.K. Code and D.A. Best, *J.Chem.Eng.Data.* **17(2)** (1972) 211-216.

Raal, J.D. and C.J. Brouckaert, *Fluid Phase Equilib.* 74 (1992) 253-270.

Raal, J.D. and A.L. Muhlbauer, *Dev.Chem.Eng. Min.Proc.* **2** (1994) 69-104.

Raal, J.D. and A.L. Muhlbauer, Phase Equilibria: Measurement and Computation, Taylor and Francis, Bristol, 1998.

Radosz, M., *Ber.Bunsenges.Phys.Chem.* **88** (1984) 859-862.

Radosz, M. "Continuous flow apparatus for measuring phase equilibria in supercritical gas-heavy hydrocarbon system" in: J.M.L Penninger *et al.* (Eds.), Supercritical Fluid Technology, Elsevier, Amsterdam, The Netherlands, 1985, pp.179.

Radosz, M., *J.Chem.Eng.Data.* **31** (1986) 43-45.

Ramjugernath, D., PhD Thesis, University of Natal, Durban, South Africa, 2000.

Rarey, J.R. and J. Gmehling, *Fluid Phase Equilib.* **83** (1993) 279-287.

Rauzy, E. and A. Peneloux, *Int.J.Thermophys.* **7(3)** (1986) 635-646.

Redlich, O. and A.T. Kister, *Ind.Eng.Chem.* **40** (1948a) 341-345.

Redlich, O. and A.T. Kister, *Ind.Eng.Chem.* **40** (1948b) 345-348.

Redlich, O. and J.N.S. Kwong, *Chem.Rev.* **44** (1953) 49.

Reid, R.C., J.M. Prausnitz and B.E. Poling, The Properties of Gases and Liquids, fourth ed., McGraw-Hill, New York, 1987.

Reisig, H., K.D. Wisotzski and G.M. Schneider, *Fluid Phase Equilib.* **51** (1989) 269-283.

Renon, H.L. and J.M. Prausnitz, *AIChE.J.* **14** (1968) 135-144.

Renon, H.L., G. Asselineau, G. Cohen and C. Raimbault, Calcul Sur Ordinateur des Equilibres Liquide-Vapeur et Liquide-Liquide, Editions Technip, 1971.

Renon, H.L., *Fluid Phase Equilib.* **2** (1978) 101.

Rice, P. and A. El-Nikheli, *Fluid Phase Equilib.* **107** (1995) 257-267.

Riddick, J.A., W.B. Bunger and T.K. Sakano, Organic Solvents: Physical Properties and Methods of Purification, fourth ed., Wiley-Interscience, New York, 1986.

Rigas, T.J., D.F. Mason and G. Thodos, *Ind. Eng. Chem.* **50(9)** 1958 1297-1300.

Roebers, J.R. and M.C. Thies, *Ind.Eng.Chem.Res.* **29(7)** (1990) 1560-1570.

Rogalski, M. and S. Malanowski, *Fluid Phase Equilib.* **5** (1980) 97-112.

Rogers, B. and J.M. Prausnitz, *Ind.Eng.Chem.Fundam.* **9** (1970) 174.

Rose, A. and E.T. Williams, *Ind.Eng.Chem.* **47(8)** (1955) 1528-1533.

Rousseaux, P., D. Richon and H.L. Renon, *Fluid Phase Equilib.* **11** (1983) 153-168.

Ruzicka, K., I. Mokbel, V. Majer, V. Ruzicka, J. Jose and M. Zabransky, *Fluid Phase Equilib.* **148** (1998) 107-137.

Saddington, A.W. and N.W. Krase, *J.Am.Chem.Soc.* **56** (1934) 353.

Sagara, H., Y. Arai and S. Saito, *J.Chem.Eng.Japan.* **54** (1972) 339-348.

Sage, B.H., J.G. Schaafsma and W.N. Lacey, *Ind.Eng.Chem.* **26** (1934) 1218-1224.

Sage, B.H. and W.N. Lacey, *Ind.Eng.Chem.* **26** (1934) 103-106.

Sameshima, J., *J.Am.Chem.Soc.* **40** (1918) 1482-1508.

Sandler, S.I., H. Orbey and B. Lee, "Equations of State" in: S.I. Sandler (Ed.), Models for Thermodynamic and Phase Equilibria Calculations, Marcel Dekker, New York, 1994, Chapter 2, pp.87-186.

Sandler, S.I., Chemical and Engineering Thermodynamics, third ed., John Wiley and Sons, New York, 1999.

Sandler, S.I. *Fluid Phase Equilib.* **210** (2003) 147-160.

Sandoval, R., G. Wilczek-Vera and J.H. Vera, *Fluid Phase Equilib.* **52** (1989) 119-126.

Sarry, M.F., *Phys.Russ.Acad.Sci.* **42** (1999) 991.

Sauermann, P., K. Holzapfel, J. Oprzynski, F. Kohler, W. Poot and T.W. de Loos, *Fluid Phase Equilib.* **112** (1995) 249-272.

Scatchard, G., *Chem.Rev.* **8** (1931) 321.

Scatchard, G. and L.B. Ticknor, *J Am.Chem.Soc.* **74** (1952) 3724.

Scheeline, H.W. and E.R. Gilliland, *Ind.Eng.Chem.* **31(8)** (1939) 1050-1057.

Schmidt, G. and H. Wenzel, *Chem.Eng.Sci.* **35** (1980) 1503-1512.

Schotte, W., *Ind.Eng.Chem.Proc.Des.Dev.* **19** (1980) 432-439.

Schwartzentruber, J. and H.L. Renon, *Fluid Phase Equilib.* **52** (1989a) 127-134.

Schwartzentruber, J. and H.L. Renon, *Ind.Eng.Chem.Res.* **28** (1989b) 1049-1055.

Schwartzentruber, J. and H.L. Renon, *Fluid Phase Equilib.* **67** (1991) 99.

Scott, D.W. and A.G. Osborn, *J.Phys.Chem.* **83** (1979) 2714.

Sebastian, H., J. Simnick, H. Lin and K. Chao, *J.Chem.Eng.Data.* **25** (1980) 246.

Shibata, S.K. and S.I. Sandler, *Ind.Eng.Chem.Res.* **28(12)** (1989a) 1893-1898.

Shibata, S.K. and S.I. Sandler, *J.Chem.Eng.Data.* **34** (1989b) 291-298.

Schreiber, L.B. and C.A. Eckert, *Ind.Eng.Chem.Proc.Des.Dev.* **10** (1971) 572.

Seo, J., J. Lee and H. Kim, *Fluid Phase Equilib.* **172** (2000) 211-219.

Sewnarain, R., MSc Dissertation, University of Natal, Durban, South Africa, 2001.

Silverman, N. and D.P. Tassios, *Ind.Eng.Chem.Proc.Des.Dev.* **23** (1984) 586.

Simnick, J., C. Lawson, H. Lin, K. Chao, *AIChE.J.* **23** (1977) 469.

Sinnot, R.K., Coulson and Richardson's Chemical Engineering: Chemical Engineering Design, fourth ed., Volume 6, Butterworth-Heinemann, Oxford, 1999.

Sivaraman, A. and R. Kobayashi, *J.Chem.Eng.Data.* **27(3)** (1982) 264-269.

Skjold-Jorgensen, S., P. Rasmussen and Aa. Fredenslund, *Chem.Eng.Sci.* **35** (1980) 2389.

Skjold-Jorgensen, S., *Fluid Phase. Equilib.* **14** (1983) 273.

Skjold-Jorgensen, S., *Fluid Phase Equilib.* **16** (1984) 317.

Skjold-Jorgensen, S., *Ind.Eng.Chem.Res.* **28** (1988) 1893.

Smith, J.M. and H.C. Van Ness, Introduction to Chemical Engineering Thermodynamics, third ed., McGraw-Hill, New York, 1975.

Smith, J.M., M.M. Abbott and H.C. Van Ness, Introduction to Chemical Engineering Thermodynamics, fifth ed., McGraw-Hill, New York, 2001.

Soave, G., *Chem.Eng.Sci* **27(6)** (1972) 1197-1203.

Soave, G., *Inst.Chem.Eng.Symp.Ser.* **56** (1979) 1.2/1-1.2/1.6.

Soave, G., *Chem.Eng.Sci.* **39** (1984) 357.

Soave, G., *Fluid Phase Equilib.* **31** (1986) 203-207.

Soave, G., A. Bertucco and L. Vecchiato, *Ind.Eng.Chem.Res.* **33** (1994) 975.

Solorzano-Zavala, M., F. Barragan-Aroche and E.R. Bazua, *Fluid Phase Equilib.* **122** (1996) 99-116.

Spencer, C.F. and R.P. Danner, *J.Chem.Eng.Data.* **17** (1972) 236-241.

Stamataki, S. and D.P. Tassios, *Rev Institut.Francais.Petrol.* **53(3)** (1998) 367-376.

Starling, K.E. and J.E. Powers, *Ind.Eng.Chem.Fundam.* **9** (1970) 531-537.

Stogryn, D.O. and J.O. Hirschfelder, *J.Chem.Phys.* **31** (1959) 1531.

Streett, W.B., *Cryogenics.* **5** (1965) 27-33.

Stryjek, R. and J.H. Vera, *Can.J.Chem.Eng.* **64** (1986a) 323-333.

Stryjek, R. and J.H. Vera, *Can.J.Chem.Eng.* **64** (1986b) 820-826.

Sutton, T.L. and J.F. Macgregor, *Can.J.Chem.Eng.* **55** (1977a) 603-608.

Sutton, T.L. and J.F. Macgregor, *Can.J.Chem.Eng.* **55** (1977b) 609-613.

Suzuki, K. and H. Sue, *J.Chem.Eng.Data.* **35** (1990) 63-66.

Swaid, I., PhD Thesis, Ruhr-Universitat, Bochum, Germany, 1984.

Swietolawski, W. and W. Romer, *Bull.Pol.Acad.Sci.(A).* (1924) 59-62.

Swietolawski, W., Ebulliometric Measurements, Reinhold, New York, 1945.

Takishima, S., K. Saiki, K. Arai and S. Saito, *J.Chem.Eng.Japan.* **19(1)** (1986) 48-56.

Tarakad, R.R. and R.P. Danner, *AIChE.J.* **23(5)** (1977) 685-695.

Tassios, D.P., *AIChE.J.* **17** (1971) 1367.

Teh, Y.S. and G.P. Rangaiah, *Trans.IChemE.* **80A** (2002) 745-758.

Thies, M.C. and M.E. Paulaitis, *J.Chem.Eng.Data.* **29** (1984) 538-440.

Todheide, K. and E.U. Franck, *Z.Physik.Chem.* **37** (1963) 387-401.

Tochigi, K., K. Kurihara and K. Kojima, *Ind.Eng.Chem.Res.* **29** (1990) 2142.

Tochigi, K., *Fluid Phase Equilib.* **104** (1995) 253.

Toghiani, H. and D.S. Viswanath, *Ind.Eng.Chem.Proc.Des.Dev.* **25(2)** (1986) 531-536.

Trebble, M.A. and P.R. Bishnoi, *Fluid Phase Equilib.* **40** (1987) 1.

Tsang, C.Y. and W.B. Streett, *J.Chem.Eng.Data.* **26(2)** (1981) 155-159.

Tsonopoulos, C., *AIChE.J.* **20(2)** (1974) 263-272.

Tsonopoulos, C. and J. Heidman, *Fluid Phase Equilib.* **29** (1986) 391.

Tsuboka, T. and T. Katayama, *J.Chem.Eng.Japan.* **8** (1975) 181-187.

Twu, C.H., D. Bluck, J.R. Cunningham and J.E. Coon, *Fluid Phase Equilib.* **69** (1991) 33-50.

Twu, C.H., J.E. Coon and J.R. Cunningham, *Fluid Phase Equilib.* **105** (1995a) 49-59.

Twu, C.H., J.E. Coon and J.R. Cunningham, *Fluid Phase Equilib.* **105** (1995b) 61-69.

Twu, C.H. and J.E. Coon, *AIChE.J.* **42** (1996) 3212-3222.

Twu, C.H., J.E. Coon and D. Bluck, *Fluid Phase Equilib.* **139** (1997) 1-13.

Twu, C.H., J.E. Coon, D. Bluck, B. Tilton and M. Rowland, *Ind.Eng.Chem.Res.* **37** (1998a) 1580-1585.

Twu, C.H., J.E. Coon, D. Bluck, B. Tilton and M. Rowland, *Fluid Phase Equilib.* **153** (1998b) 29-44.

Twu, C.H., J.E. Coon, D. Bluck, B. Tilton and M. Rowland, *Fluid Phase Equilib.* **158** (1999) 271-281.

Twu, C.H., W.D. Sim and V. Tassone, *Fluid Phase Equilib.* **183-184** (2001) 65-74.

Twu, C.H., B. Tilton and D.Bluck, "The Strengths and Limitations of Equation of State Models and Mixing Rules", 2006. Available online from: http://www.simsciessor.com/us/eng/

Usdin, E. and J.C. McAuliffe, *Chem.Eng.Sci.* **31** (1976) 1077.

Valderrama, J.O., *Ind.Eng.Chem.Res.* **42** (2003) 1603-1618.

Valderrama, J.O. and V.H. Alvarez, *Fluid Phase Equilib.* **226** (2004) 149-159.

van der Waals, J.D., PhD Thesis, University of Leiden, The Netherlands, 1873.

van Laar, J.J., *Z.Phys.Chem.* **72** (1910) 723-751.

van Laar, J.J., *Z.Phys.Chem.* **83** (1913) 599-608.

Van Ness, H.C., *Chem.Eng.Sci.* **10** (1959) 225-228.

Van Ness, H.C., S.M. Byer and R.E. Gibbs, *AIChE.J.* **19(2)** (1973) 238-244.

Van Ness, H.C., F. Pedersen and P. Rasmussen, *AIChE.J.* **24(6)** (1978) 1055-1063.

Van Ness, H.C. and M.M. Abbott, *Ind.Eng.Chem.Fundam.* **17** (1978) 66-67.

Van Ness, H.C. and M.M. Abbott, Classical Thermodynamics of Non-Electrolyte Solutions: With Applications to Phase Equilibria, McGraw-Hill, New York, 1982.

Van Ness, H.C., *Pure.Appl.Chem.* **67(6)** (1995) 859-872.

Van Nhu, N., A. Liu, P. Sauermann and F. Kohler, *Fluid Phase Equilib.* **145** (1998) 269-285.

Van't Hof, A., S.W. De Leeuw, C.K Hall and C.J. Peters, *Molecul.Phys.* **102(3)** (2004) 301-317.

Vera, J.H. and J.M. Prausnitz, *Chem.Eng.J.* **3** (1972) 1-13.

Vetere, A., *Fluid Phase Equilib.* **62** (1991) 1-10.

Vetere, A. *Fluid Phase Equilib.* **218** (2004) 33-39.

Vidal, J., *Chem.Eng.Sci.* **33** (1978) 787-791.

Vidal, J., *Fluid Phase Equilib.* **13** (1983) 15.

Voros, N.G. and D.P. Tassios, *Fluid Phase Equilib.* **91** (1993) 1-29.

Voutsas, E.C., N. Spiliotis, N.S. Kalospiros and D.P. Tassios, *Ind.Eng.Chem.Res.* **34(2)** (1995) 681-687.

Voutsas, E.C., C. Boukouvalas, N.S. Kalospiros and D.P. Tassios, *Fluid Phase Equilib.* **116** (1996) 480-487.

Wagner, Z. and I. Wichterle, *Fluid Phase Equilib.* **33** (1987) 109.

Wakeham, W.A., G. St.Cholakov, R.P. Stateva, "Consequences of Property Errors on the Design of Distillation Columns", presented at the 14th Symposium on Thermophysical Properties, NIST, Boulder, USA, 2000.

Walas, S.M., Phase Equilibria in Chemical Engineering, Butterworth Publishers, Massachusetts, 1985.

Walther, D., B. Platzer and G. Maurer, *J.Chem.Thermodyn.* **24** (1992) 387-399.

Wang, W., Y. Qu, C.H. Twu and J.E. Coon, *Fluid Phase Equilib.* **116** (1996) 488-494.

Washburn, R., *J.Am.Chem.Soc.* **41** (1919) 729-741.

Weber, W., S. Zeck and H. Knapp, *Fluid Phase Equilib.* **18** (1984) 253-278.

Wei, W.S. and R.J. Sadus, *AIChE.J.* **46** (2000) 169-196.

Weidlich, U. and J. Gmehling, *Ind.Eng.Chem.Res.* **26** (1987) 1372.

Wendland, M., H. Hasse and G. Maurer, *J.Supercrit.Fluids.* **6** (1993) 211-222.

Whiting, W. and J.M. Prausnitz, *Fluid Phase Equilib.* **9** (1982) 119.

Wichterle, I., *Fluid Phase Equilib.* **2** (1978) 59-78.

Wiesniewska, B., J. Gregorowicz and S. Malanowski, *Fluid Phase Equilib.* **86** (1993) 173-186.

Wiesniewska-Goclowska, B. and S. Malanowski, *Fluid Phase Equilib.* **180** (2001) 103-113.

Williams, R.B. and D.L. Katz, *Ind.Eng.Chem.* **46** (1954) 2512

Williamson, A.G., "Phase Equilibria of two-component systems and multi-component systems. Part 1" in: B. Le Neindre and B. Vodar (Eds.), Experimental Thermodynamics, Butterworths, London, 1975, Volume 2, Chapter 16, pp. 749-786.

Wilson, G.M. and C.H. Deal, *Ind.Eng.Chem.Fundam.* **1** (1962) 20.

Wilson, G.M., *J.Am.Chem.Soc.* **86** (1964) 127.

Wilson, G.M., *Adv.Cryogen.Eng.* **9** (1964) 168-176.

Wisniak, J., *Ind.Eng.Chem.Res.* **32** (1993) 1531-1533.

Wisniak, J., *Ind.Eng.Chem.Res.* **33** (1994) 177-180.

Wisotzski, K.D., PhD Thesis, Ruhr-Universitat, Bochum, Germany, 1984.

Wohl, K., *Trans.AIChE.* **42**, (1946) 215.

Won, K.W. and J.M. Prausnitz, *Ind.Eng.Chem.Fundam.* **12** (1973) 459.

Wong, D.S.H and S.I. Sandler, *AIChE.J.* **38(5)** (1992) 671-680.

Wong, D.S.H., H. Orbey and S.I. Sandler, *Ind.Eng.Chem.Res.* **31**(1992) 2033-2039.

Wong, K.F. and C.A. Eckert, *Ind.Eng.Chem.Fundam.* **10** (1971) 20.

Wu, G.W., N.W. Zhang, X.Y. Zheng, H. Kubota and T. Makita, *J.Chem.Eng.Japan.* **21** (1988) 25-29.

Xu, Z. and S.I. Sandler, *Ind.Eng.Chem.Res.* **26** (1987a) 601-606.

Xu, Z. and S.I. Sandler, *Ind.Eng.Chem.Res.* **26** (1987b) 1234.

Yamaguchi, T., *J.Tokyo.Chem.Soc.* **34** (1913) 691.

Yan, W., M. Topphoff, C. Rose and J. Gmehling, *Fluid Phase Equilib.* **162** (1999) 97-113.

Yang, T., G.J. Chen, W. Chan and T.M. Guo, *Chem.Eng.J.* **67** (1997) 27-33.

Yang, Q. and C. Zhong, *Fluid Phase Equilib.* **192** (2001) 103-120.

Yerazunis, S., J.D. Plowright and F.M. Smola, *AIChE.J.* **10(5)** (1964) 660-665.

Yorizane, M., S. Yoshimura, H. Masuoka, Y. Miyano and Y. Kakimoto, *J.Chem.Eng.Data.* **30** (1985) 174-176.

Young, C.L., "An Experimental Method for Studying Phase Behaviour of Mixtures at High Temperatures and Pressures." in: M.L. McGlashan(Ed.), Chemical Thermodynamics (A Specialist Periodical Report), The Chemical Society, London, 1978, Volume 2, Chapter 3, pp. 71-104.

Yu, J. and B. Lu, *Fluid Phase Equilib.* **34** (1987) 1.

Yuan, K.S., B.C.Y. Lu, C.K. Hoj and A.K. Keshpande, *J.Chem.Eng.Data.* **8** (1963) 549, as retrieved from the Dortmund Data Bank, DDBST Software and Separation Technology GmbH, DDB Software Package Version 1999, Oldenburg, 1999.

Zabaloy, M.S. and J.H. Vera, *Ind.Eng.Chem.Res.* **35(3)** (1996) 829-836.

Zabaloy, M.S. and J.H. Vera, *Ind.Eng.Chem.Res.* **37(5)** (1998) 1591-1597.

Zhong, C. and H. Matsuoka, *Fluid Phase Equilib.* **158-160** (1999) 283.

Zieborak, K., *Z.Physik.Chem.* **231** (1966) 248-258.

Zielke, F and D.A. Lempe, *Fluid Phase Equilib.* **141** (1997) 66.

Zudkevitch, D., *Chem.Eng.Comm.* **116** (1992) 41-65.

APPENDIX A

DESCRIPTION OF HPVLE MEASUREMENT METHODS

A.1 Static Methods

Static methods have been favoured for VLE measurements by researchers such as Abbott (1978), Marsh (1978) and Williamson (1975) in their respective review papers, particularly at higher pressures. It has been proposed that static equipment (except for the auxiliary features) is generally simpler than that of the HPVLE dynamic type and more significantly, that the condition of a true equilibrium can be more reliably obtained with the static method (Marsh, 1989).

Static methods can be broadly classified as static analytical methods, static synthetic methods and static combined methods; each of which will be dealt separately.

A.1.1 The Static Analytical Method

A.1.1.1 Description of the Static Analytical Method

In the static analytical method, illustrated in Figure A.1, the components are charged into a closed and evacuated cell of either fixed or variable-volume. Evacuation of the contents of the static cell is achieved through the use of a vacuum system that is coupled to the cell and this is necessitated due to system pressure being highly sensitive to the presence of any air or volatile impurities in the closed cell. The liquid components are degassed and are either pumped into the cell or "flushed" into the cell by the volatile component or a compressed gas. The components are then agitated through the use of internal magnetic stirring, mechanical rocking or shaking to ensure that there is sufficient contact between the vapour and liquid phases to speed up the attainment of equilibrium.

The measurements obtained are usually isothermal, as a result of immersion of the equilibrium cell in an isothermal fluid bath of air, gas, water or silicone oil (for higher temperatures), *etc.* It is imperative that the system is isolated from all possible interferences to negate the possibility of exchange of material or thermal energy with the surroundings *i.e.* the creation of vertical or axial thermal gradients.

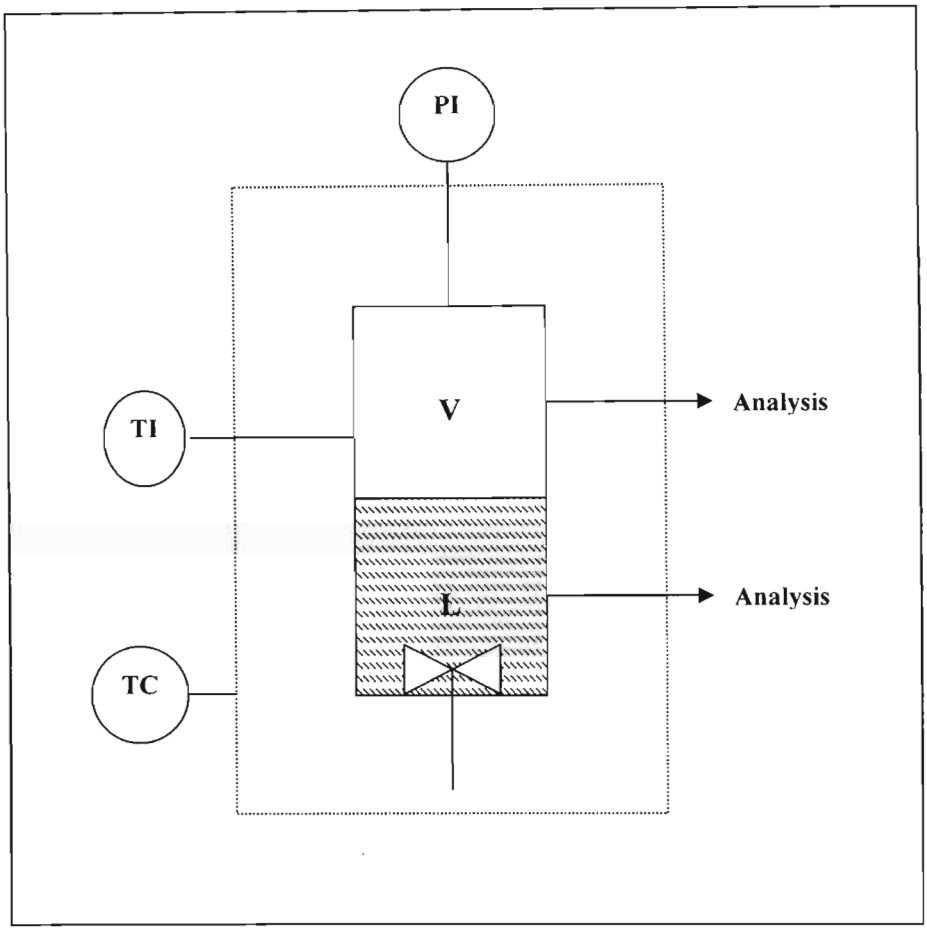

Figure A.1. Schematic diagram of a typical Static Analytical apparatus: **V**, vapour phase; **L**, liquid phase; **PI**, pressure indicator (sensor); **TC**, temperature control system receiving feedback from the temperature sensor to regulate the bath temperature; **TI**, temperature probe in the cell body.
Samples of vapour and/ or liquid are taken from appropriate sampling points for subsequent analysis.

To this end, different strategies have been employed; as in the apparatus of Ng and Robinson (1978), where isothermal conditions were obtained with a 2.5 cm thick aluminum jacket, which housed eight vertically-mounted heaters.
Isothermal fluid baths (air, nitrogen, water, oil, *etc.*) are also a popular choice for isothermal control as was employed in the equipment of Rogers and Prausnitz (1970), where the interior of the isothermal bath was also copper-lined to promote intimate thermal contact between the walls of the bath and heat transfer medium *i.e.* the fluid (air) to ensure that no thermal gradients were formed.

After the required temperature has been reached, the mixture is maintained at this temperature, until it has been ascertained that the system has reached a state of equilibrium. The pressure of the system can be varied through the addition or withdrawal of system components or by changing the cell volume with a piston (for variable-volume static cells). Prior to the withdrawal

of samples of the equilibrium phases for analysis, the fluid mixture is allowed to achieve a state of rest where the agitation of the cell is discontinued to allow for the proper disengagement of the phases (Dohrn and Brunner, 1995). After being sampled, the phases are quantified by analytical techniques such as gas chromatography or mass spectrometry.

For static methods, the vapour phase composition determination in the form of sampling and analysis is difficult, time-consuming and represents the greatest uncertainty in the technique. An alternative approach is to obtain an incomplete data set *i.e.* P-T-x measurements, where the vapour phase composition is obtained through computation from thermodynamic relations (Gibbs-Duhem equation).

A.1.1.2 Advantages of the Static Analytical Method

It has been claimed that if the sampling of the equilibrium phases can be effected through a simple and reliable means, then static methods would be the most inexpensive and accurate VLE measuring equipment (Fornari *et al.*, 1990). Apart from considerations of sampling simplifications, the other advantages afforded by static analytical methods over other methods include the following:

(a) The attainment of the *equilibrium condition* by static analytical methods is considered to be more representative than that obtained by the other methods, such as constant-pressure methods (Marsh, 1989).

(b) Static analytic methods are more amenable in terms of design capability of obtaining VLE data at *very high pressures* as opposed to dynamic methods *i.e.* maximum operating pressures of up to 200 and 350 MPa are reported in the literature (Raal and Muhlbauer, 1994) for the static apparatus of Konrad *et al.* (1983) and Todheide and Franck (1963), respectively.

(c) Since, the equilibrium cell is of a fixed-volume (constant-volume static cells) or can be of variable-volume (variable-volume static cells) design, static methods can be used to obtain *isotherms, isobars, isopleths and P-V-T data* (Ramjugernath, 2000).

A.1.1.3 Disadvantages of the Static Analytical Method

The static method, although simpler in principle than the other methods, has many experimental difficulties, which can result in the acquisition of VLE data of poor quality due to the following factors:

(a) Proper and scrupulous care must be taken beforehand to ensure that all the *dissolved gaseous content* has been removed from the introduced liquid components and that the components are of the highest purity, as this method is indeed highly intolerant of the presence of small amounts of impurities or foreign gases. Degassing is necessitated due to the contribution of the partial pressures of dissolved gases to the partial pressure of the volatile components in the mixture resulting in erroneous values for equilibrium pressures. This effect is greatly enhanced at low pressures (Abbott, 1986), where the vapour pressure of the volatile component *i.e.* the vapour density is small. Degassing can be done *in situ* or prior to the sample introduction into the equilibrium chamber. Techniques for degassing include vacuum sublimation (Bell *et al*, 1968), distillation at low temperatures (Van Ness and Abbott, 1978) and freezing/evacuation/thawing cycles (Maher and Smith, 1979b).

(b) The second major difficulty experienced with this method is *sampling without disturbing the equilibrium condition*, especially for the vapour phase. For static methods, the sampling of the liquid or vapour phases through static sampling ports results in a change in the volume of the cell and a pressure drop, which adversely affect the equilibrium pressure, temperature and the phase compositions. Also, at low pressures the vapour phase density is so small that it is only with great difficulty that a representative equilibrium sample can be obtained.

Consequently, complex and often expensive sampling techniques are employed in an attempt to prevent any disturbance of the established equilibrium during the sampling process. The size of the pressure fluctuations induced by vapour or liquid phase sampling is by no means negligible, as pressure fluctuations as high as 10 kPa have been reported by Besserer and Robinson (1971) in the literature.

Numerous techniques have been devised to prevent any perturbation of the equilibrium condition during sampling. Early methods included that of direct mercury injection into the equilibrium cell during the withdrawal of samples (Kobayashi and Katz, 1953), which was a fairly unattractive method, due to the toxicity of mercury vapour. The use of large cell volumes (Sagara *et al.*, 1972) helped to dampen the pressure drop experienced, however, with the advent of an increase in the size of the mixture volumes required, this resulted in significant additional costs, especially for rare or expensive chemicals. For variable-volume cells with a moveable

piston, the pressure drop during sampling can be avoided by altering the internal cell volume, hence compensating for the pressure disturbance.

Attempts have also been made with regards to decreasing the size of the sample withdrawn for analysis with the assumption that negligible perturbation of the equilibrium condition in the cell occurs, which does not affect the results obtained (Fornari *et al.*, 1990). The use of capillaries (Wagner and Wichterle, 1987), special sampling valves (Christov and Dohrn, 2002) such as HPLC valves or quick-acting pneumatic or electromagnetic valves (Figuiere *et al.*, 1980) and detachable micro-cells (Legret *et al.*, 1981) have been employed for this purpose. However, sampling through capillaries can lead to differential vaporisation (Christov and Brunner, 2002) especially for mixtures with widely varying boiling points (as discussed below), due to the pressure drop along the capillary section. This can be avoided to some extent by ensuring that the pressure is restricted at a small section at the end of the capillary just before entry into the chromatograph.

In light of the above difficulties, trends for many researchers in static analytic methods with regards to the sampling of the phases has been to completely eliminate the sampling of the vapour phase in a static semi-analytical method where P-T-x measurements are obtained. From the theoretical treatment of VLE data, this is made possible by the fact that if the gas phase nonidealities can be modelled with great confidence, the physical measurement of the vapour phase is unnecessary. This is due to the criterion of the test for the thermodynamic consistency of experimental VLE data *i.e.* the Gibbs-Duhem relation, making one of the measurements of the P-T-x-y set redundant, thus allowing for the computation of the vapour phase. However, this computation procedure renders the use of Gibbs-Duhem relation invalid for consistency testing of the experimental data, as a result of its prior use in the computation procedure for the incomplete data set.

(c) An additional problem experienced during sampling is the *partial condensation or the vaporization of the liquid sample* components during sampling. This is quite noticeable for mixtures containing components which have large differences in volatility *i.e.* volatile + non-volatile systems, as is the case for supercritical + subcritical mixtures. The flashing of the lighter (more volatile) components of the liquid phase during the sampling procedure results in the sample not being representative of the equilibrium composition. This then becomes a problem of homogenizing the liquid sample without partial condensation of one of the components.
Modifications to existing static sampling mechanisms were undertaken by researchers such as Kalra *et al.* (1978), where a four-port ball valve was used firstly to isolate a portion of the liquid sample, then to allow for a heated stream of helium gas to circulate the sample until it was

completely vaporised, after which the valve port could be switched to allow for the flow of the sample into a gas chromatograph for analysis. A double-acting Ruska pump ensured that the cell pressure and temperature remained constant during sampling by simultaneously controlling the movement of both the upper and lower pistons. Recent methods employed to ensure that the sampled liquid phase is representative includes the use of a jet mixer (Muhlbauer and Raal, 1991), which served to vaporise and homogenise the liquid sample prior to gas chromatographic analysis.

(d) *Long equilibrium times* are a daunting prospect for an experimenter and for many static equipment designs equilibrium times as long as 12 hours (Raal and Muhlbauer, 1994) have been reported in literature. Incorporating a more effective mechanism for the agitation of the cell contents can reduce this. However, the latter can both adversely affect the establishment of a true equilibrium and further complicate the cell design.

A.1.1.4 Static Analytical equipment in the literature

A selection of the static analytic apparatus extracted from literature (Raal and Muhlbauer, 1994) is provided in Table A.1. The notable features of Table A.1 are the maximum operating limits for pressure and temperature, equilibration time and sample size. Due to space limitations, only the first author is mentioned in Table A.1. The information omitted in the table (-), has not been provided or been made available by the author in the respective literature sources.

With regards to the distinctive features of the static equipment presented in Table A.1, a short summary can be provided as follows:

(a) The *cell interior volumes* vary from quite small *i.e.* 50 cm^3 for Figuiere *et al.* (1980) to as large as 2000 cm^3 for Reiff *et al.* (1987). As discussed earlier, a large cell volume was a strategy employed to dampen the effects of the pressure drop whilst sampling the phases. Consequently, it can be observed that with the large cell volumes of their equipment, Sagara *et al.* (1972), Klink *et al.* (1975), Ashcroft *et al.* (1983) and Reiff *et al.* (1987) employed this "dampening strategy".

(b) *The maximum operating temperature* is relatively low, when compared to dynamic methods, for synthetic analytical methods since isothermal control is limited to the temperature limits of the thermo-regulating fluid medium, for control strategies where isothermal fluid baths are used (which accounts for the majority). Apart from the above, experimenters like Ng and Robinson

(1978) used internally-mounted electrical heaters for this purpose, for which the effects of AC radiative heat transfer would then become a factor.

(c) A favoured *material of construction* was that of grade 316 stainless steel; due to its high tensile strength, minimal thermally-induced strength, machineability, non-magnetic properties and the excellent corrosion-resistant properties, to name a few.

(d) The use of thermocouples as *thermal sensors* was initially highly favoured as opposed to other types of sensors, probably due to the ruggedness and economic benefits associated with this type of sensor. However, later researchers (as indicated by the last few entries in Table A.1) gave preference to the use of the more accurate and linear platinum resistance thermometers (Pt-100's), which were by then being constructed to withstand those conditions of a more severe environment *i.e.* higher temperatures.

(e) *Pressure transducers* are more widely used as pressure sensing devices due to their ease of incorporation into an electronic display with computer linkup (RS-232 ports) and a pressure feedback-control system together with the high level of accuracy.

(f) *Equilibrium times* are often fairly long for static equipment due to the nature of the method *i.e.* there is no circulation of the phases to facilitate interphase mass and thermal exchanges, necessary for equilibration. To decrease equilibration time, some researchers incorporated internal magnetic stirrers in their designs. Kalra and Robinson (1975) used a Teflon®-coated magnetic stirrer for their cell, where the stirrer was driven by an external aluminum-encased magnetic assembly driven by variable-speed DC motor. The designs of Figuiere *et al.* (1980), Legret *et al.* (1981) and Guillevic *et al.* (1983) all featured a magnetic stirrer rotating in a magnetic field induced by coils outside the cell.

(g) The *size of the vapour and the liquid samples* is determined by the sampling mechanism and by the minimum amount that is required for the analytical instrument, which is quite small for gas chromatography. A sample volume of 60 μL was required by Ashcroft *et al.* (1983) for gas chromatographic analysis.

Table A.1. Selection of Static Analytical equipment in the literature.

Author	Cell Volume (cm^3)	Material of Construction [b]	Operating Range		Measurement Device		Equilibr. Time	Sample Size	
			Temp (K)	Press (bar)	Temp [c]	Press [d]	(min)	Vap. (µl)	Liq. (µl)
Rigas (1958)	VV [a]	304/416 SS	423	14	TC	B	–	0.2	0.75
Todheide (1963)	150	–	623	3500	TC	B	60	0.2 - 0.3 µg	0.2 - 0.3 µg
Rogers (1970)	150	SS	423	1000	TC	PT/DWP	–	VV	VV
Besserer (1971)	10/115	316 SS	310	80	TC	PT	5/10 cycles	1 $mg.mol^{-1}$	1 $mg.mol^{-1}$
Sagara (1972)	500	SS	103	100	TC	B	60	–	–
Klink (1975)	800	316 SS	–	–	–	DWP	300/1500	–	–
Kalra (1975)	250	316 SS	338	345	TC	PT	–	–	–
Ng (1978)	150	316 SS	315	175	TC	B	180	12	–
Figuiere (1980)	50	SS	673	400	TC	PT	–	1	1
Legret (1981)	100	SS	673	1000	TC	PT	10	15	15
Bae (1981)	300	304 SS	323	100	PRT	B	120	8	8

[a] Variable-Volume.
[b] SS = Stainless Steel,; MS = Manganese Steel; N 90 = Ninomic 90 SS
[c] TC = Thermocouple; PRT = Platinum Resistance Thermometer; TS = Thermistor; QT = Quartz Thermometer.
[d] B = Bourdon Gauge; PT = Pressure Transducer; DWP = Dead Weight Piston Gauge; PRSPG = Precision Resistance Pressure Strain Gauge.

Table A.1. Selection of Static Analytical equipment in the literature (cont).

Author	Cell Volume (cm^3)	Material of Construction [b]	Operating Range		Measurement Device		Equilibr. Time	Sample Size	
			Temp (K)	Press (bar)	Temp [c]	Press [d]	(min)	Vap. (µl)	Liq. (µl)
Konrad (1983)	100	N 90	293/473	2000	TC	–	–	50	50
Ashcroft (1983)	883	MS	333	690	RT	PT	180	0.06	0.06
Guillevic (1983)	50	316 SS	558	70	TC	PT	–	–	–
Swaid (1984)	–	N 90	300/450	2000	TC	B	–	–	–
Huang (1985)	VV [a]	Sapphire	310/477	185	TC	PT	–	–	–
Nakayama (1987)	270	–	450	200	TC	B	720	100	250
Wagner (1987)	65	SS	323	90	QT	PT	–	–	–
Reiff (1987)	2000	–	473	300	RT	–	–	–	–
Baba-Ahmed(1999)	43	H C276	77[e]	400	PRT	PT	120 - 180	–	–

[a] Variable-Volume.

[b] Material of Construction, SS = Stainless Steel,; MS = Manganese Steel; N 90 = Ninomic 90 SS; H C276 = Hastelloy C-276.

[c] TC = Thermocouple; PRT = Platinum Resistance Thermometer; TS = Thermistor; QT = Quartz Thermometer.

[d] B = Bourdon Gauge; PT = Pressure Transducer; DWP = Dead Weight Piston Gauge; PRSPG = Precision Resistance Pressure Strain Gauge.

[e] Minimum operating temperature for cryogenic studies.

In terms of the sampling of the vapour and liquid phases, which proved to be quite problematic for early researchers, different approaches for a solution to this problem were attempted by the following researchers: Rogers and Prausnitz (1970), Besserer and Robinson (1971), Kalra and Robinson (1975), Kalra *et al.* (1978), Ng and Robinson (1978), Figuiere (1980), Bae *et al.* (1981), Legret *et al.* (1981), Ashcroft *et al.* (1983), Guillevic *et al.* (19830, Konrad *et al.* (1983) and Nakayama *et al.* (1987).

A.1.2 The Static Synthetic Method

As opposed to analytical methods, the uniqueness of static synthetic methods, also known as non-analytic methods, arises from the complete absence of any provisions for sampling hence eliminating all the difficulties associated with the latter. Static analytic methods can be further subdivided as visual synthetic methods, non-visual synthetic methods or synthetic methods using the material balance.

A.1.2.1 Description of the Static Synthetic Method

In typical static synthetic methods, mixtures of known amounts of the degassed components are prepared and then quantitatively transferred to a temperature-controlled, variable-volume or fixed-volume equilibrium cell. This is achieved in a stepwise process, which allows for the system to equilibrate between the steps. The use of metered injection pumps allows for an accurate measurement of the stoichiometric amounts of each component added to the cell since accurate knowledge of the overall composition is required for the computation of the phase compositions.

The static synthetic method for a variable-volume type apparatus has been represented diagrammatically in Figure A.2. After the addition of the mixture to the equilibrium cell, the system pressure or temperature is then varied to ensure that the mixture is initially homogenous. Internal magnetic stirring (Fischer and Gmehling., 1994) has been frequently incorporated in the equilibrium cell design to assist with mass transfer. The system pressure or temperature is then changed until phase separation of the homogenous phase occurs (using visual or non-visual techniques).

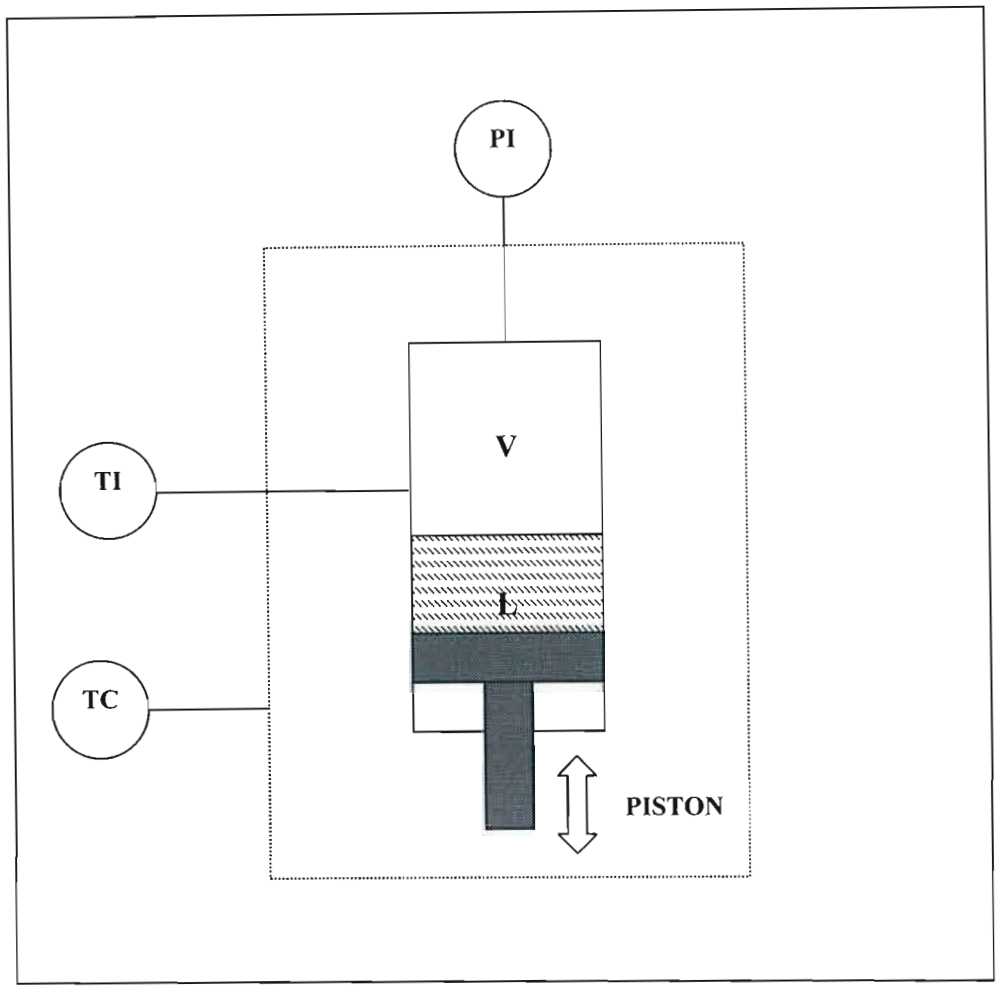

Figure A.2. Schematic diagram of a variable-volume Static Synthetic apparatus: **V**, vapour phase; **L**, liquid phase; **PI**, pressure indicator (sensor), **TC**, temperature control system (isothermal bath); **TI**, temperature probe in the cell body.

Provisions are made in the design for the controlled variation of the interior cell volume (*e.g.* a piston). There are no sample points for the vapour and liquid phases, as no sampling is required for synthetic methods.

The experimental analysis of equilibrium mixtures is surpassed by a means to synthesise the latter through the variation of system pressure or temperature or by changes of composition *i.e.* the total pressure measurement method (visual) and the P-x method (non-visual), respectively. The pressure and temperature of the "synthesised mixture" is then noted as soon as incipient phase separation is observed in the cell (visual methods) or determined by monitoring the pressure-volume relationship (non-visual methods) or by visually measuring phase volumes (material balances). It is then necessary, as part of the experimental procedure, to readjust the system pressure or temperature, with the onset of phase separation in the system, to again obtain a homogenous state to prevent layering and de-mixing of the phases (Raal and Muhlbauer, 1994). The mole fractions of the mixture components in the cell can be precisely calculated from the known amounts of each substance initially fed into the equilibrium cell. The pressure

and temperature, at which phase separation starts, together with the component mole fraction define a point on the phase envelope. In this manner, the temperature or pressure is adjusted until phase separation is detected, to obtain points on the P-V-T phase envelope.

The results obtained for the HPVLE static synthetic methods for which the pressure and the temperature are varied whilst holding the composition constant, are in the form of isopleths or constant-composition phase boundaries. The *method of temperature variation* involves, as its name implies, variation of the temperature through values of constant pressure to obtain points for the P(T)-isopleth.

The converse method *i.e.* the *method of pressure variation* involves the variation of the pressure with constant values of temperature to obtain values on the T(P)-isopleth. To obtain meaningful results *i.e.* mole fraction-pressure (x_i - P) and mole fraction- temperature (x_i -T) curves from the isopleths, a technique of cross-plotting from the two sets of isopleths (Raal and Muhlbauer, 1994), coexistence equations (Gibbs and Van Ness, 1972) or the use of iterative calculations based on equilibrium relations (Harris, 2004) can be employed. The accuracy of the final form of the data hinges upon accurate determination of feed compositions, pressures, temperatures, volumes and the calculation procedure used.

As mentioned above, static synthetic methods are of three types, visual, non-visual or material balance-based methods, each of which will be discussed separately below.

Visual Synthetic Methods

In *visual synthetic methods*, the incipient formation of a new phase (dew point, bubble point or critical point) is detected by visual or optical observation of the resulting cloudiness, droplet or meniscus-formation in a view cell *i.e.* an equilibrium cell with transparent windows. Visual synthetic methods typically involve the use of equipment that is of the variable-volume type (except for the "total pressure measurement method") with suitable provisions for the accurate determination of the cell volume. The direct experimental “dew and bubble-point" method is a notable visual synthetic method and a detailed description of the method can be found in the review paper of Malanowki (1982b). The measurements are usually in the form of P-V-T data for a system of constant overall composition with either pressure (isothermal) or temperature (isobaric) being varied for the constant-composition sample. In the isothermal version of the method, when a liquid of a given composition in a closed system is decompressed under isothermal conditions from an initial pressure value to its saturated vapour pressure at that temperature, an infinitesimal amount of vapour forms. The latter is known as the "bubble-point" as it corresponds to the initial formation of bubbles in the liquid. Continued decompression results in the increased formation of the vapour bubbles and eventually the formation of the pure

vapour. The point where the vapour is compressed and the appearance of micro-sized droplets of liquid condensate occurs corresponds to the "dew-point". The dew and bubble-point method is applicable to binary mixtures in two-phase regions and for the three-phase regions, various graphical techniques can be used (Huang *et al.*, 1985).

The first dew and bubble-point apparatus in open literature was that of Cailletet (1877) as described for investigations on the liquefaction of ethene. A similar investigation was conducted by Kuenen (1895) for binary mixtures of ethane and nitrous oxide. In both types of studies, mercury was used to both confine the sample and to vary the volume of the cell, which was kept at a constant temperature in an isothermal bath. An internal stirrer was used to facilitate the attainment of equilibrium. The pressure and volume of the system was recorded at the dew and bubble points. The much later design of de Loos *et al.* (1986) was also based on the Cailletet apparatus.

In the apparatus of Kay (1936), the cell consisted of a thick-walled glass capillary tube, which was firstly evacuated and then filled with mercury to remove any air in the system. The pure liquid components were firstly degassed and then mixed together to form mixtures of known composition. The sample was then introduced into the cell by removing some of the mercury. The sample, over the mercury in the cell, was then set in a mercury-filled compressor connected to a manifold and heated to the desired temperature. An electromagnetic stirrer served to agitate the sample continuously. Pressure changes were then made via the manifold through the variation of the pressure of the gas in the mercury reservoir. The bubble point was observed visually as the first bubble of vapour that appeared as the pressure above the liquid sample was slowly decreased. The dew point was determined by the formation of minute black spots on the capillary wall as the pressure of a completely vapourized sample was increased. Kay also obtained the densities of the saturated liquid and vapour phases studied.

Liphard and Schneider (1975) obtained phase equilibria and critical region data for the binary mixtures of carbon dioxide and squalane with an optical high-pressure cell for temperatures up to 423 K and pressures up to 100 MPa. The cell had an internal volume of 7.8 cm^3 and was constructed from stainless steel and sealed with a copper ring. The liquid mixture in the cell was stirred through the use of a magnetic stirrer. Two sapphire windows served to allow for visual observation of the phase transitions. The pressurizing system consisted of a piston through which the pressure from a rotating pump (with liquid decane) was transmitted. The squalane was introduced into the cell with a preweighed syringe. The carbon dioxide was fed into the cooled equilibrium cell from a high-pressure cylinder, the mass of which was obtained by difference. The mixture temperature and pressure were then adjusted to obtain a single phase

initially, after which the determination of the phase transition proceeded with a variation of the pressure (isobaric) or temperature (isothermal).

The equipment of Occhiogrosso *et al.* (1986) was designed for VLE measurements of carbon dioxide systems. Results were obtained in the form of pressure-composition isotherms. The equilibrium cell was constructed from 316 stainless steel and had a working cell volume of 45 cm^3. The visual determination of phase transitions was made possible through the use of a fibre-light pipe illuminated quartz window. The cell contents were pressurised by a moveable piston fitted with Viton® o-rings and driven by a syringe-type pressure generator with silicone oil as the pressurizing fluid through which the pressure was transmitted. In going from a single-phase to the two-phase mixture, the dew point, bubble point or mixture critical point was observed. The dew and bubble points were determined as explained before, however, for the mixture critical point, this was defined as the pressure and temperature at which a critical opalescence was observed for a slight change in either pressure or temperature. Also at the critical point, a slight change in either pressure (< 30 kPa) and/or temperature (< 0.1 K), caused the single supercritical phase to separate into a 50 % volume liquid and a 50 % volume vapour phase. In the above fashion, Ochiogrosso *et al.* (1986) were able to measure bubble points, dew points and critical points with the visual dew and bubble-point method.

Another method included in this classification scheme of visual equipment is that of the "total pressure measurement method" (Nagahama, 1996), which is a less popular variation of the dew and bubble-point method. In this method, the amounts of the components added to the cell, and not the cell volume, are varied for isothermal conditions until the formation of a new phase is visually detected *i.e.* pressure versus composition isotherms are obtained.

The applications of the visual synthetic method, apart from phase equilibrium studies, include the study of complicated multicomponent phase equilibrium behaviour, the measurement of the solubility of gases in electrolyte solutions and solid-fluid equilibria determinations (Dohrn and Brunner, 1995).

Non-Visual Methods

In the non-visual method, the accurate monitoring of the physical properties of a system is employed as a means to detect phase transitions in the system and measurements are made along an isothermal or isobaric path for a constant-composition sample. This method allows for the indirect determination of the dew and bubble-points. An example of the application of this method is a monitoring of the pressure-volume relationship for isothermal conditions as a plot

for a variable-volume cell, for which the volume at any instant is known accurately. Any observed discontinuities or breaks in the pressure-volume plot, which is shown in Figure A.3, correspond to phase transitions (the bubble point, dew point or mixture critical point). This method for phase transition detection is claimed to be more accurate than a visual means of phase transition detection (Dohrn and Brunner, 1995).

Any combination of the system variables typically (P-V), (T-V) or (P-x) is monitored to allow for the determination of the phase transition points. Sage and co-workers (Sage *et al.*, 1934) designed two types of cells for the acquisition of VLE data by the indirect dew and bubble-point method. The first cell (Sage and Lacey, 1934) was of the isothermal and the constant-volume type where measurements were obtained as more of a second component was added in the form of a series of additions to a known amount of the usually less volatile component in the cell.
The cell was also mechanically rocked to facilitate the attainment of equilibrium. The P-T-x relationships for the saturated vapour phase were determined in a different "dew-point cell" where the condensation of the liquid or its disappearance was observed as the dew point. The system pressure was then measured and the bubble point was obtained as the discontinuity in the plot of pressure versus composition. Disappearance was detected through the use of a thermocouple.

In a variation of the non-visual technique, Sage *et al.* (1934) designed a second cell, which was of the variable-volume type where the composition of the mixture that was charged would remain constant and the pressure-volume relationship would be studied for the isothermal conditions. The variation in volume could be achieved through the addition or removal of mercury from the equilibrium cell, allowing the volume of the sample above the mercury to be defined. The equilibrium cell contents were agitated to speed up the attainment of equilibrium. The dew and bubble points were determined as the discontinuities in the curves of specific volume versus equilibrium pressure.

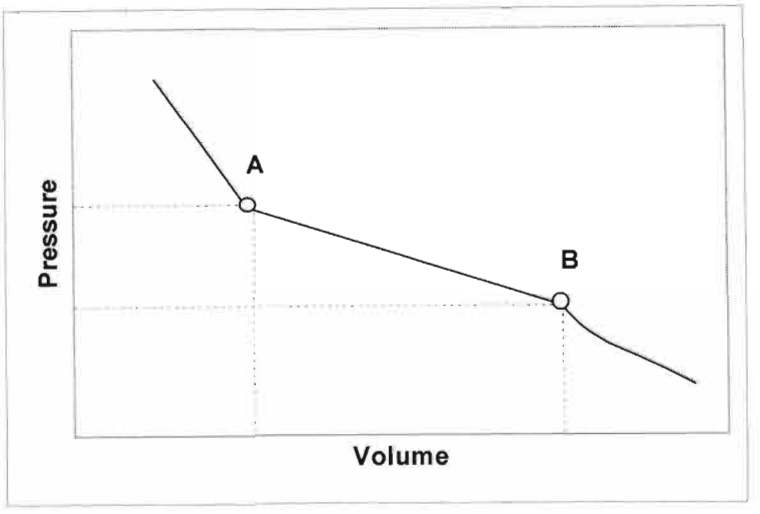

Figure A.3. Typical P-V diagram for isothermal conditions: **A**: bubble point; **B**: dew point.

The equipment of Meskel-Lesavre *et al.* (1981) was based on the design of a variable-volume cell for the simultaneous determination of VLE data and saturated liquid molar volumes for pressures up to 5 MPa and temperatures up to 373 K. The equipment was designed for bubble-point determinations through the use of a small and light equilibrium cell (so as to facilitate gravimetric measurements on a balance), a piston with a hydraulic drive and a means for the introduction of the gaseous component. The equilibrium cell was constructed from titanium and was essentially a piston-cylinder assembly, the movement of which, was controlled with the displacement of a pressurizing fluid, whose mass could be accurately determined by a balance. The liquid samples could be degassed into the cell by vacuum crystallization, after which the cell is accurately weighed. The cell is then placed under the hydraulic piston drive in the liquid thermostat. The equilibrium cell also contained an electromagnetic stirrer to agitate the liquid mixture whilst the pressure of the cell was increased. The cell pressure was determined as a function of the total cell volume and to increase the accuracy of the results, a correction for the thermal expansion and the compressibility of the hydraulic fluid was taken into account. The bubble point was indicated by the discontinuity in the P-V plot. The liquid molar volumes of pure components and the excess molar volumes for mixtures were determined simultaneously with the bubble point from the P-V plot. From the coordinates of this bubble point, the liquid molar volumes could be obtained, where the liquid mole fraction corresponded to the total mole fraction obtained at the phase transition.

The equipment of Meskel-Lesavre *et al.* (1981) allowed for measurements of multicomponent mixtures as well. The apparatus was suitable for VLE measurements for systems formed by components that have large discrepancies in their vapour pressures *i.e.* a high relative volatility.

The equilibrium cell of Meskel-Lesavre *et al.* (1981) was modified for elevated pressures and temperatures by Rousseax *et al.* (1983), where a bellows was used to replace the piston. As for the equipment of Meskel-Lesavre *et al.* (1981), VLE and saturated liquid molar volumes were determined. As in the previous design, the cell was small and light to allow for gravimetric measurements. The internal volume of the cell was variable to allow for a cell volume between 0.008 dm^3 and 0.014 dm^3. The equilibrium cell consisted of a bellows containing the mixture and a pressurizing cell enclosing the bellows. The entire assembly was housed in an air bath. The system pressure, at a constant temperature, was recorded as a function of mixture volume, the composition of which was known accurately by weighing each component.

The suitability of an indirect determination of mixture critical points by monitoring system variables (P-V-T-x) was established as not being satisfactory by Rousseax *et al.* (1983), where it was acknowledged that provided that conditions were not too close to the critical point, the pressure-cell volume plot would display a well-defined break point or discontinuity indicating the bubble point. Rousseax *et al.* (1983) also commented on the use of the above two methods to obtain the bubble point. The first was to increase the system pressure from a lower value (the low to high approach) or by decreasing it through a rapid compression to a pressure higher than the bubble pressure (the high to low approach). Although the curves of P versus V cannot be distinguished for biphasic mixtures, the time for equilibration between the phases is shorter when decreasing the pressure *i.e.* vapourization is shorter than liquefaction, based on the relative entropies of the two-phase transitions.

The equipment of Gibbs and Van Ness (1972) differs from the indirect dew and bubble-point methods as breaks in the various plots of system variables (P-V-T-x) are not monitored for the detection of phase transitions. The equipment consisted of a constant-volume glass cell in a temperature bath, into which accurately dispensed volumes of components where added from metered piston injectors. In this type of method, the feed volumes of the added components are accurately monitored as they added to the cell to form an accurately known overall composition. In the same fashion as for conventional static analytic measurements, the equilibrium pressure was monitored for each composition change under isothermal conditions. The mixture was then stirred and allowed to equilibrate, until there were no detectable changes in the system pressure. In this fashion, total composition pressure data were generated. The dew point can be calculated by means of the solution of the coexistence equation (Van Ness, 1964).

The designs of Kolbe and Gmehling (1985), Rarey and Gmehling (1993) and that of Fischer and Wilken (2001) were based on the design of Gibbs and Van Ness (1972). These designs featured automation of the entire equipment and precision computer-controlled piston injection pumps

and allowed for the accurate measurement of data in the dilute regions. In these methods, the pressure of different overall mixture compositions is measured for a constant temperature. The total compositions are determined from the known amounts of the liquid components injected into the equilibrium cell by the stepping motor-driven injection pumps. The liquid phase compositions are calculated through the use of mass and volume balance equations which are related to the equilibrium relations (VLE) of the phases.

Synthetic methods using the material balance

This is the least popular technique and is based upon the principle that in the Gibbs Phase Rule, systems which possess two degrees of freedom (for multiple coexisting fluid phases of binary and ternary mixtures), where the pressure and temperature are fixed, have constant phase compositions. In terms of the method (Fontalba, 1984), the indirect determinations of the phase compositions (x and y) and the vapour and saturated liquid molar volumes (V_s^L and V_s^V) are obtained by solving four mass balance equations relating the four unknown variables to the measured quantities of the overall amounts of the components (n_1, n_2) and the phase volumes (V^L and V^V) at fixed pressures and temperatures. Two different cell loads will produce different cell volumes, which can then be accurately measured. This technique relies on the measurement of phase volumes typically through interface level measurements, obtained visually or by monitoring thermal conductivities (Fontalba *et al.*, 1984) and consequently incorporates the use of sight glasses or windows in the apparatus. The material balance method can be used to calculate the phase compositions from accurately measured phase densities and the total volume for the different cell loadings, (DiAndreth *et al.*, 1987).

The equipment of DiAndreth *et al.* (1987) allowed for the measurement of complex ternary and quaternary phase equilibria in the form of liquid-liquid-gas and liquid-liquid-liquid-gas equilibria. Critical points were also obtained for gas-liquid and liquid-liquid mixtures by the observation of critical opalescence. The cell was of the variable-volume visual type and consisted of a sapphire window for observations of the volumes of the individual phases.
The cell consisted of a moveable piston, with water as the pressurizing fluid, and the cell was pressurized by a syringe pump. The cell volume could be varied from 9.94 - 29.02 cm^3 and was determined, as a function of piston displacement, by the position of an indicator wire attached to the piston. The equilibrium time was around 4 - 6 hours. The meniscus heights of the phases were measured with a cathetometer. The volumes of the coexisting phases were calculated from the meniscus heights.

The equipment of Laugier (1990) was another example of a material balance-based method. It was based on the design of Fontalba *et al.* (1984) but was modified to allow for the visual observation of the cell contents. The use of non-visual techniques for phase interface positions in the cell *i.e.* a thermal conductivity probe (Fontalba *et al.*, 1984) is suitable for VLE but not for LLE. With the inclusion of sapphire windows, visual observation of phase separation was possible. The cell was also light as for Meskel-Lesavre *et al.* (1981) and Rousseax *et al.* (1984) to allow for the weighing of the cell for composition determinations. The relative positions of the coexisting phases in the cell were determined through the use of an optical window and a cathetometer.

A.1.2.2 Advantages of the Static Synthetic Method

(a) The most blatant advantage of all synthetic methods over others is the *exclusion of sampling* and all the complexities and uncertainties associated with the sample withdrawal, preparation and analysis, which were dealt with in previous sections.

(b) With the *exclusion of complex and expensive sampling equipment* and analytical equipment, together with the simple design of the equipment (variable-volume cells), the total cost of the experimental equipment is usually relatively quite moderate.

(c) The experimental method is fairly *simple and straightforward*, with operator time greatly reduced and no requirement for sampling procedures.

(d) There are *no long equilibration times* to endure with synthetic equipment during the VLE measurements as phase separation is the desired result and so this method is limited only by the observation (visual or material balance) or detection (non-visual) times for the new phase formations. The system is, however, allowed to equilibrate prior to the additions of components from the piston injector, when changing the composition in the cell.
This allows for *isopleths to be generated both rapidly and reliably i.e.* a complete P (T)-isopleth can be readily obtained from just a single charging of the equilibrium cell.

(e) Synthetic methods are used as alternatives in situations *where analytical methods are not applicable or successful.* Since isotherms or isobars near the critical region have quite small gradients, any disturbance of the system (due to sampling) can result in large fluctuations in the phase compositions.
Also, synthetic methods are applicable when a phase separation is difficult to quantify by analytical methods due to the coexisting phases having similar densities *i.e.* near or at critical

points and even in "barotropic systems", which under certain conditions, have phases that have the same densities.

(f) The static synthetic method of the non-visual type easily *lends itself to automation*, as is the case in the equipment of Rarey and Gmehling (1993). The inherent advantages of automation are reduced operator time, more rapid generation of data, precise control over the injection of the components into the cell via a precision injection pump, which is very important for a stoichiometric technique.
In the equipment of Rarey and Gmehling (1993), which is of the non-visual type, all the experimental variables are logged into the computer, which then regulates the injection of the pure components into the cell based on feedback from the cell pressure sensor. The data is logged automatically and the output is analysed and the results are computed.

(g) The equipment of Meskel-Lesavre *et al.* (1981) and Rousseax *et al.* (1983) allowed for the *accurate determination of saturated molar volumes* at constant temperature and pressure as a function of composition. This allows for the calculation of partial molar volumes for the testing of mixing rules for equations of state. The data also gives an estimate of the effect of pressure on the nonideality in the liquid phase in the form of the Poynting correction.

A.1.2.3 Disadvantages of the Static Synthetic Method

(a) When applied to multicomponent systems, the use of the synthetic method *provides less information*. P, T and x envelopes can be obtained but not the tie lines (which provide vital information about phase behaviour) without the requirement of additional experiments having to be performed such as refractive index measurements (Dohrn and Brunner, 1995).

(b) A limitation of the visual synthetic method is that it is not applicable for *the study of iso-optic* systems. These types of systems have coexisting phases with approximately the same optical properties such as refractive indices and this makes the detection of phase separation through visual observation virtually impossible.

(c) Even when systems are amenable to be studied by visual synthetic methods, the *precise visual detection of phase changes* as a function of pressure and temperature is quite challenging. A finite amount of vapour at the bubble point or liquid at the dew point must be produced to allow for visual detection. Consequently at the bubble point, the small amount of material in the vapour bubble is ignored and conversely at the dew point, the small amount of material in the dew that is formed is also ignored (Occhiogrosso *et al.*, 1986). As a result, in the detection of

the phase transitions, the temperature or pressure corresponding to the transition point may be erroneous as a result of overcompensation in attempting to view the bubble or dew points. This is exemplified in the possible deposition of the liquid phase at its dew point as a thin film on the interior walls of the equilibrium cell and not as a more easily visible mist in the view cell. This poses a great problem to experimenters observing dew points and this problem is described as unavoidable by Raal and Muhlbauer (1994) as a temperature gradient must be induced between the gaseous phase and the immediate environment (even if well-agitated) when it is cooled or heated. As a result of inaccurate observation and recording of phase transitions, erroneous equilibrium P-V-T values are obtained.

(d) The use of static synthetic techniques is limited to *equilibrium states near critical or at critical states* only *i.e.* where the gradients of the isotherms $\left(\frac{\partial P}{\partial z}\right)_T$ or isobars $\left(\frac{\partial T}{\partial z}\right)_P$ are small. This is because of slopes of isobars and isotherms have large gradients away from the critical state *i.e.* the properties of the system are very concentration dependent, consequently, any errors in the overall composition (z) will have a profound effect on the results.

(e) As for the static analytical method, the static synthetic method is also highly *intolerant of any dissolved gases* or impurities in the introduced samples or the presence of any air in the cell prior to the experiment. Consequently, the same exhaustive liquid degassing and cell evacuation techniques are also necessary for static synthetic techniques.

(f) The direct visual determination of the dew and bubble points *is limited to the study of two-phase regions* and for studies of three or more phase regions, the accuracy of the determination is limited by the use of graphical or numerical methods for interpolation (Malanowski, 1982b).

(g) The use of view glasses in visual methods and in material balance-based methods for high pressures presents a *difficulty with regards to the proper sealing* of materials such as glass or sapphire into the equipment *i.e.* the window-metal interface. This further complicates the cell design.

A.1.2.4 Static Synthetic equipment in the literature

Some of the more common designs of static synthetic equipment (both high and low-pressure designs) available in the literature are presented in Table A.2. Due to space limitations, only the first author is listed and equilibrium times have not been presented (which could not be found for the large majority of the equipment). For columns with two materials of construction, the

principle material of construction of the cell is listed first and the second is the material for the cell windows. For variable-volume cells, the maximum internal cell volume or the cell volume working range is listed under cell volume.

A summary of the important aspects of the equipment listed in Table A.2 is provided below:

(a) The majority of the contemporary static synthetic equipment constructed is of the *non-visual variable-volume and fixed-volume type*, as opposed to the visual type, which has largely become obsolete, due to the limitations associated with the accurate visual detection of phase transitions (as mentioned above).
The use of accurate methods to monitor the system pressure, temperature, volume and to determine phase compositions allows for the use of computational methods to determine phase equilibrium compositions (Fischer and Wilken, 2001). Although visual observation is not used for the principal determination of phase transitions, many of the non-visual type designs still incorporate view cells due to the complex nature of high-pressure mixtures, where the formation of multiple phases is difficult to predict. However, the use of visual methods for critical region studies has been favoured by researchers such as Liphard and Schneider (1975), de Loos *et al.* (1986), Occhiogrosso *et al.* (1986) with the use of the "critical opalescence" visual method.

There have been very few designs based on the material balance method, due to the many uncertainties and the limitations of this method. For this type of equipment, only three notable designs, that of Fontalba *et al.* (1984), Di Andreth and Paulaitis (1987) and Laugier (1990) have been documented.

(b) The *popular choice of transparent material for the windows* of the equilibrium cell itself has been naturally-occurring or synthetic sapphire. This is due to the durability and robustness of the material at very high pressures (where the use of glass would be unsafe).

(c) The studies of *critical phenomena necessitates high pressures*, consequently the pressure ranges of the equipment is quite high for most cases *i.e.* up to 200 MPa for Konrad *et al.* (1983) and Matzik and Schneider (1985).

(d) *Internal agitation* through the use of magnetically coupled stirrers was a common feature for most of the static synthetic designs, as in the design of Matzik and Schneider (1985), to speed up the attainment of equilibrium.

Table A.2. Selection of Static Synthetic equipment in the literature.

Author	Cell Volume (cm^3)	Type of Cell [a]	Material of Construction [b]	Operating Range		Measurement Device	
				Temp (K)	Press (bar)	Temp [c]	Press [d]
Gibbs (1972)	–	Non-Visual (FV)	Glass	–	–	–	–
Liphard (1975)	7.8	Visual (VV)	SS & Sapphire	–	–	TC	B
Meskel-Lesavre (1981)	–	Non-Visual (FV)	TT	373	50	TC	PT
Konrad (1983)	–	Non-Visual (VV)	N90 & Sapphire	450	2000	TC	–
Rousseax (1983)	–	Non-Visual (VV)	SS	573	600	TC	B/PT
Fontalba (1984)	60	Material Balance (VV)	TT alloy	433	450	TC	PT
Kolbe (1985)	180	Non-Visual (FV)	Glass	423	10	QT	PT
de Loos (1986)	–	Visual (FV)	SS & Glass	473	200	PRT	MN
Ochiogrosso (1986)	45	Visual (VV)	316 SS & Quartz	535	700	PRT	PT
Di Andreth (1987)	9.94 - 29.02	Material Balance (VV)	–	273	500	PRT	B
Laugier (1990)	10	Material Balance (VV)	TT alloy & Sapphire	353	200	TC	PT
Rarey (1993)	–	Non-visual (FV)	SS	368	30	PRT	PT

[a] In parenthesis: (VV) = Variable-Volume Cell; (FV) = Fixed -Volume Cell.
[b] SS = Stainless Steel; N 90 = Nimonic 90 SS; TT = Titanium.
[c] TC = Thermocouple; PRT = Platinum Resistance Thermometer; TS = Thermistor.
[d] B = Bourdon gauge; PT = Pressure Transducer; PRPSG = Precision Resistance Pressure Strain Gauge; MN = Manometer.

(e) *The pressurization of the cell contents* with a variable-volume design was mostly achieved with the use of a piston or bellows, where the latter was used for higher pressures (Rousseax *et al.*, 1983). The pressure from the primary source (hand pump, screw press, *etc.*) was indirectly transmitted to the cell through the use of a suitable pressurizing or hydraulic fluid, which varied from researcher to researcher *e.g.* silicone oil was used by Konrad *et al.* (1983) and octane by Fontalba *et al.*(1984).

(f) The *interior cell volumes* and hence the sizes of the cells were quite small, in particular those of Meskel-Lesavre *et al.* (1981), Rousseax *et al.* (1983), Fontalba *et al.* (1984) and Laugier *et al.* (1990). This was to facilitate the weighing of the cells on an analytical balance.

A.1.3 The Static Combined Method

A.1.3.1 Description of the Static Combined Method

Static analytical methods are not suitable for investigations of the VLE properties of mixtures at or near the critical region, where the isobars and isotherms have small gradients. Deiters and Schneider (1986) noted that the equilibrium condition *i.e.* phase compositions of the system in the near critical region is highly sensitive to the smallest of fluctuations in temperature and pressure (induced by sampling of the phases, *etc.*). Consequently, the synthetic method, as opposed to the analytical method, is favoured for the study of critical region phase behaviour. Conversely, for phase conditions away from the critical region, where the isotherms and isobars have large gradients, the synthetic method is less accurate than the static synthetic type since any errors in overall composition measurement can lead to large temperature errors in the computed data.

Many researchers have attempted to combine features from both types of apparatus into a single versatile piece of equipment, which would allow for the acquisition of phase equilibrium data both away from and near the critical region. This search for static equipment that would allow for data acquisition near or away from the critical region culminated in the development of the static combined method. In such a method provision is made for both the sampling of the phases, visual observation of the cell contents, and also for the accurate determination of the cell volume.

The advantages and disadvantages of this method would be roughly equivalent to those for both static analytic and static synthetic methods; however, these would now roughly be combined.

A.1.3.2 Static Combined equipment in the literature

There have been very few reports on the use of the highly specialised static combined methods in the literature and a selection of the successful designs are presented in Table A.3. For those columns with two materials of construction, the principle material of construction of the cell is listed first and the second is the material for the cell windows. Equilibrium times have not been presented as these could not be found for the selection of the equipment designs that have been presented here.

Notable features of the static combined designs listed in Table A.3 are the following:

(a) As with the static synthetic method, *sapphire was the common choice* for the cell window construction material and has been used by all the researchers listed, except Schotte (1980).

(b) A combination of *visual and non-visual methods* for the determination of the phase transitions by the static synthetic method was used by the researchers. Huang *et al.* (1985) employed the method of visual observation of the phase transitions in the cell (cloudiness or droplet formation). Japas and Franck (1985), on the other hand, obtained pressure-temperature plots for constant cell volumes, where a break point was observed at the phase transition. As a result of the difficulties experienced when attempting to visually detect phase transitions (the point of de-mixing), Reisig *et al.* (1989) opted for the pressure-volume plot to determine the phase transition.

(c) In the analytical operational mode, the use of capillaries was favoured; however, this choice presented the uncertainties that were discussed in Section A.1.2.3 with regards to differential vapourization.

Table A.3. Selection of Static Combined equipment in the literature.

Author	Cell Volume (cm^3)	Sampling	Material of Construction [b]	Operating Range		Measurement Device	
				Temp (K)	Press (bar)	Temp [c]	Press [d]
Schotte (1980)	265	–	Glass	523	55	TC	–
Wisotzski (1984)	–	Sampling Capillary	Sapphire Windows	373	3000		PT
Huang (1985)	45 [a]	Sampling Valve	Sapphire	477	185	TC	PT
Japas (1985)	–	Sampling Capillary	Nickel alloy & Sapphire	673	2500	TC	PT
Reisig (1989)	–	Sampling Capillary	Cu-Be Alloy & Sapphire	300	3000	PRT	–

[a] The maxinum internal volume of a variable-volume cell.

[b] SS = Stainless Steel; N 90 = Nimonic 90 SS; TT = Titanium; Cu-Be = Copper-Beryllium.

[c] TC = Thermocouple; PRT = Platinum Resistance Thermometer; TS = Thermistor.

[d] B = Bourdon gauge; PT = Pressure Transducer; PRPSG = Precision Resistance Pressure Strain Gauge; MN = Manometer.

A.2 Dynamic Methods

In HPVLE dynamic methods, either one or both of the phases are circulated (single pass or flow) or recirculated (phase recirculation) continuously through the use of pumps into a temperature-controlled equilibrium chamber. The two principal subdivisions of HPVLE dynamic methods, which are inherently analytical, are the single pass and phase recirculation methods; both of which will be described in detail separately in the sections below.

A.2.1 The Single Vapour Pass Method

This method was the first of those classified under HPVLE dynamic methods *i.e.* the original HPVLE dynamic method. It has largely become the less favoured method of choice for dynamic HPVLE determinations due to the inherent uncertainties and experimental difficulties associated with its use.

A.2.1.1 Description of the Single Vapour Pass Method

In the single pass or semi-flow method, as its name implies, only one phase is flowing and the other phase remains stationary in the equilibrium chamber. A natural choice for the flowing component is indeed the more volatile component in the form of the gaseous phase (as it is easily pumped) consequently, this method is also known as the pure gas circulation method. A schematic of the method is shown in Figure A.4.

In this method, the gaseous stream (at a controlled pressure) is passed through two cells in series that contain the liquid phase (at a controlled temperature) to generate isobaric or isothermal data. The first of these cells is a presaturator, which serves to facilitate the attainment of an equilibrium condition for the gaseous phase when it encounters the liquid phase in the equilibrium chamber *i.e.* the second cell. As the gaseous component is circulated through the liquid phase through the action of a pump, the amount of the dissolved gas content in the liquid phase increases until equilibrium is reached.

A requirement for obtaining reliable results from this method is that the gaseous phase should pass through the liquid phase completely in as short a time period as possible to "ensure a rapid approach to equilibrium" (Tsang and Streett, 1981).

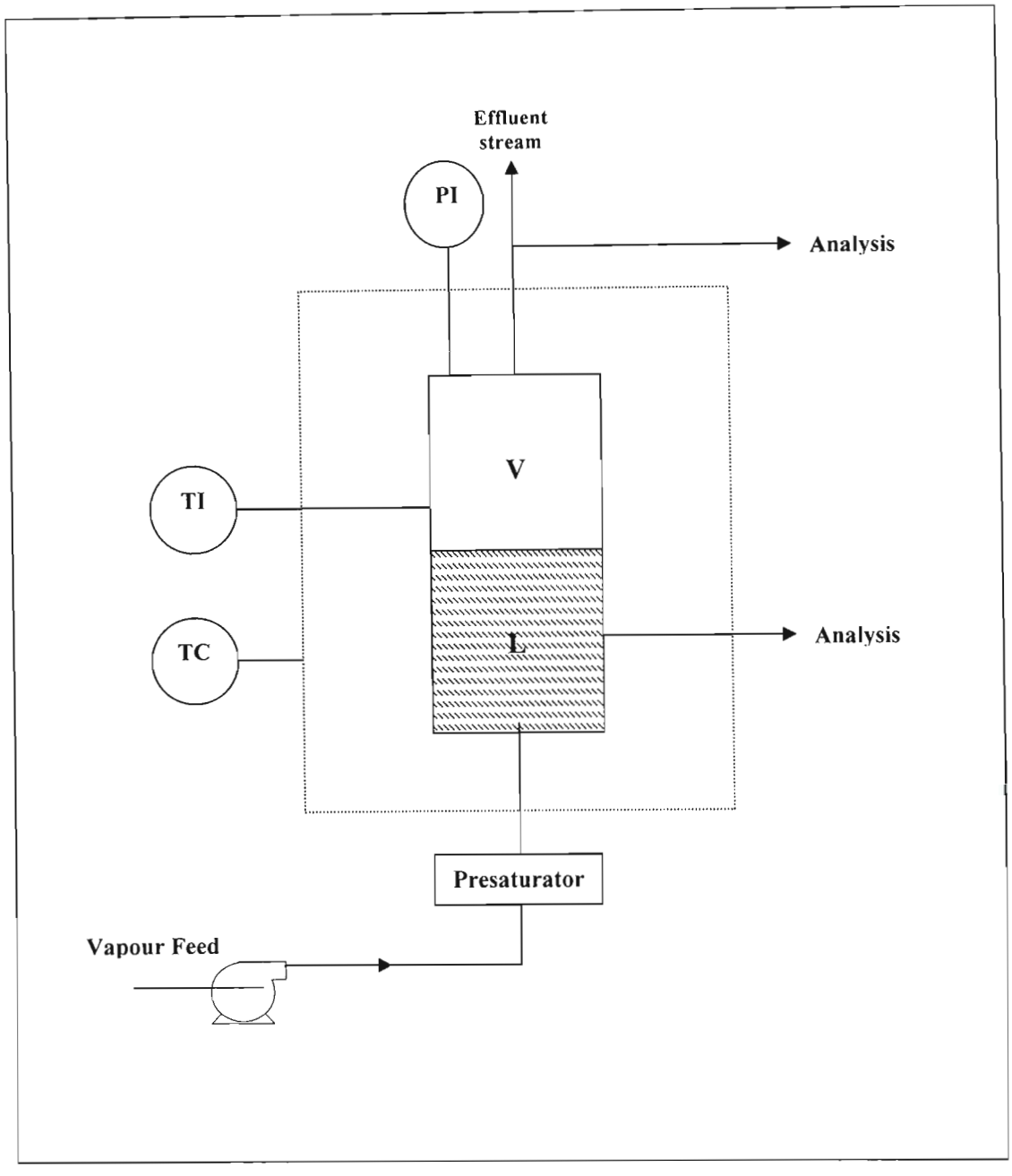

Figure A.4. Schematic diagram of a Single Vapour Pass apparatus: **V**, vapour phase; **L**, liquid phase; **TC**, temperature control system (isothermal bath for liquid component); **PI**, pressure indicator (sensor); **TI**, temperature probe in the cell body.

Equilibrium times as short at 15 minutes have been reported in the literature by researchers such as Young (1978). In reality, this time will depend on mass transport and momentum transfer coefficients in the two phases, as well as the equilibrium solubility of the system.

When equilibrium has been reached, the vapour phase is sampled by reducing its pressure and directing it to a trap (by diverting a portion of the effluent flow exiting the cell), where it is usually condensed and sampled as a liquid. The amount of gas sampled through the trap can be determined volumetrically through the use of a wet test meter (Dohrn and Brunner, 1995). The

liquid phase samples are obtained directly as a take-off from the equilibrium chamber where the samples are drawn off through tubes, depressurised and analyzed.

A.2.1.2 Advantages of the Single Vapour Pass Method

(a) The method and the associated equipment are both fairly *straightforward and inexpensive*, as this was the original form of the dynamic method.

(b) The *equilibrium times* claimed by many researchers for this method are much shorter than those required for other methods.

(c) The method finds favourable use for *the study of mixtures where the gaseous component is present in much higher concentrations* than the liquid phase.

(d) The gas-liquid equilibria or gas solubility data obtained with this method serves to allow *for the calculation of the second virial coefficients (B_{12})* as function of temperature. The *correction parameter (K_{12}) for the energy parameter* of the Kilhara intermolecular potential model can also be calculated from the experimental data.

A.2.1.3 Disadvantages of the Single Vapour Pass Method

(a) *Large quantities* of the gaseous component are required, which is a limiting factor when rare or expensive gases are used. Also, the liquid component has to be constantly discharged from the equilibrium cell; consequently one liquid charging of the cell provides a minimal amount of data (as opposed to *e.g.* the static synthetic method). The method, although economical with regards to time, is not economical with regards to use of chemical components.

(b) The experimental method (due to the principle of its operation) is limited to pure component gas and liquid systems and with further *restrictions being placed on the nature of the phases* that can be used. The partial pressure of the liquid must be low at the temperature of interest, less than 0.1 bar (Young, 1978); consequently this method is limited to conditions far from the critical region. The components (gas and liquid) must also not display high or low mutual solubility, as this compromises the attainment of a true equilibrium condition. In particular, ensuring effective agitation becomes a problem when one phase is poorly soluble in the other.

(c) The major uncertainty for this method relates to *whether a true equilibrium has indeed been attained*. Although a steady state can be detected in the system, in terms of the steady system

variables, this state may or may not represent a true equilibrium. This uncertainty is intimately related to the *flow rate of the gaseous component* that must be controlled both accurately and judiciously and can become a vital factor in limiting the accuracy of the method. A *high gas flow rate* will result in a more rapid saturation of the liquid with the gas and also results in a significant diminution of the contact time available for the gaseous phase to achieve saturation and equilibration. This is attributed to the major resistance to mass transfer being in the liquid phase, which will therefore take a longer time to dissolve in the gas bubbles.
Low gas flow rates will often allow for better saturation of the gas phase, however, the converse occurs for the liquid phase. The problem of an optimal flow rate is coupled with the problem of high solubility of the gas in the liquid or *vice versa.*
If the condition necessary for equilibrium *i.e.* saturation of both phases is not attained, erroneous phase equilibrium measurements are obtained.

(d) *Droplet entrainment* is possible where the effluent stream exiting the equilibrium chamber has droplets of the liquid phase (which is at a different composition) entrained in the vapour phase. The subsequent sampling and analysis of which will yield erroneous results.

(e) *Long equilibrium times* are experienced by researchers employing this method. Saddington and Krase (1934) carried out the bubbling procedure for a time period of 3 - 24 hours; 15 hours after which samples were taken. Miller and Dodge (1940) experienced equilibrium times of at least 26 hours.

A.2.1.4 Single Vapour Pass equipment in the literature

The use of the single vapour pass dynamic method has reported by various researchers in literature sources and a few examples of which are presented in Table A.4. Where the maximum operating pressures and temperatures for the equipment has not been provided, the maximum conditions employed in the experimental studies are listed (see footnotes of Table A.4).

The following general comments about the equipment presented in Table A.4 can be made:

(a) The *long equilibrium times*, especially for early researchers such as Saddington and Krase (1934) and Miller and Dodge (1940) were necessitated to ensure that complete saturation of the liquid phase (where the principal resistance to mass transfer lies) by the gas has been achieved. In the equipment of Miller and Dodge, the gaseous component was bubbled through the liquid component in two presaturators before the gas entered the equilibrium cell.

Table A.4. Selection of Single Vapour Pass Dynamic equipment in the literature.

Author	Cell Volume (cm^3)	Material of Construction [a]	Equilibr. Time (min)	Operating Range		Measurement Device	
				Temp (K)	Press (bar)	Temp [b]	Press [c]
Saddington (1934)	–	SS	1080 - 2340	523 [d]	300 [d]	TC	DWP
Miller (1940)	–	–	1560	–	–	–	–
Chen (1974a)	–	410 SS	–	143 - 278 [d]	130 [d]	TC	B
Garber (1979)	–	Copper	–	260 [d]	120 [d]	PRT	B
Huang (1988)	–	SS	–	573 [d]	50 [d]	TC	B
Legret (1983)	–	–	–	423	200	TC	B
Saddington (1934)	–	–	–	523 [d]	300 [d]	TC	DWP
Miller (1940)	–	SS	1080 - 2340	–	–	–	–

[a] SS = Stainless Steel; N 90 = Nimonic 90 SS; TT = Titanium.
[b] TC = Thermocouple; PRT = Platinum Resistance Thermometer; TS = Thermistor.
[c] B = Bourdon gauge; PT = Pressure Transducer; DWP = Dead Weight Piston Gauge.
[d] Maximum operating conditions in the experimental studies.

(b) Many of the researchers attempted to *disprove any internal inconsistency* of their data by examining the equilibrium phase compositions as a function of the variation in the gas flow rate (Huang *et al.*, 1988), however, no relationship was found between the two. For a flow-type cell, a steady-state condition may not always represent a true equilibrium (Garber and Ziegler, 1979) consequently tests for internal consistency provide validation of a true equilibrium state.

(c) The *data commonly measured* by the equipment was that of gas-liquid equilibria (Garber and Ziegler, 1979), partition coefficients and even dew-point loci.

A.2.2 The Single Vapour and Liquid Pass Method

A.2.2.1 Description of the Single Vapour and Liquid Pass Method

The gaseous and liquid streams are fed separately upstream of the equilibrium cell via the high-pressure metering pumps to a mixer, where the phases are concurrently contacted at a controlled pressure and temperature. A schematic of the method is shown in Figure A.5. The purpose of the mixer is to promote interphase mass transfer through the provision of mechanical energy. The mixed streams are then heated until the desired operating temperature is attained. The pre-heated combined stream is then passed into the downstream equilibrium chamber, where phase disengagement occurs to generate a liquid and vapour phase. The two phases exit separately from the equilibrium cell and the streams are diverted to allow for samples of both phases to be withdrawn, depressurized, collected and analyzed on a continual basis.

The pressure adjustment is effected by controlling the effluent stream of the top phase in the equilibrium cell. Two low-pressure separators, one for each phase, effects the separation of each phase into a vapour and liquid. In this way, there are four samples generated *i.e.* a set of vapour and equilibrium samples for each phase. The equilibrium compositions of the phases are then calculated from the weights of the measured vapour and liquid samples using a material balance (Radosz, 1985).

The determination of the interface between the phases has traditionally been achieved through the use of visual methods; however, in recent times some non-visual methods such as the AC impedance bridge technique (Hochgeschurtz *et al.*, 1993) have been successfully employed in this respect. The level of the interface between the phases in the equilibrium cell can be adjusted through the use of the bottom phase expansion valve.

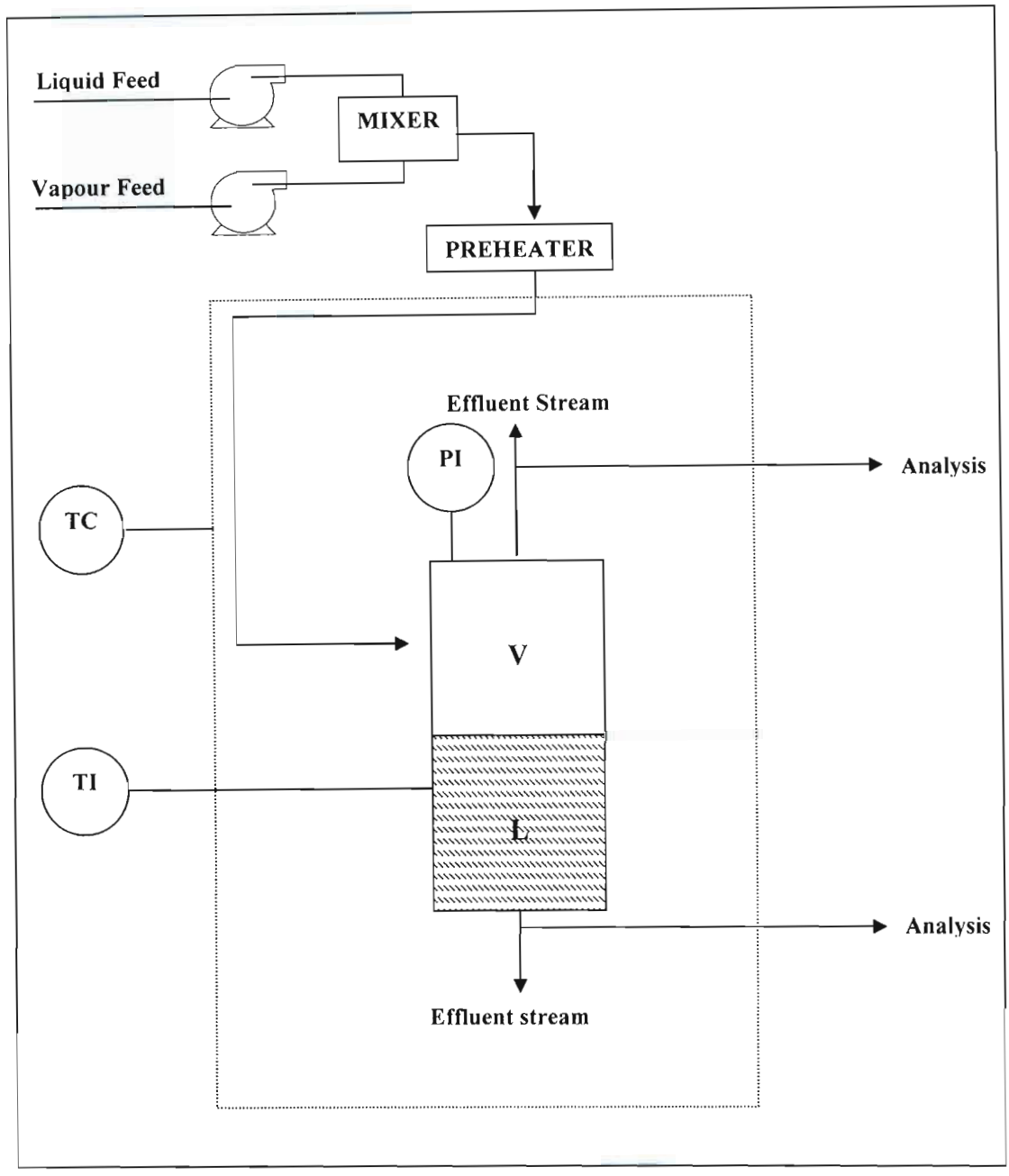

Figure A.5 Schematic diagram of a Single Vapour and Liquid Pass apparatus: **V**, vapour phase; **L**, liquid phase; **TC**, temperature control system; **PI**, pressure indicator (sensor); **TI**, temperature probe in the cell body.

A.2.2.2 Advantages of the Single Vapour and Liquid Pass Method

(a) The *minimization of the thermal degradation* of thermally sensitive materials and also of any chemical cracking or polymerization at elevated temperatures is the most distinct advantage offered by this method. This is made possible due to the short residence times of the

components in the actual heated temperature zone of the apparatus as well as the continuous flow of the components throughout the apparatus so that if any decomposition does occur, the decomposition products are removed from the system on a continuous basis.

(b) The method has the advantage that the *sampling of the liquid and vapour phases does not disturb the equilibrium* as this achieved by diverting the respective phase streams which exit the equilibrium cell for subsequent sampling and analysis. Consequently, the sampling mechanisms present in these types of systems are relatively uncomplicated and free of the uncertainties and design complications inherent in the static analytical method.

(c) The *ease of the handling and mixing of heavy compounds*, together with the allowance for obtaining *large samples* is another added benefit of this method. The heavy materials can be pumped directly from a reservoir and then preheated and mixed with the gaseous phase, prior to entry into the equilibrium cell where it exits as an effluent stream after equilibration.
The sample size can be increased by increasing the experimental run time and in this way the amount of accumulated material in the samplers can be increased.

A.2.2.3 Disadvantages of the Single Liquid and Vapour Pass Method

(a) The method is only applicable for those systems where the *time needed to attain a state of equilibrium for the components used is short* since the residence time of the mixture in the equilibrium chamber is short. Consequently, the researcher faces uncertainties as to whether a true equilibrium has been reached in one pass.

(b) There are a *number of experimental challenges* that are experienced with this method:
(1) Ensuring that contamination of the experimental mixture does not occur due to the operation of the pumps.
(2) The determination of complete phase separation in the equilibrium cell *i.e.* the detection of the interface.
(3) The prevention of droplet entrainment in the effluent streams.
(4) The elimination of pressure gradients within the equilibrium cell.

(c) Excellent *control over the feed rate and the liquid level* is necessary to keep the amounts of both components fixed. However, it has been claimed by a few researchers including Inomata *et al.* (1986) that the equilibrium phase composition is independent of initial feed rates of the components.

(d) The *treatment of the phases* (cooling and decompression) during the sampling process has to be performed meticulously to avoid large errors for measured and calculated values.

A.2.2.4 Single Vapour and Liquid Pass equipment in the literature

The use of this method has quite steadily increased as a result of interest in supercritical fluid extraction studies and also the study of thermally sensitive materials at elevated temperatures, as mentioned above. A selection of some of the successful designs of single vapour and liquid pass equipment is presented in Table A.5. For those columns with two materials of construction, the principle material of construction of the cell is listed first and the second is the material used for the cell windows.

The important conclusions regarding the nature of the equipment presented in Table A.5 are the following:

(a) The large majority of the research investigations involved *conditions at elevated pressures and to a greater extent elevated temperatures* as this method was particularly suitable for such studies (see above). This stemmed from great interest in the study of the model coal compounds and those present in coal liquefaction process streams. Simnick *et al.* (1977) studied hydrogen and tetralin binary mixtures at high pressures and temperatures for hydro-treating processes as for coal liquefaction. The design of Lin *et al.* (1985) had a temperature limit of 710 K and was used for the study of aqueous solutions and coal fluids.

(b) The *use of view windows and even variable-volume cells* was employed by later researchers who designed single vapour and liquid pass equipment. The use of transparent windows in the cell would allow for visual monitoring of the liquid level (Lin *et al.*, 1985), for the observation of coexisting phases of multicomponent mixtures and for mixture critical point determinations by the "critical opalescence method" (Thies and Paulaitis, 1984). Materials used for window construction included sapphire (Lin *et al.*, 1985) and aluminosilicate glass (Thies and Paulaitis, 1984).

(c) Provisions for preventing the *entrainment of liquid droplets* in the vapour stream and to a lesser extent, the entrainment of vapour in the sampled liquid, were an important and integral feature of the single vapour and liquid pass equipment. In the equipment of Simnick *et al.* (1977), vapour bubble entrainment in the sampled liquid phase was prevented by maintaining a small vapour space in the equilibrium cell.

Table A.5. Selection of Single Vapour and Liquid Pass equipment in the literature.

Author	Cell Volume (cm^3)	Material of Construction [a]	Operating Range		Measurement Device		Equilibr. Time	Sample Size
			Temp (K)	Press (bar)	Temp [b]	Press [c]	(min)	Vap. (µl)
Simnick (1977)	90	316 SS	703	250 [d]	TC	B	–	500/1200
Sebastion (1980)	–	–	583 [d]	–	TC	B	–	1320/1860
Thies (1984)	60	316 SS & Glass	723	350	PRT	B	–	–
Lin (1985)	10	316 SS & Sapphire	710	250	TC	B	0.3 - 0.6	500/1000
Inomata (1986)	30	316 SS	710 [d]	230 [d]	TC	B	–	300/1140
Niesen (1986)	250	316 SS	623	100	PRT	B	–	–
Briones (1987)	60	SS	373	346	TC	B	–	–
Roebers (1990)	10 - 50 (VV)	450 SS	673	350	–	–	–	–

[a] SS = Stainless Steel; N90 = Nimonic 90 SS.

[b] TC = Thermocouple; PRT = Platinum Resistance Thermometer; TS = Thermistor; QT = Quartz Thermometer.

[c] B = Bourdon Gauge; PT = Pressure Transducer; DWP = Dead Weight Piston Gauge; PRSPG = Precision Resistance Pressure Strain Gauge.

[d] Maximum operating conditions in the experimental studies.

The entrainment of liquid droplets in the vapour phase was prevented by a demister pad in the equilibrium cell, which prevents any entrained liquid droplets from escaping overhead. The equipment of Inomata *et al.* (1986) also featured a demister pad and an inclined inlet nozzle to prevent liquid droplet entrainment in the vapour phase.

(d) The *liquid level control in the equilibrium cell* was another important experimental variable, which had to be controlled accurately to allow for steady state conditions and to prevent vapour entrainment in the liquid phase. A capacitor sensor was used in the equipment of Simnick *et al.* (1977), where the output (as the liquid level) was displayed on an oscilloscope screen. Lin *et al.* (1985) employed a visual means to monitor and control the liquid level. The liquid level in the equipment of Inomata *et al.* (1986) was maintained at a fixed position by means of an overflow-type self-control system equipped with a backpressure regulator.

(e) Various strategies were employed *for the preheating and mixing* of the feed components prior to entry into the equilibrium cell. This is a very important consideration to facilitate the attainment of equilibrium within the apparatus. The combined feed streams in the equipment of Simnick *et al.* (1977) were heated in a section of tubing with a notched twisted ribbon along its length to promote mixing of the streams.
The equipment of Inomata *et al.* (1986) consisted of a separate preheater and a static mixing section. After the components were initially concurrently contacted, the mixture was fed into a preheater, in which there were two sections. The first section was an electrically-heated tube to allow for the rapid heating of the mixture. The second section consisted of a tube immersed in an air bath and allowed for an adjustment of the mixture temperature to the desired equilibrium temperature. The mixture was then fed into a static mixer *i.e.* a coiled length of tubing for the proper mixing of the components.

A.2.3 Phase Recirculation Methods

In recirculation methods, as its name implies, as opposed to circulation or single pass methods, one or both phases is/are recirculated to achieve equilibrium conditions within the apparatus. Phase recirculation methods can be subdivided into vapour phase recirculation, liquid phase recirculation and liquid and vapour phase recirculation methods and will be described in greater detail in the sections to follow.

A.2.3.1 Description of Phase Recirculation Methods

The general features of phase recirculation equipment are shown in Figure A.6. The diagram that is shown is that for two-phase recirculation; the operation of single-phase recirculation is similar but with the absence of one of the recirculation loops. The components are charged into the equilibrium cell until the desired liquid level has been attained. The temperature and the pressure of the mixture is controlled at predetermined values whilst one or both of the phases is/are continuously withdrawn, recirculated in external loops by pumps and finally sampled when equilibrium has been reached.

In *single-phase recirculation*, the vapour or liquid phase is recirculated (withdrawn continually and passed back) through the equilibrium cell through the action of a recirculating pump. A popular choice for the recirculated phase is that of the vapour phase, judging from the number of research publications for the different types of single-phase recirculation apparatus (Raal and Muhlbauer, 1998). The latter method has been employed for investigations at low temperatures or cryogenic conditions (Nagahama, 1996).
When liquid phase recirculation is the method employed, it is indeed imperative that there is no partial vapourization of the recirculating liquid phase in any part of the recirculating lines. To this end, the lines are temperature-controlled to be below that of the bubble-point of the liquid. As opposed to its vapour recirculating analog, it is not employed for studies at subzero conditions since maintaining the recirculating vapour phase below its bubble point is extremely difficult.

As was the case with single vapour pass methods, liquid phase recirculation is commonly used for measuring the solubilities of gases in liquids (GLE) but with greater success than the former method. The vapour recirculation is achieved through the vapour phase entering the equilibrium chamber at the bottom and bubbling through the liquid phase as the vapour moves upwards. The recirculation of the phases is achieved through the use of recirculating pumps.

The recirculation operation allows for excellent countercurrent contacting between the liquid and vapour phases for interphase mass transfer and equilibrium to be achieved fairly rapidly. The sampling of one of the phases (the non-recirculated phase) directly from the equilibrium chamber has to be performed in single-phase recirculation, whilst the recirculated phase can easily be sampled by diversion of the phase through the external recirculation loop.

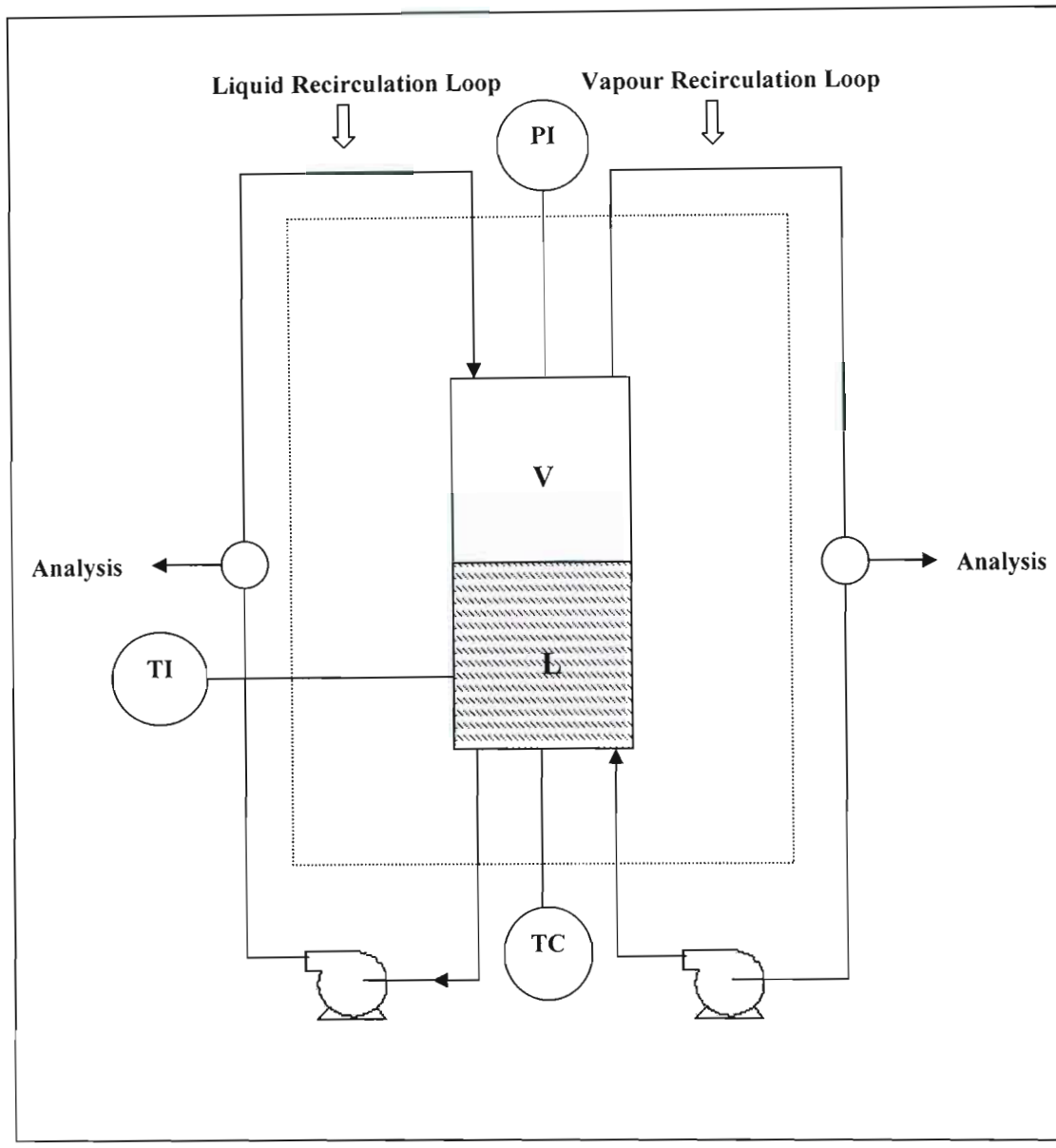

Figure A.6. Schematic diagram of a Phase Recirculation apparatus: **V**, vapour phase; **L**, liquid phase; **TC**, temperature control system; **PI**, pressure indicator (sensor); **TI**, temperature probe in the cell body.

As was the case for the single vapour pass or semi-flow method, special liquid sampling devices are required for the sampling of the liquid phase from the equilibrium chamber in the vapour phase recirculation method. The liquid phase is usually sampled through the use of capillaries.

In *two-phase recirculation*, there is both liquid and vapour phase recirculation. The liquid phase recirculation is achieved by an arrangement where the liquid phase enters the cell at the top and flows downwards through the vapour phase. The vapour recirculation is achieved by the vapour phase entering the equilibrium chamber at the bottom and bubbling through the liquid phase as it moves upwards. The recirculation of the phases is effected through the use of recirculating pumps, which are ideally pulsation-free and magnetically-driven. The recirculation operation

allows for an excellent countercurrent contacting between the liquid and vapour phases for interphase mass transfer and equilibration to be achieved fairly rapidly. However, to aid this process some researchers have employed the use of internal stirrers in the equilibrium chamber *e.g.* Kubota *et al.* (1983).

Due to the nature of the method, the condensation of the recirculating vapour phase and any vapourization of the recirculating liquid phase must be avoided. Strategies to prevent this have included the monitoring and regulation of the temperature in strategic positions in the apparatus *i.e.* three temperature-controlled zones (Raal and Muhlbauer, 1998). The first of these zones is the equilibrium chamber and the second is that of the vapour recirculation loop, which is heated at a temperature higher than that of the equilibrium temperature. The third zone is the liquid recirculation loop, which is maintained at a temperature lower than that of the equilibrium cell.

In two-phase recirculation methods, the liquid and vapour phases can be sampled by diverting a portion of the recirculating phases from the external recirculation loop into sampling loops in the form of commercially available external gas-liquid chromatograph six-port valves, which allow for the sampling volume of the six-port valve loop to be filled isobarically, eliminating problems relating to the differential vapourization of samples due to a pressure drop along the sampling space (as for sampling with capillaries). Vibrating tube densitometers can also be incorporated into the recirculation loops to allow for the densities of the recirculating phase to be obtained.

In other designs of two-phase recirculation equipment, the recirculation loops are used only for internal mixing only and not for sampling, which is achieved through static sampling ports *i.e.* directly from the equilibrium chamber such as in the designs of Behrens and Sandler (1983), Ng and Robinson (1979) and Radosz (1986). Consequently, for these types of methods, where the direct sampling from the equilibrium chamber (as for the static method) is employed, the associated pressure drop whilst sampling must be avoided. Radosz (1984, 1986) modified his apparatus for this purpose through the addition of a variable-volume cylinder to the vapour phase recirculation loop. There have even been designs of phase recirculation apparatus that have featured an ingenious design allowing for an option as to which phase is to be recirculated *i.e.* vapour or liquid, as in the apparatus designs of Kubota *et al.* (1983), Hsu *et al.* (1985) and Wu *et al.* (1988). Two-phase recirculation has been commonly employed in the study of high-temperature VLE, analogous to continuous flow methods, but with greater certainty of the attainment of equilibrium

A.2.3.2 Advantages of Phase Recirculation Methods

(a) The principle of the operation of the dynamic method allows for an excellent contacting between the phases and results in an *equilibrium state being attained quite fast*. Equilibrium times as short as 10 minutes have been reported by some researchers for both single and two-phase recirculation equipment designs, as shown in Tables (A.6) and (A.7). The use of internal stirring complements the rapid attainment of equilibrium by this method.

(b) With the contacting of the phases *not being limited to a single pass but repeated passes*, the approach to equilibrium for phase recirculation is much more reliable than that for a single pass. Consequently, as opposed to single pass or flow methods, for which there are indeed significant uncertainties with regards to the attainment of equilibrium (especially with regards to the vapour phase), phase recirculation greatly reduces uncertainties in this regard.

(c) The method is *extremely economical* with regards to the use of chemical components and the amount of data that can be obtained with a single charging of the liquid component. In this way, large quantities of the gaseous component are not wasted since both phases are recirculated in a closed loop (with the exception of the sampling loop).

(d) The *limitations placed upon the nature of the components* for use in single pass methods are largely eliminated in phase recirculation methods as liquids with high partial pressures can be investigated, with the latter allowing for studies at or near the critical region.

(e) There is some degree of *flexibility offered in terms of the sampling arrangement* for the recirculated phases with regards to the use of capillaries, gas chromatograph valves, variable-volume cylinders, *etc.*

(f) The measurement of liquid and vapour phase densities as well as phase compositions (Kim *et al.*, 1989) allows for the possibility of testing equations of state (EOS) and EOS mixing rules.

A.2.3.3 Disadvantages of Phase Recirculation Methods

(a) The method inherently suffers from some of the *same experimental challenges as those of the single pass method i.e.* maintaining a constant liquid level in the equilibrium cell, preventing droplet entrainment and pressure gradient formation due to the circulating pump. The latter experimental difficulty is particularly pertinent to this method, whose principle of operation is highly dependent upon the action of the circulating pump, which in order to produce flow

requires a pressure differential or gradient. However, it is asserted by some authors (Raal and Muhlbauer, 1998) that this factor is negligible in terms of the quality of the final data when compared to that obtained by static methods.

(b) The *recirculation loops allow for the possibility* of obtaining samples without disturbing the equilibrium condition, however, the incorporation of such loops often adds great complexity to the design of the equipment.

(c) Since the mixture "approaching equilibrium" is *recirculated through a pump body*, concerns over possible contamination of the equilibrium mixture are raised due to the pump lubricant and stuffing boxes, together with the creation of stagnant spaces or regions of entrapped material due to the inefficiency of the pump.

(d) The *need for a well-working pump* is critical for the success of the method as the range of performance for the recirculation pump should be sufficient over wide ranges of pressure and temperature, in which range it should not exhibit a large pressure drop (which is very difficult to avoid). Pulsations exhibited by the pump must also be minimal.

(e) *All the components of the equipment* in thermal contact with the equilibrium chamber have to be housed together in a thermostat *i.e.* a uniform temperature environment, so as to avoid any thermal gradients, partial vapourization or condensation in the recirculating lines. Preventing the partial condensation of the vapour phase (temperature-controlled zones) is also subject to a great deal of experimental uncertainty. This is due to the vapour phase being superheated along the recirculating line but having to dissipate this superheat (using heat exchangers) prior to re-entry into the equilibrium chamber to prevent non-equilibrium vapourization of the liquid phase.

(f) For *studies at or near the critical region*, the two factors in **(d)** and **(e)** severely compromise the suitability of the method for this type of application as very small fluctuations in pressure and temperature are intolerable, as this leads to changes in the phase behaviour.

A.2.3.4 Phase Recirculation equipment in the literature

The popularity of phase recirculation methods has increased due to the commercial availability of magnetically-driven pumps, which have better performance characteristics and also allow for the complexity of the phase recirculation loops to be somewhat reduced. This is coupled with an increasing interest in VLE studies at cryogenic conditions in the form of studies on fluorinated hydrocarbons, for which vapour-phase recirculation equipment has found great applicability.

Selections of the successful or significant designs of single-phase recirculation and two-phase recirculation equipment have been extracted from literature and are presented separately in Tables A.6 and A.7, respectively. The same conventions as for Tables (A.1) - (A.5) apply here, where applicable.

A short summary is provided for a description of the distinctive and most notable features of the equipment designs as follows:

Single-Phase Recirculation equipment (Table A.6)

(a) The noticeable *absence of liquid phase recirculation equipment*, with only two researchers in the form of Kim *et al.* (1986) and Walther *et al.* (1992) being selected from the literature sources and being listed. This attests to the relative ease of designing equipment around the principle of the vapour phase as the recirculated phase relative to liquid recirculation designs.

(b) The first significant feature of the various designs of equipment presented in Table A.6 is the difference in the *sampling strategies that were employed by the various researchers* to obtain representative vapour and liquid equilibrium samples. In the vapour recirculation design of Fredenslund *et al.* (1973), a unique liquid sampling device was developed which served to inspire designs of a similar nature in the works of Meister (1985), Bae *et al.* (1981), Ng and Robinson (1978) and Muhlbauer (1990). The liquid sampling device of Fredenslund *et al.* (1973) consisted of a 5 mm 304 SS rod with a 3.5 μL hole drilled vertically through the rod near its tip. When the rod was inserted into the equilibrium cell, the vertical hole was completely immersed in the liquid phase. The motion of the rod was controlled by the action of a piston coupled to the rod. The withdrawal and analysis of the sample was achieved by the activation of the piston, which resulted in the withdrawal of the rod from the liquid phase into the equilibrium cell wall, which had sample ports drilled into it, through which a carefully controlled stream of helium gas flowed. In this position, the hole in the rod was directly aligned with the flow path of the gas stream, which was then transported by the carrier gas and flushed to the gas chromatograph for subsequent analysis.

The equipment of Tsang and Streett (1981) was an example of a design where the researcher chose to sample one the phases through the use of capillaries. The liquid phase was withdrawn directly from the equilibrium cell and the vapour phase was sampled from the top of the vapour recirculation pump. To prevent partial condensation, the sampling valves and the recirculating lines were heated with electrical tape. The liquid phase was then vapourized through throttling the phase through the sampling valve and was then introduced into a GC sampling valve, from where it could be analysed.

Table A.6. Selection of Single-Phase Recirculation equipment in the literature.

Author	Cell Volume (cm^3)	Cell [a]	Operating Range		Measurement Device		Equilibr. Time	Sample Size	
			Temp (K)	Press (bar)	Temp [b]	Press [c]	(min)	Vap. (µl)	Liq. (µl)
Vapour Recirculation									
Aroyan (1951)	–	304 SS	143 - 298	550	TC	B	120	500 000	500 000
Williams (1954)	–	304 SS	200 [d]	550	TC	B	–	–	–
Streett (1965)	–	–	15 [d]	35	TC	–	–	–	–
Chang (1967)	100	SS	122 - 172	52	TC	B	120	–	–
Fredenslund (1973)	–	304 SS & Quartz	97 - 298	350	PRT	DWP	180	–	3.5
Nasir (1980/81)	250 (VV)	SS	423 - 623	275	TC	PT	–	–	2000
Tsang (1981)	10	–	273 - 523	2000	PRT	–	5 - 10	–	–
Dorau (1983)	168	SS	70 - 298	200	PRT	B	–	–	–
Pozo De Fernandez (1984)	–	Pyrex Tubing	323 - 523	80	PRT	–	10 - 15	–	–
	–	SS & Sappire	323 - 523	290	PRT	–	10 - 15	–	–
	–	SS	323 - 523	510	PRT	–	10 - 15	–	–

[a] SS = Stainless Steel.
[b] TC = Thermocouple; PRT = Platinum Resistance Thermometer; TS = Thermistor; QT = Quartz Thermometer.
[c] B = Bourdon Gauge; PT = Pressure Transducer; DWP = Dead Weight Piston Gauge; PRSPG = Precision Resistance Pressure Strain Gauge.
[d] Minimum operating temperature for cryogenic studies.
[e] Maximum operating conditions in the experimental studies.

Table A.6. Selection of Single-Phase Recirculation equipment in the literature (cont).

Author	Cell Volume (cm^3)	Cell [a]	Operating Range		Measurement Device		Equilibr. Time	Sample Size	
			Temp (K)	Press (bar)	Temp [b]	Press [c]	(min)	Vap. (µl)	Liq. (µl)
Vapour Recirculation									
Weber (1984)	230	SS & Glass	223 - 300	180	PRT	B	–	–	–
Meister (1985)	50	SS & Glass	70 - 290	350	PRT	DWP	–	–	–
	–	SS & Glass	295- 470	400	PRT	DWP	–	–	–
Freitag (1986)	100	H C276 & Glass	258 - 373	276	TC	B	30	–	–
Chou (1990)	100	–	343 - 388	245	TC	B	60	30	30
Jin (1993)	–	–	123 [d]	29	TC	–	–	–	–
Bobbo (1998a)	–	306 SS & Glass	240 - 350	100	PRT	B	–	–	–
Liquid Recirculation									
Kim (1986)	100	316 SS & Glass	423	137	TC	PT	10	25	0.5
Walther (1992)	37.5	Glass windows	300 - 420	300	PRT	B	–	–	–

[a] SS = Stainless Steel; H C276 = Hastelloy C-276.
[b] TC = Thermocouple; PRT = Platinum Resistance Thermometer; TS = Thermistor; QT = Quartz Thermometer.
[c] B = Bourdon Gauge; PT = Pressure Transducer; DWP = Dead Weight Piston Gauge; PRSPG = Precision Resistance Pressure Strain Gauge.
[d] Minimum operating temperature for cryogenic studies.
[e] Maximum operating conditions in the experimental studies.

Table A.7. Selection of Two-Phase Recirculation equipment in the literature.

Author	Cell Volume (cm^3)	Cell [a]	Operating Range		Measurement Device		Equilibr. Time	Sample Size	
			Temp (K)	Press (bar)	Temp [b]	Press [c]	(min)	Vap. (µl)	Liq. (µl)
Muirbrook (1965)	200	403 SS	233 - 303	1250	TC	B	–	–	–
Behrens (1983)	1000	–	283 - 373	>70	PRT	PT	240-480	2000	2000
King (1983)	300	SS	773	500	TS	B	–	11 500	34 700
Kubota (1983)	106	304 SS	283 - 353	800	–	B	120	–	–
Radosz (1984)	60	–	283 - 533	350	PRT	PT	15	100	100
Morris (1985)	100	–	311 - 588	147	TC	PT	10-15	20 - 250	0.5
Yorizane (1985)	150	304 SS	263 - 298	>80	–	B	–	–	–
Takishima (1986)	700	–	308	>100	QT	B	60	–	–
D'Souza (1988)	100	SS	318 - 353	170	PRT	–	60	300/10 000	300/10 000
Inomata (1988)	750	316 SS	313 - 413	60	TC	PT	–	–	–
Adams (1988)	1000	Sapphire	300 - 400 [d]	14 - 129 [d]	–	–	5-10	455	1.8
Jennings 1989)	40	SS	308 - 333 [d]	16 - 94 [d]	TS	–	–	1	0.2

[a] SS = Stainless Steel .

[b] TC = Thermocouple; PRT = Platinum Resistance Thermometer; TS = Thermistor; QT = Quartz Thermometer.

[c] B = Bourdon Gauge; PT = Pressure Transducer; DWP = Dead Weight Piston Gauge; PRSPG = Precision Resistance Pressure Strain Gauge.

[d] Maximum operating conditions in the experimental studies.

Table A.7. Selection of Two-Phase Recirculation equipment in the literature (cont).

Author[a]	Cell Volume (cm^3)	Cell [b]	Operating Range		Measurement Device		Equilibr. Time	Sample Size	
			Temp (K)	Press (bar)	Temp [c]	Press [d]	(min)	Vap. (µl)	Liq. (µl)
Weber (1989)	65	300 SS	300 - 670	190	PRT	B	480	20	1
Kim (1989)	150	316 SS & Glass	430 [d]	250 [d]	PRT	PT	10	100	1
Shibata (1989)	100	–	423	345	TC	DWP	30 - 45	–	–
Fink (1990)	80	H C276	308 - 353 [d]	8 - 112 [d]	TC	PT	–	–	–
Suzuki (1990)	–	–	453	250	TC	B	–	10 000	750
Park (1991)	50	316 SS	420	680	TC	–	10	20	1

[a] SS = Stainless Steel; H C276 = Hastelloy C-276.

[b] TC = Thermocouple; PRT = Platinum Resistance Thermometer; TS = Thermistor; QT = Quartz Thermometer.

[c] B = Bourdon Gauge; PT = Pressure Transducer; DWP = Dead Weight Piston Gauge; PRSPG = Precision Resistance Pressure Strain Gauge.

[d] Maximum operating conditions in the experimental studies.

The apparatus of Dorau *et al.* (1983) featured the direct sampling of both the vapour and liquid samples from the equilibrium chamber through the use of capillary tubes. The samples were extracted from the equilibrium chamber into evacuated flasks, which were connected to the capillaries via rapid connection coupling fittings. To ensure that the liquid samples were indeed representative of the equilibrium composition, the volume of the flasks used had to be greater than that of the volume of the capillary lines.

Pozo De Fernandes and Street (1984) later discovered that the previous design of Tsang and Streett (1981) was flawed in that simply heating the sampling valve could not eliminate the cooling effect and subsequent partial condensation of the less volatile liquid components as it was throttled to a low-pressure state. Consequently, the low-pressure sampling cell, together with the sampling valves had to be temperature-controlled in a separate chamber at a suitable temperature higher than that of the equilibrium cell.

Weber *et al.* (1984) experienced similar difficulties as Tsang and Streett (1981) in attempting to ensure that representative liquid phase samples were flushed to the GC for analysis. To this end, the capillary tubing and the valves had to be heated to ensure a complete sample vapourization. The vapour phase was collected in an evacuated 2 litre SS vessel, where it was maintained at below its dew point pressure at ambient conditions.

Freitag and Robinson (1986) used needle valves, which were similar in design to those used by Kalra and Robinson (1975) in their static analytic apparatus. The liquid sample was extracted directly from the equilibrium cell and the vapour sample was obtained from the recirculation line, upstream of the pump. Sampling of the liquid phase was achieved through the use of a 90 cm long capillary tube (with a 0.23 mm internal diameter), where the liquid sampling valve was located at the end of the tube and the front tip of the tube protruded into the bottom of the equilibrium cell. A strategy to minimize dead volume in the capillary tube was employed by the researchers in the form of a 0.15 mm diameter wire being inserted into the tube. The researchers asserted that this arrangement allowed for the optimal acquisition of representative low-pressure vapour samples from the high-pressure liquid phase withdrawn from the equilibrium cell. This was achieved through the sample in its entirety being obtained as it flashed through the capillary and the needle valve. This low-pressure state sample was then circulated to ensure that it was indeed uniform prior to its analysis by gas chromatography.

In the liquid phase recirculation design of Kim *et al.* (1986), the sampling valves were used to directly inject samples of the phases into a gas chromatograph.

The experimental apparatus of Chou *et al.* (1990) was another example of an apparatus that had featured sampling of the vapour and liquid phases directly from the equilibrium cell through the use of appropriate sampling devices. The equilibrium cell contained separate connections for the sampling ports of each phase and each port had specially designed sampling micro-cells with internal volumes of 30 μL, similar to those of Legret *et al.* (1981). After the collection of a sample of the appropriate phase, the micro-cells were detached from the ports and attached to a sample analysis system (a temperature-controlled micro-cell oven and a gas chromatograph). The micro-cell was attached to a variable-volume bellows in the assembly, which served as both a flash vessel and a pump to ensure the recirculation of the flashed sample through the gas chromatograph sample valve until it was homogenous and ready for analysis.

(c) The *pressure and temperature ranges* of the equipment listed in Table A.6 vary widely from one researcher to the next *i.e.* 93 K - 298 K for Fredenslund *et al.* (1983) as opposed to 273 K - 523 K for Tsang and Streett (1981). This demonstrates the wide applicability of this method over wide pressure and temperature ranges. However, it can be observed from Table 2.6 that the method of vapour phase recirculation has almost exclusively found application at subzero temperatures. Various strategies were employed by researchers to attain low temperatures in their equipment.

The cooling system of Fredenslund *et al.* (1973) consisted of a thermostat with liquid nitrogen as the coolant fluid. The liquid nitrogen was dispensed from a glass Dewar (as an intermediate storage vessel) to a vapourizer in the thermostat, where the use of a fan ensured that the vapourized liquid nitrogen blew over an electric heater connected to a temperature controller. The nitrogen (now at the desired temperature) then flowed around the equilibrium cell and the 'spent nitrogen' was then passed through a series of concentric annular spaces to serve as thermal insulation for the equilibrium cell after it had been used as a temperature-regulating fluid medium. The control of temperature achievable with this setup was ± 0.01 K.

(d) A favoured *material of construction* as for the static analytic method (see Section A.1) was stainless steel (various grades). High-pressure glass and sapphire viewing windows were also incorporated into the designs of some of the researchers such as Pozo De Fernandez *et al.* (1984) and Weber *et al.* (1984), respectively, to enable visual observation of the contents of the equilibrium cell.

Two-Phase Recirculation equipment (Table A.7)

(a) The *recirculation of the phases* by various means is an interesting feature of the equipment. In one of the earliest designs, that of Muirbrook *et al.* (1965), the phases were recirculated in external loops through the action of specially-constructed vane pumps.
The equipment of Behrens *et al. (1983)* featured phase recirculation with magnetically-driven double-acting pumps, which were designed and constructed by the experimenters.
A novel feature in the recirculation of phases was the provision for choosing the phase to be recirculated, which was incorporated in the equipment design of Kubota *et al.* (1983). This provision was incorporated in the form of a six-port valve, which in the appropriate position, allowed a single high-pressure pump to recirculate the phase of choice. The latter operational principle of Kubota and co-workers inspired the later designs of Wu *et al.* (1988) and Hsu *et al.* (1985).

(b) To improve the approach to equilibrium *i.e.* for a more rapid approach, some researchers have incorporated an *additional means for achieving phase agitation* in the equilibrium cell.
The equilibrium cell of Behrens *et al.* (1983) contained a magnetically coupled internal stirrer, which was driven by an external motor indirect drive system.
Similarly, the designs of Kubota *et al.* (1983), King *et al.* (1983), Takishima *et al.* (1986), Inomata *et al.* (1988) and Suzuki *et al.* (1990) also featured internal stirring.

A unique experimental apparatus was developed by Yorizane *et al.* (1985) which contained two equilibrium cells. The two cells (each with internal volumes of 150 cm^3) were connected to each other at their top and bottom ends by means of flexible stainless steel tubing. The purpose of this design was to achieve agitation of the phases by maintaining one cell in a fixed position whilst the other was lifted and raised by a mechanical device. This motion resulted in a flow of liquid as a function of the relative position of the two cells and a subsequent reverse movement of the vapour phase to equalize the pressure in the other cell. This perturbation of the system resulted in good contacting of the phases.

(c) As with single-phase apparatus, mention has to be made with regards to the sampling strategies of the various researchers. Behrens *et al.* (1983) withdrew phase samples directly from the equilibrium chamber with capillaries and asserted that this method proved more successful than in-line sampling bombs and multiple port gas chromatographic sampling valves in the recirculation lines. During sampling, the recirculation pumps were turned off to avoid pressure disturbances.

Kubota *et al.* (1983) designed an apparatus such that the analysis system was at a low pressure *i.e.* a pressure reduction was necessary from the high-pressure equilibrium section. A sample of the recirculating phase was trapped in a four-port (two-way) valve, from where it could then be transferred to a low-pressure analysis system.

Radosz (1984, 1986) employed the use of a variable-volume cylinder in the recirculation loop of the top phase so that no pressure disturbance was experienced during the sampling process. The phase samples were taken directly from the equilibrium chamber via capillaries. The liquid samples were then vapourized and homogenized in a 100 cm^3 chamber located downstream of the sampling valves.

The equipment of Yorizane *et al.* (1985) had sampling sections between the tubes connecting the two cells (each with three valves). Two of the three valves were used to isolate the sample and the third, a three-way valve between the other two, was used to transfer the sample to the sample chamber, into which it was expanded at a low pressure.

APPENDIX B

THERMODYNAMICS FUNDAMENTALS

B.1 Correlations for second virial coefficients

B.1.1 Correlations based on the Pitzer-Curl Relation

The correlation developed by Pitzer and Curl for nonpolar gases is based on the following form:

$$\frac{BP_c}{RT_c} = B^{(0)} + \omega B^{(1)} \tag{3.75}$$

The $B^{(0)}$ and $B^{(1)}$ terms that have been proposed in several correlations are as follows:

(a) Pitzer and Curl (1957)

$$B^{(0)} = 0.1445 - \frac{0.33}{T_r} - \frac{0.1385}{T_r^2} - \frac{0.0121}{T_r^3} \tag{B.1}$$

$$B^{(1)} = 0.073 + \frac{0.46}{T_r} - \frac{0.5}{T_r^2} - \frac{0.097}{T_r^3} - \frac{0.0073}{T_r^8} \tag{B.2}$$

(b) Abbott (1975)

$$B^{(0)} = 0.083 - \frac{0.422}{T_r^{1.6}} \tag{B.3}$$

$$B^{(1)} = 0.139 - \frac{0.172}{T_r^{4.2}} \tag{B.4}$$

(c) Tsonopoulos (1974)

$$B^{(0)} = 0.1445 - \frac{0.33}{T_r} - \frac{0.1385}{T_r^2} - \frac{0.0121}{T_r^3} - \frac{0.000607}{T_r^8} \tag{B.5}$$

$$B^{(1)} = 0.0637 + \frac{0.331}{T_r^2} - \frac{0.423}{T_r^3} - \frac{0.008}{T_r^8} \tag{B.6}$$

The use of the generalized Pitzer-Curl correlation and related forms for the evaluation of the cross virial coefficients for mixtures can be obtained through the use of the following relation:

$$\frac{BP_{cij}}{RT_{cij}} = B_{ij}^0 + \omega B_{ij}^0 \tag{B.7}$$

where P_{cij} and T_{cij} are the cross pseudo-critical properties. These can be evaluated as follows:

$$T_{cij} = \left(T_{c,i} + T_{c,j}\right)^{0.5}\left(1 - k_{ij}\right) \tag{B.8}$$

$$V_{cij} = \left[\frac{V_{c,i}^{1/3} + V_{c,j}^{1/3}}{2}\right]^3 \tag{B.9}$$

$$Z_{cij} = \left(\frac{Z_{c,i} + Z_{c,j}}{2}\right) \tag{B.10}$$

$$\omega_{cij} = \left(\frac{\omega_{c,i} + \omega_{c,j}}{2}\right) \tag{B.11}$$

$$P_{cij} = \frac{RZ_{cij}T_{cij}}{V_{cij}} \tag{B.12}$$

For Equations (B.8) - (B.12), the terms T_{cij} , V_{cij}, Z_{cij}, ω_{cij}, P_{cij} are the cross pseudo-critical temperature, volume, compressibility correction factor, acentric factor and pressure, respectively.

The quantity k_{ij} is a binary interaction parameter, which can be estimated or obtained from various literature sources (Reid *et al.*, 1987).

The Pitzer-Tsonopoulos correlation (1974) was based on an extension of the original Pitzer-Curl approach as follows:

$$\frac{BP_c}{RT_c} = B^{(0)} + \omega B^{(1)} + B^{(2)} \tag{3.76}$$

where the $B^{(0)}$ and $B^{(1)}$ terms are unchanged as have been presented in Equations (B.5) and (B.6).

For non-hydrogen bonding polar compounds, Tsonopoulos proposed the following term:

$$B^{(2)} = \frac{a}{T_r^6} \tag{B.13}$$

where a is an empirical parameter with negative values to account for the experimental observations that polar compounds have more negative virial coefficients than their homomorphs (nonpolar equivalents in terms of similar molecular structure) for the same value of ω and T_r.

For hydrogen-bonding compounds, $B^{(2)}$ now consists of two terms that are added:

$$B^{(2)} = \frac{a}{T_r^6} - \frac{b}{T_r^8} \tag{B.14}$$

where a and b are empirical parameters with positive values.

Cross virial coefficients are evaluated in the same manner, as described in Equation (B.7), and for polar + polar binary mixtures, the mixing rules for a and b are as follows;

$$a_{ij} = \left(\frac{a_i + a_j}{2}\right) \tag{B.15}$$

$$b_{ij} = \left(\frac{b_i + b_j}{2}\right) \tag{B.16}$$

B.1.2 Correlations based on an Extended Corresponding States Method

The correlation of Tarakad and Danner (1977) consisted of the following form:

$$\frac{BP_c}{RT_c} = B^{(0)}_{\text{simple fluid}} + B^{(0)}_{\text{size-shape}} + B^{(0)}_{\text{polar correction}} \tag{3.77}$$

where

$$B^{(0)}_{\text{simple fluid}} = 0.1445 + \frac{0.330}{T_r} - \frac{0.1385}{T_r^2} - \frac{0.0121}{T_r^3} - \frac{0.000607}{T_r^8} \tag{B.17}$$

$$B^{(0)}_{\text{size-shape}} = \left(-0.00787 + \frac{0.0812}{T_r^2} - \frac{0.0646}{T_r^3}\right)\overline{R} - \left(\frac{0.0347}{T_r^2} - \frac{0.000149}{T_r^7}\right)\overline{R}^2 \tag{B.18}$$

$$B^{(0)}_{\text{polarity effect}} = -\left(\frac{0.028}{T_r^7}\right)\Phi_i \tag{B.19}$$

For mixtures, the following mixing rules apply:

$$\overline{R}_{cij} = \left(\frac{\overline{R}_{ci} + \overline{R}_{cj}}{2}\right) \tag{B.20}$$

$$P_{cij} = \frac{4T_{cij}\left(\frac{P_{ci}V_{ci}}{T_{ci}} + \frac{P_{cj}V_{cj}}{T_{cj}}\right)}{\left(V_{ci}^{1/3} + V_{cj}^{1/3}\right)^3} \tag{B.21}$$

$$\Phi_{cij} = \left(\frac{\Phi_{ci} + \Phi_{cj}}{2}\right) \tag{B.22}$$

B.1.3 Correlations based on a Statistical Mechanical-Extended Corresponding States Method

In the method of Hayden and O'Connell (1975), the pure component and cross virial coefficients are provided as the sum of two principal contributions:

$$B_{ij} = B_{ij}^{F} + B_{ij}^{D} \tag{3.78}$$

The terms in Equation (3.78) are equivalent to the following:

$$B_{ij}^{F} = \left(B_{non-polar}^{F}\right)_{ij} + \left(B_{polar}^{F}\right)_{ij} \tag{3.79}$$

$$B_{ij}^{D} = \left(B_{bound}^{D}\right)_{ij} + \left(B_{metastable}^{D}\right)_{ij} + \left(B_{chemical}^{D}\right)_{ij} \tag{3.80}$$

The superscript "F" refers to the molecular interactions from the weak physical forces *i.e.* between relatively "free" molecules and the superscript "D" refers to interactions due to the strong chemical forces between molecules *i.e.* "bound" or "dimerized" molecules.

The individual contributions to the second virial coefficients can be obtained from the temperature-dependent correlations shown below:

$$\left(B_{nonpolar}^{F}\right)_{ij} = b_{0ij}\left[0.94 - \frac{1.47}{\left(T_{ij}^{*'}\right)} - \frac{0.85}{\left(T_{ij}^{*'}\right)^{2}} - \frac{1.015}{\left(T_{ij}^{*'}\right)^{3}}\right] \tag{B.23}$$

$$\left(B_{polar}^{F}\right)_{ij} = -b_{0ij}\mu_{ij}^{*'}\left[0.74 - \frac{3.0}{\left(T_{ij}^{*'}\right)} + \frac{2.1}{\left(T_{ij}^{*'}\right)^{2}} - \frac{2.1}{\left(T_{ij}^{*'}\right)^{3}}\right] \tag{B.24}$$

$$\left(B_{metastable}\right)_{ij} + \left(B_{bound}\right)_{ij} = b_{0ij}A_{ij}\exp\left(\frac{\Delta h_{ij}}{T_{ij}^{*}}\right) \tag{B.25}$$

$$\left(B_{chemical}\right)_{ij} = b_{0ij}E_{ij}^{'}\left[1 - \exp\left(\frac{1500\,n_{ij}}{T}\right)\right] \tag{B.26}$$

$$\frac{1}{T_{ij}^{*'}} = \frac{1}{T_{ij}^{*}} - 1.6\,\omega_{ij} \tag{B.27}$$

$$T_{ij}^{*} = \frac{T}{\left(\frac{\varepsilon_{ij}}{k}\right)} \tag{B.28}$$

The temperature-independent parameters used in Equations (B.23) - (B.28) are as follows:

$$b_{oij} = 1.26184\,\sigma_{ij}^{3} \tag{B.29}$$

$$\begin{aligned} \mu_{ij}^{*'} &= \mu_{ij}^{*} && \mu_{ij}^{*} < 0.04 \\ &= 0 && 0.04 < \mu_{ij}^{*} < 0.25 \\ &= \mu_{ij}^{*} - 0.25 && \mu_{ij}^{*} \geq 0.25 \end{aligned} \tag{B.30}$$

$$A_{ij} = -0.3 - 0.05\,\mu_{ij}^{*} \tag{B.31}$$

$$\Delta h_{ij} = 1.99 + 0.2\left(\mu_{ij}^{*}\right)^{2} \tag{B.32}$$

$$\mu_{ij}^{*} = \frac{7243.8\mu_i\,\mu_j}{\left(\frac{\varepsilon_{ij}}{k}\right)\sigma_{ij}} \tag{B.33}$$

$$E_{ij} = \exp\left[\eta_{ij}\left(\frac{650}{\left(\frac{\varepsilon_{ij}}{k}\right)+300} - 4.27\right)\right] \qquad \text{for } \eta_{ij} < 4.5 \tag{B.34}$$

or

$$E_{ij} = \exp\left[\eta_{ij}\left(\frac{42800}{\left(\frac{\varepsilon_{ij}}{k}\right)+22400} - 4.27\right)\right] \qquad \text{for } \eta_{ij} \geq 4.5 \qquad (B.35)$$

where T is the temperature (K), $\left(\frac{\varepsilon_{ij}}{k}\right)$ is the characteristic energy for the i-j interaction (K), σ_{ij} is the molecular size ($\mathring{A}$), μ_i is the dipole moment of component i (Debye), η_{ij} is the association parameter $(i = j)$ or solvation parameter $(i \neq j)$ and ω_{ij} is the nonpolar acentric factor.

For $i = j$, the parameters $\left(\frac{\varepsilon_{ii}}{k}\right)$, σ_{ii} and ω_{ii} can be obtained from pure component properties as follows:

$$\omega_{ii} = 0.006026\,R_{D,i} + 0.02096\,R_{D,i}^2 - 0.001366\,R_{D,i}^3 \qquad (B.36)$$

$$\left(\frac{\varepsilon_{ij}}{k}\right) = \left(\frac{\varepsilon_{ij}}{k}\right)'\left[1 - \xi c_1\left(1 - \frac{\xi(1+c_1)}{2}\right)\right] \qquad (B.37)$$

$$\sigma_{ij} = \sigma_{ii}'\,(1+\xi c_2)^{\frac{1}{3}} \qquad (B.38)$$

where

$$\left(\frac{\varepsilon_{ii}}{k}\right)' = T_{c,i}\left(0.748 + 0.91\,\omega_{ii} - \frac{0.4\,\eta_{ii}}{2+20\,\omega_{ii}}\right) \qquad (B.39)$$

$$\sigma_{ii}' = (2.44 - \omega_{ii})\left(1.0133\frac{T_{c,i}}{P_{c,i}}\right) \qquad (B.40)$$

$$\xi = 0 \quad \text{for } \mu_i < 1.45 \qquad (B.41)$$

or

$$\xi = \frac{1.7941 \times 10^{7} \mu_i^4}{\left[\left(2.882 - \frac{1.882\,\omega_{ii}}{0.03 + \omega_{ii}}\right) T_{ci} \left(\sigma_{ii}^{'}\right)^6 \left(\frac{\varepsilon_{ii}}{k}\right)^{'}\right]} \quad \text{for } \mu_i \geq 1.45 \qquad \text{(B.42)}$$

$$c_1 = \frac{16 + 400\,\omega_{ii}}{10 + 400\,\omega_{ii}} \qquad \text{(B.43)}$$

$$c_2 = \frac{3}{10 + 400\,\omega_{ii}} \qquad \text{(B.44)}$$

The pure component (i) properties that are required for Equations (B.36) - (B.44) are $T_{c,i}$, the critical temperature (K); $P_{c,i}$, the critical pressure and $R_{D,i}$, the mean radius of gyration ($\mathring{A}$).

The cross parameters $\left(\frac{\varepsilon_{ij}}{k}\right)$, $\sigma_{ij}^{'}$ and $\omega_{ij}\,(i \neq j)$ are calculated from mixing rules and pure component parameters as follows:

$$\omega_{ij} = \frac{1}{2}\left(\omega_{ii} + \omega_{jj}\right) \qquad \text{(B.45)}$$

$$\left(\frac{\varepsilon_{ij}}{k}\right)^{'} = \left(\frac{\varepsilon_{ij}}{k}\right)^{'} \left(1 + \xi^{'} c_1^{'}\right) \qquad \text{(B.46)}$$

$$\sigma_{ij} = \sigma_{ij}^{'} \left(1 - \xi^{'} c_2^{'}\right) \qquad \text{(B.47)}$$

For Equation (B.46):

$$\left(\frac{\varepsilon_{ij}}{k}\right)^{'} = 0.7\left[\left(\frac{\varepsilon_{ii}}{k}\right)\left(\frac{\varepsilon_{jj}}{k}\right)\right]^{\frac{1}{2}} + 0.6\left[\left(\frac{\varepsilon_{ii}}{k}\right)^{-1}\left(\frac{\varepsilon_{jj}}{k}\right)^{-1}\right]^{-1} \qquad \text{(B.48)}$$

$$\sigma_{ij}^{'} = \left(\sigma_{ii}\,\sigma_{ij}\right)^{\frac{1}{2}} \qquad \text{(B.49)}$$

$$\xi' = \frac{(\mu_i)^2\left(\frac{\varepsilon_{jj}}{k}\right)^{\frac{2}{3}}(\sigma_{jj})^4}{\left(\frac{\varepsilon_{ij}}{k}\right)'(\sigma_{ij}')^6} \qquad \text{for } \mu_i \geq 2 \text{ and } \mu_j = 0 \quad \text{(B.50)}$$

or

$$\xi' = \frac{(\mu_j)^2\left(\frac{\varepsilon_{ii}}{k}\right)^{\frac{2}{3}}(\sigma_{ii})^4}{\left(\frac{\varepsilon_{ij}}{k}\right)'(\sigma_{ij}')^6} \qquad \text{for } \mu_j \geq 2 \text{ and } \mu_i = 0 \quad \text{(B.51)}$$

or

$$\xi' = 0 \qquad \text{for all other values of } \mu_j \text{ and } \mu_i \quad \text{(B.52)}$$

$$c_1' = \frac{16 + 400\,\omega_{ij}}{10 + 400\,\omega_{ij}} \quad \text{(B.53)}$$

$$c_2' = \frac{3}{10 + 400\,\omega_{ij}} \quad \text{(B.54)}$$

B.2 Excess thermodynamic functions

The fundamental excess property relation can be represented as follows:

$$d\left[\frac{G^E}{RT}\right] = -\left[\frac{H^E}{RT^2}\right]dT + \left[\frac{V^E}{RT}\right]dP + \sum_{i=1}^{n} \ln\gamma_i dx_i \quad \text{(3.81)}$$

where the terms in the above relation have been described in Chapter 3.

The temperature dependence of the excess Gibbs energy can be obtained from Equation (3.81) to yield the following form of the Gibbs-Helmholtz equation:

$$H^E = -RT^2\left[\frac{\partial\left(G^E/RT\right)}{\partial T}\right]_{P,x_i} \tag{B.55}$$

With the availability of VLE data at one or more temperatures *i.e.* isothermal data sets, the value for H^E can be obtained by graphical means. The data are first regressed with a suitable G^E correlation to allow for the values of $\left(\frac{G^E}{RT}\right)$ to be computed, which are plotted against T in a linear fashion to obtain the H^E values. Important considerations in the use of this method are the linearity of the plot and the temperature range over which the H^E value is obtained.

The excess entropy *i.e.* S^E can then be obtained from a simple substitution with the following:

$$G^E = H^E - TS^E \tag{B.56}$$

B.3 Liquid phase activity coefficient models

B.3.1 The Margules Equations

The original form of the Margules equations (1895) can be made equivalent to power series expansions of the activity coefficients for a binary mixture in composition as follows:

$$\ln\gamma_1 = \sum_{k=1}^{n}\alpha_k\, x_2^{\beta_k} \qquad (\beta_k > 1) \tag{B.57}$$

$$\ln\gamma_2 = \sum_{k=1}^{n}\alpha'_k\, x_1 \qquad (\beta_k > 1) \tag{B.58}$$

where α_k and α'_k are the empirical parameters.

By combining the above, a generalized form for the Margules equations in terms of an expansion of A, B, C and higher-order empirical terms can be obtained as shown in Equation (B.59).

$$\left(\frac{G^E}{RTx_1x_2}\right) = (A_{21}x_1 + A_{12}x_2) + x_1x_2(B_{21}x_1 + B_{12}x_2) + x_1^2x_2^2(C_{21}x_1 + C_{12}x_2) + \ldots \quad \text{(B.59)}$$

The activity coefficients for the general form of the Margules equation are the following:

$$\ln\gamma_1 = x_2^2\left[A_{12} + 2x_1(A_{21} - A_{12}) + x_1x_2\left[B_{12} + 2x_1(B_{21} - B_{12})\right] + x_1^2x_2^2\left[C_{12} + 2x_1(C_{21} - C_{12})\right]\right]$$

$$+ x_2^2x_1(x_2 - x_1)\left[(B_{21}x_1 + B_{12}x_2) + 2x_1x_2(C_{21}x_1 + C_{12}x_2)\right] \quad \text{(B.60)}$$

$$\ln\gamma_2 = x_1^2\left(A_{21} + 2x_2(A_{12} - A_{21}) + x_1x_2\left[B_{21} + 2x_2(B_{12} - B_{21})\right] + x_1^2x_2^2\left[C_{21} + 2x_2(C_{12} - C_{21})\right]\right)$$

$$+ x_1^2x_2(x_1 - x_2)\left[(B_{21}x_1 + B_{12}x_2) + 2x_1x_2(C_{21}x_1 + C_{12}x_2)\right] \quad \text{(B.61)}$$

From the above, it can be seen that the Margules equations can have any number of terms, which is dependent upon the truncation of the series expansion. If the number of the parameters desired is an odd number, then the truncated form of the infinite series is obtained by setting the parameters corresponding to (n) and $(n+1)$ as being equal and neglecting the higher-order coefficient terms.

The three-suffix form can be obtained by setting the B and C terms of Equation (B.59) equal to zero, obtaining the following:

$$\left(\frac{G^E}{RTx_1x_2}\right) = A_{21}x_1 + A_{12}x_2 \quad \text{(B.62)}$$

The four-suffix form is obtained by setting $B_{21} = B_{12} = B$ to obtain the following:

$$\left(\frac{G^E}{RTx_1x_2}\right) = A_{21}x_1 + A_{12}x_2 + Bx_1x_2 \quad \text{(B.63)}$$

B.3.2 The van Laar Equation

In the original formulation of the van Laar equation (1910, 1913), the adjustable parameters A'_{12} and A'_{21}, were related to the parameters of the van der Waals equation of state (a and b) through the following:

$$A'_{12} = \frac{b_1}{RT}\left(\frac{\sqrt{a_1}}{b_1} - \frac{\sqrt{a_2}}{b_2}\right)^2 \tag{B.64}$$

$$A'_{21} = \frac{b_2}{RT}\left(\frac{\sqrt{a_1}}{b_1} - \frac{\sqrt{a_2}}{b_2}\right)^2 \tag{B.65}$$

However, the formulation of the van Laar equation through the use of the van der Waals equation of state is not theoretically valid as the values of the parameters A'_{12} and A'_{21} do not correspond with the values that are obtained for the van der Waals parameters from theory *i.e.* the values for a and b:

$$a = \frac{27R^2T_c^2}{64P_c} \tag{B.66}$$

$$b = \frac{RT_c}{8P_c} \tag{B.67}$$

where

$$\frac{\sqrt{a}}{b} = 3\sqrt{3P_c} \tag{B.68}$$

From Equation (B.68), it can be inferred that for two components with approximately the same critical pressure, the terms A'_{12} and A'_{21} in Equations (B.64) and (B.65) are zero, hence $\left(\frac{G^E}{RTx_1x_2}\right)$ is zero *i.e.* an ideal mixture. Also, the degree of nonideality should increase as a function of the difference in critical pressure. The above two requirements for the van Laar equation based on the van der Waals equation of state are generally not true, resulting in Equations (B.64) and (B.65) not being valid. Consequently, the van Laar equation is not accorded the status of having a theoretical basis, despite the original derivation having proposed

the above relation between the van Laar parameters and those of the van der Waals equation of state.

B.3.3. The Wilson Equation

The local composition concept of Wilson (1964) can be represented as follows:

$$\frac{x_{ji}}{x_{ii}} = \frac{x_j \exp\left(-\frac{\lambda_{ji}}{RT}\right)}{x_i \exp\left(-\frac{\lambda_{ii}}{RT}\right)} \tag{3.118}$$

Applying the local composition concept to a binary mixture, the following equations are obtained:

$$\frac{x_{21}}{x_{11}} = \frac{x_2 \exp\left(-\frac{\lambda_{21}}{RT}\right)}{x_1 \exp\left(-\frac{\lambda_{11}}{RT}\right)} \tag{B.69}$$

$$\frac{x_{12}}{x_{22}} = \frac{x_1 \exp\left(-\frac{\lambda_{12}}{RT}\right)}{x_2 \exp\left(-\frac{\lambda_{22}}{RT}\right)} \tag{B.70}$$

Using the local composition concept, Wilson obtained the local volume fraction as the following for a binary mixture:

$$\xi_1 = \frac{x_{11} V_1}{x_{11} V_1 + x_{21} V_2} \tag{B.71}$$

$$\xi_2 = \frac{x_{22} V_2}{x_{22} V_2 + x_{12} V_1} \tag{B.72}$$

In Equations (B.71) and (B.72), ξ_1 is the local volume fraction of component 1 as the central molecule and ξ_2 is the local volume fraction of component 2 as the central molecule, respectively.

Wilson then modified the original athermal expression of Flory and Huggins for G^E :

$$\frac{G^E}{RT} = \sum_{i=1}^{n} x_i \frac{\varphi_i}{x_i} \tag{B.73}$$

where

$$\varphi_i = \frac{x_i V_i}{\sum_{i=1}^{n} x_j V_j} \tag{B.74}$$

In Equation (B.73), the first composition (x_i) represents the probability of an i molecule and the second term (φ_i) represents the probability of the interaction of an i molecule being with another i molecule.

Instead of using the average volume fraction (φ_i), Wilson used the local volume fraction to obtain the following expression:

$$\frac{G^E}{RT} = x_1 \frac{\xi_1}{x_1} + x_2 \frac{\xi_2}{x_2} \tag{B.75}$$

It can be seen from Equation (3.118) that if $\lambda_{ji} = \lambda_{ii}$, then the local volume fraction, shown in Equations (B.71) and (B.72), is simply equal to the average volume fraction expression of Flory and Huggins, alluding to the simplifications inherent in the theory of Flory and Huggins.

Substituting Equations (B.71) and (B.72) into (B.75) and defining the simplifying terms, Λ_{12} and Λ_{21}, yields the following:

$$\frac{G^E}{RT} = - x_1 \ln(x_1 + \Lambda_{12} x_2) - x_2 \ln(x_2 + \Lambda_{21} x_1) \tag{3.119}$$

B.3.4. The NRTL Equation

The NRTL model (1969) was based on the "local composition" concept of Wilson (1964) and the two-liquid theory of Scott (Hildebrand and Scott, 1964).

The local composition was defined for a binary mixture, in an analogous fashion to that of Wilson, as:

$$\frac{x_{21}}{x_{11}} = \frac{x_2 \exp\left(-\alpha_{12}\frac{g_{21}}{RT}\right)}{x_1 \exp\left(-\alpha_{12}\frac{g_{11}}{RT}\right)} \tag{B.76}$$

$$\frac{x_{12}}{x_{22}} = \frac{x_1 \exp\left(-\alpha_{12}\frac{g_{12}}{RT}\right)}{x_2 \exp\left(-\alpha_{12}\frac{g_{22}}{RT}\right)} \tag{B.77}$$

The next step in the development of the theory was the application of the two-liquid theory of Scott (1956), which postulated that for a binary mixture, the property of the mixture can be determined as the average of the properties of two imaginary fluid structures, known as molecular clusters or cells.

Each of these consist of molecules of either type 1 or type 2 as the central molecule and in each of these molecular cells, the central molecules are surrounded by molecules of these two types in proportions which are dependent upon the Gibbs energies of interaction (g_{ij}) between the central molecule (j) and surrounding molecules (i). In accordance with the two-liquid theory of Scott, the mixture property can be found as:

$$M = x_1 M^{(1)} + x_2 M^{(2)} \tag{B.78}$$

where $M^{(1)}$ and $M^{(2)}$ are the mixture properties for cells 1 and 2, respectively. The properties of the two mixtures are independent of one another.

Renon and Prausnitz applied the two-liquid theory for the calculation of the mixture residual Gibbs energy (G^R) through the use of the mixture excess Gibbs energy (G^E), as shown below:

$$G^E = G^R - x_1 G_1^R - x_2 G_2^R \tag{B.79}$$

where G_1^R and G_2^R are the residual Gibbs energies for the pure components.

From two-liquid theory:

$$G^R = x_1\left(G^R\right)^{(1)} + x_2\left(G^R\right)^{(2)} \tag{B.80}$$

The residual Gibbs energy of the two cells from the two-liquid theory can then be represented as:

$$\left(G^R\right)^{(1)} = x_{11}g_{11} + x_{21}g_{21} \tag{B.81}$$

$$\left(G^R\right)^{(2)} = x_{22}g_{22} + x_{12}g_{12} \tag{B.82}$$

where g_{11} and g_{22} are the Gibbs energies associated with the interactions of the pure substances in the imaginary liquid *i.e.* between like molecules and $g_{12} = g_{21}$ are the Gibbs energies associated with the interactions between unlike molecules in the imaginary fluids.

For the pure fluids, the residual Gibbs energy is equal to the Gibbs energy of the pure substances:

$$G_1^R = \left(G^R\right)^{(1)}_{pure} = g_{11} \tag{B.83}$$

$$G_2^R = \left(G^R\right)^{(2)}_{pure} = g_{22} \tag{B.84}$$

Substituting Equations (B.80) - (B.84) into (B.79), and using the relations shown below:

$$x_{11} + x_{21} = 1 \tag{B.85}$$

$$x_{12} + x_{22} = 1 \tag{B.86}$$

allows for the following expression for G^E to be obtained:

$$G^E = x_1x_{21}\left(g_{21} - g_{11}\right) + x_2x_{12}\left(g_{12} - g_{22}\right) \tag{B.87}$$

Substituting the expressions for the local mole fractions in Equations (B.76) and (B.77) into (B.87) and introducing simplifying terms, the final expression for the NRTL expression is obtained:

$$\frac{G^E}{RT} = x_1 x_2 \left[\frac{\tau_{21} G_{21}}{x_1 + G_{21} x_2} + \frac{\tau_{12} G_{12}}{x_2 + G_{12} x_1} \right] \tag{3.132}$$

B.4 Infinite dilution activity coefficients (γ_i^∞) from the extrapolation of VLE data

The work of Gatreaux and Coates (1955) related γ_i^∞ values to the partial derivative of pressure with respect to the liquid phase composition. The work of Pividal *et al.* (1992) modified the expression of Gatreaux and Coates for use at low pressures and moderate temperatures to obtain the following:

$$\gamma_i^\infty = \varepsilon_1^\infty \left(\frac{P_2^{sat}}{P_1^{sat}} \right) \left[1 + \left(\frac{1}{P_2^{sat}} \right) \left(\frac{\partial P}{\partial x_1} \right)_T^{x_1 = 0} \right] \tag{B.88}$$

$$\varepsilon_i^\infty = \exp \left[\frac{(B_{11} - V_1)(P_2^{sat} - P_1^{sat}) + \delta_{12} P_2^{sat}}{RT} \right] \tag{B.89}$$

$$\beta_2 = 1 + P_2^{sat} \left(\frac{B_{22} - V_2}{RT} \right) \tag{B.90}$$

$$\delta_{ij} = (2B_{12} - B_{11} - B_{22}) \tag{3.73}$$

In the above relations for components 1 and 2, the B_{11} and B_{22} terms are the pure component virial coefficients and B_{12} is the second virial cross coefficient. V_1 and V_2 are the saturated liquid molar volumes. Ultimately, the accuracy of the determined γ_i^∞ values depends upon the determination of the partial derivative in Equation (B.88) *i.e.* $\left(\frac{\partial P}{\partial x_1} \right)_T^{x_1 = 0}$. The method of Ellis and Jonah (1962) for the determination of the latter quantity was modified by Maher and Smith (1979a).

In accordance with the method of Maher and Smith (1979a), the P versus x_1 data are converted to deviation pressure (P_D) versus x_1 values through the following:

$$P_D = P - \left[P_2^{sat} + \left(P_1^{sat} - P_2^{sat}\right)x_1\right] \tag{B.91}$$

The above equation can be differentiated by taking the limit as $x_1 \to 0$ to obtain the following:

$$\left(\frac{P_D}{x_1 x_2}\right)_{x_1=0} = \left(\frac{\partial P}{\partial x_1}\right)_{x_1=0} - P_1^{sat} + P_2^{sat} \tag{B.92}$$

The term on the left-hand side of Equation (B.92) is obtained by extrapolating a linear plot of $\left(\frac{P}{x_1 x_2}\right)_{x_1=0}$ versus x_1 to $x_1 = 0$. In the event that the slope of this plot is not linear, it was suggested by Maher and Smith (1979a) that a plot of $\left(\frac{x_1 x_2}{P}\right)$ versus x_1 be used instead. With the evaluation of the partial derivative, the γ_1^{∞} values can be determined. The value of γ_2^{∞} is then determined in an analogous fashion.

B.5. Equations of State (EOS)

B.5.1 Benedict-Webb-Rubin-Starling (BWRS) EOS

The form of the BWRS equation can be represented as follows:

$$\begin{aligned} P = {} & RT\rho + \left(B_o RT - A_o - \frac{C_o}{T^2} + \frac{D_o}{T^3} - \frac{E_o}{T^4}\right)\rho^2 + \left(bRT - a - \frac{d}{T}\right)\rho^3 \\ & + \alpha\left(a + \frac{d}{T}\right)\rho^6 + \left(\frac{c}{T^2}\right)\rho^3\left(1 + \gamma\rho^2\right)\exp\left(-\gamma\rho^2\right) \end{aligned} \tag{B.93}$$

where ρ is the density. $A_o, B_o, C_o, D_o, E_o, a, b, c, d, \alpha$ and γ are the adjustable parameters.

To extend the BWRS EOS for the treatment of mixtures, mixing rules for the parameters are used as follows:

$$A_o = \sum_{i=1}^{n}\sum_{j=1}^{n} x_i x_j \left(1 - k_{ij}\right)\left(\sqrt{A_{oi} A_{oj}}\right) \tag{B.94}$$

$$B_o = \sum_{i=1}^{n} x_i B_{oi} \tag{B.95}$$

$$C_o = \sum_{i=1}^{n}\sum_{j=1}^{n} x_i x_j \left(1 - k_{ij}\right)\left(\sqrt[3]{C_{oi} C_{oj}}\right) \tag{B.96}$$

$$D_o = \sum_{i=1}^{n}\sum_{j=1}^{n} x_i x_j \left(1 - k_{ij}\right)\left(\sqrt[4]{D_{oi} D_{oj}}\right) \tag{B.97}$$

$$E_o = \sum_{i=1}^{n}\sum_{j=1}^{n} x_i x_j \left(1 - k_{ij}\right)\left(\sqrt[5]{E_{oi} E_{oj}}\right) \tag{B.98}$$

$$K = \left[\sum_{i=1}^{n} x_i \left(\sqrt[3]{K_i}\right)\right]^3 \quad \text{for} \quad K = a, b, c, d, \alpha \tag{B.99}$$

$$k_{ii} = 0 \tag{B.100}$$

B.6. Consistency Index for the Direct TC Test of Van Ness (1995)

Table B.1. Consistency Index for VLE data.

Index	RMSD for $\left(\ln\frac{\gamma_1}{\gamma_2}\right)$	
1	> 0	≤ 0.025
2	> 0.025	≤ 0.050
3	> 0.050	≤ 0.075
4	> 0.075	≤ 0.100
5	> 0.100	≤ 0.125
6	> 0.125	≤ 0.150
7	> 0.150	≤ 0.175
8	> 0.175	≤ 0.200
9	> 0.200	≤ 0.225
10	> 0.225	

The values range from 1 for highly consistent data to 10 for data of very poor quality.

APPENDIX C

C.1 Gas chromatograph operating conditions and detector calibrations

A Shimadzu GC-14 gas chromatograph unit, equipped with dual packed column injection ports and dual flame ionization detectors, was employed for all the qualitative chemical purity determinations and the quantitative sample analyses conducted in this study. A Porapak® Q column was employed for the 1-propanol + 2-butanol and cyclohexane + ethanol VLE investigations and a SE-30 column was used for the 1-propanol + n-dodecane and 2-butanol + n-dodecane determinations.

C.1.1 Operating conditions

The gas chromatograph operating conditions for the cyclohexane + ethanol (1), 1-propanol + 2-butanol (2), 1-propanol + n-dodecane (3) and 2-butanol + n-dodecane (4) systems are presented in Table C.1.

Table C.1. Gas chromatograph operating conditions for the systems studied.

Operating conditions	(1)	(2)	(3)	(4)
Carrier gas	Helium	Helium	Helium	Helium
Carrier gas flow ($ml.min^{-1}$)	30	30	30	30
Temperature control mode	Isothermal	Isothermal	Isothermal	Isothermal
Injector temperature (°C)	150	220	220	220
Column temperature (°C)	230	180	180	180
Detector temperature (°C)	250	250	250	250
Experimental run times (min)	10	5	5	5

C.1.2 Detector calibrations

The flame ionization detector was calibrated for all the systems through the use of the area ratio method of Raal and Muhlbauer (1998). The necessary plots for this calibration procedure, as was described in Chapter 6, are shown in Figures (C.1)-(C.8) for the systems studied.

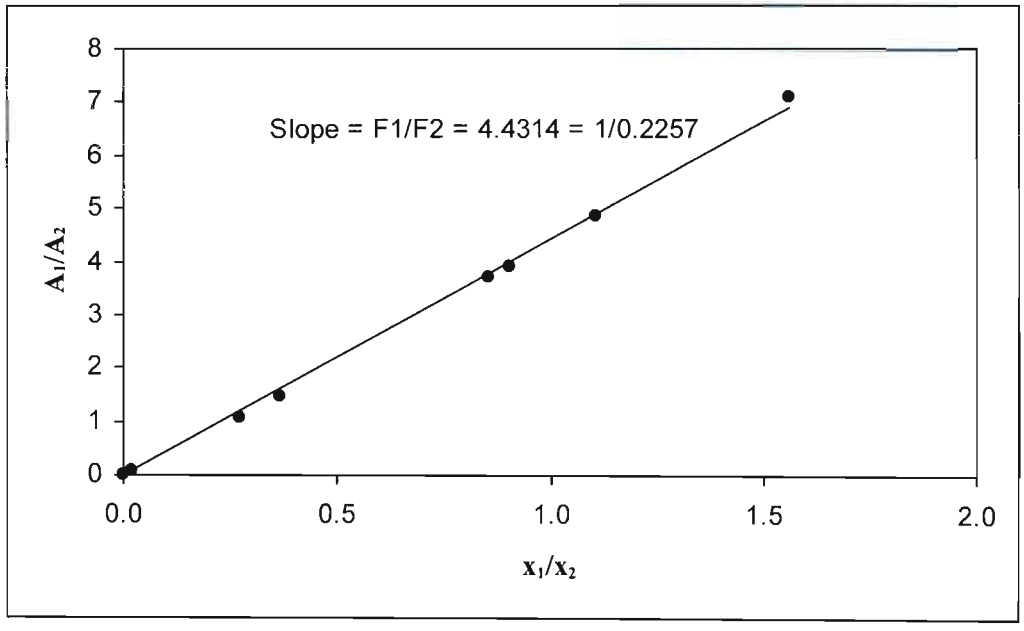

Figure C.1. A_1/A_2 versus x_1/x_2 for the cyclohexane (1) + ethanol (2) system.

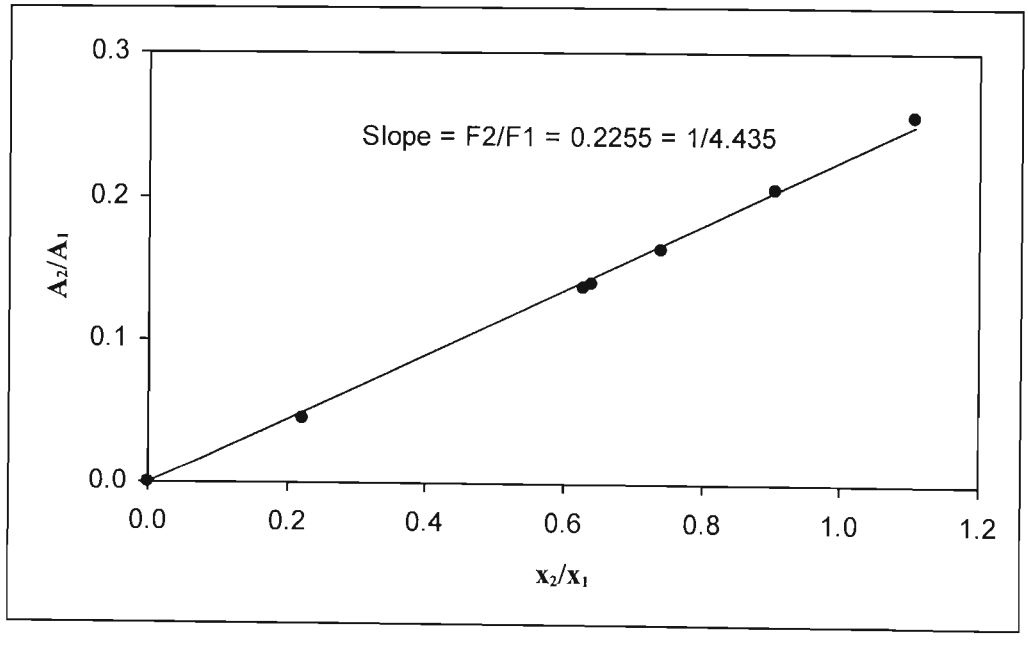

Figure C.2. A_2/A_1 versus x_2/x_1 for the cyclohexane (1) + ethanol (2) system.

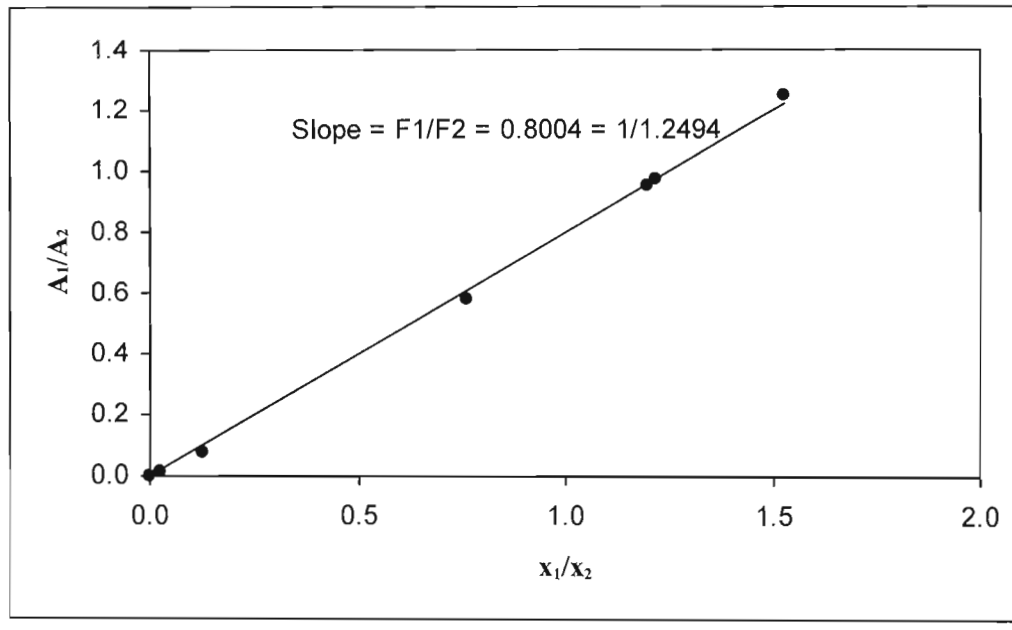

Figure C.3. A_1/A_2 versus x_1/x_2 for the 1-propanol (1) + 2-butanol (2) system.

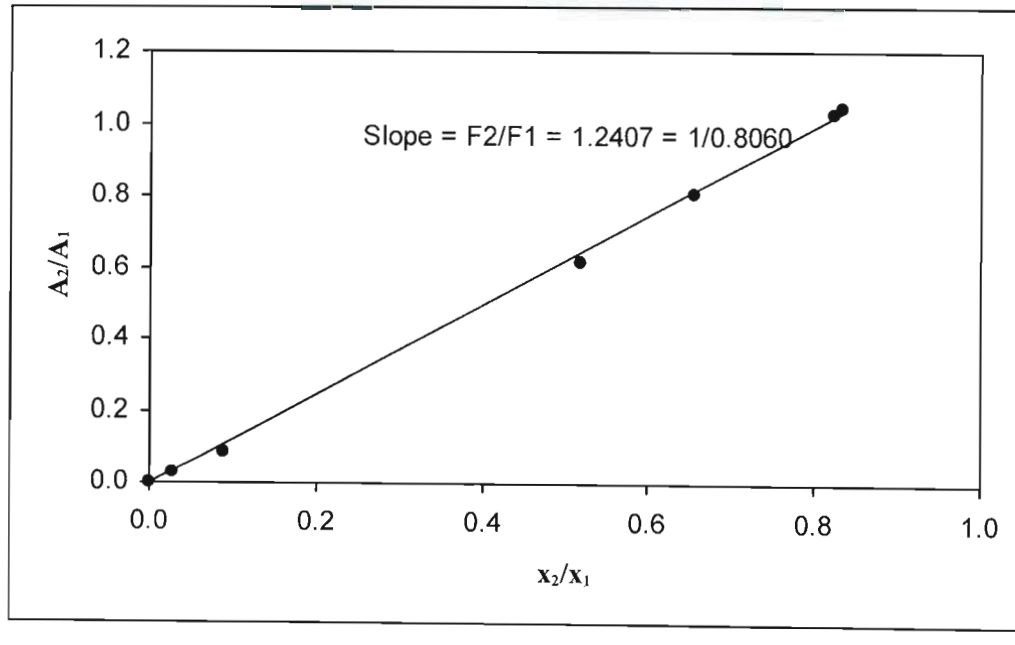

Figure C.4. A_2/A_1 versus x_2/x_1 for the 1-propanol (1) + 2-butanol (2) system.

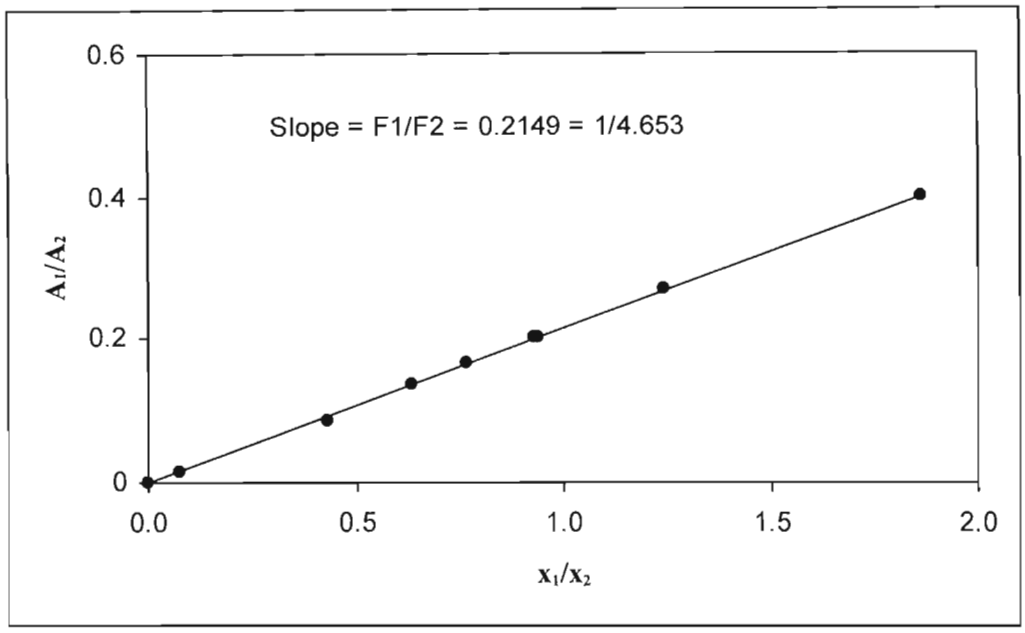

Figure C.5. A_1/A_2 versus x_1/x_2 for the 1-propanol (1) + n-dodecane (2) system.

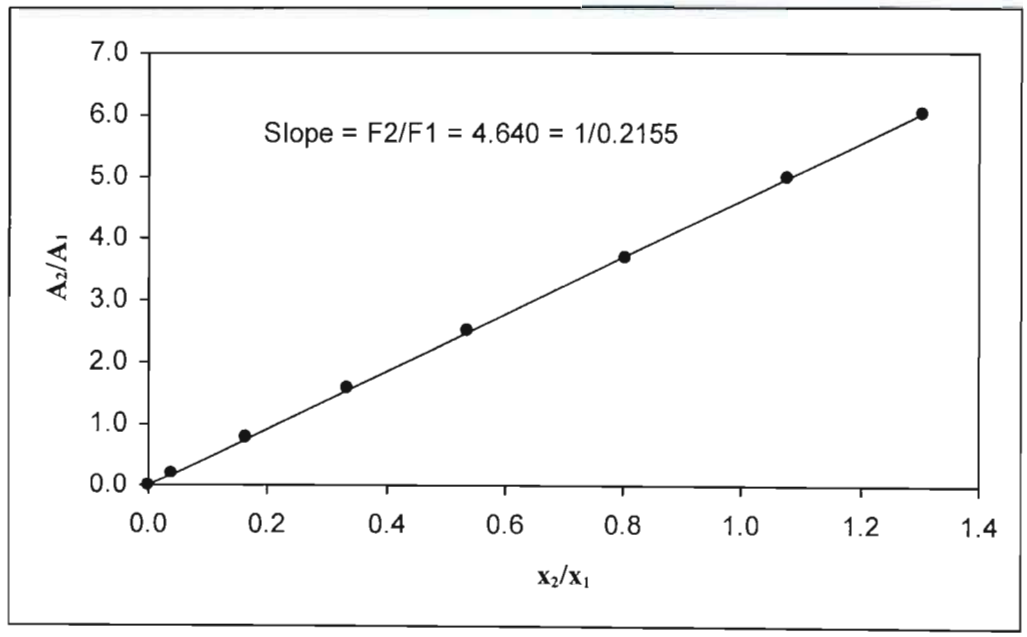

Figure C.6. A_2/A_1 versus x_2/x_1 for the 1-propanol (1) + n-dodecane (2) system.

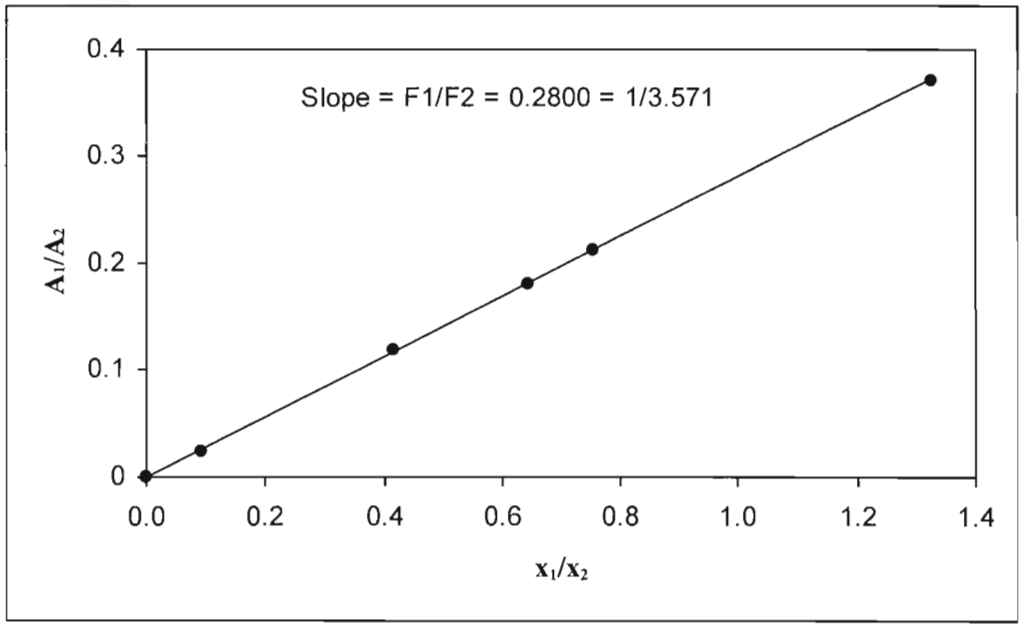

Figure C.7. A_1/A_2 versus x_1/x_2 for the 2-butanol (1) + n-dodecane (2) system.

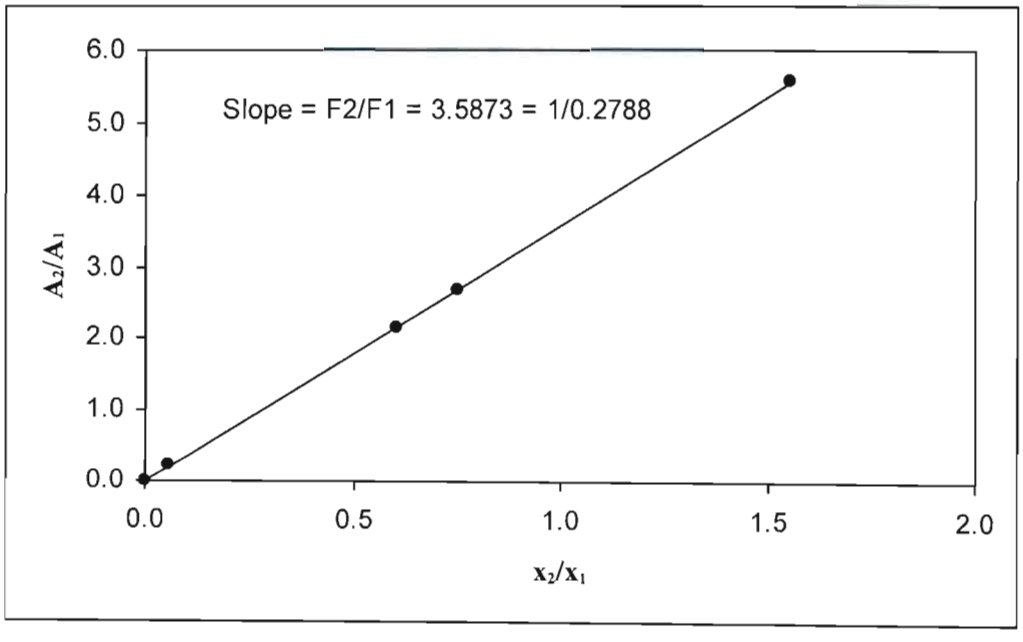

Figure C.8. A_2/A_1 versus x_2/x_1 for the 2-butanol (1) + n-dodecane (2) system.

APPENDIX D

THE OPTIMIZATION ROUTINES

D.1. Vapour Pressure correlations

The vapour pressure correlations employed were the Antoine, Cox, Frost-Kalkwarf, modified Frost-Kalkwarf and the Wagner equations. The Nelder-Mead Simplex algorithm was employed within the technical computing framework of the MATLAB® (version 7.0.1) workspace for all the vapour pressure fits. A separate treatment of the models used will be presented below so as to provide a platform for a comparison of the computational efficiency (times, sensitivity to initial guess, *etc.*) and correlative efficiency *i.e.* fit of the equation to the models.

D.1.1 The Antoine Equation

For the correlation of the vapour pressure data of the saturated hydrocarbons (n-alkanes and cyclohexane), the Antoine equation proved to be the most computationally efficient and provided excellent fits for $P \leq 100\,\text{kPa}$. In the fitting procedure, the Antoine equation was highly insensitive to the initial guess and was observed to converge to a solution quite rapidly *i.e.* between 5 and 10 seconds. However, at elevated pressures and for the alkanols, it proved weaker in this regard, as did the other correlations.

D.1.2 The Cox Equation

The use of the Cox equation necessitated the assignment of a reference pressure (P_{ref}) and reference temperature (T_{ref}) for the use of the equation. As in the fitting procedure of Chirico *et al.* (1989), the reference pressure was atmospheric *i.e.* $P_{ref} = 101.325\,\text{kPa}$ such that the reference temperature is the normal boiling point of the substance *i.e.* $T_{ref} = T_b$. The Cox equation was the most sensitive of all the vapour pressure correlations to the initial guess, which if very different from the optimal parameters, would not produce convergence. This is due to the relative order of magnitude of its parameters, especially C. Consequently, an effective strategy was to use the parameters from an initial data fitting procedure, where the guess is rather crude, as the refined parameter estimates for a second optimization routine. The Cox equation was in all cases the least computationally efficient with computational times of up to 50 seconds.

D.1.3 The Frost-Kalkwarf Equation

The Frost-Kalkwarf was also sensitive to the initial guess as for the Cox equation but less so. The same strategy was employed where an initial optimization was used to obtain refined parameter estimates for the final optimization. It provided an excellent overall performance with regards to computational times and for the fits of the data sets.

D.1.4 The Modified Frost-Kalkwarf Equation

Despite the claims of the DIPPR Compilation Project (Daubert and Jones, 1990) that values of $E = 2$ or $E = 6$ can be used for the relation, it was found that in many cases with $E = 6$ *i.e.* the Riedel equation (Sandler, 1999), convergence could not be achieved. Consequently, $E = 2$ was used in the fitting of this equation for all the substances, which as for the Frost-Kalkwarf equation, gave an excellent fit to the data.

D.1.5 The Wagner Equation

As the Antoine equation, the Wagner relation was also quite insensitive to the initial parameter estimates. However, the Wagner equation was slightly less computationally efficient than the Antoine equation and produced results of quite similar or slightly inferior accuracy. The longer computational times can be attributed to it being a four-parameter equation. The "2.5-5" and "3-6" forms of the Wagner equation were tested for differences; however, none were significantly apparent. The "3-6" form of the Wagner equation was used in the fitting procedure.

D.2. Vapour-Liquid Equilibrium correlations

The Levenberg-Marquardt algorithm was employed for the minimization of the objective functions in the BUBL P and BUBL T routines for γ_i - ϕ_i methods and the Nelder-Mead Simplex algorithm was used for the BUBL P computations in the ϕ_i - ϕ_i method.

D.2.1. The Gamma-Phi (γ_i - ϕ_i) Method

In general, the BUBL P computations were much more efficient than the BUBL T calculations. The results for the latter were highly sensitive to the values of the vapour pressure correlation constants employed in the formulation of the objective function.

The initial parameter estimates used for the Wilson, T-K Wilson and NRTL models was 5000 $J.mol^{-1}$ for both parameters. For the UNIQUAC and the modified UNIQUAC equations, an initial guess of 5000 and -5000 $J.mol^{-1}$ was used for the parameters, as was recommended by Gess *et al.* (1991).

D.2.1.1 The Wilson Equation

The Wilson equation was computationally efficient with most iterations under 30 seconds in the BUBL P and BUBL T calculations and the equation fitted excellently to most of the data sets. The Wilson equation was insensitive to the initial guesses for the parameters.

D.2.1.2 The T-K Wilson Equation

The T-K Wilson was slightly less computationally efficient than Wilson equation as it required longer iteration times but was also not sensitive to the initial guesses

D.2.1.3 NRTL Equation

The NRTL was sensitive to the initial guess for α_{ij}, even within the accepted value range of 0.1 - 0.5 and also converged slightly slower to a solution than the Wilson equation.

D.2.1.4 UNIQUAC and modified UNIQUAC Equations

The UNIQUAC equation proved to be the least computationally efficient and was slightly sensitive to initial parameter estimates. The lattice coordination number was set at a value of 10, as recommended by Prausnitz *et al.* (1980).

D.2.2. The Phi-Phi (ϕ_i - ϕ_i) Method

The mixing rules that were employed for the correlation of the isothermal data were the Huron-Vidal (HV) and the modified Huron-Vidal mixing rules *i.e.* MHV1 and MHV2 in conjunction with the PRSV EOS and the Wilson equation. In general, the computations were quite efficient and stable with the OF being minimized by the Nelder-Mead Simplex method. However, the success of the correlation with the models was dependent upon a judicious approach in the assignment of the initial parameter guesses.

D.2.2.1 The HV MR

The original HV approach was the least computationally efficient of the all the models and was also sensitive to the initial parameter estimates. The HV MR model struggled to converge to a proper solution for the alkanol + n-dodecane systems and consequently proper results were not achievable with the HV model for this type of system.

D.2.2.2 The MHV1 MR

The MHV1 approach was much more efficient than the HV MR model but took slightly longer to converge to a solution than the MHV2 approach. It was also considerably less sensitive to the initial parameter estimates than the HV model and initial guesses of 5000 $J.mol^{-1}$ were used for both the parameters.

D.2.2.3 The MHV2 MR

Despite the quadratic form for the α_m parameter in the mixing rules, which has to be solved first before a value for a_m can be obtained, the MHV2 model proved to be the most computationally efficient. The model was also fairly insensitive to the initial guesses for the parameters and values of 5000 $J.mol^{-1}$ were used for both parameters.

APPENDIX E

E.1 Formats used for the reference citations

(a) For a journal publication:

Author/s, *Journal name* **Volume (Issue number)** (year) page number/s.

(b) For a conference presentation:

Author/s, "Title of presentation", Conference Title, Organization, Country, year.

(c) For a book:

Author/s, Title of book, edition, Publisher, Publishing Company Location, year, page numbers.

(d) For a chapter in a multi-author book:

Author/s, "Chapter title" in: (Editor/s), Title of book, Publisher, Publishing Company location, year, Volume number, Chapter number, page numbers.

(e) For an online internet resource:

Resource information. Available online from: website address.

E.2. Contractions used for the journal names

Adv.Chem.Ser.	Advances in Chemical Series
Adv.Cryogen.Eng.	Advances in Cryogenic Engineering
AIChE.J.	American Institute of Chemical Engineers Journal
Am.Chem.Soc.Symp.Ser.	American Chemical Society Symposium Series
Ann.Phys.Chem.	Annual Review of Physical Chemistry

Austr.J.Chem.	Australian Journal of Chemistry
Austr.J.Sci.Res.	Australian Journal of Scientific Research
Ber.Bunsenges.Phys.Chem.	Berichte Der Bunsen-Gesellschaft fur Physikalische Chemie
Bull.Pol.Acad.Sci.	Bulletin of the Polish Academy of Sciences
Bull.Japan.Petrol.Inst.	Bulletin of the Japan Petroleum Institute
Can.J.Chem.Eng.	Canadian Journal of Chemical Engineering
Chem.Eng.Comm.	Chemical Engineering Communications
Chem.Eng.J.	Chemical Engineering Journal
Chem.Eng.Sci.	Chemical Engineering Science
Chem.Eng.Technol	Chemical Engineering and Technology
Chem.Proc.Eng.	Chemical Engineering Progress
Chem.Eng.Progr.Symp.Ser.	Chemical Engineering Progress Symposium Series
Chem.Rev.	Chemical Reviews
Collect.Czech.Chem.Commun.	Collection of Czechoslovak Chemical Communications
Compt.Rend.	Comptes Rendus Hebdomadaire des Seances de l'Academie des Sciences
C.R.Acad.Sci.	Comptes Rendus de l' Academie des Sciences
Dev.Chem.Eng.Min.Proc.	Developments in Chemical Engineering and Mineral Processing
Fluid Phase Equilib.	Fluid Phase Equilibria
Ind.Eng.Chem.	Industrial and Engineering Chemistry
Ind.Eng.Chem.Anal.Ed.	Industrial and Engineering Chemistry Analytical Edition
Ind.Eng.Chem.Fundam.	Industrial and Engineering Chemistry Fundamentals

Ind.Eng.Chem.Res.	Industrial and Engineering Chemistry Research
Ind.Eng.Chem.Proc.Des.Dev.	Industrial and Engineering Chemistry Process Design and Development
Int.J.Phys.Chem.	International Journal of Physical Chemistry
Int.J.Thermophys.	International Journal of Thermophysics
Int.J.Energy.Research.	International Journal of Energy Research
J.Am.Chem.Soc.	Journal of American Chemical Society
J.Chem.Thermodyn.	Journal of Chemical Thermodynamics
J.Chem.Ed.	Journal of Chemical Education
J.Chem.Eng.Japan.	Journal of Chemical Engineering of Japan
J.Chem.Phys.	Journal of Chemical Physics
J.Phys.Chem.	Journal of Physical Chemistry
J.Sci.Intrum.	Journal of Scientific Instruments
J.Serb.Chem.Soc.	Journal of Serbian Chemical Society
J.Supercrit.Fluids.	Journal of Supercritical Fluids
J.Tokyo.Chem.Soc.	Journal of Tokyo Chemical Society
Molecul.Phys.	Molecular Physics
Philos.Mag.	Philosophical Magazine
Pure.Appl.Chem.	Pure and Applied Chemistry
Rev.Institut.Francais.Petrol.	Revue de Institut Francais du Petrole
Rev.Sci.Instrum.	Review of Scientific Instruments
Trans.AIChE.	Transactions of the American Institute Chemical of Engineers
Trans.IChemE.	Transactions of the Institution of Chemical Engineers

Z.Physik.Chem.	Zeitschrift fur Physikalische Chemie

UNIVERSITY OF KWAZULU-NATAL

DEVELOPMENT OF A NOVEL APPARATUS FOR VAPOUR-LIQUID EQUILIBRIUM MEASUREMENTS AT MODERATE PRESSURES

2006

PRASHANT REDDY